MEDICAL RADIOLOGY

Diagnostic Imaging

A. L. Baert
M. Knauth
K. Sartor

Imaging in Transplantation

A. Bankier
Editor

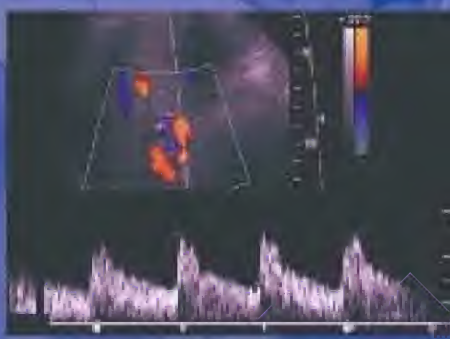

Springer

MEDICAL RADIOLOGY

Diagnostic Imaging

Editors:
A. L. Baert, Leuven
M. Knauth, Göttingen
K. Sartor, Heidelberg

Alexander A. Bankier (Ed.)

Imaging in Transplantation

With Contributions by

H. Antretter · A. A. Bankier · T. Franquet · M. Freund · N. Grenier · N. Heaton
P. Jaksch · D. Kienzl · J. B. Kruskal · J. E. Kuhlman · C. Kulinna-Cosentini · G. Laufer
S. Mehrain · P. Merville · G. Pasticier · I. Pedrosa · V. Raptopoulos · J. Sierra
O. Tucker · K. M. Unsinn · G. A. Zamboni

Foreword by

A. L. Baert

With 213 Figures in 424 Separate Illustrations, 99 in Color and 15 Tables

Springer

Alexander A. Bankier, MD
Director of Functional Respiratory Imaging
Beth Israel Deaconess Medical Center
Harvard Medical School
330 Brookline Avenue
Boston, MA 02215
USA

Medical Radiology · Diagnostic Imaging and Radiation Oncology
Series Editors:
A. L. Baert · L. W. Brady · H.-P. Heilmann · M. Knauth · M. Molls · C. Nieder · K. Sartor

Continuation of Handbuch der medizinischen Radiologie
Encyclopedia of Medical Radiology

Library of Congress Control Number: 2006930914

ISBN 978-3-540-40229-9 Springer Berlin Heidelberg New York

This work is subject to copyright. All rights are reserved, whether the whole or part of the material is concerned, specifically the rights of translation, reprinting, reuse of illustrations, recitations, broadcasting, reproduction on microfilm or in any other way, and storage in data banks. Duplication of this publication or parts thereof is permitted only under the provisions of the German Copyright Law of September 9, 1965, in its current version, and permission for use must always be obtained from Springer-Verlag. Violations are liable for prosecution under the German Copyright Law.

Springer is part of Springer Science+Business Media

http//www.springer.com
© Springer-Verlag Berlin Heidelberg 2008
Printed in Germany

The use of general descriptive names, trademarks, etc. in this publication does not imply, even in the absence of a specific statement, that such names are exempt from the relevant protective laws and regulations and therefore free for general use.

Product liability: The publishers cannot guarantee the accuracy of any information about dosage and application contained in this book. In every case the user must check such information by consulting the relevant literature.

Medical Editor: Dr. Ute Heilmann, Heidelberg
Desk Editor: Ursula N. Davis, Heidelberg
Production Editor: Kurt Teichmann, Mauer
Cover-Design and Typesetting: Verlagsservice Teichmann, Mauer

Printed on acid-free paper – 21/3180xq – 5 4 3 2 1 0

Foreword

Organ transplantation is considered one of the major advances in modern medicine and surgery of recent decades.

Thousands of patients all over the world owe their lives to the revolutionary surgical techniques and new methods in immunosuppression applied in human transplantation, which is also a supreme example of human interindividual solidarity.

As in most other domains of modern medicine, radiological imaging plays a major role in the correct selection of donors and donor organs, as well as in the optimal therapeutic management and care of the transplanted patients.

I am very much indebted to A. Bankier for accepting the challenging task of editing a much needed volume dedicated to all radiological aspects of organ transplantation in humans. This book is the result of a very successful collaboration between a group of international experts in the field and offers a comprehensive overview of all radiological issues relevant to all those involved in the care of transplanted patients.

I congratulate the editor and contributing authors for this outstanding, well researched, and superbly illustrated book.

I am convinced that this volume on a hot clinical topic will be of great interest to both radiologists in training and certified radiologists, as well as to transplant surgeons and medical specialists with an interest in transplantation.

I sincerely hope that it will meet with the same success as the many other volumes previously published in the series, Medical Radiology – Diagnostic Imaging.

Leuven

Albert L. Baert

Preface

By the time I started my medical internship – which, despite many grey hairs on my head, is not too long ago – the "art" of transplantation was a somewhat esoteric subdiscipline of medicine reserved for a handful of experts based in highly specialized academic institutions. Although this core of transplantation medicine still exists today, substantial progress in the field of surgical transplantation techniques and post-transplantation care has brought transplant recipients beyond the boundaries of specialized centers into a much wider medical environment. As a consequence, organ recipients, notably after bone marrow, kidney, liver, and heart transplantation, are now seen in the daily practice of many general practitioners and, thereby, of many general radiologists. The primary aim of this book, therefore, was to provide the non-specialized radiologist with an easily accessible and comprehensive manual covering essential and routine-relevant diagnostic topics in the imaging of transplantation.

The second aim of this book was fostered by personal experience. Throughout my radiological practice in the field of transplantation, I have witnessed the simple impossibility of providing meaningful diagnostic and clinical care in the absence of a sincere devotion to strong interdisciplinary collaboration. This conviction is mirrored in the structure of this book. The radiological chapters are all preceded by clinical chapters aimed at embedding radiological information in the indispensable background of clinical knowledge. The second aim of this book, thus, was to enforce a multidisciplinary approach to diagnostic imaging in the field of transplantation medicine.

The book's third aim was to increase awareness of the open issues in transplantation medicine. Despite the tremendous advances that transplantation has made over the last decade, substantial problems remain. Many of these problems have moved from the early post-transplantation period into the mid- and long-term follow-up of transplant recipients, and thereby into the fields of chronic allograft rejection, chronic infection, sequels of chronic high-dosed medication, and transplant-unrelated co-morbidity. Without any doubt, radiological techniques have a key role to play in all of these areas; hence, sufficient attention from the radiologist to these still emerging and ever expanding issues is required, as are adequate related training efforts in this field. Hopefully, this volume will contribute a modest part to this effort.

I will not end this preface without expressing my gratitude to the individuals who have – voluntarily or not – substantially contributed to making this book happen. I would first like to thank all the authors involved in this work. I strongly believe that the quality of their contributions has made this a comprehensive, informative, and up-to-date contribution to the field of transplantation medicine. I would then like to thank

my fellows and residents. They have missed their teacher quite a bit during the "hot" periods of this project, and they paid me back, not by complaining, but by asking pertinent questions and by providing me with interesting cases. I would like to thank Peter Jaksch and Walter Klepetko from the Lung Transplantation Unit of my home University of Vienna, Austria. Their clinical and surgical competence, combined with their reliability, have made our daily collaboration a productive and enjoyable partnership. I owe my deep gratitude to Pierre Alain Gevenois, Department of Radiology, and Marc Estenne, Lung Transplantation Unit, both at the Hôpital Erasme, University of Brussels, Belgium. Their support, expertise, and friendship have aided our fruitful research collaboration in the field of lung transplantation over the past decade. Without their ongoing input, many things would simply not have happened. I would also like to thank Christiane Knoop, Alain Van Muylem, and Denis Tack, all from the same institution, for satisfying my often intrusive (and most likely annoying) avidity for their help and knowledge.

It is to Ursula N. Davis at Springer-Verlag that I sincerely apologize for my sometimes more than undulating working rhythm, a rhythm she tolerated with admirable patience and humor. Without her moral support and her enduring determination, I would not have made it through this project.

I am also grateful to Prof. Albert L. Baert, AZ Gasthuisberg, University of Leuven, Belgium, who put his paternal trust in me to get this volume accomplished.

My final thanks go to my children. Particularly during the final phases of this book project, their father had – as worded by a reasonably impatient daughter – his "head in the clouds," while he should have been caring for the really important things in life such as homework and ball games…

Boston

Alexander A. Bankier

Contents

Solid Organ Transplantation: Past, Present, and Future Challenges

1

Christiane Kulinna-Cosentini and Alexander A. Bankier

CONTENTS

1.1 Historical Overview

The dream of curing illness and injury by transplanting tissues or entire organs is probably as old as the history of healing itself. Transplantation began indeed many centuries ago as a primitive practice and has since evolved into a modern medicine reality.

C. Kulinna-Cosentini, MD
Department of Radiology, Medical University of Vienna, Waehringer Guertel 18–20, 1090 Vienna, Austria
A. A. Bankier, MD
Director of Functional Respiratory Imaging, Beth Israel Deaconess Medical Center, Harvard Medical School, 330 Brookline Avenue, Boston, MA 02215, USA

The earliest evidence of an orthotopic autograft (organ is placed in its normal anatomic position) has been preserved from the Bronze Age. A circular disk of bone was removed from the calvarium to relieve intracranial pressure and later replaced as an autograft (Sharma and Unruh 2004). Written accounts from Egypt, China and India dating back many centuries describe manifold experimentations in grafting (Sharma and Unruh 2004). Potters of the Koomas caste in India reported that around 800 BC, the surgeon Susrata grafted a new nose from skin flaps (Transweb 2000). In the sixteenth century, reports of tissue autograft transplantation (transplants using the patient's own tissue) were more congruent to our current scientific standards. Tagliocozzi from Italy successfully transplanted skin flaps from the patient's own arms to re-create their nose (rhinoplasty) (Calne 1963; Transweb 2000). It was not until a couple of centuries later that successful allografts (transplants from one human individual to another) or xenografts (from animal to human individual) were carried out: in 1668 van Meeneren (Transweb 2000) documented the first successful bone graft, whereby bone from a dog's skull was used to repair a defect in human cranium. The modern age of organ transplantation began in the twentieth century with Alexis Carrel, based on his pioneering work devoted to vascular replacement. He described the method of joining blood vessels by replacing the artery with a segment of a vein in the early 1900s (Sharma and Unruh 2004). An organ perfusion system created by Carrel and Charles Lindbergh led to the development of cardiopulmonary bypasses, thus making open heart surgery a reality (Sharma and Unruh 2004). The kidney was the first vital organ to be successfully transplanted. In 1933, the Russian surgeon Veronoff performed the first human allograft (kidney from mother to son) without the benefit of tissue typing. The procedure failed, the kidney never functioned, and the

16-year-old boy died from rejection 22 days later (Sharma and Unruh 2004). In 1954, Joseph Murray achieved the first successful kidney transplantation from one identical twin to another without using anti-rejection drugs (Houston Chronicle 2004; Transweb 2000). In 1962 the first cadaveric kidney transplant was performed (Transweb 2000). The organ functioned for 21 months. This was made possible thanks to 6-mercaptopurine, the first useful immunosuppressive drug. Soon after the first successful kidney transplantations, other organ transplantations followed: in 1963 James Hardy transplanted the first lung (Gift of Life Donor Program 2004). In 1966 there was the first simultaneous pancreas/kidney transplantation and 1 year later the first successful liver transplantation followed (Barber 2003; Gift of Life Donor Program 2004).

There was a period of 62 years from the first experimental cardiac transplantation in animals at the University of Chicago in 1905 until the first successful human heart transplantation on 3 December 1967 by Christian Barnard (Gift of Life Donor Program 2004; Sharma and Unruh 2004). The transplant recipient was a 54-year-old man with end-stage ischemic heart disease; the donor was a young man with severe brain injury. The recipient initially recovered but subsequently died of pseudomonas pneumonia 18 days later. After multiple attempts of cardiac transplantation with poor outcomes, the 1-year survival during the 1970s improved from 22% in 1968 to 65% in 1978 (Sharma and Unruh 2004). This success occurred because of improved management of infectious complications, the aggressive diagnosis and treatment of rejection, and better donor and recipient selection.

1.2 Organ Procurement for Transplantation

A worldwide shortage of donor organs has led to the development of national and international systems for organ procurement and allocation. Such systems promote organ donation and ensure fair distribution of available donor organs through a combination of legislation, organ exchange organizations (OEOs), transplant coordinators, publicity campaigns, donor cards, and professional training programs (de Meester 1997).

Although these measures have decreased inappropriate organ allocation, the problem of donor organ shortage is far from being solved. Most early transplant programs were operated locally, and waiting lists were short. Therefore, suitable recipients could often not be found for the available organs (Cohen and Wight 1999). This issue promoted centralized organizations aimed to coordinate organ procurement and allocation in larger geographic perspectives. The OEOs were generated for this requirement, ensuring the best possible match between donor and recipient, and prioritizing the most urgent cases.

Most OEOs operate on a national basis such as in Italy or Spain (Cohen and Wight 1999). Other European countries, for example Austria, Belgium, Germany, Luxembourg and the Netherlands, operate together and are organized by the Eurotransplant Foundation (Cohen and Wight 1999). The United Kingdom Transplant Support Service Authority (UKTSSA) serves the UK and Ireland; and Scandia Transplant serves Denmark, Finland, Iceland, Norway and Sweden. In the USA, the national organization is the result of an alliance between regional agencies, known as the Organ Procurement and Transplantation Network (OPTN). Eurotransplant is the largest OEO in Europe and serves an area of 500,000 km^2 and a population of 116 million. In contrast Scandia Transplant serves an area of 1,100,000 km^2 and a population of 24 million, whereas the OEO of Spain covers an area of 500,000 km^2 and serves 40 million (Cohen and Wight 1999).

Cadaveric organ donation remains the most important graft source for organ transplantation. The concept of brain stem death is essential to the process of cadaveric heart-beating organ donation (Department of Health 1983). Potential donors include any patient deeply unconscious on a ventilator as a result of severe irreversible brain injury of known etiology or patients who have suffered spontaneous intracerebral hemorrhage, acute neurological trauma and cerebral anoxia from different causes. The first step following identification of a potential organ donator is the assessment of clinical signs of brain death (Kaufmann and Lynne 1986). Brain stem death must be recognized by two independent physicians not involved in the organ procurement team. These two physicians should perform two sets of brain stem function tests, before brain stem death is confirmed (Kaufmann and Lynne 1986). In a deeply comatose patient, maintained on a ventilator, the criteria to be satisfied that brain stem death has occurred are (Royal College of Physicians Working Party 1995):

- Fixed and dilated pupils not responding to bright light
- Absent corneal reflexes
- No motor response to painful stimuli
- No reflex activity unless of spinal cord origin
- No oculocephalic reflex (doll's eyes)
- Absent vestibulo-ocular reflexes
- No gag or cough reflex to bronchial stimulation by the passage of a suction catheter
- No respiratory movements (without mechanical ventilation until arterial pCO_2 rises above 60 mmHg.

Ingestion of alcohol, neurodepressant drugs or metabolic abnormalities such as hypernatremia can mimic the clinical picture of brain death. So it is an absolute condition that sufficient time should pass by for the effect of any such drug intoxication to wear off before performing brain stem testing.

If the diagnosis of brain death is confirmed and consent to remove the organs and/or tissues has been obtained, the transplant coordinator arranges an appropriate time for this procedure. At this point "patient care" becomes "donor maintenance," and the intention is to keep optimal organ function for the benefit of the recipient. Organs of donors can be lost at this stage if management is difficult and time-consuming. So high medical and nursing care is as fundamental at this stage as is the management by the transplant coordinator. On one hand, the transplant coordinators are responsible for the local organization of organ donation and communication with OEO; on the other hand, they have to determine, if they travel to a donating hospital, whether the organs are suitable for transplant when a potential donor becomes available. The donor's medical history is carefully examined and the medical status is evaluated for possible further investigations. All relevant information is sent to the OEO for eventual allocation of the available organs.

The consent of the living donors is regulated by law in most countries (Fluss et al. 1997). Frequently, this consent must be legally binding and written (Terasaki 1991), and only few countries allow the consent to be informed and oral (Terasaki 1991). In most countries, medical examination for suitability of organs is required by law, and in a few countries it is indicated in local technical guidelines (Fluss et al. 1997).

In all but one European country, consent for a donation from the deceased donor is embedded in a binding law (Land and Cohen 1992). Most countries have a donor register in place, which can differ from country to country: a dedicated register of donors, non-donors or combined registers (Cohen and Wight 1999).

1.3 Patient Selection for Transplantation

1.3.1 Donor Selection Criteria

The criteria for cadaver organ selection are regulated by technical guidelines in most countries in Europe, with only nine having binding selection criteria in place (European Commission 2003). Figure 1.1 shows the different factors included in the risk assessment in the different countries and the manner in which they are regulated (binding requirements, technical guidelines or not regulated). In contrast, there is consensus in the use of a number of biological tests, which are routinely determined beforehand: human immunodeficiency virus antibody (anti-HIV) 1 and 2, hepatitis C virus antibody (anti-HCV), hepatitis B virus antibody (anti-HBV), hepatitis B antigen (Ag-HBs), cytomegalovirus (CMV), Treponema pallidum. However, this does not apply for some other tests, for example toxoplasmosis, human immunodeficiency virus antigen (Ag-HIV), human T-cell leukemia virus (HTLV).

1.3.2 Recipient Selection Criteria

All recipients undergo a comprehensive pretransplantation medical and psychological evaluation, during which emphasis is placed on the cardiovascular system to determine operative risks and physiologic age (Stratta et al. 2005). Patients then are discussed at a multidisciplinary pretransplantation selection committee meeting, with candidacy for transplantation determined by group decision (Stratta et al. 2005). Patients are then admitted on a waiting list. In the context of current organ shortage, there is a continuous debate about whether elderly patients should go onto the national waiting lists, or be part of specially designed schemes to which older or marginal organs, e.g., kidney, are preferentially allocated (Oniscu et al. 2004). In 1999,

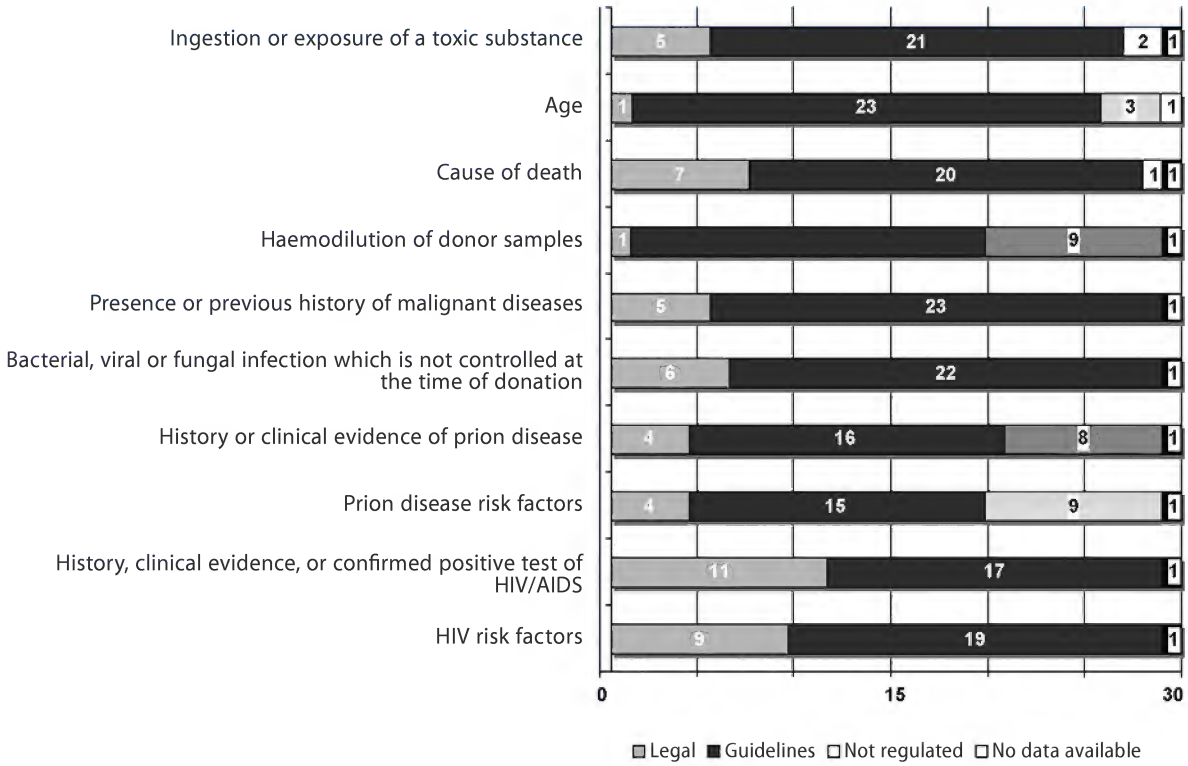

Fig. 1.1. Risk assessment criteria (European commission 2003)

Eurotransplant Leiden started the Eurotransplant Senior Program (ESP) "old for old" to give older patients with renal insufficiency the possibility of kidney transplantation (Schlieper et al. 2001). The aim is to use kidneys from donors older than 65 years for recipients older than 65 years. Kidney transplantations in older recipients have been performed with good results (Cantarovich et al. 1994; Sola et al. 1998).

1.4 Immune Responses to Allografts/Xenotransplantation

Matching the tissues of an organ donor and those of the recipient is wanted because the immune system attacks foreign tissue. This process is called rejection. Some patients, however, are too ill to wait for a highly compatible donor, so tissue matching is often not optimal. For organs that cannot be donated from a living family member (e.g., heart), a highly compatible donor is rarely available. With the use of immunosuppressive therapy, the success of transplantation is less affected by the compatibility of the donor (Gibbs 1997). It is nonetheless mandatory to find a donor whose tissue type matches the recipient's tissue type as closely as possible (Matas and Schnitzler 2004; Talbot and Manas 1997).

Tissue type is determined by molecules on the surface of every cell in the body. These molecules are called human leukocyte antigens (HLA) or the major histocompatibility complex (Petersdorfet et al. 1998; Villard 2006). Each person has unique HLAs. The HLAs on the cells of the transplant signal to the body that this tissue is foreign, when a person receives a transplant, and stimulate an immune response. The recipient's blood usually is screened for antibodies against the tissues of the specific potential donor. If these antibodies are present severe rejection is expected, and transplantation will not be performed in these cases (Matas and Schnitzler 2004; Talbot and Manas 1997).

Even if tissue types are closely matched, transplanted organs are usually rejected unless preventive measures are taken. Rejection, if it occurs, can begin soon after transplantation – acute rejection – but can

also occur after weeks, months or years, then called delayed rejection (Gibbs 1997). Rejection can usually be controlled by using drugs called immunosuppressants (Schwartz and Damashek 1959).

Immunosuppressive drugs inhibit immune function by targeting both T- and B-cell responses through blockage of cellular proliferation induced by alloantigen stimulation, and by inhibition of the cytokine production necessary for such stimulation (Villard 2006). Optimal immunosuppressive therapy should balance mandatory immunosuppression while preserving immunity against environmental antigens such as bacterial and viral infections (Villard 2006).

Many different types of immunosuppressants can be used to prevent or control rejection. Most of them, including steroids, suppress the entire immune system (Merck 2003). Antilymphocyte globulin, antithymocyte globulin, and monoclonal antibodies suppress only specific parts of the immune system. Immunosuppressants must be taken for an indefinite period. High doses are usually necessary for the first few weeks, and after that smaller doses can usually prevent rejection (Stark et al. 2002; Villard 2006).

1.4.1 Xenotransplantation

Xenotransplantation is the transplantation of organs between different species. Current research is aimed at using pigs as donors by genetically manipulating their immune system so that their organs are accepted by humans (Schmoeckel et al. 1996). Some ethicists give precedence to human needs so they focus on the outcome that best serves the interests of patients and, if successful, xenotransplants could save thousands of human lives. But some questions remain to be answered: including that if there are chances for successful transplantation, what is the risk of transmitting diseases or infections from the animal to the patient.

1.5 Role of Imaging in Transplantation

Radiology is an essential part of a successful transplantation program. Careful donor selection and thorough preoperative evaluation are necessary to avoid any risk for the donor, to minimize complications and to ensure graft function. The role of the radiologist and the different imaging techniques is to define the conditions in which graft donation is contraindicated and to identify anatomic variations that may alter the surgical approach. Exact evaluation of the following individuals and situations in the field of organ transplantation is important for radiologic imaging: (1) the living donor, (2) the cadaveric donor, (3) the recipients, (4) the diagnosis of graft dysfunction, and (5) the diagnosis and treatment of complications.

1.5.1 Evaluation of Living Donors

In living donor transplantation, preoperative evaluation of the donor includes accurate determination of the organ volume, which is crucial to ensure adequate perfusion of both donor and recipient organ, e.g., the liver. Determination of the exact vascular anatomy of the living donor is mandatory, because identification of the replaced or accessory arteries may alter the surgical approach. For that purpose digital subtraction angiography (DSA), helical computerized tomography (CT) angiography or magnetic resonance (MR) angiography can be used. Although DSA and CT have similar results, helical CT or MRI is preferred today due to its non-invasiveness. The definition of the venous anatomy is poorer with DSA than with CT (Burgos et al. 2004).

An additional advantage in using helical CT or MRI is the detection of incidental tumors (Hiramoto et al. 2003) in the organ itself or in other organs.

1.5.2 Evaluation of Cadaveric Donors

An abdominal ultrasound is mandatory in the evaluation of cadaveric donors, especially to exclude chronic diseases of the donor organ and to exclude incidental tumors. Tosaka et al. (1990) reported a prevalence of 0.04 of incidental renal cell carcinoma (RCC) in the general population. However, this prevalence appears to be higher in the cadaveric potential population (Carver et al. 1999). Intraparenchymatous RCC are usually not detected during graft inspection in bench, so renal ultrasound (US) of the donor is essential.

1.5.3 Recipient Evaluation

The most crucial imaging data to be gathered before organ transplantation are about vascular anatomy and the vascular status of the recipient. Are there any abnormalities, such as anatomic variants, which influence the surgical procedure? Is there any atheromatosis or occlusion that could preclude anastomosis viability? Vascular evaluation of the recipient is indicated in patients with claudication or previous vascular surgery, and in asymptomatic patients older than 60 years with vascular risk factors, bruits or asymmetric pulses in the lower limbs (Burgos et al. 2004). A combination of Doppler-ultrasound and helical CT angiography is adequate. Two main indications for MR angiography are evaluation of the vascular anatomy of multiple vessels or vascular abnormalities in the operation area, and exclusion of stenosis in the iliac arteries, e.g., in renal transplantation, so as not to provoke insufficient organ perfusion after transplantation (Burgos et al. 2004).

Another reason for ultrasound or helical CT is to exclude incidental carcinoma. For example, the prevalence of RCC in the dialysis population is higher than in the general population, ranging between 1.5% and 2.6% (Miller et al. 1989; Terasawa et al. 1994). A close relationship also has been reported between acquired cystic kidney disease (ACKD) and RCC, which is four- to six-fold greater than the risk in the general population. Preoperative lung CT, e.g., in patients with cystic fibrosis, is used to study the texture of lung parenchyma and identify areas of maximal lung destruction, bullous disease, and pleural affections that might affect decisions regarding which lung should be explanted first for transplantation or the selection of donor lungs (Marom et al. 1999). Other reasons for lung CT are detection of lung nodules or adenopathy, that might be suggestive of malignancy, and to detect findings that are suggestive of infections (e.g., aspergillosis).

1.5.4 Diagnosis of Graft Function

The absence of graft function in the immediate post-transplant period makes a Doppler ultrasound necessary to exclude vascular thrombosis or stenosis of the pretransplantation vessel. No arterial flow in the graft is suggestive of arterial thrombosis, and the presence of systolic flow with inversion of diastolic flow is diagnostic of venous thrombosis. If there is suggestion of artery stenosis in Doppler ultrasound, the diagnosis should be confirmed by DSA, CT angiography or MR angiography. If obstruction or hemodynamic stenosis are diagnosed early in the postoperative period, surgical repair may be successful.

DSA has served as the gold standard to make this diagnosis. However, the invasiveness of DSA makes it less attractive as a diagnostic tool in the early postoperative period. Color Doppler sonography has been proposed as an alternative means of detecting such complications, but many authors have reported frequent false-negative sonographic examinations, primarily due to flow-through collateral vessels after thrombosis of the artery.

Multi-phasic multidetector CT allows, in a single examination, a comprehensive evaluation of potential liver donors and of graft recipients. 3D-CTA with maximum intensity projection, multiplanar reconstructions, shaded surface display, and volume rendering techniques has become a strong competitor for DSA. The new development of multislice CT (MSCT) allows scan times fast enough to image the liver during a pure arterial phase of contrast opacification. This offers the possibility of 3D CTA for a variety of clinical applications.

1.5.5 Diagnosis and Treatment of Complications

Most complications occur in the early postoperative phase. Thus, clinicians should be mindful of the possibility of obstruction, bleeding or acute rejection.

Ultrasonography is the technique of choice for the diagnosis of post-transplant fluid collections such as pleural effusion, lymphocele, abscess, hematoma or urinoma. It can also be used therapeutically to drain these fluid collections. Furthermore ultrasound is used for guidance to collect biopsy samples to exclude necrosis or acute rejection in pathology. Sometimes ultrasonographic findings may be misleading, so further investigation with helical CT is required, especially for acute bleeding or graft stenosis. In this case early interventional re-vascularization may rescue the graft, obviating the need for re-transplantation. The degree of parenchymal ischemia can be assessed with contrast-enhanced CT.

Pathologies not affecting the transplanted organ but influencing further therapeutic decisions such as infections and/or other comorbidities, e.g., pneu-

monia, are other reasons for performing postoperative imaging such as chest X-ray or lung CT.

1.6 Ethical and Economical Issues in Organ Transplantation

Most ethical issues in transplantation result from the need for more organs. The debate focuses on the fair share of the organs and on the attempt to increase the number of available organs. At the First International Congress on Ethics, Justice and Commerce in Transplantation held in Ottawa, Canada in 1989, consensus was reached on several resolutions, including commercialism (buying and selling of human organs and tissues is unacceptable), potential donors (patients in a persistent vegetative state should not be considered donors), organ retrieval (alleged criminal activity to obtain organs for transplant is abhorrent), and organ allocation (distribution of organs must be equitable). Prolonging life through transplantation is desirable, but it must take place within an ethical framework (Program Committee 1990).

1.6.1 What are some Ethical Issues in Transplantation Today?

Before recipients are added to the waiting list, they are evaluated by a specialized health care team at the transplant hospital. Several tests and evaluation criteria are used for recipient selection. The same criteria are applied to everyone who is referred for a transplant (**the justice principle**). This means treatment should be given without regard to factors such as race, age, gender or any other irrelevant aspect of a patient's persona. Moreover, it should have the rather general virtues of fairness, honesty, balance, and the lack of prejudice.

The **utility principle** means that the probability of a successful outcome is aimed. It looks towards the ambition of achieving the greatest good for the greatest number. It can lead, for example, to the decision that a highly expensive form of treatment for an individual with a poor prognosis should be withheld in favor of a cheaper treatment (of perhaps less dramatic benefit).

All patients have complex medical conditions so each individual patient is evaluated within these broad criteria (**the beneficence principle**). The likely benefits of any treatment are balanced against the possible risks before any treatment decision is made. This allows us quite ethically to recommend a course of treatment with significant potential risks if we are satisfied that the potential benefits, and the likelihood that the benefit will occur, more than balance the risk.

Now as ever there are lots of discussions focused on a patient's age in transplantation. Should younger patients be transplanted before older patients? In the recent past, chronologic age was a contraindication both for organ donation and transplantation. However, similar to trends in the overall general population, there has been an increasing, yet disproportionate, shift towards increasing numbers of older donors and recipients in for example kidney transplantation (Stratta et al. 2005).

So, the concept of age matching has become popular as a method of optimizing usage in elderly donors and recipients (Pessione et al. 2003). The results of kidney transplantation in elderly recipients are in reality very similar to those in younger recipients, particularly when considering death-censored analysis (Pessione et al. 2003). Controversially, a number of studies have shown that the use of older donor kidneys transplanted into younger recipients results in inferior outcomes, which suggests that donor age is a more important risk factor than recipient age (Pessione et al. 2003).

Debates continue surrounding transplantation for alcoholism, smoking, drug abuse, and other behaviors that led to the need for transplant. Can past behavior be a sufficient basis for excluding potential transplant recipients or should these people be eligible for transplantation if they change their behavior? Because of the limited resource of donated organs, transplant donation should also be considered from the life-style perspective of the potential recipient.

1.6.2 Defining the Components of Costs

In this age of expensive medical care, many people wonder whether financial compensation for organ donation would be too expensive. In fact saving lives means saving money. Kidney transplants are cheaper than dialysis over prospective lifetimes and

they pay for themselves within 2–3 years (Loubeau et al. 2001; Matas and Schnitzler 2004; Schweitzer 1998). Most of the costs of dialysis are paid by the Federal government through the End Stage Renal Disease (ESRD) program. Thus, any increase in organ supply automatically reduces costs to the Federal government.

Direct costs include the operation itself, fees for medication, the stay on intensive care units and the costs for preoperative tests.

Indirect costs consist of the economic consequences of lost or impaired ability to work or engage in leisure activities, such as lost income and household costs related to domestic maintenance and chores as well as to dependant care (Klarenbach et al. 2006).

Some countries have fixed costs and other countries, especially in Europe, calculate the components of transplantation for each individual case. To get a rough idea of costs, a kidney transplantation without any complication and a hospital stay of 20 days is calculated in Austria to be about € 40,000, whereas a liver transplantation costs about € 70,000. In Germany, a kidney transplantation was calculated to be € 50,000, and a liver transplantation € 120,000 (Rotondo 1995).

In US, average billed charges per transplantation in 1999 consisted of different categories, such as evaluation of recipient, candidacy, procurement, hospital, physician, follow-up, and immunosuppressants. For a kidney transplantation without the first three categories (operation and hospital stay only) the charge is about $ 80,900; for liver transplantation, $ 195,600. These arbitrarily chosen numbers mirror the high geographical variability of transplantation-related costs.

References

Barber N (2003) The nasty side of organ transplantation. A short history of human and xeno transplanting. http://www.geocities.com/organdonate/AAACh18HistoryofHumanandXeno.html

Burgos F, Pascual J, Marcen R, Garcia-Navas R, Gomez V, Ortuno J (2004) The role of imaging techniques in renal transplantation. World J Urol 22:399–404

Calne RY (1963) Introduction and history. Renal transplantation. Edward Arnold, London, pp 3–4

Cantarovich D, Giral-Classe M, LeSant J (1994) Renal transplantation from cadaver donors over 60 years old. Clin Transplant 237:237–242

Carver B, Zibari G, McBride V (1999) The incidence and implications of renal cell carcinoma in cadaveric renal transplants at the time of organ recovery. Transplantation 67:1438–1440

Cohen B, Wight C (1999) A European perspective on organ procurement: breaking down the barriers to organ donation. Transplantation 68(7):985–990

de Meester J (1997) Organization of donation and organ allocation. In: Chapman JR DM, Wight C (eds) Organ and tissue donation for transplantation, Vol 226. Edward Arnold, London

Department of Health (1983) Cadaveric organs for transplantation. a code of practice including the diagnosis of brain stem death. Department of Health, London. http://www.dh.gov.uk/en/PublicationsAndStatistics/LettersAndCirculars/HealthServiceCirculars/DH_4003033

European Commission (2003) Directorate-General and Consumer Protection Public Health and Risk Directorate Unit C6 Health Measures. Human organ transplantation in Europe: an overview. http://ec.europa.eu/health/ph_threats/human_substance/documents/organ_survey.pdf

Fluss S, Dickens BM, King AR (1997) Legislation on organ and tissue donation. In: Chapman JRDM, Wight C (eds) Organ and tissue donation for transplantation, Vol. 95. Edward Arnold, London

Gibbs P (1997) Transplant immunology – for surgeons. In: Forsythe J (ed) Transplantation surgery. Saunders, Edinburgh, pp 63–88

Gift of Life Donor Program (2004) History of organ and tissue donation and transplantation. www.donors1.org

Hiramoto J, LaBerge J, Hirose R (2003) Live donor renal transport using kidney with arteriographic evidence of mild renovascular disease. Clin Transplant 16:24–29

Houston Chronicle (2004) A brief history of transplants. www.chron.com/content/chronicle/special/transplant/history.html

Kaufmann H, Lynne J (1986) Brain death. Neurosurgery 19:850–856

Klarenbach S, Garg A, Vlaicu S (2006) Living organ donors face financial barriers: a national reimbursement policy is needed. CMAJ 174(6):797–798

Land W, Cohen B (1992) Post mortem and living donation in Europe-transplant laws and activities. Transplant Proc 24:2165

Loubeau P, Loubeau J, Jantzen R (2001) The economics of kidney transplantation versus hemodialysis. Prog Transplant 11:291–297

Marom E, McAdams H, Palmer S et al (1999) Cystic fibrosis: usefulness of thoracic CT in the examination of patients before lung transplantation. Radiology 213(1):283–288

Matas A, Schnitzler M (2004) Payment for living donor (vendor) kidneys: a cost-effectiveness analysis. Am J Transplant 4(2):216–221

Merck (2003) Principles of transplantation: suppression of the immune system (2003) www.merck.com/mmhe/print/sec16/ch187/ch187b.html

Miller L, Soffer O, Nannan V (1989) Acquired renal cystic kidney disease in end stage renal disease: an autopsy study of 155 cases. Am J Nephrol 9:322–328

Oniscu G, Brown H, Forsythe J (2004) How old is old for transplantation? Am J Transplant 4:2067–2074

Pessione F, Cohen S, Durand D, Hourmant M, Kessler M, Legendre C (2003) multivariate analysis of donor risk fac-

tors for graft survival in kidney transplantation. Transplantation 75:361–367
Petersdorf E, Gooley T, Anasetti C, Martin P, Smith A, Mickelson EM (1998) Optimizing outcome after unrelated marrow transplantation by comprehensive matching of HLA class I and II alleles in the donor and recipient. Blood 92:3515–3520
Program Committee (1990) Ethics, justice and commerce in transplantation: the epilogue. Transplant Proc 22(3):1054
Rotondo R (1995) www.transplantationen-information.de
Royal College of Physicians Working Party (1995) Criteria for the diagnosis of brain stem death. Working party review. J R Coll Phys 29:381–382
Schlieper G, Ivens K, Voiculescu A, Luther B, Sandmann W, Grabensee B (2001) Eurotransplant Senior Program "old for old": results from 10 patients. Clin Transplant 15:100–105
Schmoeckel M, Nollert G, Shahmohammadi M (1996) Human decay accelerating factor successfully protects pig hearts from hyperacute rejection by human blood. Trans Proc 28:768–769
Schwartz R, Damashek W (1959) Drug induced immunological tolerance. Nature 183:1682–1683
Schweitzer E (1998) The shrinking renal replacement therapy "break-even" point. Transplantation 66(8):s5
Sharma S, Unruh H (2004) History of adult transplantation. www.emedicine.com/med/topic3497.htm
Sola R, Guirado L, Lopez N (1998) Renal transplantation with limit donors: to what should the good results obtained be attributed? Transplantation 66:1159
Stark K, Gunther M, Schonfelf C, Tullius S, Bienzle U (2002) Immunisations in solid-organ transplant recipients. Lancet 359:957–965
Stratta R, Sundberg AK, Rohr MS, Adams P (2005) Optimal use of older donors and recipients in kidney transplantation. Surgery 139(3):324–333
Talbot D, Manas D (1997) Matching the graft to the recipient. In: Forsythe J (ed) Transplantation surgery. Saunders, Edinburgh, pp 45–62
Terasaki P (1991) History of transplantation: thirty-five recollections, Vol. 341. UCLA TT Laboratory, Los Angeles
Terasawa Y, Suzuki Y, Morita M (1994) Ultrasonic diagnosis of renal cell carcinoma in hemodialysis patients. J Urol 152:846–850
Tosaka A, Ohya D, Yamada K (1990) Incidence and properties of renal masses and symptomatic renal cell carcinoma detected by abdominal ultrasound. J Urol 144:1097–1100
Transweb. History of Transplantation (2000) www.transweb.org/reference/timeline/historytable.htm
Villard J (2006) Immunity after organ transplantation. Swiss Med Wkly 136:71–77

Heart Transplantation

2

2.1 Epidemiological, Clinical and Surgical Considerations

Herwig Antretter and Guenther Laufer

CONTENTS

H. Antretter, MD, Professor
G. Laufer, MD, Professor
Klinische Abteilung für Herzchirurgie, Universitätsklinik für Chirurgie, Anichstrasse 35, 6020 Innsbruck, Austria

2.1.1 History and Epidemiology

Heart transplantation (HTX) has evolved over the past 39 years from a rarely performed experimental procedure to a clinically well established therapy with an excellent circumoperative outcome regarding survival and quality of life. It was Christiaan Barnard who performed unexpectedly the first successful human-to-human heart transplant (allograft) on 3 December, 1967 at Groote Schuur Hospital in Cape Town, South Africa (Barnard 1967, 1968); however, outstanding efforts to develop this surgical therapy were made by Norman Shumway and Richard Lower at Stanford University (Lower and Shumway 1960; Shumway et al. 1966) over a long period of time. Norman Shumway himself performed the fourth heart transplant in the world in January 1968, which was the first adult human to human heart transplantation in the United States.

In this early era most of the first 100 procedures failed (Bailey 2000) and patients who survived were only short-term survivors. Subsequently cardiac transplantation nearly disappeared from clinical practice in the early 1970s. Major efforts were concentrated at the Stanford University and Dr. Shumway and his group again applied new concepts, especially in immunosuppression (cyclosporin A), that subsequently led to the reappearance of this therapy in the early 1980s (Jamieson et al. 1979). Other important impacts were the development of improved procurement protocols allowing transplantation of hearts from remote donors (Watson et al. 1979). Caves established in Stanford the transvenous technique for serial sampling of the myocardium for rejection surveillance by using a bioptome (Caves et al. 1974). Finally a histologic system for grading cardiac allograft rejection was first described by Margaret Billingham at Stanford University (Billingham 1985).

Cardiac allotransplantation has rapidly increased with more than 70,000 transplant procedures to date. It is an established treatment modality for selected patients with end-stage heart failure who are not responding to any other maximal medical or surgical therapy; however, its availability remains limited. As there are many potential candidates for this life-saving therapy and the shortage of suitable donor organs is profound, careful selection of possible recipients is important in order to obtain excellent long-term results and not to waste one of the relatively fixed number of donor organs.

To achieve good results is not only a matter of surgical techniques, it depends on appropriate patient selection, adequate donor management, organ procurement and the prevention of perioperative complications. It should be emphasized, however, that surgical performance and the application of appropriate techniques are necessary prerequisites for treatment success.

As long as we have to use human organs there will be a tremendous shortage of donor organs worldwide. Due to increasing waiting lists, a result of the broadening of acceptance criteria, it is imperative to restrict this therapeutic option to those who have the poorest prognosis and therefore the greatest need. Thus these patients will derive the maximum benefit.

2.1.2 Pre-Surgical Evaluation: Recipient Evaluation and Selection

Because of the donor shortage appropriate selection of potential transplant recipients is of great importance. They should have an unacceptably high predicted short-term mortality or a very low quality of life despite aggressive medical therapy or after all other surgical therapies have failed. The candidate evaluation has to focus on pre-operative risk factors and on all additional factors that can negatively influence the post-transplant outcome.

The overwhelming majority suffer from either ischemic cardiomyopathy or idiopathic dilated cardiomyopathy in combination with intractable heart failure (Hosenpud et al. 1997). But there is also an increasing proportion of patients who develop cardiac allograft vasculopathy several years after HTX awaiting a second HTX (retransplantation). Finally the number of children with congenital heart diseases on transplant waiting lists both early after birth and later as a grown up with congenital heart disease (GUCH) is increasing. Other infrequent indications for enrolment to cardiac transplantation, such as electrical storm (Dubin et al. 2003; Greene et al. 2000), are depicted in Table 2.1.1.

For candidate selection several factors have to be assessed: low left ventricular (LV) ejection fraction, right ventricular dysfunction, the New York Heart Association (NYHA) functional class, ventricular arrhythmias, measurement of functional capacity with determination of maximal oxygen consumption, hemodynamic measurements, pulmonary capillary resistance and the neurohumoral activation resulting from congestive heart failure (elevated plasma norepinephrine levels) (Aaronson et al. 1997; Doval et al. 1996; Gradman and Deedwania 1994; Mancini et al. 1991; Stevenson et al. 1990).

Absolute contraindications to cardiac transplantation are obviously all concomitant diseases with poor prognosis and a short expected life span, such as neoplasm, severe cerebral illness, and generalized severe peripheral vascular disease. Other contrain-

Table 2.1.1. Indications for cardiac transplantation. Causes of end-stage heart failure (the percentage in *parentheses* represents the amount of patients in our clinical cohort who underwent cardiac transplantation between 1997 and 2004)

Indications for HTX at University Hospital Innsbruck	1.1.1997–31.12.2004
Ischemic cardiomyopathy	89 (53.3%)
Idiopathic dilated cardiomyopathy	55 (32.9%)
Valvular heart disease	11 (6.6%)
Hypertrophic obstructive cardiomyopathy	2 (1.2%)
Restrictive cardiomyopathy	1 (0.6%)
Electrical storm	1 (0.6%)
Arrhythmogenic right ventricular dysplasia	1 (0.6%)
Cardiac allograft vasculopathy (retransplantation)	3 (1.8%)
Congenital heart disease	4 (2.4%)
Transposition of great arteries	3
Ebstein's malformation	1
Total	**167 patients**

dications are severe obesity, severe osteoporosis, irreversible pulmonary parenchymal disease, mental illness and drug abuse (alcohol, tobacco, and illicit drugs).

Also the presence of any active life-threatening infection is traditionally an absolute contraindication to cardiac transplantation, except mediastinitis following implantation of a ventricular assist device or a previously treated endocarditis. These situations are consistent with good outcome despite a higher correlation of post-transplant mediastinal infection.

Additionally an elevated fixed pulmonary hypertension with a pulmonary vascular resistance of more than 6 Wood units is a contraindication for orthotopic heart transplantation.

Relative contraindications should be considered on an individual basis [psychosocial instability, a documented noncompliance and diabetes with evidence of end-organ dysfunction (nephropathy, neuropathy, retinopathy)]. Chronic cardiac hepatopathy, caused by severe heart failure resulting from prolonged recurrent congestion and/or impaired arterial perfusion, is a common entity in patients evaluated for HTX. Hepatic dysfunction generally normalizes within several weeks following HTX, is consistent with good long-term survival and seems therefore to be a benign, potentially reversible disease (Dichtl et al. 2005).

A history of prior malignancy increases the risk of a subsequent fatal malignancy following HTX (DiSalvo et al. 1998). Cardiac transplantation may be considered, however, if there is no evidence of residual, recurrent or metastatic disease for a sufficiently long period, which means the malignancy is cured (Kirklin et al. 2002a). By the way all patients should be screened appropriately for malignancy by CT scan of cranium and chest, abdominal ultrasound and exact physical examination.

Currently it is our general policy normally not to transplant patients older than 70 years. The elderly population is the fastest growing segment in all western industrial countries and a fundamental change has been taking place recently regarding open heart interventions in elderly patients with acceptable morbidity, mortality and improved quality of life. Therefore, well-selected recipients older than 70 years with single organ damage, that is a failing heart, can be evaluated for transplantation (Blanche et al. 1996) and can yield clinical results comparable to those of younger patients (Marelli et al. 2002).

Other basic considerations regarding a good candidate for heart transplantation are sufficient motivation and compliance by the patient and positive support from the family or any other relatives.

2.1.2.1 Complications Before Transplantation – Artificial Heart

Patients awaiting heart transplantation are normally in the New York Heart Association Class III–IV, showing different symptoms of heart failure, hemodynamic compromise, and exercise capacity. Frequent re-evaluation and close medical surveillance are mandatory during their time on the waiting list for HTX. Despite aggressive medical treatment mortality remains high for those with end-stage heart disease. The proportion of patients undergoing transplant on an urgent basis has continued to increase (Hankins and Mancini 2001). At least 10%–25% of listed patients die on the waiting list prior to HTX.

If there is clear evidence of worsening prompt hospital admission for intensive therapy is necessary. As the availability of a suitable donor heart is not predictable, hemodynamic deterioration is first treated with intravenous inotropic support. When the low-cardiac-output syndrome continues to be refractory, patients are put on a mechanical circulatory device for temporary mechanical support. This "bridge to transplantation" concept enables patient stabilization, withdrawal of intravenous medication (inotropic agents, catecholamines, calcium sensitizers) and rehabilitation (Antretter et al. 2002a). During chronic mechanical circulatory support a low level of exercise is possible and the patients are able to walk around, to leave hospital and sometimes they are followed up by heart failure specialists in an outpatient clinic. Nearly 25% of the most recent cohort transplanted from 1 January, 2001 to 30 June, 2003 were on some type of mechanical circulatory support (Taylor et al. 2004).

Several systems are now available for circulation support. Ventricular assist devices (VAD) are mechanical pumps that can take over the circulatory function of the left ventricle (LVAD), the right ventricle (RVAD) or both ventricles (biventricular assist device – BVAD). The patient's native heart remains in place, and the VADs are implanted in a heterotopic position. Connection between the heart chambers and the great vessels is usually achieved

using cannulae. The pumps are designed for either intracorporeal implantation (within the body) or paracorporeal placement (outside the body – in most cases paraumbilical). According to the design blood flow is either pulsatile (pulsatile pumps, for example: Pierce-Donachy Thoratec VAD, HeartMate XVE-LVAS, Novacor LVAD, Berlin Heart Excor) or non-pulsatile (centrifugal pumps: Medtronic Bio-Medicus, ECMO – extracorporeal membrane oxygenation; axial flow pumps: MicroMed DeBakey, Berlin Heart Incor, HeartMate II, Impella).

The total artificial heart (TAH) is designed for orthotopic heart replacement, and is thus capable of replacing the function of the entire heart. The artificial pumps are implanted orthotopically after the patient's diseased native heart has been removed. Currently there are only pulsatile designs available (CardioWest TAH, AbioCor IRH, Penn State TAH). A total artificial heart is indicated in patients with severe aortic valve insufficiency, intractable ventricular arrhythmias, an acquired ventricular septal defect, or irreversible biventricular failure requiring a high pump output (Renlund 2004).

Berlin Heart offers several miniaturized editions of VADs down to a pump chamber size of 10 ml in order to apply the concept of "bridge to transplantation" to the small cohort of children and babies suffering from severe congestive heart failure who are not responding to aggressive medical therapy (Hetzer et al. 1998).

2.1.3 Operation

2.1.3.1 Cardiac Donor and Procurement

In order to expand the number of potential donors, selection criteria have been modified over the years with the aim of recruiting older donors as well. Like recipient selection, the evaluation of potential donor hearts depends on universally accepted objective criteria that may be modified by the particular circumstances and program-based trends within each case.

The ideal donor is young, has no history of cardiac symptoms or coronary risk factors and the mechanisms of injury did not affect heart function at the time of donor evaluation. Longer periods of previous cardiac instability (cardiac arrest, cardiac resuscitation, hypotension, hypoxemia, arrhythmias) are taken into consideration during evaluation, however the actual hemodynamics are of decisive importance for full acceptance of the organ for transplantation.

It is our policy to evaluate every single potential donor by transthoracic or transesophageal echocardiography to exclude cardiac anomalies or congenital heart defects, to assess valve morphology and function, chamber size, wall thickness, and ejection fraction, and to evaluate wall motion abnormalities. In addition, if there is a suspicion of coronary heart disease we try to obtain a coronary angiography, which is frequently logistically impossible. Then it is of great importance to accurately inspect the coronary arteries during organ harvesting. If there are some doubts or visible plaques we generally disclaim the organ. If this situation is foreseeable, an experienced cardiac surgeon has to carry out explantation of the donor organ.

Valuable information is provided by a 12-lead ECG, the insertion of a central venous catheter (for volume status) and in marginal donors a Swan-Ganz catheter (for complete hemodynamic status).

The use of moderate inotropes to maintain a stable output in donors is not a contraindication, but high doses of catecholamines over a longer period can jeopardize the donor myocardium leading to impaired post-transplant function.

It is clear that all laboratory findings and serological test results have to be checked and if there are adverse findings (for example, positive results for anti-HIV) the donor has to be refused.

The upper age limit of donors varies between transplant centers: the older the donor the more extensive the evaluation that is needed. Most centers have an upper age limit of 55 years although some centers have extended this to 65 years of age (Kirklin et al. 2002b). In special cases it is important that donor age is not viewed in absolute terms, but considered along with other important variables such as donor cardiac dysfunction, projected ischemia time, and the recipient's clinical condition. The risk of early mortality after HTX from donors older than 40 years is increased nearly threefold and is multifactorial in nature (Lietz et al. 2004). The use of older donor hearts is associated with an increase in the incidence of transplant vasculopathy at 1 year.

If the organ recipient is in a critically ill and life-threatening status we would also accept a marginal donor for transplantation.

There are of course donors who appear unacceptable at initial evaluation (Copeland 1995). Hemodynamic collapse and cardiac arrest are the natural history of brain death. Therefore, aggressive optimization of the donor must immediately follow the diagnosis of brain death until organ procurement can take place (Poston and Griffith 2004). Organ donors have been reported to have severely depressed circulating levels of free triiodothyronine (T_3) resulting in left ventricular dysfunction (Novitzky et al. 1987). Acute thyroid hormone supplementation before organ harvesting has a hemodynamic benefit, improving the global left ventricular function. Therefore, correction of the hypothyroid environment may result in improved ventricular function (Dyke et al. 1991). Pulmonary artery catheterization and echocardiography can provide guidance on appropriate fluid management. Large doses of inotropes are often the result of hormonal deficiencies that develop after brain death.

For that reason some centers have developed a standardized aggressive approach to donor management that allows functional resuscitation of dysfunctional organs which initially fall outside the transplant acceptance criteria (Boucek et al. 1993; Laks 1995; Wheeldon et al. 1995).

Absolute contraindications for using a potential donor include previous myocardial infarction, severe echocardiographic ventricular dysfunction, severe coronary artery disease (detected by coronary angiogram), intractable ventricular arrhythmia and positive HIV status. Relative contraindications include, among others, positive hepatitis B or C serology, sepsis, history of metastatic cancer, evidence of cardiac contusion, prolonged hypotension, non-critical coronary artery disease, and a history of intravenous drug abuse (Miniati and Robbin 2002).

Finally there is no doubt that careful donor selection is a key to successful heart transplantation (Copeland 1995) and satisfactory post-transplant long-term follow-up.

2.1.3.2 Donor Cardiectomy

After median sternotomy the pericardium is opened in a reversed T-shape fashion and suspended by stay sutures. The heart is examined for evidence of cardiac injury, coronary heart disease and global right and left ventricular contractility.

Then the pericardium is incised over the superior vena cava (SVC) and the vein is dissected circumferentially. Here, care has to be taken not to injure the azygos vein and the sinoatrial node. A suture is passed around the SVC but not tied. Next, the inferior vena cava (IVC) is circumferentially freed from the pericardial reflection.

The ascending aorta is dissected from the pulmonary trunk and circumferentially freed.

After abdominal surgeons have completed their preparations, 25,000 units heparin is administered by the anesthesiologist via a central line. A purse-string suture is placed on the ascending aorta and a cardioplegia cannula is inserted. The suture around the SVC is ligated, the IVC is occluded by a vessel clamp and the heart is allowed to beat empty. Then the IVC is transected. After three to five heartbeats the aorta is cross-clamped immediately before the brachiocephalic trunk and the cardioplegia is started at a pressure-controlled infusion rate. Either the left atrial appendage or one upper lung vein is partially divided to permit the escape of warm blood from the lung and heart.

Usually 2 l of 4°C cold Celsior® cardioplegic solution (Pasteur Merieux, IMTIX – Transplant Unit, Lyon, France) is infused; this was specifically developed for heart transplantation as a perfusion and cold storage solution.

During cardioplegic infusion the heart is topically and continuously cooled with cold saline.

Excision starts inferiorly by retracting the heart upwards and transecting the inferior and superior right as well as the inferior and superior left pulmonary veins (usually at the pericardial reflection – if the lungs are not retrieved). Subsequently, proceeding upwards, the SVC is cut through caudal to the tied suture without injuring the sinus node, the right and left pulmonary arteries are transected and finally the aorta is transected just proximal to the aortic cross-clamp (Fig. 2.1.1).

If the lungs are also retrieved, a modified heart-explantation technique is used. The left atrial incision is made in the middle, between the atrioventricular groove and the orifice of the left pulmonary veins. This incision is extended clockwise to the orifice of the right pulmonary veins in order to preserve enough left atrial tissue for the later left atrial anastomosis as well as enough tissue for the creation of atrial cuffs for the lung transplantation. In this case the pulmonary trunk is transected immediately in front of the bifurcation into the pulmonary arteries.

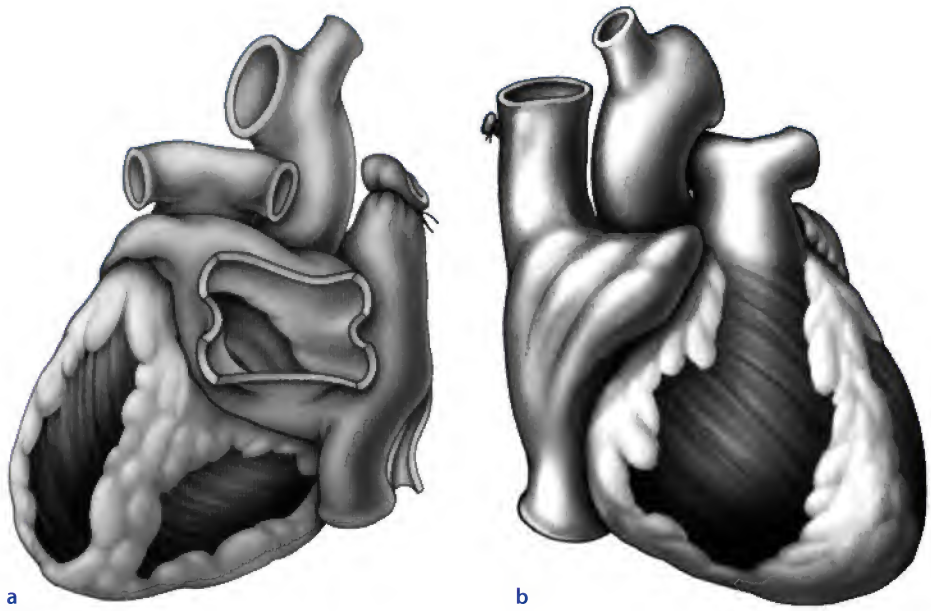

Fig. 2.1.1a, b. Donor cardiectomy. **a** Excised heart and preliminary preparation for the biatrial implantation technique. Ligation of the superior vena cava, incision through the inferior vena cava towards the right atrial appendage. [From Kirklin JK, Young JB, McGiffin DC (2002c) The heart transplant operation. In: Kirklin JK, Young JB, McGiffin DC (eds) Heart transplantation. Churchill Livingstone, New York, with permission.] **b** Excised donor heart with additional length of the superior vena cava for the bicaval implantation technique. [From Kirklin JK, Young JB, McGiffin DC (2002c) The heart transplant operation. In: Kirklin JK, Young JB, McGiffin DC (eds) Heart transplantation. Churchill Livingstone, New York, with permission]

If additional aorta is necessary for the recipient procedure (for example, in pediatric heart transplantation procedures), the transection and following harvest are extended down to the arch vessels (Brown et al. 1996).

After removal of the organ, the heart is placed in a basin filled with cold saline and quickly inspected. If there is an open foramen ovale it is closed there and then in the operating room with a 5-0 prolene suture from either the right or left side. All other preparations are done immediately before implantation.

The heart is then placed into a sterile bag filled with Celsior® solution, all air is evacuated and a ligature is placed around it. We place the first bag into two additional sterile bowel bags, which are tied separately. Protected by three separate sterile layers, the organ is then placed and buried in a container filled with crushed ice. Under these conditions, the myocardial metabolism is significantly reduced, by both diastolic arrest after infusion of crystalloid cardioplegic solution and hypothermic storage at about 2–5°C. With this method, which is currently the only one used for heart preservation, 4–5 h of ischemia time is generally accepted to be safe (Yacoub et al. 1990).

Before leaving the donor hospital the explanting surgeon briefly informs the implanting surgeon in the recipient hospital about special findings, about the exact cross-clamp time, and the estimated arrival time of the donor explant team.

2.1.3.3 Orthotopic Cardiac Transplantation

2.1.3.3.1 Recipient Cardiectomy

We usually start the recipient operation when the donor team has inspected the organ and has started to explant the donor heart. A careful synchronization between donor heart procurement and the beginning of the recipient's operation can avoid unnecessary long organ ischemia time.

The recipient is scrubbed from neck to feet and draped in the same manner as for standard heart lung machine operations. Consequently the whole groin area is accessible (for femoral cannulation).

After standard median sternotomy, opening and suspension of the pericardium, the typically en-

larged heart is cannulated for connection with the heart lung machine in the usual fashion after systemic heparinization: an arterial cannula in the ascending aorta and two venous caval cannulae. A right angle SVC cannula is inserted directly into the SVC 1 cm above the cavoatrial junction close to the orifice of the azygos vein, and then a tape is passed around. The IVC has to be cannulated low, through the right atrium just above the connection with the IVC and far lateral, to allow an adequate atrial cuff after heart excision. Also the IVC is surrounded with tape.

Cardiopulmonary bypass (CPB) is established but not before the arrival of the donor heart organ, except if the patient's hemodynamic status deteriorates rapidly.

If the recipient had previous open heart surgery (a situation not uncommon for heart transplant recipients) we usually dissect the common femoral artery and femoral vein for a short distance in one of the groins. Umbilical tapes are placed around the vessels and everything is prepared for emergency femoral cannulation. Cardiopulmonary bypass can be established immediately if there are serious complications during chest reopening or stepwise division of fibrous adhesions.

Surgical intervention in repeat sternotomy procedures requires sternal division with an oscillating saw. As there are often distinct adhesions between the posterior surface of the sternum and the heavily enlarged heart, injuries (especially of the right ventricle) are not unusual. Therefore, the surgeon has to be aware of that problem and should have experience in reoperative procedures.

After arrival of the donor team, CPB is started and the patient is cooled down to 28°C. Both caval tapes are snared and the aorta is cross-clamped. The right atrium is opened just lateral to the base of the right appendage. The incision is extended inferiorly nearly to the atrioventricular groove and further down to the lateral side of the coronary sinus. It is important to leave enough atrial cuff around the IVC cannula. The right atriotomy is extended superiorly around the atrial appendage to the interatrial septum. Incision of the interatrial septum opens the left atrium.

The aorta is then cut through above the aortic valve and this should be done carefully in order not to injure the right pulmonary artery, which lies directly behind the aorta. After that the pulmonary trunk is transected as proximally as possible.

The heart is then pulled laterally or superiorly and the left atrium is divided: starting at the septum and superiorly and inferiorly the incision is continued along the atrioventricular groove close to the mitral valve to the base of the left atrial appendage, which is also removed. Cardiectomy is now completed. After the diseased heart is removed from the pericardial space both atrial cuffs are trimmed according to the expected size of the donor atrias (Fig. 2.1.2); bleeding in the connective tissue of the atrial cuffs or between the aorta and pulmonary trunk is cauterized. Finally a drainage catheter is implanted into the left upper pulmonary vein through a purse string suture to permit evacuation of blood from left atrium, especially if the left atrial anastomosis has closed this space and blood removal becomes impossible by pump suction (Kirklin and Barratt-Boyes 1993; McCarthy et al. 1996).

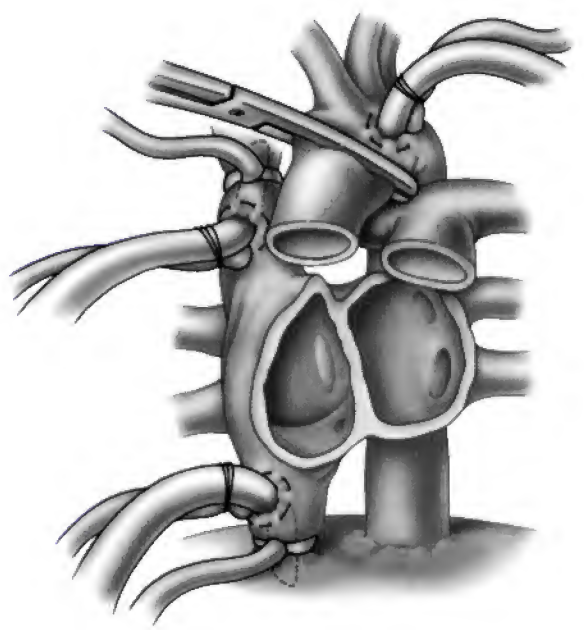

Fig. 2.1.2. Recipient cardiectomy. Intraoperative situation after recipient cardiectomy, before starting the standard bi-atrial heart implantation technique. Note the insertion of the venous cannulae into the superior vena cava (*SVC*) and inferior vena cava (*IVC*) and of the arterial cannula into the ascending aorta, which is cross-clamped immediately before the brachiocephalic trunk. [From Kirklin JK, Young JB, McGiffin DC (2002c) The heart transplant operation. In: Kirklin JK, Young JB, McGiffin DC (eds) Heart transplantation. Churchill Livingstone, New York, with permission]

2.1.3.3.2 Preparation of the Donor Organ

The donor heart is removed from the ice-filled storage box, the outermost plastic bag is opened, the sterile medium bag is carefully lifted out of the outermost bag with a clamp and then placed into a sterile basin. Then the middle plastic box is again opened with sterile scissors and the innermost bag is obtained in the same manner as before. This bag too is opened with sterile scissors and the heart is removed and placed in a new sterile basin for preparation.

First the pulmonary artery is separated from the aorta but one has to be careful not to injure the left main coronary artery. The incision in the left atrial appendage is closed with a polypropylene running suture. If the biatrial technique is employed for implantation the SVC is also closed with a 4-0 polypropylene running suture. It is of great importance not to jeopardize the donor sinoatrial node. The pulmonary artery is then transected at the bifurcation.

The heart is turned over and the bridge of atrial wall between superior and inferior pulmonary veins on either side is removed, as is the bridge between the left and right pulmonary vein orifices in order to create one large left atrial opening. All irregular ends of the pulmonary veins are trimmed away (Fig. 2.1.1a).

Finally the implanting surgeon again looks for a patent foramen ovale and also inspects the aortic and mitral valves for congenital or acquired abnormalities.

2.1.3.3.3 Standard Biatrial Transplantation Technique

This technique is the original procedure initially described by Lower and Shumway (Lower and Shumway 1960; Shumway et al. 1966). Implantation of the donor heart starts with the anastomosis connecting the left atrial cuff of the donor heart to the remnant left atria of the patient heart. (Fig. 2.1.3a). The assistant holds the donor heart left-sided in the chest, enabling the implanting surgeon to make a left inferior anastomosis with a continuous running suture. After reaching the atrial septum inferiorly, anastomosis of the left atrium is then finished by the other end of the suture closing the superior left atrium and the atrial septum. Size discrepancies can be balanced easily. During the implantation topical cooling of the donor heart with ice slush is important for maintaining hypothermia. Then the donor right atrium is opened from the lateral aspect of the IVC to the base of the right atrial appendage. Again a polypropylene suture is used for the right-sided running suture line, starting superiorly at the top of the right atrial donor incision and passing through the top of the recipient right atrial cuff. This suture line is then brought inferiorly along the septum, where deep bites have to be taken (Fig. 2.1.3b). After reaching the IVC near to the inferior cannula, the anastomosis is then continued with the other end of the suture. Starting at the top, the stitches are then brought down, connecting the anterolateral aspects of both remnant right atrias.

Stay sutures are placed wherever necessary. Surplus atrial tissue has to be excised to create competent atrial anastomoses.

Next the pulmonary anastomosis is performed with a 4-0 polypropylene running suture. To avoid kinking of the new pulmonary trunk the proper length has to be measured and the vessels are trimmed. Again at the left lateral side of the recipient, pulmonary artery suturing starts with first completing the back wall and finally the anterior wall. It is important to prevent rotation of the pulmonary artery.

At this point we start systemic rewarming. The aortic anastomosis is carried out in the same fashion as the pulmonary anastomosis (Fig. 2.1.3c). The end-to-end anastomosis between donor aorta and patient aorta is made by continuous whipstitch (also 4-0 polypropylene). As there are often great size discrepancies, compensation is necessary either by opening the donor aorta for about 1 cm or by excision of a triangle on the anterior wall of the recipient aorta.

After that air is removed from the heart and the aortic clamp is removed (Kirklin and Barratt-Boyes 1993). We do not perform the aortic anastomosis prior to the pulmonary anastomosis, as is carried out in many transplant units to reduce graft ischemic time. Instead, we accept a few extra minutes and perform the sometimes difficult pulmonary anastomosis in a bloodless operation field.

2.1.3.3.4 Bicaval Anastomosis Technique

The initial and still widespread technique of standard biatrial transplantation described by Lower and Shumway (1960) has undergone some surgical modifications to reduce disadvantages of the original method.

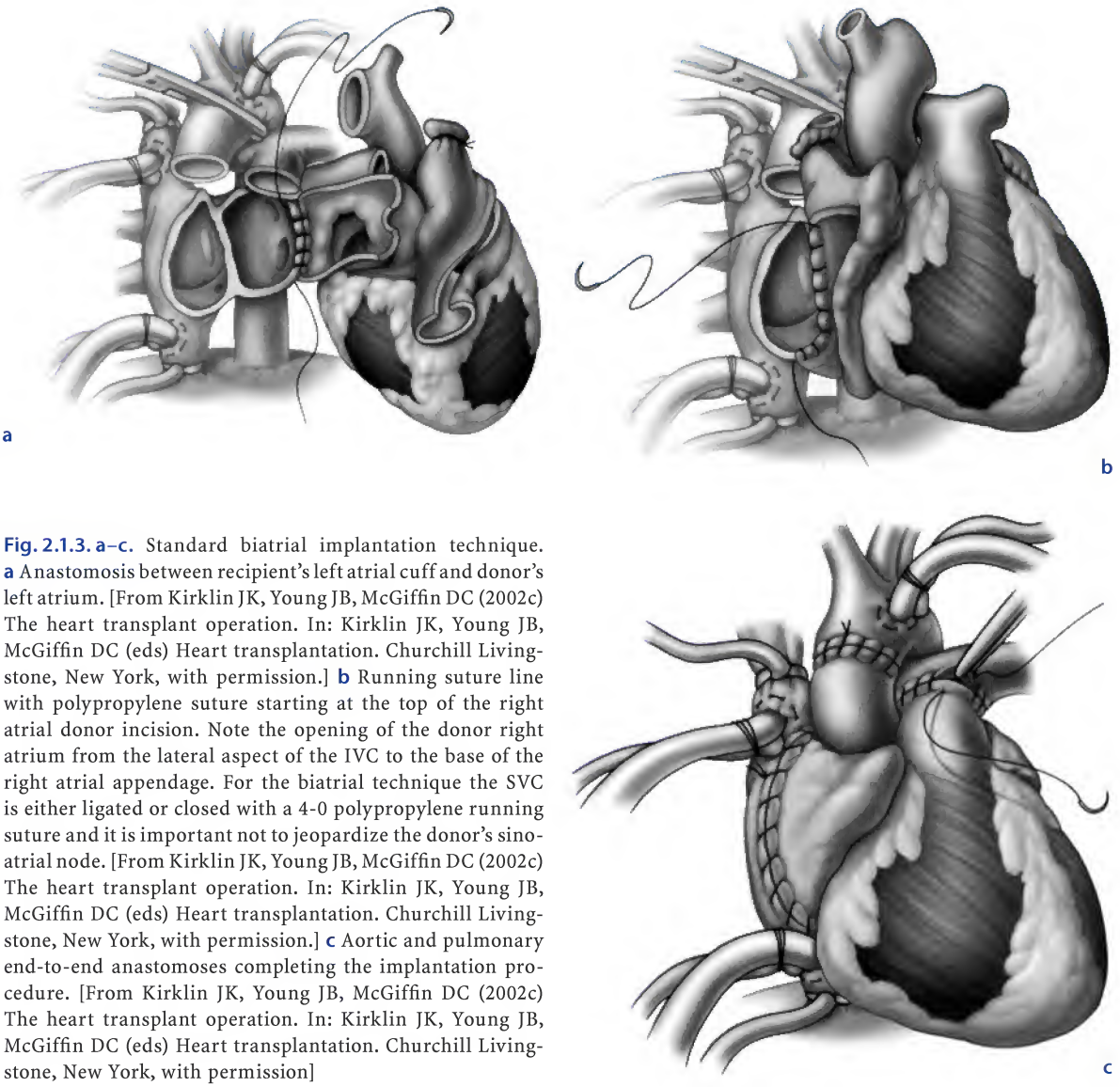

Fig. 2.1.3. a–c. Standard biatrial implantation technique. **a** Anastomosis between recipient's left atrial cuff and donor's left atrium. [From Kirklin JK, Young JB, McGiffin DC (2002c) The heart transplant operation. In: Kirklin JK, Young JB, McGiffin DC (eds) Heart transplantation. Churchill Livingstone, New York, with permission.] **b** Running suture line with polypropylene suture starting at the top of the right atrial donor incision. Note the opening of the donor right atrium from the lateral aspect of the IVC to the base of the right atrial appendage. For the biatrial technique the SVC is either ligated or closed with a 4-0 polypropylene running suture and it is important not to jeopardize the donor's sinoatrial node. [From Kirklin JK, Young JB, McGiffin DC (2002c) The heart transplant operation. In: Kirklin JK, Young JB, McGiffin DC (eds) Heart transplantation. Churchill Livingstone, New York, with permission.] **c** Aortic and pulmonary end-to-end anastomoses completing the implantation procedure. [From Kirklin JK, Young JB, McGiffin DC (2002c) The heart transplant operation. In: Kirklin JK, Young JB, McGiffin DC (eds) Heart transplantation. Churchill Livingstone, New York, with permission]

As a consequence of the biatrial operation, the patient has two sinus nodes, an innervated recipient and a denervated donor node. They are isolated electrically from each other by the atrial running suture line (Fig. 2.1.3c). Frequently it is possible to see the activity of both sinus nodes on an ECG.

The great disadvantage of the biatrial technique is distortion of the atrial geometry, which is associated with atrioventricular valve insufficiency, atrial arrhythmias, and postoperative bradycardia (Melton et al. 1999). This technique also damages internodal pathways. Tricuspid regurgitation is present in a high percentage of patients, and mitral regurgitation can also be observed in many (Angermann et al. 1990) despite normal valve leaflet structures.

These observations led to the development of the bicaval anastomotic technique. Left atrial anastomosis is carried out as prescribed above (see Sect. 2.1.3.3.3). Then separately the SVC and IVC are anastomosed with the intact right donor atrium in an end-to-end fashion with continuous whip stitch using a 4-0 and 5-0 polypropylene suture respectively (Fig. 2.1.4). Care has to be taken to avoid an angulation or stenosis (Morgan and Edwards 2005) of the SVC, which can create a pressure gradient or increase the difficulty of passing a bioptome

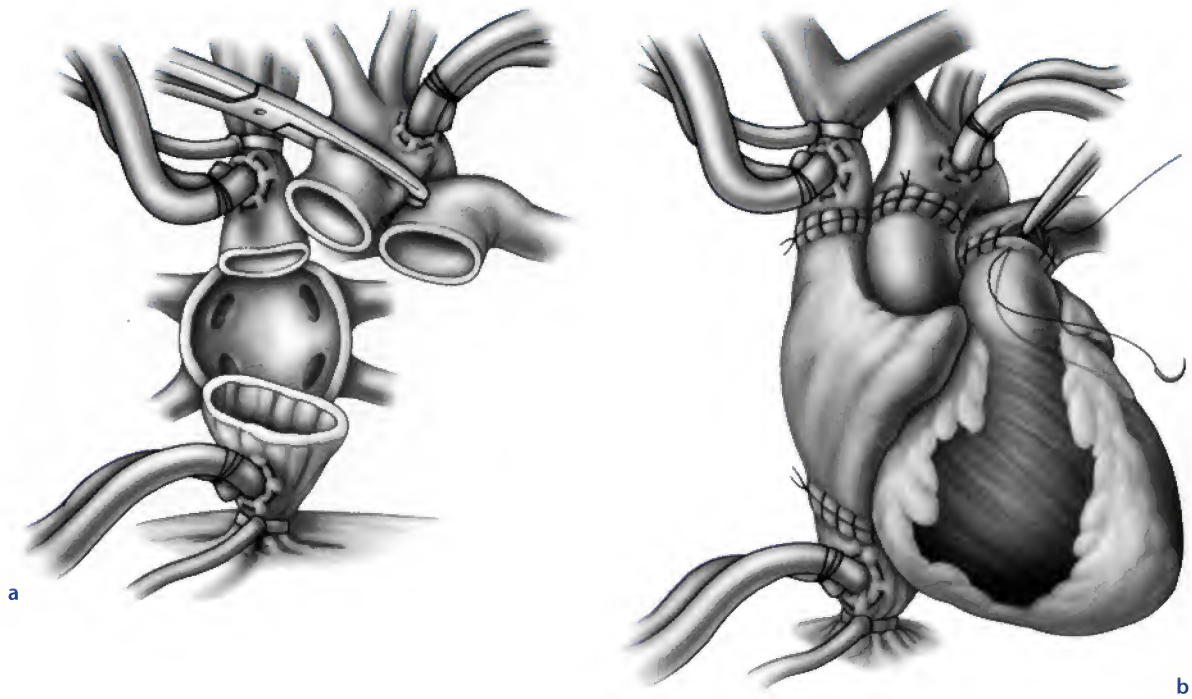

Fig. 2.1.4a, b. Bicaval anastomosis technique. **a** Recipient cardiectomy: also the right atrium is resected with the cuffs of the SVC and IVC left in place. [From Kirklin JK, Young JB, McGiffin DC (2002c) The heart transplant operation. In: Kirklin JK, Young JB, McGiffin DC (eds) Heart transplantation. Churchill Livingstone, New York, with permission.] **b** SVC and IVC are separately anastomosed with the intact right donor atrium in an end-to-end fashion. Aorta and pulmonary artery are dealt with as described for the standard biatrial orthotopic technique. [From Kirklin JK, Young JB, McGiffin DC (2002c) The heart transplant operation. In: Kirklin JK, Young JB, McGiffin DC (eds) Heart transplantation. Churchill Livingstone, New York, with permission]

during performance of endomyocardial biopsies (Kirklin et al. 2002c).

By maintaining the atrial shape, sinus node function is preserved and there is less tricuspid insufficiency than in the biatrial technique. The bicaval technique is also helpful if there are large discrepancies between the donor's and the recipient's atria.

Although this technique is associated with longer cross-clamp and donor ischemia times, the bicaval implantation procedure has significantly reduced the need for permanent pacemaker implantation in contrast to the standard biatrial technique (Deleuze et al. 1995; Meyer et al. 2005).

2.1.3.3.5 Total Orthotopic Heart Transplantation Technique

The technique of total orthotopic cardiac transplantation was introduced by Yacoub et al. (1990) and Dreyfus et al. (1991) and in it both donor atria remain, intact with separate anastomoses of pulmonary and caval veins. By using this implant technique harvesting of the donor heart needs some modifications: the bridge of the posterior left atrial wall has to be kept intact, and the pulmonary veins are joined on each side.

The recipient heart explantation is more extensive compared with other techniques. After circumferential transection of the venae cavae, the left atrium is completely removed leaving only one left-sided and one right-sided atrial cuff. These two cuffs include the ostia of the pulmonary veins.

Implantation of the heart starts with the anastomosis between the left atrial cuff and the corresponding orifice of the left donor atrium; subsequently, the right pulmonary veins are anastomosed in the same manner to the corresponding right orifice of the left donor atrium. The following implantation is then performed in the usual fashion.

Potential complications of this technique include bleeding from the pulmonary anastomoses, which are often accessible with difficulty. As there is also

a higher incidence of (left) atrial thrombosis in the enlarged resultant atria with the biatrial or bicaval technique (Derumeaux et al. 1995), the total orthotopic transplant technique can prevent thrombotic complications.

All cardiac transplantations are completed in the same fashion. After successful termination of cardiopulmonary bypass, post-bypass bleeding is stopped by infusion of protamine, fresh frozen plasma and, if necessary, platelet units (as many of the patients are pretreated with oral anticoagulants). Meticulous surgical hemostasis is essential for preventing postoperative pericardial tamponade necessitating surgical revision. Temporary epicardial pacemaker wires are placed in the anterior right ventricular wall and if needed in the right atrial wall. The chest is drained with pericardial and mediastinal chest tubes and if there are pleural effusions or the pleural spaces have been opened during the procedure pleural chest tubes are also inserted. Chest closure is then carried out in the same manner used for standard open heart procedures.

2.1.3.3.6 Heart Transplantation in Neonates and Children – Pediatric Cardiac Transplantation

The main indication for heart transplantation in neonates is hypoplastic left heart syndrome, which is a lethal malformation if left untreated. Other indications are all cardiomyopathies following complex congenital anomalies with or without staged surgical reconstruction or palliative operations. The underlying anatomy and pathology in children is complex as a large variety of inborn cardiac anomalies may be present. Most pediatric cases undergo several surgical procedures to correct congenital heart defects or to improve the hemodynamic condition with palliative surgery (Schmid et al. 2005).

Highly experienced in neonatal heart transplantation is the Loma Linda group. They started their program of neonatal cardiac allograft transplantation in 1985 after the spectacular baboon heart xenotransplantation in Baby Fae in 1984 (Bailey et al. 1985).

They subsequently presented impressive immediate-term results in 142 transplanted infants regarding operative survival, long-term outcome, growth potential and the quality of life in older survivors (Bailey et al. 1993; Razzouk et al. 1996; Scheule et al. 2002).

The operative cardiac transplant technique is nearly the same as described above adapted to the underlying congenital disease. In hypoplastic left heart syndrome hypothermic circulatory arrest is necessary to enable the aortic anastomosis and reconstruction of the aortic arch using donor tissue.

Older infants requiring heart transplantation often suffer from dilated cardiomyopathy as a consequence of viral myocarditis. Cardiac transplantation is carried out in the same fashion as in grown-ups.

Postoperative complications are the same in children and adults. Rejection, infection, graft vasculopathy, lymphoproliferative disease, and impairment of kidney function are common problems in long-term outcome (Bailey et al. 1995; Penn 1993; Starnes et al. 1989).

A special pediatric problem is growth after heart transplantation. The majority of pediatric candidates for heart transplantation have sub-optimal growth parameters. Poor hemoperfusion during a prolonged pretransplant waiting period, nutrient malabsorption, decreased renal perfusion with induced diuresis, hemodynamic instability with ischemic injury to the hypothalamic pituitary axis with resultant insufficiencies of one or more of the growth-promoting hormones can compromise growth parameters. Factors influencing post transplant growth include age, graft function and glucocorticoid use (Hathout and Chinnock 2004).

The number of transplantations in pediatric patients at many institutions is limited by donor organ shortage. This is best reflected in the number of deaths on the waiting list, which is 25%–40% in pediatric patients and therefore higher than for adult cardiac transplant recipients (Groetzner et al. 2005).

Between July 1996 and June 2005, 11 children underwent heart transplantation at our institution (mean age 9.7±5.7 years, median 10 years, range 8 months to 16 years), with the youngest baby, weighing 6.1 kg at the time of transplantation, having LVAD implantation ("bridge to transplantation") 13 days prior to HTX. Five patients (45.4%) of our transplanted pediatric population needed mechanical circulatory assist prior to HTX.

2.1.3.3.7 Heterotopic Cardiac Transplantation

Heterotopic heart transplantation (h-HTX) was clinically established by Barnard and Losman (1977), who first implanted an auxiliary heart. The

donor heart is placed in the right pleural cavity and anastomosed to the recipient's own myopathic organ (Fig. 2.1.5).

Today this method has relatively few specific indications and is only rarely performed (Cooper and Taniguchi 1996). The greatest disadvantage of this method is the ongoing deterioration of the recipient's poorly contracting heart leading to massive problems during long-term follow-up (Antretter et al. 2002b) (Fig. 2.1.6). In addition, the results of h-HTX are generally inferior to those of orthotopic HTX (Kirklin et al. 2002c).

Presently there is only one basic indication for h-HTX: a markedly elevated pulmonary vascular resistance in the recipient (Newcomb et al. 2004), that is not responding to vasodilative pharmacologic agents. The fixed pulmonary hypertension is one of the leading problems during orthotopic HTX resulting in immediate right heart failure (Klima et al. 2005). The auxiliary heart, acting in parallel with the recipient's own heart (which is the situation in

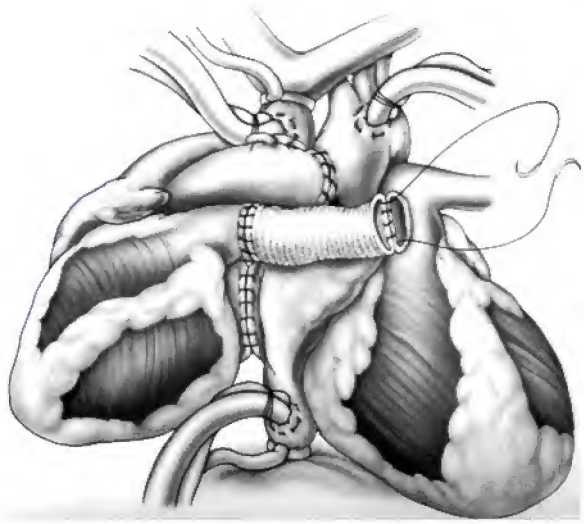

Fig. 2.1.5. Heterotopic cardiac transplantation. The donor's left atrium is anastomosed to the corresponding opening in the native left atrium. Donor superior vena cava is then anastomosed end-to-side to the anterolateral aspect of the recipient's SVC near the junction of the right native subclavian and innominate veins. The donor's aorta is then anastomosed end-to-side to the anterolateral aspect of the native ascending aorta. Finally the donor's pulmonary artery is lengthened with an appropriately sized woven graft (Hemashield prosthesis), which is then anastomosed end-to-side to the anterior aspect of the native pulmonary artery. [From Kirklin JK, Young JB, McGiffin DC (2002c) The heart transplant operation. In: Kirklin JK, Young JB, McGiffin DC (eds) Heart transplantation. Churchill Livingstone, New York, with permission]

Fig. 2.1.6. a Chest radiograph showing the left-sided massive dilated orthotopic native heart in a 35-year-old patient who had a heterotopic heart transplantation 19 years previously [right sided, the heterotopic graft with an abandoned old epicardial pacemaker lead which was previously used for graft rejection monitoring (*arrow*)]. Heterotopic heart transplantation was carried out because of markedly elevated pulmonary vascular resistance. **b** In 1999 the patient presented clinical signs of acute forward failure: ECG showed ventricular fibrillation of his own heart, while the heterotopic graft was in regular sinus rhythm. Transthoracic echocardiography (TTE) revealed severe regurgitation through the incompetent aortic and mitral valves, resulting in a severe decrease in cardiac output. In 2001 the patient's own native heart was removed and the heterotopic graft was transferred into the orthotopic position. Chest radiograph before discharge shows the heterotopic graft after the "transfer operation" in the orthotopic position. The patient is now in NYHA class 0–I. The *arrow* shows the old epicardial pacemaker lead, previously used for rejection monitoring

h-HTX), can manage the elevated pulmonary resistance only with the continuous support of the native right ventricle.

Since diagnosis of fixed pulmonary hypertension will be reassessed in the near future because of the extended use of ventricular assist devices, which show remarkable improvement of so-called fixed pulmonary hypertension, the indications for h-HTX will probably drop down to extremely rare cases, if ever.

Since 1993 – in a continuous series of 234 cardiac transplants performed at our institution – only one h-HTX (0.4%) has been necessary.

2.1.4 Perioperative Complications and Problems

There are some complications which can lead to an initial failure of the transplanted heart. Bleeding from the anastomoses, which is sometimes a major concern, requires a careful search for the source especially as many patients take oral anticoagulants up until the transplantation and therefore suffer from coagulopathy. Massive volume substitution (blood or plasma) after separation from cardiopulmonary bypass (CPB) can lead to right heart failure.

Another common problem is early right heart failure following transplantation because of elevated pulmonary resistance in the recipient. The right ventricle of the donor is not adapted to this elevated pulmonary pressure and is therefore not able to function effectively (Klima et al. 2005).

This can be a serious problem especially if there is a substantial discrepancy in size between donor and recipient (> 30%) or if the donor's right ventricle is affected by myocardial contusions.

Other reasons for right and (also left) heart failure are air embolism into the coronary arteries after separation from CPB because of inadequate removal of air, prolonged cold ischemia time or imperfect preservation or storage of the retrieved organ.

In most circumstances pharmacological therapy with pulmonary vasodilators and inotropic drugs can solve the problem. If not, a mechanical circulatory assist by external RVAD or ECMO should be considered. In recipients with high pulmonary vascular resistance as the principal cause of right ventricular failure, we prefer to use venoarterial ECMO support.

Many patients suffer from rhythm disturbances early after transplantation. Commonly they have a junctional rhythm until normal sinus activity reoccurs. Intravenous isoproterenol therapy early after transplantation can maintain the heart rate about 100–120 beats per minute, optimizing the cardiac output and preventing arrhythmias. Epicardial (atrio-)ventricular pacing is an alternative to pharmacological therapy. Asymptomatic, transient atrial arrhythmias are common with an incidence of about 20%–25% during hospital stay. Ventricular arrhythmias are more common than atrial arrhythmias (incidence up to 60%) and reflect the ischemic and reperfusion injury (prolonged ischemia time), hypokalemia or hypomagnesemia.

The transplanted heart is characterized by autonomic denervation, therefore chronotropic incompetence and, often during intermittent episodes of allograft rejection, sinus node dysfunction are not abnormal – especially in the early postoperative period.

The incidence of permanent pacemaker implantation varies between 6% and 23% (Melton et al. 1999) using the biatrial technique. If necessary a rate-responsive pacing system should be implanted as chronotropic incompetence is the rule. With the use of the bicaval anastomosis technique, the incidence of permanent pacemaker implantation diminished to less than 5%.

In a series of 136 consecutive patients being transplanted with the bicaval anastomosis technique in our department only one (0.7%) needed permanent pacemaker implantation (AAI mode) because of sinus node dysfunction.

Further common postoperative complications include superficial wound infection or deep sternal infection (retrosternal infection – mediastinitis). Prophylactic antimicrobial therapy should therefore be routinely employed. Deep wound infection in an immunocompromised patient always indicates a life-threatening situation and requires both extensive surgical intervention and aggressive antimicrobial therapy.

2.1.4.1 Physiology of the Transplanted Heart

Cardiac transplantation provides remarkable rehabilitation. But it is fundamentally important to remember that cardiac allografts do not function normally. Exercise tolerance may be much less than in normal individuals.

The transplanted heart is completely denervated, therefore no longer supplied by sympathetic and parasympathetic nerves. Denervation leads to a reduced augmentation of peripheral vascular resistance (Mohanty et al. 1987), impairment of renin–angiotensin–aldosterone regulation, a tendency to hypertension (decrease in the vagal inhibitory effect on sympathetic output) and the absence of angina pectoris (Stark et al. 1991). Denervation causes a higher resting heart rate (elimination of vagal-mediated parasympathetic influences).

But there are indications that some heart transplant patients reinnervate their cardiac allograft. Late after transplantation some patients feel angina pectoris, which suggests the partial reestablishment of afferent reinnervation (Kirklin et al. 2002d).

2.1.5 Cardiac Retransplantation

The recipient's half-life (time to 50% survival) after heart transplantation is 8.8 years for adults and more than 10 years for children (Boucek et al. 1999; Hosenpud et al. 1999). The overall retransplantation rate varies from 2.2% to 4.4% in the transplant population (Boucek et al. 1999; Hosenpud et al. 1999) enjoying a prolonged survival. Therefore, a subpopulation of them will redevelop heart failure eventually necessitating a retransplantation.

Primary allograft failure because of recipient pulmonary hypertension, severe or ongoing acute rejection, intractable donor arrhythmias, depressed donor heart function, and technical problems requires urgent or early retransplantation (Razzouk 2000).

The indication for late retransplantation is predominantly (accelerated) coronary graft disease (cardiac allograft vasculopathy, transplant vasculopathy – see Sect. 2.1.7). Because of ongoing immunological reactions in the coronary vessels some patients develop severe diffuse, mostly three-vessel vasculopathy with histopathologically characteristic concentric fibrointimal hyperplasia (Schnetzler et al. 1998). This atherosclerotic process frequently results in silent myocardial infarctions (denervation of the transplanted heart) with subsequent congestive heart failure. These patients benefit only from cardiac retransplantation. As conventional coronary angiography is insufficiently insensitive, intravascular ultrasound (IVUS) is now routinely used for annual or biannual surveillance of heart transplant recipients. IVUS allows for the measurement of intimal area, lumen area, plaque morphology, vessel remodeling, and progression of disease over time (Konig et al. 2000; Miniati and Robbin 2002; Poelzl et al. 2005).

The technique of retransplantation is nearly the same as for primary transplantation with excision of the old graft along the suture lines of the previous anastomoses. If not carried out in the first procedure, bicaval anastomosis for the right atrium can be done in the repeat procedure in order to prevent arrhythmias, tricuspid valve insufficiency and right-sided heart dysfunction. As retransplantation is a second surgical intervention, expertise in reoperative procedures are of importance.

Survival rates after retransplantation depend on several factors: emergency retransplantation has a worse survival with markedly increased operative mortality (Razzouk et al. 1998; Schnetzler et al. 1998). Elective retransplantation has a long-term outcome comparable to that of primary transplantation, especially in patients with transplant-related coronary artery disease (John et al. 1999; Razzouk et al. 1998; Schnetzler et al. 1998). Progress is being made, with an increase in survival rates and an increased time between primary transplantation and the retransplant procedure (Hosenpud et al. 1999).

As there is a distinct shortage of donor organs some propose that retransplantation should not be allowed, in order to save the lives of patients waiting for their first transplant (Collins and Mozdzierz 1993). There are substantial moral, ethical, and financial concerns regarding the fairness of cardiac retransplantation; therefore, a rational approach to cardiac retransplantation is essential.

2.1.6 Strategies of Immunosuppression

Several immunosuppressive protocols pursue the same goal: to prevent rejection of the transplanted allograft (reduction of the intensity of the immune response to a degree that allows acceptance of the allograft) without increasing the risk of subsequent infection. Since the clinical introduction of the more specific immunosuppressive agent cyclosporin

(CsA; now known as ciclosporin) (Calne 1979) the risk of infections has decreased dramatically. Nevertheless ineffective immunosuppression is related to allograft rejection or infection.

Actually basic immunosuppressive therapy consists of an induction therapy with polyclonal antithymocyte globulin for the first 3–5 days post transplant. Methylprednisolone is administered intraoperatively before opening the aortic cross-clamp and is tapered postoperatively. When oral medication is possible, prednisolone is given and gradually reduced. Most patients leave our hospital 4 weeks after transplantation with a daily dosage of 0.3 mg/kg. In order to minimize the negative side-effects of long-term steroid application (Cushing's habitus, weight gain or obesity, osteoporosis, hypertension, diabetes, peptic ulcer disease, hyperlipidemia and psychiatric disorders) we try to withdraw it as early as possible. But in fact it is not clear whether this approach will improve survival and quality of life.

The classic antimetabolite azathioprine (AZA) is added to the other immunosuppressive drugs with a daily dosage of 1.5–2 mg/kg and has to be adjusted according to the white blood cell (WBC) count. Because of its myelosuppressive potential it has to be reduced when leucopenia occurs (fewer then 4,000 WBC/mm^3).

After stabilization of renal function we generally start with ciclosporin on day 3–5 after transplantation, with an initial daily dosage of 5 mg/kg orally divided into twice-daily doses. Later on, dosage is adjusted to the measured trough drug levels, which should be around 200–250 ng/ml early after transplantation and between 150 and 200 ng/ml in the first half year after transplantation, with target trough levels of between 100 and 150 ng/ml during long-term follow-up.

Immunosuppressive therapy following cardiac transplantation is therefore divided into three different phases:

1. Initial high-dose immunosuppression to facilitate graft acceptance and prevent early acute rejection episodes.
2. Chronic maintenance therapy.
3. Treatment of established cardiac allograft rejection with augmented immunosuppression during short- and long-term follow-up.

Modification of the standard triple drug therapy (CsA, AZA, corticosteroids) is not unusual and the clinical introduction of other potent immunosuppressive drugs such as mycophenolate mofetil (MMF) (Kobashigawa et al. 1998), tacrolimus (FK 506) (Taylor et al. 1999), sirolimus (Ikonen et al. 2000), and everolimus (Eisen et al. 2005; Tuzku et al. 2002) is the beginning of a tailored individual immunosuppressive therapy while minimizing toxicity.

2.1.7 Endomyocardial Biopsy, Acute and Chronic Rejection

The key to managing rejection is early diagnosis, before myocyte necrosis and stimulation of vascular endothelial cell proliferation. Rapid diagnosis allows immediate modification of the recipient's immunosuppressive therapy.

To date the standard method for determining acute rejection is endomyocardial biopsy (EMB), an invasive procedure obtaining at least four to six myocardial tissue specimens from different right ventricular locations. Samples are subsequently histologically examined and classified according to the International Society for Heart and Lung Transplantation (ISHLT) scheme (Billingham et al. 1990). Interpretation of the tissue by an experienced pathologist gives valuable information about the sufficiency of the present immunosuppressive therapy.

EMBs are therefore routinely scheduled after transplantation at fixed intervals. Repeated biopsies are necessary after diagnosed and treated rejections in order to document the resolution.

After needle punction and cannulation of the right internal jugular vein (guidewire, sheath) (alternative: subclavian or femoral veins), a bioptome is inserted (in adults: size 7–9 French), advanced to the right atrium, rotated to the left lateral side of the patient, and directed through the tricuspid valve to the right ventricular septum. The jaws are opened, the ventricular septum is touched, the jaws are closed and the bioptome is slowly withdrawn along with the specimen. Biopsy procurement is normally done under fluoroscopic guidance in an operating room or cardiac catheterization laboratory. Alternatively EMBs can be performed under echocardiographic guidance.

Despite EMB being a very safe procedure in the hands of skilled surgeons or cardiologists, it is an expensive, invasive technique, and an inconvenient, unpleasant experience for the patient with inherent

dangers [risk of ventricular perforation with subsequent pericardial tamponade, tricuspid valve injury, bleeding complications at the site of puncture of jugular or subclavian vein (venous hematoma, carotid or subclavian artery puncture), rhythm disturbances (malignant ventricular arrhythmia, supraventricular arrhythmia, transient complete heart block), pneumothorax, and nerve paresis].

Alternatives of non-invasive rejection monitoring have been developed to supplement or replace EMB and are now established in some transplant units: monitoring and recording of intramyocardial electrogram (IMEG) amplitude with telemetry function (monitoring) using a permanent, implanted pacemaker system (Iberer et al. 1998; Warnecke et al. 1992). With this tool it will be possible to abandon EMB, which is important for infants or children, in whom routine EMB cannot be performed (Müller et al. 1993).

Clinical manifestations of acute rejections are unspecific, and most episodes of cardiac rejection are asymptomatic, often only detected by EMB. If there are clinical symptoms, they can be divided into three categories:

1. Constitutional symptoms: fever, malaise, myalgias, and flu-like symptoms.
2. Signs of cardiac irritation: different forms of arrhythmias.
3. Signs and symptoms of cardiac dysfunction and low cardiac output (Kirklin et al. 2002e).

The treatment of acute rejection employs intravenous steroids as a first-line therapy for a grade 2 or more biopsy. Symptomatic patients with arrhythmias, fever or hemodynamic changes are often treated despite lesser grade biopsy results.

Chronic rejection of the cardiac allograft – also called cardiac allograft vasculopathy (CAV), transplant vasculopathy (Tx-CAD), transplant-associated coronary artery disease or graft arteriosclerosis – is one of the main causes of morbidity, mortality and limited long-term results after heart transplantation. It is a diffuse concentric intimal thickening composed primarily of smooth muscle cells which narrow or focally obstruct the coronary arteries of the transplanted heart. In early stages macrophages and lymphocytes typically accumulate in subendothelial areas. CAV may affect vessels along their entire length, and intimal thickening may thus be seen in large and small arteries. The elastic lamina remains largely intact, and calcification is infrequent. Lipids may also be a prominent component of the thickened intima (Yun et al. 2001). Myocardial infarction and interstitial fibrosis result from CAV.

Endothelial injury from immune and non-immune factors triggers multiple deleterious events, including platelet aggregation, endothelial adhesion molecule overexpression, and antibody- and complement-mediated endothelial damage. T-lymphocytes and macrophages firmly adhere to the damaged endothelium, migrate through the basement membrane and stimulate medial smooth muscle cell proliferation and their migration into an expanded intima (Libby 1996). A brain-dead donor, donor heart ischemia, postperfusion inflammation, immune factors, acute rejection, cytomegalovirus, hypertension, and hyperlipidemia all entail endothelial cell injury, which causes CAV development ("response to injury" hypothesis). The collective injury culminates in diffuse intimal thickening within the coronary vasculature.

The prevalence of angiographic CAV increases 10% with each year of post-transplant follow-up. Data from the ISHLT Transplantation Registry show a prevalence of 7.8% and 20.8% at 1 and 5 years of follow-up, respectively (Segovia 2002). Average survival after diagnosis of significant CAV ranges between 2 and 4.2 years (Cantin et al. 2002).

The diagnostic approach to CAV is intravascular ultrasound (IVUS). It can image both the lumen and the intima and identify the luminal area, the maximal intimal thickness, the intimal area, and the intimal index (Eisen 2004).

Treatment of CAV consists of percutaneous transluminal coronary angioplasty and stenting (predominantly drug eluting stents), coronary bypass surgery (which is not successful for this disease) and medical therapy (pravastatin, proliferation signal inhibitors: sirolimus and everolimus). Definitive therapy for selected patients with end-stage CAV is retransplantation.

2.1.8 Infections After Cardiac Transplantation

Infections play an important role in solid organ transplantations. Besides the usual pathogenic organisms, immunocompromised patients are susceptible to infections with organisms that are normally not pathogenic or only sometimes pathogenic.

In addition there is always the possibility of transmitting pathogens with the organ during transplan-

tation, resulting in infections in the early postoperative period during intensified immunosuppression (donor transmitted infectious disease – bacterial, viral or fungal transmission).

The course of infectious disease is often atypical in immunocompromised organ recipients, with a retarded inflammatory response due to immunosuppression. This results in a delay in diagnosis and institution of adequate therapy.

Next, special infections can induce malignant transformations. The post-transplantation lymphoproliferative disorder (PTLD) is a malignant disorder associated with B-cell proliferation induced by Ebstein–Barr virus (EBV) (Aull et al. 2004; Gray et al. 1995; Höfer et al. 2005). EBV has also been implicated in the induction of leiomyosarcoma although the exact mechanisms of oncogenesis are not yet known (Bonatti et al. 2005).

Finally infection with cytomegalovirus (CMV), another member of the human herpes virus family, can be an important cause of severe and sometimes life-threatening disease. Sources of CMV infection in all recipients are either the graft (primary infection of a CMV-seronegative recipient or superinfection of a CMV-seropositive recipient infected with a different strain of virus from a seropositive donor organ) or reactivation of endogenous latent infection in the immunosuppressed host. Seronegative recipients also are at risk of infection via sexual transmission. Transfer of the virus by blood or blood products remains unclear (Antretter et al. 2004).

Different clinical courses are possible after contact with CMV: from asymptomatic infection to CMV syndrome (fever, indisposition, fatigue, unspecific gastrointestinal symptoms, leucopenia, thrombocytopenia, elevated liver function tests) and CMV disease (organ manifestation with the pathologic evidence of CMV in tissue biopsy or blood).

Controversy remains over whether CMV infection can induce acute graft rejection (through increased HLA class II antigen expression) or if intensified immunosuppression early after transplantation and after treatment of rejection predisposes patients to CMV infection. Heart allograft recipients with CMV infection have been shown to have significantly lower survival rates, more frequent acute cellular, vascular and chronic allograft rejections, and subsequently a higher association with accelerated heart allograft vascular disease (transplant vasculopathy) than patients without infection (Antretter et al. 2004; Bonatti et al. 2004).

Infectious complications persist as a major cause of death, especially within the first year of heart transplantation (Hosenpud et al. 2000). Within the first month of transplantation, infections are usually of nosocomial bacterial origin, including *Pseudomonas aeruginosa*, *Staphylococcus aureus*, *Enterococci*, and Enterobacteriaceae. These organisms can cause pneumonia, urinary tract and wound infections. Later infections are commonly caused by viruses and opportunistic fungi (e.g., *Pneumocystis*, *Candida*, and *Aspergillus*) (Miniati and Robbin 2002).

2.1.9 Long-Term Survival After Heart Transplantation

Survival following orthotopic heart transplantation has improved tremendously since the introduction of this treatment modality in the late 1960s. In our institution perioperative mortality is actually 2.6%, 1-year survival 96% and 5-year survival 80% (Fig. 2.1.7). Death within a hospital stay occurred with a mean of 16.2± 8.8 days and causes of death were predominantly infection, early graft failure and multi organ failure. During long-term follow-up major causes of death are allograft coronary artery disease and malignancy. The overwhelming majority (83%) of our long-term survivors are in excellent

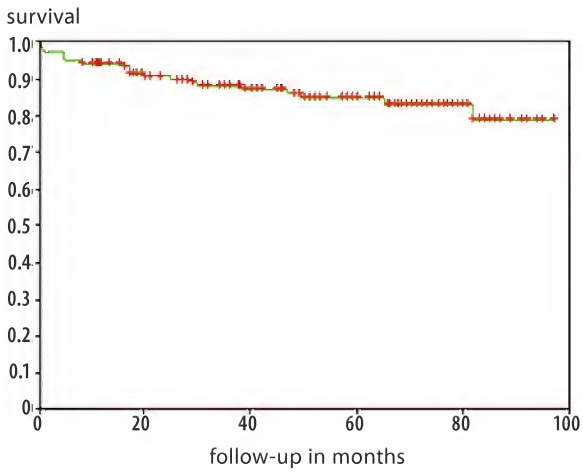

Fig. 2.1.7. Survival following cardiac transplantation (Department of Cardiac Surgery, Department of Transplant Surgery, Medical University Innsbruck, Austria). January 1997 – December 2004, $n = 166$ patients

condition (NYHA I) with no major limitations in physical activity.

According to the ISHLT database, after the first post-transplantation year mortality rate is constant at approximately 4% per year (Hosenpud et al. 2000) with a patient half-life (time to 50% survival) of 9.8 years.

2.1.10 Conclusion

Heart failure is an epidemic disease with increasing prevalence and thousands of patients die annually with-end stage heart failure – many of whom are on the waiting list for heart transplantation. Therefore, appropriate donor and recipient selection is of great importance in gaining maximum benefit for the affected population. Radical alternatives to transplantation, such as partial left ventricular resection (Batista et al. 1996; McCarthy et al. 1997), dynamic cardiomyoplasty (Magovern and Simpson 1996; Moreira et al. 1996), permanent left ventricular assist device implantation (Griffith et al. 1996), biventricular pacing (Linde et al. 2003) and cell transplantation, have been investigated intensively or are under investigation in order to obtain wider clinical application. Some of these alternatives will probably progress into a true alternative to transplantation.

Unfortunately, the success of heart transplantation has only magnified the shortage of donor organs, which will continue to be a tremendous problem. Remarkable relief of donor organ shortage will be achieved in the future when cross-species transplantation becomes available. Xenotransplantation may eventually solve today's problems of a long waiting list with a substantial pretransplant mortality. But there are still important unsolved questions regarding the use of xenogenic organs for transplantation.

References

Aaronson KD, Schwartz JS, Chen T-M et al (1997) Development and prospective validation of a clinical index to predict survival in ambulatory patients referred for cardiac transplant evaluation. Circulation 95:2660–2667

Angermann EC, Spes CH, Tammen A et al (1990) Anatomic characteristics and valvular function of the transplanted heart: transthoracic versus transesophageal echocardiographic findings. J Heart Transplant 9:331–338

Antretter H, Hangler H, Hoefer D et al (2002a) Totaler und partieller Herzersatz – Trends und Entwicklungen. J Kardiol 9:3–13

Antretter H, Poelzl G, Margreiter J et al (2002b) Successful transfer of a cardiac allograft from a heterotopic to an orthotopic position 16 years after heart transplantation. Transplantation 74:540–543

Antretter H, Hoefer D, Hangler H et al (2004) Long-term outcome of cytomegalovirus high risk patients after heart transplantation: comparison between two prophylactic regimes – a single center experience. Eur Surg 36:113–120

Aull MJ, Buell JF, Trofe J et al (2004) Experience with 274 cardiac transplant recipients with posttransplant lymphoproliferative disorder: a report from the Israel Penn International Transplant Tumor Registry. Transplantation 78:1676–1682

Bailey LL (2000) Current opinion in heart transplantation: an introduction: editorial commentary. Curr Opin Organ Transplant 5:115–117

Bailey LL, Nehlsen-Canarella SL, Consepcion W et al (1985) Baboon-to-human cardiac xenotransplantation in a neonate. J Am Med Assoc 254:3321–3329

Bailey LL, Gundry SR, Razzouk AJ et al (1993) Bless the babies: one hundred fifteen late survivors of heart transplantation during the first year of life. The Loma Linda University Pediatric Heart Transplant Group. J Thorac Cardiovasc Surg 105:805–814

Bailey LL, Zuppan CW, Chinnock RE et al (1995) Graft vasculopathy among recipients of heart transplantation during the first 12 years of life. The pediatric heart transplant group. Transplant Proc 27:1921–1925

Barnard CN (1967) The operation. South African Med J 41:1271–1274

Barnard CN (1968) Human cardiac transplantation: an evaluation of the first two operations performed at the Groote Schuur Hospital, Cape Town. Am J Cardiol 22:791–803

Batista RJV, Santos JLV, Takeshita N et al (1996) Partial left ventriculectomy to improve left ventricular function in end-stage heart disease. J Cardiac Surg 11:96–97

Billingham ME (1985) Endomyocardial biopsy detection of acute rejection in cardiac allograft recipients. Heart Vessels Suppl 1:86–90

Billingham ME, Cary NRB, Hammond ME et al (1990) A working formulation for the standardization of nomenclature in the diagnosis of heart and lung rejection. J Heart Lung Transplant 9:587–593

Blanche C, Takkenberg JJM, Nessim S et al (1996) Heart transplantation in patients 65 years of age and older: a comparative analysis of 40 patients. Ann Thorac Surg 62:1442–1447

Bonatti H, Tabarelli W, Ruttmann E et al (2004) Impact of cytomegalovirus match on survival after cardiac and lung transplantation. Am Surg 70:710–714

Bonatti H, Hoefer D, Rogatsch H et al (2005) Successful management of recurrent Epstein-Barr virus-associated multilocular leiomyosarcoma after cardiac transplantation. Transplant Proc 37:1839–1844

Boucek MM, Mathis CM, Kanakriyeh MS et al (1993) Donor shortage: use of the dysfunctional donor heart. J Heart Lung Transplant 12:186–190

Boucek MM, Faro A, Novick RJ et al (1999) The registry of the International Society for Heart and Lung Transplantation: third official pediatric report – 1999. J Heart Lung Transplant 18:1151–1172

Brown ME, Sarris GE, Oyer PE (1996) Cardiac donor evaluation, retrieval, and matching to recipient. In Smith JA, MacCarthy PM, Sarris GE, Stinson EB, Reitz BA (eds) The Stanford manual of cardiopulmonary transplantation. Futura, Armonk, pp 15–30

Calne RY (1979) Immunosuppression for organ grafting – observations on cyclosporin A. Immunolog Rev 46:113–124

Cantin B, Gao SZ, Kwok BWK et al (2002) Prognosis of patients with significant angiographically diagnosed cardiac allograft coronary disease. J Heart Lung Transplant 21:96

Caves PK, Billingham ME, Stinson EB et al (1974) Serial transvenous biopsy of the transplanted human heart. Improved management of acute rejection episodes. Lancet 1:821–826

Collins EG, Mozdzierz GJ (1993) Cardiac retransplantation: determining limits. Heart Lung 22:206–212

Copeland JG (1995) Only optimal donors should be accepted for heart transplantation: protagonist. J Heart Lung Transplant 14:1038–1043

Cooper DKC, Taniguchi S (1996) Heterotopic heart transplantation – indications, surgical techniques and special considerations. In: Cooper DKC, Miller LW, Patterson GA (eds) The transplantation and replacement of thoracic organs. Kluwer, Dordrecht, pp 353–365

Deleuze PH, Benvenuti C, Mazzuccotelli JP et al (1995) Orthotopic cardiac transplantation with direct caval anastomosis: is it the optimal procedure? J Thorac Cardiovasc Surg 109:731–737

Derumeaux G, Habib G, Schleifer DM et al (1995) Standard orthotopic heart transplantation versus total orthotopic heart transplantation. A transesophageal echocardiography study of the incidence of left atrial thrombosis. Circulation 92II:196–201

Dichtl W, Vogel W, Dunst KM et al (2005) Cardiac hepatopathy before and after heart transplantation. Transplant Int 18:697–702

DiSalvo T, Naftel D, Kasper EK et al (1998) The differing hazard of lymphoma vs. other malignancies in the current era – a multi institutional study [abstract]. J Heart Lung Transplant 17:70

Doval HC, Nul DR, Grancelli HO et al (1996) Nonsustained ventricular tachycardia in severe heart failure: independent marker of increased mortality due to sudden death. Circulation 94:3198–3203

Dreyfus G, Jebara V, Mihaileanu S et al (1991) Total orthotopic heart transplantation: an alternative to standard technique. Ann Thorac Surg 52:1181–1184

Dubin AM, Berul CI, Bevilacqua LM et al (2003) The use of implantable cardioverter-defibrillators in pediatric patients awaiting heart transplantation. J Card Fail 9:375–379

Dyke CM, Yeh T, Lehman JD et al (1991) Triiodothyronine-enhanced left ventricular function after ischemic injury. Ann Thorac Surg 52:14–19

Eisen HJ (2004) Pathogenesis and management of cardiac allograft vasculopathy. Curr Opin Organ Transplant 9:448–452

Eisen H, Kobashigawa J, Starling RC (2005) Improving outcomes in heart transplantation: the potential of proliferation signal inhibitors. Transplant Proc 37 [Suppl. 4S]:4–17

Gradman AH, Deedwania PC (1994) Predictors of mortality in patients with heart failure. Cardiol Clin 12:25–35

Gray J, Wreghitt TG, Pavel P et al (1995) Ebstein-Barr virus infection in heart and heart/lung transplant recipients: incidence and clinical impact. J Heart Lung Transplant 14:640

Greene M, Newman D, Geist M et al (2000) Is electrical storm in ICD patients the sign of a dying heart? Outcome of patients with clusters of ventricular tachyarrhythmias. Europace 2:263–269

Griffith BP, Kormos RL, Nastala CJ et al (1996) Results of extended bridge to transplantation: window into the future of permanent ventricular assist devices. Ann Thorac Surg 61:359–365

Groetzner J, Reichart B, Roemer U et al (2005) Results of pediatric cardiac transplantation – long-term results of a 15-year experience. Thorac Cardiovasc Surg 53 [Suppl 2]:149–154

Hankins S, Mancini DM (2001) Listing and treatment of status 1 patients. Curr Opin Organ Transplant 6:216–221

Hathout EB, Chinnock RE (2004) Growth after heart transplantation [Editorial]. Pediatr Transplant 8:97–100

Hetzer R, Loebe M, Potapov EV et al (1998) Circulatory support with pneumatic paracorporeal ventricular assist device in infants and children. Ann Thorac Surg 66:1498–1506

Höfer D, Bonatti H, Poelzl G et al (2005) Cecal perforation as a rare initial manifestation of posttransplant lymphoproliferative disorder after cardiac transplantation. J Heart Lung Transplant 24:505–506

Hosenpud JD, Bennett LE, Keck BM et al. (1997) The registry of the International Society for Heart and Lung Transplantation: fourteenth official report – 1997. J Heart Lung Transplant 16: 691–712

Hosenpud JD, Bennett LE, Keck BM et al (1999) The registry of the International Society for Heart and Lung Transplantation: sixteenth official report – 1999. J Heart Lung Transplant 18:611–626

Hosenpud JD, Bennett LE, Keck BM et al (2000) The registry of the International Society for Heart and Lung Transplantation: seventeenth official report – 2000. J Heart Lung Transplant 19:909–931

Iberer F, Grasser B, Schreier G et al (1998) Introducing a new clinical method for noninvasive rejection monitoring af-

ter heart transplantation to clinical practice: analysis of paced intramyocardial electrograms. Transplant Proc 30:895–899
Ikonen TS, Gummert JF, Hayase M et al (2000) Sirolimus (rapamycin) halts and reverses progression of allograft vascular disease in non-human primates. Transplantation 70:1773–1780
Jamieson SW, Burton NA, Bieber CP et al (1979) Cardiac-allograft survival in primates treated with cyclosporin A. Lancet 10:545
John R, Chen JM, Weinber A et al (1999) Long-term survival after cardiac retransplantation: a twenty-year single-center experience. J Thorac Cardiovasc Surg 117:543–555
Kirklin JW, Barratt-Boyes BG (1993) Primary cardiomyopathy and cardiac transplantation. In: Kirklin JW, Barratt-Boyes BG (eds) Cardiac surgery. Churchill Livingstone, New York, pp 1655–1681
Kirklin JK, Young JB, McGiffin DC (2002a) Recipient evaluation and selection. In: Kirklin JK, Young JB, McGiffin DC (eds) Heart transplantation. Churchill Livingstone, New York, pp 198–231
Kirklin JK, Young JB, McGiffin DC (2002b) The donor heart. In: Kirklin JK, Young JB, McGiffin DC (eds) Heart transplantation. Churchill Livingstone, New York, pp 293–338
Kirklin JK, Young JB, McGiffin DC (2002c) The heart transplant operation. In: Kirklin JK, Young JB, McGiffin DC (eds) Heart transplantation. Churchill Livingstone, New York, pp 339–352
Kirklin JK, Young JB, McGiffin DC (2002d) Physiology of the transplanted heart. In: Kirklin JK, Young JB, McGiffin DC (eds) Heart transplantation. Churchill Livingstone, New York, pp 353–372
Kirklin JK, Young JB, McGiffin DC (2002e) Cardiac allograft rejection. In: Kirklin JK, Young JB, McGiffin DC (eds) Heart transplantation. Churchill Livingstone, New York, pp 464–520
Klima U, Ringes-Lichtenberg S, Warnecke G et al (2005) Severe right heart failure after heart transplantation. A single-center experience. Transplant Int 18:326–332
Kobashigawa J, Miller L, Renlund D et al (1998) A randomized active-controlled trial of mycophenolate mofetil in heart transplant recipients. Mycophenolate mofetil investigators. Transplantation 66:507–515
Konig A, Theisen K, Klauss V (2000) Intravascular ultrasound for assessment of coronary allograft vasculopathy. Z Kardiol 89 [Suppl 9]:45–49
Laks H (1995) Only optimal donors should be accepted for heart transplantation: antagonist. J Heart Lung Transplant 14:1043-1046
Libby P (1996) Transplantation associated arteriosclerosis: potential mechanisms. In: Tilney N, Storm T, Paul L (eds) Transplantation biology: cellular and molecular aspects. Lippincott-Raven, Philadelphia, pp 577–586
Lietz K, John R, Mancini DM et al (2004) Outcomes in cardiac transplant recipients using allografts from older donors versus mortality on the transplant waiting list. J Am Coll Cardiol 4:1553–1561
Linde C, Braunschweig F, Gadler F et al (2003) Long-term improvements in quality of life by biventricular pacing in patients with chronic heart failure: results from the multisite stimulation in cardiomyopathy study (MUSTIC). Am J Cardiol 91:1090–1095
Losman JG, Barnard CN (1977) Hemodynamic evaluation of left ventricular bypass with a homologous cardiac graft. J Thorac Cardiovasc Surg 74:695–708
Lower RR, Shumway NE (1960) Studies on orthotopic transplantation of the canine heart. Surgical Forum 11:18–19
Magovern GJ, Simpson KA (1996) Clinical cardiomyoplasty: review of the ten-year United States experience. Ann Thorac Surg 61:413–419
Mancini DM, Eisen H, Kussmaul W et al (1991) Value of peak exercise oxygen consumption for optimal timing of cardiac transplantation in ambulatory patients with heart failure. Circulation 83:778–786
Marelli D, Laks H, Kobashigawa JA et al (2002) Seventeen-year experience with 1,083 heart transplants at a single institution. Ann Thorac Surg 74:1558–1566
McCarthy PM, Smith JA, Siegel LC et al (1996) Cardiac transplant admission, anesthesia and operative procedures. In: Smith JA, MacCarthy PM, Sarris GE, Stinson EB, Reitz BA (eds) The Stanford manual of cardiopulmonary transplantation. Futura, Armonk, pp 31–61
McCarthy PM, Starling RC, Wong J et al (1997) Early results with partial left ventriculectomy. J Thorac Cardiovasc Surg 114:755–763
Melton IC, Gilligan DM, Wood MA et al (1999) Optimal cardiac pacing after heart transplantation. PACE 22:1510–1527
Meyer SR, Modry DL, Bainey K et al (2005) Declining need for permanent pacemaker insertion with the bicaval technique of orthotopic heart transplantation. Can J Cardiol 21:159–163
Miniati DN, Robbin RC (2002) Heart transplantation: a thirty-year perspective. Annu Rev Med 53:189–205
Mohanty PK, Thomas MD, Arrowood JA et al (1987) Impairment of cardiopulmonary baroreflex after cardiac transplantation in humans. Circulation 75:21
Moreira LFP, Stolf NAG, Braile DM et al (1996) Dynamic cardiomyoplasty in South America. Ann Thorac Surg 61:413–419
Morgan JA, Edwards NM (2005) Orthotopic cardiac transplantation: comparison of outcome using biatrial, bicaval, and total techniques. J Card Surg 20:102–106
Müller J, Warnecke H, Spiegelsberger S et al (1993) Reliable noninvasive rejection diagnosis after heart transplantation in childhood. J Heart Lung Transplant 12:189–198
Newcomb AE, Esmore DS, Rosenfeldt FL et al (2004) Heterotopic heart transplantation: an expanding role in the twenty-first century? Ann Thorac Surg 78:1345–1351
Novitzky D, Cooper DKC, Reichart B (1987) Hemodynamic and metabolic responses to hormonal therapy in brain-dead potential organ donors. Transplantation 43:852–854
Penn I (1993) Incidence and treatment of neoplasia after transplantation. J Heart Lung Transplant 12:328–336
Poelzl G, Ullrich R, Huber A et al (2005) Capillary deposition of the complement fragment C4d in cardiac allograft biopsies is associated with allograft vasculopathy. Transplant Int 18:313–317
Poston RS, Griffith BP (2004) Heart transplantation. J Intensive Care Med 19:3–12
Razzouk AJ (2000) Cardiac retransplantation. Curr Opin Organ Transplant 5:154–157
Razzouk AJ, Chinnock RE, Gundry SR et al (1996) Transplantation as primary treatment for hypoplastic left heart syndrome: intermediate-term results. Ann Thorac Surg 62:1–8
Razzouk AJ, Chinnock RE, Dearani JA et al (1998) Cardiac

retransplantation for graft vasculopathy in children: should we continue to do it ? Arch Surg 133:881–885
Renlund DG (2004) Building a bridge to heart transplantation. N Engl J Med 351:849–851
Scheule AM, Zimmermann GJ, Johnston JK et al (2002) Duration of graft cold ischemia does not affect outcomes in pediatric heart transplant recipients. Circulation 106:163–167
Schmid C, Tjan TDT, Scheld HH (2005) Techniques of pediatric heart transplantation. Thoracic Cardiovasc Surg 53 [Suppl 2]:141–145
Schnetzler B, Pavie A, Dorent R et al (1998) Heart retransplantation: a 23-year single-center clinical experience. Ann Thorac Surg 65:978–983
Segovia J (2002) Update on cardiac allograft vasculopathy. Curr Opin Organ Transplant 7:240–251
Shumway NE, Lower RR, Stofer RC (1966) Transplantation of the heart. Adv Surg 2:265–284
Stark RP, McGinn AL, Wilson RF (1991) Chest pain in cardiac transplant recipients. Evidence of sensory reinnervation after cardiac transplantation. N Engl J Med 324:1791–1794
Starnes VA, Bernstein D, Oyer PE et al (1989) Heart transplantation in children. J Heart Transplant 8:20–26
Stevenson LW, Tillisch TH, Hamilton M et al (1990) Importance of hemodynamic response to therapy in predicting survival with ejection fraction ≤20% secondary to ischemic or nonischemic dilated cardiomyopathy. Am J Cardiol 66:1348–1354
Taylor DO, Barr ML, Radovancevic B et al (1999) A randomised, multicenter comparison of TAC and CsA immunosuppressive regimes in cardiac transplantation: decreased hyperlipidemia and hypertension with TAC. J Heart Lung Transplant 18:336
Taylor DO, Edwards LB, Boucek MM et al (2004) The registry of the International Society for Heart and Lung Transplantation: twenty-first official adult heart transplant report – 2004. J Heart Lung Transplant 23:796–803
Tuzku EM, Schoenhagen P, Starling RC et al (2002) Impact of everolimus on allograft vasculopathy: the SDZ RAD/heart intravascular ultrasound study. J Heart Lung Transplant 21:68
Warnecke H, Müller J, Cohnert T et al (1992) Clinical heart transplantation without routine endomyocardial biopsy. J Heart Lung Transplant 11:1093–1102
Watson DC, Reitz BA, Baumgartner WA et al (1979) Distant heart procurement for transplantation. Surgery 86:56–59
Wheeldon DR, Potter CDO, Oduro A et al (1995) Transforming the "unacceptable" donor: outcomes from the adoption of a standardized donor management technique. J Heart Lung Transplant 14:734–742
Yacoub M, Mankad P, Ledingham S (1990) Donor procurement and surgical techniques for cardiac transplantation. Semin Thorac Cardiovasc Surg 2:153–161
Yun JJ, Fischbein MP, Laks H et al (2001) Chronic rejection of transplanted hearts. Curr Opin Organ Transplant 6:205–210

2.2 Imaging in Heart Transplantation

Janet E. Kuhlman

CONTENTS

2.2.1 Introduction

Heart transplantation is a procedure usually reserved for patients less than 65 years of age with severe, end-stage heart failure that is no longer manageable with conventional treatment. Radiologic imaging plays an integral and ongoing part in the selection and evaluation process, both prior to and following heart transplantation. Imaging is essential during the pre-surgical phase; critical in the immediate post-surgical period; and important for surveillance during the early and later follow-up stages.

There are a growing number of patients with refractory heart failure. In the US, an estimated 4.7 million patients suffer from congestive heart failure (Massad 2004). These patients have a life expectancy that is shortened (80% mortality at 5 years), unless they qualify for and receive a cardiac transplant (Massad 2004; Winkel et al. 1999). For patients with New York Heart Association Class IV heart failure, 1-year mortality without transplantation approaches 50%, while 1-year mortality with cardiac transplantation is only 10%–15% (Massad 2004). Improved long-term survival after cardiac transplantation is now possible due to improved surgical techniques, and earlier detection and more successful management of complications including allograft rejection; immunosuppression-facilitated infection and malignancy; and accelerated graft atherosclerosis. Survival remains approximately 40%–50% at 10 years (Hosenpud et al. 1999; Massad 2004; Shiba et al. 2004; Taylor et al. 2004).

While the number of medical centers performing cardiac transplantation continues to grow, the shortage of donor hearts continues to limit the availability of this type of surgery particularly in the US, where only 2000–2700 procedures a year are performed (Massad 2004; Poston and Griffith 2004; Winkel et al. 1999). Worldwide, an estimated 4000 cardiac transplantations are performed annually (Taylor et al. 2004). As of May 2004, 66,000 heart transplantations have been reported to the International Society for Heart and Lung Transplantation (Hosenpud et al. 1999; Taylor et al. 2004).

J. E. Kuhlman, MD
Professor, Department of Radiology, Thoracic Imaging Section, University of Wisconsin Medical School, E3/311 CSC, 600 Highland Ave., Madison, WI 53792-3252, USA

2.2.2 Complications of Cardiac Transplantation – An Overview

Patients who undergo heart transplantation face a lifetime of therapy with potent immunosuppressive agents. Aggressive immunosuppression is meant to stave off the onset of allograft complications such as graft failure, rejection, and accelerated coronary atherosclerosis; but in the process these agents make the transplant recipient highly vulnerable to opportunistic infections and malignancies (Knollmann et al. 2000a; Leung 1999).

Complications of infection, malignancy, allograft rejection and cardiac allograft vasculopathy can occur at any time after cardiac transplantation, but the risk and frequency of these complications correlate with the severity of the immunosuppression and the length of time from surgery. It is helpful, therefore, to categorize complications into three periods: those that occur during the immediate post-surgical period; those that are most likely to appear during the first year post-transplantation; and those that are increasingly seen after the 1-year anniversary of transplantation (Hosenpud et al. 1999; Knollmann et al. 2000a; Leung 1999).

In the first 30 days after cardiac transplantation, primary graft failure accounts for 41% of mortalities, followed by multi-organ system failure (13%) and non-CMV infection (14%) (Taylor et al. 2004). During this period, recipients also face complications related to cardiothoracic surgery and median sternotomy, and post-operative infection (Knisely et al. 1999; Knollmann et al. 2000a; Leung 1999).

After the first 30 days, episodes of acute rejection are a concern for the first year, so immunosuppression remains high and opportunistic infections may take hold (Hosenpud et al. 1997, 1999; Knollmann et al. 2000a; Leung 1999). During the first year post-transplantation, non-CMV infection causes 35% of mortalities, graft failure 19% and acute rejection 12% (Taylor et al. 2004). Once the 1 year mark has passed, other long-term complications surface, including accelerated atherosclerotic disease especially in the coronary arteries of the donor heart and secondary malignancies (Knollmann et al. 2000a; Leung 1999). After 5 years, cardiac allograft vasculopathy is the most common cause of death (30%), then malignancy (24%), and non-CMV infection (10%) (Taylor et al. 2004).

2.2.3 Cardiac Transplantation – The Pre-Surgical Evaluation

Due to the shortage of donor organs, pre-surgical evaluation of heart transplant candidates remains thorough and the waiting period for surgery remains long.

Candidates for transplantation have refractory heart failure with marked left ventricular decompensation due to a variety of etiologies including coronary artery disease (45%); cardiomyopathy (45%) – idiopathic, hypertensive, peripartum, or viral; valvular heart disease (3%–4%); and congenital heart disease (2%) (Taylor et al. 2004; Winkel et al. 1999). Candidates are typically less than 65 years of age (although older patients have been transplanted at some centers) and have an estimated 2-year survival of less than 60% without transplantation (Kirklin et al. 2004).

In addition to cardiac function studies, radiologic evaluation of candidates prior to cardiac transplantation includes screening patients with several imaging modalities to exclude active infection, occult malignancy and to assess vital organ function. Patients with severe or irreversible organ damage from pulmonary hypertension or other pulmonary diseases, liver or kidney failure are usually not candidates for transplantation; nor are those with extensive cerebrovascular or peripheral vascular disease (Massad 2004). Pre-operative imaging studies may include: nuclear renal scanning to assess kidney function; ventilation-perfusion imaging to assess lung function; mammography to exclude breast cancer; abdominal ultrasound or CT to assess the liver, pancreas, gallbladder, gastrointestinal (GI) tract, and kidney, as well as to look for aortic aneurysms; carotid ultrasound to evaluate for carotid stenosis; dental Panorex and sinus films to look for infection and dental disease (Kirklin et al. 2004).

Chest radiographs and/or chest CT are used to exclude active lung infection, or occult malignancy, and to look for signs of pulmonary hypertension or pulmonary thromboembolic disease (Leung 1999; Winkel et al. 1999). In addition, the radiologist should note any findings that might complicate thoracic surgery such as adhesions from previous median sternotomy, aortic aneurysms or dissection, and pulmonary artery variants. Surgical anastomoses between the donor organ and the recipient will involve the aorta and pulmonary artery, and pathology or variants in these

vessels may complicate or prohibit transplantation. In addition, accelerated atherosclerosis of aortic aneurysms with increased rates of expansion and high rupture rates occurs in cardiac transplant recipients, possibly related to corticosteroid and immunosuppression therapy exposure (Englesbe et al. 2003). Therefore, the radiologist must be alert to this detectable complication and note the presence of even small aortic aneurysms in the chest or abdomen on preoperative imaging examinations of heart transplant candidates, so that these aneurysms may be followed closely and undergo early elective repair (Englesbe et al. 2003). Screening for aortic aneurysms has now become routine at most cardiac transplant centers (Englesbe et al. 2003).

Finally, an increasing number of patients with end-stage heart failure are being maintained temporarily or more long-term with mechanical circulatory support such as left ventricular assist devices (LVADs). The presence of an LVAD prior to transplantation (19%) makes the subsequent cardiac transplantation procedure more difficult, and LVADS are associated with their own complications that may affect perioperative mortality, including infection, stroke, and bowel compromise (Kirklin et al. 2004; Poston and Griffith 2004; Taylor et al. 2004) (Fig. 2.2.1). However, these bridges to transplantation have improved the survival and outcome of many patients with end-stage heart failure, allowing them their chance at transplantation (Poston and Griffith 2004).

2.2.4 Cardiac Transplantation – Overview of the Operation

Most heart transplants performed today are orthotopic transplantations, with heterotopic transplantation being rarely used. In an orthotopic heart transplantation, a median sternotomy is performed and the recipient's native heart is excised and replaced by a donor heart. When the native heart is excised, two techniques may be used: the traditional, atrial-to-atrial cuff technique or the newer, bicaval method. In the older, traditional approach, the surgeon leaves behind in the recipient a cuff of the right atrium, a cuff of the left atrium with pulmonary veins intact, a short segment of ascending aorta, and a short segment of main pulmonary artery. These are anastomosed to the harvested, donor organ. The superior vena cava of the donor heart is tied off just above the right atrium and a short segment of the

a

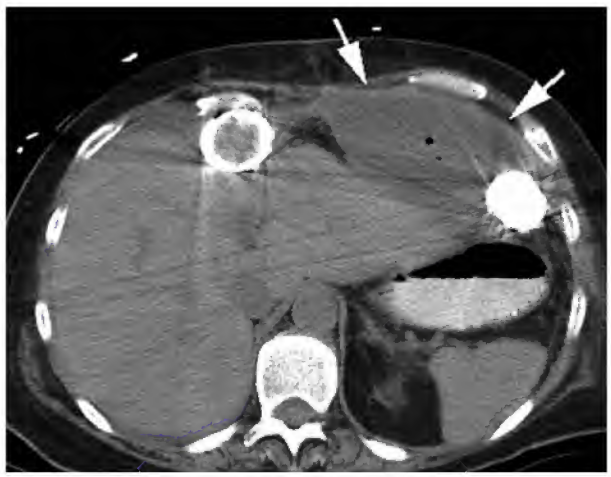

b

Fig 2.2.1a, b. Pre-surgical phase – complication of bridge support devices. A 57-year-old woman with end-stage heart failure due to giant cell myocarditis awaiting heart transplant. As a bridge to heart transplantation, a left ventricular assist device (*LVAD*) was placed to support the patient's heart function until a suitable cardiac donor became available. **a** A left-side-down decubitus view of the abdomen showed a large amount of free intraperitoneal air 10 days after placement of the LVAD. At surgery, a small perforation in the transverse colon was identified beneath the LVAD. **b** A follow-up abdominal CT 2 months later identified a large fluid collection between the two drive lines of the LVAD. Percutaneous aspiration of the collection revealed pus that grew coagulae-negative *Staphylococcus*. Cardiac transplantation was delayed and could not be performed before the patient died of complications. Although LVADs are placed to support and improve the cardiac status of patients awaiting heart transplantation and do so in many patients, these devices carry their own complications that can delay or preclude transplantation

donor inferior vena cava is used in the attachment to the right atrium (Henry et al. 1989; Knisely et al. 1999; Rodeheffer and McGregor 1992; Thorsen and Goodman 1988).

In the newer, bicaval technique, the recipient's right atrium is completely excised. The donor's right atrium is left intact and anastomoses are made between the donor's and recipient's superior and inferior venae cavae. Anastomoses between the donor's and recipient's left atrium, aorta and pulmonary artery are similar to the traditional technique (Poston and Griffith 2004; Shanewise 2004). The bicaval technique has resulted in improved survival at some transplant centers and has become the preferred method except in very young children, because it is associated with fewer atrial, mitral and tricuspid valve complications (Kirklin et al. 2004; Poston and Griffith 2004).

With respect to imaging, the anatomic configuration of the orthotopic cardiac transplant has a typical appearance on chest CT, especially if the older surgical technique has been used (Henry et al. 1989; Knisely et al. 1999). Often most noticeable is a gap or increased distance between the donor heart's ascending aorta and both the native superior vena cava and the native main pulmonary artery. The main pulmonary artery at the anastomosis between donor and recipient may appear angulated and high-riding. There may also be differences noted between the diameters of the native and donor aortas and pulmonary arteries. Sometimes these discrepancies are so great that graft material must be used at the anastomosis sites and this is visible on CT as encircling radiodense material (Henry et al. 1989; Knisely et al. 1999). If the traditional approach is used, the tied-off donor superior vena cava is identified as a remnant medial to the native superior vena cava (see Figs. 2.2.7c, d, 9c, d). At the right and left atrial cuff anastomoses between native an donor hearts, a slight constriction may be evident. Differences in diameter at the inferior vena cava anastomosis between donor organ and recipient may also be noted.

2.2.5 Cardiac Transplantation – The Immediate Post-Surgical Period

During the first 30 days after cardiac transplantation, primary failure of the donor heart is the most common cause of death, and usually manifests as right heart dysfunction (Poston and Griffith 2004). Multi-organ failure and peri-operative infection are the second and third most common causes of death in the first 30 days (Poston and Griffith 2004; Taylor et al. 2004). Other complications encountered in the peri-operative period include those attributable to cardiothoracic surgery and median sternotomy, as well as the more specific surgical misadventures that can occur with cardiac organ transplantation.

Non-specific complications that are seen immediately after major cardiothoracic surgery include: pneumothorax, pneumopericardium, pneumomediastinum, myocardial infarction, pulmonary edema, overwhelming sepsis, stroke, and pulmonary embolism (Fig. 2.2.2). Hemothorax, hemopericardium, and mediastinal bleeding may also occur and be severe and life-threatening, requiring re-exploration. Gastrointestinal problems including ulcers, pancreatitis, cholecystitis, diverticulitis, and bowel

Fig 2.2.2. Immediate post-surgical phases – stroke. A 55-year-old woman 14 days status post orthotopic heart transplant for constrictive/restrictive cardiomyopathy developed an acute embolic occlusion of the right middle cerebral artery trunk. Head CT demonstrated a large infarct in that right middle cerebral artery distribution with compression of the ventricles and some midline shift

perforation are not uncommon due to the stress of major surgery and the high-dose corticosteroids employed for immunosuppression (Knisely et al. 1999; Winkel et al. 1999).

More specifically in heart transplant recipients, bleeding, leaks, and frank rupture can occur at the anastomosis sites; the most critical of which is the aortic anastomosis, particularly if there is a marked difference in diameter between the donor and recipient aorta (Knisely et al. 1999; Reitz et al. 1982) (Fig. 2.2.3). In addition, acute or chronic breakdown at the aortic anastomosis can lead to aortic dehiscence, dissection, and pseudoaneurysm formation (Henry et al. 1989; Knollmann et al. 2000a; Knosalla et al. 1996). Pseudoaneurysms can also form at two additional sites in the cardiac transplant patient: at the cannulation sites used for cardiopulmonary bypass and at the endomyocardial biopsy sites in the right ventricle, taken to look for rejection (Knisely et al. 1999). Although most of these complications occur in the immediate post-operative period, some can occur months to years later (Knisely et al. 1999). Aortic dissection, when it occurs in the heart transplant patient (1%–2%), usually involves the recipient's native aorta, although rare cases of dissection involving the donor's aorta have been reported (Schellemans et al. 2004). Dissection can occur in the immediate peri-operative period usually due to mismatches in donor–recipient vessel size or years later when they may be due to infection or accelerated atherosclerosis (Schellemans et al. 2004).

The post-operative chest film in the cardiac transplant patient is often difficult to interpret, especially in the immediate post-surgical period. The heart size frequently appears enlarged, but this may be misleading and not a good indicator of donor heart function (see Figs. 2.2.3a, 2.2.6a). Because the smaller donor heart is placed within the intact, but larger, native pericardium, the cardiac silhouette often remains enlarged on chest films for months after transplantation, not due to cardiomegaly of the donor organ, but due to pericardial fluid that fills the larger pericardial sac (Knisely et al. 1999). The size of the cardiac silhouette usually returns to normal over the course of many months. A right double density may also be seen in some cardiac transplant recipients due to the anastomosis of donor and recipient right atria used in the traditional atrial–atrial approach (Knisely et al. 1999; Shirazi et al. 1983).

2.2.6 Cardiac Transplantation – The First Year

2.2.6.1 Immunosuppression – An Overview

A variety of potent immunosuppression agents are used in cardiac transplantation to stave off allograft rejection. New and more effective combination therapies are being developed all the time. Typically some combination of three types of agents is employed: corticosteroids; calcineurin inhibitors that prevent interleukin-2 transcription [ciclosporin A or FK506 (Tacrolimus); and antimetabolite agents (azathioprine, mycophenolate mofetil) (Eisen and Ross 2004; Massad 2004; Poston and Griffith 2004; Winkel et al. 1999). In an attempt to reduce the development of cardiac allograft vasculopathy, newer anti-fibrosing, anti-proliferative agents such as rapamycin (sirolimus) and everolimus have recently been added to calcineurin inhibitors in clinical trials (Eisen and Ross 2004; Poston and Griffith 2004). Some centers still use induction therapy at the time of transplantation with anti-lymphocyte antibody (45%) or to a lesser extent OKT3 (monoclonal T-cell antibody) (5%), due to the latter's association with an increased risk of malignancy and post-transplant lymphoproliferative disorders (PTLD) (Haldas et al. 2002; O'Neill et al. 2004; Taylor et al. 2004). Newly developed monoclonal antibodies (basiliximab and daclizumab) that block the interleukin-2 receptor site are being investigated as additional immunosuppressant agents (Massad 2004).

2.2.6.2 Acute Allograft Rejection

Signs and symptoms of acute allograft rejection include increasing shortness of breath and weakness, indicating worsening heart failure and ventricular decompensation. The first episode of acute rejection may occur within a week of transplantation or within the first few months (Poston and Griffith 2004). Acute rejection is mediated through both cellular and humoral pathways, particularly those that involve the CD4 T cell (Poston and Griffith 2004).

Rejection can now be detected early by endomyocardial biopsy, which is employed according to a reg-

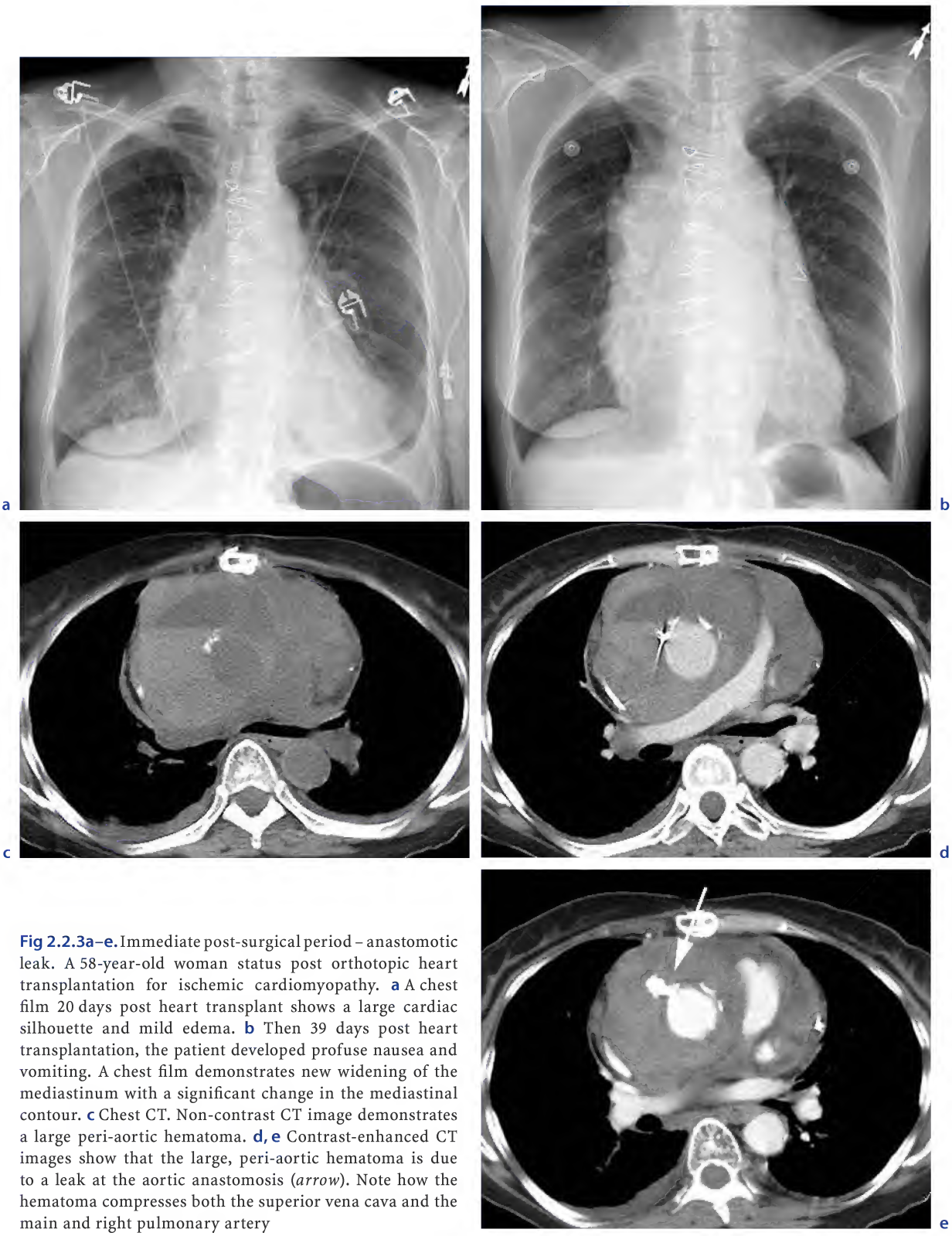

Fig 2.2.3a–e. Immediate post-surgical period – anastomotic leak. A 58-year-old woman status post orthotopic heart transplantation for ischemic cardiomyopathy. **a** A chest film 20 days post heart transplant shows a large cardiac silhouette and mild edema. **b** Then 39 days post heart transplantation, the patient developed profuse nausea and vomiting. A chest film demonstrates new widening of the mediastinum with a significant change in the mediastinal contour. **c** Chest CT. Non-contrast CT image demonstrates a large peri-aortic hematoma. **d, e** Contrast-enhanced CT images show that the large, peri-aortic hematoma is due to a leak at the aortic anastomosis (*arrow*). Note how the hematoma compresses both the superior vena cava and the main and right pulmonary artery

ular surveillance schedule. A transvenous approach is used and the septal wall of the right ventricle is the preferred site for endomyocardial sampling. Features of rejection include infiltration of the heart muscle by lymphocytes and myocardial cell necrosis (Knisely et al. 1999; Poston and Griffith 2004; Winkel et al. 1999). Complications of right ventricular biopsy can occur and include: bleeding, venous thrombosis, pneumothorax, injury to the tricuspid valve, coronary artery fistula, arrhythmias, right ventricular perforation and pseudoaneurysm formation (Fig. 2.2.4 and see Fig. 2.2.6b) (Knisely et al. 1999; Winkel et al. 1999; Yamani and Starling 2000).

When detected by biopsy, rejection is treated aggressively by increasing the level of immunosuppression and the dose of corticosteroids (Winkel et al. 1999). In severe cases, additional agents such as antithymocyte globulin, OKT3, cyclophosphamide, methotrexate, vincristine, tacrolimus, rapamycin, or mycophenolate mofetil may be required (Knisely et al. 1999; Massad 2004; Poston and Griffith 2004; Winkel et al. 1999). Anti-T cell agents such as antithymocyte (ATG) and OKT3 (monoclonal T-cell antibody) are being used less often in primary induction as such agents cause such profound immunosuppression that the risk opportunistic infection and malignancy are increased (O'Neill et al. 2004). At many centers, these latter agents are now reserved for severe cases of rejection that have failed to respond to the first-line agents or in those patients whose renal dysfunction limits the use of nephrotoxic calcineurin inhibitors (O'Neill et al. 2004; Poston and Griffith 2004).

Allograft rejection can occur at any time following cardiac transplantation, even years later, thus necessitating some degree of life-long immunosuppression. However, cases are most frequent during the first several months after surgery, gradually declining in number after 6 months to 1 year (Kobashigawa et al. 1993; Winkel et al. 1999). Acute rejection as the cause of death occurs in

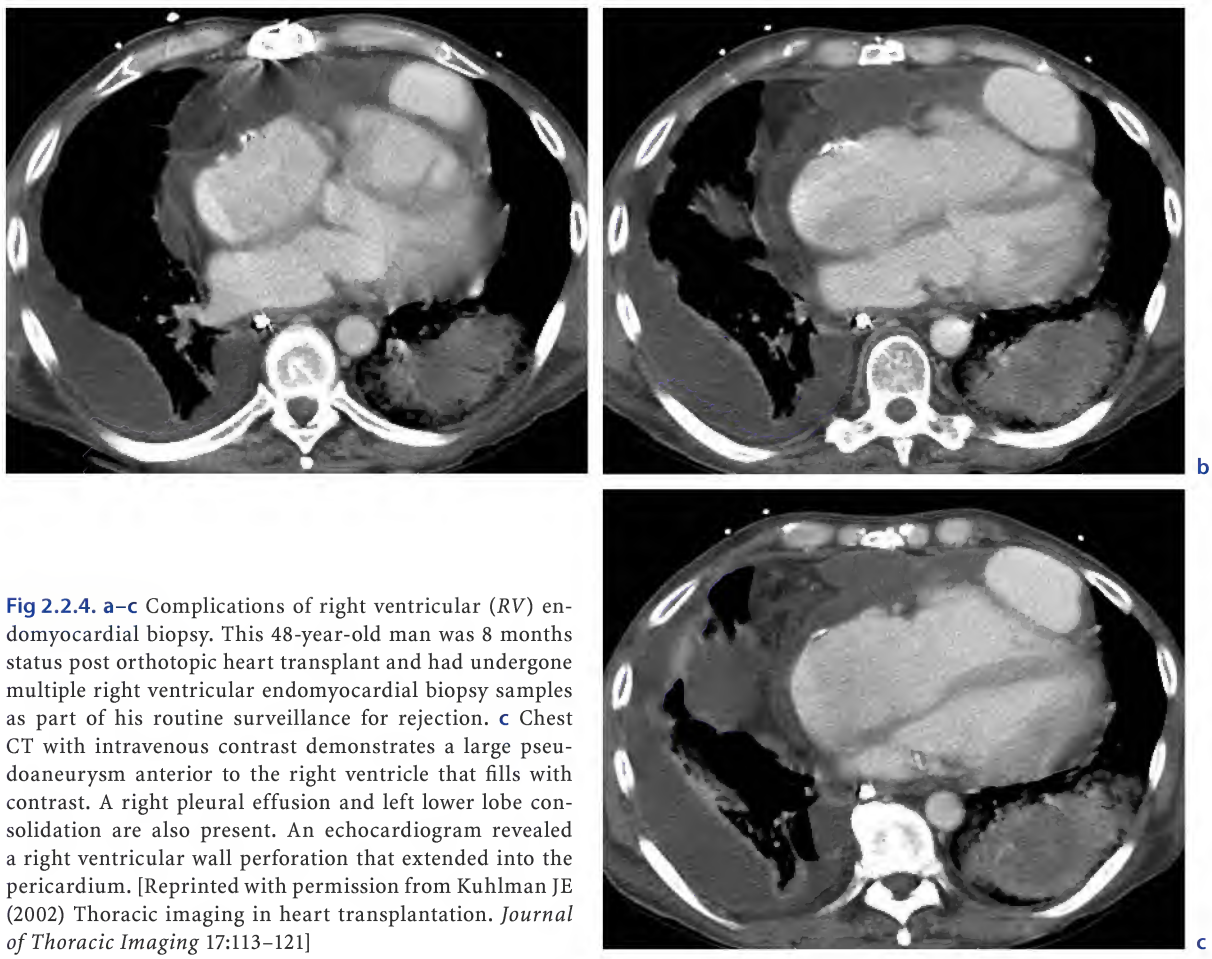

Fig 2.2.4. a–c Complications of right ventricular (*RV*) endomyocardial biopsy. This 48-year-old man was 8 months status post orthotopic heart transplant and had undergone multiple right ventricular endomyocardial biopsy samples as part of his routine surveillance for rejection. **c** Chest CT with intravenous contrast demonstrates a large pseudoaneurysm anterior to the right ventricle that fills with contrast. A right pleural effusion and left lower lobe consolidation are also present. An echocardiogram revealed a right ventricular wall perforation that extended into the pericardium. [Reprinted with permission from Kuhlman JE (2002) Thoracic imaging in heart transplantation. *Journal of Thoracic Imaging* 17:113–121]

only 3% of heart transplant patients who have survived 18 months from the time of transplantation (Kobashigawa et al. 1993).

2.2.7 Infection

The risk of infection is ever present in the cardiac transplant patient. However, because immunosuppression is greatest during the first 3–6 months following transplantation, this period is also the most dangerous for severe, life-threatening infection (Leung 1999; Petri 1994).

A variety of common and opportunistic pathogens cause infection in heart transplant patients including: bacteria, viruses, fungi, protozoa, and mycobacterium. Also of concern is reactivation of infection. CMV infection in the donor heart may cause serious infection in the sero-negative recipient following transplantation. Dormant tuberculosis in the recipient may become active under immunosuppression (Winkel et al. 1999).

In the immediate post-surgical period, infections are most likely to be due to bacteria and fungi. The lungs are the most common site affected with nosocomial pneumonias (Fishman and Rubin 1998; Leung 1999; Miller et al. 1993; Winkel et al. 1999). *Staphylococcus aureus*, *Pseudomonas aeruginosa* and *Klebsiella pneumoniae* are frequent causes of pneumonia that may be severe and progress to lung abscess (Austin et al. 1989; Knollmann et al. 2000a; Petri 1994).

Post-operative complications including sternal wound and mediastinal infection are also a problem, occurring in 7% of cardiac transplant recipients (Miller et al. 1993). On chest CT, retrosternal fluid and/or air collections are common within the first 2 weeks of surgery and sampling may be required to determine if these are infected or not (Fig. 2.2.5) Persistent retrosternal fluid and/or air collections on CT after 2 weeks from surgery are indicative of infection (Jolles et al. 1996). Mediastinal abscesses often demonstrate rim enhancement with intravenous contrast. Complications of chronic mediastinal infections include sinus tracts and fistula, as well as pseudoaneurysm formation of the aorta (Knisely et al. 1999; Levin et al. 2004). Line sepsis, groin infections, and bed sores can be problematic in the transplant recipient as well (Massad 2004).

After the immediate post-surgical period, but during the first 6 months after transplantation, other opportunistic pathogens begin to emerge as threats including fungi such as *Candida albicans*, *Aspergillus*, *Cryptococcus* and *Coccidioides*; viruses such as CMV; and other unusual infections due to *Legionella*, *Nocardia*, and protozoa as in *Pneumocystis carinii* pneumonia (Leung 1999; Massad 2004; Millet et al. 1993; Thaler and Rubin 1996) (Figs. 2.2.6–2.2.8). Prophylaxis with trimethoprim/sulfamethoxazole is used to prevent infections such as *Pneumocystis carinii* and *Nocardia*, but these still occur (Leung 1999; Thaler and Rubin 1996) (Figs. 2.2.7, 2.2.8). Prophylaxis with antiviral agents to prevent CMV infection have been used as well in heart transplant recipients (Massad 2004). Despite these advances, opportunistic infections that occur during this period of greatest immunosuppression are often severe, and readily disseminate including to the soft tissues, muscles, liver, spleen, kidneys, and central nervous system (Knollmann et al. 2000a) (Figs. 2.2.6, 2.2.8). Primary infections can also occur in the sinuses and mastoid air cells, and then spread to the CNS (Knollmann et al. 2000a).

Beyond 6 months, the threat of infection is directly related to the severity of immunosuppression required to prevent rejection (Thaler and Rubin 1996). As the dose of corticosteroids and other immunosuppressant agents is lowered, the risk of opportunistic infection decreases, but it is never eliminated. Opportunistic infections still occur, but community-acquired pneumonias may become more common.

CMV continues to be an important pathogen in heart transplant patients (Massad 2004; Rubin 2000). Not only does CMV cause disseminated viremia, it is also a significant cause of pneumonitis, myocarditis, and GI infections including hepatitis, esophagitis, enteritis, and colitis (Rubin 2000). CMV may also play a role in provoking episodes of rejection, cardiac allograft vasculopathy and PTLD (Rubin 2000).

CMV may be transmitted to the seronegative recipient by a seropositive donor or CMV can reactivate in the seropositive recipient as the result of immunosuppression especially if anti-lymphocyte antibody therapy is employed (Rubin 2000). Ganciclovir is the first-line treatment for CMV infections, but resistant strains may require additional drugs.

Imaging findings of CMV infection are usually nonspecific and overlap with other infections and disease processes. CMV pneumonitis has a variety of appearances, but most commonly presents similar to an

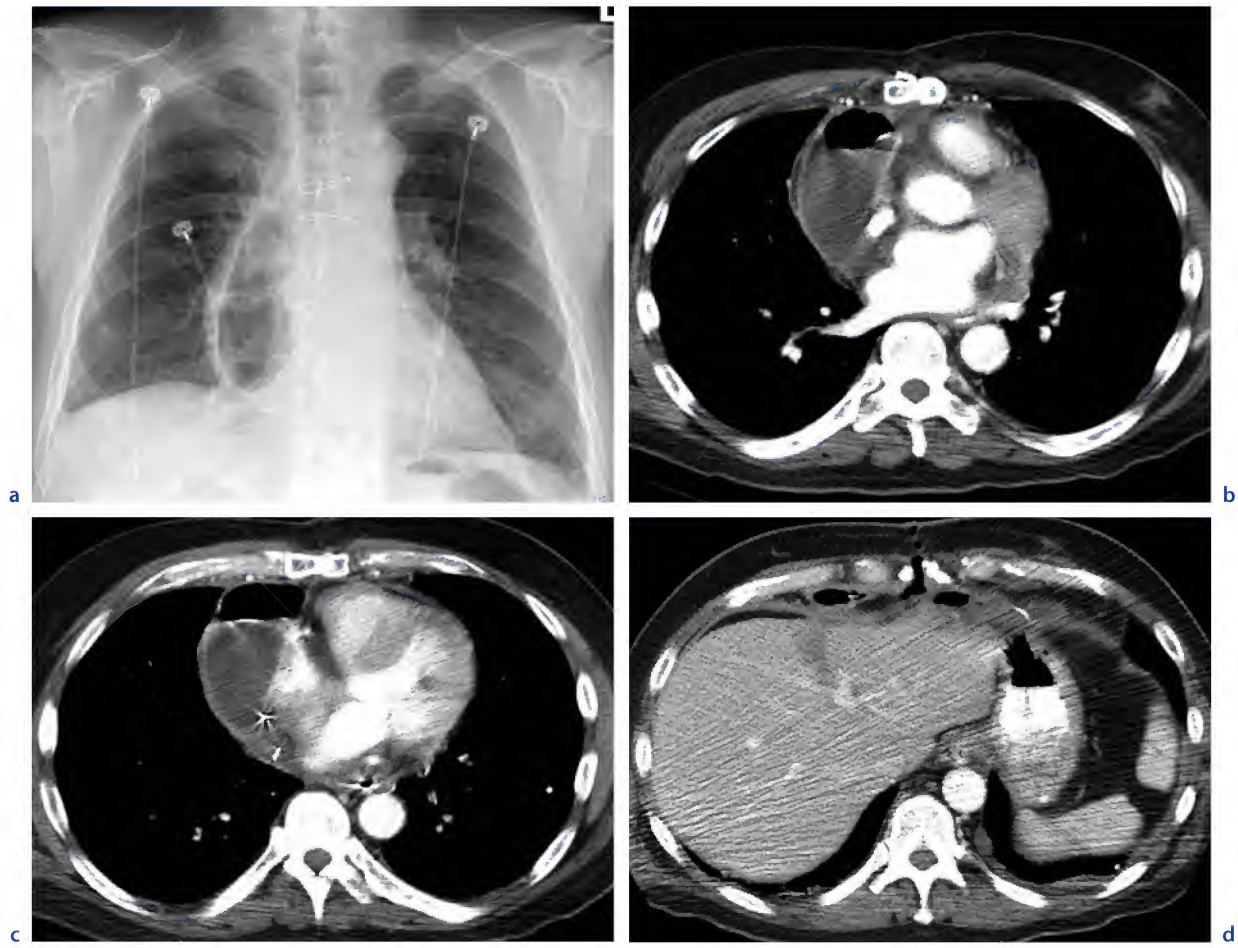

Fig 2.2.5a–d. Peri-operative complications in the first 30 days – mediastinal abscess. After 9 $^{1}/_{2}$ months of bridge support with a left ventricular assist device (*LVAD*), this 55-year-old man underwent an orthotopic heart transplant for ischemic cardiomyopathy. **a** On post-operative day 6, a chest film showed a new, large, air collection in the mediastinum. **b–d** Chest CT with intravenous contrast demonstrated a large air-fluid collection with rim enhancement adjacent to the heart transplant. The collection extended from the mediastinum to the base of the heart and tracked out the upper abdominal wall through the surgical incision. On surgical re-exploration, a mediastinal abscess was found that communicated with and originated from the upper abdomen where a small bowel perforation was identified close to the exit site of the old LVAD drive line

atypical pneumonia with patchy or diffuse bilateral lung infiltrates on chest radiographs. On CT, CMV may mimic *Pneumocystis carinii* pneumonia with diffuse or patchy ground glass opacities, but it may also demonstrate reticular, reticular-nodular and more focal airspace opacities (Knisely et al. 1999).

Gastrointestinal manifestations of CMV that are most often detected with imaging are esophagitis and colitis. On CT, esophagitis appears as diffuse esophageal wall thickening. Ulcerations are often detected on swallowing studies or endoscopy. Patients with CMV colitis may demonstrate marked, diffuse colonic wall thickening which is indistinguishable from other severe forms of colitis such as ischemic colitis or pseudomembranous colitis.

Invasive fungi, most commonly in the form of aspergillus, are important pathogens in the immunocompromised heart transplant recipient (Knisely et al. 1999; Knollmann et al. 2000a; Leung 1999). The lung is a frequent site of initial fungal infection, particularly in the case of invasive pulmonary aspergillosis (IPA). However, dissemination of fungal infections beyond the lungs is common and may manifest as abscesses in the liver, spleen, kidneys, adrenal glands, skin and central nervous system (Knisely et al. 1999; Knollmann et al. 2000a) (Fig. 2.2.6).

On chest radiographs and CT, IPA appears as one or more nodular opacities. On CT, the CT halo sign may be seen; a zone of ground glass opacity surrounding the nodule (Fig. 2.2.6). The nodular

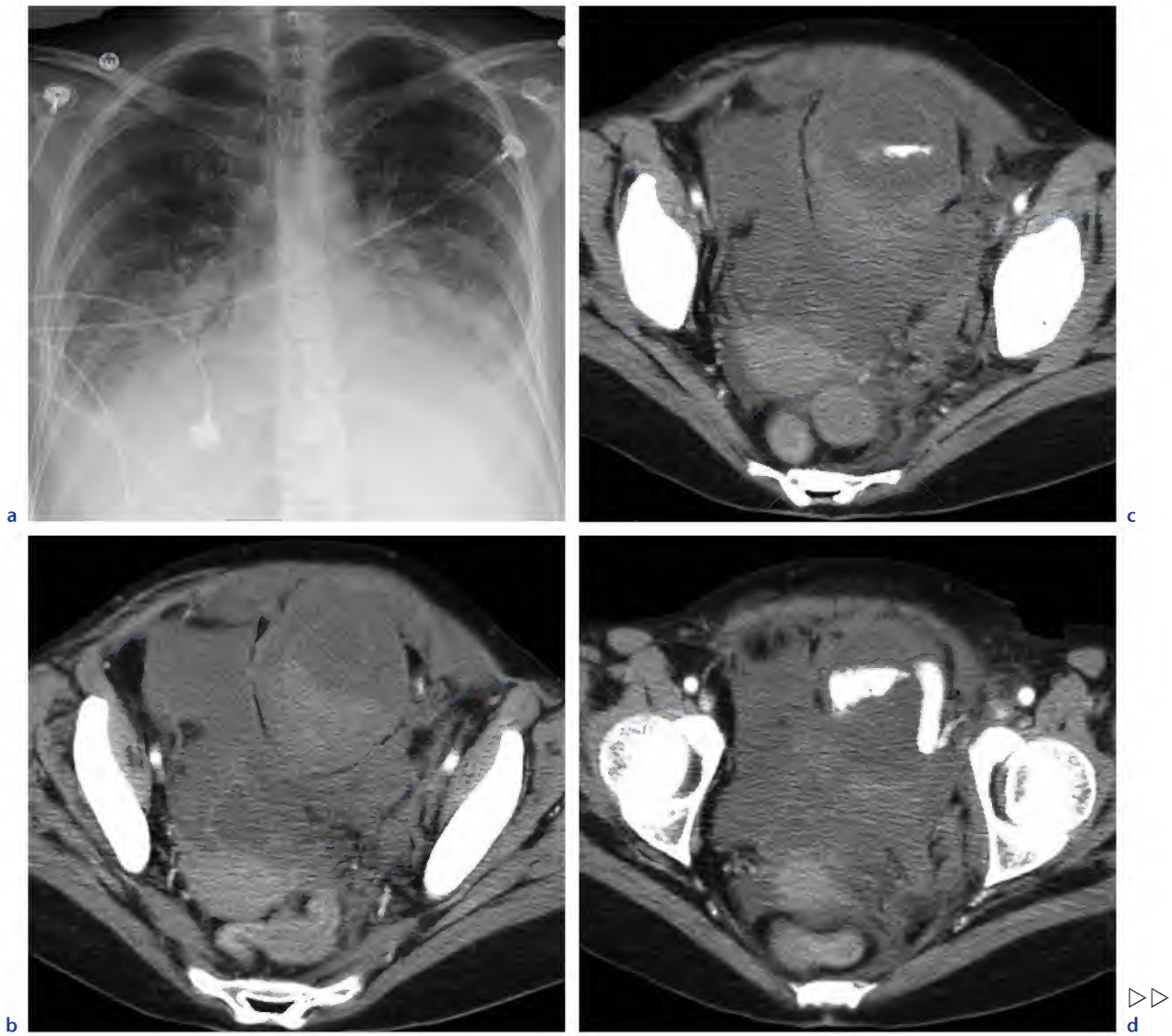

Fig 2.2.6a–j. Disseminated aspergillosis. A 39-year-old woman 1 month out from orthotopic heart transplantation for giant cell myocarditis. **a** A chest film taken during the first week after transplantation demonstrates non-specific edema and an enlarged cardiac silhouette. Early rejection was found on endomyocardial biopsy and the patient was treated with a pulse of corticosteroids, OKT3 and plasmapheresis. **b–d** During the first month following transplantation, the patient developed abdominal pain and a drop in her hematocrit, after a right ventricular endomyocardial biopsy was attempted via a femoral approach. An abdominal-pelvic CT scan shows a large pelvic hematoma with active bleeding and extravasation of intravenous contrast from the left common femoral vein as a complication of this procedure. **e–g** One month following transplantation, the patient developed fever, weakness, diarrhea, headache and pain and redness in her right eye. A chest CT demonstrates multiple inflammatory nodules and masses, some with a surrounding ground glass zone or "CT halo" suspicious for invasive pulmonary aspergillosis. Subsequent lung biopsy of one nodule grew *Aspergillus fumigatus*. **h–j** MRI scan of the brain demonstrated multiple fungal abscesses. **h, i** T2-weighted MRI images show multiple, scattered high signal foci. **j** Post-gadolinium-enhanced image shows multiple ring enhancing lesions. The patient was found to have disseminated aspergillosis with pneumonia, myocarditis, chorioretinitis, and central nervous system involvement. Fungal infection in the heart transplant patient is often disseminated

e

f

g

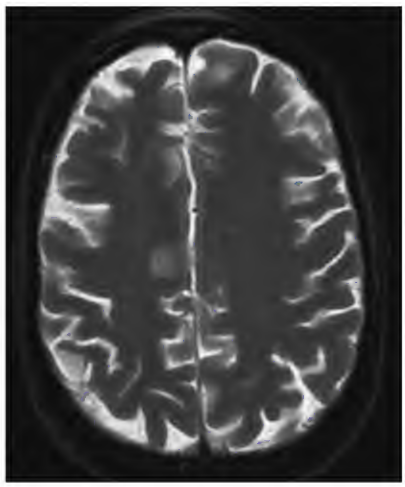

h

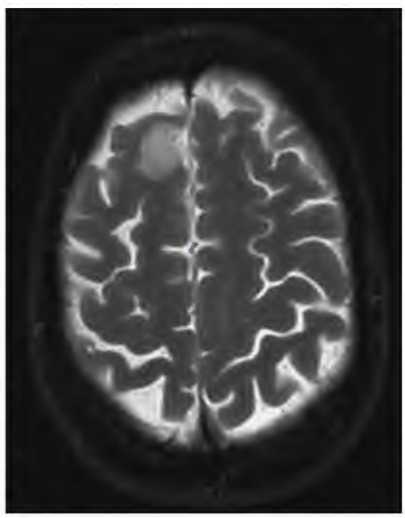

i

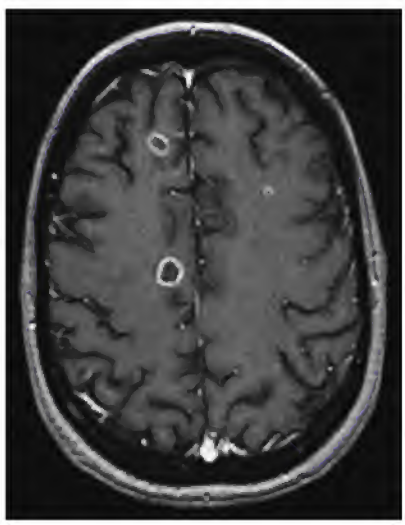

j

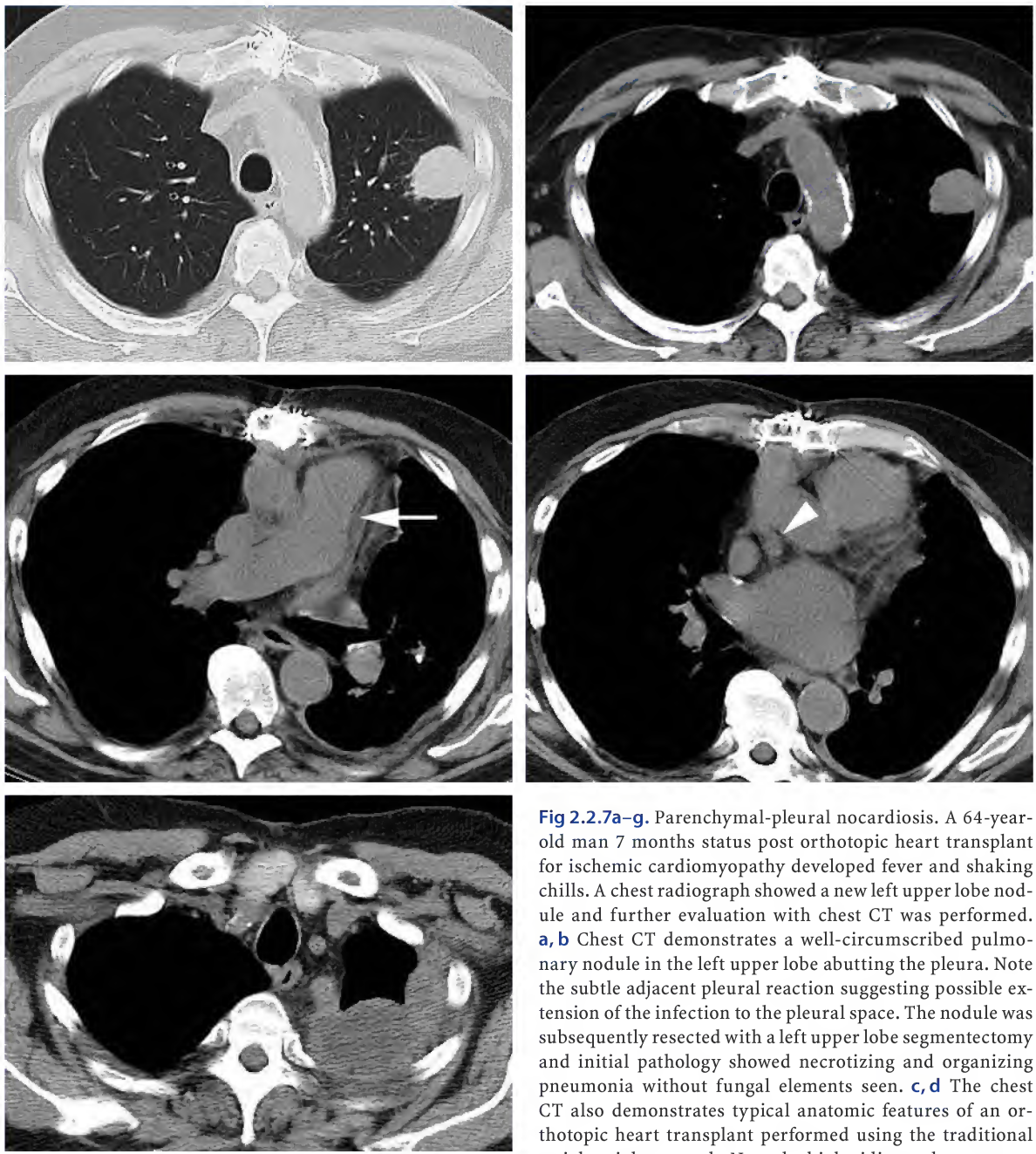

Fig 2.2.7a–g. Parenchymal-pleural nocardiosis. A 64-year-old man 7 months status post orthotopic heart transplant for ischemic cardiomyopathy developed fever and shaking chills. A chest radiograph showed a new left upper lobe nodule and further evaluation with chest CT was performed. **a, b** Chest CT demonstrates a well-circumscribed pulmonary nodule in the left upper lobe abutting the pleura. Note the subtle adjacent pleural reaction suggesting possible extension of the infection to the pleural space. The nodule was subsequently resected with a left upper lobe segmentectomy and initial pathology showed necrotizing and organizing pneumonia without fungal elements seen. **c, d** The chest CT also demonstrates typical anatomic features of an orthotopic heart transplant performed using the traditional atrial-atrial approach. Note the high-riding pulmonary artery and its angulated appearance at the pulmonary artery anastomosis site (*arrow*). Note the increased space between the donor's aorta and the recipient's superior vena cava and note the remnant of the donor's superior vena cava located medial to the recipient's superior vena cava (*arrowhead*). **e** One month after the left upper lobe segmentectomy, the patient returned with fever, chills and chest pain. A repeat chest CT demonstrated a loculated, empyema in the left upper hemithorax.

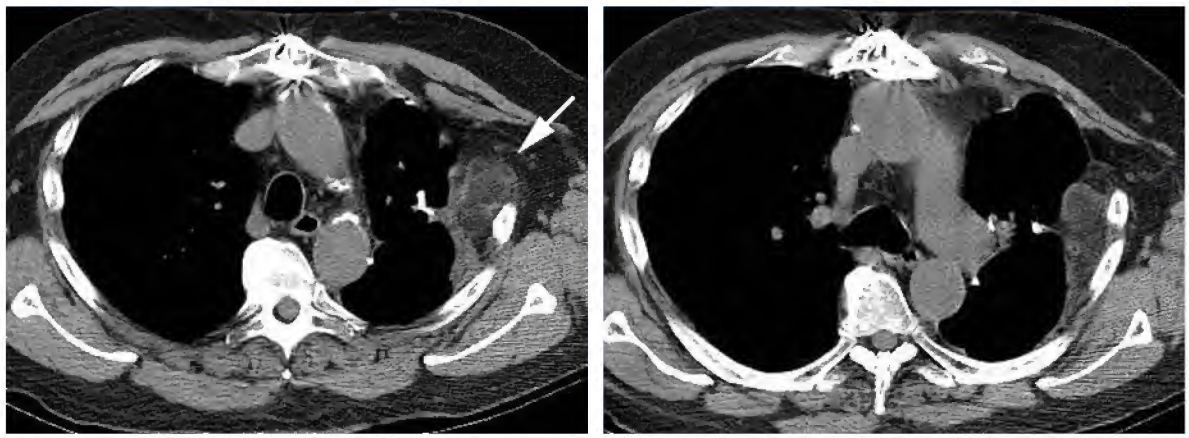

f g

f, g The patient underwent chest tube and subsequent open drainage followed by thoracic muscle flap closure (*arrow*). Nocardia was recovered from the empyema space

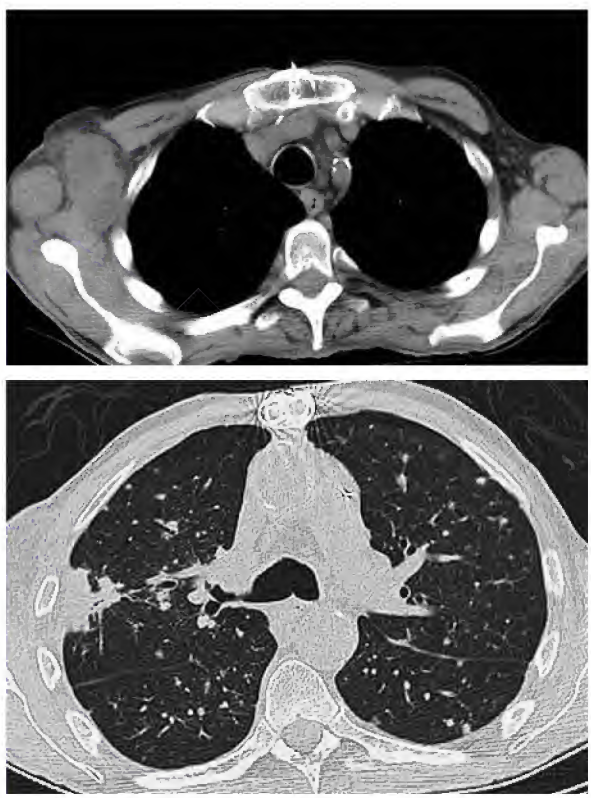

a b

Fig 2.2.8a, b. Pulmonary and extrapulmonary nocardiosis. A 57-year old man, 7 years status post orthotopic heart transplant for ischemic cardiomyopathy, developed pain in his right axilla with a palpable lump. **a, b** Chest CT demonstrated a large abscess in the right axilla, as well as many, bilateral, small pulmonary nodules and one larger mass on the right. The right axillary abscess was aspirated and cultures of the aspirate and of sputum grew *Nocardia nova*

opacities of IPA may go on to cavitate (Knisely et al. 1999). Other causes of nodules and cavitary nodules in a heart transplant recipient besides invasive fungal infection include septic emboli, *Staphylococcus aureus* abscesses, and infections due to more unusual organisms such as *Nocardia* and *Rhodococcus equi* (Kwak et al. 2003) (Figs. 2.2.7, 2.2.8).

2.2.8 Cardiac Transplantation – After 1 Year

After the 1-year anniversary of cardiac transplantation, the risk of acute rejection and opportunistic infection diminishes, but other threats emerge, the most serious of which is cardiac allograft vasculopathy. Accelerated atherosclerosis of the coronary arteries is the cause of death of 19% of transplant recipients that have lived to this period, followed by secondary malignancies as the cause of death in 15%. Infection accounts for only 10% of deaths and rejection 7% at this stage. Strokes account for 4% of deaths and myocardial infarction 3% (Knollmann et al. 2000a). In patients who have undergone multiorgan, heart-lung transplantation, an additional complication of chronic transplant rejection is the development of bronchiolitis obliterans syndrome in the lungs (Banakier et al. 2003) (Fig. 2.2.9).

In longer term survivors, the incidence of malignancy increases. By 7 years, 24% of heart transplant

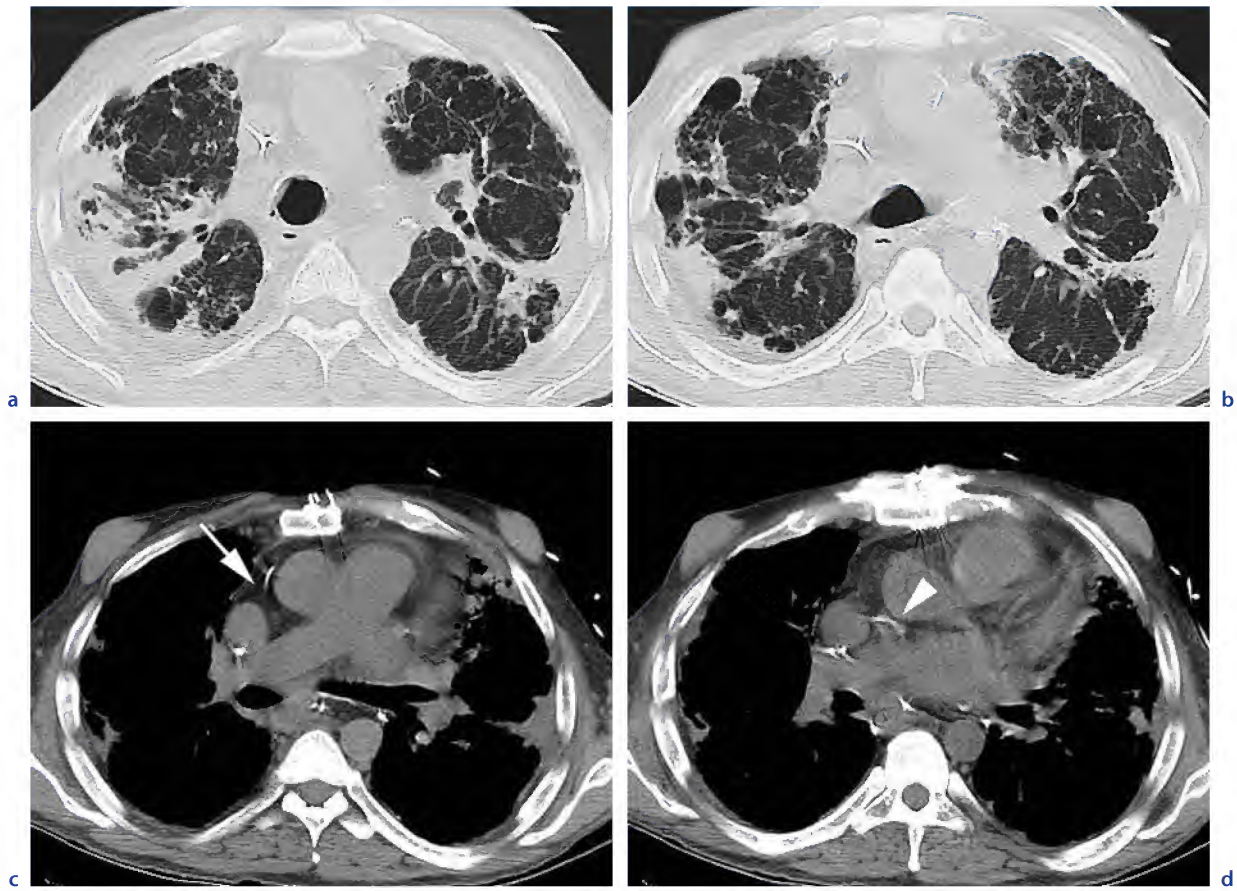

Fig 2.2.9a–d. Bronchiolitis obliterans and pulmonary fibrosis. A 42-year-old man with a history of heart/lung transplantation for Eisenmenger syndrome 10 years ago, now with increasing shortness of breath. **a, b** Chest CT shows changes of end-stage bronchiolitis obliterans and pulmonary fibrosis secondary to chronic lung rejection. **c, d** Note typical anatomic configuration of heart transplantation performed with the atrial-atrial method. There is an increased space between the donor aorta and the recipient superior vena cava (*arrow*). Note the remnant of the donor superior vena cava (*arrowhead*)

patients have developed a malignancy; 18% have developed skin cancer; 4.4% lymphoma (Massad 2004; Taylor et al. 2004).

2.2.9 Cardiac Allograft Vasculopathy of the Coronary Arteries

Vasculopathy of the coronary arteries in the donor heart that is accelerated and progressive is a mark of chronic rejection, and continues to be a significant obstacle to long-term survival of cardiac transplant recipients (Knollmann et al. 2000a; Massad 2004; Taylor et al. 2004). Half of all patients who are 5 years out from cardiac transplantation demonstrate some evidence of coronary vasculopathy, and cardiac allograft vasculopathy is the leading cause of mortality in cardiac transplant recipients who are at least 1 year out from surgery (Gao et al. 1989; Massad 2004; O'Neill et al. 2004; Poston and Griffith 2004; Valantine 2004). The cause is unknown, but may be multifactorial involving immunologic triggers of rejection; non-immunologic causes such as hypertension, diabetes and hyperlipidemia; and complications of immunosuppressive therapy such as CMV infection (Valantine 2004). The process is characterized by rapidly progressive, diffuse, concentric narrowing of the coronary arteries, both epicardial and proximal vessels, that results from proliferation of smooth muscle cells, extracellular matrix, macrophages, and lymphocytes in the intima of the coronary arteries, especially the smaller vessels (Billingham 1989; Massad 2004;

Poston and Griffith 2004; Valantine 2004). Myocardial ischemia is the consequence, and currently there is no effective treatment short of retransplantation (Knisely et al. 1999; Valantine 2004; Winkel et al. 1999).

New imaging techniques for monitoring the progression of coronary allograft vasculopathy include intracoronary ultrasound, MRI, and cardiac CT. Although coronary angiogram and intracoronary ultrasound remain the mainstay of diagnosis they are invasive techniques. MRI and cardiac CT are being investigated as alternative non-invasive techniques for monitoring cardiac transplant recipients for evidence of rejection and allograft vasculopathy (Almenar et al. 2003; Bae et al. 2004). Cardiac CT can be used to provide a calcium index score of the coronary arteries that can be followed over time and may correlate with the severity of coronary disease shown by intracoronary ultrasonography and coronary angiography (Barbir et al. 1999; Knollmann et al. 2000b; Lazem et al. 1997; St Goar et al. 1992). In addition, cardiac CT using high-speed, EKG-gated, multidetector CT technology can produce CT coronary angiograms that are the equivalent to those obtained by conventional angiography (Bae et al. 2004).

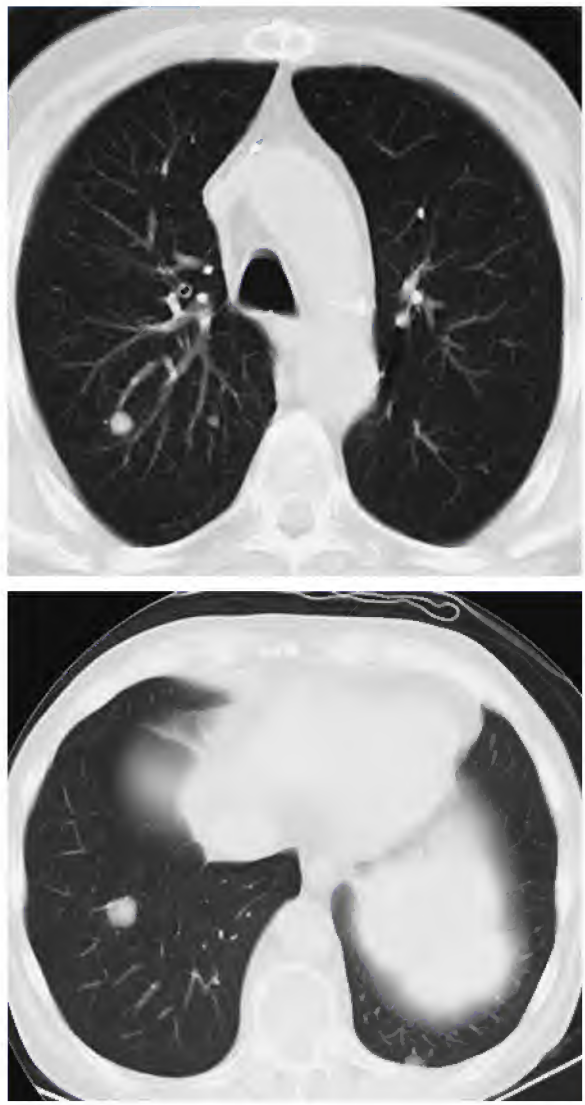

Fig 2.2.10a,b. Post transplant lymphoproliferative disorder (*PTLD*). This 61-year-old man's chest CT demonstrated multiple, new lung nodules 8 months status post cardiac transplantation. Open lung biopsy showed lymphoproliferative disorder. [**a** Reprinted with permission from: Kuhlman JE (2004) The immunocompromised host: chest. In: Husband JE, Reznek RH (eds) *Imaging in oncology*, 2nd edn, Chap 58. Taylor and Francis, London, pp1337–1362]

2.2.10 Post-Transplant Malignancy

Heart transplant recipients also face an increased risk for malignancy including skin cancers, PTLD including lymphoma, and Kaposi sarcoma (Knollmann et al. 2000a; Penn 1979; Shiba et al. 2004; Winkel et al. 1999). Once the heart transplant recipient is more than 1 year out from transplantation, malignancy is second only to cardiac allograft vasculopathy as the most common cause of death (Knollmann et al. 2000a). By 7 years post-transplantation, the incidence of malignancy is 24%, with 18% of survivors having skin cancer (Taylor et al. 2004).

Post-transplant B-cell disorders include lymphoid hyperplasia, PTLD, and malignant lymphoma (mostly non-Hodgkin in type) (Figs. 2.2.10, 2.2.11). They occur in 2%–6% of cardiac transplant recipients and PTLD is associated with Epstein-Barr virus infection and immunosuppression (Armitage et al. 1991; Higgins et al. 2003; Knisely et al. 1999; Young et al. 1989). Manifestations of PTLD may be focal or disseminated (Knollmann et al. 2000a). Organs as diverse as the brain, lung, heart, liver, kidneys, spleen, GI tract, and lymph nodes may be involved (Haldas et al. 2002; Knollmann et al. 2000a). Thoracic manifestations include pulmonary nodules, reticulonodular opacities, and masses. Associated adenopathy may or may not be

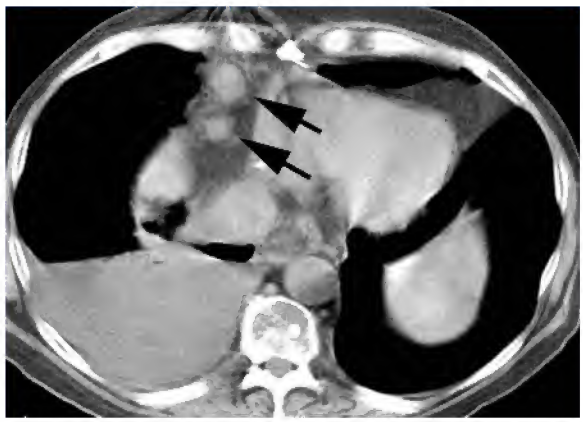

Fig 2.2.11. Post-transplant lymphoma. This 64-year-old man developed shortness of breath 13 months status post cardiac transplantation. CT shows a large right pleural effusion and adenopathy, including in the right paracardiac region (*arrows*). Thoracentesis of the pleural effusion identified monoclonal large cell lymphoma on cytology. [Reprinted with permission from Kuhlman JE (2002) Thoracic imaging in heart transplantation. *Journal of Thoracic Imaging* 17:113–121]

present, with presentation more often extranodal in type (Haldas et al. 2002; Haramati et al. 1993; Knisely et al. 1999).

The incidence of other organ cancers such as lung cancer in heart transplant recipients is similar to that in the general population, with similar risk factors (Bagan et al. 2005; Potaris et al. 2005; Shiba et al. 2004). Lung cancer does arise in cardiac transplant recipients (~1%), particularly those who have been smokers (Bagan et al. 2005; Knisely et al. 1999; Potaris et al. 2005) (Fig. 2.2.12). In this immunosuppressed patient population, lung cancer tends to be aggressive once the tumor has spread to the lymph nodes (Bagan et al. 2005). When diagnosed at an advanced stage, lung cancer in this patient population carries a poor prognosis (Bagan et al. 2005; Delcambre et al. 1996; Goldstein et al. 1996; Johnson et al. 1998; Leung 1999; Pham et al. 1995). The mean time to diagnosis of lung cancer following cardiac transplantation varies among reported series (mean 3488 months with a range of 1.5–180 months) (Bagan et al. 2005; Delcambre et al. 1996; Goldstein et al. 1996; Johnson et al. 1998; Leung 1999; Pham et al. 1995; Potaris et al. 2005). Although advocated by some, the role of CT screening for lung cancer in heart transplant patients has yet to be determined (Delcambre et al. 1996; Johnson et al. 1998). However, reports suggest that if lung cancer is detected at an early stage in this

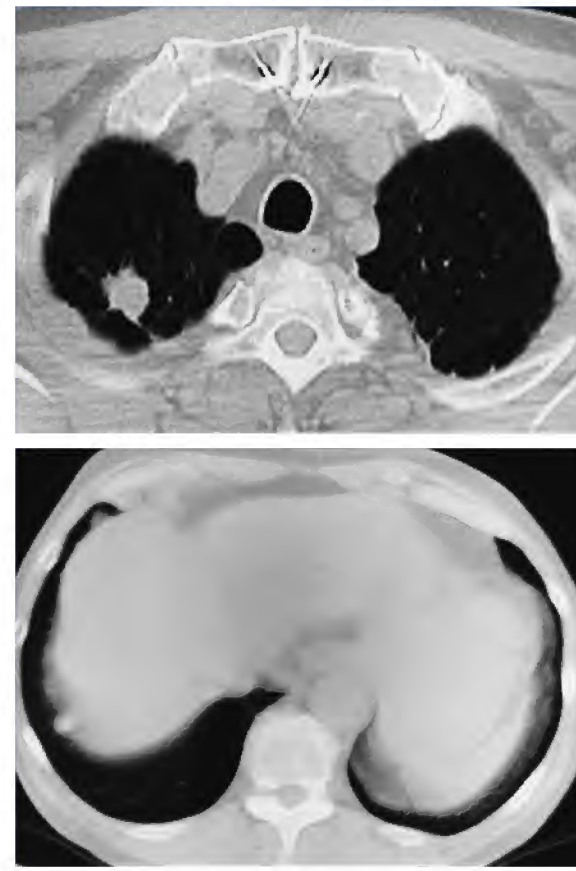

Fig 2.2.12a,b. Lung cancer arising in a heart transplant recipient. A 61-year-old man, 4 months status post orthotopic heart transplantation for dilated cardiomyopathy with a new lung mass found on chest radiography. The patient was a former smoker. Chest CT shows a speculated mass in the right lung apex and multiple metastases studding the pleural surface of the right hemidiaphragm. Biopsy of the right upper lobe mass revealed squamous cell carcinoma of the lung. [Reprinted with permission from Kuhlman JE (2002) Thoracic imaging in heart transplantation. *Journal of Thoracic Imaging* 17:113–121]

patient population, resection improves survival, despite an increased risk of peri-operative infection (Bagan et al. 2005).

2.2.11 Other Complications of Therapy

The heart transplant recipient is at risk for a number of other non-immunologic complications of therapy. Complications of corticosteroid therapy

are legion and include: obesity, glucose intolerance, hypertension, hyperlipidemia, poor wound healing, cataracts, personality changes including psychosis, gout, osteoporosis, insufficiency fractures, avascular necrosis, peptic ulcer disease, and lipomatosis (mediastinal, extrapleural, and upper back buffalo hump) (Knollmann et al. 2000a; Winkel et al. 1999). Complications of azathioprine therapy include bone marrow suppression, cholestatic jaundice, and pancreatitis. Adverse effects of ciclosporin A and calcineurin inhibitors include hypertension, hyperkalemia, renal tubular acidosis, renal failure, hepatic failure, tremor, hirsutism, seizures, hypertrichosis, gingival hyperplasia, anxiety, and conjunctivitis (Massad 2004; Winkel et al. 1999). Central nervous system leukoencephalopathy can result from high-dose ciclosporin A and tacrolimus (Knollmann et al. 2000a). Rapamycin, due to its anti-fibrosing qualities, may increase the risk of wound dehiscence and seroma formation. It may also foster hyperlipidemia and cases of interstitial pneumonitis have been reported (Massad 2004; Poston and Griffith 2004).

References

Almenar L, Igual B, Martinez-Dolz L, Arnau MA, Osa A, Rrueda J, Palencia M (2003) Utility of cardiac magnetic resonance imaging for the diagnosis of heart transplant rejection. Transplant Proc 35:1962–1964

Armitage JM, Kormos RL, Stuart RS et al (1991) Post-transplant lymphoproliferative disease in thoracic organ transplant patients: ten years of cyclosporine-based immunosuppression. J Heart Lung Transplant 10:877–886

Austin JH, Schulman LL, Mastrobattista JD (1989) Pulmonary infection after cardiac transplantation: clinical and radiologic correlations. Radiology 172:259–265

Bae KT, Hong C, Takahashi N, Gutierrez F, Shakey A, Hirsch R, Canter CE (2004) Multi-detector row computed tomographic angiography in pediatric heart transplant recipients: initial observations. Transplantation 77(4):599–602

Bagan P, Assouad J, Berna P, Souilamas R, Barthes F, Riquet M (2005) Immediate and long-term survival after surgery for lung cancer in heart transplant recipients. Ann Thorac Surg 79:438–442

Barbir M, Bowker T, Ludman PF, Mitchell AG, Wood D, Yacoub M (1994) Ultrafast computed tomographic scanning for detection of coronary disease in cardiac transplant recipients. Am J Cardiol 74:941–944

Billingham ME (1989) Graft coronary disease: the lesion and the patients. Transplant Proc 21:3665–3666

Bnakier AA, Muylem AV, Scillia P, De Maertelaer V, Estenne M, Genevois PA (2003) Air trapping in heart-lung transplant recipients: variability of anatomic distribution and extent at sequential expiratory thin-section CT. Radiology 229:737–742

Delcambre F, Pruvot FR, Ramon P et al (1996) Primary bronchogenic carcinoma in transplant recipients. Transplant Proc 28:2884–2885

Gao SZ, Schroeder JS, Alderman EL et al (1989) Prevalence of accelerated coronary artery disease in heart transplant survivors: comparison of cyclosporine and azathioprine regimens. Circulation 80:100–105

Eisen H, Ross H (2004) Optimizing the immunosuppressive regimen in heart transplantation. J Heart Lung Transplant 23:S207–S213

Englesbe MJ, Wu AH, Clowes AW, Zierler RE (2003) The prevalence and natural history of aortic aneurysms in heart and abdominal organ transplant patients. J Vasc Surg 37:27–31

Fishman JA, Rubin RH (1998) Infection in organ – transplant recipients. N Engl J Med 338:1741–1751

Goldstein DJ, Austin JHM, Zuech N et al (1996) Carcinoma of the lung after heart transplantation. Transplantation 62:772–775

Haldas J, Wang W, Lazarchick J (2002) Post-transplant lymphoproliferative disorders: T-cell lymphoma following cardiac transplant. Leukemia Lymphoma 43(2):447–450

Haramati LB, Schulman LL, Austin JHM (1993) Lung nodules and masses after cardiac transplantation. Radiology 188:491–497

Henry DA, Corcoran HL, Lewis TD et al (1989) Orthotopic cardiac transplantation: evaluation with CT. Radiology 170:343–350

Higgins CD, Swerdlow AJ, Smith JD, Hunt BJ, Thomas JA, Burke MM, Crawford DH, Yacoub MH (2003) Risk of lymphoid neoplasia after cardiothoracic transplantation: the influence of underlying disease and human leukocyte antigen type and matching. Transplantation 75:1698–1703

Hosenpud JD, Bennett LE, Keck BM, Fiol B, Novick RJ (1997) The registry of the International Society for Heart and Lung Transplantation: fourteenth official report – 1997. J Heart Lung Transplant 16:691–712

Hosenpud JD, Bennett LE, Keck BM, Fiol B, Boucek MM, Novick RJ (1999) The Registry of the International Society for Heart and Lung Transplantation: sixteenth official report – 1999. J Heart Lung Transplant 18:611–626

Johnson WM, Baldursson O, Gross TJ (1998) Double jeopardy: lung cancer after transplantation. Chest 113:1720–1723

Jolles H, Henry DA, Roberson JP, Cole TJ, Spratt JA (1996) Mediastinitis following median sternotomy: CT findings. Radiology 201:463–466

Kirklin JK, McGiffin DC, Pinderski LJ, Tallaj J (2004) Selection of patients and techniques of heart transplantation. Surg Clin N Am 84:257–287

Knisely BL, Mastey LA, Collins J, Kuhlman JE (1999) Imaging of cardiac transplantation complications. RadioGraphics 19:321–339

Knollmann FD, Hummel M, Hetzer R, Felix R (2000a) CT of heart transplant recipients: spectrum of disease. RadioGraphics 20:1637–1648

Knollmann FD, Bocksch W, Spiegelsberger S, Hetzer R, Felix R, Hummel M (2000b) Electron-beam computed tomography in the assessment of coronary artery disease after heart transplantation. Circulation 101:2078–2082

Knosalla C, Weng Y, Warnecke H et al (1996) Mycotic aortic aneurysms after orthotopic heart transplantation. J Heart Lung Transplant 15:827–839

Kobashigawa JA, Kirklin JK, Naftel DC et al (1993) The Transplant Cardiologists Research Database Group: pretransplantation risk factors for acute rejection after heart transplantation – a multi-institutional study. J Heart Lung Transplant 12:355–366

Kuhlman JE (2002) Thoracic imaging in heart transplantation. J Thoracic Imag 17:113–121

Kuhlman JE (2004) The immunocompromised host: chest. In: Husband JE, Reznek RH (eds) Imaging in oncology, 2nd edn, chap 58. Taylor and Francis, London, pp 1337–1362

Kwak EJ, Strollo DC, Kulich SM, Kusne S (2003) Cavitary pneumonia due to *Rhodococcus equi* in a heart transplant recipient. Transplant Infect Dis 5:43–46

Lazem F, Barbir M, Banner N, Ludman P, Mitchell A, Yacoub M (1997) Coronary calcification detected by ultrafast computed tomography is a predictor of cardiac events in heart transplant recipients. Transplant Proc 29:572–575

Leung AN (1999) Invited Commentary: Scientific exhibit. RadioGraphics 19(2):340–341

Levin T, Suh B, Beltramo D, Samuel R (2004) Aspergillus mediastinitis following orthotopic heart transplantation: case report and review of the literature. Transplant Infectious Disease 6:129–131

Massad MG (2004) Current trends in heart transplantation. Cardiology 101:79–92

Miller LW, Schlant RC, Kobashigawa R, Kubo S, Renlund DG (1993) 24th Bethesda conference: cardiac transplantation. Task force 5: complications. J Am Coll Cardiol 22:41–54

O'Neill JO, Taylor DO, Starling RC (2004) Immunosuppression for cardiac transplantation. The past, present, and future. Transplant Proc 36 [Suppl 2S]:309S–313S

Penn I (1979) Tumor incidence in human allograft recipients. Transplant Proc 11:1047–1051

Petri WA Jr (1994) Infections in heart transplant recipients. Clin Infect Dis 18:141–148

Pham SM, Kormos RL, Landreneau RJ et al (1995) Solid tumors after heart transplantation: lethality of lung cancer. Ann Thorac Surg 60:1623–1626

Poston RS, Griffith BP (2004) Heart transplantation. J Intensive Care Med 19(1):3–12

Potaris K, Radovancevic B, Thomas CD, Gregoric I, Vaporciyan AA, Riggs SA, Radovancevic R, Vaugh WK, Frazier OH (2005) Lung cancer after heart transplantation: 17-year experience. Ann Thoracic Surg 79:980–983

Reitz BA, Fowles RE, Ream AK (1982) Cardiac transplantation. In: Ream AK, Fogdall RP (eds) Acute cardiovascular management, anesthesia, and intensive care. Lippincott, Philadelphia, Pa., pp 549–567

Rodeheffer RJ, McGregor CGA (1992) The development of cardiac transplantation. Mayo Clin Proc 67:480–484

Rubin RH (2000) Prevention and treatment of cytomegalovirus disease in heart transplant patients. J Heart Lung Transplant 19:731–735

Schellemans C, Tack W, Vanderheyden M (2004) Acute type A aortic dissection in a cardiac allographt recipient: case report and review of the literature. Heart 90:1256–1258

Shanewise J (2004) Cardiac transplantation. Anesthesiology Clin N Am 22:753–765

Shiba N, Chan MCY, Kwok BW, Valantine HA, Robbins RC, Hunt SA (2004) Analysis of survivors more than 10 years after heart transplantation in the cyclosporine era: Stanford experience. J Heart Lung Transplant 23(2):155–164

Shirazi KK, Amendola MA, Tisnado J et al (1983) Radiographic findings in the chest of patients following cardiac transplantation. Cardiovasc Intervent 6:1–6

St Goar FG, Pinto FJ, Alderman EL et al (1992) Intracoronary ultrasound in cardiac transplant recipients: in vivo evidence of "angiographically silent" intimal thickening. Circulation 85:979–987

Taylor DOES, Edwards LB, Boucek MM, Trulock EP, Keck BM, Hertz MI (2004) The registry of the international society for heart and lung transplantation: twenty-first official adult heart transplant report – 2004. J Heart Lung Transplant 23(7):796–803

Thaler SJ, Rubin RH (1996) Opportunistic infections in the cardiac transplant recipient. Curr Opin Cardiol 11:191–203

Thorsen MK, Goodman LR (1988) Extracardiac complications of cardiac surgery. Semin Roentgenol 23:32–48

Valantine H (2004) Cardiac allograft vasculopathy after heart transplantation: risk factors and management. J Heart Lung Transplant 23:S187–S193

Winkel E, DiSesa VJ, Costanzo MR (1999) Advances in heart transplantation. Dis Mon 45(3):62–87

Yamani MH, Starling RC (2000) Long-term medical complications of heart transplantation: information for the primary care physician. Cleveland Clinic J Med 67:673–680

Young L, Alfieri C, Hennessy K et al (1989) Expression of Epstein-Barr virus transformation-associated genes in tissues of patients with EBV lymphoproliferative disease. N Engl J Med 321:1080–1085

Renal Transplantation: Epidemiological, Clinical, Radiological and Surgical Considerations

3

Nicolas Grenier, Pierre Merville, and Gilles Pasticier

CONTENTS

3.1 Epidemiological Considerations

Worldwide, the population treated with renal replacement therapy reached almost 1.7 million at the end of 2003, representing approximately 1.3 million patients who undergo dialysis and 400,000 patients who are alive with a kidney transplant (Lameire et al. 2005). The number of patients treated for end-stage renal disease doubled during the last decade in the United States and Europe, where dialysis consumes about 2% of health care budgets, with < 0.1% of these patients requiring treatment (De Vecchi et al. 1999). Based on the European Renal Association–European Dialysis and Transplant Association registry (25 countries of the European Union), approximately 360,000 patients are undergoing renal replacement therapy, with 66% of them on dialysis and 34% living with a functioning graft; the percentage of kidneys transplanted from living donors varies widely among the European countries, between < 10% to > 50%. (ERA–EDTA Registry: ERA–EDTA 2003, Annual report. Amsterdam, The Netherlands, 2004, Academic Center.)

Renal transplantation represents the treatment of choice for chronic renal insufficiency. It not only improves the patients' quality of life but significantly prolongs their survival compared to those

N. Grenier, MD
Professor, Service d'Imagerie Diagnostique et Interventionnelle de l'Adulte, Groupe Hospitalier Pellegrin, Place Amélie-Raba-Léon, 33076 Bordeaux Cedex, France
P. Merville, MD
Professor, Département de Néphrologie, Unité Médicale de Néphrologie Transplantation Rénale, Groupe Hospitalier Pellegrin, place Amélie-Raba-Léon, 33076 Bordeaux Cedex, France
G. Pasticier, MD
Département d'Urologie, Groupe Hospitalier Pellegrin, Place Amélie-Raba-Léon, 33076 Bordeaux Cedex, France

remaining on hemodialysis (Wolfe et al. 1999). The advances made in immunosuppressive therapies have provided constant improvement of short-term graft survival, which now exceeds 90% 1 year after transplantation (Cecka 2002). In contrast, graft half-life had improved very little, remaining around 7.5–9.5 years until the early 1990s. Over the past 10 years, this situation has changed, with significantly prolonged graft survival for large cohorts of renal graft recipients. The half-life of engrafted cadaveric kidneys increased from 7.5 years in 1988 to 13.8 years in 1996 (Hariharan et al. 2000), with progressively improved renal function over time (Gourishankar et al. 2003).

The principal cause of graft loss after the first year is chronic allograft nephropathy (CAN), followed by patient death, late acute rejections, nephropathy recurrence and polyomavirus infection (Hariharan 2001). However, prolongation of graft survival also means extended exposure of the patient to side-effects associated with immunosuppressive therapies, mainly infections and cancers, and other late-onset cardiovascular, bone and/or metabolic complications. The first year after transplantation is special, as it is characterized by the highest rates of acute rejection and opportunistic infections, such as cytomegalovirus. In this review, we successively address the presurgical evaluation of the patient, the operation itself and its possible complications, then the early (first year) and late (after the first year) medical complications.

3.2 Presurgical Evaluations

3.2.1 Evaluation of the Graft Recipient

The pretransplantation work-up is aimed at determining whether the patient's general condition can tolerate the surgical intervention and whether local conditions permit graft implantation, and the latter orients the choice of the technique to be used.

3.2.1.1 The General Work-Up

Physical examination is conducted to evaluate the patient's general condition, weight, body type and medical history. Weight loss for overweight patients is strongly recommended. It is important to establish the existence and size of a possible inguinal hernia, especially in men. The existence of abdominal and/or pelvic scars, resulting from previous interventions, has an impact on the side of transplantation: the left side is chosen for patients who have undergone surgery for appendicitis-associated peritonitis and/or a right inguinal hernia with insertion of prosthetic material.

All men should undergo digital rectal examination to search for a suspicious prostate nodule. In France, the circulating prostate-specific antigen (PSA) concentration is systematically determined as of 50 years (45 years in the case of a family history of prostate cancer). Particular importance is accorded to normal-for-age PSA values and biopsy samples are taken when the least doubt exists, as the development of a preexisting prostate cancer could be facilitated by immunosuppressive therapy. The remainder of the patient's general condition is evaluated during a consultation with the anesthesiologist.

3.2.1.2 Local Examination

The local status of the lower urinary tract and blood vessels to be attached to the graft is evaluated essentially through imaging explorations.

3.2.1.2.1 The Lower Urinary Tract

Retrograde cystography is mandatory to assess bladder morphology and function. The bladder capacity must be assessed because it is often decreased, depending on the degree of urine output before transplantation. Bladder diverticulum and vesicoureteral reflux must be excluded because they could facilitate urinary infection during the post-transplantation period. Such abnormalities should be treated during or before the transplantation. Finally, bladder-output function and urethral morphology during voiding can be examined during cystouretrography.

3.2.1.2.2 Status of the Vasculature

For young recipients (< 50 years old) who have not been on dialysis for a prolonged period and thus

have a low probability of developing arterial lesions, Doppler examination of the lower limbs suffices. If the Doppler examination appears abnormal, contrast-enhanced imaging should be performed; the choice between computed tomography angiography (CTA) and magnetic resonance angiography (MRA) depends on residual renal function. However, for patients older than 50 years and at any age after several years of dialysis a precise evaluation of arterial status is critical. Prolonged dialysis may induce extensive arterial calcifications, mainly in the lower aorta and iliac vessels, sometimes rendering arterial anastomosis extremely difficult. The site, the severity and the degree of extension of these calcifications, and the presence of arterial stenoses directly influence the choice of the implantation site. Today, the best technique to determine arterial wall status is non-enhanced multidetector-row CT (MDCT) with axial sections and coronal reformations. For lumen patency assessment the choice between contrast-enhanced CTA and MRA, as above, depends on residual renal function.

3.2.2 Evaluation of the Donor

Examination of the kidney to be engrafted depends on the donor's status, i.e., either being maintained in a state of brain death (cadaveric) or living. We are concerned here exclusively with the renal morphology explorations obtained with different imaging techniques.

3.2.2.1 Evaluation of Cadaveric Donor Kidneys

No consensus has been reached for the assessment of the renal status of cadaveric donors: it can be based on simple abdominal ultrasonography (US) or contrast-enhanced CT. As the diagnosis of cerebral death moves towards requiring cerebral contrast-enhanced CT angiography, helical CT now plays an increasing role for that purpose.

3.2.2.2 Evaluations of Living-Donor Kidneys

The aim of these evaluations is the assessment of kidney anatomy, volume and function, determination of the number of renal arteries and veins, and overall examination of the anatomy of the entire excretory system. MDCT scanners offer a shorter image-acquisition time, thinner collimation and better spatial resolution than single detector-row CT scanners. They also provide more precise anatomical coverage, increased contrast enhancement of the arteries and greater longitudinal spatial resolution. Dual-phase MDCT angiography combined with three-dimensional (3D) post processing enables minimally invasive and highly accurate depiction of preoperative donor anatomy. The MDCT protocol includes unenhanced acquisitions to detect urolithiasis, followed by acquisitions after iodine enhancement as follows: during the vascular phase (25–30 s), to assess the number and location of renal arteries; during the tubular phase (65–75 s), to assess the number and length of renal veins, renal morphology and volume; and during the excretory phase (2–10 min), to assess the morphology of the upper excretory system.

In a recent study based on 94 renal donors, four-slice MDCT visualized 107 of the 114 renal arteries and 95 of the 98 renal veins confirmed at surgery, but 7 accessory arteries were missed in 6 donor kidneys, yielding respective MDCT sensitivities and specificities of 66% and 100%, 75% and 100%, and 50% and 100%, and overall accuracy of 94%, 97% and 99%, for the identification of variant anatomy of renal arteries, veins and ureters, respectively (Sahani et al. 2005).

According to a recent comparative study between multislice helical CTA and gadolinium-enhanced MRA (on 31 donors), CTA with 3D reconstruction seems more accurate than MRA for assessing the anatomy of renal arteries and veins: CTA visualized 33 arteries and 32 veins (100% sensitivity), while MRA revealed 32 arteries and 31 veins (97% sensitivity). CTA detected all five accessory renal arteries, while MRA detected only one. CTA also identified all three accessory renal veins, while MRA identified two. CTA had sensitivities of 97% and 47% for left lumbar and left gonadal veins, respectively, while the corresponding MRA sensitivities were 74% and 46% (Bhatti et al. 2005). Because nephron-underdosing and donor kidney–recipient body size mismatch can lead to poor allograft function, Saxena et al. (2004) evaluated the relationship between MRI-determined donor kidney volume and post-transplantation graft function: transplantation of donor–recipient pairs with a volume:weight ratio $< 2\ cm^3/kg$ was associated with significantly poorer graft function.

3.3 Current Surgical Techniques

3.3.1 Graft Preparation

The graft is placed in a recipient containing conservation solution and ice; this is the cold ischemia period. Graft preparation consists of excising the cortical fat of the kidney to better assure that the renal parenchyma is healthy (good nerve and blood supply), and to identify all suspicious lesions that must be removed and subjected to histological examinations. Then the vascular pedicle is dissected and all of its collateral vessels are ligated. Short right renal veins can be lengthened by excising an elongation or patch of the contiguous vena cava with the right kidney, to obtain an artery and a vein of about the same lengths. The renal artery is dissected, preserving an aortic patch for its branching. In the case of multiple renal arteries of the same caliber and in close proximity, a common aortic patch is conserved. The ureter is then isolated and carefully dissected to preserve its fatty envelope, which guarantees its good vascularization. Finally, to assure the absence of any leaks, the arterial and venous trunks of the graft are perfused with the conservation solution via a small cannula.

3.3.2 Graft Preservation

The usual kidney storage solutions use an impermeant solute, such as phosphate, lactobionate, glucose, sucrose or raffinose. There is less agreement about the need for other minor components used to minimize acidosis or oxidative reperfusion injury, or enhance regeneration following revascularization. At present, the best known solutions are University of Wisconsin (UW), histidine-tryptophan ketoglutarate (HTK, Custodiol®) or Celsior®.

Two methods are described for kidney preservation: the most common is an initial flushing followed by ice storage and the second is continuous hypothermic pulsatile perfusion, mainly used for non-heart-beating donors. In all cases, the period of cold ischemia should be as short as possible, especially with marginal donors or elderly kidneys.

3.3.3 Transplantation

3.3.3.1 Surgical Approach

Some teams systematically implant the first graft on the right because of the more superficial iliac vessels; others prefer implanting a right kidney on the left and left kidney on the right so that the renal pelvis and ureter are placed anteriorly, thereby facilitating subsequent nephrostomy should it be necessary. Epigastric vessels are dissected and conserved should reimplantation of a polar artery be required.

3.3.3.2 Vascular Anastomoses (Fig. 3.1)

The arterial axis is first palpated to evaluate the quality of its wall. Arterial and venous dissection is limited to segments to be used for anastomoses. In most cases, the renal vein is attached to the external iliac vein. The arterial anastomosis is more variable: end-to-side to the external iliac, most often above the venous implantation, or to the primary iliac artery; sometimes end-to-end to the hypogastric artery, when taken from a living donor, because the graft's artery does not have an aortic patch. All these sites can be used in combination when multiple arteries are reimplanted, even the epigastric artery for the small isolated polar branches.

Once the anastomoses have been completed, the artery and vein are unclamped, with recording of the 'warm' ischemia time (corresponding to the time needed to establish the anastomoses). The moment of kidney reloading is crucial because it allows evaluation of: (1) the quality of renal revascularization (without hypoperfused zones); (2) the good positioning of the vessels, without arterial bending or 'kinking' of the artery (which can be a source of circulatory disorders or stenosis) or without venous tension; (3) the absence of flow disturbances detected by palpation of the artery or vein; (4) the absence of leaks at the anastomosis sites or the small hilum branches. The kidney is then placed in its definitive position on the psoas, after once again confirming the optimal positioning of the vessels.

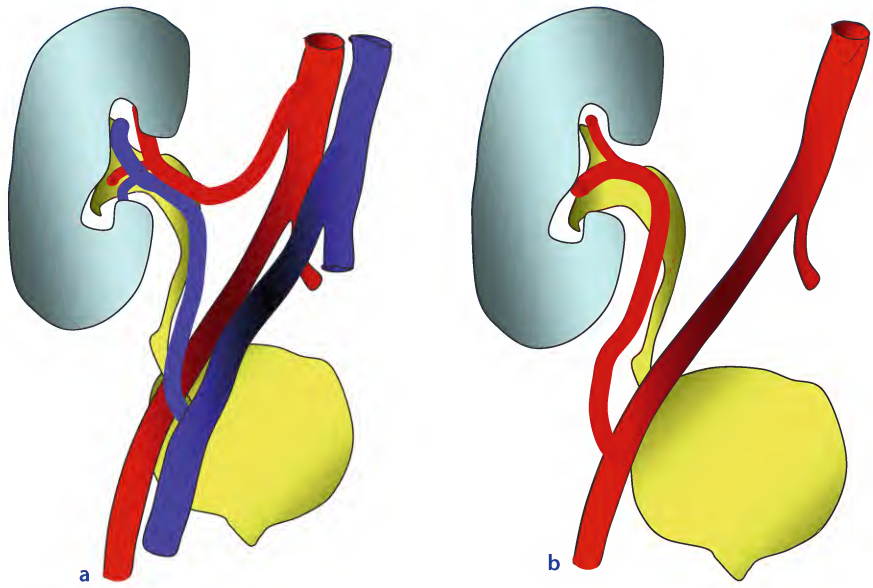

Fig. 3.1a,b. Vascular and ureterovesical anastomoses. The renal vein is attached to the external iliac vein. The arterial anastomosis is variable: **a** end-to-side to the primary iliac artery, or **b** to the external iliac artery, most often above the venous implantation

3.3.3.3 Anastomosis of the Ureter

The type of ureterovesical anastomosis chosen depends on the initial radiological images, the condition of the graft's ureter and intra-operative observations (quality of exposure, the healthy appearance of the bladder, compliance during filling via a catheter).

As a general rule, the ureterovesical anastomosis is made using the Lich–Gregoir technique, with an extravesicular approach: the fat and muscle layers of the bladder are incised over 3–4 cm, causing extrusion of the mucosa without opening it; the ureter is reimplanted into the lowest portion of the bladder mucosa; the bladder wall is closed above the ureter without compressing it, thereby creating an anti-reflux system. The Leadbetter–Politano technique, which corresponds to an intravesicular reimplantation with the creation of a submucosal tunnel, is preferred when the bladder is small. In the case of a technical problem, a double-J stent is left in place to stabilize the anastomosis.

In rare cases (the bladder cannot be reached because the ureter is too short), it is possible to reestablish urinary continuity by using the recipient's ureter; a classical pyeloureteral anastomosis is protected by a double-J stent, according to the Andersen–Hynes pyeloplasty technique.

3.4 Radiological Assessment of the Graft

US is the most useful technique for early and late transplant follow-up. Implantation of the graft within the iliac fossa improves its accessibility and makes possible the use of high-frequency probes, which provide high-resolution and high Doppler sensitivity. On gray-scale US, the normally functioning grafted kidney shows the same corticomedullary differentiation as a native kidney (Fig. 3.2a, b). High-frequency probes (10–15 MHz) show clear separations of all the kidney compartments: the cortex, the outer medulla and the inner medulla, with a decreasing echogenicity gradient from the capsule to the papilla (Fig. 3.2c). The pyelocaliceal system is visible within the sinus fat but color Doppler helps distinguish it from blood vessels. Walls of the renal pelvis can appear slightly thickened during the early postoperative period.

Color Doppler is now essential for detection of intra- or extrarenal arterial or venous abnormalities. The entire graft, and venous and arterial anastomoses can be imaged with a 3.5- to 5-MHz probe (Fig. 3.3). A high-frequency (7.5–14 MHz) probe allows examination by generating high-resolution images of the anterior distal intrarenal vasculature (interlobular and arcuate arteries), which are bet-

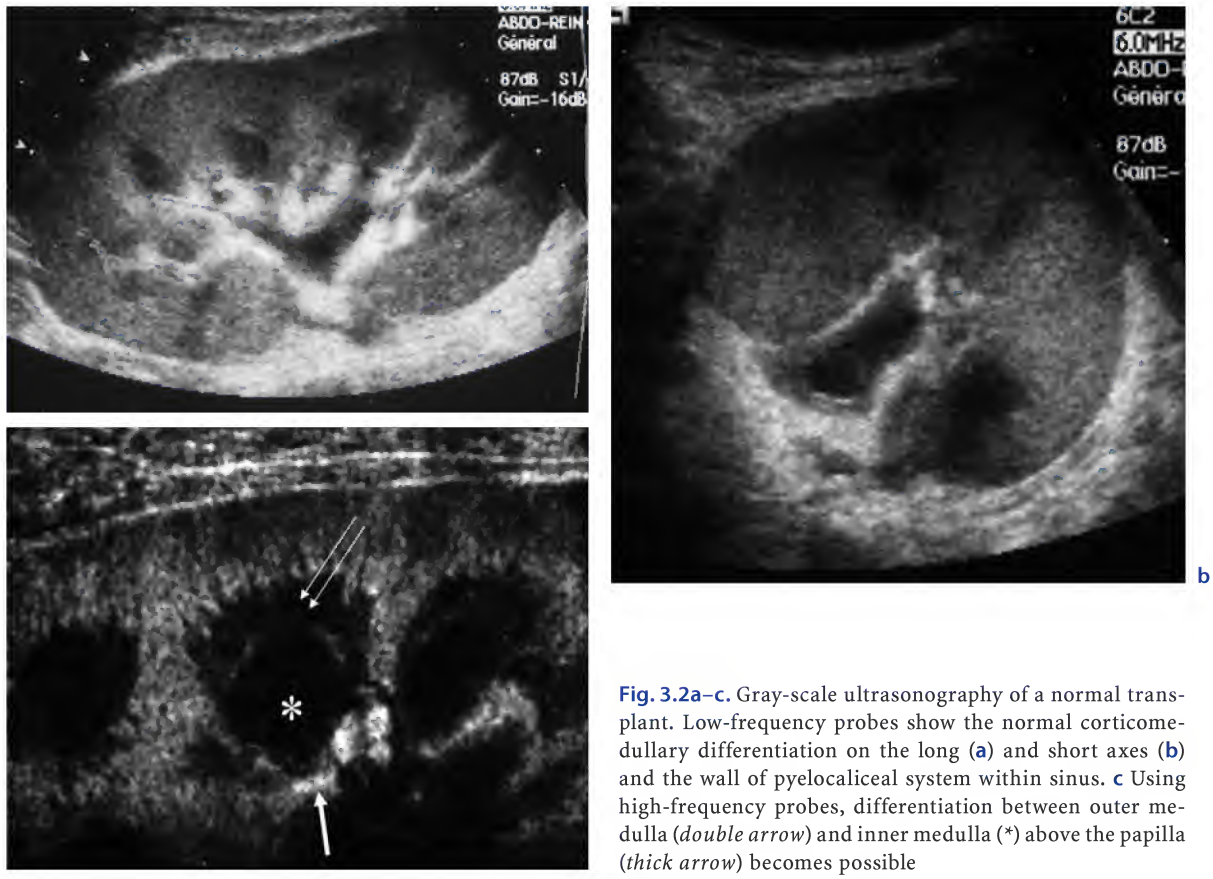

Fig. 3.2a–c. Gray-scale ultrasonography of a normal transplant. Low-frequency probes show the normal corticomedullary differentiation on the long (**a**) and short axes (**b**) and the wall of pyelocaliceal system within sinus. **c** Using high-frequency probes, differentiation between outer medulla (*double arrow*) and inner medulla (*) above the papilla (*thick arrow*) becomes possible

ter delineated with the power mode (Fig. 3.4). Color mapping of the graft must be performed in all cases. Using low pulse repetition frequency, the perfusion of the graft cortex must be homogeneous and complete to the capsule. Spectral sampling of renal artery flow and interlobar arteries at two or three levels of the graft is also mandatory in all cases. The renal artery velocity profile is analyzed and the peak systolic velocity, after angle correction, is measured. Flow sampling of interlobar arteries enables calculation of the resistivity index (RI).

MRI of the renal graft is performed with body phased-array coils, using adequate sequences for visualizing successively the renal parenchyma and its environment, the vascular tree, and the excretory system. Today, MRI protocols assure complete evaluation of the entire graft, including renal parenchyma morphology and perfusion, the vascular tree and the excretory system (Fig. 3.5). On T_1-weighted (T1w) (spin-echo or gradient-echo) sequences, the normal corticomedullary differentiation is visible on normally functioning kidneys: the medulla generates a lower signal intensity (SI) than the cortex. On T_2-weighted (T2w) sequences (usually obtained with a fast spin-echo technique), the medulla generates a higher SI. Gadolinium (Gd) injection gives an accurate delineation of perfused and non-perfused areas of the graft and high-resolution 3D MR angiograms can be obtained for the entire arterial tree – from the iliac axis to the third- or fourth-order branches. However, the distal vascular tree (from interlobar to interlobular arteries) cannot be visualized. The same 3D sequence must be repeated 5 min after Gd injection (or later if necessary) to obtain MR urograms and furosemide injection is generally not necessary for that purpose.

CT has always played a minor role in kidney transplant imaging because it requires normal renal function for analysis of the renal parenchyma or renal vessels. However, the dose of iodine contrast medium now required with MDCT is lower, making it possible to broaden its indications. Association of early acquisitions, during the arterial phase, and late acquisitions, during the excretory phase, provides complete information about the graft (Sebastia et al. 2001).

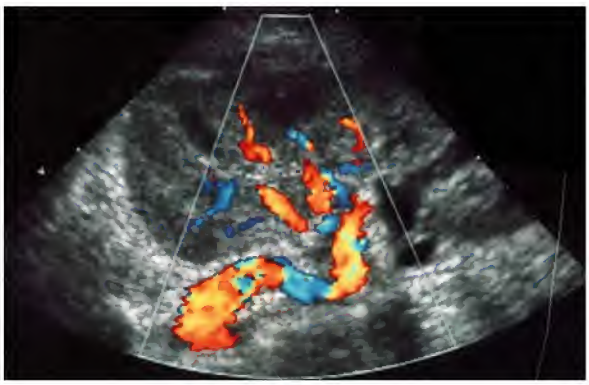

a

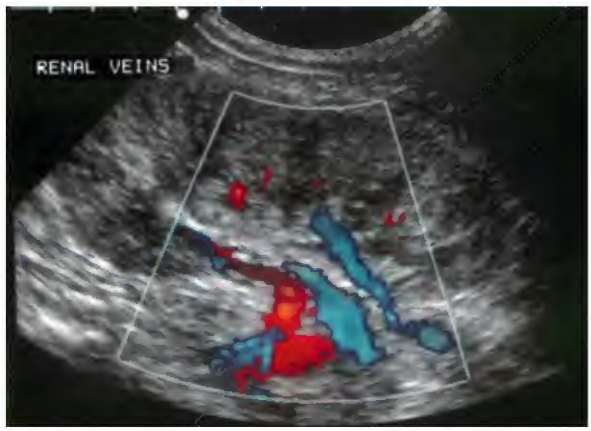

b

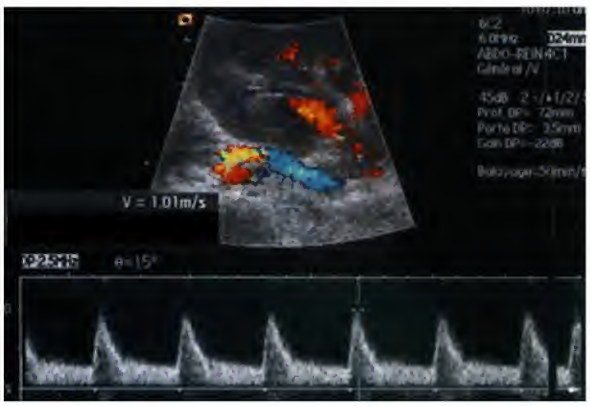

c

Fig. 3.3a–c. Color flow ultrasonography of the renal pedicle shows a unique renal artery implanted on the primary iliac artery (**a**) and two renal veins implanted on the external iliac vein (**b**). **c** The flow on the renal artery shows low resistance and systolic velocities between 80 and 120 cm/s

a

b

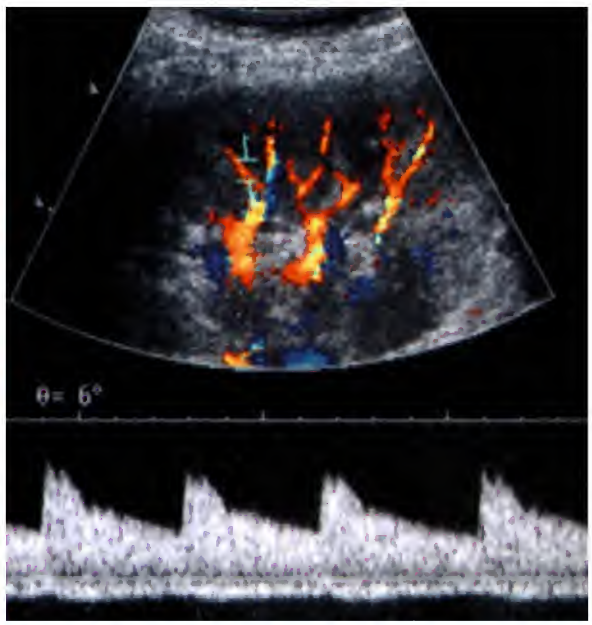

c

Fig. 3.4a–c. Color flow ultrasonography of the intrarenal vasculature. Using the power mode, with a low-frequency probe (**a**), the vasculature must be harmonious, without any defect. With a high-frequency probe (**b**), the cortical interlobular vessels must be visualized until the capsule. **c** Spectral sampling of interlobar arteries show a low resistivity of the flow

Fig. 3.5a–d. MR imaging of a normal transplant with fat-saturated T1-weighted (**a**) and T2-weighted (**b**) sequences. Post-gadolinium 3D MR angiography (**c**) and 3D MR urography sequences (**d**) provide a complete visualization of anastomotic sites

3.5 Early Postoperative Phase

We consider complications occurring during the first year after transplantation to be early and those developing subsequently to be late.

3.5.1 Early Graft Complications

3.5.1.1 Urological Complications

Urological complications can be a source of morbidity and sometimes mortality after kidney transplantation. Their incidence has decreased considerably over the past decade. The current urological complication rate ranges from 4% to 7% (Gogus et al. 2002; Kocak et al. 2004) and death is highly unusual. Many of these complications are of a technical origin, resulting from difficulties encountered during retrieval or implantation of the graft.

3.5.1.1.1 Urinary Fistula

The urinary fistula frequency ranges from 1% to 5%. It is the most common early complication, occurring during the first 2 weeks after transplantation. The majority of urinary leaks are attributed to ureteral ischemia. Maintaining ureteral blood supply by not

dissecting the periureteral connective tissue is a very delicate technical aspect of surgery and a major point of contention for urologists. The other causes of urinary leaks are failure of ureterovesical anastomosis or a missed ureteral duplication. Leakage may be suspected when increasing volumes of a clear liquid are collected by drains, while diuresis tends to decline during the days following surgery. Determination of fluid electrolytes, ingestion of methylene blue thereafter found in the fluid collected and US showing a perirenal fluid collection can confirm the diagnosis.

US usually finds a well-defined anechoic collection at the lower pole of the kidney or intraperitoneal fluid when the transplant is implanted intraperitoneally (Fig. 3.6). Rarely, urinoma is located within the perineum or the thigh. This fluid appears hypointense on unenhanced MR T1w and hyperintense on T2w sequences. T2w MR urography shows the collection and the entire dilated excretory system. This collection may rapidly increase in size between two examinations. The differential diagnosis includes lymphoceles, which usually occur later, after the 4th week post-transplantation. Chemical analysis of the fluid, aspirated under US control, may suggest the diagnosis if the creatinine concentration is higher than that in blood. However, the definitive diagnosis of urinoma is based on the demonstration of an extravasation of contrast medium into the collection after intravenous injection. This can be obtained with Gd-enhanced MRI, iodine-enhanced CT or radionuclides. Urine collection contamination by the contrast agent or the radiotracer often requires delayed imaging (5–15 min after injection) (Fig. 3.6). Cystography or antegrade pyelography may be necessary, if the diagnosis is still in doubt, before performing surgery (Fig. 3.7).

a

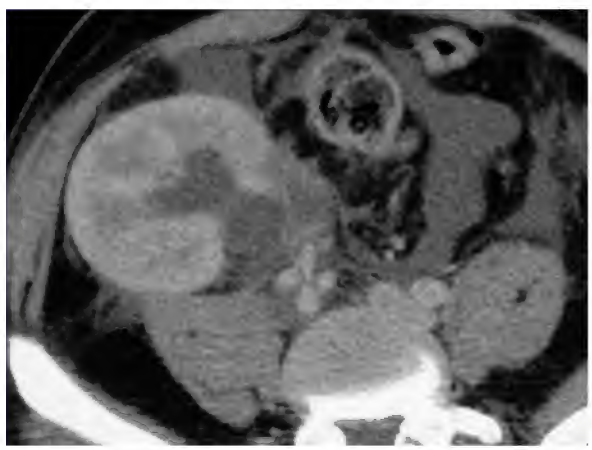

b

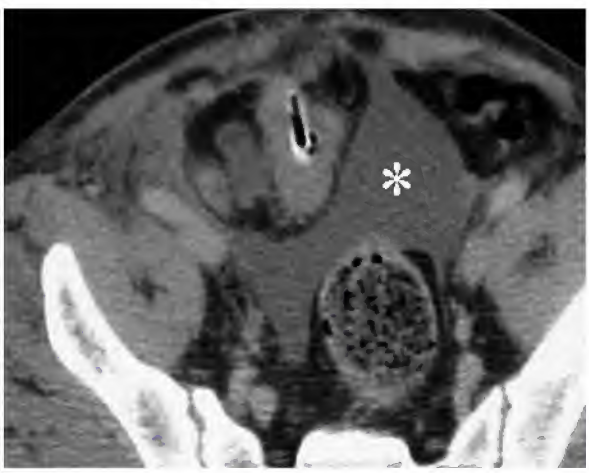

c

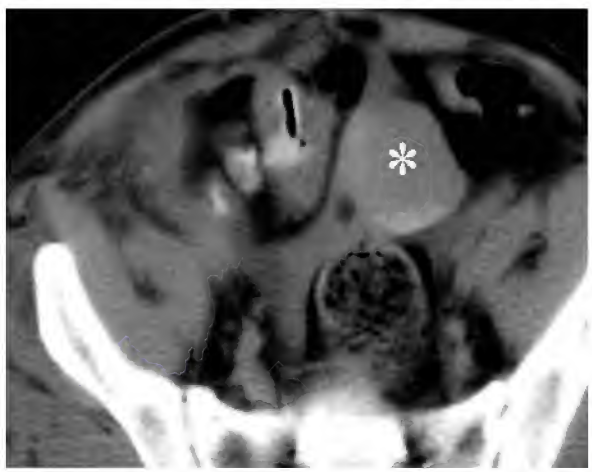

d

Fig. 3.6a–d. Urinary leak secondary to ureteral ischemia. Ultrasonography (**a**) shows a fluid collection between the lower pole of the transplant and the bladder. **b** On contrast-enhanced CT, fluid is noted around the graft and within the peritoneal cavity. The pelvic fluid collection (*) has a water density at the early phase after contrast injection (**c**) but enhances at the late phase (**d**) due to the urinary leak of contrast medium

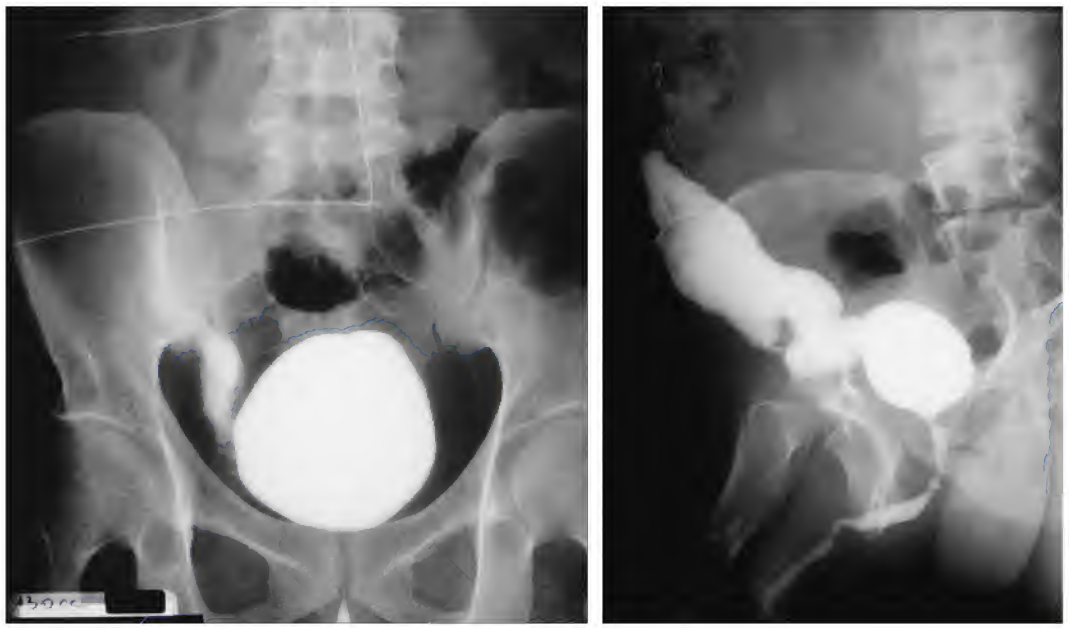

a b

Fig. 3.7a,b. Urinary leak secondary to failure of ureterovesical anastomosis. Retrograde (**a**) and voiding cystography (**b**) show extravasation of contrast agent from the bladder

Whereas the treatment of most of these leaks is surgical, small ones can be treated by nephrostomy and/or ureter stenting (for approximately 6–10 weeks) (Matalon et al. 1990), keeping in mind that the endoscopic approach can be very delicate, owning to the position of the newly created ureteral orifice and the normal inflammatory reaction present during the days following transplantation. Percutaneous antegrade introduction of a ureteral stent into the renal cavities can be difficult and even dangerous, if they are not dilated. Open surgery consists of reimplanting the ureter, with the technique to be used chosen as a function of its remaining healthy length: repair of the ureterovesical anastomosis when the ureter is sufficiently long, or, if not, a pyeloureteral or ureteroureteral anastomosis to the recipient's own ureter.

3.5.1.1.2 Ureteral Stenosis

This complication develops somewhat later (several months) and its frequency tends to increase with time, 5% at 1 year and 10% at 5 years. In 80% of the cases, it is the consequence of progressive fibrosis of the ureterovesical anastomosis (probably secondary to sequelae after ureteral ischemia) but it can also result from inflammatory infiltration of the ureter wall during rejection, thereby explaining why most of these stenoses are located in the lower third of the ureter, close to the ureteral anastomosis. The differential diagnosis includes: surgical error causing a tight anastomosis or a kinking phenomenon when the ureter is too long; intraluminal causes of obstruction, such as lithiasis or blood clot; and extraluminal compression by perigraft fluid collections.

The diagnosis is suspected when decreased renal function is associated with dilatation of the collecting system on US (Fig. 3.8). However, such dilatation may be passive, due to two phenomena: either a full bladder, requiring repeated US after complete voiding or bladder catheterization, or a loss of smooth-muscle tonus secondary to ureteral denervation. Unfortunately, this latter mechanism is difficult to confirm; usually it occurs very early after transplantation and dilatation is observed during follow-up, despite persistently normal renal function.

Differentiation between obstructive and non-obstructive pyelocaliectasis remains difficult and Doppler RI measurement is neither sensitive nor specific in transplanted kidneys (Platt et al. 1991). Renal scintigraphy may characterize the obstruction when the tracer accumulates within the collecting system on delayed images and by measuring increased clearance time after furosemide injection.

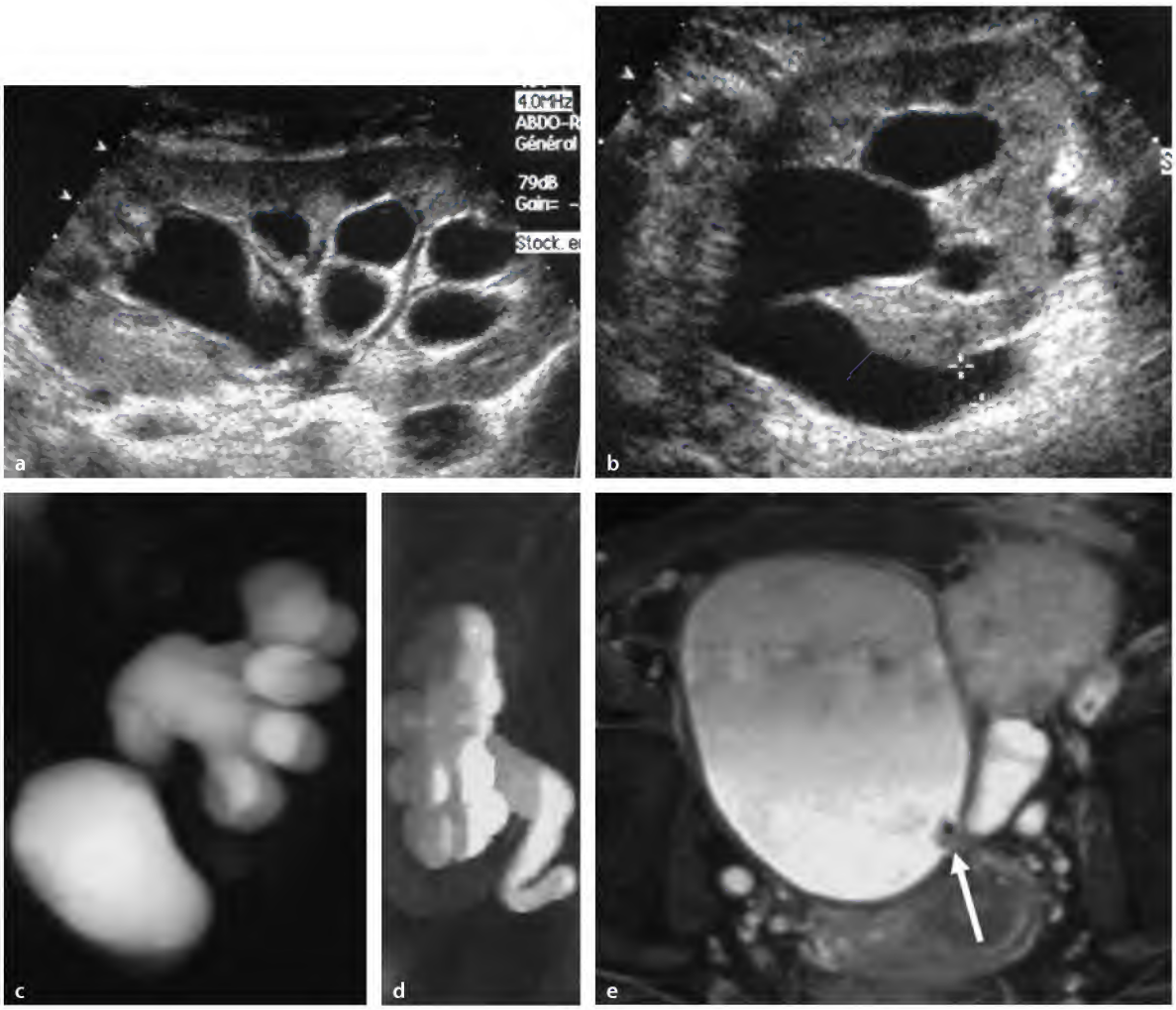

Fig. 3.8a–e. Urinary obstruction at the level of the uterovesical anastomosis. Sonography shows a dilatation of pyelocaliceal system (**a**) and ureter of renal graft (**b**). Ureteropyelectasis is well visualized on 3D T2w (**c**) and Gd-enhanced T1w (**d**) MR images. T2w axial section (**e**) shows a thickened anastomosis due to fibrotic tissue (*arrow*)

When obstruction is suspected, visualization of the entire upper urinary tract is mandatory to determine its exact location and cause. The least invasive method for that purpose is MR urography because most of these patients have decreased renal function (Fig. 3.8). CT urography may be an alternative, when renal function is not too severely impaired, but X-ray excretory urography should no longer be performed because of its high rate of obtaining interpretable images of the lower ureter. With MRI, both type of sequences (T2w and Gd-enhanced T1w) have to be obtained. When dilatation is sufficient, T2w sequences demonstrate the entire collecting system up to the anastomosis or the site of obstruction. If not, T1w Gd-enhanced sequences, with delayed acquisitions, usually do. Antegrade opacification after nephrostomy is also possible and constitutes the first therapeutic step. This urine diversion allows normalization of renal function, and radiological opacification demonstrates the site and length of the stenosis.

In the rare cases of extended and/or multiple stenoses, surgical reimplantation is required and the rules given above for fistula treatment should be followed. Most of the time, the stenosis is short and located in the ureterovesical anastomosis zone, and endoscopic repair, which is more successful the earlier it is undertaken, should be attempted. For the highly unusual immediate postoperative stenoses, the simple insertion of a double-J stent for 4 weeks

can be sufficient. For the late events, endoscopic dilatation may be sufficient; most often, incision is required either antegrade under endoscopic guidance or retrograde under endoscopic and radiological control using a dilatation balloon equipped with an incising electrode (Acucise™ procedure). In all cases, a large caliber (10–14G Fr) indwelling stent should be left in place for 4–6 weeks.

3.5.1.1.3 Graft Infection

Urinary infections are common during the first month following transplantation. They are usually nosocomial bacterial infections, sometimes facilitated by the presence of catheters, which can lead to real pyelonephritis of the graft or the development of renal or perirenal abscesses. Sometimes, perigraft abscesses may be secondary to bacterial contamination of a preexisting fluid collection (hematoma, lymphocele or urinoma). The most frequently encountered microorganisms are: *Staphylococcus aureus*, *Escherichia coli*, enterococci and *Candida albicans*. Infections can be prevented by strict implementation of standard hygiene rules and, perhaps, antibiotic prophylaxis. Pelvic pain and graft tenderness are associated with fever and elevated white blood cell counts. However, it must be kept in mind that immunosuppression may attenuate these clinical and biological signs.

US, using B-mode and Doppler techniques, should be performed first, and will show a perigraft collection (Fig. 3.9), often extending towards superficial planes, which, in this context, must always be considered infected. Thin or coarse echoes, sediment, septa and a thickened hypervascularized peripheral

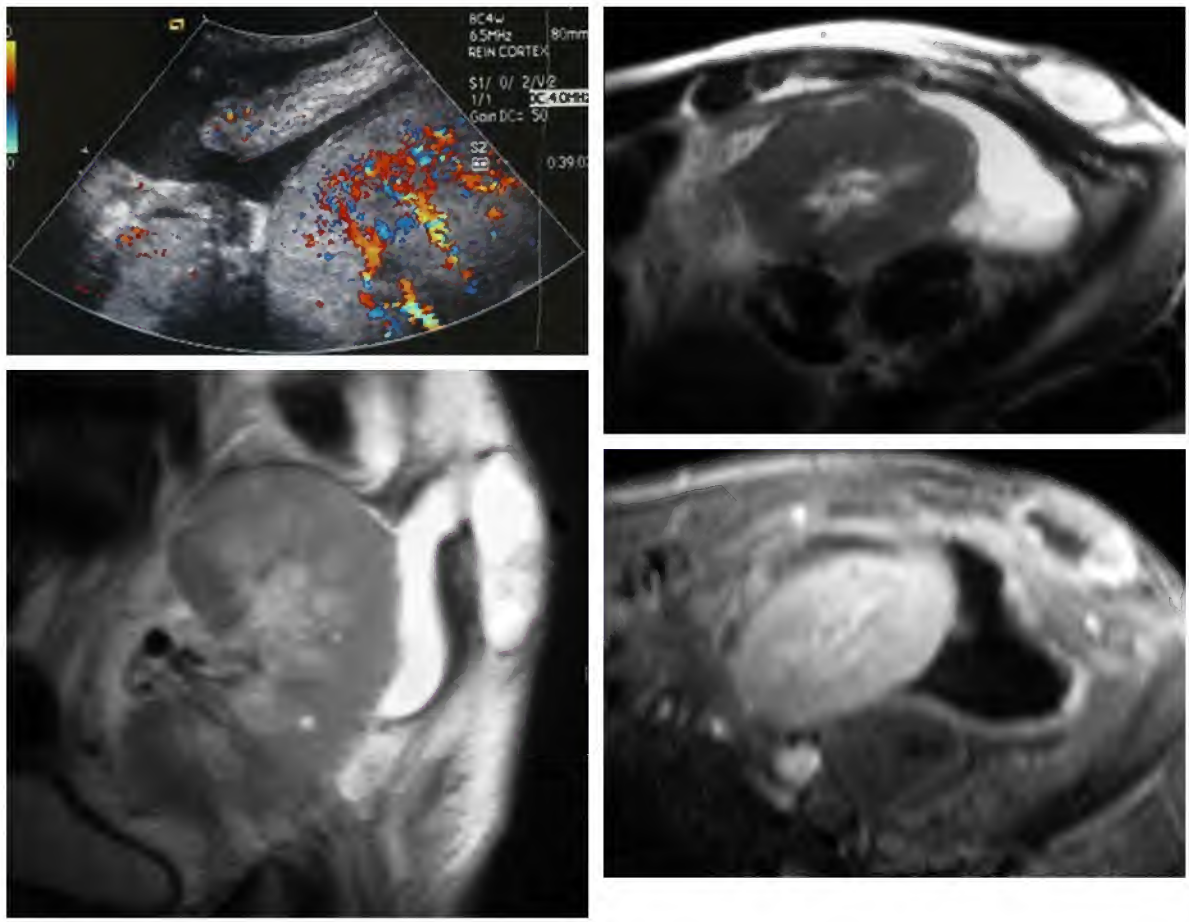

Fig. 3.9a–d. Perirenal abscess in a patient with graft tenderness and fever. **a** A fluid collection is seen around the graft on color flow sonography, extending through the disrupted abdominal wall to subcutaneous tissues. This fluid collection is confirmed by MR imaging on axial (**b**) and coronal (**c**) T2w sequences. **d** Peripheral wall of the collection and superficial soft tissue are enhancing after Gd injection

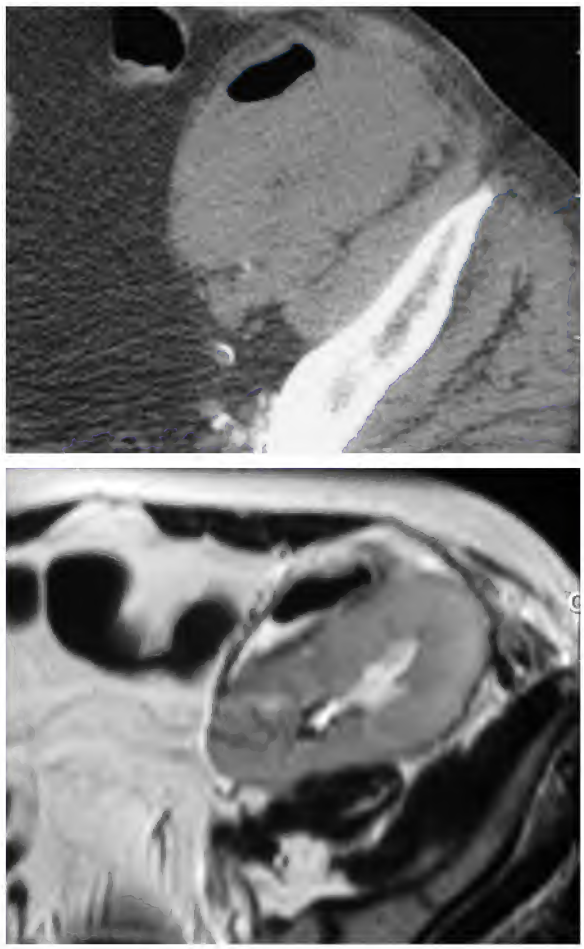

Fig. 3.10a,b. Perigraft infection with a perirenal fluid collection containing gas on **a** non-enhanced CT and **b** T2w MR imaging

wall are evocative of infection. When infection of a perigraft collection is suspected, contrast-enhanced MRI or CT will help to assess their exact extension before treatment. On MR images, the contents appear slightly hyperintense on T1w sequences and intermediate on T2w sequences; Gd-enhanced images reveal signal enhancement of the peripheral wall and peripheral soft tissues. Presence of gas within the fluid on CT scans is highly suggestive of infection (Fig. 3.10). Fluid aspiration from these collections, under US control, may be necessary for confirmation of the diagnosis, and optimal treatment combines percutaneous or surgical drainage and systemic antibiotic therapy.

Renal parenchyma infection may be seen as an increased graft volume and/or areas of decreased or increased echogenicity with decreased flow on color Doppler examination (Fig. 3.11). The power

Fig. 3.11a–c. Pyelonephritis of the transplant. **a** A hypoechoic triangular area is detected at the upper pole of the graft on sonography with **b** a hypoperfusion on the color Doppler mode. **c** Contrast-enhanced CT shows several foci of parenchymal infection (courtesy of Dr O. Hélénon, Paris)

mode may be more sensitive for detection of these hypoperfused zones (Nilsson et al. 1998). But these features are not specific and can reflect focal infarcts or acute rejection. Gd-enhanced MRI and enhanced CT are able to distinguish between infection and infarction in most cases, because enhancement is observed in the former and not in the latter, except for a thin peripheral capsular rim. But imaging is not able to differentiate between infection and rejection. Once a renal abscess has developed, enhanced CT or MR imaging shows a non-enhancing intrarenal collection.

Recurrent graft infections may also be secondary to persistent ureteral reflux into the graft, due to a technical failure of ureteral implantation. Retrograde cystography remains the technique of choice to demonstrate this reflux.

Urinary infections with *Corynebacterium urealyticum* are uncommon but can expose the transplant to complications, such as ureteral obstruction, renal abscess formation or progressive destruction of the graft (Dominguez-Gil et al. 1999). Risk factors for this infection include prolonged ureteral or bladder catheterization and urological manipulations. *Corynebacterium*-induced inflammation of the urothelium produces bacterial incrustation in struvite (magnesium-ammonium-phosphate) crystals. Color-Doppler US detects these urothelial calcifications that produce a twinkling artifact within the bladder and/or the upper urinary tract (Fig. 3.12).

3.5.1.1.4 Perigraft Fluid Collections

In addition to those associated with fistulas and perigraft abscesses discussed above, these fluid build-ups can be constituted of blood and/or lymph. Postsurgical lymphorrhea causing a lymphocele is avoided, above all by preventive measures. This complication is even more unusual when vessel dissection is limited during the transplantation and combined with careful lymphostasis. Should it occur early despite those precautions, drains should be kept in place for several days to avoid collection formation.

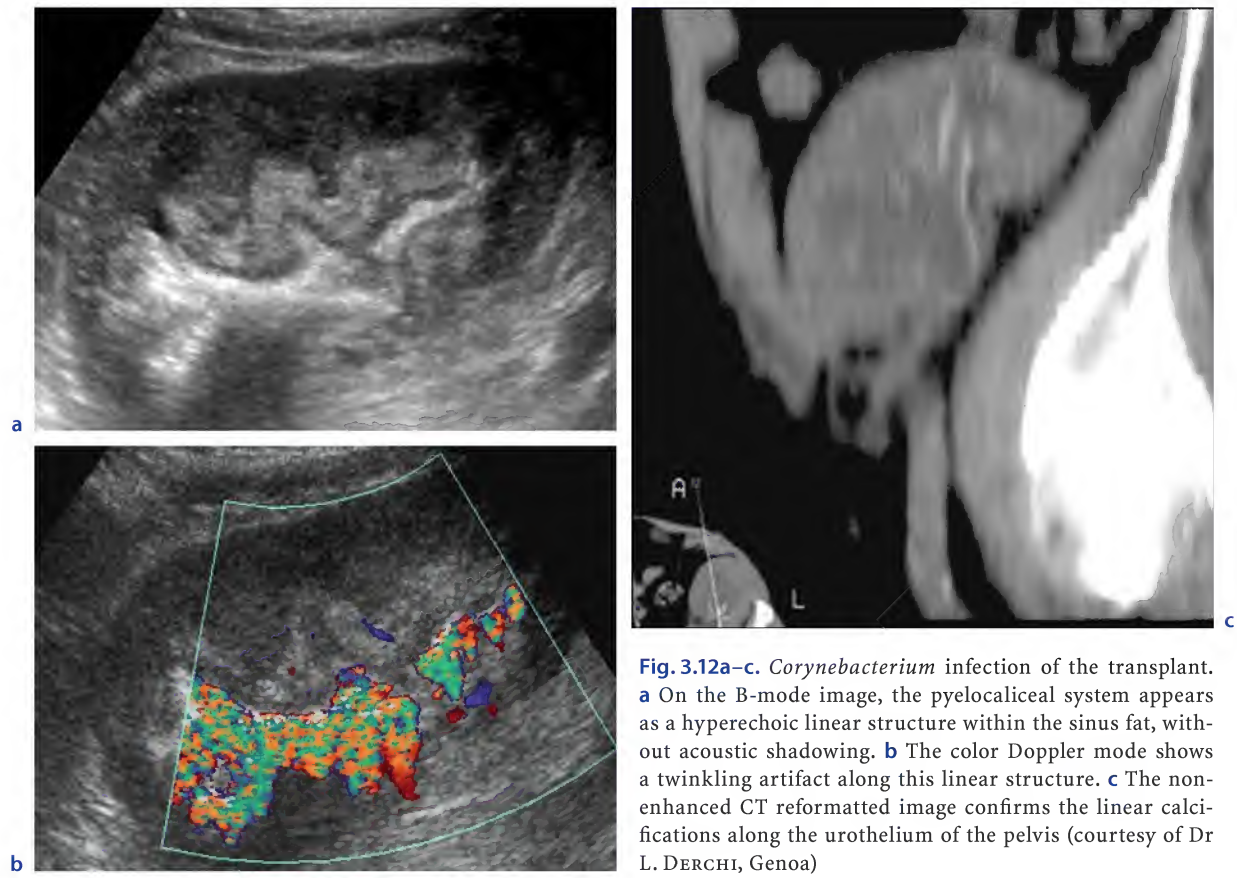

Fig. 3.12a–c. *Corynebacterium* infection of the transplant. **a** On the B-mode image, the pyelocaliceal system appears as a hyperechoic linear structure within the sinus fat, without acoustic shadowing. **b** The color Doppler mode shows a twinkling artifact along this linear structure. **c** The non-enhanced CT reformatted image confirms the linear calcifications along the urothelium of the pelvis (courtesy of Dr L. Derchi, Genoa)

Unfortunately, lymphoceles remain the most frequent cause of perigraft collections, occurring in 1%–20% of renal graft recipients, usually after the 4th week post-transplantation. These cystic lesions are often small in volume and have no effect on the kidney. Sometimes, their volume may increase causing ureteral or venous compression. The radiological appearance of a lymphocele is similar to that of seromas but the latter appear immediately after surgery and regress spontaneously.

On ultrasonograms, a lymphocele appears as a well-defined anechoic collection (Fig. 3.13a). A few septa may be observed. CT density values (Fig. 3.14) and SI on MR sequences (Fig. 3.13) are typical of simple fluids, without any enhancement after contrast injection. Fluid aspiration is usually unnecessary and is done only when a urinoma is suspected; it allows determination of the creatinine level, which is the same as that in blood, and the aspirate contains a few lymphocytes.

When a lymphocele is responsible for ureteral or venous compression, radical therapy is essential. Simple aspiration and drainage are ineffective because they do not prevent lymph leakage. Therefore, percutaneous drainage (Fig. 3.14c) must be combined with sclerosis of the cavity by repeated instillations of doxycycline, tetracycline, acetic acid, alcohol or povidine–iodine. Although single session sclerotherapy and 1-day catheter drainage are usually sufficient for lymphoceles < 150 ml, multiple sessions until daily drainage falls below 10 ml are necessary for larger ones (Karcaaltincaba et al. 2005). Despite the high success rate (around 97%) provided by this approach, recurrence may occur in 20% of the patients. Montalvo et al. (1996) instilled povidine–iodine twice daily in 18 lymphoceles in renal grafts, and observed no complications and two recurrences treated percutaneously; no surgery was needed. However, in renal transplants, the proximity of vascular and excretory structures to the cavity raises the risk of complications, such as vascular thrombosis of the renal pedicle (Adani et al. 2005). This is the reason why, in many institutions, intraperitoneal marsupialization under laparoscopy remains the preferred therapeutic approach in this context.

Hematomas account for approximately 9% of peritransplant collections and usually occur during the immediate postoperative period, due to surgery. The other main causes are:

- Early renal biopsy complicated by a cortical pseudoaneurysm, which may increase in size and subsequently rupture in the perirenal space; this complication occurs immediately (24–48 hours) or several weeks after biopsy.
- Graft rupture secondary to severe acute rejection, which occurs in 3%–6% of renal transplants and during the first 2 weeks after transplantation. This diagnosis must be suspected when anuria is associated with abdominal pain at the graft level, graft swelling and hypotension or shock.
- More exceptional causes, including breakdown of the arterial anastomosis or rupture of an arterial aneurysm (mycotic or not).

During the early postoperative period, hematomas are echogenic collections without flow on US images and are hyperattenuated on unenhanced CT images (Fig. 3.15). These patterns tend to change with time, with the collection becoming less echogenic, and its density decreases, resembling a lymphocele. In this setting, MRI is more specific, showing high intensity on both T1w and T2w sequences (Neimatallah et al. 1999). Extravasation of the contrast agent can be visualized with US, after injection of microbubbles or with MRI, after Gd injection. Pretherapeutic MRA is useful to search for the cause of the hematoma and, more specifically, arterial complications, such as aneurysms or pseudoaneurysms.

According to their etiology, hemorrhagic complications must be managed either surgically, when they result from rupture of the graft or the arterial anastomosis, or radiologically, by embolization, when they are the consequence of a pseudoaneurysm rupture or an arteriovenous fistula. If the hematoma is sufficiently large to cause ureteral obstruction, surgical evacuation is mandatory.

3.5.1.2 Vascular Complications

3.5.1.2.1 Renal Artery Thrombosis

Arterial thrombosis is very unusual, occurring in < 1% of renal graft recipients, but is extremely severe, leading in most cases to graft loss. It occurs early after transplantation, caused by a hypercoagulable state, hypotension, hyperacute rejection, immunosuppressive therapy or a surgical complication: anastomotic occlusion, arterial dissection, renal artery kinking when it is too long or torsion of the renal artery when implanted intraperitoneally.

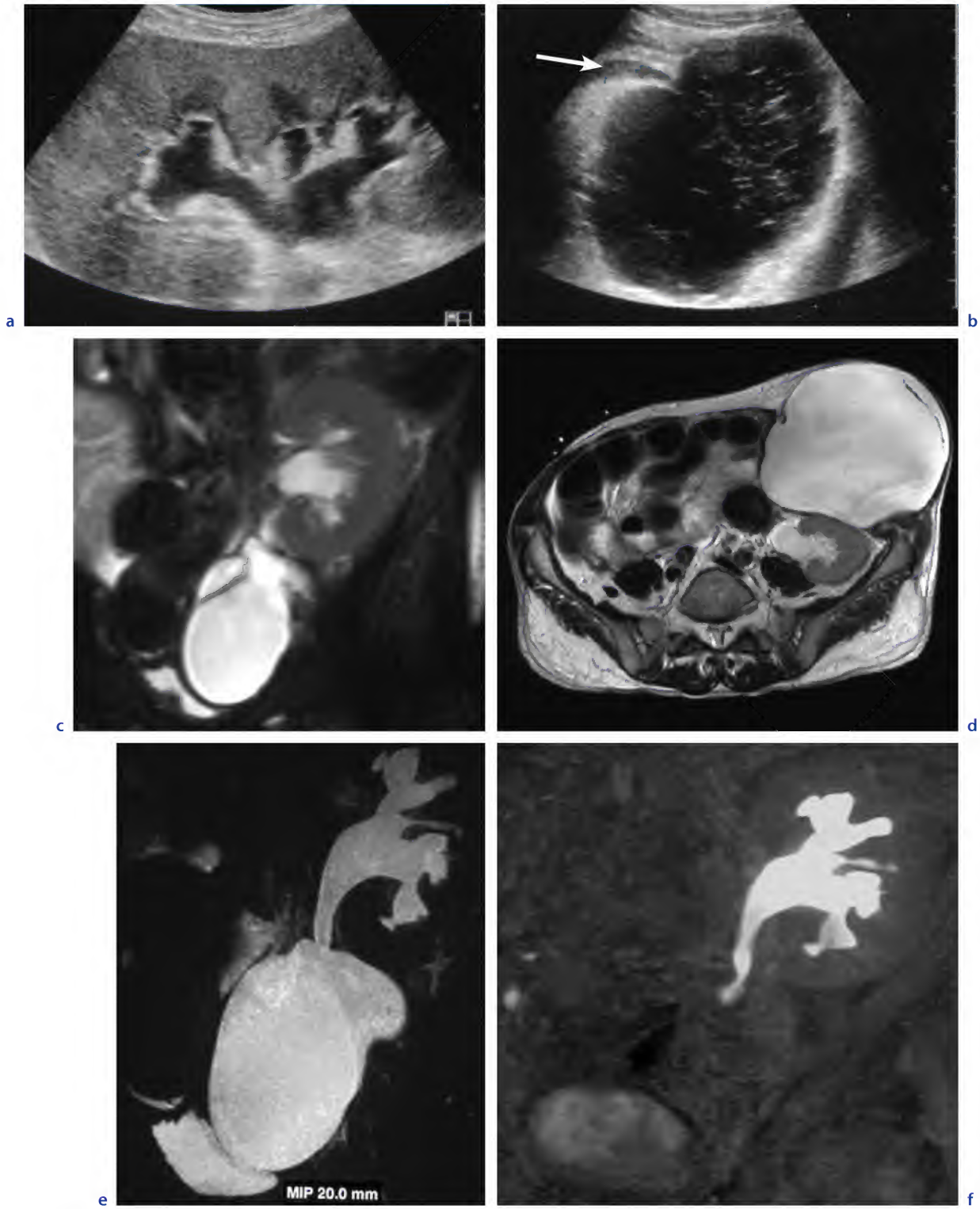

Fig. 3.13a–f. Perigraft lymphocele responsible for urinary obstruction. On sonography, the pyelocaliceal system (**a**) and the ureter (**b**) (*arrow*) are dilated due to a pelvic fluid collection showing thin septas. On T2w coronal (**c**) and axial (**d**) MR images, the collection seats below and in front of the lower pole of the kidney, compressing the ureter. The lymphocele and the obstructed excretory cavities are superimposed on the T2w MR urographic image (**e**) whereas only the latter appear on the Gd-enhanced T1w MR urographic image (**f**) demonstrating the location of compression

Fig. 3.14a–f. Perigraft lymphocele. **a, b** The perirenal fluid collection appears with a homogeneous water density on contrast-enhanced CT, without any visible peripheral wall. **c** A direct opacification of the collection was necessary before drainage and sclerosis

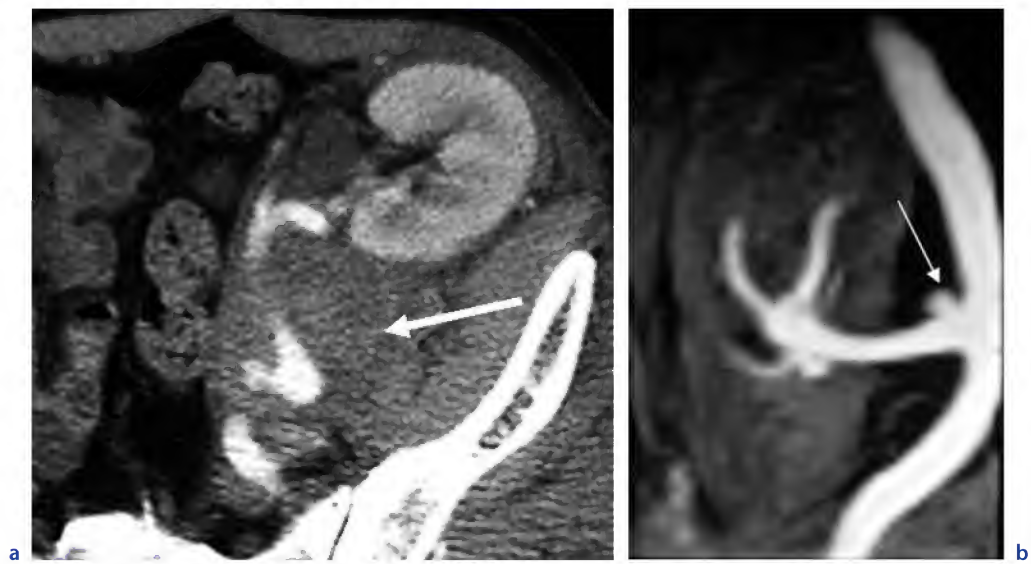

Fig. 3.15a, b. Perigraft hematoma secondary to the rupture of a mycotic aneurysm. **a** Contrast-enhanced CT shows a dense collection (*thick arrow*) at the lower pole of the transplant surrounding the renal artery. **b** Gd-enhanced MR angiography shows the aneurysm close to the arterial anastomosis (*thin arrow*)

Its diagnosis is suspected soon after transplantation, when severe renal impairment is associated with anuria. Confirmation is easily obtained with color flow Doppler US (Fig. 3.16) showing arterial flow in the iliac artery and sometimes in an arterial stump, absence of flow within the entire graft, which is swollen and hypoechoic, and a persistent 'to-and-fro' flow pattern within renal veins (Grenier et al. 1991, 1997). If confirmation is necessary, Gd-enhanced MRI examination can demonstrate the complete devascularization of the graft (Hélénon et al. 1992).

Only rapid reintervention, within 12 h for surgical thrombectomy, can save the graft and does so in half of the cases. Percutaneous endovascular revascularization has been described for allograft salvage, but only for late thrombosis (Juvenois et al. 1999).

3.5.1.2.2 Infarctions

Segmental infarcts can also be due to segmental or reimplanted accessory renal artery thrombosis or be associated with acute rejection. They are usually

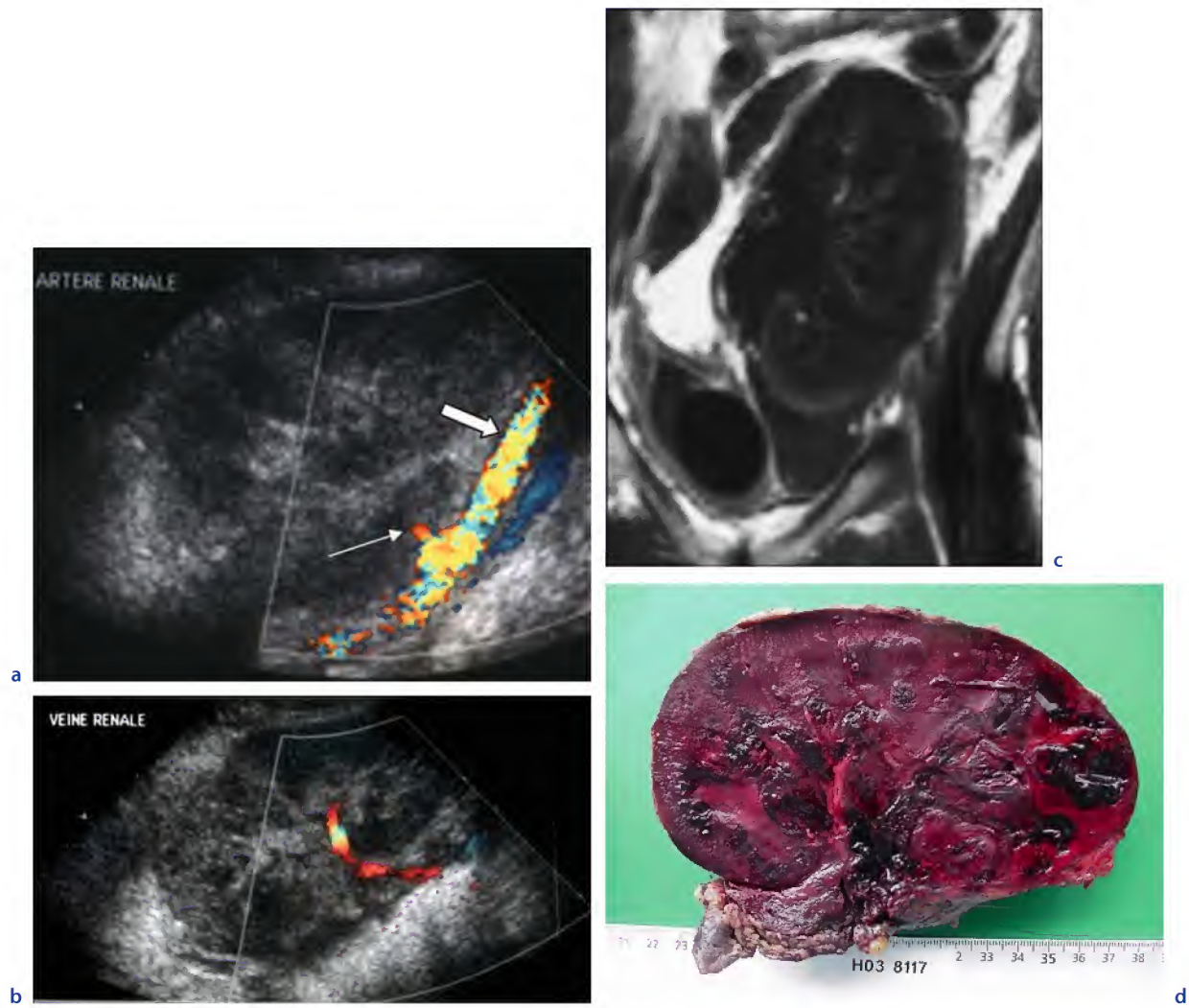

Fig. 3.16a–d. Renal artery thrombosis. **a** The iliac artery appears patent (*thick arrow*) on the sagittal section with color flow sonography, whereas no flow is detected within the graft. The stump of the occluded renal artery is visible (*thin arrow*). **b** More medially, the renal vein is also patent with a to-and-fro flow (with successive blue and red encoding). **c** The contrast-enhanced MR image shows an absence of enhancement within the entire graft. **d** Complete necrosis of the graft was confirmed by the macroscopic examination

asymptomatic and renal function impairment depends on their size. As mentioned above, color flow Doppler US is not specific to infarction, showing wedge-shaped areas of decreased or increased echogenicity without flow (Dodd et al. 1991; Grenier et al. 1997) (Fig. 3.17). These features can also be seen in hypoperfused segments secondary to graft infection. Injection of ultrasound contrast agents may help differentiate between these two entities, with infarctions showing no passage of microbubbles within the non-perfused areas (Lefevre et al. 2002). Similarly, contrast-enhanced MR images and CT scans demonstrate the absence of enhancement within the infarcted segments, except for the subcapsular cortex corticis (Neimatallah et al. 1999; Sebastia et al. 2001).

3.5.1.2.3 Renal Artery Stenosis

The frequency of renal artery stenosis (RAS) in transplanted kidneys varies from 1% to 23% (Bruno et al. 2004). These values depend on the method used for the diagnosis. When color flow US is used systematically, every month during the first year, the rate can be as high as 12.4% (Wong et al. 1996). RAS may represent around 75% of all post-transplant vascular complications (Bruno et al. 2004). It develops during the 3 years following surgery, most often during the first year. End-to-end anastomoses (on the internal iliac artery) are now used very rarely because anastomotic stenoses are more common (threefold higher risk) (Jordan et al. 1982).

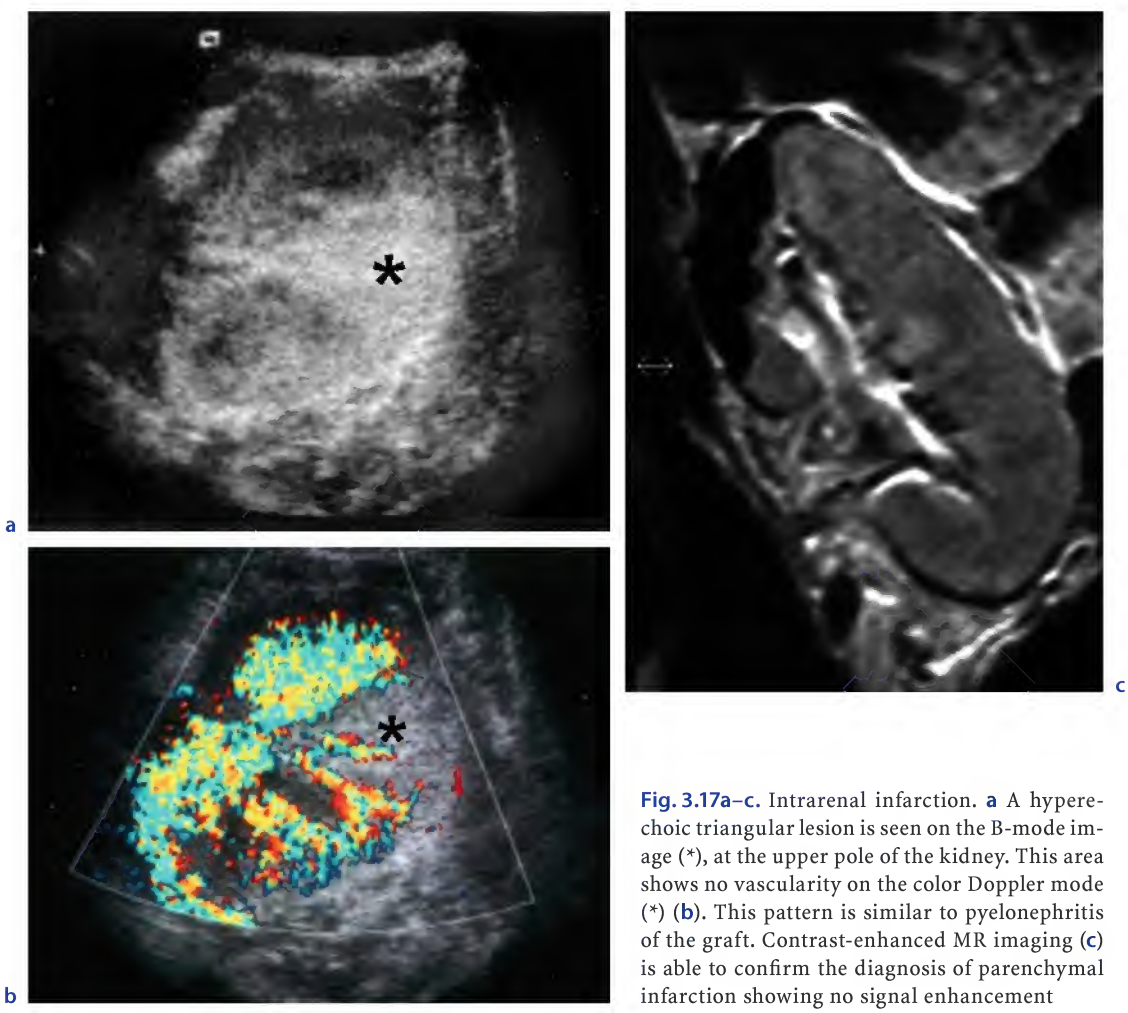

Fig. 3.17a–c. Intrarenal infarction. **a** A hyperechoic triangular lesion is seen on the B-mode image (*), at the upper pole of the kidney. This area shows no vascularity on the color Doppler mode (*) (**b**). This pattern is similar to pyelonephritis of the graft. Contrast-enhanced MR imaging (**c**) is able to confirm the diagnosis of parenchymal infarction showing no signal enhancement

With end-to-side anastomosis made using an arterial patch (cadaveric donor) or without a patch (living donor), stenoses are usually located far from the anastomosis, occurring predominantly in the proximal portion of the arterial trunk. Stenoses may also arise in the recipient's iliac artery.

Their origin is multifactorial: an atherosclerotic plaque in the donor's renal artery or in the recipient's iliac artery; dissection, kinking or twisting of the renal artery (due to excessive vessel length); malpositioning of the graft; flow turbulences generating intimal hyperplasia; graft perfusion catheter during cannulation causing intimal damage; wall ischemia due to excessive dissection with destruction of vasa vasorum. It is also possible that prolonged cold ischemia may play a role in the development of RAS through ischemia-reperfusion injury (Halimi et al. 1999; Patel et al. 2001). The role of an immunological mechanism remains controversial: Wong et al. (1996) found a higher RAS frequency in patients developing rejection; but, when compared to a control group, no difference was found between living-related and cadaver kidney transplantation (Merkus et al. 1993). However, several cases of spontaneous RAS regression tend to support such a mechanism (Chan et al. 1985).

Severe hypertension with or without allograft dysfunction is the most frequent clinical symptom. Hypertension is a common feature in transplant recipients (up to 80%). Therefore, as for native kidneys, RAS is specifically suspected when hypertension develops suddenly, rapidly becomes more severe and resistant to medical therapy, and is associated with graft dysfunction without any other cause or when associated with an audible bruit over the graft (Palleschi et al. 1980; Rijksen et al. 1982). It may account for around 1%–5% of post-transplant hypertension. However, at present, early RAS are often detected systematically with color flow US, despite no blood pressure or renal function change.

US now enables close early and late monitoring of all renal grafts after transplantation, making it

a

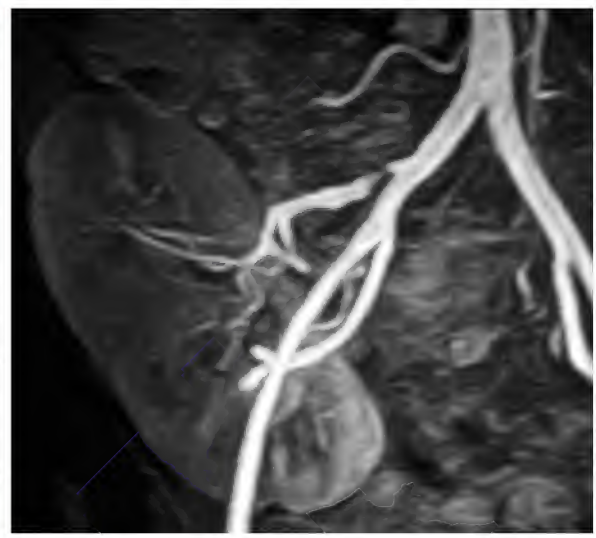

c

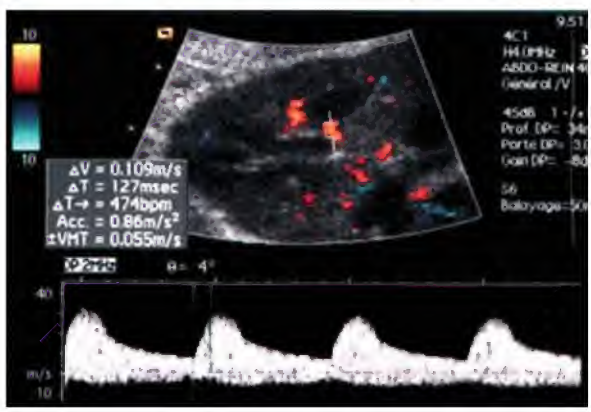

b

Fig. 3.18a–c. Renal artery stenosis. **a** On color flow sonography, an aliasing phenomenon is present at the proximal portion of the renal artery (*arrow*). **b** The spectral waveform shows an increased peak systolic velocity (2.8 m/s) with spectral broadening. On the intrarenal interlobar arteries, the ascension time is increased at 127 ms. **c** Gd-enhanced MR angiography confirms the post-ostial renal artery stenosis

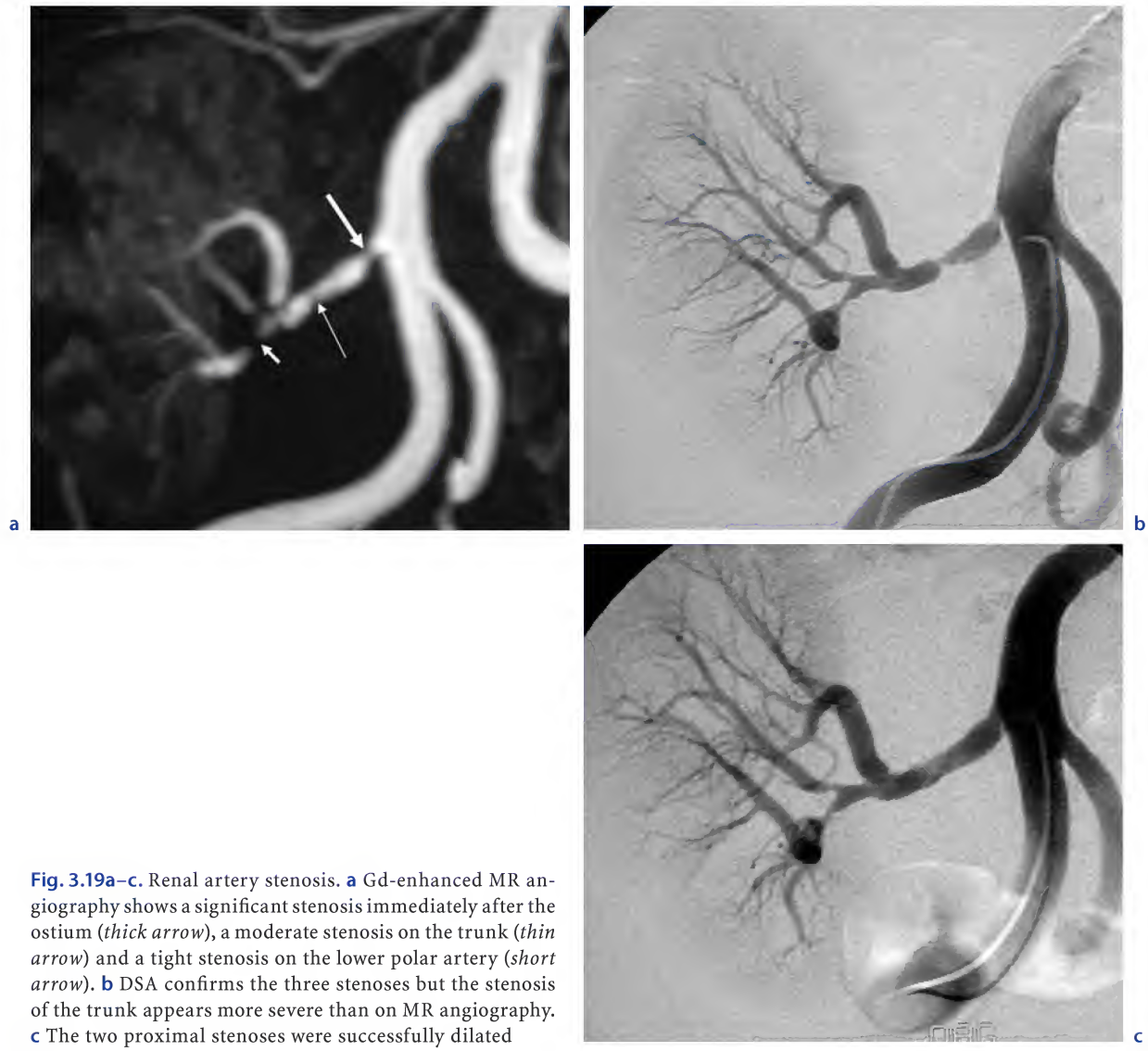

Fig. 3.19a–c. Renal artery stenosis. **a** Gd-enhanced MR angiography shows a significant stenosis immediately after the ostium (*thick arrow*), a moderate stenosis on the trunk (*thin arrow*) and a tight stenosis on the lower polar artery (*short arrow*). **b** DSA confirms the three stenoses but the stenosis of the trunk appears more severe than on MR angiography. **c** The two proximal stenoses were successfully dilated

possible to detect the development of iliac or the renal artery stenoses (Figs. 3.18, 3.19). Both velocity-profile changes, responsible for spectral broadening and perivascular color artifact, and systolic acceleration must be observed to make this diagnosis. A systolic velocity threshold of 190–200 cm/s (Grenier et al. 1991; Loubeyre et al. 1997) or a systolic velocity ratio between renal and external iliac arteries of 1.5 (Loubeyre et al. 1997) has been proposed for significant stenoses. Using these criteria, Doppler techniques appear to be highly sensitive but less specific (Erley et al. 1992). When the renal artery is too long, kinking is easily demonstrated on the color display but only spectral sampling is able to confirm the presence of a stenosis. Because stenoses are sometimes located on reimplanted accessory renal arteries, full knowledge of a precise surgical report is mandatory before examination so that these accessory vessels will not be left unexplored.

Finally, diagnosis of iliac artery stenosis requires systematic Doppler waveform analysis of the common iliac artery above the renal anastomosis. As described for native kidneys, intrarenal sampling of interlobar arteries and looking for dampened waveforms may help detect severe proximal stenosis (Gottlieb et al. 1995). Those authors showed that the acceleration time was significantly prolonged in patients with a severe proximal arterial stenosis (p=0.0004) (Fig. 3.18b). Using a threshold accelera-

tion time of 0.10 s or subjective assessment of dampening of the waveforms resulted in an accuracy of 95%. However, these intrarenal features are less useful in transplanted kidneys because the proximal changes are more easily accessible than in native kidneys.

Specificity is lower than sensitivity, meaning that a second examination has to be performed when arterial stenosis is suspected. MRA is the most suitable for that purpose because it is not invasive. Flow-sensitive MRA techniques, using time-of-flight or phase-contrast sequences, were the first to be proposed (Cahen et al. 1996; Gedroyc et al. 1995). But now, only 3D Gd-enhanced acquisitions are recommended (Fang and Siegelman 2001; Ferreiros et al. 1999) (Figs. 3.18c, 3.19a). Using body phased-array coils and a parallel imaging technique, these sequences provide high-quality angiograms with excellent reproducibility. The sensitivity and specificity of MRA in detecting signifi-

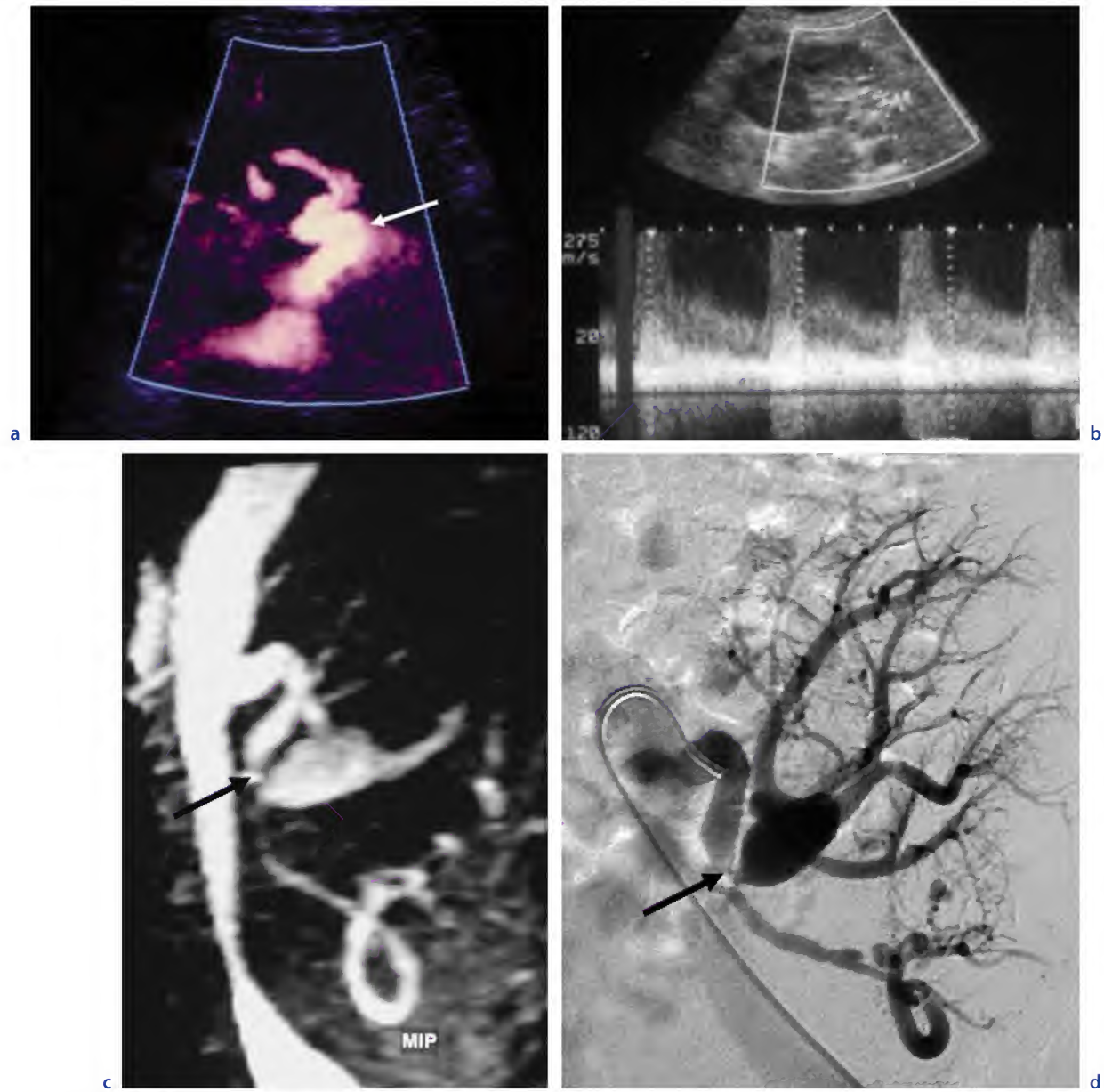

Fig. 3.20a–d. Kinking of the renal artery. **a** On power Doppler sonography the renal artery appears with a narrowing at the site of plicature (*arrow*). **b** Spectral waveform shows a severe spectral broadening with a high peak systolic velocity (2.75 m/s). **c** MR angiography and **d** DSA confirm the kinking phenomenon with a severe stenosis (*arrows*) and post-stenotic dilatation

cant stenoses were 100% and 98%, respectively, and interobserver kappa concordance values exceeded 0.85 (Ferreiros et al. 1999). Overestimation of the degree of stenosis has often been reported for native renal arteries, but this point has never been addressed in renal grafts to the best of our knowledge. Based on a questionnaire, Omary et al. (2000) showed that MRA results had considerable impact on the referring physician's management of patients with renal dysfunction, by avoiding invasive procedures in 39% of patients. Stenoses due to kinking of the renal artery (Fig. 3.20) and stenoses of the iliac arteries and (Fig. 3.21) are also well demonstrated by MRA.

Helical CT (Hofmann et al. 1999) using 16- to 64-multidetector rows offers high resolution for RAS diagnosis. However, its role in transplanted kidneys has been poorly demonstrated, probably because of the nephrotoxicity of iodine contrast agents. However, in patients with normal renal function, it seems an acceptable alternative to MRA.

Captopril-sensitized renography has been a popular non-invasive screening procedure for RAS diagnosis. However, despite its relatively good sensitivity (75%), the procedure is severely limited by its poor specificity (67%) (Erley et al. 1992). It seems that this technique might have a better role in predicting outcome after revascularization (Shamlou et al. 1994).

Digital subtraction angiography (DSA) provides a definitive diagnosis of RAS and serves as the first step for percutaneous revascularization. It should only be performed when angioplasty has been decided. The lowest amount of iodine contrast agent must be used. When renal function is impaired, intra-arterial injection of CO_2 or Gd-chelate can be proposed (Spinosa et al. 1998, 2002). Rotational angiography may also be used to find the optimal incidence for RAS analysis and catheterization (Hagen et al. 2005).

Percutaneous transluminal angioplasty, with or without stent placement, is the preferred primary treatment of RAS, when medical therapy can no longer control blood pressure and/or renal function progressively deteriorates (Fig. 3.19). Artery stenting is an effective method for recurrent stenosis (Sierre et al. 1998). The technical success rate of angioplasty varies from 94% to 100% and the clinical success rate from 82% to 94% (Beecroft et al. 2004; Patel et al. 2001). At 3, 6 and 12 months following engraftment Beecroft et al. (2004) calculated primary patency rates (±95% CI) of 94±6%, 72±12% and 72±12%, respectively. Secondary patency rates (±95% CI) at the same times were: 100%, 85±10% and 85±10%, respectively. Only two complications were observed (groin hematoma and pseudoaneurysm). The reported midterm patency (mean of 30 months) reached 100% (Beecroft et al. 2004; Sierre et al. 1998).

a

b

Fig. 3.21a, b. Stenosis of the iliac artery. **a** On power Doppler sonography the iliac artery appears with a stenosis (*arrow*) above the anastomosis with renal artery (*double arrow*). **b** MR angiography confirms the site of stenosis

3.5.1.2.4 Renal Vein Thrombosis

Acute venous thrombosis occurs in approximately 1%–4% of renal transplant recipients and usually during the early postoperative period. Clinical findings depend on whether the onset is progressive or abrupt and whether thrombosis is complete or incomplete. When it is complete and abrupt, graft pain and swelling are observed, associated with oliguria and proteinuria. Acute venous thrombosis is often due to faulty surgical technique, hypovolemia, hypercoagulation state or renal vein compression by a perigraft fluid collection as predisposing factors. It may also be a complication of postoperative lower limb or iliac vein thrombosis extending into the renal vein.

Diagnosis of renal vein thrombosis is difficult. On Doppler images, no venous flow is present and arterial flow appears decreased and highly resistive, showing protodiastolic or holodiastolic reflux (Fig. 3.22). On B-mode, the kidney is often enlarged and sometimes heterogeneous. Direct visualization of the thrombus within the renal vein and its extension into the iliac vein is possible (Fig. 3.23). When seen later, transcapsular collaterals may have developed that drain venous flow towards the iliac veins (Fig. 3.24). In difficult cases, using either unenhanced "white blood" axial gradient-echo or Gd-enhanced T1w MRI sequences may help visualize the venous thrombus.

In the case of partial venous thrombosis, anticoagulants administration is usually sufficient. However, when confronted with early complete thrombosis, rapid surgical revascularization is required but, if too severe, transplantectomy may be necessary. Percutaneous thrombectomy, associated with anticoagulation, has also been proposed (Melamed et al. 2005).

3.5.1.2.5 Vascular Complications of Biopsy

Intrarenal arteriovenous fistulas and pseudoaneurysms occur in approximately 1%–18% of the grafts after percutaneous transplant biopsies. Most of them are asymptomatic and resolve spontaneously. But they may be responsible for severe perirenal hemorrhage (usually due to rupture of a peripheral pseudoaneurysm) or hematuria. Their detection is now based on color flow US and their treatment, when symptomatic, on transcatheter embolization.

Pseudoaneurysms present as localized vessel dilatations, anechoic on B-mode US, with a rotative flow inside on color-encoded images (Dodd et al. 1991) and, when isolated, with a to-and-fro flow pattern of the spectral waveform in the neck (Fig. 3.25). However, they are rarely isolated and most of them are associated with an arteriovenous shunt. These shunts are responsible for enlargement of the supply artery and draining vein associated with high-grade turbulence (Fig. 3.26a). This turbulent flow creates perivascular vibration, which appears on color flow US as an area of random color encoding of perivascular tissues, enhanced in systole, the so-called the perivascular artifact (Grenier et al. 1991; Middleton et al. 1989). On arterial spectral waveforms of feeding arteries, the flow profile is severely altered, with increased velocities and decreased RI (Hubsch et al. 1990) (Fig. 3.26b, c). When the shunt-

a

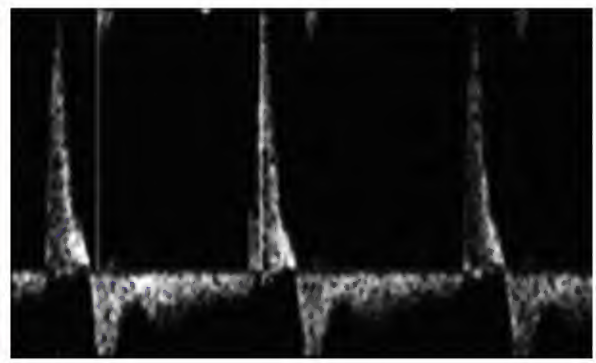

b

Fig. 3.22a,b. Renal vein thrombosis. **a** On the diastolic color flow image, all the arteries show a blue color compatible with a reversed flow. **b** The spectral waveform shows a holodiastolic reflux evocative of renal vein thrombosis

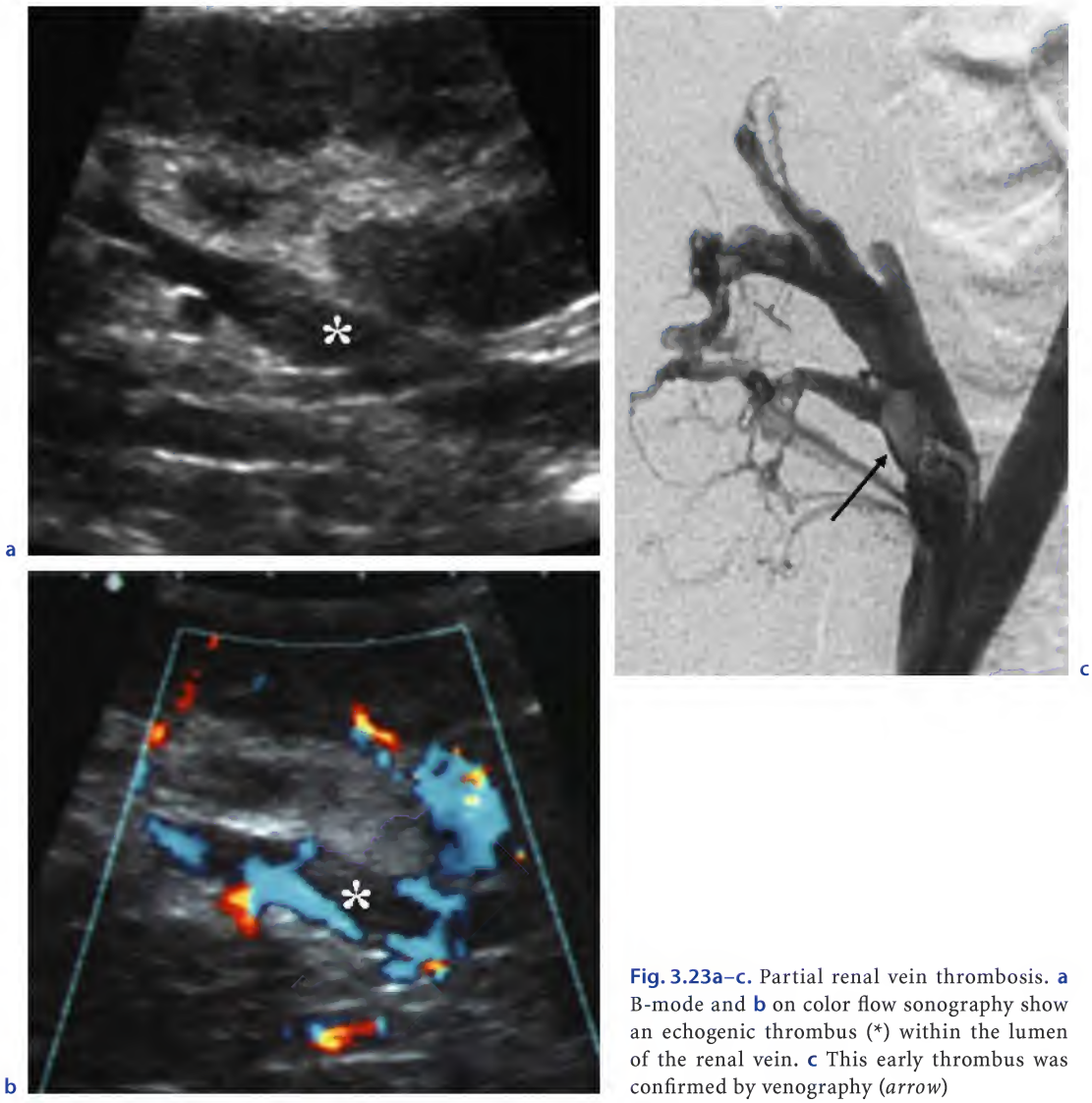

Fig. 3.23a–c. Partial renal vein thrombosis. **a** B-mode and **b** on color flow sonography show an echogenic thrombus (*) within the lumen of the renal vein. **c** This early thrombus was confirmed by venography (*arrow*)

ing effect is important, a "steal" phenomenon may be observed within the graft with decreased, or even reversed, diastolic flow, within adjacent non-feeding segmental arteries. Venous flow resembles arterial flow with systolic enhancement (Fig. 3.27).

When a clinical complication occurs, arteriovenous fistulas and pseudoaneurysms can be effectively treated by transcatheter embolization, using superselective catheterization, which is a very efficient technique, providing a 95% technical success rate (Perini et al. 1998). To avoid occlusion of normal renal branches and to preserve renal function, microcoils are positioned as far as possible into the feeding artery(ies) of the fistula or into the neck of the pseudoaneurysm using coaxial catheters.

3.5.1.2.6 Parenchymal Necrosis

Allograft necrosis is a rare and extremely severe complication. It results from defective distal perfusion occurring immediately after graft implantation (primary non-function) or as a consequence of severe acute tubular necrosis (ATN) or acute rejection. It is most often limited to the cortex (cortical necrosis) or extends into the medulla (total necrosis).

In cortical necrosis, the graft may appear normal on gray-scale ultrasonograms, when imaged early, or show a hypoechoic cortex. This hypoechogenicity may be limited to the outer cortex, run along the capsule or cover the entire outer and inner cortex thick-

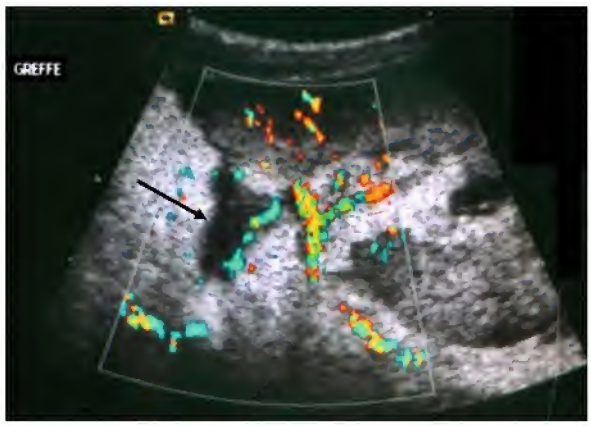

a

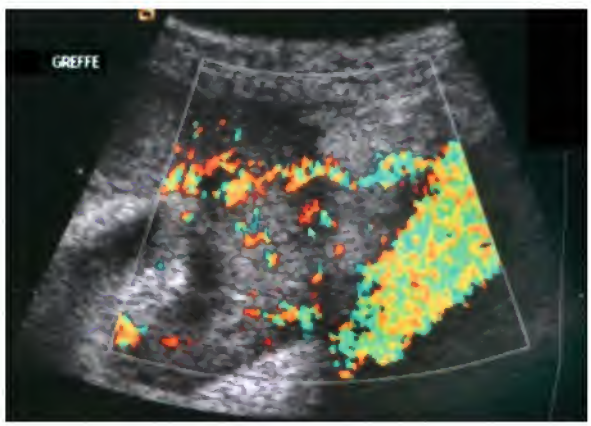

b

c

Fig. 3.24a–c. Renal vein thrombosis. **a** Color flow sonography shows thrombosed segmental veins within the renal sinus (*arrow*) and **b** transcapsular venous drainage, towards the external iliac vein, at the lower pole of the kidney. **c** The venous phase of renal DSA shows the absence of venous drainage through the normal renal vein and a heterogeneous renal parenchyma

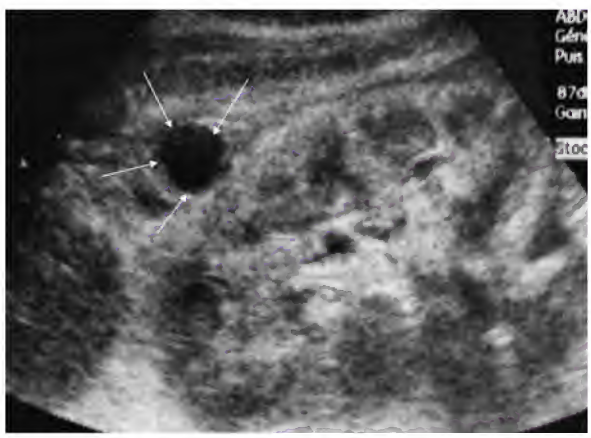

a

Fig. 3.25a,b. Post-biopsy pseudoaneurysm. **a** On gray scale sonography, an anechoic area appears at the anterior aspect of the graft (*arrows*). **b** The color flow sonography shows that this lesion is circulating with a typical "to-and-fro" spectral pattern

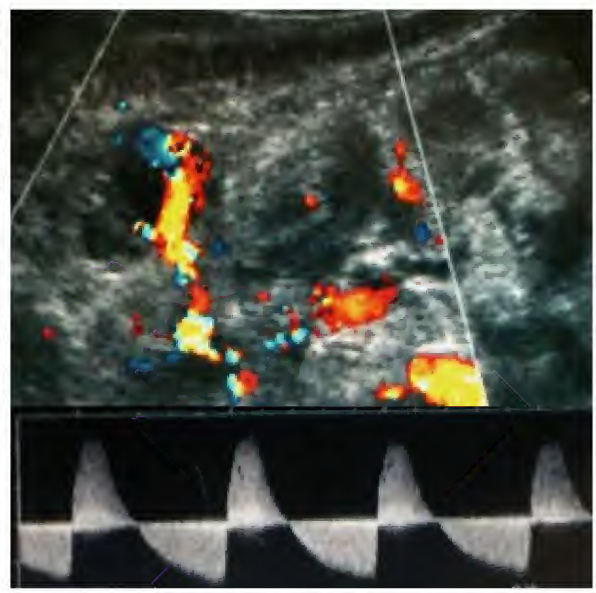

b

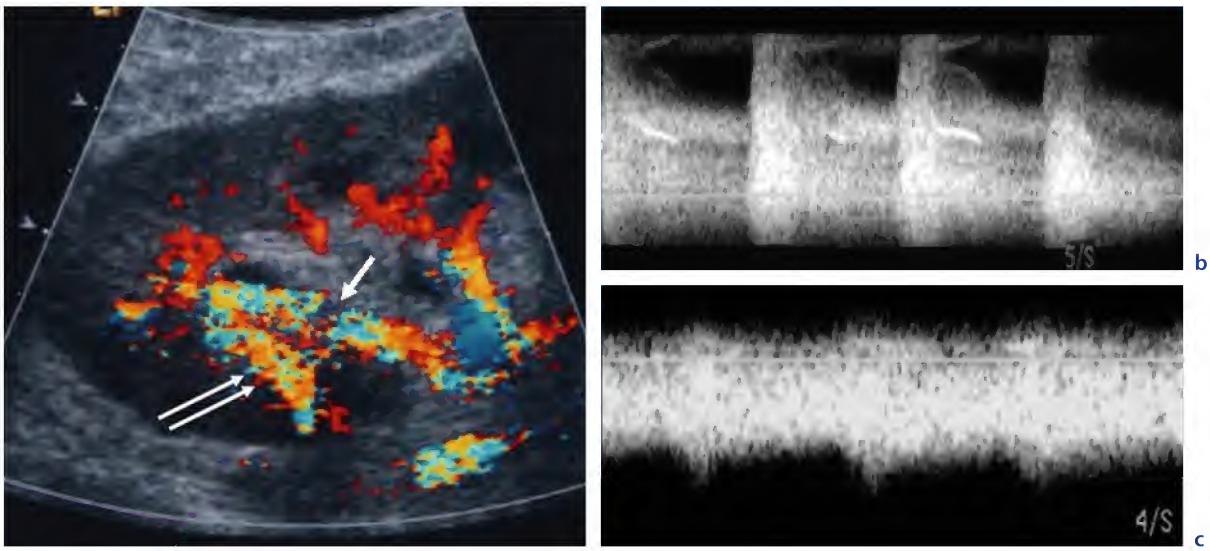

a b c

Fig. 3.26a–c. Post-biopsy arteriovenous fistula. **a** At the upper pole of the kidney graft, two vessels appear enlarged with high velocities on color flow sonography. Spectral sampling allows separation of the afferent artery (*arrow*) and the efferent vein (*double arrow*). **b** Arterial waveform shows increased velocities, spectral broadening and low resistance. **c** Venous waveform shows increased flow and arterial modulation

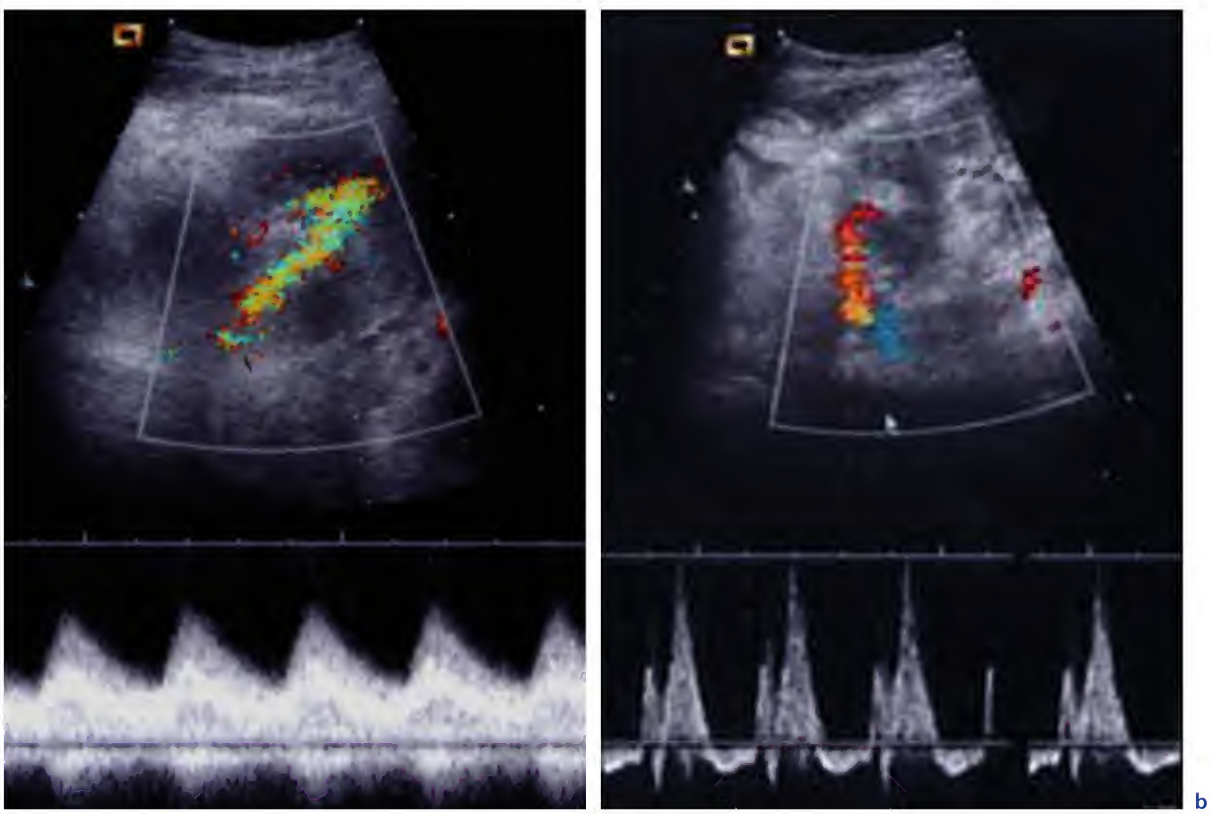

a b

Fig. 3.27a,b. Post-biopsy arteriovenous fistula with steal phenomenon. **a** Color flow sonography on the lower pole of the graft shows an arteriovenous fistula with increased velocities and spectral broadening on spectral waveform. **b** Arterial flow at the upper pole is characterized by a holodiastolic reflux due to a steal phenomenon, which disappeared after embolization of the shunt

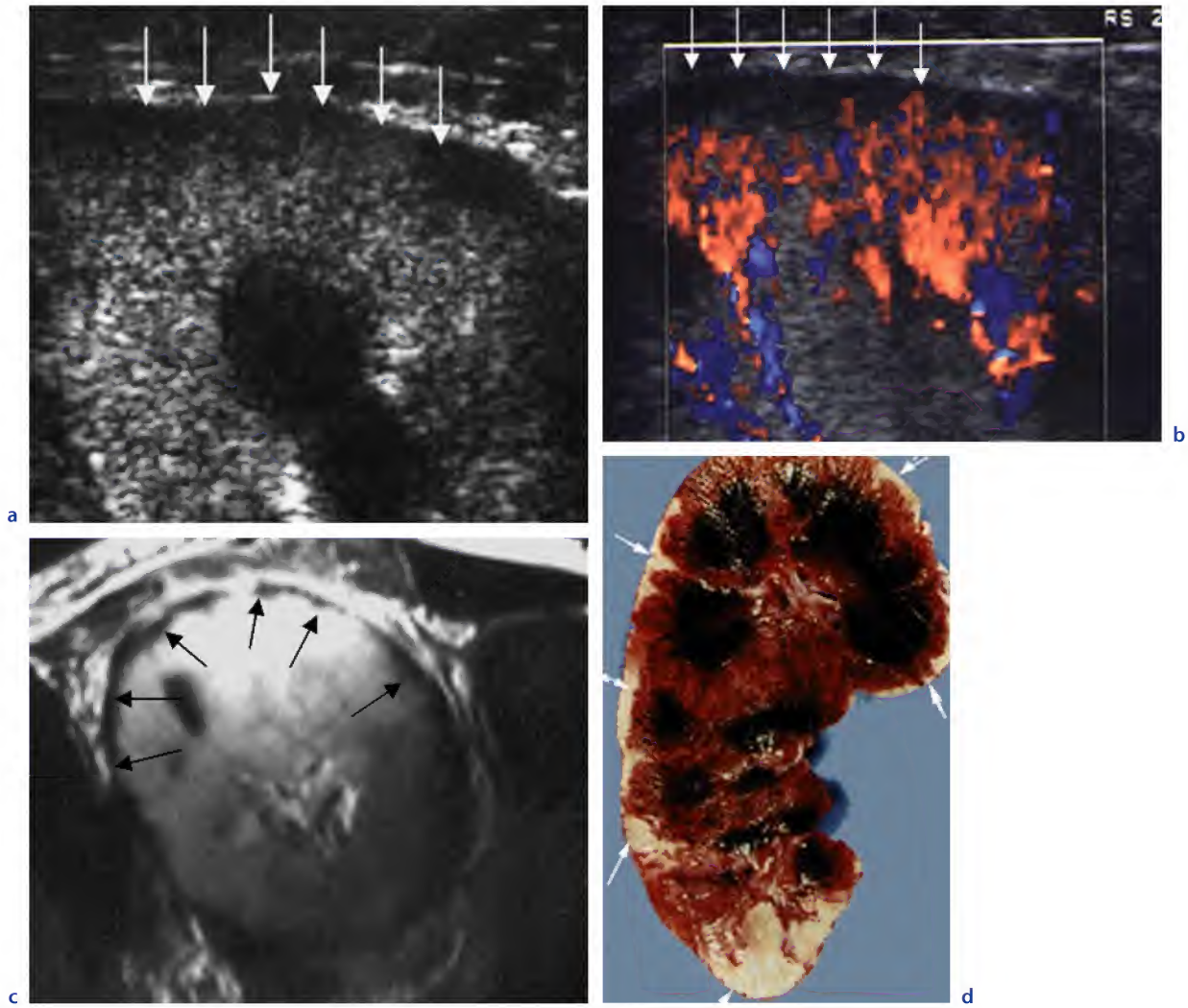

Fig. 3.28a–d. Partial cortical necrosis. The outer cortex (*arrows*) of this graft appears hypoechoic on gray scale image (**a**) and devascularized on color flow sonography (**b**), using a high-frequency probe. **c** The Gd-enhanced MR sequence confirms the absence of enhancement within the outer cortex. **d** Macroscopic specimen from a similar outer cortical necrosis from an other patient [Fig. 3.29d reprinted with permission from HÉLÉNON et al (1992) *RadioGraphics* 12:21–33]

ness (Fig. 3.28a). Using a high-frequency probe with color Doppler flow, the anterior cortex appears to be partially or entirely devascularized (Fig. 3.28b). In the case of partial cortical necrosis, limited to the outer cortex, interlobular vessels do not reach the capsule. In the case of complete cortical necrosis, interlobular vessels are no longer seen. When necrosis extends into the medulla, no flow is seen in the entire parenchyma, while the main arteries and veins remain patent in the pedicle and sinus.

However, prudence is necessary when making the diagnosis of perfusion defects based on power Doppler US, because the absence of detectable flow at the interlobular level does not always correspond to cortical areas that lack perfusion on MR images (MARTINOLI et al. 1996), as mentioned earlier. This lack of correspondence explains why MRI confirmation is always required.

Gd-enhanced MRI clearly shows the type (hemorrhagic or not) and in-depth extension of the parenchymal devascularization (HÉLÉNON et al. 1992) (Figs. 3.28c, 3.29). In hemorrhagic cortical necrosis, the cortex may appear hyperintense on T1w images and hypointense on T2w sequences. When non-hemorrhagic, the cortex is hyperintense on T2w images.

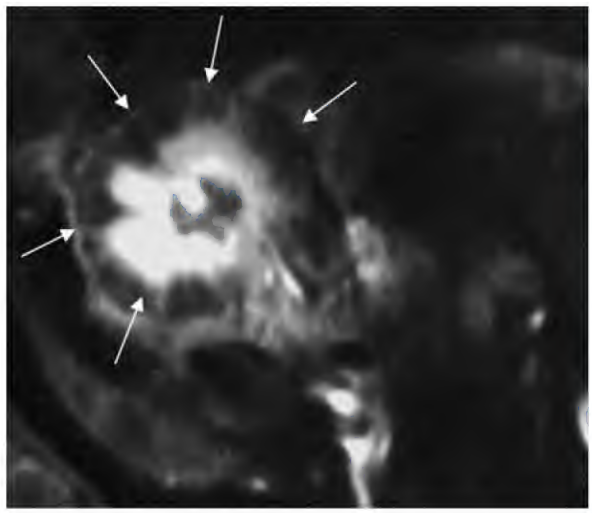

a

b

Fig. 3.29a,b. Complete cortical necrosis. **a** On this transverse Gd-enhanced TIw image the medulla is enhancing normally whereas the cortex remains unenhanced (*arrows*). **b** Macroscopic specimen from a similar cortical necrosis from another patient [Fig. 3.28b reprinted with permission from HÉLÉNON et al. (1992) *RadioGraphics* 12:21–33]

3.5.1.3 Medical Complications

3.5.1.3.1 Clinical Considerations

Different causes can be responsible for the failure or deterioration of renal graft function.

Primary non-function is characterized by immediate anuria without subsequent improvement. It is favored by certain risk factors: elderly donor, hypertension, prolonged ischemia, kidneys from children implanted into adults.

ATN is characterized by delayed recovery of renal function. It becomes manifest 12–24 h after revascularization as anuria or renal insufficiency with preserved diuresis. In particular, it is favored by the donor's age and vascular history, intensive care of the donor (hemodynamic status) and drugs used, difficulties encountered during organ excision (multiple organs), perfusion and cooling fluids used, duration of cold ischemia. ATN is extremely frequent after cadaveric donor transplantation. Conversely, it is unusual in living-donor transplantation because of the very short cold ischemia time. It resolves spontaneously over the first 2 weeks, depending on the degree of ischemia–reperfusion injury.

Acute rejection, in the majority of cases, is mediated by T lymphocytes and modern immunosuppressant therapies are able to prevent it more and more frequently. The actual acute rejection rate is 10%–15%, whereas 20 years ago it was at 30%–40%. In certain cases, humoral rejections can occur. They are characterized by involvement of the peritubular capillaries, to which complement component C4d adheres, and the appearance of circulating antibodies directed against the donor. Acute rejection remains the primary cause of graft loss in the short term and represents, above all, a major risk factor for the development of chronic graft dysfunction. Clinical signs are few in number and become manifest late, with a painful and enlarged graft, markedly diminished diuresis and febricula. Notably, a serum creatinine rise of $>20\%$ is an important warning signal. Imaging is useful for the differential diagnosis, as it reveals abnormalities of the large vessels or the excretory pathway.

The definitive diagnosis and the severity of the episode are provided by a renal biopsy showing lymphocyte infiltration of the tubules and the interstitium, with vascular lesion(s) in the most severe cases. First-line therapy consists of high-dose corticosteroids and, in the case of corticoresistant rejec-

tion, administration of anti-lymphocyte globulins or monoclonal antibody OKT3. Acute cellular rejection is reversible in the majority of cases.

The possibility of drug nephrotoxicity has to be excluded, either directly caused by calcineurin inhibitors (ciclosporin, tacrolimus) or more indirectly amplified by drug interactions. Again, the definitive diagnosis is provided by the biopsy, showing acute or chronic lesions associated with calcineurin-inhibitor-induced nephrotoxicity.

3.5.1.3.2 Imaging

Except for severely injured kidneys with primary non-function, distinguishing clinically between these medical entities may be difficult and, unfortunately, imaging techniques have not yet played a major role in alleviating that difficulty, thereby still justifying renal biopsies. In severe primary non-function, cortical or corticomedullary parenchymal necrosis must be detected with Gd-enhanced MRI (see above).

Many US features have been described as being highly suggestive of acute rejection: enlarged graft, effacement of the central sinus–echo complex, enlargement of pyramids, increased or decreased cortex echogenicity, loss of corticomedullary differentiation, thickened collecting system walls (Fig. 3.30). Unfortunately, these features are subjective and not specific, and have low reproducibility. Their limited negative-predictive value, between 17% and 50%, precludes any useful application in practice (Frick et al. 1981; Fried et al. 1983; Hoddick et al. 1986; Hricak et al. 1987; Kelcz et al. 1990; Linkowski et al. 1987).

Similarly, after initial promising results of duplex Doppler RI measurements, no correlation could be established between a high RI, >0.75 or >0.80, and acute vascular rejection (Allen et al. 1988; Don et al. 1989; Genkins et al. 1989; Kelcz et al. 1990; Linkowski et al. 1987). In fact, a RI rise >0.80 can be observed in each of these medical complications. This finding is not surprising because the changed cortical microcirculation is a non-specific parameter of renal transplant dysfunction. Pathological processes, such as acute rejection or ATN, affect the microcirculation first, either because direct injury affects the vessel wall or interstitial edema-induced narrowing of the capillary lumen occurs. However, the extent of the RI increase directly reflects the degree of cortical hypoperfusion (Fig. 3.31). Thus,

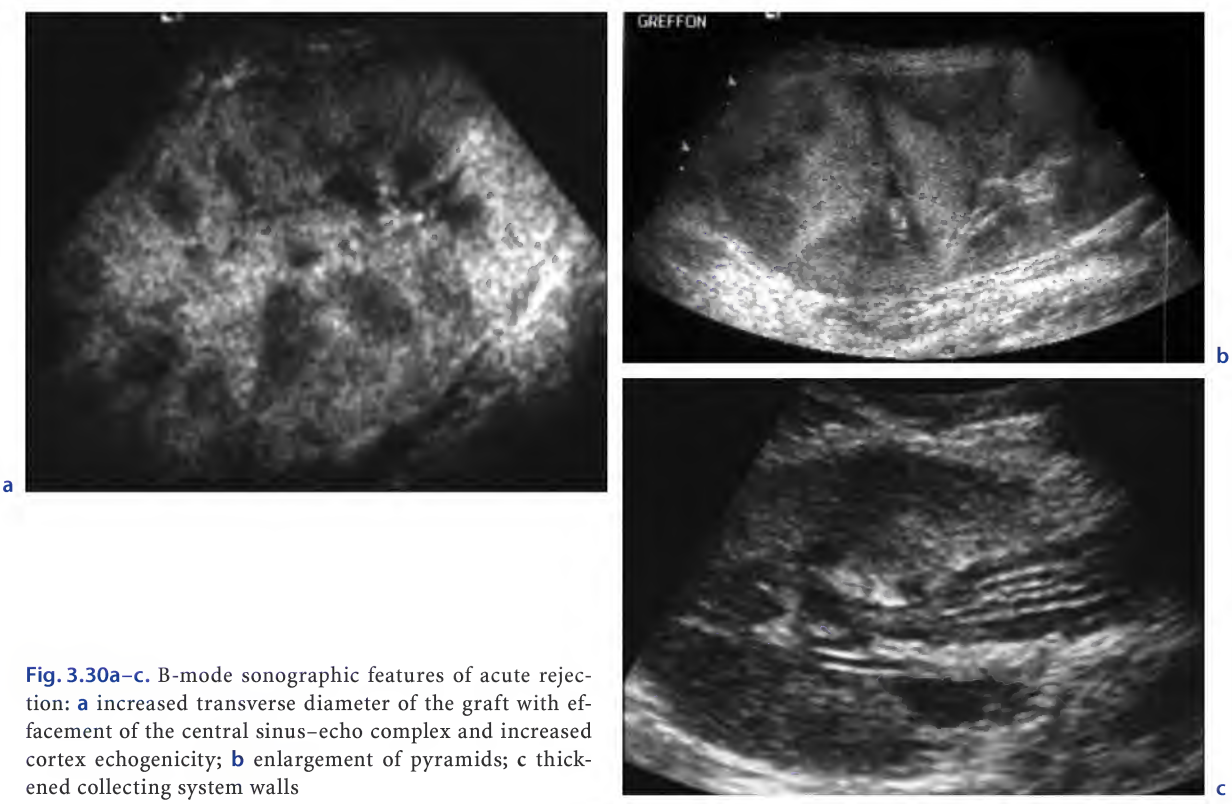

Fig. 3.30a–c. B-mode sonographic features of acute rejection: **a** increased transverse diameter of the graft with effacement of the central sinus–echo complex and increased cortex echogenicity; **b** enlargement of pyramids; **c** thickened collecting system walls

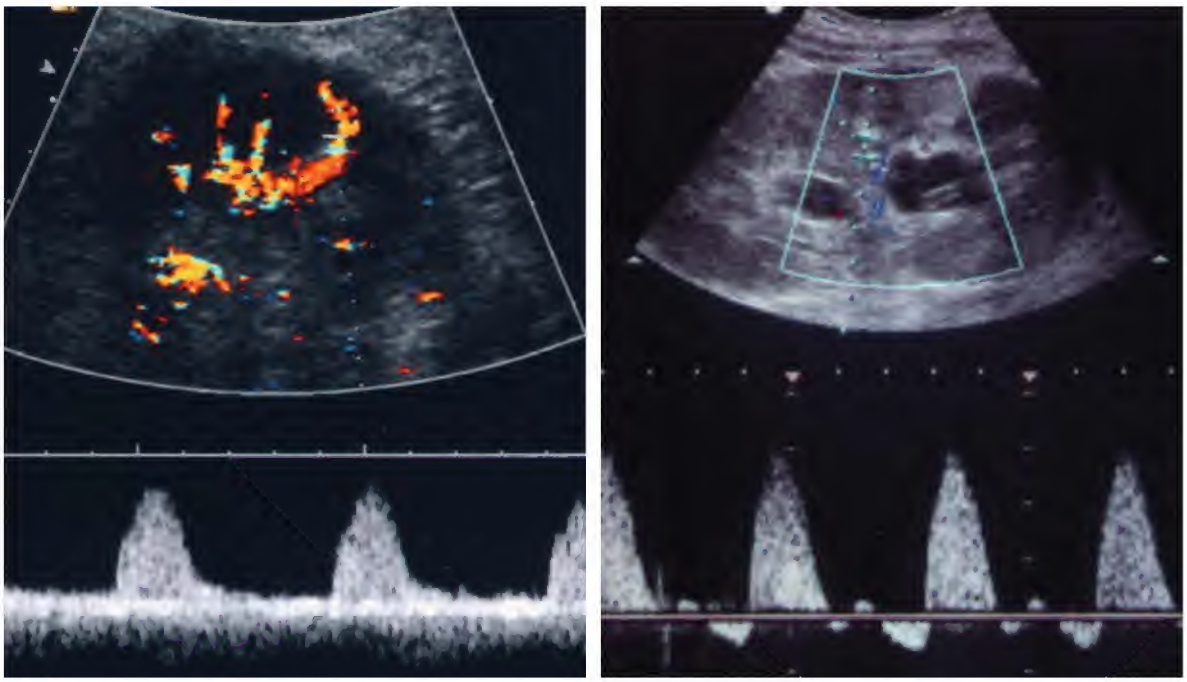

a b

Fig. 3.31a,b. Increase of intrarenal resistances with an absence of telediastolic flow in an acute rejection episode (**a**) and a proto- and telediastolic reflux in severe acute tubular necrosis (**b**)

it was thought that the degree of RI increase might be associated with the clinical outcome: in the most severe cases, protodiastolic or even holodiastolic reverse flow, evocative of severe acute rejection, severe ATN or renal vein thrombosis, is associated with a poor functional prognosis (Kaveggia et al. 1990). However, our study comparing RI measurement and power Doppler did not identify RI measurements as being statistically significant in determining prognosis at 12 months post engraftment (Trillaud et al. 1998).

Power Doppler US using high-frequency transducers to delineate cortical blood flow visualizes the dense cortical interlobular pedicles all the way to the cortex cortices (Martinoli et al. 1996). In renal grafts with impaired function, focal or diffuse absence of interlobular signals can be observed (Fig. 3.32). These changes can be reversed with treatment and are associated with a prediction of poor functional recovery at 12 months (Trillaud et al. 1998).

Findings on MR T1w sequences detecting these entities overlap too. The graft may or may not be enlarged. Initially, based on early experimental and clinical studies, decreased corticomedullary differentiation (CMD) on T1w sequences was considered specific to acute rejection (Hricak et al. 1986; Rholl et al. 1986). Now, this feature is considered non-specific for any nephropathy (Neimatallah et al. 1999). Proposed mechanisms are either lower cortical signal intensity due to edema or increased medullary SI resulting from decreased tubular flow or deposition of protein or blood components (e.g., hemoglobin). The intensity of the CMD decrease was initially shown to be associated with the degree of renal insufficiency and supposedly absent when serum creatinine reached 3.0 mg/dl (Semelka et al. 1994). However, in acute renal failure (ARF), CMD may remain preserved, at least within 2 weeks of developing ARF, and its degree seems now to be independent of the serum creatinine level (Chung et al. 2001). Similarly, signal changes on T2w images are highly variable.

Distinction between acute rejection and ATN is also difficult when radionuclide ($^{99}Tc^{m}$-MAG3) scintigraphy is used (el-Maghraby et al. 1998). Diagnosis is based on delayed and diminished radiotracer uptake associated with progressive parenchymal accumulation and retention, with no evidence of its excretion (Dubovsky et al. 1995). Delayed transit with delayed time to maximal activity (T_{max}), delayed time to one-half maximal activity $T½$ and high 20/3 min ratio are the main quantitative parameters used. Although the ability of these uptake

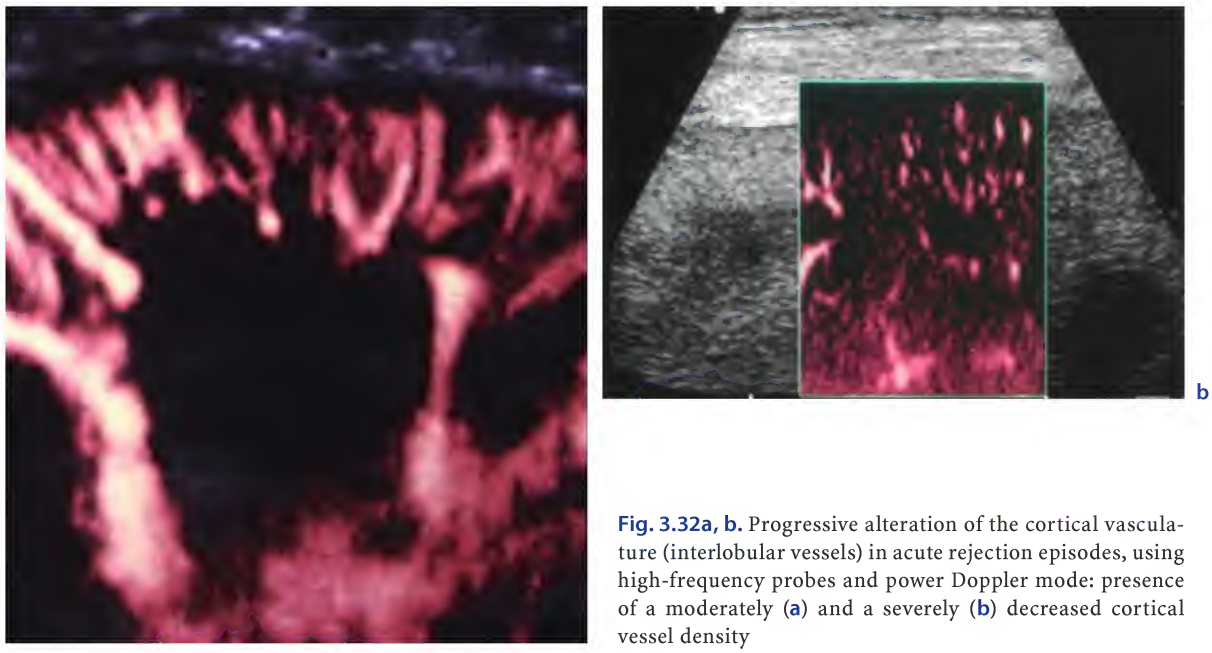

a b

Fig. 3.32a, b. Progressive alteration of the cortical vasculature (interlobular vessels) in acute rejection episodes, using high-frequency probes and power Doppler mode: presence of a moderately (**a**) and a severely (**b**) decreased cortical vessel density

indices and excretion parameters to differentiate between acute rejection and ATN is poor (Brown et al. 2000; el-Maghraby et al. 1998), they reflect the severity of renal dysfunction. Both entities are best distinguished on the basis of serial studies obtained over several days or weeks. Pertinently, concerning ATN, the graft usually attains its lowest perfusion and function levels by 48 h post-transplantation, and they improve thereafter, whereas renal perfusion and function generally decline progressively in acute rejection (el-Maghraby et al. 1998).

3.5.2 Early Patient Complications

3.5.2.1 Infectious Complications

Infections are the major cause of morbidity and mortality during the first year following kidney transplantation: 80% of grafted patients experience at least one infectious episode. The risk of infection is associated, in particular, with: the cumulative dose of immunosuppression, nosocomial environmental factors (water, operating room, air conditioning), the presence of foreign materials (central and urinary catheters), and the patient's nutritional and metabolic status (diabetes, renal insufficiency, cardiac insufficiency).

Any clinical picture suggestive of infection in a graft recipient has to be explored rapidly and an etiological diagnosis obtained without delay. Bronchoalveolar lavage for atypical pneumopathy, lumbar puncture for neurological symptoms, even incomplete, or organ biopsy must be performed in any doubtful situation.

3.5.2.1.1 Infections During the First 6 Months

The first 6 months after transplantation represents the time during which the patient is the most exposed to opportunistic infections.

Cytomegalovirus (CMV) Infections

CMV infections differ according to whether they are primary (positive donor–negative recipient), with a risk of 70%, or a reactivation or reinfection (positive recipient), with a lower risk of around 20%–30% in the absence of any prophylaxis. Furthermore, CMV infection is distinguished from CMV disease, according to the presence or not of clinical manifestations: fever, arthralgias, myalgias, leukopenia, elevated transaminases; and organ involvement in the most severe forms: pneumopathy (20%), colitis or acute pancreatitis. The diagnosis is based on a weekly polymerase chain reaction (PCR) search for virus in the blood or pp65-antigen determination in leukocytes (CMV antigenemia) during the first few

months following transplantation. In addition to its direct effects, CMV infection can favor superinfection with opportunistic microbes (*Pneumocystis*) and chronic graft dysfunction.

Thin-section CT findings of CMV pneumonia in immunocompromised patients are usually bilateral and difficult to assess on chest radiographs. The three main features shown by thin-section CT are areas of ground-glass opacification (66% of the patients), predominating in the upper lobes (Fig. 3.33), multiple nodules (59%) and areas of air-space consolidation (59%). Other findings are thickening of bronchovascular bundles, tree-in-bud appearance and pleural effusion (Franquet et al. 2003).

Protozoan Infections

These infections are much less common. *Pneumocystis jiroveci*, formerly *carinii*, (the most frequent) is responsible for bilateral alveolar interstitial hypoxia-inducing pneumonia. Its frequency has been sharply lowered by prophylaxis (trimethoprim–sulfamethoxazole, pentamidine aerosols). The typical findings are diffuse bilateral interstitial infiltrates, most severe in the perihilar regions. As the disease progresses, alveolar infiltrates may also develop. CT scanning may demonstrate typical features including perihilar ground-glass opacities (Fig. 3.34), often in a patchy or topographical distribution, with infected areas scattered throughout the normal lung parenchyma (Franquet et al. 2003).

Toxoplasmosis produces poorly specific symptoms or neurological signs (encephalitis, cerebral abscess), pneumopathy and/or chorioretinitis.

Bacterial Infections

Frequently caused by atypical bacteria (*Listeria monocytogenes*, *Legionella*, *Nocardia*, *Mycobacterium tuberculosis* or atypical mycobacteria), they are rare and difficult to diagnose.

Fungal Infections

Aspergillosis is the most common, often associated with an environmental factor (exposure to dusts). Spore inhalation is the main route by which *Aspergillus* infections are contracted. This fungus affects the lungs, the sinuses, and the peripheral and central nervous systems. The prognosis is usually poor, despite the availability of appropriate antimicrobial agents (amphotericin B, itraconazole, voriconazole).

Since the clinical signs of invasive aspergillosis are non-specific and often non-existent, radiological and laboratory evaluations are key diagnostic tools (Ergin et al. 2003). CT is very valuable for making an early diagnosis, is useful for demonstrating rhinosinusitis and involvement of other tissues, such as cerebral aspergillosis and skeletal

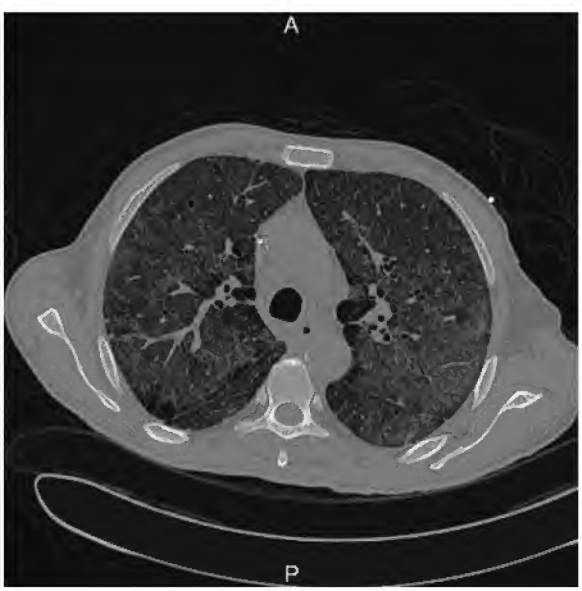

Fig. 3.33. Cytomegalovirus pneumonia. CT of the lung shows a ground-glass opacification predominating in the upper lobes with subpleural micronodules on the right side

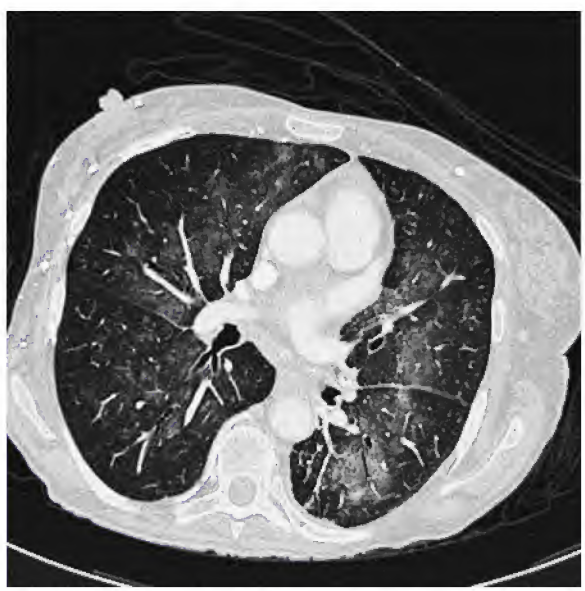

Fig. 3.34. Pneumocystis pneumonia. CT scanning of the lung demonstrates typical features including perihilar ground-glass opacities in a patchy distribution

invasion, and it can be used to guide biopsy procedures. Semi-invasive aspergillosis or chronic necrotizing aspergillosis is characterized on CT by unilateral or bilateral segmental areas of consolidation, or multiple nodular opacities or both. These findings are non-specific, most commonly mimicking those of reactivation tuberculosis (Franquet et al. 2004). Excavation is possible in these forms (Fig 3.35a).

In angio-invasive aspergillosis, characterized histologically by invasion and occlusion of small- to medium-sized pulmonary arteries by fungal hyphae, typical CT findings consist of nodules surrounded by a halo of ground-glass attenuation (halo sign) (Fig. 3.35b) or pleural-based wedge-shaped areas of consolidation. The air-crescent sign in angio-invasive aspergillosis is usually seen during convalescence.

In *Aspergillus* bronchopneumonia, also known as airway-invasive aspergillosis, which occurs in up to 10% of patients developing invasive pulmonary aspergillosis, CT scans show centrilobular nodules and branching linear or nodular opacities giving a tree-in-bud appearance (Fig. 3.35c). The centrilobular nodules have a patchy distribution in the lung (Franquet et al. 2004).

Aspergillosis may also develop within the spine (Fig. 3.36), within the pelvis, with tubo-ovarian masses or ureteral compression, or within the renal graft, as a fungus ball (saprophytic colonization of a cavity by fungal hyphae, without invasion of the adjacent tissues) (Johnston et al. 2004).

Cryptococcosis, histoplasmosis, coccidioidomycosis or mucormycosis are extremely rare.

3.5.2.1.2 Infections Occurring After 6 Months

Their frequency is higher than in the general population. They can be community-acquired infections or caused by opportunistic microbes, therefore vaccines without live virus, using either attenuated or killed virus, are recommended.

a

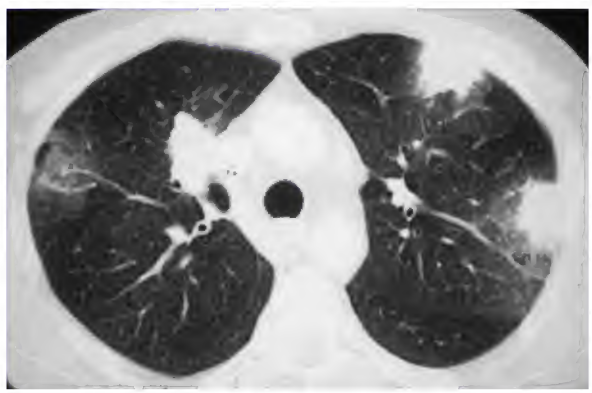

b

c

Fig. 3.35a–c. Aspergillosis of the lung in transplanted patients. **a** Semi-invasive aspergillosis with a large excavated lesions. **b** Angio-invasive aspergillosis : CT shows typical findings consisting of nodules surrounded by a halo of ground-glass attenuation (halo sign) **c** Airway-invasive aspergillosis: CT scans show centrilobular nodules and branching linear or nodular opacities giving a tree-in-bud appearance (fig 3.35c: Courtesy of Dr Ph. Grenier, Paris).

Fig. 3.36. Aspergillosis of the spine. On the sagittal T1w MR image a mass is visible, developing within the epidural space of the medullary canal, at the posterior aspect of the sac. Note the hyperintensity of two intervertebral disks at the same level. Aspergillosis was confirmed at surgery

3.5.2.2 Early Cancers

Post-transplantation lymphoproliferative syndromes, for all grafts combined, have an overall frequency of 2%, and represent a major progressive complication of organ transplantations. For kidney transplants, this rate reaches its peak during the first year (0.5%) and stabilizes over the following years (1.2% at 5 years). This complication is addressed in greater detail with the other malignant complications in the following chapter.

3.6 Long-Term Follow-Up

3.6.1 Late Complications of the Graft

3.6.1.1 Chronic Allograft Nephropathy (CAN)

CAN can be defined as a progressive deterioration of renal function appearing several months after transplantation, independently of acute rejection, another nephrotoxicity phenomenon or recurrence of the initial nephropathy with a suggestive histological appearance (Halloran et al. 1999). Four types of lesions can be found in graft biopsy samples: hyperplasia of the vessel intima, tubular atrophy, interstitial fibrosis and/or allograft glomerulonephritis. Different scores have been devised to classify CAN according to its severity. The most widely used is the Banff classification, based on the extent of the fibrosis and the tubule lesions in the cortical zone (Racusen et al. 1999). It is important to have access to tools able to evaluate CAN at an early stage, before the appearance of any clinical signs, because studies based on systematic biopsies showed that 25% of the patients had CAN lesions as early as month 3 post-transplantation (Legendre et al. 1998).

The mechanism leading to CAN development is complex and poorly understood, bringing together causes dependent on and independent of the allogeneic reaction. Its natural history shows that it comprises two very distinct phases: an early phase (first year), with an exponential increase of fibrotic interstitial lesions and tubular atrophy; and a late phase (after the first year), during which lesions caused by the nephrotoxicity of anti-calcineurins (ciclosporin, tacrolimus) predominate and play a major role after 3 years post-transplantation.

Kidneys suffering from CAN are decreased in size and have poorer corticomedullary differentiation and, sometimes, mild dilatation of the renal calices and pelvis. Most imaging techniques focus on the loss of parenchymal vascularity in the cortex to recognize this entity. However, neither RI measurement nor evaluation of intrarenal vessel density with power Doppler mode helps to identify transplants developing CAN. Recently, several authors tried to obtain more quantitative data by calculating depth-corrected fractional areas (percentage of the area of colored pixels relative to the total region of interest

area) on transverse slices and the distance from the most peripheral color pixels to the surface of the transplant during systole (Nankivell et al. 2002). They showed that a maximal fractional area < 17.3% could diagnose CAN with 88% specificity and 86% positive-predictive value, and severe CAN with 87% sensitivity and 95% negative-predictive value. A to-capsule distance > 5 mm was less sensitive (49%) but more specific (91% alone and 97% when combined with the fractional area). On radionuclide images, CAN is characterized by non-specifically diminished tracer uptake (Dubovsky et al. 1995).

Although RI measurements have no value for this diagnosis, they could have a prognostic value for long-term allograft outcomes: Radermacher et al. (2003) showed that renal arterial RI ≥0.80, measured at least 3 months after transplantation, was associated with poor subsequent allograft performance and death.

3.6.1.2 Recurrence of the Initial Nephropathy

Glomerular nephropathies represent the primary cause of chronic renal insufficiency (CRI) and are the principal entities that recur in the graft. According to the type of glomerulonephritis, the risk of recurrence ranges from 6% to 19% (Hariharan et al. 1999), which corresponds to the third cause of graft loss (after CAN and patient death with a functional graft), and it rises with the duration of the transplant. Focal or segmental hyalinosis, membranoproliferative glomerulonephritis, IgA nephropathy, membranous glomerulonephritis, diabetic nephropathy, lupus nephropathy and glomerulonephritis with anti-glomerular basement membrane antibodies bear the highest and most severe (loss of the graft) risks of recurrence. Finally, certain non-glomerular nephropathies can recur, such as hemolytic uremic syndrome or primary oxalosis.

3.6.1.3 Graft Infections

The frequency of polyomavirus interstitial nephritis is 3%–5% in the population of renal graft recipients. When confronted with a deterioration of renal function, the diagnosis is made based on a biopsy, showing the characteristic tubular epithelium lesions, confirmed by immunohistochemistry (simian virus-40 labeling), that are often associated with inflammatory cell infiltration into the interstitium. PCR on blood and urine is useful for screening and monitoring, as is urinalysis to search for infected cells (decoy cells). Imaging does not play any role in this diagnosis. Therapy is disappointing and combines lowering the doses of immunosuppressants and perhaps low-dose cidofovir in light of its nephrotoxicity (Ramos et al. 2002).

3.6.1.4 Calculus Disease

Based on the United States Renal Data System, which reported their retrospective records of 42,096 renal transplant recipients between 1994 and 1998, the incidence of urolithiasis was 0.11% for males and 0.15% for females (Abbott et al. 2003). At the time of calculus discovery, 67% had kidney stones and 33% ureteral stones. Uric acid stones are much less common than calcium calculi. The stones can be transplanted from cadaveric or living donors or develop de novo, favored either by metabolic disorders (tertiary hyperparathyroidism, hypercalciuria, hypocitraturia) or infection (*Proteus mirabilis*), or the presence of a foreign body in the urinary tract (double-J stent) (Crook and Keoghane 2005).

Stones can be easily detected by US, when located in the pyelocaliceal system or within the ureter, or when they have migrated, facilitated by the subsequent dilatation. In difficult cases, unenhanced CT may help (Fig. 3.37).

Fig. 3.37. Intracaliceal stones in an old renal transplant presenting with three cortical cysts

Extracorporeal shock-wave lithotripsy (ESWL) has been used successfully to treat renal and ureteral transplant stones. The stone may be directly accessed for percutaneous removal by nephrostomy or ureteroscopy, which can be difficult because of the ureteral anastomosis, and, if necessary, by a combined percutaneous and retrograde technique (Crook and Keoghane 2005).

3.6.2 Late Patient Complications

3.6.2.1 Cardiovascular Complications

Cardiovascular disease is a major cause of morbidity and the primary cause of death of kidney-graft recipients. In Europe, the frequencies of coronary disease, cerebrovascular disease and peripheral vascular disease after renal transplantation are 6%–14%, 1.4%–2.6% and 2.7%–6.3%, respectively (Nankivell et al. 2002). In the United States, 15 years after transplantation, the respective frequencies are 23%, 15% and 15% (Kasiske et al. 1996).

The risk of a cardiovascular event is 5 times higher for renal transplant recipients than in the general population. Nevertheless, the graft seems to prolong life expectancy compared to patients on hemodialysis while awaiting a compatible graft (even for groups with cardiovascular risk factors) (Wolfe et al. 1999). The fight against cardiovascular mortality requires better control of its risk factors: hypertension, lipid disorders, obesity, tobacco use, hyperhomocysteinemia and immunosuppressive therapy.

3.6.2.2 Hypertension

Hypertension is very common, particularly in kidney-transplant recipients, affecting 60%–85% of them. Its origin is multifactorial: CAN, graft-artery stenosis, presence of the native kidneys, immunosuppressive regimen (corticosteroids, calcineurin inhibitors) and/or nephropathy recurrence in the graft. Blood pressure is a major factor predictive of graft survival (Opelz et al. 1998). Numerous clinical trials have demonstrated the efficacy of good blood-pressure control against cardiovascular mortality in the general population, but its impact on graft survival is unknown.

The majority of antihypertensive agents can be prescribed to renal transplant recipients. The most frequently used are calcium-channel blockers and angiotensin-converting enzyme inhibitors or angiotensin II-receptor antagonists. Doppler US of the graft should be performed before starting antihypertensive treatment to eliminate graft-artery stenosis as the cause of hypertension (Rengel et al. 1998).

3.6.2.3 Malignancies

The overall risk of developing a cancer is multiplied by 100 for renal transplant recipients compared to the general population. The cumulative frequency of malignancies varies according to the type of cancer and the time after transplantation (Behrend et al. 1997). In Europe, the overall frequency of cancers, 10 years after engraftment, is 20%–30%. The mean age at the time of cancer diagnosis is 41 years, with a mean interval after transplantation of 5 years (Penn 2000b).

The most common malignancies in Europe are skin cancers, followed by solid tumors and lymphomas. With the exception of skin and lip cancers, the incidences of the most common malignancies seen in the general population are not higher. But frequencies are higher for some relatively rare tumors, including post-transplant lymphomas and lymphoproliferative disorders (PTLD), Kaposi's sarcoma (KS), renal carcinomas, in situ carcinomas of the uterine cervix, hepatobiliary carcinomas, anogenital carcinomas and various sarcomas (excluding KS) (Penn 2000a).

3.6.2.3.1 Skin Cancers

Cutaneous malignancies are the most common in kidney transplant recipients in occidental countries. The mean time to their occurrence is 8 years for patients undergoing transplantation during their fourth decade and 3 years for those grafted after their sixth decade. In contrast to the general population, squamous cell cancer is more frequent (two-thirds of the tumors) than basal cell carcinoma and its cumulative incidence can reach 30% at 20 years.

KS, malignant melanoma and Merkel tumors also occur much more frequently in renal graft recipients than in the general population. Finally,

anogenital carcinomas represent 3% of the cancers in graft recipients. As a consequence, anogenital lesions (warts, condylomas) that can undergo rapid local then regional extension should systematically be sought in regular physical examinations. Their prognosis is much more dismal than for the general population and they are responsible for 5% of the deaths of kidney graft recipients (Penn 2000b).

3.6.2.3.2 Solid Tumors

Solid tumors include all cancers that are of neither cutaneous nor hematological origin. Most renal cancers developing in renal graft recipients are clear-cell carcinomas, with 90% occurring in native kidneys and 10% in renal allografts (Fig. 3.38). They become apparent 2–258 months (average 75 months) after transplantation. Invasive KS involving the renal graft has also been described (Diaz-Candamio et al. 1998). Many renal carcinomas result from underlying kidney disease in renal allograft recipients. Two predisposing causes have been identified: analgesic nephropathy and acquired cystic disease (ACD) of the recipients' native kidneys. Analgesic nephropathy is known to cause cancers, mostly transitional cell carcinomas, in various parts of the urinary tract. ACD arises in 30%–95% of patients on

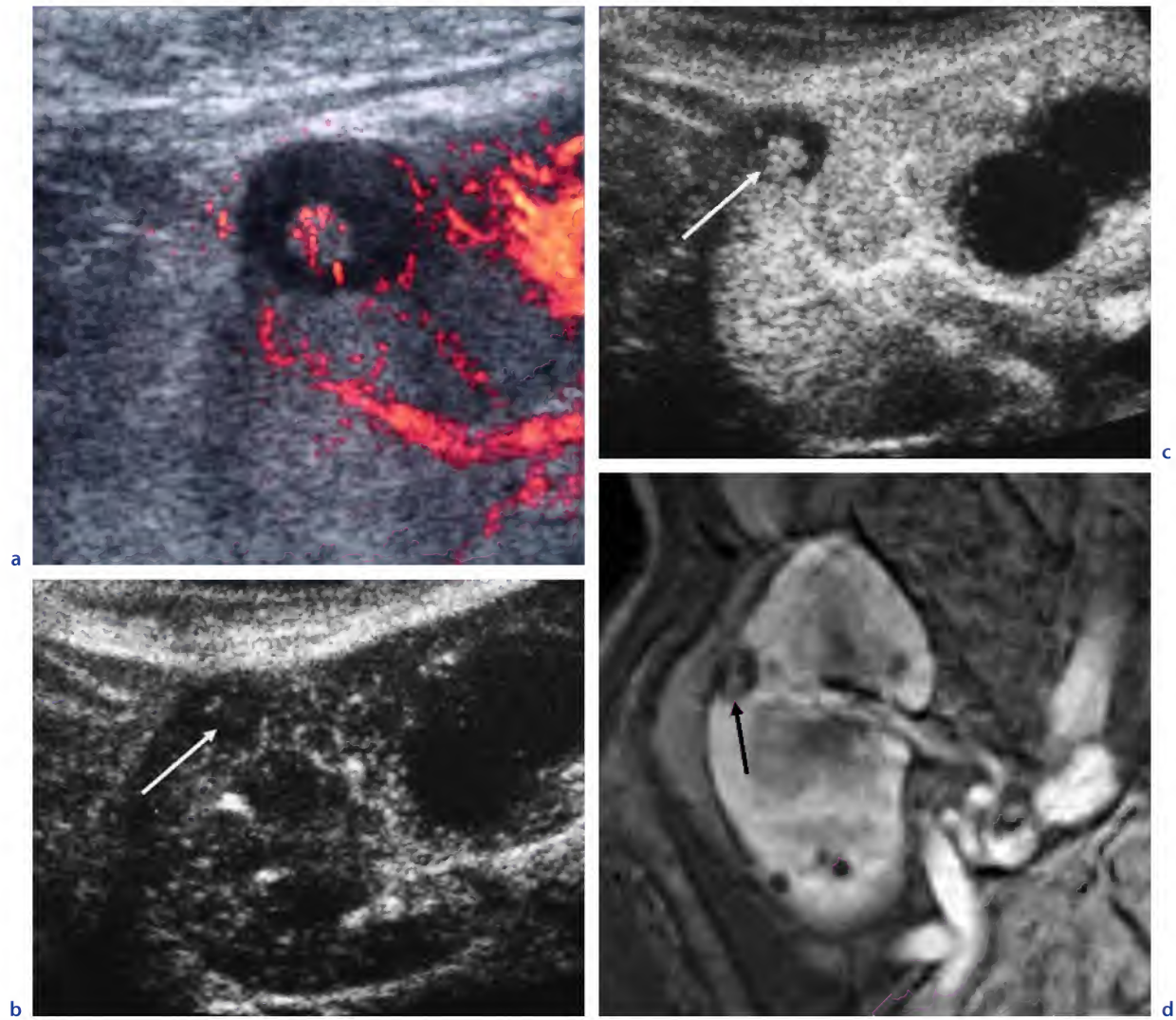

Fig. 3.38a–d. Intracystic renal cell carcinoma. Systematic sonographic follow-up of the graft revealed an atypical renal cyst with a hypervascularized nodule within it (**a**) which was confirmed by contrast-enhanced sonography at the arterial phase (**b**) and at the parenchymal phase (**c**) and by Gd-enhanced MR imaging (**d**) (*arrows*)

long-term hemodialysis and is complicated by renal adenocarcinomas, which develop 30- to 40-fold more often than in the general population, but the exact incidence of these ACD-related carcinomas in renal transplant recipients is not known. Whereas most renal cancers in transplant recipients develop in the context of ACD (Heinz-Peer et al. 1995), screening tests are not justified (Heinz-Peer et al. 1998).

Hence, patients presenting with micro- or macrohematuria should undergo exploratory procedures to actively search for cancer at the level of native and transplanted kidneys, looking for a renal or urothelial tumor. US and CT, when renal function is normal, or US and MRI, when it is impaired, can provide the necessary information about the renal parenchyma and the entire excretory system (Fig. 3.39). When ACD is present, MRI seems better able than US to visualize simple and complex lesions within native kidneys (Heinz-Peer et al. 1998). Radical nephrectomy or nephroureterectomy is recommended for native kidney tumors. Conservative percutaneous radiofrequency (RF) techniques should be considered for tumors developing within the graft (Goeman et al. 2006).

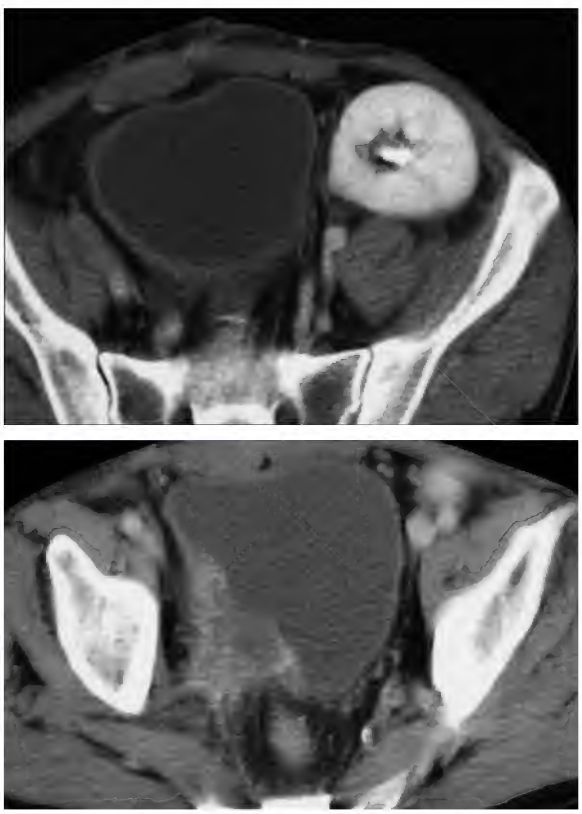

a

b

Fig. 3.39a, b. Development of an invasive bladder cancer, in a transplanted patient, with invasion of the extravesical fat

Uterine cervix carcinomas occurred in 10% of the women with post-transplant cancers. In situ lesions comprised at least 70% of cases, justifying regular pelvic examinations and cervical smears for post-adolescent female organ-transplant recipients (Penn 2000a).

The majority (73%) of hepatobiliary tumors are hepatocellular carcinomas; many of them are preceded by hepatitis B virus infection.

3.6.2.3.3 Post-transplantation Lymphoproliferative Disorders/ PTLD

PTLD are the third most common cancer in graft recipients in Europe. For renal transplant recipients, their frequency is 1%–2%, or 30–50 times higher than that for the general population, and they represent 21% of the malignancies, as opposed to 5% for the general population. These pathologies cover a large spectrum of hematological proliferations, ranging from benign hyperplasia to undifferentiated lymphoma. They are very often induced by Epstein–Barr virus (EBV), whose infection is favored by the immunosuppressive therapy.

Their distribution differs from that seen in the general population: non-Hodgkin's lymphoma, often an extranodal form with multiple sites at onset, represents 93% of the lymphomas in graft recipients versus 65% in the general population; Hodgkin's lymphoma and myeloma represent, respectively, 3% and 4% of the PTLD versus 10% for both of these hemopathies in the general population.

Two peaks of their frequencies are seen: one early, during the first months following transplantation (0.5% the first year), and the other years later (0.04% and per year). The greater majority of these lymphomas start as B-lymphocyte proliferations.

Three types of EBV-induced lymphoproliferations can be distinguished.

Benign polyclonal B-cell proliferation (55%) is characterized by a benign proliferation of B lymphocytes, without cytogenetic anomalies or immunoglobulin-gene rearrangement. It is a form of infectious mononucleosis that appears several weeks after an intensification of the immunosuppressive regimen.

Polyclonal B-cell proliferation with malignant characteristics (30% of lymphomas) has a clinical picture at onset similar to that of benign proliferations.

Monoclonal malignant B-cell proliferations are often extranodal (15% of the cases).

Their overall prognoses are less favorable than for the general population with the overall mortality rate for lymphoma in renal transplant recipients exceeding 50%, and the usual anti-neoplastic agents are less effective than in non-transplanted individuals.

The principal sites of involvement are the liver, brain, lymph nodes, lung and gastrointestinal tract. Detailed description of the radiological features of lymphomatous lesions within all these organs is beyond the scope of this review. In the abdomen, extranodal disease is more frequent than nodal and splenic involvement. Abdominal involvement is significantly less frequent among renal transplant recipients than among liver or heart recipients (Pickhardt and Siegel 1999). Most of these abdominal lesions are adequately visualized by contrast-enhanced CT: splenic or hepatic low-attenuation lesions, localized circumferential wall-thickening of the gastrointestinal tract (with or without aneurysmal dilatation of involved bowel loops) and mesenteric infiltration (Pickhardt and Siegel 1999).

The renal graft itself can also be involved. Most of the time, the lesion develops within the renal hilum, infiltrating the perirenal fat and encasing renal arteries and veins (Fig. 3.40). The tumor tissue may spread into the sinus, then into the renal parenchyma or towards the perirenal fat. Less often, renal involvement resembles multiple renal nodules. Involvement of the native kidneys and the bladder is also possible (Bellin et al. 1995).

These locations are difficult to assess ultrasonographically at the early phase and only dilatation of the collecting system may be seen. When visible, they appear as hypoechoic masses with hyperechoic components within the hilum and sinus. Color Doppler is able to identify encasement of renal vessels.

On CT scans, the lymphomatous tissues show low attenuation (20–30 HU) and moderate enhancement after iodine contrast-medium injection. On MR images, they exhibit a relatively typical signal intensity pattern: a hilar mass hypointense on T1w and T2w sequences, traversed by renal vessel with minimal enhancement (Ali et al. 1999). Sometimes, a hyperintensity is seen on T2w images and the enhance-

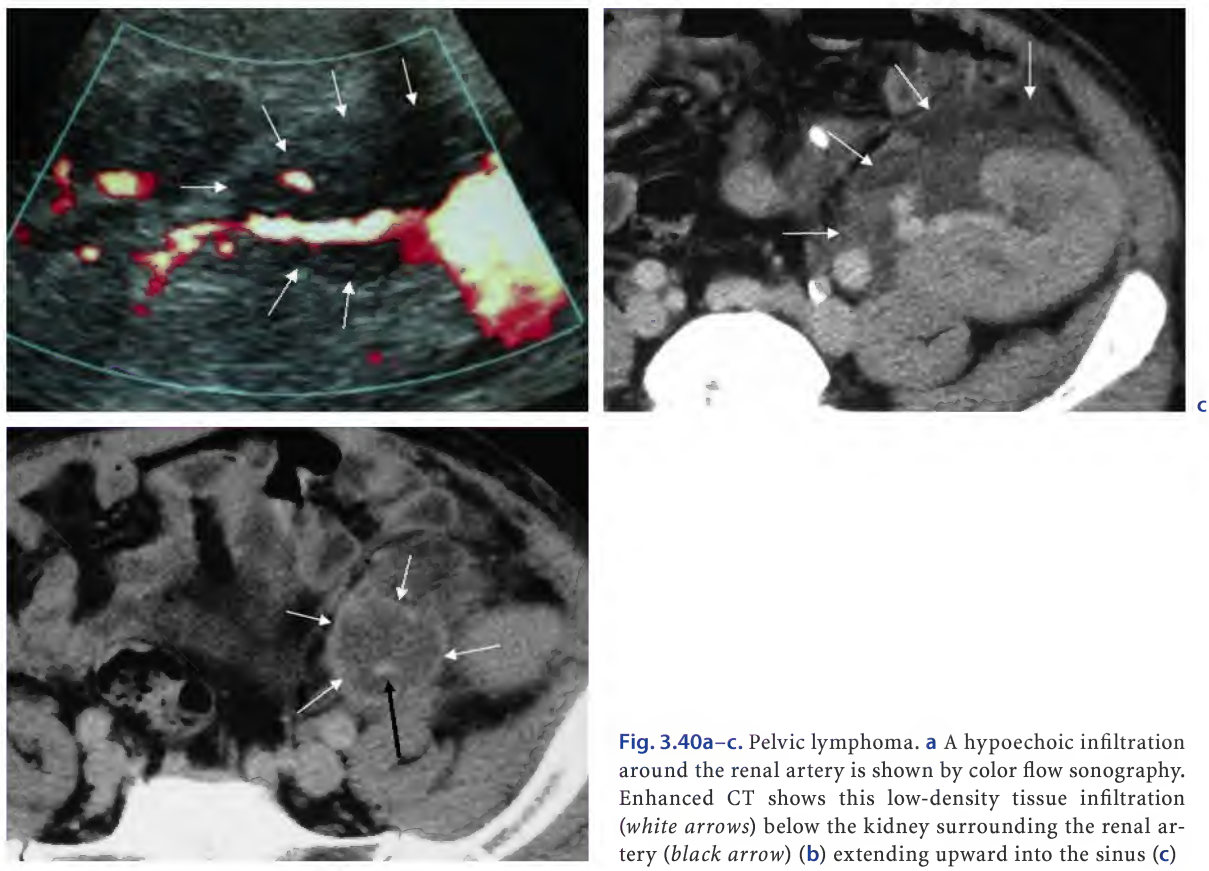

Fig. 3.40a–c. Pelvic lymphoma. **a** A hypoechoic infiltration around the renal artery is shown by color flow sonography. Enhanced CT shows this low-density tissue infiltration (*white arrows*) below the kidney surrounding the renal artery (*black arrow*) (**b**) extending upward into the sinus (**c**)

a

b

Fig. 3.41a,b. Abdominal lymphoma with retroperitoneal (**a**) and splenic (**b**) localization

ment may be more prominent during the early phase after Gd injection (Claudon et al. 1998). Other sites include retroperitoneal nodes, liver and spleen (Fig. 3.41). The definitive diagnosis is based on image-guided percutaneous biopsy, which can be difficult if the mass is limited to the hilum.

3.6.2.4 Late Infections

Chronic infections with hepatitis B or C virus (HBV, HCV), CMV, EBV or human papillomavirus (HPV) are seen in 10% of renal transplant recipients. These infections can affect the graft (CMV) or other organs (liver for HBV and HCV), or contribute to the development of a malignant complication (EBV, HPV). In addition, carriers of *M. tuberculosis* before engraftment might experience reactivation after transplantation.

Among kidney transplant recipients, the 5%–10% who experienced immunological complications (acute then chronic graft rejection) and, as a consequence, were exposed to intense immunosuppressive therapy during the first year become more susceptible to developing opportunistic infections (*Pneumocystis jiroveci*, *Listeria monocytogenes*, *Nocardia asteroides*, *Cryptococcus neoformans* or *Aspergillus*). Therefore, it is extremely important to take preventive measures, i.e., vaccinations and prophylaxis.

3.7 Emergent Imaging Techniques

3.7.1 Perfusion Studies

As mentioned above, renal perfusion is decreased during acute rejection. Color-flow US only qualitatively evaluates this parenchymal perfusion. A more quantitative approach can be obtained by using spin-labeling with MRI or contrast-enhanced dynamic studies with US or MRI.

Renal perfusion can be measured using pulsed arterial spin labeling (or spin tagging) with endogenous water used as a diffusible tracer (Golay et al. 2004). With this technique, a perfusion-weighted image can be generated by the subtraction of an image in which inflowing spins have been labeled from an image obtained without spin labeling. Quantitative perfusion maps can then be calculated (in ml/min per 100 g of tissue) when T1 of the tissue and efficacy of labeling are known. This method was applied to a model of acute rejection in rats at 4.7 T (Wang et al. 1998). During severe rejection, the renal cortex-perfusion rate in allogeneic kidneys was very low (undetectable) compared to the value in syngeneic kidneys. Moreover, the renal cortex-perfusion rate determined by MRI was significantly correlated with histological rejection. However, these methods are complex to implement in a clinical setting and their concordance with established methods has never been adequately assessed. Hence, their impact in clinical practice remains uncertain.

Use of first-pass dynamic contrast-enhanced imaging acquisitions makes quantification of absolute

or relative renal perfusion possible. The most widely used technique for that purpose is MRI, whereas US with microbubble injection is still in its infancy (Lefevre et al. 2002). MR technical and methodological issues for quantification of renal perfusion have been extensively described elsewhere (Grenier et al. 2006). Gd chelates (Sharma et al. 1995) and iron oxide (Gaschen et al. 2001) have been used for that purpose, with the latter being restricted to the vascular compartments during the first pass, while the former diffuses within the interstitial space and the glomeruli. These bolus tracking techniques have the advantage of being less prone to movement artifacts than spin-labeling techniques. Using superparamagnetic particles of iron-oxide (SPIO), Beckmann et al. (1996) showed that perfusion rates correlated significantly with the histological score of acute and chronic rejections.

First-pass Gd-enhanced acquisitions allow, in the same time, to measure glomerular filtration rate. Several models have been proposed and GFR maps can also be calculated but validation with reference methods is still required (Fig. 3.42).

3.7.2 Blood Oxygen-Level-Dependent (BOLD) MRI

The outer medulla is particularly sensitive to hypoxia because the active reabsorption process within the thick ascending loop of Henle requires a high level of oxygen consumption (Brezis and Rosen 1995). Therefore, decreased medullary blood flow or increased tubule reabsorption may induce medullary hypoxia and secondary ischemia.

This BOLD MRI approach was discussed in detail in a recent review (Grenier et al. 2003). Using a multi-echo gradient-echo sequence, R2* maps can be obtained showing a higher R2* within the medulla (i.e., lower pO_2) (Fig. 3.43). The BOLD technique does not measure pO_2 directly but allows intrarenal R2* (1/T2*) measurements that are closely associated with the deoxyhemoglobin concentration. Therefore, absolute R2* values cannot be used in practice.

Sadowski et al. (2005) showed that medullary R2* values were significantly lower (corresponding to increased oxygen concentration, probably due to decreased consumption) in patients with acute graft

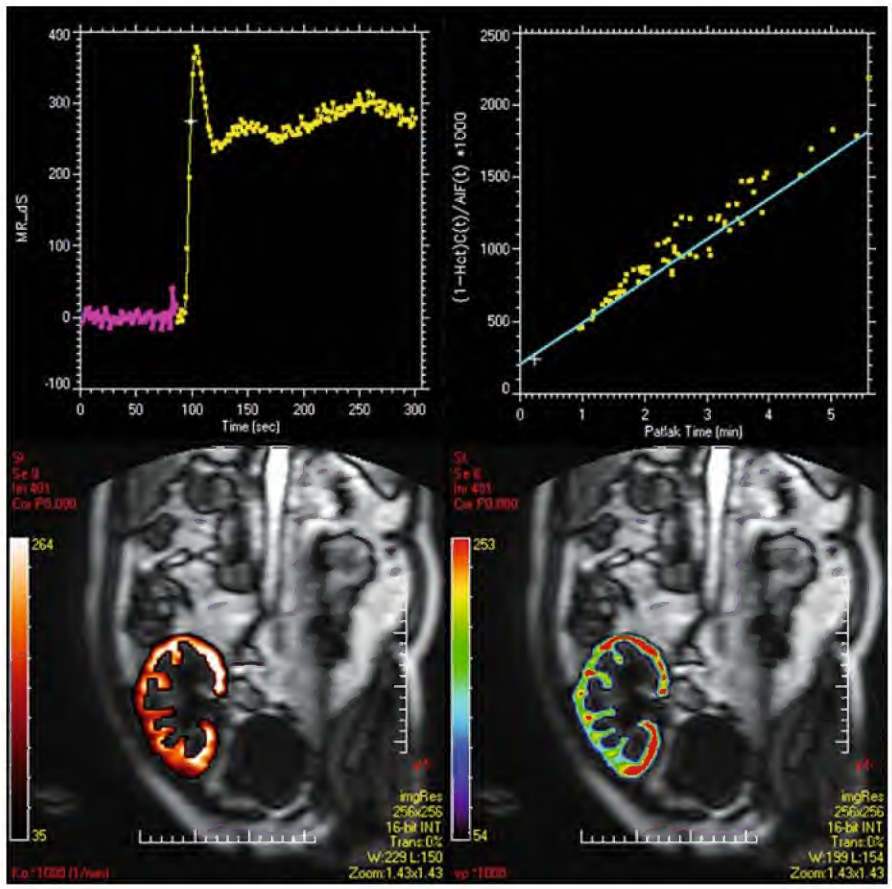

Fig. 3.42a–d. Example of dynamic Gd-enhanced fast 3D sequence making it possible to obtain signal intensity time curve on the cortex (**a**). Taking into account the arterial input function, after conversion of signal intensity into concentration, and applying the Rutland-Patlak method, a plot can be obtained (**b**) allowing calculating functional maps of glomerular filtration rate (**c**) and of cortical blood volume (**d**)

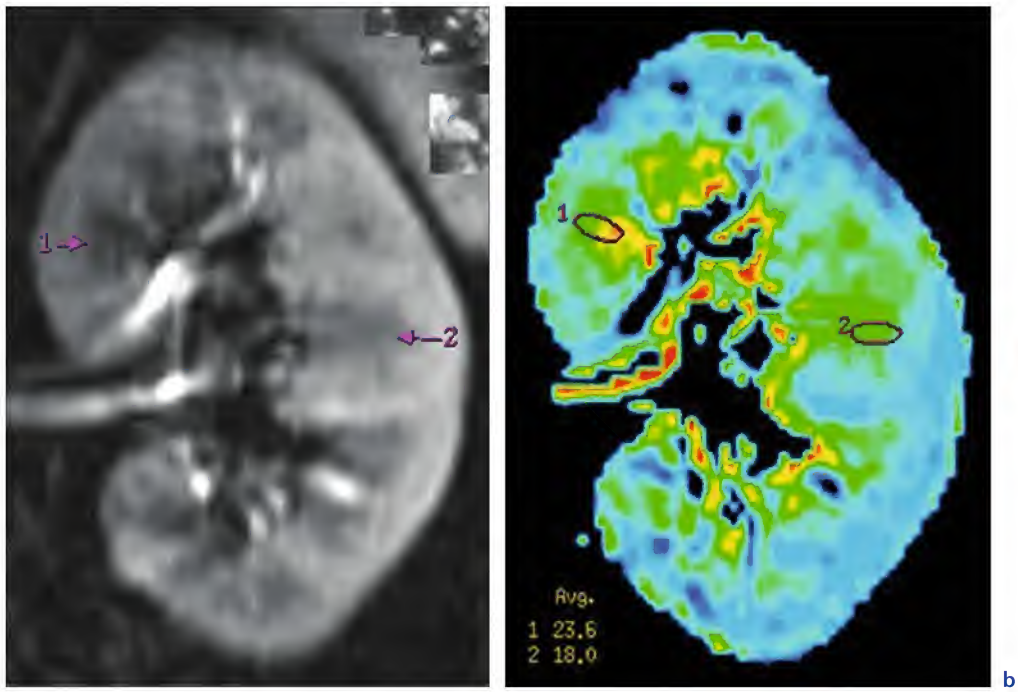

a b

Fig. 3.43a,b. BOLD sequence on a normally functioning renal graft. The coronal T1w gradient echo image shows the normal cortico-medullary differentiation. On the calculated R2* map, higher values of R2* are displayed in the medulla reflecting lower pO_2. [Reprinted with permission from Sadowski et al. (2005) *Radiology* 236:911–919]

rejection than in normally functioning kidneys and in transplants with ATN, with a threshold value of 18/s for separation of these groups. On the other hand, cortical R2* values were significantly higher in ATN than in acute rejection.

3.7.3 Diffusion MRI

Water movements related to transport during reabsorption and concentration–dilution functions can be studied by measuring the diffusion characteristics of the kidney. However, diffusion imaging is a challenging technique within the kidney due to the extreme sensitivity of diffusion-weighted sequences to several sources of artifacts. Apparent diffusion coefficient (ADC) values are higher in the cortex than the medulla and medullary diffusion is anisotropic (Ries et al. 2001) (Fig. 3.44). Using a renal transplantation model in rats, Yang et al. (2004) demonstrated at 7 T that cortical and medullary ADC values were significantly lower in allografts than isografts. Preliminary results in patients indicated a low variability of cal-

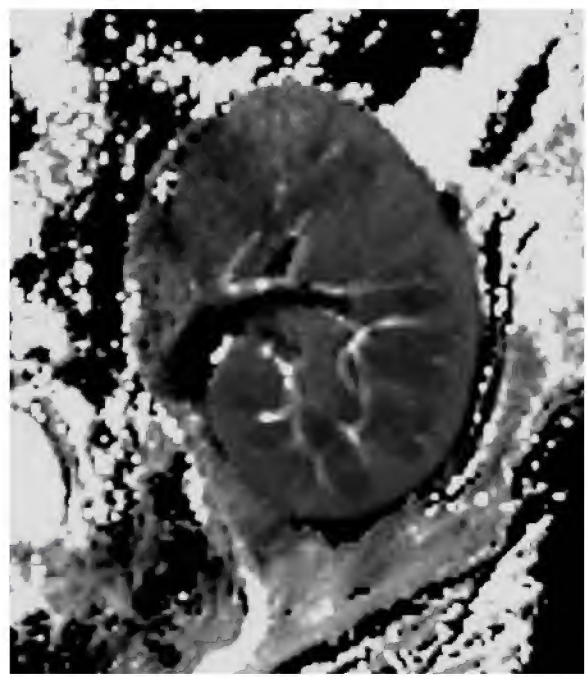

Fig. 3.44. Apparent diffusion (*ADC*) trace map of a normal renal transplant showing higher ADC values in the cortex than in the medulla

culated ADC and showed a significant inverse relationship between serum creatinine and ADC values (Thoeny et al. 2006). However, the exact role of this method in evaluating the diagnosis and prognosis of acute renal diseases remains to be defined.

3.7.4 Macrophage Labeling with USPIO

Macrophages, virtually absent in normal kidneys, may infiltrate renal tissues in specific nephropathies, such as acute proliferative types of human and experimental glomerulonephritides (Cattell 1994), renal graft dysfunctions (rejection and ATN) (Grau et al. 1998) or acute ischemic disease (Ysebaert et al. 2000) and non-specific kidney diseases, such as hydronephrosis. Today, in clinical practice, the degree of inflammatory response in the kidney can only be approached by renal biopsy. Ultra-small superparamagnetic particles of iron oxide (USPIO) are nanoparticles that have a long half-life in the bloodstream (2 h in rats; 36 h in humans) and, several hours after intravenous injection, are avidly captured by extrahepatic cells with phagocytic activity which include circulating monocytes and resident macrophages that are present in most tissues.

Several models of experimental nephropathies in rats were used to demonstrate the detectability of intrarenal macrophagic activity in vivo (Hauger et al. 2000). Models of acute (Yang et al. 2001; Ye et al. 2002) and chronic graft rejection (Beckmann et al. 2003) in rats showed diffuse homogeneous SI decreases in the three renal compartments (Fig. 3.45). Conversely, signal diminution was found only within the medulla in a model of ischemia–reperfusion, with no change within the cortex (Jo et al. 2003). The degree of SI decrease was always correlated with the number of macrophages within each renal compartment and disease severity.

The results of the first clinical study on 12 patients were recently reported (Hauger et al. 2007). MRI was performed 3 days after USPIO injection (Sinerem®, Guerbet Group) to ensure getting rid of signal changes from the vascular blood volume, knowing that USPIO's half-life in blood is 36 h in humans. A significant SI decrease only within the medulla was observed in patients with ATN, whereas patients with acute rejection had diffuse SI decreases (Fig. 3.46). Those preliminary clinical findings seem to corroborate experimental observations and call for larger multicenter clinical trials and evaluation of imaging 2 days after injection to shorten the time to diagnosis.

3.8 Conclusion

The culmination of more than a century of trials and errors, renal transplantation, as it is practiced today, is a relatively simple intervention that gives excellent results as long as a rather strict procedure is re-

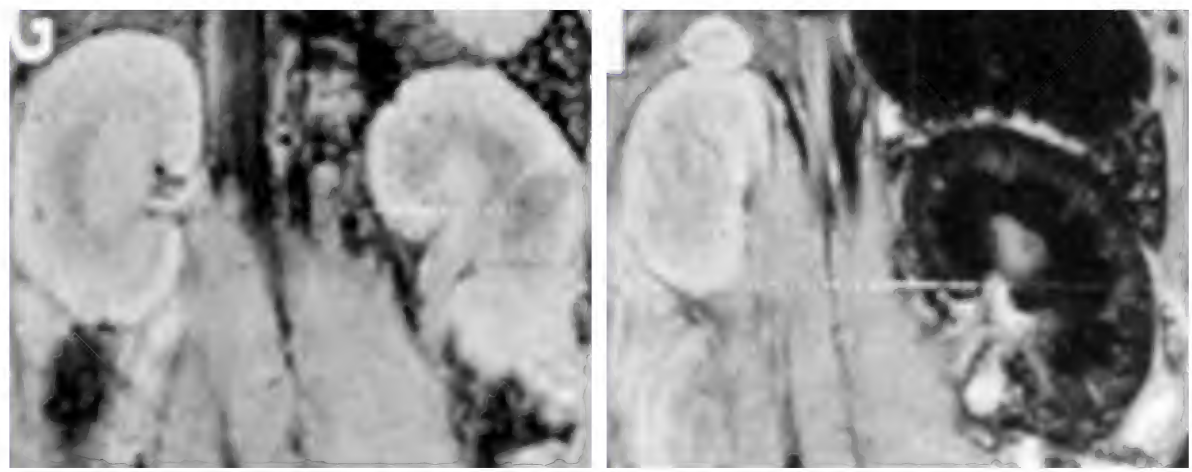

Fig. 3.45a,b. USPIO-enhanced MR imaging in a rat model of allogeneic left renal transplantation before (**a**) and 24 h after (**b**) injection of particles. On the post-injection image, the parenchyma of the left kidney shows a decreased signal intensity due to the intrarenal phagocytosis of iron oxide particles secondary to acute rejection. [Reprinted with permission from Ye et al. (2002) *Kidney Int* 61:1124–1135]

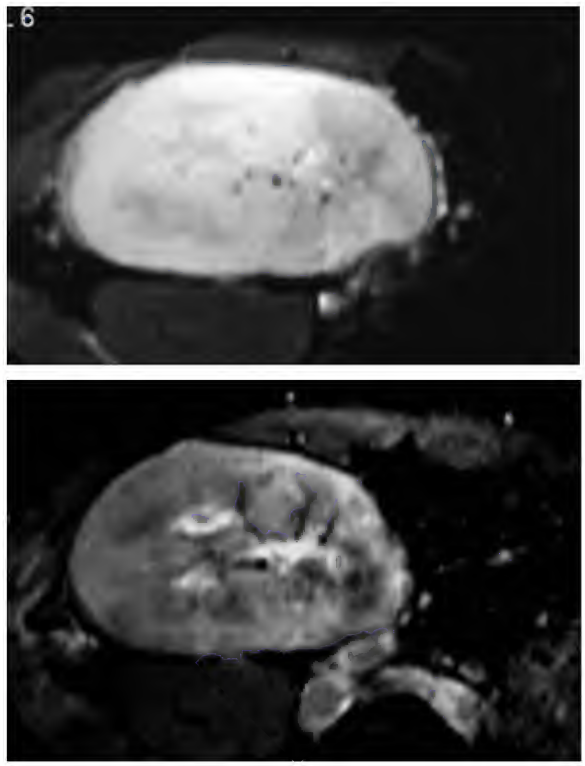

Fig. 3.46a,b. Sinerem®-enhanced MR imaging of a patient with acute rejection. The T2*w axial images obtained before (**a**) and 72 h after (**b**) injection of iron oxide particles show a decrease of signal intensity in all kidney compartments on the post-injection image due to the intrarenal infiltration of macrophages

spected. It requires a multidisciplinary approach to the patient, harmoniously combining the competencies of the nephrologist, radiologist, and urologist. This close-knit association and the contribution of each specialist before and after surgery should optimize the chances of successful transplantation and limit perioperative complications. Moreover, should the latter fail, the multidisciplinary approach contributes to achieving optimal treatment. The spectrum of late complications is quite broad, and awareness and understanding of them are important to assure good management of transplanted patients. This management requires systematic screening for risk factors, reasonable preventive drug use, an active vaccination policy, and aggressive and rapid treatment of events as they arise. It also means that patient education must start early, even before transplantation, with emphasis placed on compliance with the regimen prescribed, life style and appropriate diet. Development of non-invasive imaging techniques has already transformed the diagnosis of many of these complications, by rapidly providing complete useful morphological information. Emerging methods, once they have found their place, will soon further enhance that knowledge by adding functional data obtained during the same imaging sessions.

References

Abbott KC, Schenkman N, Swanson SJ et al (2003) Hospitalized nephrolithiasis after renal transplantation in the United States. Am J Transplant 3:465–470

Adani GL, Baccarani U, Bresadola V et al (2005) Graft loss due to percutaneous sclerotherapy of a lymphocele using acetic acid after renal transplantation. Cardiovasc Intervent Radiol 28:836–838

Ali MG, Coakley FV, Hricak H et al (1999) Complex post-transplantation abnormalities of renal allografts: evaluation with MR imaging. Radiology 211:95–100

Allen KS, Jorkasky DK, Arger PH et al (1988) Renal allografts: prospective analysis of Doppler sonography. Radiology 169:371–376

Beckmann N, Joergensen J, Bruttel K et al (1996) Magnetic resonance imaging for the evaluation of rejection of a kidney allograft in the rat. Transpl Int 9:175–183

Beckmann N, Cannet C, Fringeli-Tanner M et al (2003) Macrophage labeling by SPIO as an early marker of allograft chronic rejection in a rat model of kidney transplantation. Magn Reson Med 49:459–467

Beecroft JR, Rajan DK, Clark TW et al (2004) Transplant renal artery stenosis: outcome after percutaneous intervention. J Vasc Interv Radiol 15:1407–1413

Behrend M, Kolditz M, Kliem V et al (1997) Malignancies in patients under long-term immunosuppression after kidney transplantation. Transplant Proc 29:834–835

Bellin MF, Fuerxer F, Bitker MO et al (1995) Tumors of the genito-urinary tract in renal transplant recipients: clinical and radiological findings. Eur Radiol 5:26–32

Bhatti AA, Chugtai A, Haslam P et al (2005) Prospective study comparing three-dimensional computed tomography and magnetic resonance imaging for evaluating the renal vascular anatomy in potential living renal donors. BJU Int 96:1105–1108

Brezis M, Rosen S (1995) Hypoxia of the renal medulla – its implications for disease. N Engl J Med 332:647–655

Brown ED, Chen MY, Wolfman NT et al (2000) Complications of renal transplantation: evaluation with US and radionuclide imaging. Radiographics 20:607–622

Bruno S, Remuzzi G, Ruggenenti P (2004) Transplant renal artery stenosis. J Am Soc Nephrol 15:134–141

Cahen R, Loubeyre P, Trolliet P et al (1996) Magnetic resonance angiography for the detection of transplant renal artery stenosis. Transplant Proc 28:2830

Cattell V (1994) Macrophages in acute glomerular inflammation. Kidney Int 45:945–952

Cecka JM (2002) The UNOS Renal Transplant Registry. Clin Transpl 1–20

Chan YT, Ng WD, Ho CP et al (1985) Reversible stenosis of the renal artery following renal transplantation. Br J Surg 72:454–455

Chung JJ, Semelka RC, Martin DR (2001) Acute renal failure: common occurrence of preservation of corticomedullary differentiation on MR images. Magn Reson Imaging 19:789–793

Claudon M, Kessler M, Champigneulle J et al (1998) Lymphoproliferative disorders after renal transplantation: role of medical imaging. Eur Radiol 8:1686–1693

Crook TJ, Keoghane SR (2005) Renal transplant lithiasis: rare but time-consuming. BJU Int 95:931–933

De Vecchi AF, Dratwa M, Wiedemann ME (1999) Healthcare systems and end-stage renal disease (ESRD) therapies – an international review: costs and reimbursement/funding of ESRD therapies. Nephrol Dial Transplant 14 [Suppl 6]:31–41

Diaz-Candamio MJ, Pombo F, Lorenzo MJ et al (1998) Kaposi's sarcoma involving a transplanted kidney: CT findings. AJR Am J Roentgenol 171:1073–1074

Dodd GD 3rd, Tublin ME, Shah A et al (1991) Imaging of vascular complications associated with renal transplants. AJR Am J Roentgenol 157:449–459

Dominguez-Gil B, Herrero JC, Carreno A et al (1999) Ureteral stenosis secondary to encrustation by urea-splitting *Corynebacterium urealyticum* in a kidney transplant patient. Nephrol Dial Transplant 14:977–978

Don S, Kopecky KK, Filo RS et al (1989) Duplex Doppler US of renal allografts: causes of elevated resistive index. Radiology 171:709–712

Dubovsky EV, Russell CD, Erbas B (1995) Radionuclide evaluation of renal transplants. Semin Nucl Med 25:49–59

el-Maghraby TA, de Fijter JW, Wasser MN et al (1998) Diagnostic imaging modalities for delayed renal graft function: a review. Nucl Med Commun 19:915–936

Ergin F, Arslan H, Azap A et al (2003) Invasive aspergillosis in solid-organ transplantation: report of eight cases and review of the literature. Transpl Int 16:280–286

Erley CM, Duda SH, Wakat JP et al (1992) Noninvasive procedures for diagnosis of renovascular hypertension in renal transplant recipients – a prospective analysis. Transplantation 54:863–867

Fang YC, Siegelman ES (2001) Complications of renal transplantation: MR findings. J Comput Assist Tomogr 25:836–842

Ferreiros J, Mendez R, Jorquera M et al (1999) Using gadolinium-enhanced three-dimensional MR angiography to assess arterial inflow stenosis after kidney transplantation. AJR Am J Roentgenol 172:751–757

Franquet T, Lee KS, Muller NL (2003) Thin-section CT findings in 32 immunocompromised patients with cytomegalovirus pneumonia who do not have AIDS. AJR Am J Roentgenol 181:1059–1063

Franquet T, Gimenez A, Hidalgo A (2004) Imaging of opportunistic fungal infections in immunocompromised patient. Eur J Radiol 51:130–138

Frick MP, Feinberg SB, Sibley R et al (1981) Ultrasound in acute renal transplant rejection. Radiology 138:657–660

Fried AM, Woodring JH, Loh FK et al (1983) The medullary pyramid index: an objective assessment of prominence in renal transplant rejection. Radiology 149:787–791

Gaschen L, Schuurman HJ, Bruttel K et al (2001) MRI and ultrasonographic detection of morphologic and hemodynamic changes in chronic renal allograft rejection in the rat. J Magn Reson Imaging 13:232–241

Gedroyc WM, Neerhut P, Negus R et al (1995) Magnetic resonance angiography of renal artery stenosis. Clin Radiol 50:436–439

Genkins SM, Sanfilippo FP, Carroll BA (1989) Duplex Doppler sonography of renal transplants: lack of sensitivity and specificity in establishing pathologic diagnosis. AJR Am J Roentgenol 152:535–539

Goeman L, Joniau S, Oyen R et al (2006) Percutaneous ultrasound-guided radiofrequency ablation of recurrent renal cell carcinoma in renal allograft after partial nephrectomy. Urology 67:199

Gogus C, Yaman O, Soygur T et al (2002) Urological complications in renal transplantation: long-term follow-up of the Woodruff ureteroneocystostomy procedure in 433 patients. Urol Int 69:99–101

Golay X, Hendrikse J, Lim TC (2004) Perfusion imaging using arterial spin labeling. Top Magn Reson Imaging 15:10–27

Gottlieb RH, Lieberman JL, Pabico RC et al (1995) Diagnosis of renal artery stenosis in transplanted kidneys: value of Doppler waveform analysis of the intrarenal arteries. AJR Am J Roentgenol 165:1441–1446

Gourishankar S, Hunsicker L, Jhangri G et al (2003) The stability of the glomerular filtration rate after renal transplantation is improving. J Am Soc Nephrol 14:2387–2394

Grau V, Herbst B, Steiniger B (1998) Dynamics of monocytes/macrophages and T lymphocytes in acutely rejecting rat renal allografts. Cell Tissue Res 291:117–126

Grenier N, Douws C, Morel D et al (1991) Detection of vascular complications in renal allografts with color Doppler flow imaging. Radiology 178:217–223

Grenier N, Claudon M, Trillaud H et al (1997) Noninvasive radiology of vascular complications in renal transplantation. Eur Radiol 7:385–391

Grenier N, Basseau F, Ries M et al (2003) Functional MRI of the kidney. Abdom Imaging 28:164–175

Grenier N, Pedersen M, Hauger O (2006) Functional and cellular MR imaging of the kidney. In: Prigent A, Piepsz A (eds) Functional imaging in nephro-urology. Dunitz, London, pp 173–196.

Hagen G, Wadstrom J, Eriksson LG et al (2005) Three-dimensional rotational angiography of transplanted renal arteries: influence of an extended angle of rotation on beam-hardening artifacts. Acta Radiol 46:170–176

Halimi JM, Al-Najjar A, Buchler M et al (1999) Transplant renal artery stenosis: potential role of ischemia/reperfusion injury and long-term outcome following angioplasty. J Urol 161:28–32

Halloran P, Melk A, Barth C (1999) Rethinking chronic allograft nephropathy: the concept of accelerated senescence. J Am Soc Nephrol 10:167–181

Hariharan S (2001) Long-term kidney transplant survival. Am J Kidney Dis 38:S44–S50

Hariharan S, Adams MB, Brennan DC et al (1999) Recurrent and de novo glomerular disease after renal transplantation: a report from Renal Allograft Disease Registry (RADR). Transplantation 68:635–641

Hariharan S, Johnson C, Breshnahan B et al (2000) Improved graft survival after renal transplantation in the united states, 1988 to 1996. N Engl J Med 342:605–612

Hauger O, Delalande C, Deminière C et al (2000) Nephrotoxic nephritis and obstructive nephropathy: evaluation with MR imaging enhanced with ultrasmall superparamagnetic iron oxide-preliminary findings in a rat model. Radiology 217:819-826

Hauger O, Grenier N, Deminière C et al (2007) USPIO-enhanced MR imaging of macrophage infiltration in native and transplanted kidneys: initial results in humans. Eur Radiol. Published online at http://www.springerlink.com/content/100472

Heinz-Peer G, Schoder M, Rand T et al (1995) Prevalence of acquired cystic kidney disease and tumors in native kidneys of renal transplant recipients: a prospective US study. Radiology 195:667–671

Heinz-Peer G, Maier A, Eibenberger K et al (1998) Role of magnetic resonance imaging in renal transplant recipients with acquired cystic kidney disease. Urology 51:534–538

Hélénon O, Attlan E, Legendre C et al (1992) Gd-DOTA-enhanced MR imaging and color Doppler US of renal allograft necrosis. Radiographics 12:21–33

Hoddick W, Filly RA, Backman U et al (1986) Renal allograft rejection: US evaluation. Radiology 161:469–473

Hofmann LV, Smith PA, Kuszyk BS et al (1999) Three-dimensional helical CT angiography in renal transplant recipients: a new problem-solving tool. AJR Am J Roentgenol 173:1085–1089

Hricak H, Terrier F, Demas BE (1986) Renal allografts: evaluation by MR imaging. Radiology 159:435–441

Hricak H, Terrier F, Marotti M et al (1987) Posttransplant renal rejection: comparison of quantitative scintigraphy, US, and MR imaging. Radiology 162:685–688

Hubsch PJ, Mostbeck G, Barton PP et al (1990) Evaluation of arteriovenous fistulas and pseudoaneurysms in renal allografts following percutaneous needle biopsy. Color-coded Doppler sonography versus duplex Doppler sonography. J Ultrasound Med 9:95–100

Jo SK, Hu X, Kobayashi H et al (2003) Detection of inflammation following renal ischemia by magnetic resonance imaging. Kidney Int 64:43–51

Johnston O, Little DM, Hickey D et al (2004) Aspergillus "fungus ball" within a cadaveric renal transplant graft. Nephrol Dial Transplant 19:1317–1318

Jordan ML, Cook GT, Cardella CJ (1982) Ten years of experience with vascular complications in renal transplantation. J Urol 128:689–692

Juvenois A, Ghysels M, Galle C et al (1999) Successful revascularization for acute renal allograft thrombosis after 32 hours of ischaemia. Nephrol Dial Transplant 14:199–201

Karcaaltincaba M, Akhan O (2005) Radiologic imaging and percutaneous treatment of pelvic lymphocele. Eur J Radiol 55:340–354

Kasiske BL, Guijarro C, Massy ZA et al (1996) Cardiovascular disease after renal transplantation. J Am Soc Nephrol 7:158–165

Kaveggia LP, Perrella RR, Grant EG et al (1990) Duplex Doppler sonography in renal allografts: the significance of reversed flow in diastole. AJR Am J Roentgenol 155:295–298

Kelcz F, Pozniak MA, Pirsch JD et al (1990) Pyramidal appearance and resistive index: insensitive and nonspecific sonographic indicators of renal transplant rejection. AJR Am J Roentgenol 155:531–535

Kocak T, Nane I, Ander H et al (2004) Urological and surgical complications in 362 consecutive living related donor kidney transplantations. Urol Int 72:252–256

Lameire N, Jager K, Van Biesen W et al (2005) Chronic kidney disease: a European perspective. Kidney Int Suppl S30–S38

Lefevre F, Correas JM, Briancon S et al (2002) Contrast-enhanced sonography of the renal transplant using triggered pulse-inversion imaging: preliminary results. Ultrasound Med Biol 28:303–314

Legendre C, Thervet E, Skhiri H et al (1998) Histologic features of chronic allograft nephropathy revealed by protocol biopsies in kidney transplant recipients. Transplantation 65:1506–1509

Linkowski GD, Warvariv V, Filly RA et al (1987) Sonography in the diagnosis of acute renal allograft rejection and cyclosporine nephrotoxicity. AJR Am J Roentgenol 148:291–295

Loubeyre P, Abidi H, Cahen R et al (1997) Transplanted renal artery: detection of stenosis with color Doppler US. Radiology 203:661–665

Martinoli C, Crespi G, Bertolotto M et al (1996) Interlobular vasculature in renal transplants: a power Doppler US study with MR correlation. Radiology 200:111–117

Matalon TA, Thompson MJ, Patel SK et al (1990) Percutaneous treatment of urine leaks in renal transplantation patients. Radiology 174:1049–1051

Melamed ML, Kim HS, Jaar BG et al (2005) Combined percutaneous mechanical and chemical thrombectomy for renal vein thrombosis in kidney transplant recipients. Am J Transplant 5:621–626

Merkus JW, Huysmans FT, Hoitsma AJ et al (1993) Renal allograft artery stenosis: results of medical treatment and intervention. A retrospective analysis. Transpl Int 6:111–115

Middleton WD, Kellman GM, Melson GL et al (1989) Postbiopsy renal transplant arteriovenous fistulas: color Doppler US characteristics. Radiology 171:253–257

Montalvo BM, Yrizarry JM, Casillas VJ et al (1996) Percutaneous sclerotherapy of lymphoceles related to renal transplantation. J Vasc Interv Radiol 7:117–123

Nankivell BJ, Chapman JR, Gruenewald SM (2002) Detection of chronic allograft nephropathy by quantitative doppler imaging. Transplantation 74:90–96

Neimatallah MA, Dong Q, Schoenberg SO et al (1999) Magnetic resonance imaging in renal transplantation. J Magn Reson Imaging 10:357–368

Nilsson A, Loren I, Persson NH et al (1998) Color Doppler energy: detection of hypoperfused areas in renal transplants. J Ultrasound Med 17:153–155

Omary RA, Baden JG, Becker BN et al (2000) Impact of MR angiography on the diagnosis and management of renal transplant dysfunction. J Vasc Interv Radiol 11:991–996

Opelz G, Wujciak T, Ritz E (1998) Association of chronic kidney graft failure with recipient blood pressure. Collaborative Transplant Study. Kidney Int 53:217–222

Palleschi J, Novick AC, Braun WE et al (1980) Vascular complications of renal transplantation. Urology 16:61–67

Patel NH, Jindal RM, Wilkin T et al (2001) Renal arterial stenosis in renal allografts: retrospective study of predisposing factors and outcome after percutaneous transluminal angioplasty. Radiology 219:663–667

Penn I (2000a) Post-transplant malignancy: the role of im-

munosuppression. Drug Saf 23:101–113
Penn I (2000b) Cancers in renal transplant recipients. Adv Ren Replace Ther 7:147–156
Perini S, Gordon RL, LaBerge JM et al (1998) Transcatheter embolization of biopsy-related vascular injury in the transplant kidney: immediate and long-term outcome. J Vasc Interv Radiol 9:1011–1019
Pickhardt PJ, Siegel MJ (1999) Posttransplantation lymphoproliferative disorder of the abdomen: CT evaluation in 51 patients. Radiology 213:73–78
Platt JF, Ellis JH, Rubin JM (1991) Renal transplant pyelocaliectasis: role of duplex Doppler US in evaluation. Radiology 179:425–428
Racusen LC, Solez K, Colvin RB et al (1999) The Banff 97 working classification of renal allograft pathology. Kidney Int 55:713–723
Radermacher J, Mengel M, Ellis S et al (2003) The renal arterial resistance index and renal allograft survival. N Engl J Med 349:115–124
Ramos E, Drachenberg C, Papademitriou J et al (2002) Clinical course of polyoma virus nephropathy in 67 renal transplant patients. J Am Soc Nephrol 13:2145–2151
Rengel M, Gomes-Da-Silva G, Inchaustegui L et al (1998) Renal artery stenosis after kidney transplantation: diagnostic and therapeutic approach. Kidney Int suppl 68: S99–S106
Rholl KS, Lee JK, Ling D et al (1986) Acute renal rejection versus acute tubular necrosis in a canine model: MR evaluation. Radiology 160:113–117
Ries M, Basseau F, Tyndal B et al (2001) Diffusion and BOLD-contrast imaging in the kidneys of diabetic rats. In: International Society of Magnetic Resonance in Medicine Glasgow
Rijksen JF, Koolen MI, Walaszewski JE et al (1982) Vascular complications in 400 consecutive renal allotransplants. J Cardiovasc Surg (Torino) 23:91–98
Sadowski EA, Fain SB, Alford SK et al (2005) Assessment of acute renal transplant rejection with blood oxygen level-dependent MR imaging: initial experience. Radiology 236:911–919
Sahani DV, Rastogi N, Greenfield AC et al (2005) Multi-detector row CT in evaluation of 94 living renal donors by readers with varied experience. Radiology 235:905–910
Saxena AB, Busque S, Arjane P et al (2004) Preoperative renal volumes as a predictor of graft function in living donor transplantation. Am J Kidney Dis 44:877–885
Sebastia C, Quiroga S, Boye R et al (2001) Helical CT in renal transplantation: normal findings and early and late complications. Radiographics 21:1103–1117
Semelka RC, Corrigan K, Ascher SM et al (1994) Renal corticomedullary differentiation: observation in patients with differing serum creatinine levels. Radiology 190:149–152
Shamlou KK, Drane WE, Hawkins IF et al (1994) Captopril renography and the hypertensive renal transplantation patient: a predictive test of therapeutic outcome. Radiology 190:153–159
Sharma RK, Gupta RK, Poptani H et al (1995) The magnetic resonance renogram in renal transplant evaluation using dynamic contrast-enhanced MR imaging. Transplantation 59:1405–1409
Sierre SD, Raynaud AC, Carreres T et al (1998) Treatment of recurrent transplant renal artery stenosis with metallic stents. J Vasc Interv Radiol 9:639–644
Spinosa DJ, Matsumoto AH, Angle JF et al (1998) Gadolinium-based contrast and carbon dioxide angiography to evaluate renal transplants for vascular causes of renal insufficiency and accelerated hypertension. J Vasc Interv Radiol 9:909–916
Spinosa DJ, Angle JF, Hartwell GD et al (2002) Gadolinium-based contrast agents in angiography and interventional radiology. Radiol Clin North Am 40:693–710
Thoeny HC, Zumstein D, Simon-Zoula S et al (2006) Functional evaluation of transplanted kidneys with diffusion-weighted and BOLD MR imaging: initial experience. Radiology 241:812-21
Trillaud H, Merville P, Tran Le Linh P et al (1998) Color Doppler sonography in early renal transplantation follow-up: resistive index measurements versus power Doppler sonography. AJR Am J Roentgenol 171:1611–1615
Wang JJ, Hendrich KS, Jackson EK et al (1998) Perfusion quantitation in transplanted rat kidney by MRI with arterial spin labeling. Kidney Int 53:1783–1791
Wolfe RA, Ashby VB, Milford EL et al (1999) Comparison of mortality in all patients on dialysis, patients on dialysis awaiting transplantation, and recipients of a first cadaveric transplant [see comments]. N Engl J Med 341:1725–1730
Wong W, Fynn SP, Higgins RM et al (1996) Transplant renal artery stenosis in 77 patients – does it have an immunological cause? Transplantation 61:215–219
Yang D, Ye Q, Williams M et al (2001) USPIO-enhanced dynamic MRI: evaluation of normal and transplanted rat kidneys. Magn Reson Med 46:1152–1163
Yang D, Ye Q, Williams DS et al (2004) Normal and transplanted rat kidneys: diffusion MR imaging at 7 T. Radiology 231:702–709
Ye Q, Yang D, Williams M et al (2002) In vivo detection of acute rat renal allograft rejection by MRI with USPIO particles. Kidney Int 61:1124–1135
Ysebaert DK, De Greef KE, Vercauteren SR et al (2000) Identification and kinetics of leukocytes after severe ischaemia/reperfusion renal injury. Nephrol Dial Transplant 15:1562–1574

Liver Transplantation

4

4.1 Epidemiological, Clinical and Surgical Considerations

Olga Tucker and Nigel Heaton

CONTENTS

4.1.1 Introduction

Liver transplantation is an established, effective and often lifesaving treatment for acute and chronic end-stage liver disease. Over the last four decades major advances in diagnosis, preoperative patient assessment, donor organ preservation, immunosuppressive therapy, surgical, anaesthetic and intensive care techniques, and improved assessment and management of postoperative complications have resulted in increased patient and graft survival. Currently patients with chronic liver disease undergoing liver transplantation have a 1-year survival of 85–96% , and a 5-year survival of greater than 70% (Busuttil and Lake 2004).

O. Tucker MD, FRCSI
Specialist Registrar, Institute of Liver Studies, King's College Hospital, Denmark Hill, London SE5 9RS, UK
N. Heaton MB, BS, FRCS
Professor of Transplant Surgery, Institute of Liver Studies, King's College Hospital, Denmark Hill, London SE5 9RS, UK

4.1.2 Epidemiology and Indications for Liver Transplantation

The first successful kidney transplant was performed in 1954 between monozygotic twins, followed by the first attempted liver transplant in 1963 (Starzl et al. 1963). However, significant intraoperative and early postoperative mortality, combined with ineffective and often toxic immunosuppressive regimes, resulted in 1-year survival rates in the 1970s of only 30%. The introduction of effective immunosuppression with cyclosporin in 1981 and subsequently tacrolimus in 1989, led to significant improvement in survival following liver transplantation, and a dramatic increase in the number of transplants being performed.

Liver transplantation is indicated for patients with end-stage chronic liver disease who have a shortened life expectancy (of less than 18 months survival) and a poor quality of life as a consequence of the severity of liver disease. The degree of liver dysfunction due to cirrhosis is assessed by the Child-Pugh point scoring system consisting of clinical and biochemical measurements including grade of encephalopathy, severity of ascites, serum bilirubin, serum albumin, and prothrombin time (Pugh et al. 1973). More recently MELD has replaced the Child-Pugh score as a predictor of death within 3 months due to chronic liver disease [MELD is based on serum creatinine, bilirubin and international normalized ratio (INR)].

Indications for transplantation include poor synthetic function, refractory ascites, subacute bacterial peritonitis, chronic encephalopathy, recurrent variceal bleeding, unacceptable quality of life, hepato-pulmonary syndrome, and a life expectancy of less than 18 months due to liver disease. The most common clinical conditions associated with cirrhosis requiring transplantation are chronic viral

hepatitis, alcohol-related liver disease, autoimmune disorders such as primary biliary cirrhosis, autoimmune hepatitis and sclerosing cholangitis, hepatocellular carcinoma, and a variety of metabolic disorders. Common causes of acute liver failure necessitating liver transplantation include non-A non-B hepatitis and paracetamol hepatotoxicity. Other indications are listed in Table 4.1.1. In children the most common indication for liver transplantation is extrahepatic biliary atresia, which accounts for approximately 50% of cases. Other indications in children include metabolic disorders such as alpha-1-antitrypsin deficiency and a variety of inborn errors of metabolism based in the liver, Alagille's syndrome, and unresectable tumours confined to the liver such as hepatoblastoma (Table 4.1.2).

Contraindications to liver transplantation include uncontrolled active extrahepatic sepsis, advanced cardiorespiratory disease, extrahepatic malignancy, active substance abuse, medical non-compliance, and significant irreversible brain injury. A history of previous abdominal surgery, the presence of portal vein thrombosis, or congenital anomalies of the inferior vena cava are no longer considered a barrier to transplantation. Co-infection with human immunodeficiency virus is also no longer considered

Table 4.1.1. Indications for liver transplantation in adults

Chronic liver disease		
Chronic parenchymal disease	Hepatitis C cirrhosis	
	Hepatitis B cirrhosis	
	Alcohol-related cirrhosis	
	Autoimmune cirrhosis	
	Cryptogenic cirrhosis	
	Haemochromatosis	
	Alpha-1-antitrypsin deficiency	
	Wilson's disease	
Cholestatic disorder	Primary biliary cirrhosis	
	Primary sclerosing cholangitis	
Acute fulminant liver failure	Hepatitis A, B, or C	
	Non-A Non-B Hepatitis	
	Toxin	Paracetamol overdose
		Antituberculosis drugs
		Non-steroidal anti-inflammatory drugs
		Anti-epileptic drugs
		Halothane
		Carbon tetrachloride
		Amanita Phylloides poisoning
		Wilson's disease
Other indications	Malignancy	Hepatocellular carcinoma
		Metastatic neuroendocrine tumour
	Cholangiocarcinoma	
	Budd-Chiari syndrome	
	Polycystic liver disease	
	Amyloidosis	
	Hepatic enzyme defects	

Table 4.1.2. Indications for liver transplantation in children

Chronic liver disease		
Cholestatic	Extrahepatic biliary atresia	
	Primary sclerosing cholangitis	
Inborn errors of metabolism	Wilson's disease	
	Alpha-1-antitrypsin deficiency	
	Glycogen storage disease	Tyrosinaemia
		Galactosaemia
		Cystic fibrosis
		Defects of fatty acid oxidation
		Other
Chronic parenchymal disease	Congenital Haemochromatosis	
	Autoimmune cirrhosis	Viral hepatitis
		Alagille's syndrome
Acute fulminant liver failure	Toxin (similar to adults)	Non-A Non-B hepatitis
		Wilson's disease
		Congenital hemochromatosis
Other indications	Neoplasm	Hepatoblastoma
		Haemangioendothelioma

to be a medical contraindication to transplantation. However, transplantation for cholangiocarcinoma and large hepatocellular carcinomas outside the Milan or University of California, San Francisco (UCSF) criteria for liver transplantation remains controversial and is at best considered experimental (Mazzaferro et al. 1996; Yao et al. 2001).

4.1.3 Preoperative Evaluation

Evaluation of patients for liver transplantation involves a multidisciplinary approach by transplant hepatologists and surgeons, dieticians, psychologists, social workers, transplant co-ordinators and radiologists. A comprehensive medical assessment is essential to determine significant co-morbid conditions that may preclude transplantation, or negatively impact on the patient's peri-operative and/or postoperative course. Evaluation of the extent of liver disease, the presence of complications of cirrhosis, and the need of urgency for transplantation are important. Routine radiological investigations include a chest radiograph to evaluate heart size and exclude parenchymal lung lesions, and abdominal ultrasonography with Doppler assessment of the liver to determine the presence of ascites, screen for hepatocellular carcinoma or other mass lesions, portal vein patency, size and direction of portal venous flow, and hepatic venous patency. The majority of transplant centres also routinely perform contrast-enhanced triple-phase chest and abdominal computed tomography (CT) to evaluate suspected hepatocellular carcinoma, other parenchymal hepatic lesions, extrahepatic disease, suspicious lymphadenopathy, severity of portal hypertension with evaluation of the extent of collateral circulation, patency of the porto-mesenteric venous system, and aberrant arterial anatomy. Further evaluation of parenchymal liver lesions can be performed with gadolinium-enhanced magnetic resonance imaging.

Liver transplantation is the best curative option in patients with hepatocellular carcinoma and

cirrhosis, but disease-free survival following surgery is dependent on accurate preoperative clinical and radiological staging. Preoperative staging for hepatocellular carcinoma includes estimation of serum alpha-fetoprotein, abdominal ultrasonography, lipiodol-enhanced abdominal CT, angiography, and MR tesla. Favourable prognostic features include single, small, encapsulated tumours without evidence of vascular invasion (Fig. 4.1.1). The presence of portal vein involvement, and satellitosis with parenchymal field change are associated with advanced stage disease. Histological features conferring a better prognosis include well differentiated tumours with no evidence of satellitosis, capsular or vascular invasion, clear resection margins and fibrolamellar subtype. Criteria for liver transplantation for hepatocellular carcinoma associated with chronic liver disease include the Milan and UCSF criteria (Table 4.1.3) (Mazzaferro et al. 1996; Yao et al. 2001). Since the adoption of the Milan criteria, 5-year survival rates of 70%–75% are reported (Llovet et al. 2005). A 1-year survival rate of 90%, a 5-year survival rate of 75% and an 11% recurrence rate have been seen in patients following transplantation fulfilling the expanded UCSF criteria (Yao et al. 2001). Non-surgical options include transarterial chemoembolization (TACE), embolization, percutaneous ablation using radiofrequency ablation or alcohol, selective internal radiation therapy, systemic chemotherapy, hormonal, gene and immunotherapy. Currently, TACE and percutaneous ablation techniques are being increasingly used for local control of hepatocellular carcinoma to attempt to stabilize or downstage tumour in patients on the waiting list for liver transplantation. The technique delivers high concentrations of a chemotherapeutic agent directly to the tumour bed combined with tumour necrosis, while minimizing ischaemia to the surrounding hepatic parenchyma. Post-treatment effects can be assessed radiologically by reduced arterialization and deposition of lipiodol in the lesion accompanied by a reduction in the serum level of alpha-fetoprotein. Preoperative tumour biopsy is not recommended unless surgical intervention is not feasible and a histological diagnosis is required. In the presence of suspected malignancy a CT thorax is mandatory to exclude metastatic disease.

Table 4.1.3. Criteria for liver transplantation in cirrhosis and hepatocelluar carcinoma

Milan criteria	Single tumour <5 cm diameter
	Up to 3 tumours <3 cm diameter
	No vascular invasion
	No extra hepatic disease
UCSF criteria	Single tumour <6.5 cm diameter
	No more than 3 tumours largest <4.5 cm
	Total diameter <8 cm

Fig. 4.1.1. Peripherally located encapsulated hepatocellular carcinoma in explanted liver

An aortoportogram or spleno-portogram is indicated if abdominal ultrasonography is inconclusive, or shows portal vein thrombosis. As discussed previously, portal vein thrombosis is not a contraindication to transplantation, but it is essential to document its extent and severity, and careful preoperative consideration is required to plan the surgical approach. Portal vein thrombectomy or reconstruction with a venous jump graft from the superior mesenteric vein using donor iliac vein is feasible. Although a surgical solution exists with portal vein thrombosis, extensive mesenteric venous thrombosis usually precludes transplantation. If the patient remains on the waiting list for transplantation for a prolonged period of time, Doppler ultrasonography should be repeated as silent thrombosis of the portal vein occurs in 13%–64% of patients (Gonzalez et al. 1993; Langnas et al. 1991).

In approximately 10% of children, extrahepatic biliary atresia is associated with the polysplenia/asplenia syndrome (Falchetti et al. 1991; Hoffman et al. 1989; Raynor et al. 1988). Features of this syndrome include polysplenia or asplenia, absence of the inferior vena cava with azygos continuation, preduodenal portal vein, midgut malrotation, situs inversus, aberrant hepatic arterial anatomy, portal vein hypoplasia, and bilobed right lung (Falchetti et al. 1991).

4.1.3.1 Organ Donation

Three types of organ donation exist: heart beating cadaveric, non-heart beating cadaveric, and living donation. The majority of organs originate from cadaveric heart beating donors diagnosed as "brain stem dead". The current world-wide shortage of cadaveric organs for transplantation and the rise in the number of patients on waiting lists have led to interest in other methods of increasing the donor pool. Options include donation after cardiac death, otherwise known as non-heart beating or deceased cadaveric donation, the use of marginal grafts (from older donors or fatty infiltration of greater than 30%), split liver transplantation, and living related liver transplantation from a relative or spouse (Figs. 4.1.2, 4.1.3). Non-heart beating donation is increasing in incidence and making a significant contribution to organ availability. However, these livers carry a higher risk of primary non-function and of ischaemic cholangiopathy particularly if the cold ischaemic time is longer than 10 h or donors are older than 60 years. Living related liver transplantation initially evolved as a technique for transplanting children from an adult donor using the left lateral segment. Over 3,000 such transplants have been performed with excellent graft survival. There have been two donor deaths and the morbidity including those of bile leak and bleeding is less than 5%. Since 1995 adult-to-adult living donation has developed using either the left or right lobes. The risk of donor death is higher than left lateral segment donation with an incidence of bile leak of 2%–5%. In the setting of living related liver transplantation, accurate preoperative assessment of liver volumes is necessary to avoid the small-for-size liver syndrome both for the donor and the recipient particularly in adult-to-adult donation. The small-for-size syndrome is a recognizable clinical syndrome, occurring in the presence of reduced mass of liver insufficient to maintain normal liver function characterized by liver dysfunction with prolonged cholestasis, coagulopathy, portal hypertension, and ascites (Tucker and Heaton 2005). It is important to realize that significant interpatient variation in liver volumes exists. In most, the right liver volume represents >50% of the total liver volume (TLV) (median, 65% of TLV), with a range of 45%–80% of TLV. The contribution of the left liver to the TLV is also variable with a range of 15%–45% of TLV, contributing ≤25% of TLV in ≥10% of the population (Abdalla et al. 2004). Total liver volume, graft volume and functional remnant liver (FRL) can be accurately measured by three-dimensional CT volume reconstruction on the basis of body surface area (BSA) and body weight (Abdalla et al. 2004; Vauthey et al. 2000). In living related liver transplantation, CT-measured TLV and FRL can be used to predict post-resection function in the normal donor liver. However, CT-volumetry-measured TLV of the recipient's liver is not a useful index of function as the liver is diseased. Values calculated from the ratio of liver graft weight to recipient body weight (GRBWR), or standardized liver volume (SLV) based on recipient BSA can be used to predict minimum adequate graft volume (Higashiyama et al. 1993; Vauthey et al. 2000). In split liver and living related liver transplantation, a GRBWR of ≥0.8% or a graft weight ratio (graft weight divided by standard recipient liver weight) of ≥30% are recommended

Fig. 4.1.2. Steatotic cadaveric liver graft

Fig. 4.1.3. Ex vivo bench split of cadaveric liver graft into anatomical right and left lobes for transplantation

to achieve patient and graft survival of greater than 90% (Kawasaki et al. 1998; Lo et al. 1999).

Mandatory preoperative radiological investigations in potential living related donors include abdominal Doppler ultrasonography, abdominal CT with accurate estimation of TLV, graft volume, and FRL, magnetic resonance cholangiography and angiography. Additional investigations including MRI liver and liver biopsy are required if steatosis is suspected. At the time of surgery an intraoperative transcystic duct cholangiogram is performed to evaluate the biliary anatomy. Intraoperative ultrasonography is also helpful in delineating segmental anatomy and major vascular structures, including the course and significant tributaries of the middle hepatic vein.

4.1.4 Postoperative Phase: Early Postoperative Complications

Early postoperative complications include primary graft non-function, primary graft dysfunction, vascular, infectious, biliary, and immunological complications (Table 4.1.4). Early graft failure otherwise known as primary graft non-function is relatively rare, occurring in 2%–5% of patients, and necessitates re-transplantation as a life-saving measure. Signs of poor graft function include continuing vasopressor support for haemodynamic instability, persistent or increasing acidosis, rising base excess and serum lactate, and haemorrhage due to persistent coagulopathy. Postoperative intra-abdominal haemorrhage in the first 48 h is a common complication occurring in 5%–10% of patients. Re-exploration may be necessary, but a definite bleeding point is identified in only 50%.

Hepatic artery thrombosis is a serious technical complication occurring in approximately 4% of adults and 8% of paediatric transplants. Early recognition of hepatic artery thrombosis with immediate surgery to re-vascularize the graft may salvage the liver. Unrecognized, it usually results in graft loss due to biliary injury and hepatic necrosis, requiring re-transplantation. Other modes of presentation include bile duct necrosis and biliary leak, or cholangitis with recurrent bacteraemia. Hepatic arterial anastomotic stenosis may also occur, and should be dealt with early by balloon angioplasty prior to developmentofgraftdysfunction.Portalveinthrombosis is a relatively rare complication in adults occurring in less than 2% but appears to be significantly higher in paediatric liver transplant recipients (Langnas et al. 1991). It presents with prolongation of the

Table 4.1.4. Postoperative complications

Early	Primary graft non-function	
	Primary graft dysfunction	
	Haemorrhage	
	Vascular complications	Hepatic artery thrombosis
		Portal vein thrombosis
	Biliary complications	Leak
		Stricture
	Bowel complications	Perforation
		Ileus
	Acute cellular rejection	
	Infection	Bacterial
		Viral
Late	Chronic cellular rejection	
	Vascular complications	Hepatic artery thrombosis
		Portal vein thrombosis
		Stenosis
	Biliary complications	Stricture

INR and persistent acidosis, and if left untreated may result in severe graft dysfunction, and therefore warrants urgent re-exploration and re-vascularization. We routinely perform a Doppler ultrasound scan on postoperative days 1 and 5 to evaluate portal vein and hepatic artery flow, and the flow characteristics. Adults who require reconstruction of aberrant hepatic arteries on the back-table prior to implantation, and all paediatric patients are routinely given low molecular weight heparin as prophylaxis against arterial and venous thrombosis once the INR level is ≤1.5, platelet count ≥30×109/l, and there is no evidence of active haemorrhage. Common variations of arterial anatomy include an accessory left hepatic artery arising from the left gastric artery, and an accessory or replaced right hepatic artery arising from the superior mesenteric artery. Patients with high resistance flow in the hepatic artery on Doppler ultrasonography are commenced on prophylactic doses of low molecular weight heparin, and a Doppler ultrasound is repeated within 24 h. Urgent radiological investigation with CT angiography and selective visceral angiography may be indicated if hepatic artery thrombosis is suspected.

Bowel perforation can occur in patients who have had previous surgery, particularly in children following Kasai port-enterostomy for extrahepatic biliary atresia, due to the presence of multiple adhesions and severity of portal hypertension at the time of transplantation combined with the small delicate calibre of bowel loops. Transmural lesions can be caused by diathermy during adhesionolysis and haemostasis particularly in the region of the duodenum, which perforate days later. Other aetiological factors include herpes simplex virus and cytomegalovirus enteritis. Cytomegalovirus infection can cause deep ulceration of the stomach, duodenum, small and large bowel. The use of steroids, immunosuppressive agents, the presence of malnutrition, a catabolic state, and intra-abdominal infection all contribute to an increased risk of bowel perforation.

Cardiorespiratory compromise with continuing inotrope support, atelectasis, lower respiratory tract infections and/or pleural effusions are common. Paralysis of the right diaphragm is a rare surgical complication, secondary to right phrenic nerve injury at the time of cross clamping the suprahepatic vena cava. Infective complications are common. Bacterial pneumonia is the most common infective complication in the immediate postoperative period caused by a wide spectrum of pathogens. Daily chest X-rays are performed in the intensive care unit, and intensive chest physiotherapy is performed. During the second postoperative week gram positive line infection is a frequent complication. Meticulous attention to sterility in line care is essential. Patients with persistent pyrexia and gram positive septicaemia should be evaluated for endocarditis by transthoracic, and transoesophageal ECHO if negative. Opportunistic infections occur including toxoplasmosis, candidiasis, aspergillosis, and *Pneumocystis carinii* pneumonia. Acute adult respiratory distress syndrome can precede transplantation in patients with fulminant hepatic failure, can occur following transplantation in association with the systemic inflammatory response and multi-organ dysfunction syndromes, or can be caused by *Pneumocystis carinii* pneumonia requiring prolonged ventilation.

Other pathogens include herpes viruses, particularly herpes simplex and varicella zoster, cytomegalovirus and Epstein Barr virus. Signs and symptoms of cytomegalovirus disease include a swinging pyrexia, a falling white cell count with relative lymphopenia, diarrhoea which may be bloody, general malaise, arthritis, hepatitis and pneumonitis. Cytomegalovirus hepatitis usually manifests during the 3rd to 8th week post-transplant. Epstein Barr virus infection may present with fever, lymphadenopathy, or hepatitis.

Acute cellular rejection is common, and usually occurs in the first month after transplantation. The majority of cases are steroid responsive. A liver biopsy is required to prove the diagnosis, and exclude other causes of graft dysfunction. Graft loss due to acute rejection is uncommon.

Postoperative biliary complications include biliary leak, stricture formation, T-tube-related problems, Roux loop, cystic duct problems related to the t-tube, roux loop, or cystic duct, preservation injury, and sphincter of Oddi dysfunction. A hand-sewn end-to-end anastomosis of the donor common hepatic duct to the recipient common bile duct with interrupted sutures is the most commonly performed technique of biliary reconstruction. It is regarded as the most physiological method. This technique also preserves the sphincter of Oddi and permits access to the biliary tree for endoscopic cholangiography if complications arise. Roux-en-Y hepaticojejunostomy with formation of a 50-cm Roux loop is generally the preferred technique for biliary reconstruction in extrahepatic biliary atresia, sclerosing cholangitis, segment grafts, small donor bile duct size, significant donor-to-recipient bile duct size discrepancy, cholangiocarcinoma, and cases of re-transplantation (Fig. 4.1.4).

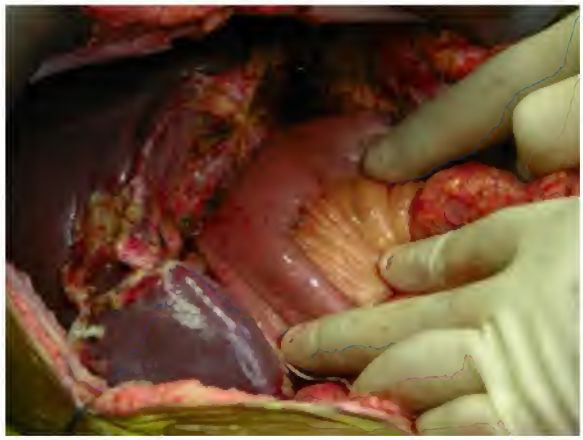

Fig. 4.1.4. Roux-en-Y hepaticojejunal anastomosis

Early biliary complications are usually technical in origin. Anastomotic leak following Roux-en-Y hepaticojejunostomy or primary duct-to-duct anastomosis can occur due to poor surgical technique, high steroid use, or ischaemic injury. Biliary strictures, which can be anastomotic or non-anastomotic in nature, may be technical in origin, but also occur secondary to graft preservation injury, donor/recipient blood group incompatibility, intraoperative injury to the bile duct blood supply, or postoperative hepatic artery thrombosis or stenosis leading to extrahepatic bile duct necrosis, bile leak, bile peritonitis and sepsis (Figs. 4.1.5, 4.1.6). Other complications following Roux-en-Y hepaticojejunostomy include postoperative haemorrhage, particularly if there is residual portal hypertension, and Roux loop perforation with peritonitis.

A T-tube can be employed to stent a duct-to-duct anastomosis, but is associated with complications in 10%–28% of cases. Adverse events include early dislodgement of the tube with leak, obstruction of the tube, cholangitis, or leak after inadvertent or planned removal. We have a selective policy of T-tube insertion when there is a significant size disparity between donor and recipient bile ducts, right lobe split liver grafts, living donor right lobe grafts, and following re-operation for bile leak with revision of the duct-to-duct anastomosis (Fig. 4.1.6). The T-tube is clamped at day 7 to 10 days postoperatively if clinical parameters and liver function tests are normal. A cholangiogram is performed at 3 months, with T-tube removal if all parameters are normal. Biliary leak following removal can be managed by observation, endoscopic placement of stents or nasobiliary catheters, or surgery. An internal stent can also be used with both duct-to-duct anastomosis and Roux-en-Y hepaticojejunostomy, but removal requires endoscopy. Disadvantages include obstruction of a small duct, stasis and ascending infection, and removal may be difficult predisposing to further complications.

Bile leak with resultant biloma and intra-abdominal infection with abscess formation can occur following reduced-sized, split and living related liver transplantation due to leak from the parenchymal cut-surface or inadvertent bile duct injury. Biliary reconstruction is by Roux-en-Y hepaticojejunostomy, and may involve two anastomoses at implantation of the left lateral segment at split or living related liver transplantation if segment II and III ducts are sepa-

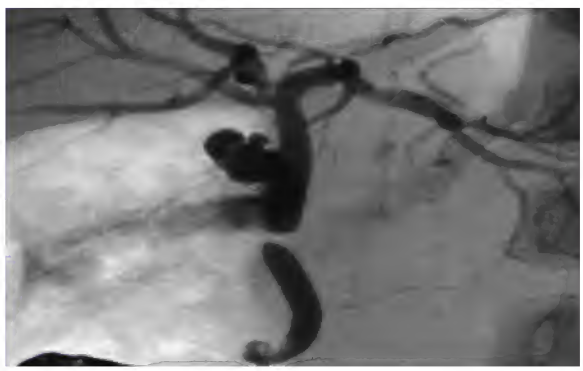

Fig. 4.1.5. Anastomotic biliary stricture

Fig. 4.1.6. Apparent anastomotic biliary stricture due to donor-to-recipient bile duct diameter discrepancy

rate. Biliary complications following living related liver transplantation can also occur due to damage to residual ducts, hepatic duct stump leak and arterial injury. The majority of cut surface leaks settle with conservative management over 4–6 weeks, but radiological guided drainage, biliary stent placement at endoscopic retrograde cholangiopancreatography (ERCP), or surgical exploration with drainage and/or reconstruction may be required.

4.1.5 Long-Term Follow-Up: Late Complications

The majority of complications following transplantation occur during the first 6 months. Late complications include vascular, biliary and immunological complications, and recurrence of primary disease (Table 4.1.4). Late hepatic artery thrombosis occurring more than 6 months after transplantation accounts for approximately 10% of late graft losses. Presentation is often subtle with mild liver dysfunction, late biliary stricture, recurrent low-grade cholangitis, bacteremia, or changes of centrilobular cell loss on liver biopsy. Some patients may present with significant complications including intrahepatic biliary necrosis, biloma, and intrahepatic abscess formation. The majority of patients settle with conservative management as collateral vessels form which reconstitute the hepatic arterial blood supply. However, re-transplantation is required if serious complications such as necrosis and/or sepsis develop.

Late portal vein thrombosis can occur, presenting with clinical features of portal hypertension, such as variceal haemorrhage. Increasing splenomegaly may be identified on follow-up ultrasound scan post-transplant. Portal hypertension may be due to technical shortcomings resulting in portal vein stenosis, or to other factors such as late rejection, portal pyaemia particularly from the biliary tree, or the development of nodular regenerative hyperplasia of the graft. Early and late portal vein thrombosis and stenosis are more common in the paediatric transplant population after segmental transplantation. Measurement of splenic size can be used as a guide to the continuing presence or development of portal hypertension following transplantation. The majority of cases can be managed conservatively as a sufficient venous collateral circulation develops. Patients with nodular regenerative hyperplasia present approximately 5 years following transplantation, and in severe cases may have ascites, oedema and bleeding oesophageal varices (Fig. 4.1.7). Radiological imaging reveals multiple hyperplastic parenchymal nodules with no evidence of perinodular fibrosis. Rarely, some of these patients develop progressive graft failure requiring re-transplantation.

Complications involving the vena cava are rare, and are usually technical in origin. Suprahepatic caval stenosis presents with hepatic outflow obstruction with lower trunk and leg oedema, portal hypertension, ascites and renal impairment. If suspected, the investigations of choice are Doppler ultrasonography, and cavography with pressure studies. The diagnosis is confirmed by the presence of a significant gradient across the stenosis. Management options include percutaneous dilation and/or caval stenting. Caval stenosis may be asymptomatic and should be excluded as a cause of graft dysfunction in patients who have undergone re-transplantation.

Anastomotic and non-anastomotic biliary strictures can develop. The majority present more than 4 weeks after surgery. Aetiological factors include injury to the vascular supply of the donor and recipient ducts, size mismatch and surgical technique. Patients may present asymptomatically with a rise in cholestatic liver enzymes or bile duct dilation on ultrasonography, with non-specific symptoms, jaundice, or cholangitis. Ultrasonography is used as a screening tool if a biliary stricture with obstruction is suspected. However, it is often of limited value as bile duct dilatation may be absent. If a T-tube is in situ, a T-tube cholangiogram can be performed. If there is a high index of suspicion in the

Fig. 4.1.7. Nodular regenerative hyperplasia in an explanted liver

presence of a negative ultrasound scan or to acquire further anatomical detail, we perform an magnetic resonance cholangiopancreatogram (MRCP) as the next investigation of choice. Selective invasive imaging procedures with ERCP or percutaneous transhepatic cholangiography can then be attempted if an end-to-end duct-to-duct anastomoses was performed with intervention in the form of balloon dilation or stenting as appropriate (Fig. 4.1.5). Following Roux-en-Y hepaticojejunostomy, percutaneous transhepatic cholangiography or radionucleotide scan are options. Management choices include endoscopic balloon dilatation with or without an endoprosthesis, or surgical intervention. Biliary reconstructive surgery with a Roux-en-Y hepaticojejunostomy is indicated if the stricture is limited to the extrahepatic biliary tree in a patient with persistent allograft dysfunction following failed endoscopic therapy.

Non-anastomotic biliary structures have a less satisfactory outcome, with approximately 50% requiring re-transplantation, with a mortality approaching 30% (Hesselink et al. 1987). Hepatic artery thrombosis has been documented in 89% of those with non-anastomotic contrast leak, 57% with a non-anastomotic stricture and 10% of those with an anastomotic stricture following transplantation (Zajko et al. 1987). In a recent study from our department, graft function returned to normal in 18%, improved in 36%, but remained abnormal in 45% of patients after Roux-en-Y hepaticojejunostomy for bile duct strictures (Sutcliffe et al. 2004). Four patients subsequently underwent re-transplantation. Hepaticojejunostomy was more likely to yield a favourable outcome if performed within 2 years of transplantation, as prolonged biliary obstruction was associated with advanced graft fibrosis. Surgery should be reserved for selected patients without histological evidence of moderate to severe graft fibrosis or significant non-biliary pathology (Sutcliffe et al. 2004). Anastomotic stricture with ascending cholangitis and prolonged obstruction leading to secondary biliary cirrhosis can occur. Late complications following Roux-en-Y hepaticojejunostomy biliary reconstruction include bowel obstruction due to adhesional obstruction of the afferent limb of the Roux loop or small bowel, and internal herniation.

Non-anastomotic biliary strictures occur secondary to hepatic artery thrombosis or stenosis, preservation injury, ABO blood group incompatibility, and chronic ductopenic rejection. They are frequently multiple. Isolated non-anastomotic strictures of the donor extra-hepatic or intra-hepatic biliary tree may be managed with endoscopic dilation and stenting. Following preservation injury complex bile pathology develops with multiple strictures, bile lakes and abscesses, and invariably results in the need for re-transplantation.

Late episodes of acute rejection are uncommon, and usually relate to poor patient compliance or inadequate levels of immunosuppression. The pathophysiology of chronic rejection is poorly understood, and can lead to graft loss. The incidence of chronic rejection has fallen progressively to approximately 5% over the past 10 years. Over-immunosuppression can lead to opportunistic bacterial infections and increased incidence of malignant disorders. Opportunistic infections such as legionellosis, nocardiosis, and tuberculosis occur between the 1st and l2th month post-transplant. Immunosuppressive treatment can be associated with Epstein Barr virus infection, and the development of post-transplantation lymphoproliferative disorder (Fig. 4.1.8).

Graft loss may occur due to recurrence of the primary disease, particularly hepatitis C virus and primary sclerosing cholangitis. Recurrence of primary sclerosing cholangitis is suspected if radiological imaging suggests intrahepatic and/or extrahepatic biliary structuring, beading and irregularity >90 days post-transplant (Graziadei et al. 1999). Histological features include fibrous cholangitis and/or fibro-obliterative lesions with or without ductopenia, biliary fibrosis, or biliary cirrhosis (Graziadei et al. 1999).

Fig. 4.1.8. Representative axial computed tomography images demonstrating extensive retrogastric and paraaortic lymphadenopathy following liver transplantation indicating post-transplantation lymphoproliferative disease

4.1.6 Conclusions

Appropriate patient selection, improved preoperative staging of disease, standardization of surgical techniques, and early diagnosis and management of postoperative complications have resulted in improved survival rates following liver transplantation in association with advances in organ preservation and immunosuppressive regimes. Close cooperation between hepatologists, intensive care physicians, surgeons and radiologists has significantly improved outcome, and will continue to promote further advances in this evolving field of transplantation.

References

Abdalla EK, Denys A, Chevalier P, Nemr RA, Vauthey JN (2004) Total and segmental liver volume variations: implications for liver surgery. Surgery 135:404–410

Busuttil RW, Lake JR (2004) Role of tacrolimus in the evolution of liver transplantation. Transplantation 77: S44–S51

Falchetti D, de Carvalho FB, Clapuyt P, de Ville de Goyet, de Hemptinne B, Claus D, Otte JB (1991) Liver transplantation in children with biliary atresia and polysplenia syndrome. J Pediatr Surg 5:528–531

Gonzalez et al. (1993)

Graziadei IW, Wiesner RH, Batts KP, Marotta PJ, LaRusso NF, Porayko MK, Hay E, Gores GJ, Charlton MR, Ludwig J, Poterucha JJ, Steers JL, Krom RAF (1999) Recurrence of primary sclerosing cholangitis following liver transplantation. Hepatology 29:1050–1056

Hesselink EJ, Slooff MJH, Schuur KH, Bijleveld CH, Gips CH (1987) Consequences of hepatic artery pathology after orthotopic liver transplantation. Transplant Proc 19:2476–2477

Higashiyama H, Yamaguchi T, Mori K, Nakano Y, Yokoyama T, Takeuchi T, Yamamoto N, Yamaoka Y, Tanaka K, Kumada K (1993) Graft size assessment by preoperative computed tomography in living related partial liver transplantation. Br J Surg 80:489–492

Hoffman et al. (1989)

Kawasaki S, Makuuchi M, Matsunami H, Hashikura Y, Ikegami T, Nakazawa Y, Chisuwa H, Terada M, Miyagawa S (1998) Living related liver transplantation in adults. Ann Surg 227:269–274

Langnas AN, Marujo W, Stratta RJ, Wood RP, Shaw BW Jr (1991) Vascular complications after orthotopic liver transplantation. Am J Surg 161:76–82

Llovet JM, Schwartz M, Mazzaferro V (2005) Resection and liver transplantation for hepatocellular carcinoma. Semin Liver Dis 25(2):181–200

Lo CM, Fan ST, Liu CL, Chan JK, Lam BK, Lau GK, Wei WI, Wong J (1999) Minimum graft size for successful living donor liver transplantation. Transplantation 68:1112–1116

Mazzaferro V, Regalia E, Doci R, Andreola S, Pulvirenti A, Bozzetti F, Montalto F, Ammatuna M, Morabito A, Gennari L (1996) Liver transplantation for the treatment of small hepatocellular carcinomas in patients with cirrhosis. N Engl J Med 334(11):693–699

Pugh RNH, Murray-Lyon IM, Dawson JL et al (1973) Transection of the oesophagus for bleeding oesophageal varices. Br J Surg 60:646–649

Raynor et al. (1988)

Starzl TE, Marchioro TL, Von Kaulla K et al (1963) Homotransplantation of the liver in humans. Surg Gynecol Obstet 117:659–676

Sutcliffe R, Maguire D, Mroz A, Portmann B, O'Grady J, Bowles M, Muiesan P, Rela M, Heaton N (2004) Bile duct strictures after adult liver transplantation: a role for biliary reconstructive surgery? Liver Transpl 10(7):928–934

Tucker ON, Heaton N (2005) The "small for size" liver syndrome. Curr Opin Crit Care 11(2):150–155

Vauthey JN, Chaoui A, Do KA, Bilimoria MM, Fenstermacher MJ, Charnsangavej C, Hicks M, Alsfasser G, Lauwers G, Hawkins IF, Caridi J (2000) Standardized measurement of the future liver remnant prior to extended liver resection: methodology and clinical associations. Surgery 127:512–519

Yao FY, Ferrell L, Bass NM, Watson JJ, Bacchetti P, Venook A, Ascher NL, Roberts JP (2001) Liver transplantation for hepatocellular carcinoma: expansion of the tumor size limits does not adversely impact survival. Hepatology 33(6):1394–1403

Yao FY, Ferrell L, Bass NM, Bacchetti P, Ascher NL, Roberts JP (2002) Liver transplantation for hepatocellular carcinoma: comparison of the proposed UCSF criteria with the Milan criteria and the Pittsburgh modified TNM criteria. Liver Transpl 8(9):765–774

Zajko AB, Campbell WL, Logsdon GA, Bron KM, Tzakis A, Esquivel CO, Starzl TE (1987) Cholangiographic findings in hepatic artery occlusion after liver transplantation. AJR Am J Roentgenol 149(3):485-489

4.2 Imaging of Liver Transplantation

Giulia A. Zamboni, Ivan Pedrosa, Jonathan B. Kruskal, and Vassilios Raptopoulos

CONTENTS

4.2.1 Introduction

Liver transplantation is an effective and definitive treatment for patients with end-stage liver disease for which no other satisfactory therapy is available. The many improvements in surgical technique and post-operative care, as well as the use of locoregional treatments to control tumor progression in hepatocellular carcinoma (HCC) patients, have increased the number of patients that are eligible for transplantation. The critical shortage of cadaveric livers has led to the use of living-donor liver transplantation. Living-donor liver transplantation was introduced in the late 1980s to address the shortage of organs for infants and children and has since gained widespread application. Adult-to-infant transplantation uses the left lateral segment, or the left lobe, which has a volume sufficient to sustain metabolic function in the recipient, and allows the donor to retain a larger volume of functional liver. The volume of the left lobe, however, is not sufficient for adult-to-adult transplantation, therefore the right lobe is harvested, and the equilibrium between the transplanted volume and the volume remaining to the donor is very delicate and crucial. Donor safety is a primary concern, and preoperative imaging plays a crucial role in donor selection and workup, providing information on liver parenchyma and vasculature anatomy and reducing surgical and post-surgical morbidity and mortality.

G. A. Zamboni, MD
I. Pedrosa, MD
J. B. Kruskal, MD, Professor
V. Raptopoulos, MD, Professor
Department of Radiology, Beth Israel Deaconess Medical Center, 330 Brookline Avenue, Boston, MA 02215, USA

4.2.2 Surgical Anatomy

- Segments
- Conventional vascular anatomy: arteries, portal and hepatic veins
- Biliary anatomy

Couinaud's surgical anatomy is based on the liver's portal and hepatic venous systems. The liver is divided by oblique-vertical planes defined by the three hepatic veins and a transverse plane through the right and left main portal branches. The middle hepatic vein

runs in the main portal fissure (Cantlie's line), which extends from the inferior vena cava to the gallbladder fossa, and divides the right and left liver. Segment I is the caudate, or Spiegel, lobe. The left hepatic vein divides the left liver into a larger paramedian sector, which includes segments III and IV, and a smaller lateral sector, including segment II. The left portal vein divides segment II from segment III and divides segment IV, which lies between the left hepatic vein and the main lobar fissure, into segments IVa (superior) and IVb (inferior). The right lobe is divided into four segments by the right hepatic vein and the right portal vein: segments V (right anteroinferior), VI (right posteroinferior), VII (right posterosuperior) and VIII (right anterosuperior) (Fig. 4.2.1).

I: caudate/Spiegel lobe
II: left posterolateral segment
III: left anterolateral segment
IVa: left superomedial segment
IVb: left inferomedial segment
V: right anteroinferior segment
VI: right posteroinferior segment
VII: right posterosuperior segment
VIII: right anterosuperior segment

The surgical line for right-lobe harvesting in living-donor liver transplantation runs 1 cm right of the middle hepatic vein and parallel to Cantlie's line, and corresponds to a relatively avascular plane (Deshpande et al. 2002; Erbay et al. 2003). For left lateral segment transplantation, the transection is performed along the main lobar fissure.

Although conventional vascular and biliary anatomy have been described, there are many variants which may be present more or less often.

In the conventional arterial anatomy of the liver, the common hepatic artery originates from the celiac trunk (Fig. 4.2.2). From the common hepatic artery arise the left gastric, gastroduodenal and proper hepatic arteries. The hepatic artery divides at the hepatic hilum into the right and left branches. The middle hepatic artery supplies the medial seg-

Fig. 4.2.2. Volume-rendered CT image of conventional hepatic arterial anatomy. The common hepatic artery (*1*) originates from the celiac axis and, after the origin of the gastroduodenal artery (*5*), becomes the proper hepatic artery (*2*). The proper hepatic artery divides into the left (*3*) and right (*4*) hepatic artery

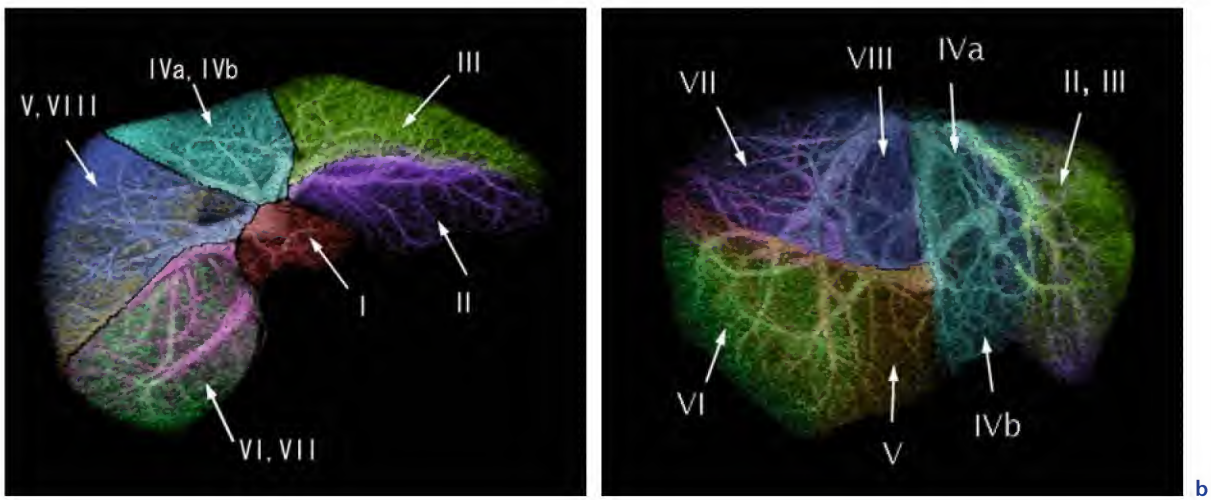

a b

Fig. 4.2.1a,b. 3D volume rendering (*VR*) of a liver with virtually divided and colored segments along vascular landmarks. **a** Inferior and **b** antero-posterior views. The middle hepatic vein divides left and right liver, while the portal vein divides superior and inferior regions

ment of the left liver (segment IV), and is usually a branch of the left hepatic artery or of the proper hepatic artery (Table 4.2.1; MICHELS 1966).

The portal vein bifurcates at the hilum into left and right pedicles (Fig. 4.2.3). The left pedicle divides into three branches for segments II, III, and IV. The right pedicle divides into anterior and posterior branches, which both bifurcate into ascending and descending branches, which supply the segments V–VIII.

Conventionally there are three hepatic veins (Fig. 4.2.4). The right hepatic vein is formed by the confluence of an anterior trunk (from segments V and VI) and a posterior trunk (from segment VII). The middle hepatic vein runs along Cantlie's line (main portal fissure) and drains the central sector of the liver: segment IV on the left and segments V and VIII on the right. The left hepatic vein arises from the confluence of a transverse vein (from segment II) and a sagittal vein (from segment IV). In 85% of

Table 4.2.1. Variants of arterial anatomy of the liver according to MICHELS (1966)

MICHELS classification of hepatic arterial anatomy		Frequency of occurrence (%)
I	Normal anatomy: proper hepatic artery originates from common hepatic artery and divides into left and right hepatic arteries	55
II	Replaced left hepatic artery arising from left gastric artery	10
III	Replaced right hepatic artery arising from superior mesenteric artery	11
IV	Replaced left hepatic artery and right hepatic artery	1
V	Accessory left hepatic artery arising from left gastric artery	8
VI	Accessory right hepatic artery arising from superior mesenteric artery	7
VII	Replaced left hepatic artery and right hepatic artery	1
VIII	Replaced right hepatic artery with accessory left hepatic artery or replaced left hepatic artery with accessory right hepatic artery	4
IX	Proper hepatic artery arising from superior mesenteric artery	4.5
X	Proper hepatic artery arising from left gastric artery	0.5

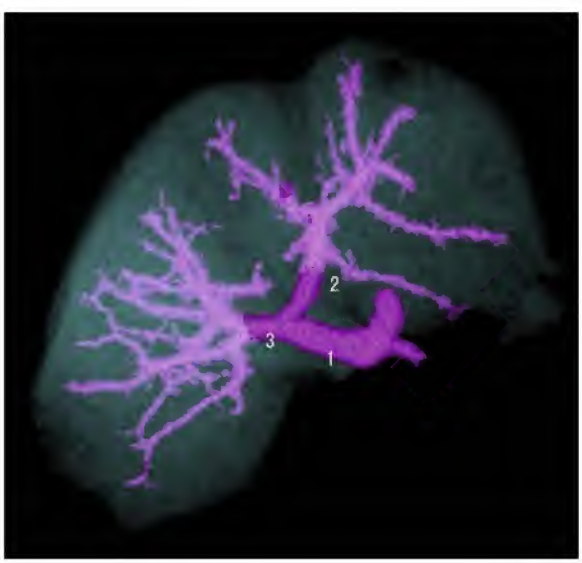

Fig. 4.2.3. Volume-rendered CT image of conventional portal vein anatomy. The main portal vein (*1*) originates from the confluence of the superior mesenteric and splenic veins, and bifurcates into the left (*2*) and right (*3*) portal veins

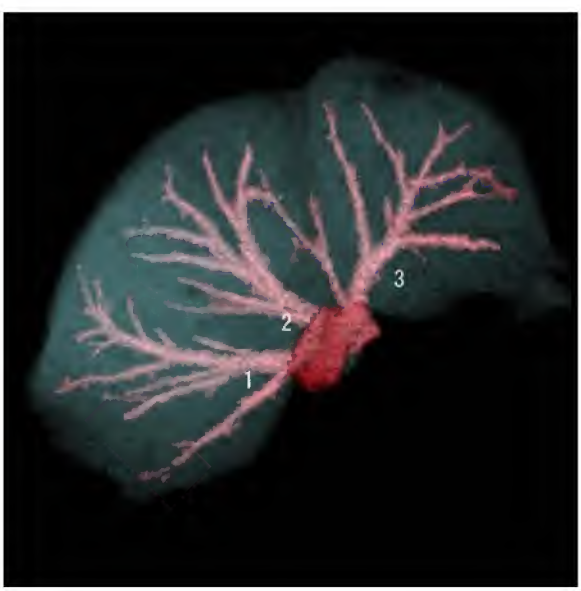

Fig. 4.2.4. Volume-rendered CT image of conventional hepatic vein anatomy: right (*1*), middle (*2*), and left (*3*) hepatic veins

Table 4.2.2. Biliary anatomy variants

Biliary anatomy (from Smadja and Blumgart 1994)		Frequency of occurrence (%)
A	Normal anatomy	57
B	Trifurcation of the common bile duct into right anterior, right posterior and left hepatic duct	12
C	Aberrant drainage of right segmental ducts into the common hepatic duct	20
D	Aberrant drainage of right segmental ducts into the left hepatic duct	6
E	Absence of hepatic duct confluence, two or more ducts from each lobe converge to form the common hepatic duct	3
F	Absence of right hepatic duct with ectopic drainage of right posterior duct into the cystic duct	2

cases the middle and left hepatic veins form a common trunk. (Deshpande et al. 2002).

A short vertical right hepatic duct and a longer horizontal left duct usually join at the hilum to form the common hepatic duct. The right duct is formed by fusion of the right anterior (from segments V and VIII) and posterior (from segments VI and VII) sectoral ducts. The left duct is formed by the fusion of the ducts from segments II and III. Segment IV most commonly drains into the left hepatic duct (Table 4.2.2). However, the biliary tree follows the conventional anatomy only in little more than half of the population.

4.2.3 Imaging Modalities

- CT
- MRI
- US

Imaging has a fundamental role in all phases of liver transplantation, and different modalities are used in combination to optimize the screening, preoperative and postoperative evaluation of the recipient and, for living-donor liver transplantation, of the donor.

For the screening of patients awaiting liver transplantation, computed tomography (CT), magnetic resonance imaging (MRI) and ultrasonography (US) have been advocated (Berry and Sidhu 2004; Chu et al. 2005; Goyen et al. 2002; Kamel et al. 2000; Mortele et al. 2003; Schroeder et al. 2005; Yeh et al. 2004).

For the preoperative evaluation of both donors and recipients, because of the high prevalence of vascular variants, accurate display of the vascular and biliary anatomy is fundamental and can be obtained with CT or MRI. CT is more commonly used because it is widely available, quicker and less expensive (Ishifuro et al. 2002; Kamel et al. 2000, 2001a; Kruskal and Raptopoulos 2002). A major disadvantage of CT is the lack of easy depiction of the biliary anatomy. Recently, however, the use of CT biliary contrast agents has been shown to markedly improve visualization of the biliary anatomy (Schroeder et al. 2006; Yeh et al. 2004). MRA can be used when there are contraindications to the use of iodinated contrast media, and magnetic resonance cholangiopancreatography (MRCP) can accurately depict the biliary anatomy (Lim and Park 2004; Sahani et al. 2004a).

US can be used intraoperatively for optimal surgical guidance.

For postoperative evaluation of donors and recipients, gray-scale and Doppler US are the initial imaging modalities used because US is cost-effective, avoids the use of ionizing radiation, and can be performed at the patient's bedside and repeatedly. When complications occur, patients can be further imaged with CT or MRI. Microbubble contrast has been reported to improve the detection of hepatic vessels when they are poorly or not visualized or when patency is suspect, and may be useful in the assessment of parenchymal complications and neoplastic disease recurrence (Berry and Sidhu 2004).

CT and MRI can be used to follow up parenchymal regeneration in both donors and recipients, allowing for evaluation of the liver volume over time (Kamel et al. 2003). US and CT can provide optimal guidance for interventional therapeutic procedures for complications.

With the advent of MDCT angiography and MRA, catheter angiography is rarely used for surgical planning, but maintains its role in interventional therapy for complications.

4.2.4 Recipients

4.2.4.1 Preoperative Imaging

- Imaging protocols
- Volume
- Hepatoma
- Portal vein thrombosis and varices
- Pertinent vascular variants
  - Hepatic artery
  - Portal vein
  - Hepatic veins

For the preoperative evaluation of potential liver transplant recipients in our institution we perform a multiphasic multidetector CT study, which enables the evaluation of parenchyma and accurate assessment of the arterial, portal venous and hepatic venous anatomy. Oral milk or water (500 ml) is used to opacify the proximal bowel. After a non-intravenously enhanced scan is performed, 200 ml of non-ionic 350 mg I/ml contrast material is administered intravenously at a 5 ml/s rate. The high iodine concentration allows better visualization of the veins. Acquisition timing is guided by bolus tracking in the aorta (enhancement threshold: 200 HU): a late arterial phase scan is initiated 10 s after the threshold is reached, then a venous phase (late portal-hepatic venous) scan is initiated with a 45-s delay from threshold; a delayed acquisition is performed after 3 min.

MR imaging is a good alternative to MDCT in those cases with contraindications to iodinated contrast (i.e., allergy). Our MR liver protocol is detailed in Table 4.2.3. Surface coils provide a superior signal-to-noise than that of the body coil embedded in

Table 4.2.3. MRI of the liver: imaging protocol[a]

Sequence	T1W IP/OOP	SSFSE/HASTE	MRCP	T2W FrFSE	TOF	LAVA
Type	SPGRE	Spin echo	Spin echo	Spin echo	SPGRE	SPGRE
Orientation	Axial	Coronal/axial	Coronal	Axial	Oblique axial	Axial
TR	175	Minimum	Minimum	2200	30	4.2
TE	2.3/5.4	60	600	84	4.7 (Min full)	1.7
Flip angle	80	155	155	180	45	10
Number of excitations	1	1	1	1	1	1
2D/3D	2D	2D	2D	2D	2D	3D
Slice thickness (mm)	8	5/4	60	7	5	4.2 (before interpolation)
Gap (mm)	2	0	–	2	10	0
Field of view	350	360/350	240	350	350	360
No. Partitions/slices	20	16	3–5	22	5	80
Phase·Freq steps	160·256	192·256	256·384	160·320	128·256	192·256
Rectangular field of view	0.75	1/0.75	1	0.75	0.75	0.75
Fat suppression	No	No	Yes	Yes	No	Yes
Echo train length	–			15	–	–
Bandwidth (kHz)	62.50	62.50	62.50	31.25	31.25	62.50

[a]1.5 T General Electric platform

the MR scanner. We do not routinely administer oral contrast material in the evaluation of liver pathology. Breath-hold imaging acquisitions reduce the total examination time and eliminate respiratory-related artifacts. A combination of T1- and T2-weighted images is obtained, followed by a dynamic acquisition during the arterial, portal venous, and delayed venous phases.

The CT scan allows accurate measurement of liver volume, which is important in assigning priority to transplant candidates: transplantation is more urgent in cirrhotic patients with small livers, who have the poorest function (Redvanly et al. 1995). The liver is isolated from surrounding structures of similar attenuation by hand-tracing, performed with a frequency dependent on the change in liver contour (Fig. 4.2.5). Usually, hand-tracing can be performed every 3–4 mm in the upper half of the liver, and every 5–6 mm in the lower half, allowing automatic interpolation between the hand-traced images (Kamel et al. 2001c). Large vessels (e.g., the inferior vena cava and extrahepatic portal vein) and major fissures (e.g., the fissure for the ligamentum teres) should be excluded. Kamel et al. (2001c) has demonstrated that the volume thus measured is well correlated to graft weight (r=0.898–0.879).

The parenchyma must be carefully screened for the presence of primary or secondary malignant disease. Most patients awaiting transplantation are cirrhotic, with a high risk of developing hepatoma, and as many as 20% of these patients will develop HCC (Fig. 4.2.6). Patients diagnosed with small hepatic cancer are moved up the transplantation list. On the basis of the natural doubling time of hepatoma, it has been suggested that patients on a transplantation list undergo screening every 6 months. Currently, the generally accepted criteria (Milan criteria; Mazzaferro et al. 1996) for transplantation in HCC patients consist of the presence of one nodule smaller than 5 cm or up to three nodules each smaller than 3 cm in the absence of detectable vascular invasion. Expansion of these criteria has been proposed, but there is no consensus yet. The sensitivity of cross-sectional imaging techniques for the detection of HCC prior to liver transplantation is variable depending on the imaging protocol and the type of pathological correlation used (Eubank et al. 2002; Krinsky et al. 2001,

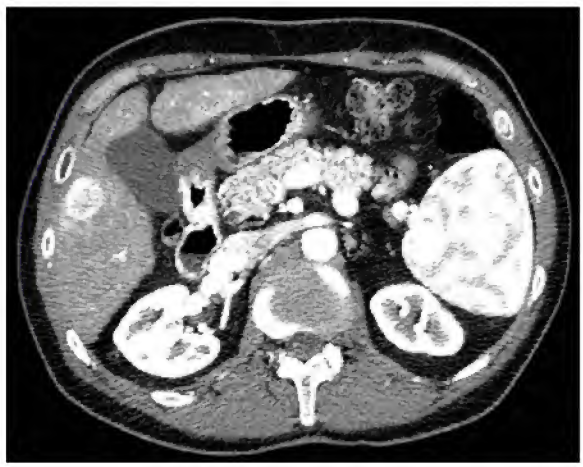

Fig. 4.2.6. A 65-year-old patient with hepatitis C and cirrhosis, awaiting liver transplantation. Multiphasic CT scan in the late arterial-early portal venous phase demonstrates a 2.3×2.3 cm hypervascular lesion in segment VI, compatible with a hepatoma

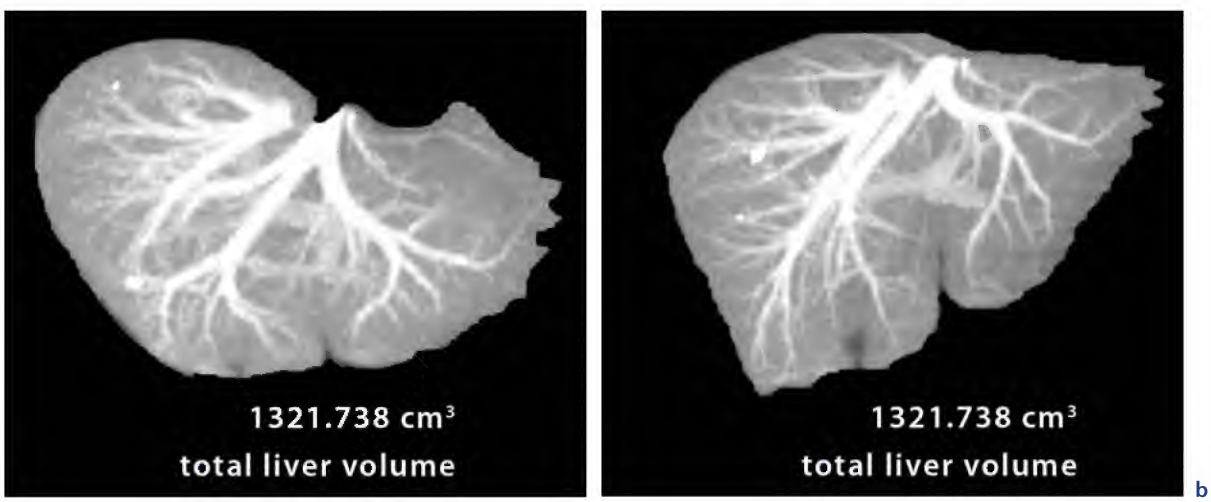

a b

Fig. 4.2.5a,b. MIP rendering of CT angiography allows accurate assessment of the liver volume

2002; Mori et al. 2002; Rode et al. 2001; Teefey et al. 2003). The reported sensitivities for CT in the detection of hepatoma range between 88% and 94%, with specificities ranging from 96% to 99% (Jang et al. 2000; Kang et al. 2003; Lim and Park 2004). A superior sensitivity of MR compared to CT and US has been reported (Eubank et al. 2002; Mori et al. 2002; Rode et al. 2001); Teefey et al. (2003) reported a superior sensitivity of US compared to MR and CT on a lesion-per-lesion basis. However, the MR protocol in this study included dynamic imaging with a 2D approach using an 8 mm slice thickness with a 2 mm interslice gap. The use of high-resolution thin-slice (2–4 mm slice thickness) dynamic MR imaging is crucial in the evaluation of the cirrhotic liver as many of the HCCs are small in size (Holland et al. 2005; Krinsky et al. 2001). The reported sensitivities for SPIO-enhanced MR imaging are 84.7% and 94.7%, on a per-lesion and a per-patient basis, respectively (Kim et al. 2006a). MRI can be used when there are contraindications to CT. For contrast-enhanced US, 96.4% sensitivity and 87.5% specificity have been reported (Nicolau et al. 2004).

Preoperative imaging can also demonstrate additional findings, for example abdominal aorta aneurysm, cholelithiasis, renal cell carcinoma, and others such as renal parenchyma disease or signs of metabolic disease that may require additional treatment (Fig. 4.2.7).

Fig. 4.2.7. Oxalosis. A 55-year-old male, affected by primary oxalosis, awaiting liver and kidney transplantation (Cochat et al. 1999). Non-intravenously enhanced CT scan demonstrates bilateral diffuse parenchymal calcification involving the cortex and medullary regions of the kidneys (nephrocalcinosis), consistent with the patient's history of oxalosis

Preoperative imaging of the liver transplant recipient should depict in detail the relevant vasculature anatomy, and reveal the presence of variants that are important for surgical planning (Table 4.2.4; Erbay et al. 2003). The most common arterial variants that are relevant in potential liver transplant recipients include replaced or accessory hepatic arteries from the superior mesenteric artery. A replaced

Table 4.2.4. Prevalence of vascular variants (adapted, from Erbay 2003)

Variants	Frequency in the population	% of all variants
Hepatic arteries	49±5	40±4
Replaced or accessory RHA	14±3	12±3
Replaced or accessory LHA	20±4	16±3
Middle artery from RHA	5±2	4±2
Other	10±3	9±3
Hepatic veins	48±5	40±5
Inferior right vein	31±5	26±4
Segment VIII vein drains to middle vein	6±2	5±2
Multiple branching	9±3	8±2
Other	2±1	2±1
Portal vein	24±4	20±4
Trifurcation	12±3	10±3
Accessory right vein	8±3	7±2
Other	4±2	3±2

Fig. 4.2.8. Coronal MIP rendering of CT angiogram shows the common hepatic artery (*arrow*) originating from the superior mesenteric artery (*arrowhead*)

(Fig. 4.2.8) or accessory (for segments V and VI; Fig. 4.2.9) right hepatic artery may originate from the superior mesentery artery or, less commonly, from the celiac axis (Fig. 4.2.10). Totally replaced common hepatic arteries originating from the superior mesenteric artery (SMA) or, even more rarely, from the aorta are rare variants; on cross-sectional imaging the replaced common hepatic artery originating from the SMA courses posterior to the portal vein. A replaced or accessory (for segments II and III) left hepatic artery, originating from the left gastric artery, on cross-sectional imaging courses along the fissure for the ligamentum venosum. The size of the recipient hepatic artery is important in planning arterial blood flow to the liver graft: a small-caliber recipient artery, 3 mm or less, or multiple small hepatic arteries supplying the liver may result in inadequate arterial supply to the graft and may require the creation of an alternative inflow source, e.g. an aortohepatic interposition graft.

Patency of the portal vein should be assessed, as portal vein thrombosis may occur in patients with end-stage cirrhosis. Portal vein thrombosis is not a contraindication to liver transplant, but requires modification of the surgical technique to create extra-anatomical venous grafts (Fig. 4.2.11).

Portal hypertension is the main cause of portal systemic collateral vessels; the most common being gastroesophageal, paraumbilical, splenorenal, and inferior mesenteric collateral vessels (Fig. 4.2.12). Pleuropericardial-peritoneal, pancreaticoduodenal, splenoazygos, and mesocaval collateral vessels are less common. The most frequent varices in patients with portal hypertension (up to 80%) are coronary collateral veins at the lesser omentum (Cho et al. 1995). For surgical planning the most important varices are those located anteriorly or in the surgical bed.

The patency of hepatic veins and the inferior vena cava should be evaluated. Transjugular intrahepatic portal-systemic shunts (TIPS), when present, should be assessed for patency and their location should be described (Fig. 4.2.13). The distal end of the TIPS should be in the right hepatic vein: when being positioned in the inferior vena cava it constitutes a contraindication to liver transplantation.

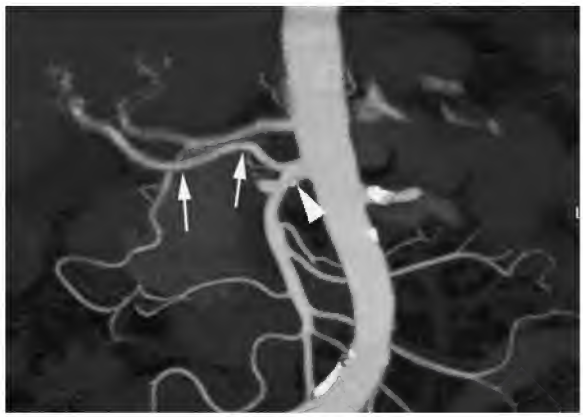

Fig. 4.2.9. Coronal MIP rendering of CT angiogram shows a replaced right hepatic artery (*arrows*) originating from the superior mesenteric artery (*arrowhead*)

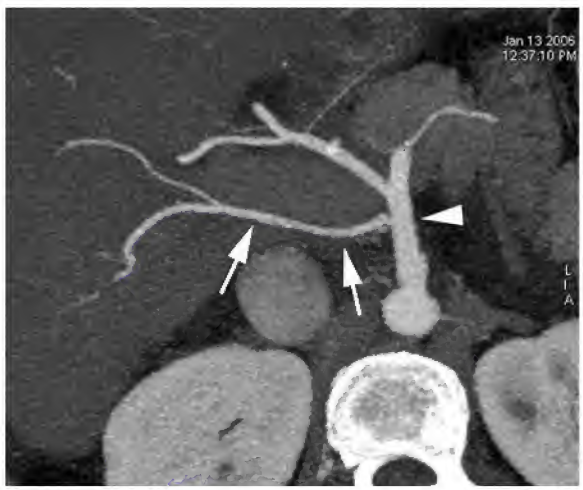

Fig. 4.2.10. Axial MIP rendering of CT angiogram shows an accessory right hepatic artery (*arrows*) originating from the celiac axis (*arrowhead*)

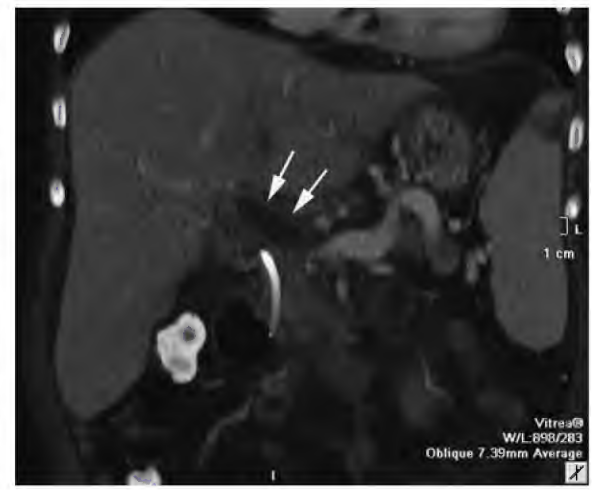

Fig. 4.2.11. Coronal MIP rendering of CT angiogram shows extensive thrombus in the occluded and distended portal vein (*arrows*)

Fig. 4.2.12. Coronal MIP rendering of CT angiogram demonstrates extensive gastroesophageal (*arrowheads*) and splenorenal (*arrows*) varices

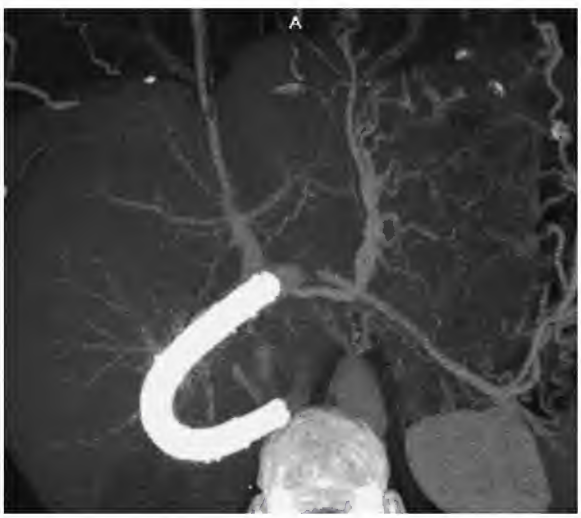

Fig. 4.2.13. Axial MIP rendering of CT angiogram allows accurate assessment of the position of the TIPS stent. The distal end of the TIPS stent is at the confluence of the right hepatic vein and inferior vena cava

The anatomy of the confluence of the hepatic veins should be described, with details on eventual anomalies. The presence of a replaced or accessory inferior right hepatic vein is important for surgical planning; its size and the distance between the main hepatic vein (at the confluence of the hepatic vein and the inferior vena cava) and the drainage site of the inferior right hepatic vein into the inferior vena cava should be carefully evaluated (Fig. 4.2.14). The presence of multiple hepatic veins draining separately into the inferior vena cava is also important for the planning of the anastomoses.

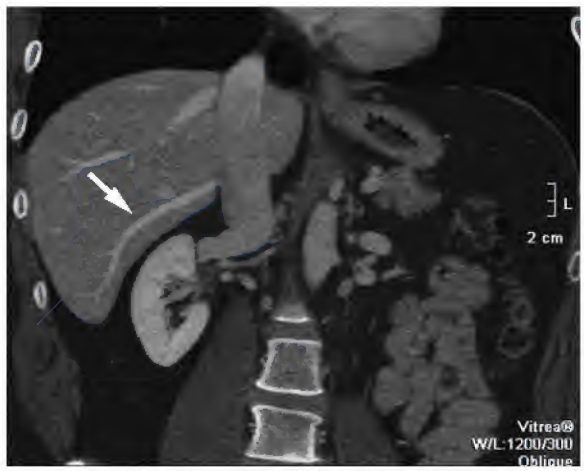

Fig. 4.2.14. Coronal MIP rendering of CT angiogram shows an accessory right inferior hepatic vein (*arrow*), draining separately into the inferior vena cava

4.2.4.2 Intraoperative Imaging

Intra-operative US

Ultrasound is used intraoperatively to assess the patency of vascular anastomoses.

4.2.4.3 Postoperative Imaging

Postoperative evaluation:

- Collections and hematomas
- Parenchymal abnormalities – rejection
- Vascular abnormalities
- Doppler US

Postoperative evaluation of the transplanted liver is routinely performed by US, with gray-scale assessment of the parenchyma and biliary tree and Doppler study of the vasculature. The normal liver transplant has a homogeneous or slightly heterogeneous pattern at US. A small amount of ascites is usually present in the early postoperative period, and commonly resolves in 7–10 days (Gemmete et al. 2006). Gas within the portal vein can be a normal finding in the early postoperative period (Federle and Kapoor 2003). Small hepatic hematomas and periportal lymphedema are also common. The appearance of hepatic hematomas on ultrasound depends on the acuity of the bleed: fresh bleeds are echogenic while 2–3 days following a bleed the appearance varies from a more solid hypoechoic appearance to that

of a multiseptated fluid collection. The bleed may be entirely intraparenchymal, subcapsular or extracapsular depending on the etiology. Periportal edema was previously considered a sign of rejection: this is no longer specific for rejection since there are many recognized causes of periportal fluid. The edema appears as fluid or low attenuation tissue encircling the main portal vein, and is often indistinguishable from postoperative fluid or even hematoma tracking up into the porta hepatis. Collections and hematomas that impair liver function or compress the hepatic vasculature require evacuation, which can be performed under US or CT guidance.

The parenchyma of the transplanted liver must be carefully assessed for the presence of abnormalities.

The differential diagnosis for diffuse parenchymal abnormalities includes rejection, ischemia, hepatitis, and cholangitis. There is no imaging finding specific for rejection, and often the only abnormal finding is heterogeneity of the liver parenchyma; the diagnosis of rejection is based on liver biopsy, which can be easily performed under US guidance.

Parenchymal heterogeneity is also present in ischemia, where it is usually accompanied by Doppler signs of arterial compromise. Recurrence of viral or autoimmune hepatitis in the transplanted liver is accompanied by biochemical evidence. Reinfection with the hepatitis C virus (HCV) occurs in nearly all patients who undergo liver transplantation for HCV cirrhosis. In the majority of patients (80%–85%) (Crossin et al. 2003), the infection does not appear to have adverse effects on the parenchyma (i.e., cirrhosis) at short-term and medium-term follow-up; long-term prognosis is still unknown. A small group of patients transplanted for HCV will develop fibrosing cholestatic hepatitis and rapidly progress to liver failure (Keeffe 2000). Cholangitis may cause diffuse parenchymal change with accompanying biliary abnormalities (Crossin et al. 2003). Other viral infections may complicate the postoperative period. In these cases, non-specific parenchymal abnormalities may be present although the diagnosis is typically performed only after biopsy (Fig. 4.2.15).

The differential diagnosis for focal liver lesions includes benign and malignant lesions (metastatic, recurrent or primary) and the parenchymal manifestations of arterial abnormalities, infarcts, and abscesses. Infarcts usually appear as round or geographic solid lesions, with central hypoechoic necrotic areas. Abscesses have thick walls and central hypoechoic areas. Infarcts and abscesses may contain intraparenchymal gas (Fig. 4.2.16).

Post-transplantation lymphoproliferative disorder has an incidence of 2%–8.4% in adult recipients, and may occur as early as 1 month after transplantation (Ben-Ari et al. 1999). It is a consequence of the chronic immunosuppression, which causes unregulated lymphoid expansion (especially of the B-cells), and it is strongly associated with Epstein-Barr virus infection. Severity of the disease ranges from benign mononucleosis to fulminant lymphoma. The most common form is the extrahepatic type, with encasement of the porta hepatis, which can be seen as hypoechoic soft tissue on US examinations.

The transplant vasculature is examined with both gray-scale and Doppler US. The most common vascular complications post liver transplantations are abnormalities involving the hepatic artery, with an incidence ranging between 4% and 25%. Risk factors for arterial complications include anastomosis to the abdominal aorta, donor arterial variants requiring multiple anastomoses, and pediatric age recipient.

The most common vascular complication is hepatic artery thrombosis, accounting for 60% of all post-transplantation vascular complications; it is associated with up to 20%–60% mortality and is the second leading cause of graft failure in the early postoperative period (Quiroga et al. 1991). Since the biliary system in the transplanted liver is only vascularized by the hepatic artery, impaired arterial supply to the graft may lead to biliary ischemia and/or necrosis. Early thrombosis can cause cholangitis, hepatic necrosis, septic shock and liver failure, and requires prompt surgical intervention. Chronic thrombosis is more benign and often not treated, as the biliary complications that it causes cannot be reversed (Gemmete et al. 2006).

Hepatic artery stenosis usually presents with elevated liver function tests or with ischemic changes in a liver biopsy. The accepted treatment for hepatic artery stenosis is balloon angioplasty.

The Doppler spectrum of the normal hepatic artery shows low vascular resistance and continuous diastolic flow: there is a rapid systolic upstroke with acceleration time inferior to 80 ms; the resistive index [(peak systolic velocity – peak diastolic velocity)/peak systolic velocity] should be between 0.5 and 0.7 (Crossin et al. 2003) (Fig. 4.2.17). Doppler criteria for diagnosing a significant hepatic artery complication are: peak systolic velocities greater than 200 cm/s, focal increase in velocity greater than threefold, resistive index less than 0.5, and acceleration time greater than 80 ms (tardus-parvus

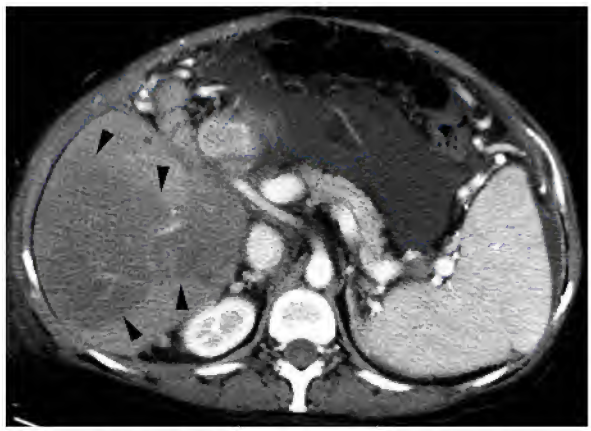

a

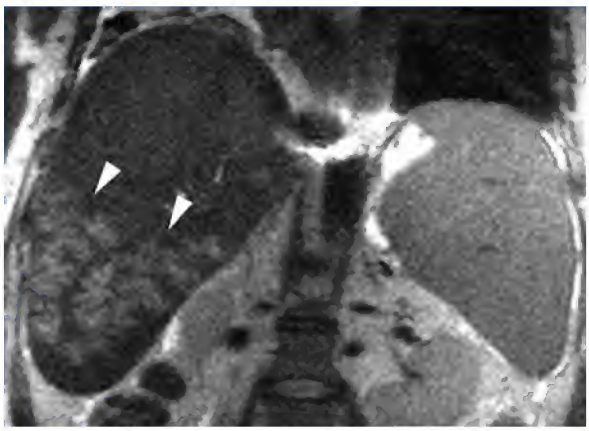

b

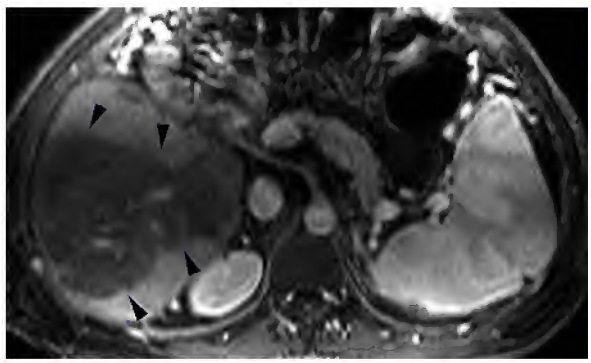

c

Fig. 4.2.15a–c. Cytomegalovirus (*CMV*) infection. A 48-year-old woman with history of ethanol abuse and cirrhosis status post living-donor right lobe liver transplant presenting with nausea, vomiting, and right lower quadrant pain. **a** Axial contrast-enhanced CT image at the level of the liver shows a large hypoenhancing area (*arrowheads*) in the liver, which does not cause mass effect or architectural distortion of the hepatic vasculature. Distinction between geographic fatty infiltration and edema/inflammation is difficult based on this finding. **b** Coronal T2-weighted single-shot fast spin echo (*SSFSE*) image shows a large heterogeneous area (*arrowheads*) of increased signal intensity in the liver. Fatty infiltration was ruled out on the basis of the imaging findings on in-phase and opposed-phase MR images (not shown). **c** Axial gadolinium-enhanced 3D fat-saturated T1-weighted gradient echo acquisition during the delayed venous phase confirms the presence of a large area with decreased enhancement (*arrowheads*) in the liver, without causing mass effect upon the hepatic vasculature. These findings were consistent with an inflammatory/ischemic process and a biopsy was recommended. Histopathologic analysis revealed hepatic necrosis secondary to acute CMV infection

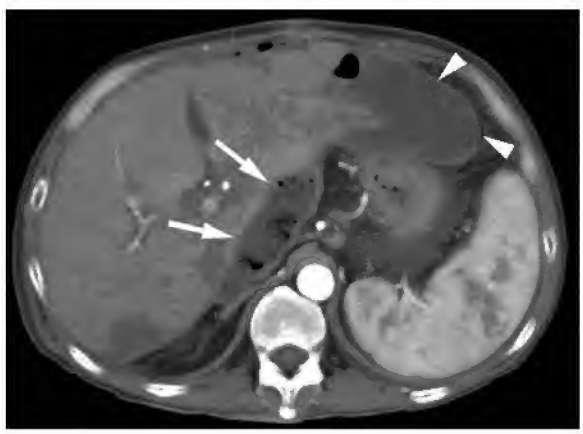

Fig. 4.2.16. A 47-year-old man with elevated alkaline phosphatase status post living-donor right hepatic lobe liver transplant and hepatic artery repair. Axial CT scan shows multifocal areas of non-enhancing liver parenchyma, consistent with infarction (*arrowheads*). On the medial edge of the liver surgical packing material (*arrows*) is seen, which simulates the appearance of a fluid collection containing gas

pattern; Crossin et al. 2003; Gemmete et al. 2006) (Fig. 4.2.18).

CT angiography (CTA) can be used in the evaluation of vascular complications (Fig. 4.2.19). Cheng et al (2004) have reported a 90% diagnostic accuracy for 3D MDCT angiography in the diagnosis of vascular complications in a pediatric population; the sensitivity and specificity were 86.7% and 100%, respectively; the positive and negative predictive values were 100% and 71.4%, respectively. Brancatelli et al (2002) have reported 100% sensitivity, 89% specificity, 95% accuracy, 92% positive predictive value, and 100% negative predictive value in an adult population.

MR angiography is very sensitive for the detection of complications in the hepatic artery although it may overestimate the amount of disease (Pandharipande et al. 2001; Stafford-Johnson et al. 1998). The sensitivity, specificity, positive predictive value, negative predictive value, and accuracy

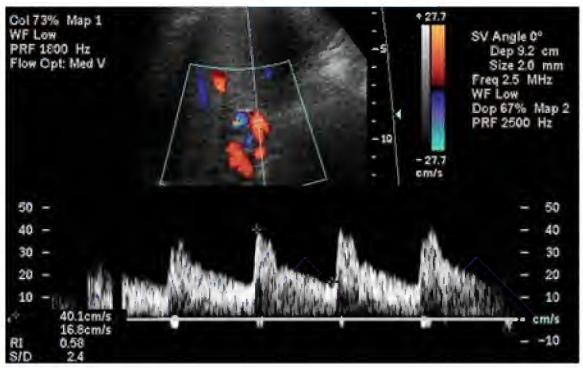

Fig. 4.2.17. Normal Doppler US waveform of the right hepatic artery, with normal resistive index (RI=0.58)

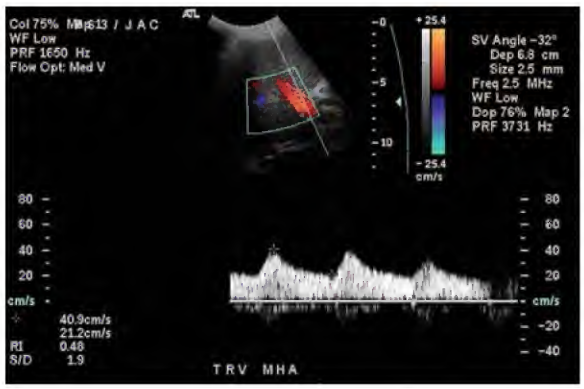

Fig. 4.2.18. Doppler US of hepatic artery stenosis showing the typical tardus-parvus waveform pattern (prolonged acceleration time, spectral broadening), with a resistive index of less than 0.5

of MR angiography in the detection of >50% stenosis or occlusion at the anastomosis are 100%, 74%, 29%, 100%, and 77%, respectively (Kim et al. 2003). Significant arterial stenosis can be reliably excluded in the presence of normal MR angiography findings (Kim et al. 2003). The diagnosis of stenosis at the anastomosis must be done with caution as metallic surgical clips may cause a pseudo narrowing of the lumen of the vessel due to susceptibility artifact. Careful review of the source MR images may help recognize this phenomenon in those cases where MIP reconstructions suggest the presence of stenosis at the anastomosis.

Lack of visualization of the hepatic artery is consistent with hepatic artery thrombosis. However, a false-positive diagnosis of hepatic artery thrombosis may result from very slow flow within this vessel. Review of the 3D dataset obtained during the portal venous phase is important when the hepatic artery is not visualized during the arterial phase to differentiate between hepatic artery thrombosis and slow flow.

A pseudoaneurysm at the anastomotic site can be seen at CTA and MRA as a round mass that enhances avidly during the arterial phase. Portions of the pseudoaneurysm may contain thrombus and therefore do not enhance after administration of contrast. Furthermore, flow within the pseudoaneurysms may be slow and hence enhancement is only appreciated during the portal or delayed venous phases.

Portal vein complications include thrombosis and stenosis, which have a 1%–2% incidence (Langnas et al. 1991) (Fig. 4.2.20).

a b

Fig. 4.2.19a,b. Axial MIP (**a**) and coronal VR (**b**) CT angiographic images show a stenosis (*arrows*) of the hepatic artery, with periportal edema and parenchymal infarcts in the left lobe (diffuse and inhomogeneously hypodense regions)

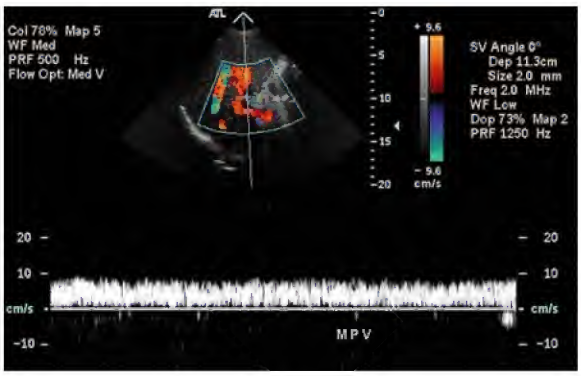

Fig. 4.2.20. Normal Doppler US of the main portal vein: flow is directed towards the liver and has normal velocity and periodicity

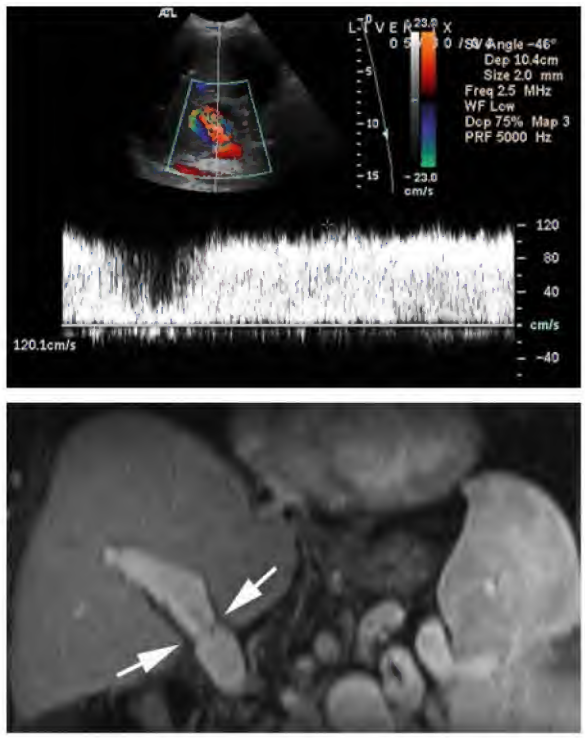

Fig. 4.2.21a,b. Mild anastomotic narrowing of the portal vein. A 50-year-old man with end-stage liver disease after orthotopic liver transplantation. **a** US color and pulsed Doppler of the right portal vein shows increased velocities within this vessel of up to 120 cm/s suggestive of proximal stenosis. **b** Coronal reconstruction of a gadolinium-enhanced 3D fat-saturated T1-weighted gradient echo acquisition during the portal venous phase shows mild narrowing of the portal vein (*arrows*) at the surgical anastomosis although there is normal enhancement of the intrahepatic portal vein. Note lack of aneurysmal dilatation of the intrahepatic portal vein, distal to the anastomosis. At catheter portography, no pressure gradient was documented in the portal vein

Portal vein thrombosis usually occurs in the early postoperative period. The portal vein may appear narrowed at US or an echogenic luminal thrombus may be recognized.

Portal vein stenosis presents with signs and symptoms of portal hypertension. US shows focal color aliasing with more than a three- to fourfold increase in velocity at the stenosis relative to the prestenotic segment.

MR imaging can be helpful to differentiate slow flow versus portal vein thrombosis in patients with inconclusive US results. TOF imaging has a sensitivity of 100% and specificity of 96% for the detection of portal vein occlusion (Finn et al. 1991). The sensitivity and specificity of gadolinium-enhanced MR for detection of portal vein stenosis are 100% and 84%, respectively, when a narrowing > 50% of its caliber is used as the diagnostic criterion (Kim et al. 2003). However, false positives are very common (Kim et al. 2003). The presence of poststenotic dilation of the portal vein, possibly caused by turbulent flow at the stenotic site, suggests long-standing severe stenosis and can help reduce the number of false-positive results (Fig. 4.2.21) (Kim et al. 2003).

Hepatic vein stenosis presents clinically with elevated liver enzymes, Budd-Chiari syndrome or coagulopathy. It is more common in segmental transplants, where it has a 4%–7% incidence (Ko et al. 2002). Ko et al. (2003) have reported that a persistent monophasic wave pattern on Doppler US is a sensitive, but not specific, finding of hepatic vein stenosis after living-donor liver transplantation (Fig. 4.2.22).

MR imaging is an excellent technique to visualize the hepatic and abdominal veins. The hepatic veins are visualized on gadolinium-enhanced MR images

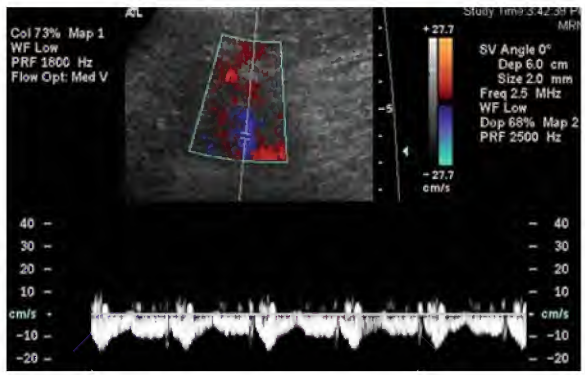

Fig. 4.2.22. Normal Doppler US of the hepatic veins demonstrating a triphasic waveform, with flow directed towards the inferior vena cava

in virtually every patient (Stafford-Johnson et al. 1998). In addition, accessory hepatic veins are readily seen on gadolinium-enhanced MR images during the delayed venous phase. MR can differentiate between stenosis and occlusion/thrombosis of the hepatic veins. In the presence of hepatic vein thrombosis, MR imaging can show abnormal increased signal intensity of the liver parenchyma in the territory drained by the occluded hepatic vein. This finding may help to estimate the amount of hepatic congestion in the occlusion of accessory hepatic veins (Fig. 4.2.23).

Inferior vena cava (IVC) complications, thrombosis and stenosis, are relatively rare (incidence lower than 1%); they are more common in the pediatric population or in cases of retransplantation. US of IVC thrombosis shows vessel narrowing or an intraluminal echogenic thrombus with no Doppler signal. IVC stenosis can occur secondary to anastomotic size discrepancy or to suprahepatic caval kinking from organ torsion. Doppler US of IVC stenosis shows a three- to fourfold increase in velocity through the stenosis compared to the prestenotic segment.

Similarly, MR imaging provides exquisite evaluation of the IVC. MR imaging can accurately detect IVC stenosis at the anastomosis. However, mild narrowing of the IVC lumen may not correlate with clinical symptoms or increased gradient at catheter venography (Stafford-Johnson et al. 1998).

Biliary complications, ischemic or non-ischemic, occur in up to 25% of transplant recipients (Letorneau and Castaneda-Zuniga 1990). Complications include leaks, strictures, stones or sludge, dysfunction of the sphincter of Oddi, malpositioning of the T-tube, and recurrent disease.

Bile leaks are usually early complications; they may originate from the anastomotic site, the cystic duct stump, the cut surface of the liver or they may be related to the T-tube (Fig. 4.2.24).

Strictures can occur at the anastomotic site, where they are caused by scar tissue, or at non-anastomotic sites, where they are most often secondary to ischemia caused by hepatic arterial lesions (Quiroga et al. 1991).

At MR imaging, the evaluation of biliary complications is based on a combination of thin-slice and thick-slab heavily T2-weighted images. Nega-

Fig. 4.2.23a-c. Right hepatic vein thrombosis. A 27-year-old female status post fulminant liver failure secondary to acetaminophen overdose followed by orthotopic liver transplant presenting now with abnormal liver function test. **a** Axial short tau inversion recovery (*STIR*) image of the upper abdomen shows abnormal increased signal intensity in the posterior aspect of the right lobe of the liver. Note the geographic appearance of the abnormal signal intensity with a sharp transition (*arrows*) between the abnormal and normal liver parenchyma suggestive of a vascular distribution of the disease process. **b** Maximum intensity projection (*MIP*) reconstruction from a gadolinium-enhanced 3D fat-saturated T1-weighted gradient echo acquisition during the delayed venous phase shows lack of enhancement of the right hepatic vein (*arrowheads*). **c** Source axial image from same acquisition as in **b** confirms the presence of thrombus in the right hepatic vein (*arrow*). Note the decreased enhancement (*arrowheads*) in the territory of the right lobe drained by the right hepatic vein

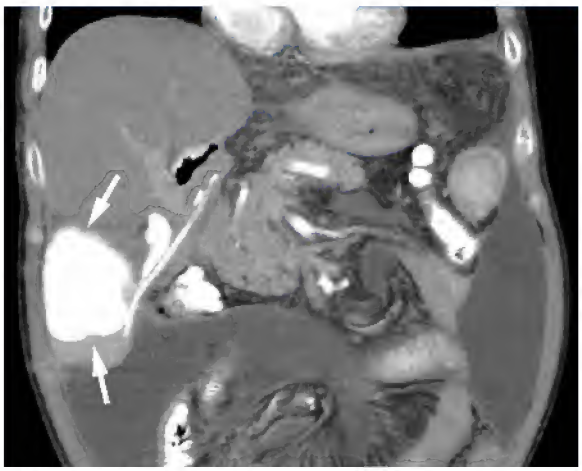

Fig. 4.2.24. Biloma. A 47-year-old man 19 days status post living, related right lobe liver transplant, with acute onset of abdominal pain. Coronal reformat of contrast-enhanced CT performed after a percutaneous cholangiogram shows a large fluid collection along the right flank (*arrows*), adjacent to the inferior liver edge, filled with contrast medium from the cholangiogram. These findings confirmed the presence of a bile leak

Fig. 4.2.25. Bile duct anastomotic stricture. A 37-year-old female status post fulminant acute hepatitis A, followed by orthotopic cadaveric liver transplant presenting now with abnormal liver function tests. Coronal thick-slab T2-weighted single-shot fast spin echo (*SSFSE*) MRCP image shows a short-segment stenosis (*arrow*) at the biliary anastomosis with upstream dilatation of the common bile duct. The remnant of the cystic duct (*arrowhead*) and a small amount of hyperintense fluid in the duodenal lumen (*asterisk*) are also seen

tive oral contrast improves the visualization of the biliary system on thick-slab T2-weighted MRCP images by decreasing the signal intensity of the overlying fluid in the stomach and duodenum. The authors routinely administer a combination of 150 ml Gastromark (Mallinckrodt Medical, St. Louis, Mo., USA) and 150 ml Readi-cat (EZEM Canada, Westbury, New York) for MRCP examinations. This preparation provides negative contrast on both T1- and T2-weighted sequences, without causing significant susceptibility artifacts (Liebig et al. 1993).

MRCP is helpful in the detection of biliary strictures, bile leaks, and biloma formation. Thick-slab MRCP images are particularly useful in the presence of biliary dilatation (Fig. 4.2.25). However, proximal biliary dilatation may be absent in the transplanted patient with stenosis at the anastomotic site (Laghi et al. 1999; Pandharipande et al. 2001). Careful analysis of thin-slice MR images can help to identify the stricture and/or leak (Fig. 4.2.26). False MR positive and negative results may occur in the presence of surgical clips due to susceptibility artifact obscuring the biliary ducts.

Non-anastomotic biliary strictures and dilations are the result of ischemic insults to the bile ducts only within the graft (Boraschi et al. 2004). Non-anastomotic strictures are probably the result of microcirculatory problems and they usually involve the hepatic duct bifurcation and progress peripherally (Boraschi et al. 2004). Sludge and stone formation within affected ducts may occur (Boraschi et al. 2004). MRCP can accurately depict biliary dilation, and the degree and level of the obstructive lesions (Boraschi et al. 2004). However, MR may underestimate the number and length of intrahepatic strictures (Boraschi et al. 2004). T2-weighted MR images demonstrate low signal intensity filling defects surrounded by hyperintense bile in approximately 50% of patients with ischemic-type biliary lesions (Boraschi et al. 2004). These filling defects correspond to a combination of partially or completely sloughed biliary epithelium and stones (Boraschi et al. 2004). Gadolinium-enhanced MR imaging shows thickening and increased enhancement of the wall in the affected bile ducts in up to 64% of transplanted patients (Boraschi et al. 2004).

MR imaging may have an advantage over endoscopic retrograde cholangiopancreatography (ERCP) in those patients with biliary strictures in whom the biliary ducts proximal to the anastomosis are not dilated and/or well opacified during the ERCP procedure. Similarly, overdistention of the biliary ducts during the injection of contrast at ERCP in patients with biliary strictures may be misinterpreted as donor-recipient size mismatch (Fig. 4.2.27).

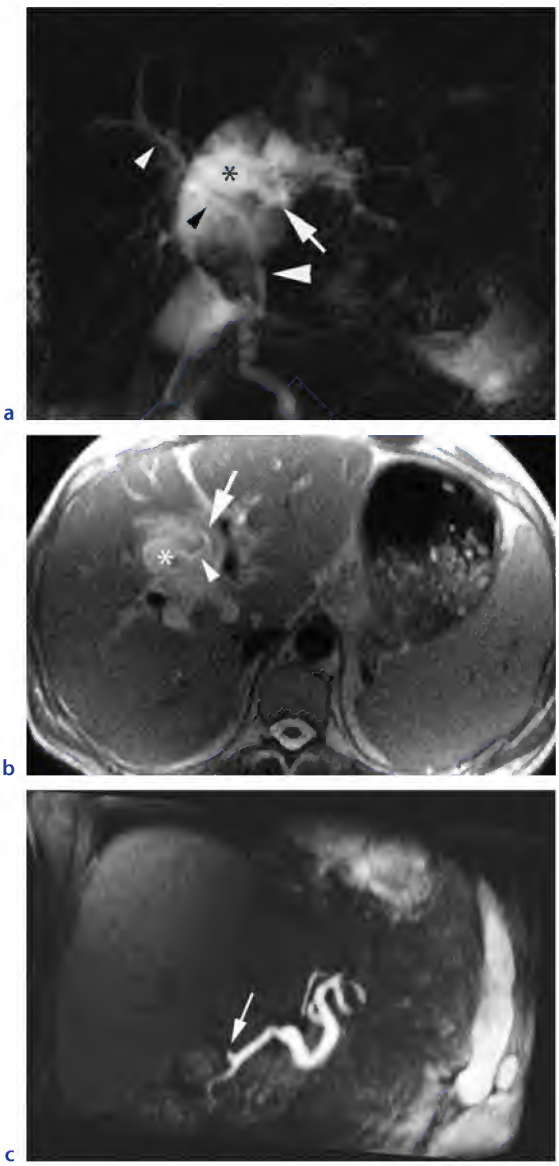

Fig. 4.2.26a–c. Hepatic artery occlusion. A 42-year-old man with history of ethanol abuse, hepatitis C, and cirrhosis status post orthotopic cadaver liver transplant and bile duct necrosis secondary to hepatic artery thrombosis. **a** Coronal thick-slab T2-weighted single-shot fast spin echo (*SSFSE*) MRCP image shows the normal extrahepatic common bile duct (*large arrowhead*) and intrahepatic right duct (*small arrowheads*). The intrahepatic left duct is seen proximally although an abrupt change in caliber is appreciated in its middle portion (*arrow*). A large hyperintense fluid collection (*asterisk*) is demonstrated in the porta hepatis overlying the bile ducts. **b** Axial T2-weighted SSFSE image at the level of the porta hepatis confirms the presence of a bile leak (*arrowhead*) from the left common duct (*arrow*). The fluid collection in the porta hepatis is again seen (*asterisk*). **c** MRA – axial maximum intensity projection (MIP) reconstruction of the hepatic artery demonstrates occlusion of this vessel at the level of the anastomosis (*arrow*)

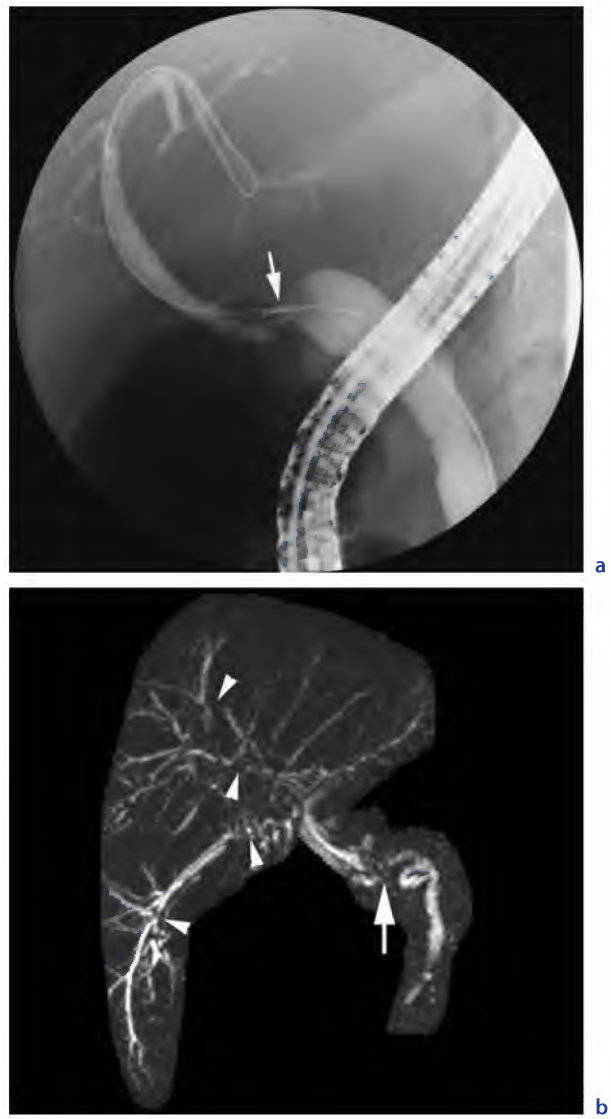

Fig. 4.2.27a,b. A 58-year-old female with history of ethanol abuse and cirrhosis status post cadaveric liver transplant and rising alkaline phosphatase. **a** Endoscopic retrograde cholangiography (*ERCP*) demonstrates a difference in caliber between the native common bile duct inferiorly and the donor hepatic duct above the anastomosis (*arrow*). This finding was interpreted as a size mismatch between the native and donor hepatic ducts. **b** Maximum intensity projection reconstruction (*MIP*) of a 3D T2-weighted respiratory-triggered fast recovery fast spin echo sequence demonstrates a stenosis (*arrow*) at the level of the anastomosis. Note the similar caliber of the donor and native extrahepatic ducts. Multiple short-segment areas of stenosis (*arrowheads*) are demonstrated in the intrahepatic ducts likely representing non-anastomotic ischemic strictures. The incongruence of the results at ERCP and MR can be explained by overdistension of the native hepatic duct produced by the injection of contrast against the anastomotic stricture. A repeated ERCP confirmed the presence of stenosis and an intrabiliary stent was placed

4.2.5 Donors

- Adult-to-child: left lateral segment
- Adult-to-adult: right lobe

Selection of the optimal donor for living-donor liver transplantation is a long and detailed process which includes clinical, laboratory, serology, histology, imaging and psychosocial evaluations of the candidate. In addition, ethical issues arise in the recipient-donor matching and throughout the post-transplantation process, especially if complications arise. Donor safety is a primary goal in living-donor liver transplantation, and imaging is fundamental for providing, with minimal invasiveness, useful information for optimal candidate selection and surgical planning. If the volume for donation is chosen inappropriately, the liver donor may be left with insufficient parenchyma to sustain metabolic function, and may need to undergo urgent liver transplantation him or herself, since presently there is no equivalent to renal dialysis for liver failure.

Preoperative imaging should evaluate the liver parenchyma, depict the relevant vascular anatomy and measure the total and lobar volumes (Kruskal and Raptopoulos 2002). Exclusion of parenchymal, vascular, and biliary abnormalities or variations that could increase surgical morbidity for partial hepatectomy is a primary concern.

The two ends of the spectrum of living-donor liver transplantation are left lateral segment (LLS) transplantation for adult-to-child donation and right lobe donation for adult-to-adult donation. In LLS transplantation, grafts tend to be large for size, with a possible risk of vascular compression and difficulties in abdominal closure. In right lobe transplantation evaluation of liver volumes is of paramount importance: the balance between providing adequate liver volume to the recipient and leaving sufficient volume to the donor to sustain metabolic function is very delicate (Guiney et al. 2003). The ideal volume for recipients is estimated based on the ratio between graft weight and recipient body weight or between graft volume and estimated liver volume of the recipient: when the transplanted parenchyma is normal, acceptable values are 0.8% graft weight/recipient body weight (Inomata et al. 2000) and 40% graft volume/estimated liver volume of the recipient (Lo et al. 1999). Remnant liver volume (RLV) is a primary concern and a recent report states that the outcome of donors with an RLV < 35% was not different from that of donors with an RLV ≥ 35%, except for transient cholestasis (Cho et al. 2006).

4.2.5.1 Preoperative Imaging

Preoperative evaluation:
- CT protocol
- Pertinent vascular variants
  - Hepatic artery
  - Portal vein
  - Hepatic veins
- Virtual hemi-hepatectomy

CT and MRI have both been successfully used in the preoperative imaging of liver donors (Chu et al. 2005; Fulcher et al. 2001; Kamel et al. 2001b; Lee et al. 2001; Schroeder et al. 2005). There is no clear consensus on which modality is best apt for performing a comprehensive evaluation of the donor liver. CT is simple, fast, accurate, widely available and very comfortable for the patient, while providing a high consistency of studies, and for these reasons it is used by most investigators. However, radiation dose and intravenous contrast are of concern. MR imaging has shown promising results as the sole preoperative imaging technique for evaluation of living adult-to-adult liver donor candidates (Lee et al. 2001). Similarly, MR imaging has been advocated as an all-in-one technique for evaluation of biliary and vascular anastomosis in the post-transplanted pediatric population (Chu et al. 2005). MR imaging is superior to standard multiphasic CT protocols for evaluation of the biliary system. MR imaging has the potential to simplify the presurgical evaluation of living donors by providing a comprehensive evaluation of the vascular and biliary anatomy. "All-in-one" CT and MR imaging protocols can accurately define the arterial and venous anatomy in living liver-donor candidates (Schroeder et al. 2005). Both CT and MR imaging protocols for evaluation of the biliary system after administration of hepatobiliary contrast agents have been proposed. Some of the advantages of MR over CT in the evaluation of potential liver donors include the lack of ionizing radiation, which is less desirable in these typically healthy young subjects, and safety of the gadolinium-based contrast agents. The latter includes a much lower incidence of contrast reactions (Shellock and Kanal 1999) and lack of nephro-

toxicity (Haustein et al. 1992; Prince et al. 1996; Rofsky et al. 1991).

At our institution preoperative evaluation of potential liver donors is performed using a multiphasic multidetector CT study that enables accurate assessment of the arterial, portal venous and hepatic venous anatomy and the performance of volume measurements. Oral milk or water (500 ml) is used to opacify the proximal bowel; other negative oral contrast mediums (e.g., Volumen, EZEM) can be alternatively used. After a non-intravenously enhanced scan is performed, non-ionic intravenous contrast material (200 ml) is administered. Acquisition timing is guided by bolus tracking in the aorta (enhancement threshold: 200 HU): early arterial scan is initiated when the threshold is reached, then a venous (late portal-early venous) scan is initiated with a 60-s delay from threshold; a delayed acquisition is performed after 3 min.

4.2.5.1.1 What to Evaluate in the Exam

The first step is to screen the liver for the presence of focal liver disease and the extent of steatosis. Focal liver lesions have been reported in up to 18% of living liver donors (Fulcher et al. 2001). The presence of malignant lesions disqualifies the candidate from donation. When benign lesions are present, their size and site must be carefully evaluated, especially if the lesion is on the surgical resection plane.

Both CT and MR can depict and characterize incidentally found liver lesions in living liver-donor candidates. In general MR imaging allows for better characterization of incidental parenchymal lesions than MDCT (Schroeder et al. 2005).

The acceptable upper limit of steatosis in a donor liver is 30%, above which there is high risk of liver dysfunction in the donor and graft nonfunction in the recipient (Marsman et al. 1996). Currently the most sensitive technique for the detection of fatty liver is MR with in- and out-of-phase sequences. Axial dual-echo in-phase and opposed-phase T1-weighted GRE images are typically used for detection of fatty infiltration and iron deposition. In the presence of fatty deposition, the liver demonstrates decreased signal intensity on opposed-phase images compared to that of the in-phase images (Fig. 4.2.28). Conversely, in the presence of iron deposition in the liver, there is decreased signal intensity on the in-phase images (acquired with a longer echo time) compared to that of the opposed-phase images (acquired with a shorter echo time) due to a susceptibility effect caused by the iron. Attenuation values at CT lower than 40 HU for the liver parenchyma are suggestive of steatosis (Fig. 4.2.29). Dual-energy CT at 140 and 80 kVp has been reported to be useful in the differentiation between focal fatty infiltration of the liver and low-density neoplastic or non-neoplastic lesions, if the iron content of the liver is not increased (Raptopoulos et al. 1991): an increase in attenuation greater than 10 HU when increasing kVp is unique to fatty infiltration. Detection of steatosis requires the potential donor to undergo liver biopsy.

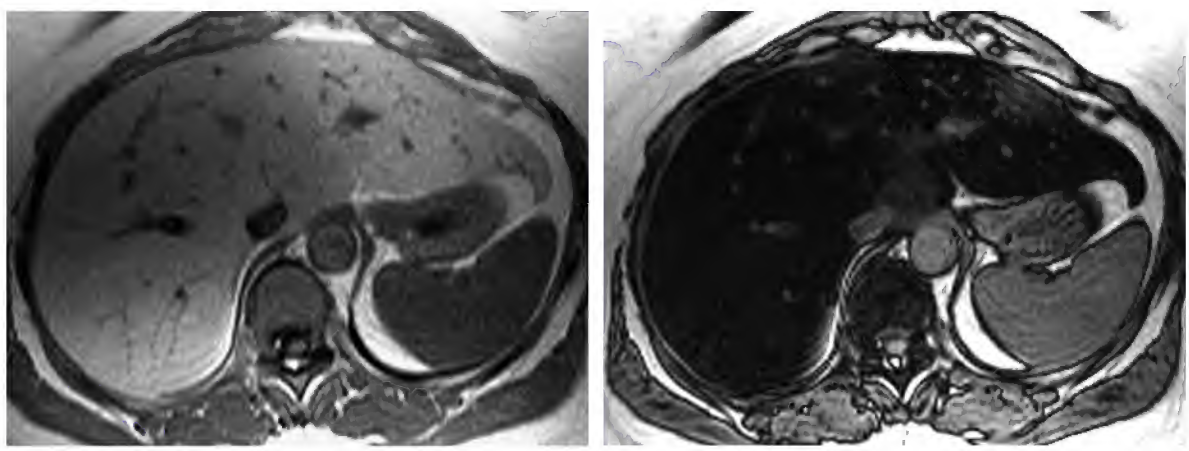

a b

Fig. 4.2.28a,b. Axial T1-weighted in-phase gradient echo image demonstrates homogeneous high signal intensity in the liver parenchyma (**a**). Axial T1-weighted opposed-phase gradient echo image shows diffuse decreased signal intensity of the liver, which is diagnostic of fatty infiltration (**b**)

Fig. 4.2.29. Unenhanced CT scan of the liver shows diffuse moderate fat infiltration of the parenchyma, which is isodense to the vessels. Mean attenuation of the liver is 42 HU

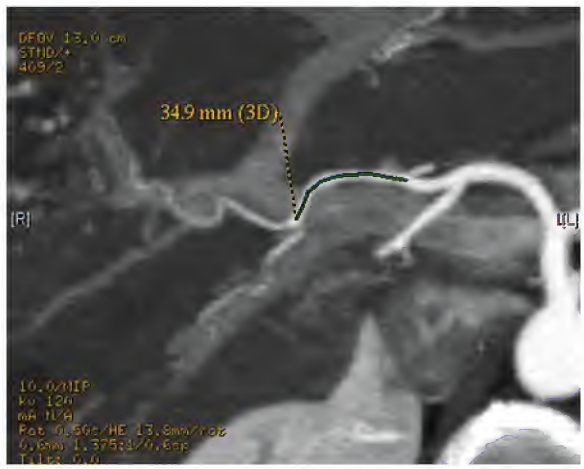

Fig. 4.2.30. Preoperative evaluation of the donor. Axial MIP image of CT angiogram allows accurate measurement of the length of the right hepatic artery before its first bifurcation

The second step is the evaluation of relevant intrahepatic vascular anatomy, with two-dimensional and three-dimensional models. Documentation of vascular abnormalities or variants, especially when intersecting the surgical resection plane, is fundamental for correct donor selection and surgical planning (Erbay et al. 2003). Schroeder et al. (2005) assessed the value of MCTA and MRI in depiction of the hepatic arterial anatomy, and compared their results to the intraoperative findings. MDCTA was deemed more accurate and reliable than MRA, with a higher number of detected variants and a higher rated image quality, likely due to the higher spatial resolution of MDCT.

4.2.5.1.2 Pertinent Arterial Anatomy Variants

(Alonso-Torres et al. 2005; Deshpande et al. 2002)

Conventional arterial anatomy might not always provide a hepatic artery with sufficient length because only part of the liver is harvested. It is important to identify the proper hepatic artery bifurcation and measure the length of the RHA or LHA before its next bifurcation (Fig. 4.2.30).

A replaced LHA (for adult-to-child donation) or RHA (for adult-to-adult donation), being usually longer, might allow a safer anastomosis (Fig. 4.2.31). On the other hand, an accessory LHA or RHA might require the creation of a dual anastomosis, as they are to be considered end arteries.

When evaluating a potential right lobe donor, the arterial supply to segment IV must be carefully evaluated, because preservation of the arterial inflow to this segment is fundamental to the prevention of liver failure in the donor. Normally, the artery for segment IV arises from the LHA, but it is not uncommon for the supply to come from the RHA, through an artery that crosses Cantlie's – and therefore the resection – line. Two arterial variants that disqualify the candidate as a potential donor are the origin of the RHA or LHA before the gastroduodenal artery origin, and the trifurcation of the common hepatic artery into gastroduodenal, right and left hepatic arteries (Fig. 4.2.32).

Fig. 4.2.31. Coronal MIP image of CT angiogram shows replaced left hepatic artery (*arrows*) originating from the left gastric artery

Fig. 4.2.32. Coronal oblique MIP image of CT angiogram shows trifurcation (*arrow*) of the common hepatic artery into gastroduodenal, right and left hepatic arteries, which disqualifies the candidate as a right lobe donor

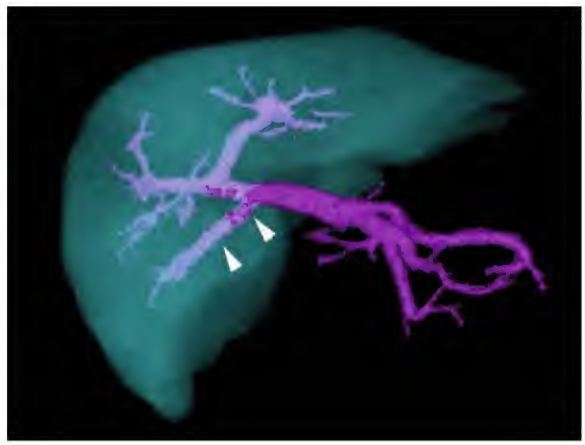

Fig. 4.2.33. Volume-rendered image of CT angiogram shows the right posterior portal vein (*arrowheads*) arising directly from the main portal vein

4.2.5.1.3
Pertinent Portal Vein Anatomy Variants

Trifurcation of the portal vein into right anterior, right posterior and left portal venous branches is an important variant, presenting in 6% of the potential donors. Knowledge of this variant is important for surgical planning, to ensure appropriate ligation in the donor and anastomosis in the recipient. One of the sectorial veins, most commonly the one supplying segments V and VIII, might originate from the left portal vein. Another variant is the right posterior portal vein arising directly from the portal vein, before its bifurcation (Fig. 4.2.33).

MR imaging provides exquisite detail of venous structures in the abdomen. High intravascular signal intensity can be achieved during the portal and delayed venous phases due to the extended intravascular phase, which has been attributed to minimal albumin binding of the gadolinium contrast agent (Vogl et al. 1992). In the study by Schroeder et al. (2005), MR imaging provided superior visualization of the portal and hepatic veins than contrast-enhanced MDCT.

4.2.5.1.4
Pertinent Hepatic Vein Anatomy Variants

Variations of the hepatic venous anatomy are observed in up to 30% of potential donors. The site of the confluence of the middle hepatic vein should be identified, because early branching and ramification of the middle hepatic vein can alter the surgical plane. One of the most common variants is a replaced or accessory inferior right hepatic vein: the size of the vein and the distance between its drainage into the inferior vena cava and that of the right hepatic vein must be measured. The locations and drainage patterns of the veins draining segments V and VIII must be carefully evaluated, because in the conventional anatomy they cross the surgical plane; their size must also be noted (Fig. 4.2.34). Veins larger than 5 mm should be preserved and anastomosed to the recipient's inferior vena cava, to avoid graft venous congestion which may lead to rejection (Fulcher et al. 2001; Fig. 4.2.35).

4.2.5.1.5
Biliary Anatomy

MR imaging of the biliary system is typically performed with a combination of thin-slice and thick-slab heavily T2-weighted images. The extrahepatic biliary system is accurately visualized with these techniques up to the level of the hepatic duct bifurcation (Fig. 4.2.36) (Schroeder et al. 2005; Taourel et al. 1996). Identification of abnormalities and/or anatomic variants of the intrahepatic biliary system with conventional T2-weighted MRCP techniques can be challenging and often inadequate, particularly in the non-dilated system (Lee et al. 2001). High-resolution 3D respiratory-triggered T2-weighted MRCP techniques are now available and may improve the visualization of the non-dilated intrahepatic biliary system (Fig. 4.2.37).

a b

Fig. 4.2.34a,b. Axial (**a**) and coronal (**b**) MIP images of the CT angiogram show the vein from segment VIII (*arrows*) draining into the middle hepatic vein

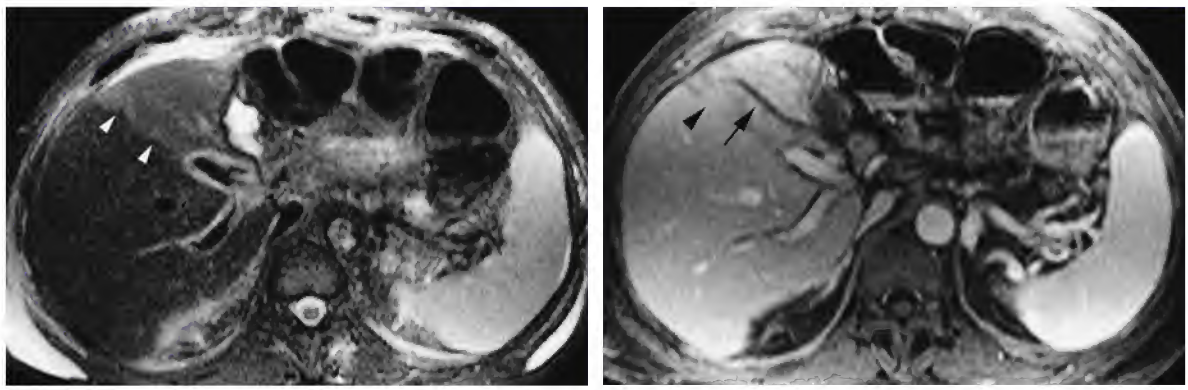

a b

Fig. 4.2.35a,b. A 50-year-old man with hepatitis C cirrhosis 2 days status post living-related orthotopic right lobe liver transplant and abnormal liver function test. **a** Axial STIR image at the level of the upper abdomen shows increase signal intensity (*arrowheads*) in the anterior aspect of the liver in a geographic distribution suggestive of a vascular abnormality. **b** Axial gadolinium-enhanced 3D fat-saturated T1-weighted gradient echo acquisition during the delayed venous phase shows heterogeneous enhancement in the same area (*arrowhead*). A non-enhancing vein (*arrow*) is demonstrated within this area and is consistent with a thrombosed branch of the middle hepatic vein. Anatomic variants in the hepatic venous system may result in impaired venous drainage if an independent anastomosis for the draining vein is not performed

While conventional CT protocols do not allow for evaluation of the intrahepatic biliary system an "all-in-one" CT imaging protocol after administration of a biliary contrast agent (CT cholangiography) has been proposed (Schroeder et al. 2005). A superior visualization of the biliary system on CT cholangiography compared to conventional T2-weighted MRCP techniques has been reported (Schroeder et al. 2005; Yeh et al. 2004). Schroeder et al. (2005) were able to visualize at least up to the second intrahepatic branch in all their liver donor candidates with a CT cholangiography protocol (Schroeder et al. 2005). In this study, MRCP allowed reliable visualization of the common duct up to its bifurcation and demonstrated only one-third of the biliary variants displayed on CT cholangiography (Schroeder et al. 2005).

The MR imaging visualization of the non-dilated intrahepatic biliary system in living liver transplant donor candidates can also be improved with administration of contrast agents that are excreted by the biliary system. MR imaging after administration of mangafodipir trisodium (Teslascan; Amersham Health, Princeton, N.J., USA) improves the visualization of anatomic variants of the intrahepatic right ductal system, which can

Fig. 4.2.36. Coronal thick-slab T2-weighted SSFSE MRCP image shows an aberrant right hepatic duct (*arrow*) draining directly into the common hepatic duct (*arrowhead*)

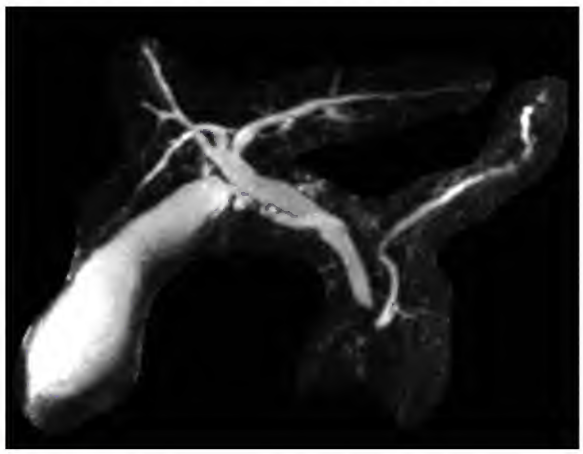

Fig. 4.2.37. Volume-rendered reconstruction of a respiratory-triggered 3D T2-weighted fast recovery fast spin echo acquisition shows a trifurcation of the intrahepatic common bile duct

be critical prior to living right lobe transplantation (Lee et al. 2004). Gadobenate dimeglumine (Gadolinium-BOPTA; Bracco, Milan, Italy) is a gadolinium-based contrast agent that is selectively taken up by hepatocytes and approximately 2%–4% of the injected dose is excreted through the biliary route (Peterstein et al. 2000; Spinazzi et al. 1999). In addition, gadolinium-BOPTA can be used for routine dynamic contrast-enhanced MR imaging and allows for multiphase imaging of the liver and MRA reconstructions (Goyen et al. 2002). These characteristics make gadolinium-BOPTA a suitable contrast agent for an "all-in-one" MR protocol (Lim et al. 2005a). Initial results have shown improved visualization of the non-dilated intrahepatic biliary system with gadolinium-BOPTA versus mangafodipir trisodium MR cholangiography (MRC) (Lim et al. 2005b). Gadolinium-BOPTA-enhanced MRC increases the diagnostic confidence of biliary anatomic variants in living donor liver transplant candidates compared to conventional T2-weighted MRCP images (Lim et al. 2005a).

4.2.5.1.6 Virtual Hepatectomy

MDCT and MRI examinations of the potential liver donor allow performance of detailed 3D reconstructions of the vascular anatomy, and accurate assessment of the ideal surgical plane (1 cm right of the middle hepatic vein, parallel to Cantlie's line). A virtual hepatectomy can be performed, to help the surgeon choose the ideal resection plane (Fig. 4.2.38). The margins of the virtually resected lobe can be manually traced similarly to the liver volume segmentation technique previously described in the paragraph on recipient preoperative evaluation (Sect. 4.2.4.1). Another easier, though less accurate, method is to create a 3D model with the superimposition of the reconstructions of the hepatic arteries, portal vein and hepatic veins and to virtually cut this 3D model along the desired resection plane. This second easier technique can be applied in most cases, but not when the technique provides borderline lobe volumes for either recipient or donor.

Accurate determination of the volumes for the right and left hepatic lobes is critical prior to split liver transplantation (Fig. 4.2.39). Both CT and MR provide accurate measurements of the liver volumes. Measurement of the liver volume is best achieved during the venous phase of the contrast-enhanced CT and MR examinations. Both CT and MR tend to overestimate the liver volume with MR being more prone to this problem (Schroeder et al. 2005). This phenomenon may be related to comparison of the estimated volumes with the weight measurement of the explanted graft, which lacks the physiologic perfusion (Schroeder et al. 2005). A conversion factor of 0.75 between the preoperative graft volume and the effective weight of the non-perfused graft has been proposed (Lemke et al. 2003; Schroeder et al. 2005).

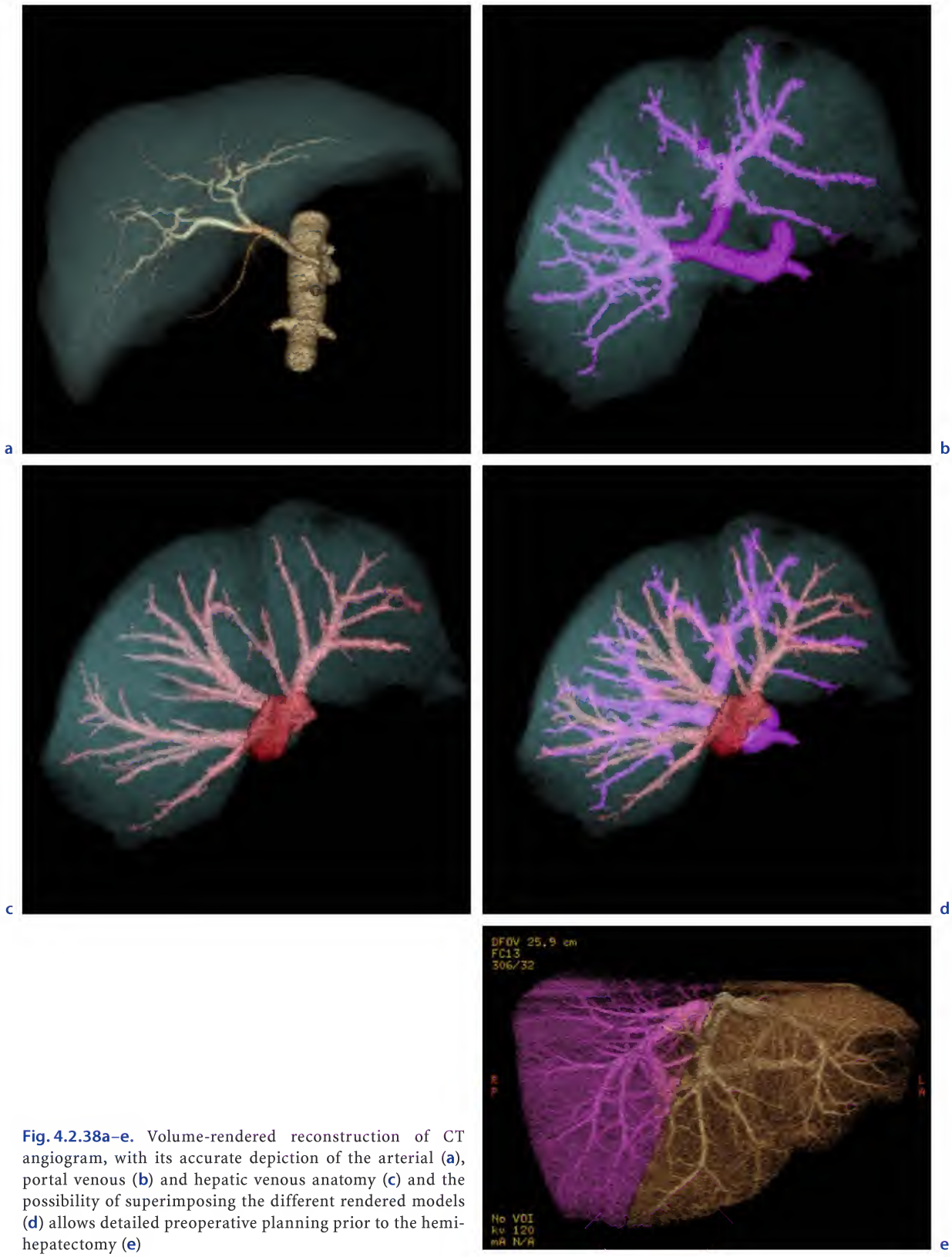

Fig. 4.2.38a–e. Volume-rendered reconstruction of CT angiogram, with its accurate depiction of the arterial (**a**), portal venous (**b**) and hepatic venous anatomy (**c**) and the possibility of superimposing the different rendered models (**d**) allows detailed preoperative planning prior to the hemihepatectomy (**e**)

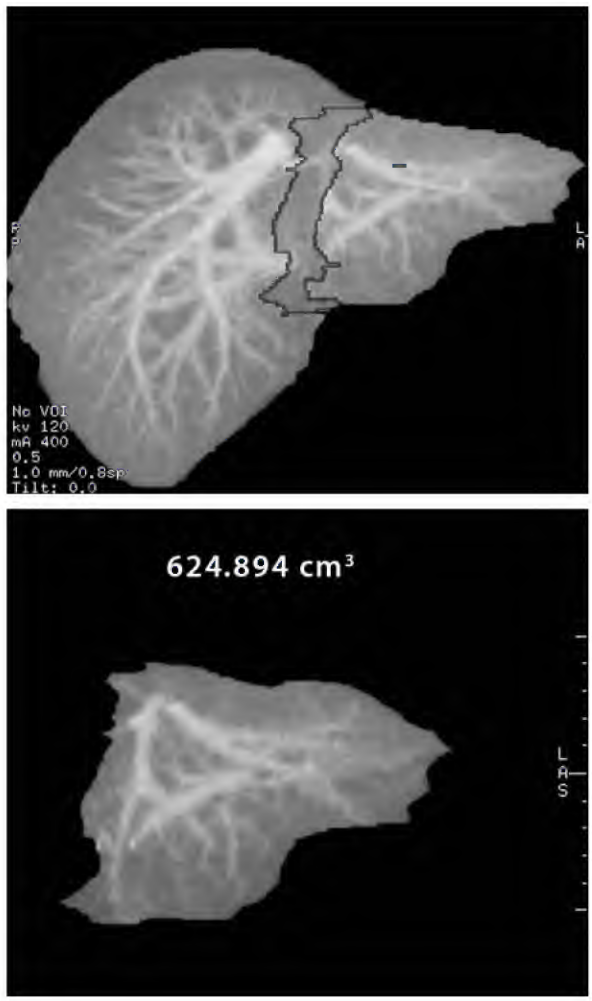

Fig. 4.2.39a,b. Small left lobe. A 33-year-old healthy male, candidate right lobe donor. The accurate volume measurements performed on the MIP reconstructions of the CT angiogram show that the patient has a small left lobe, and therefore is unsuitable for right lobe donation

4.2.5.2 Intraoperative Imaging

Intra-operative
- US

Ultrasonography is used intraoperatively for the evaluation of the donor vasculature and the final assessment of the optimal resection plane (Chong 2004). The liver surface can be marked under US guidance with an argon laser, at first with dots that appear on the US scan as an echogenic interface with strong posterior acoustic shadowing (Bassignani et al. 2001). This acoustic shadowing allows evaluation of the intrahepatic course of the resection plane. When the proper resection plane is confirmed, a line that connects the dots can be traced and used for resection.

4.2.5.3 Postoperative Imaging

Postoperative
- Complications
- Intervention
- Volumes

Postoperative evaluation of the liver donor is performed routinely with US, to assess the onset of complications such as fluid collections or hematomas at the resection site. The most commonly reported donor complication is bile leak (Pomfret et al. 2001; Renz and Busuttil 2000). A collection along the resection plane is not uncommon, but usually resolves spontaneously.

Imaging can provide useful guidance for the treatment of these postoperative complications: US and CT can be used to guide the drainage of collections and hematomas, while vascular and biliary complications are often managed with interventional radiology procedures. Regeneration of the liver can be followed by CT or MRI, which allow measurement of the parenchymal volume and assessment of its progressive increase (Kamel et al. 2003) (Fig. 4.2.40). Insufficient remnant volume to the donor is probably the most severe complication, as the only treatment for liver insufficiency would be urgent transplantation.

References

Alonso-Torres A, Fernandez-Cuadrado J, Pinilla I et al (2005) Multidetector CT in the evaluation of potential living donors for liver transplantation. Radiographics 25(4):1017–1030

Bassignani MJ, Fulcher AS, Szucs RA et al (2001) Use of imaging for living donor liver transplantation. Radiographics 21(1):39–52

Ben-Ari Z, Amlot P, Lachmanan SR et al (1999) Posttransplantation lymphoproliferative disorder in liver recipients: characteristics, management, and outcome. Liver Transpl Surg 5(3):184–191

Berry JD, Sidhu PS (2004) Microbubble contrast-enhanced ultrasound in liver transplantation. Eur Radiol 14 [Suppl 8]:P96–P103

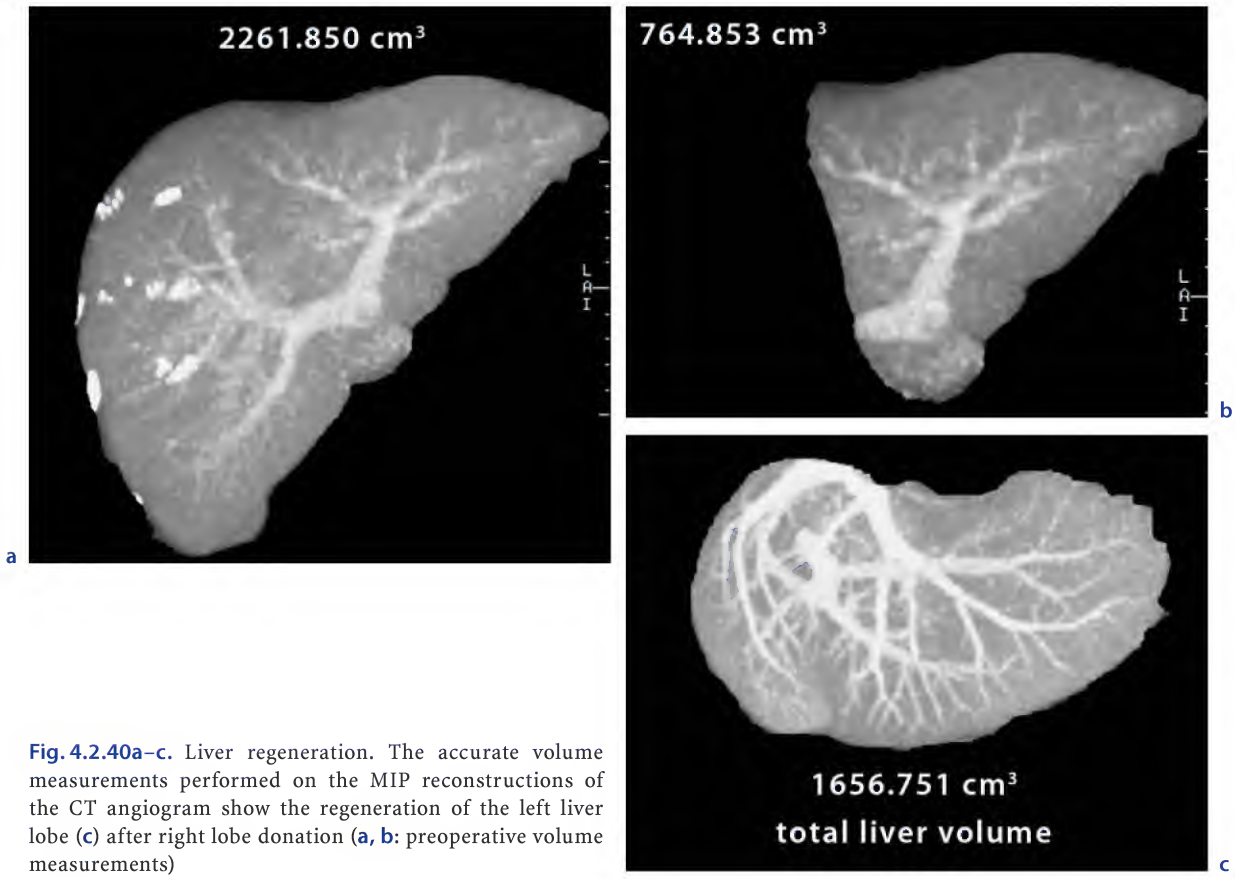

Fig. 4.2.40a–c. Liver regeneration. The accurate volume measurements performed on the MIP reconstructions of the CT angiogram show the regeneration of the left liver lobe (**c**) after right lobe donation (**a, b**: preoperative volume measurements)

Boraschi P, Donati F, Gigoni R et al (2004) Ischemic-type biliary lesions in liver transplant recipients: evaluation with magnetic resonance cholangiography. Transplant Proc 36:2744–2747

Brancatelli G, Katyal S, Federle MP et al (2002) Three-dimensional multislice helical computed tomography with the volume rendering technique in the detection of vascular complications after liver transplantation. Transplantation 27;73(2):237–242

Cheng YF, Chen CL, Huang TL et al (2004) 3DCT angiography for detection of vascular complications in pediatric liver transplantation. Liver Transpl 10(2):248–252

Cho JY, Suh KS, Kwon CH et al (2006) Outcome of donors with a remnant liver volume of less than 35% after right hepatectomy. Liver Transpl 12(2):201–206

Cho KC, Patel YD, Wachsberg RH et al (1995) Varices in portal hypertension: evaluation with CT. Radiographics 15(3):609–622

Chong WK (2004) Ultrasound evaluation of liver transplants. Abdom Imaging 29(2):180–188

Chu WC, Yeung DT, Lee KH et al (2005) Feasibility of morphologic assessment of vascular and biliary anatomy in pediatric liver transplantation: all-in-one protocol with breath-hold magnetic resonance. J Pediatr Surg 40:1605–1611

Cochat P, Gaulier JM, Koch Nogueira PC et al (1999) Combined liver-kidney transplantation in primary hyperoxaluria type 1. Eur J Pediatr 158 [Suppl 2]:S75–S80

Crossin JD, Muradali D, Wilson SR (2003) US of liver transplants: normal and abnormal. Radiographics 23(5):1093–1114

Deshpande RR, Heaton ND, Rela M (2002) Surgical anatomy of segmental liver transplantation. Br J Surg 89(9):1078–1088

Erbay N, Raptopoulos V, Pomfret EA et al (2003) Living donor liver transplantation in adults: vascular variants important in surgical planning for donors and recipients. AJR Am J Roentgenol 181(1):109–114

Eubank WB, Wherry KL, Maki JH et al (2002) Preoperative evaluation of patients awaiting liver transplantation: comparison of multiphasic contrast-enhanced 3D magnetic resonance to helical computed tomography examinations. J Magn Reson Imaging 16:565–575

Federle MP, Kapoor V (2003) Complications of liver transplantation: imaging and intervention. Radiol Clin North Am 41(6):1289–1305

Finn JP, Edelman RR, Jenkins RL et al (1991) Liver transplantation: MR angiography with surgical validation. Radiology 179:265–269

Fulcher AS, Szucs RA, Bassignani MJ et al (2001) Right lobe living donor liver transplantation: preoperative evaluation of the donor with MR imaging. AJR Am J Roentgenol 176(6):1483–1491

Gemmete JJ, Mueller GC, Carlos RC (2006) Liver transplantation in adults: postoperative imaging evaluation and interventional management of complications. Semin Roentgenol 41(1):36–44

Goyen M, Barkhausen J, Debatin JF et al (2002). Right-lobe living related liver transplantation: evaluation of a comprehensive magnetic resonance imaging protocol for assessing potential donors. Liver Transpl 8:241–250

Guiney MJ, Kruskal JB, Sosna J et al (2003) Multi-detector row CT of relevant vascular anatomy of the surgical plane in split-liver transplantation. Radiology 229(2):401–407

Haustein J, Niendorf HP, Krestin G et al (1992) Renal tolerance of gadolinium-DTPA/dimeglumine in patients with chronic renal failure. Invest Radiol 27:153–156

Holland AE, Hecht EM, Hahn WY et al (2005) Importance of small (≤20-mm) enhancing lesions seen only during the hepatic arterial phase at MR imaging of the cirrhotic liver: evaluation and comparison with whole explanted liver. Radiology 237:938–944

Inomata Y, Uemoto S, Asonuma K et al (2000) Right lobe graft in living donor liver transplantation. Transplantation 69(2):258–264

Ishifuro M, Horiguchi J, Nakashige A et al (2002) Use of multidetector row CT with volume renderings in right lobe living liver transplantation. Eur Radiol 12(10):2477–2483

Jang HJ, Lim JH, Lee SJ et al (2000) Hepatocellular carcinoma: are combined CT during arterial portography and CT hepatic arteriography in addition to triple-phase helical CT all necessary for preoperative evaluation? Radiology 15(2):373–380

Kamel IR, Raptopoulos V, Pomfret EA et al (2000) Living adult right lobe liver transplantation: imaging before surgery with multidetector multiphase CT. AJR Am J Roentgenol 175(4):1141–1143

Kamel IR, Kruskal JB, Keogan MT et al (2001a) Multidetector CT of potential right-lobe liver donors. AJR Am J Roentgenol 177(3):645–651

Kamel IR, Kruskal JB, Pomfret EA et al (2001b) Impact of multidetector CT on donor selection and surgical planning before living adult right lobe liver transplantation. AJR Am J Roentgenol 176(1):193–200

Kamel IR, Kruskal JB, Warmbrand G et al (2001c) Accuracy of volumetric measurements after virtual right hepatectomy in potential donors undergoing living adult liver transplantation. AJR Am J Roentgenol 176(2):483–487

Kamel IR, Erbay N, Warmbrand G et al (2003) Liver regeneration after living adult right lobe transplantation. Abdom Imaging 28(1):53–57

Kang BK, Lim JH, Kim SH et al (2003) Preoperative depiction of hepatocellular carcinoma: ferumoxides-enhanced MR imaging versus triple-phase helical CT. Radiology 226(1):79–85

Keeffe EB (2000) Liver transplantation at the millennium. Past, present, and future. Clin Liver Dis 4(1):241–255

Kim BS, Kim TK, Jung DJ et al (2003) Vascular complications after living related liver transplantation: evaluation with gadolinium-enhanced three-dimensional MR angiography. AJR Am J Roentgenol 181:467–474

Kim YK, Kwak HS, Kim CS et al (2006a) Hepatocellular carcinoma in patients with chronic liver disease: comparison of SPIO-enhanced MR imaging and 16-detector row CT. Radiology 238(2):531–541

Ko EY, Kim TK, Kim PN et al (2003) Hepatic vein stenosis after living donor liver transplantation: evaluation with Doppler US. Radiology 229(3):806–810

Ko GY, Sung KB, Yoon HK et al (2002) Endovascular treatment of hepatic venous outflow obstruction after living-donor liver transplantation. J Vasc Interv Radiol 13(6):591–599

Krinsky GA, Lee VS, Theise ND et al (2001) Hepatocellular carcinoma and dysplastic nodules in patients with cirrhosis: prospective diagnosis with MR imaging and explantation correlation. Radiology 219:445–454

Krinsky GA, Lee VS, Theise ND et al (2002) Transplantation for hepatocellular carcinoma and cirrhosis: sensitivity of magnetic resonance imaging. Liver Transpl 8:1156–1164

Kruskal JB, Raptopoulos V (2002) How I do it: pre-operative CT scanning for adult living right lobe liver transplantation. Eur Radiol 12(6):1423–1431

Laghi A, Pavone P, Catalano C et al (1999) MR cholangiography of late biliary complications after liver transplantation. AJR Am J Roentgenol 172:1541–1546

Langnas AN, Marujo W, Stratta RJ et al (1991) Vascular complications after orthotopic liver transplantation. Am J Surg. 161(1):76–82

Lee VS, Morgan GR, Teperman LW et al (2001) MR imaging as the sole preoperative imaging modality for right hepatectomy: a prospective study of living adult-to-adult liver donor candidates. AJR Am J Roentgenol 176:1475–1482

Lee VS, Krinsky GA, Nazzaro CA et al (2004) Defining intrahepatic biliary anatomy in living liver transplant donor candidates at mangafodipir trisodium-enhanced MR cholangiography versus conventional T2-weighted MR cholangiography. Radiology 233:659–666

Lemke AJ, Brinkmann MJ, Pascher A et al (2003) [Accuracy of the CT-estimated weight of the right hepatic lobe prior to living related liver donation (LRLD) for predicting the intraoperatively measured weight of the graft.] Rofo 175:1232–1238

Letourneau JG, Castaneda-Zuniga WR (1990) The role of radiology in the diagnosis and treatment of biliary complications after liver transplantation. Cardiovasc Intervent Radiol 13(4):278–282

Liebig T, Stoupis C, Ros PR et al (1993) A potentially artifact-free oral contrast agent for gastrointestinal MRI. Magn Reson Med 30:646–649

Lim JH, Park CK (2004) Hepatocellular carcinoma in advanced liver cirrhosis: CT detection in transplant patients. Abdom Imaging 29(2):203–207

Lim JS, Kim MJ, Kim JH et al (2005a) Preoperative MRI of potential living-donor-related liver transplantation using a single dose of gadobenate dimeglumine. AJR Am J Roentgenol 185(2):424–431

Lim JS, Kim MJ, Jung YY, Kim KW (2005b) Gadobenate dimeglumine as an intrabiliary contrast agent: comparison with mangafodipir trisodium with respect to non-dilated biliary tree depiction. Korean J Radiol 6:229–234

Lo CM, Fan ST, Chan JK et al (1999) Minimum graft volume for successful adult-to-adult living donor liver transplantation for fulminant hepatic failure. Transplantation 62(5):696–698

Marsman WA, Wiesner RH, Rodriguez L et al (1996) Use of fatty donor liver is associated with diminished early patient and graft survival. Transplantation 62(9):1246–1251

Mazzaferro V, Regalia E, Doci R et al (1996) Liver transplantation for the treatment of small hepatocellular carcinomas in patients with cirrhosis. N Engl J Med 334:693–699

Michels NA (1966) Newer anatomy of the liver and its variant blood supply and collateral circulation. Am J Surg 112(3):337–347

Mori K, Scheidler J, Helmberger T et al (2002) Detection of malignant hepatic lesions before orthotopic liver transplantation: accuracy of ferumoxides-enhanced MR imaging. AJR Am J Roentgenol 179:1045–1051

Mortele KJ, Cantisani V, Troisi R et al (2003) Preoperative liver donor evaluation: imaging and pitfalls. Liver Transpl 9(9):S6–S14

Nicolau C, Vilana R, Bru C (2004) The use of contrast-enhanced ultrasound in the management of the cirrhotic patient and for detection of HCC. Eur Radiol 14 [Suppl 8]:P63–P71

Pandharipande PV, Lee VS, Morgan GR et al (2001) Vascular and extravascular complications of liver transplantation: comprehensive evaluation with three-dimensional contrast-enhanced volumetric MR imaging and MR cholangiopancreatography. AJR Am J Roentgenol 177:1101–1107

Petersein J, Spinazzi A, Giovagnoni A et al (2000) Focal liver lesions: evaluation of the efficacy of gadobenate dimeglumine in MR imaging – a multicenter phase III clinical study. Radiology 215:727–736

Pomfret EA, Pomposelli JJ, Lewis WD et al (2001) Live donor adult liver transplantation using right lobe grafts: donor evaluation and surgical outcome. Arch Surg 136(4):425–433

Prince MR, Arnoldus C, Frisoli JK (1996) Nephrotoxicity of high-dose gadolinium compared with iodinated contrast. J Magn Reson Imaging 6:162–166

Quiroga J, Colina I, Demetris AJ et al (1991) Cause and timing of first allograft failure in orthotopic liver transplantation: a study of 177 consecutive patients. Hepatology 14(6):1054–1062

Raptopoulos V, Karellas A, Bernstein et al (1991) Value of dual-energy CT in differentiating focal fatty infiltration of the liver from low-density masses. AJR Am J Roentgenol 157(4):721–725

Redvanly RD, Nelson RC, Stieber AC et al (1995) Imaging in the preoperative evaluation of adult liver-transplant candidates: goals, merits of various procedures, and recommendations. AJR Am J Roentgenol 164(3):611–617

Renz JF, Busuttil RW (2000) Adult-to-adult living-donor liver transplantation: a critical analysis. Semin Liver Dis 20(4):411–424

Rode A, Bancel B, Douek P et al (2001) Small nodule detection in cirrhotic livers: evaluation with US, spiral CT, and MRI and correlation with pathologic examination of explanted liver. J Comput Assist Tomogr 25:327–336

Rofsky NM, Weinreb JC, Bosniak MA et al (1991) Renal lesion characterization with gadolinium-enhanced MR imaging: efficacy and safety in patients with renal insufficiency. Radiology 180:85–89

Sahani D, D'souza R, Kadavigere R et al (2004a) Preoperative hepatic vascular evaluation with CT and MR angiography: implications for surgery. Radiographics 24(5):1367–1380

Schroeder T, Malago M, Debatin JF et al (2005) "All-in-one" imaging protocols for the evaluation of potential living liver donors: comparison of magnetic resonance imaging and multidetector computed tomography. Liver Transpl 11:776–787

Schroeder T, Radtke A, Kuehl H et al (2006) Evaluation of living liver donors with an all-inclusive 3D multi-detector row CT protocol. Radiology 2006 Jan 26; [Epub ahead of print]

Shellock FG, Kanal E (1999) Safety of magnetic resonance imaging contrast agents. J Magn Reson Imaging 10:477–484

Smadja C, Blumgart LH (1994) The biliary tract and the anatomy of biliary exposure. In: Blumgart LH (ed) Surgery of the liver and biliary tract, 2nd edn. Churchill Livingstone, London

Spinazzi A, Lorusso V, Pirovano G et al (1999) Safety, tolerance, biodistribution, and MR imaging enhancement of the liver with gadobenate dimeglumine: results of clinical pharmacologic and pilot imaging studies in nonpatient and patient volunteers. Acad Radiol 6:282–291

Stafford-Johnson DB, Hamilton BH, Dong Q et al (1998) Vascular complications of liver transplantation: evaluation with gadolinium-enhanced MR angiography. Radiology 207:153–160

Taourel P, Bret PM, Reinhold C et al (1996) Anatomic variants of the biliary tree: diagnosis with MR cholangiopancreatography. Radiology 199:521–527

Teefey SA, Hildeboldt CC, Dehdashti F et al (2003) Detection of primary hepatic malignancy in liver transplant candidates: prospective comparison of CT, MR imaging, US, and PET. Radiology 226:533–542

Vogl TJ, Pegios W, McMahon C et al (1992) Gadobenate dimeglumine – a new contrast agent for MR imaging: preliminary evaluation in healthy volunteers. AJR Am J Roentgenol 158:887–892

Yeh BM, Breiman RS, Taouli B et al (2004) Biliary tract depiction in living potential liver donors: comparison of conventional MR, mangafodipir trisodium-enhanced excretory MR, and multi-detector row CT cholangiography-initial experience. Radiology 230(3):645–651

Lung Transplantation

5

5.1 Epidemiological, Clinical and Surgical Considerations

Peter Jaksch

CONTENTS

P. Jaksch, MD
Department of Thoracic Surgery, Transplantation Unit, Medical University of Vienna, Waehringer Guertel 18–20, 1090 Vienna, Austria

5.1.1 Introduction

The first human lung transplantation (LuTX) was performed by Dr James Hardy (Hardy et al. 1963) in June 1960 at the University of Mississippi in a patient with unresectable lung cancer and obstructive pneumonitis. The patient received immunosuppression with azathioprine (Aza) and irradiation, but he died due to renal failure after 17 days.

Surgeons in the United States, Canada and Europe performed about 40 human lung transplantations between Hardy's operation and the end of 1980. But success was limited by anastomotic healing problems immediately after the operation, technical complications, infections and the inability to differentiate infection from rejection. Improvement of bronchial anastomotic healing was achieved by

introducing ciclosporin (CsA) and reducing the dose of corticosteroids.

In 1983 the Toronto Lung Transplant Group (1986) performed the first single-lung transplantations for patients with end-stage chronic obstructive pulmonary disease and advanced pulmonary fibrosis. Their technique was later expanded to bilateral sequential single-lung transplantation for patients with bronchiectasis and cystic fibrosis.

More recently, use of living donors for lobar allografts has been demonstrated to be a useful alternative for selected patients who require isolated lung transplantation.

5.1.1.1 Survival, Indications and Contraindications

Despite the wide acceptance of LuTX as a treatment option for patients with end-stage lung disease, the long-term outcome of this procedure is inferior compared with the results of other solid organ transplants. However, at experienced transplant centres 1-year survival rates have increased recently, achieving more than 85% in selected patients. Survival rates depend on recipient age, underlying disease, physical status at the time of transplantation, comorbidities and other factors (Fig. 5.1.1) (Hertz et al. 2002).

To date more then 15,000 lung transplantations have been performed worldwide, indications have been expanded (Fig. 5.1.2; Table 5.1.1) and more patients are being accepted as recipients despite being older or having comorbidities.

The main indications (Glanville and Estenne 2003) are chronic obstructive pulmonary disease (COPD), idiopathic pulmonary fibrosis (IPF), primary (PPH) and secondary pulmonary (SPH) hypertension and cystic fibrosis (CF), but also rare diseases (Saleem et al. 2005) such as lymphangi-

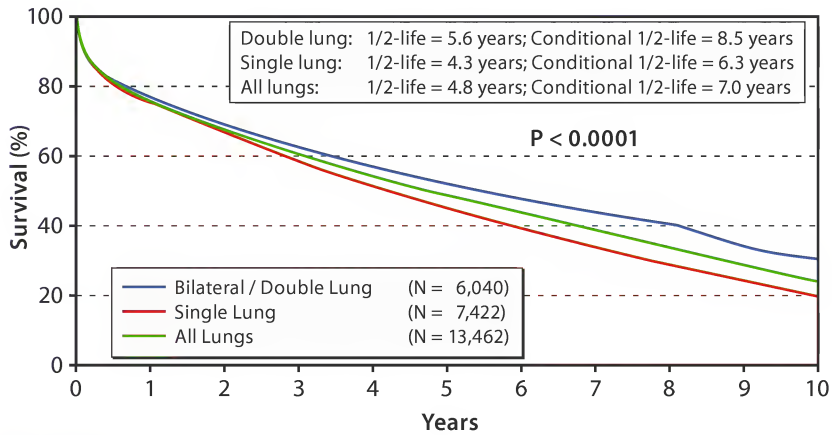

Fig. 5.1.1. Adult lung transplantation: survival

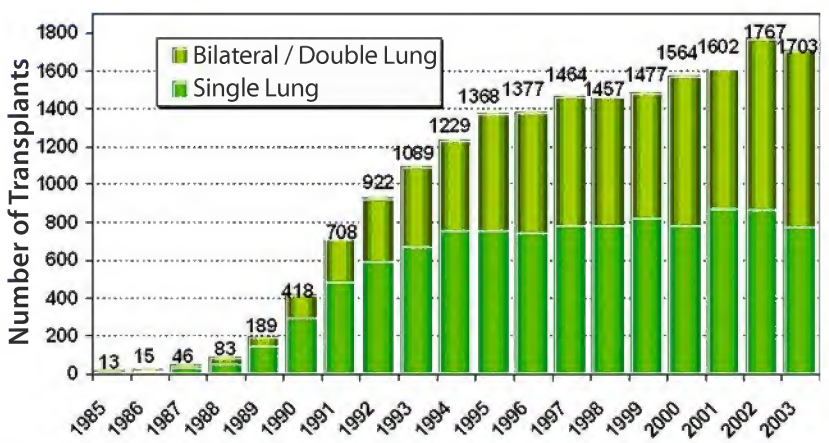

Fig. 5.1.2. Number of lung transplants reported by year and procedure type

Table 5.1.1. Indications for lung transplantation

Lung emphysema/COPD
Cystic fibrosis
Idiopathic pulmonary fibrosis
Alpha-1-antitrypsin deficiency
Primary pulmonary hypertension
Re-transplantation
Secondary pulmonary hypertension
Lymphangioleiomyomatosis
Langerhans' cell histiocytosis
Sarcoidosis

oleiomyomatosis (LAM), Langerhans' histiocytosis, alveolar cell carcinoma and sarcoidosis have gained more acceptance as indications for transplantation.

Absolute (Boe et al. 2003) contraindications to LuTX include serious dysfunction of the kidney and liver, active extrapulmonary infection, current tobacco use or other substance abuse (e.g. alcohol, narcotics), progressive neuromuscular disease and active malignancy within the past 5 years.

Relative contraindications include medical conditions of the recipients that are felt to potentially impact on the long-term outcome and should be optimally treated and well controlled prior to surgery [diabetes mellitus, systemic hypertension and peptic ulcer disease, osteoporosis, age, body mass index (BMI) < 18 or > 25–30 kg/m^2, steroid dose > 20 mg/day].

5.1.1.2 Immunosuppression

The majority (Knoop et al. 2003) of lung transplant recipients receive a triple-drug maintenance regimen including calcineurin inhibitors [CsA or tacrolimus (Tac)], cell-cycle inhibitors [mycophenolate mofetil (MMF), sirolimus, everolimus] and steroids (Fig. 5.1.3). Equal proportions receive CsA and Tac. There is also a trend to prescribe MMF instead of Aza. Steroid withdrawal is uncommon even 5 years after transplantation. The use of induction therapy with poly- or monoclonal antibodies is discussed controversially and differs between transplant centres.

A high-dose intravenous steroid pulse is the standard treatment for uncomplicated acute rejection. A switch from CsA to Tac is the first treatment step of refractory acute rejection followed by high-dose steroids or antilymphocyte agents, total lymphoid irradiation or extracorporeal photopheresis.

The treatment of chronic rejection is challenging and includes different strategies such as modification of the maintenance regimen, augmentation of the immunosuppressive medication, addition of inhaled immunosuppressant or other immunomodulatory treatments.

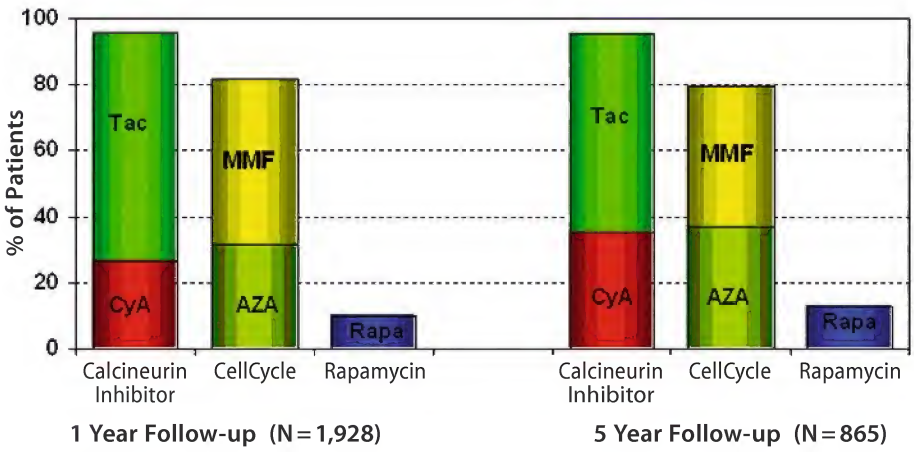

Fig. 5.1.3. Adult lung recipients. Maintenance immunosuppression at time of follow-up for follow-ups between January 2001 and June 2004

5.1.1.3 Transplant Procedures

Single-lung transplantation is the most common form of transplantation used in patients with COPD and IPF. Due to organ scarcity other TX techniques, such as lobar and split lung transplantation, are used and allow the use of living donors especially in younger patients.

Double-lung TX is mandatory for all infectious lung diseases, for example cystic fibrosis, chronic infected obstructive lung diseases and in most cases of severe pulmonary hypertension.

Bilateral LuTX is performed as two subsequent single LuTXs, replacing one side after the other through a transverse thoracosternotomy or through minithoracotomies.

Combined (Boe et al. 2003) heart-lung transplantation is indicated in cases of end-stage lung disease with irreversible heart failure and in patients suffering from complex Eisenmenger's syndrome.

5.1.2 Pretransplant Evaluation and Imaging

5.1.2.1 Recipient Evaluation

Different imaging techniques play an important role in evaluating patients for lung transplantation, predicting transplant risk and searching for comorbidities.

The following radiological investigations are performed routinely in lung transplant candidates:

- Chest CT and radiograph
- Thoracoabdominal CT scan
- Abdominal ultrasound
- Ventilation/perfusion scan especially for single LuTX
- Sinus CT (in cystic fibrosis).

Radiology, together with pathology, is necessary to establish the accurate diagnosis of the candidate's lung disease. In combination with functional diagnostic methods, imaging methods are important for calculating the loss of functional lung tissue, finding the optimal time of referral and finally helping to decide the appropriate surgical technique in each distinct case.

For patients with emphysema (Slone et al. 1998), imaging studies have been useful for selecting patients for surgical interventions, such as bullectomy and lung volume reduction surgery (LVRS), both methods being used as bridging techniques to LuTX.

5.1.2.2 Donor Evaluation

Typically a donor is an intubated ventilated patient; brain death diagnosis should be initiated and the transplant team be sent information about the patient's history and cause of death. A recent chest radiograph is performed to evaluate infectious or posttraumatic lesions and to compare donor and recipient size and measured or calculated lung volume.

Basic criteria for consideration for lung donation now comprise an organ donor with a lack of significant pulmonary disease, although donors with mild asthma may be accepted, and a chest radiograph demonstrating one clear lung field. A multiorgan donor with pneumonia or severe contusion to one lung may be a satisfactory single-lung donor.

Pneumonia, trauma, pneumothorax, hematothorax, effusions and solid tumours are radiographically visible.

Aspiration, atelectasis and pneumonia are common in potential donors, and therefore endotracheal suctioning, percussion, turning for postural drainage and occasional manual lung inflation are critically important. Mucopurulent secretions are frequent in donors with a normal chest radiograph and do not preclude lung donation.

The current definition of brainstem death is based on coma, absent brainstem reflexes and apnoea, with the criteria for organ donation listed in Table 5.1.2.

Table 5.1.2. Minimum donor criteria for organ donation. From Boe et al. (2003)

Patient meets criteria for brainstem death
Absence of malignancy with metastatic potential
Absence of sepsis or communicable disease

5.1.3 Imaging During the First 3 Months After Transplantation

5.1.3.1 Normal Appearance

5.1.3.1.1 At the ICU

After arrival at the intensive care unit (ICU) patients are always monitored by arterial and Swan–Ganz catheter measurements. Arterial blood-gas, cardiac output and urine production are measured and the position of the endotracheal tube has to be checked.

Sometimes extracorporeal membrane oxygenation (ECMO) or cardiopulmonary bypass is required, especially in patients with pulmonary hypertension, to protect the pulmonary circulation and the left ventricle from volume overload. After single-lung TX double-lumen tracheal tubes are sometimes used to ventilate both lungs separately for some hours to avoid hyperinflation of the native emphysematous lung.

Chest tubes are obligatory for the first few days: two tubes are placed on each transplanted side. The quantity and quality of the fluid have to be monitored and postoperative bleeding has to be detected by measuring the haemoglobin value of the pleural fluid.

The first thoracic radiograph, which is performed immediately after arrival at the ICU, gives important information (see Table 5.1.3). It provides evidence relating to the presence of oedema or atelectasis, pneumothorax, lung expansion and size, and position of the diaphragm and mediastinum. If some form of lung shadowing is recognized, a differential diagnosis has to be made and the resulting therapeutic interventions have to be initiated (see Sect. 5.1.4).

Table 5.1.3. Interpretation of chest radiograph shadowing post lung transplant

	Time after transplantation (h)	
	<24	>24
Diffuse	Overhydration Reperfusion injury	Overhydration Rejection Late reperfusion injury
Localised	Surgical residua Localized graft injury Haemorrhage pleural fluid accumulation	Pneumonia Pleural fluid accumulation
Lobar	Vascular problem Obstructing clot	Vascular problem Sputum plug Pneumonia

5.1.4 Complications

5.1.4.1 Complications of the First 24 H

5.1.4.1.1 Size Mismatch

Size mismatch of donor lung and recipient hemithorax can cause mechanical and infectious problems. Therefore, a careful pretransplant evaluation of donor lung size is essential to reduce postoperative problems. If the implanted lung is too large, atelectasis can occur with subsequent severe infection problems. Possible solutions to overcome this problem include intraoperative size reduction or use of single lobes.

A mismatch of 25%–30% is acceptable but size mismatch less than 10% would be ideal (Massard et al. 1993).

Chest radiograph, thoracic CT and lung function with body plethysmography are important to assess the size of donor and recipient lungs, one of the most important criteria for defining the matching donor.

5.1.4.1.2 Pneumothorax

See Sect. 5.1.4.2 for complication after 24 h.

5.1.4.1.3 Reperfusion Oedema/Reimplantation Response (RIR)

The reimplantation response is a type of noncardiogenic pulmonary oedema resulting from the unavoidable trauma associated with transplantation (Montefusco and Veith 1986). The aetiology is unknown but considered to be secondary to a com-

bination of surgical trauma, ischaemic damage to capillaries, denervation, and interruption of lymphatic drainage, surfactant deficiency and different coagulation factor disturbances (Collins 2000).

Some degree of reperfusion oedema is present in almost all lung transplant recipients.

Management of this problem includes exclusion of other differential diagnoses (particularly pulmonary venous obstruction) and supportive therapy in terms of oxygen, NO and the avoidance of fluid overloading. However, running the patient dry in these early days can lead to significant short- and long-term renal impairment.

Radiographically, a diffuse alveolar pattern of infiltration or reticulonodular change is identified in the perihilar and basilar regions of the transplanted lung. Abnormalities are first detected on the chest radiograph at 24–48 h postoperatively. The changes reach a peak before day 4 and begin to resolve by day 5. In the majority of cases, complete resolution should be achieved by day 14. The differential diagnosis of this alveolar and interstitial infiltration also includes acute rejection and pneumonic infiltration. Localized densities can occur for a variety of reasons.

Histologically diffuse alveolar damage (DAD) or BOOP-like reactions (BOOP is bronchiolitis obliterans organizing pneumonia) are described. Any change in the chest X-ray beginning after day 5 should be assumed to be due to some other cause such as infection or rejection.

Use of CT scan seems of no diagnostic benefit; X-ray investigation together with the clinical picture, histology and time course should fix a diagnosis of RIR.

5.1.4.2 Early Complications (< 1–2 Months)

5.1.4.2.1 Pneumothorax, Transient Air Leak and Pleural Effusions

All patients experience pleural effusion ipsilateral to the transplanted lung in the postoperative period that requires drainage with thoracostomy tubes. In the initial phase after lung transplantation, pleural drainage is haemorrhagic in most patients but tends to self-limit and becomes progressively less haemorrhagic until becoming serous after 7 days (Judson et al. 1996).

Postoperative pleural complications occur in up to 22%. The most frequent complications are pneumothorax and empyema (Herridge et al. 1995). During post-transplant follow-up, the majority of surviving patients have residual pleural alterations detectable with CT. These alterations do not seem to worsen the progress of these patients, although they may be an inconvenience should re-transplantation be required.

Haemothorax and persistent air leak are associated with increased postoperative mortality. Chest CT shows pleural alterations in most patients 12 months after transplantation (Ferrer et al. 2003).

5.1.4.2.2 Phrenic Nerve Injury (PNI)

Injury of the phrenic nerve can be caused from stretching or direct instrumentation of the nerve and occurs after double-lung transplantation in up to 40% in different degrees. Paralysis of the diaphragm results in prolonged ventilation time and longer ICU time (Sheridan et al. 1995; Ferdinande et al. 2004).

Radiologic signs of PNI are atelectasis of the lower lobe or raised diaphragm.

Sheridan et al. (1995) evaluated 27 lung transplant recipients and found 8 with phrenic nerve injury, an incidence of 30%. An increased hospital stay was noted in these patients. In most cases, the event occurred in patients with bilateral LuTX and had little impact on lung function.

5.1.4.2.3 Reimplantation Response (RIR)

See Sect. 5.1.4.1.3.

5.1.4.2.4 Acute Rejection (AR)

Acute rejection (AR) of the lung manifests pathologically as infiltration of mainly lymphocytes in the perivascular and peribronchial/peribronchiolar regions. It is graded according to the intensity of the infiltrating cells and to the extent of lung parenchyma involvement. Air space oedema and mononuclear cells are also present features.

Acute rejection of the lung is graded according to the International Society for Heart Lung Transplantation (ISHLT) Working Formulation (Yousem

et al. 1996). Acute rejection consists of five grades ranging from A0 (no rejection) to A1–A4 (minimal to severe AR).

A diagnosis of AR should only be made when other possible causes of abnormal function or radiological shadowing are excluded histologically, microbiologically and clinically. Common differential diagnoses are infections and in the early postoperative period acute lung injury or reperfusion injury (Zenati et al. 1990). Usually AR develops during the first 6 months after transplantation, but any decrease in lung function or infiltrate on chest X-ray should be suspected as AR even years after transplantation.

In addition, AR tends to arise after the 5th postoperative day, in contrast to the reimplantation response that tends to become manifest within the first 48 h.

The clinical diagnosis of acute lung rejection includes the presence of fever, infiltrates on the chest radiograph, decreased oxygen uptake, exclusion of infection (by bronchial lavage, BAL) and a rapid improvement of symptoms after an IV steroid bolus but in some cases no clinical or radiological signs develop and AR is only diagnosed histologically. Almost all lung transplant patients experience at least one episode of AR.

Although the chest X-ray is relatively insensitive and nonspecific in the diagnosis of acute pulmonary rejection, it may be the first hint that rejection is occurring. Chest X-ray may be normal in 50%, others may show peribronchial thickening, areas of increased opacity, pleural effusions or consolidations (Ward and Muller 2000).

A radiographic response to treatment may confirm the suspicion of rejection. In most cases rejection is confirmed by transbronchial biopsy.

Findings on CT scan and HRCT are nonspecific and have a low positive predictive value. Herber et al. (2001) reported ten patients with proven AR, ground glass opacities, bronchial wall thickening, septal thickening, dilatation of the bronchus, pleural effusions and centrilobular densities with a specificity of 30%–50%.

5.1.4.3 Infection

Infection is a frequent cause of mortality and morbidity in lung transplant recipients. Direct communication of the transplanted lung with the atmosphere and impaired mucociliary action in an immunocompromised patient predispose them to bacterial, viral and fungal infections. Within the first postoperative month, bacteria and fungi are common causes of infection, while viral infections are common in the 2nd and 3rd months (Tables 5.1.4, 5.1.5). Transplanted infections of the donor or persisting microorganisms of the recipient, especially after single-lung transplant are sources of early postoperative infections. Although bacteria are responsible for the majority of infections following lung transplantation, fungal infections are associated with the highest mortality (Alexander and Tapson 2001).

Collins and co-workers (2000) identified 39 patients with 45 pneumonias. Of these 45 pneumonias, the most common single infectious organisms were *Cytomegalovirus* in 15 pneumonias, *Pseudomonas* in 7 pneumonias, and *Aspergillus* in 8 pneumonias. The most common CT findings of pneumonia were consolidation in 82%, ground glass opacification in 76%, septal thickening in 73%, pleural effusion in 73%, multiple nodules in 56%, and single nodules in 4% of pneumonias. There were no significant differences in the prevalence of findings among bacterial, viral and fungal pneumonias (Ward and Muller 2000).

Radiographic findings are often nonspecific and usually do not distinguish pneumonia from rejection, unless findings are present in the native lung. CT is useful for early detection of pneumonia and is helpful in directing bronchoscopy or transbronchial biopsy, and is very useful in following response to therapy.

5.1.4.3.1 Bacterial Infection

Bacterial pneumonia accounts for the majority of infections, generally occurring in the first 2 months. *Pseudomonas* and *Klebsiella* are the most common pathogens. The radiologic features of infection are generally nonspecific and sometimes subtle but CT, and in particular HRCT, is very helpful when making the diagnosis, showing consolidation, ground glass opacification and nodularity. The nodularity may have a tree-in-bud pattern (Collins et al. 2000). Diagnosis should be confirmed by bacteriology taken from bronchoalveolar lavage; transbronchial biopsy should be performed to distinguish pneumonia from AR, diffuse alveolar damage (DAD) or BOOP.

Table 5.1.4. Timeline of complications following lung transplantation that may require intensive care unit treatment (from Lau et al. 2004). (*BOS* Bronchiolitis obliterans syndrome, *CMV* cytomegalovirus, *GI* gastrointestinal)

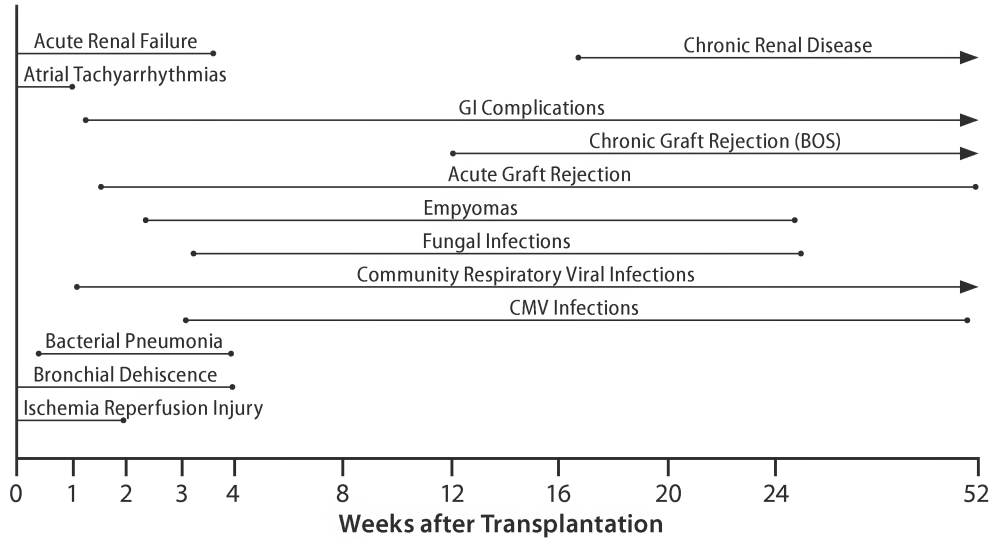

Table 5.1.5. Relevant infections after lung transplantation grouped according to type and frequency. (*CMV* Cytomegalovirus, *EBV* Epstein–Barr virus, *HIV* human immunodeficiency virus, *HHV* human herpes virus, *HSV* herpes simplex virus, *RSV* respiratory syncytial virus, *VZV* varicella zoster virus)

Group	Frequent	Infrequent
Bacterial	Bacterial bronchitis and/or pneumonia *Pseudomonas aeruginosa* Enterobacteriaceae *Staphylococcus aureus* *Enterococcus* *Haemophilus influenzae* Paranasal sinusitis Gastroenteritis	Atypical pneumonias Tuberculosis Nontuberculous mycobacteriosis Nocardiosis Anaerobic infections (actinomyces, etc.)
Viral	Herpes virus infections CMV EBV HSV VZV Viral respiratory tract infection Rhinovirus Parainfluenza virus Influenza virus RSV Adenovirus Viral gastroenteritis	HIV infection JC virus infection Polyoma BK virus infection HHV6? HHV7? Hepatitis B and C
Fungal	*Aspergillus fumigatus/niger/flavus* *Candida* species	Mucormycosis *Cryptococcal* infection *Penicillium* infection
Protozoa		*P. carinii* pneumonia Toxoplasmosis

5.1.4.3.2 Fungal Infection

Fungal (Kubak 2002) infections are a significant cause of postoperative morbidity and mortality in lung transplant recipients. The lung recipient remains continuously open to the environment and to the myriad of fungal spores and pathogens.

Early fungal infections are related to surgical complications or derived from the implanted lung; fungal infections after months 1–6 reflect opportunistic, relapsed, or residual infections. Late fungal infections are usually associated with treatments for chronic rejection or bronchial airway mechanical abnormalities.

Most frequent fungal infections in lung transplant recipients are related to *Aspergillus* species, followed by *Candida* and *Cryptococcus*. Infection with *Aspergillus* species can present in different forms, such as tracheobronchitis, bronchopneumonia, bronchocentric granulomatosis, angioinvasive disease, allergic bronchopulmonary aspergillosis, acute eosinophilic pneumonia, mycetoma and empyema. The identification of high-risk patients (preoperatively and postoperatively) is essential in implementing prophylactic or pre-emptive management.

The most frequent CT pattern in patients with invasive fungal infection is a combination of nodules, consolidation and ground glass opacities. The angioinvasive type of aspergillosis often has a typical CT appearance of a mass with surrounding ground glass opacity or halo sign. These masses or nodules may be multiple and some may go on to cavitate.

5.1.4.3.3 Viral Infection

Cytomegalovirus (CMV) pneumonia was the second commonest infection in transplant recipients with a very high mortality, occurring in up to 50% of patients in some series. It may be difficult to distinguish CMV infection from AR since the clinical signs and symptoms are usually similar; however, the timing of symptoms may provide a clue to the diagnosis as being CMV infection, which rarely occurs within the first 2 weeks after transplantation.

The chest radiograph in patients with CMV pneumonia may be normal or show ground glass opacities or reticulonodular opacities. HRCT is more sensitive and may help to guide the appropriate site for biopsy. The HRCT features of CMV infection include ground glass opacities, nodules which may tend to coalesce and consolidations.

When only ground glass opacification is seen on CT, *Pneumocystis carinii* pneumonia and AR should also be considered in the differential diagnosis.

5.1.4.3.4 Tuberculosis

Infections may be caused by reactivation of a primary infection in the recipient, reactivation of a lesion from the donor lung, or as a primary infection. The (Morales et al. 2005) increase in the number of solid organ transplants has resulted in an increased incidence of opportunistic infections, including infection by typical and atypical mycobacteria, with the risk of developing tuberculosis. Pretransplant chemoprophylaxis with isoniazid has become increasingly common in an attempt to prevent the disease. The source of infection in tuberculosis (TB) may be difficult to identify. There are few reports on TB in lung transplantation (Baldi et al. 1997; Miller et al. 1995).

The incidence of infections with tuberculosis ranges from 6.5% to 10%. In a series from Spain Morales and co-workers (2005) found a rate of 2.6% with a high mortality of 42.8% due to failing or not successfully completed treatment.

Malouf and Glanville (1999) found an incidence of 9% (23 patients of 261) with mycobacterial infections, 19 cases with pulmonary (*M. avium complex* $n=13$, *M. tuber* $n=2$, *M. abscessus* $n=2$, *M. asiaticum* $n=1$ and *M. kansasii* $n=1$) and 6 with extrapulmonary infections. Most episodes were treated and graft function improved in most cases. They concluded that mycobacterial infections, particularly due to nontuberculous mycobacteria, are relatively common after lung transplantation and may be an unrecognized cause of graft dysfunction.

Schulman et al. (1997) published two cases of pulmonary tuberculosis, both 3 months after bilateral lung transplantation, and found radiographically a narrowing of the middle lobe bronchus of the right lung caused by an endobronchial granulomatous mass (n=1) and a focal cluster of small nodules in the upper lobe of the left lung and small bilateral pleural effusions (n=1).

5.1.4.3.5 Bronchial Problems/Anastomotic Problems

The most common airway problems are anastomotic dehiscence and bronchial stenosis due to strictures. The reason is mostly a lack of perfusion of the bronchial tree, as the donor airways depend on a retrograde pulmonary-to-bronchial arterial circulation until revascularization of the bronchus wall occurs. Ischaemia is greater on the right main bronchus than on the left, therefore anastomotic healing is better on the left and early stenotic problems or dehiscence occur on the right anastomosis more frequently than on the left side. In the early years of transplantation the en bloc technique was mainly performed with a high incidence of tracheal dehiscence, which prompted the development of bilateral lung transplantation.

To reduce the risk of ischaemic airway problems the steroid dose was lowered in the early postoperative period and surgical tricks such as omental wrap or different sutures types were tried.

Airway dehiscence can be suspected when a pneumothorax with a persistent air leak occurs some days after the operation or anastomotic wound healing problems are detected via bronchoscopy.

Radiographically dehiscence can be detected by the presence of extrapulmonary peribronchial air on chest X-ray or CT. Using thin-section CT, small amounts of extraluminal air can be found and can lead to early interventions such as endobronchial stenting before infectious problems occur.

Delayed bronchial problems such as stenosis can be suspected when atelectasis occurs weeks or months after transplantation. Diagnosis of stenosis has to be confirmed by bronchoscopy and CT. Reasons for late bronchial stenotic problems are chronic infectious problems due to ischaemia and strictures due to shrinking bronchial walls.

5.1.5 Long-Term Follow-Up

5.1.5.1 Normal Appearance

In double-lung recipients the chest X-ray can appear without any pathology. If a size reduction has to be performed intraoperatively stapler devices can be seen. A raised diaphragm could give a hint of phrenic nerve injury. Pleural thickening is mostly seen on the lower parts of the lungs.

In single-lung recipients hyperinflation of the native lung in COPD patients can be observed. In contrast in IPF recipients the transplanted lung can impose hyperinflated.

5.1.5.2 Long-Term Complications

5.1.5.2.1 Chronic Rejection/BO(S)

Chronic rejection (bronchiolitis obliterans, BO) is the single most important cause of chronic allograft dysfunction and of late mortality after lung transplantation. It is an inflammatory disorder of the small airways leading to obstruction and destruction of pulmonary bronchioles and severe obstructive airway disease. This condition is difficult to prove using biopsy specimens, because BO may be patchy in distribution; therefore, a clinical term, bronchiolitis obliterans syndrome (BOS), has been in use for >10 years to describe the progressive decrease of pulmonary function (Verleden 2005). Following the ISHLT grading system BOS is graded BOS grade 0, 0p, 1, 2 and 3, depending on the decrease of forced expiratory volume in 1 s (FEV_1) compared to the best reproducible value reached after transplantation.

The recent incidence of chronic lung dysfunction due to BO is about 60% at 5 years post transplantation and this is one of the main indications for retransplantation.

Immune-mediated injury has been recognized as the leading cause of BOS, but recently nonimmune mechanisms, such as gastro-oesophageal reflux, have been recognized as potential cofactors. The results of various treatment options have generally been frustrating, therefore early diagnosis is needed to prevent or reverse progression of disease.

Bronchiolitis obliterans usually begins later than 3 months following transplant and manifests as dyspnoea, obstruction of the airways, recurrent lower tract infections and a rapid progression over months with a clinical course similar to that of COPD.

Several potential early markers such as lung function, BAL analysis, analysis of exhaled gases, breath condensate and CT are known and routinely

used to assess the time course of changes and to predict the decrease in lung function and the risk for BOS.

The radiographic features of BO are: peribronchial and interstitial opacities, bronchial dilatation, decreased vascular markings with areas of hyperinflation (best detected on expiratory CT), peripheral patchy consolidation and multiple pulmonary nodules 0.5–1.5 cm in diameter. The presence of air trapping on expiratory HRCT is a good indicator of the bronchiolar obliteration. In patients with BOS, areas with obstructed airways cannot empty and remain more radiolucent, while in areas that have normal airways the density increases during the expiratory phase. In a study by Bankier et al. (2001) five of six patients with initial false-positive findings (with significant air trapping but an $FEV_1 > 80\%$ of baseline) later developed BOS, which suggests that expiratory CT may contribute to the early detection of the condition. Conversely, air trapping has a very high negative predictive value, i.e. a low score of air trapping in a patient with declining lung function makes the diagnosis of BOS very unlikely. Quantification of air trapping using expiratory HR showed a good correlation between BOS grade and percentage of expiratory trapping, with a cut-off level of more than 32% as an early indicator for BO (Bankier et al. 2001).

5.1.5.2.2 Infections

See Sect. 5.1.4.3.

5.1.5.2.3 Post-Transplant Lymphoproliferative Disease (PTLD)

PTLD is a typical complication with an incidence of about 1%–3% and an onset 8–12 months post-transplantation. It is associated with EBV infection and induced through T-cell suppression due to CsA, Tac or MMF. Most cases are B-cell lymphoma with a significantly higher incidence after lung transplantation compared to other organs. PTLD can involve multiple organ systems, commonly lymph nodes cervical, GI tract, particularly distal small bowel, proximal colon or multicentric, or the lungs as a solitary mass, multiple nodules or as hilar lymph adenopathy.

Reduction of immunosuppressive medication, chemotherapy and B-cell antibodies are all therapeutic options.

Diagnosis is suspected on radiography and CT scan, but is confirmed by open lung biopsy or transbronchial biopsy.

5.1.5.2.4 Malignancies

An increased risk of developing certain malignancies is a recognized complication of organ transplantation. The patterns and incidence of malignancy in transplant recipients differ from those in the general population and are substantially influenced by the specific type of allograft and immunosuppressive therapy received (Penn 1993). The Registry of the International Society for Heart and Lung Transplantation has reported the incidence of malignancy at 1-year follow-up after lung transplantation to be 4.3%, with 50.7% due to lymphoproliferative disorders, and at 5-year follow-up to be 7.7%, with 17.8% due to lymphoproliferative disorders and 50.7% due to skin malignancies (Hosenpud et al. 2000).

Bronchogenic carcinoma develops in the native lung of transplant recipients with emphysema and pulmonary fibrosis at frequencies of 2% and 4%, respectively. The carcinomas most commonly manifest as a pulmonary nodule or mass on chest radiographs, with more nodules seen on CT scans (Collins et al. 2002). This rate is similar to that in other high-risk populations (e.g. elderly smokers with emphysema or other chronic lung disease). The majority of cancers are associated with a poor prognosis. The most common imaging manifestations are a solitary pulmonary nodule or mass.

5.1.5.2.5 Complications of the Native Lung

McAdams and co-workers (2001) published a series of 111 single-lung recipients and complications occurred in 17 (15%) recipients, most commonly due to infections or lung cancer, and this caused serious morbidity or mortality in 12 (71%) of the 17 patients affected. Infectious complications typically manifested as lobar or segmental opacities on chest radiographs or CT scans. Lung cancer manifested as a solitary, circumscribed nodule, multiple nodules, or a hilar mass.

Hyperinflation of the native lung is a specific problem of recipients of a single lung for COPD. Due to the progression of the underlying disease the obstruction increases and subsequent air trapping re-

sults in hyperinflation of the old lung and compression of the transplanted lung, producing increasing dyspnoea during exercise. Lung volume reduction surgery is the only therapeutic option, and perhaps endobronchial volume reduction is a future option in such cases.

5.1.5.2.6 Recurrence of the Underlying Disease

Recurrence of the primary disease in the transplanted lung has been reported for several diseases, for example sarcoidosis, pulmonary Langerhans' cell histiocytosis, giant cell interstitial pneumonia, LAM and bronchioloalveolar carcinoma.

Sarcoidosis is the most commonly reported recurrent disease. Milman et al. (2005) reported a recurrence rate of 50% in seven lung-transplanted patients without clinical significance.

Dauriat et al. (2006) described a recurrence rate of histiocytosis X (HX) of about 20% in 39 transplant recipients. The present authors transplanted 12 patients with histiocytosis X: 3 of them developed a recurrence during the first 3 years postoperatively, 1 received a re-transplantation and HX relapsed again 12 months after the redo surgery.

Boehler (2001) has reported that 1 in 34 patients transplanted for LAM developed recurrence of underlying disease.

There is controversy regarding whether bronchioloalveolar carcinoma should be accepted as an indication for LuTX. A recurrence of the disease within the donor lungs was noted in four of seven lung-transplanted patients by Garver et al. (1999). At the University of Birmingham Zorn et al. (2003) transplanted nine patients with bronchioloalveolar carcinoma and just two of them were free from recurrence.

In all cases of suspected recurrence of the primary lung disease standard radiography together with changes in lung function can give a hint of relapse, but a CT scan and transbronchial biopsy are necessary to confirm the diagnosis.

5.1.5.2.7 Bronchial or Tracheal Stenosis

See Sect. 5.1.4.3.5

5.1.5.2.8 Pulmonary Nodules

Schulman and co-workers (2000) assessed clinical and radiographic findings of pulmonary nodules and masses after lung and heart-lung transplantation. In total, 159 patients were followed by serial chest radiographs for a median of 27 months. Single or multiple lung nodules or masses were noted at chest radiography in 15 (9.4%) of 159 patients. Imaging findings and causes of these nodules and masses were reviewed retrospectively.

Infection was found in 10 (6%) of 159 patients. Specific pathogens (11 pathogens in 10 patients) were *Aspergillus* ($n=4$), *Mycobacteria* ($n=4$), and other bacteria ($n=3$). Noninfectious causes were found in 5 (3%) of the patients and included B-cell lymphoma ($n=2$), bronchogenic carcinoma ($n=2$), and pulmonary infarcts ($n=1$). Nodules and masses appeared a median of 11 months after transplantation (range: 0.2–36 months). Five patients (33%) had single lesions; the other ten (67%) patients had multiple lesions (range 2–50). *Aspergillus* lesions were most commonly located in the upper lobes, were cavitary in three of four patients, and all were fatal. Nodules and masses arose in the transplanted lung in 12 (80%) of the patients, and in the native lung in 3 (20%) of the patients (2 bronchogenic carcinoma, 1 *M. tuberculosis* simulating bronchogenic carcinoma).

Nodules and masses detected by chest radiography are not uncommon (9.4%) after lung and heart-lung transplantation. Infectious are more common than noninfectious causes of post-transplant nodules and masses. Specific clinical and imaging characteristics may provide clues to the aetiology (Schulman et al. 2000).

5.1.5.2.9 New Entities and Rarities

5.1.5.2.9.1 Fibrosis of the Upper Lobe

Konen et al. (2003) published HRCT findings in seven lung transplant recipients who developed a progressive lung fibrosis, predominantly in the upper lobes with relative sparing of the basal segments. This radiographic feature may represent a specific and rare type of rejection in lung transplant recipients. Clinical, laboratory, microbiological and

pathological studies did not reveal any specific findings that could explain a common mechanism in this group of patients.

5.1.5.2.9.2 Sirolimus-Induced Pneumonitis

Interstitial pneumonitis (Garrean et al. 2005) is an ill-defined side-effect of sirolimus, a new immunosuppressant drug recently introduced for patients after solid organ transplantation. Lymphocytic alveolitis and radiologic BOOP are the key findings in sirolimus-associated pneumonitis. Sirolimus withdrawal was associated with recovery within 6 months. Published first as occurring in patients after kidney transplantation, one case report describes a stable heart-lung transplant recipient who developed a pulmonary infiltrate that reversed after ceasing sirolimus therapy (McWilliams et al. 2003).

5.1.6 Imaging of Interventional Complications

5.1.6.1 Transbronchial Biopsies (TBB)

Scheduled bronchoscopies are performed routinely during the first year after transplantation at most transplant centres. Inspection of the anastomotic sutures, control of anastomotic wound healing, BAL with microbiologic cultures and transbronchial biopsies are taken to document lung tissue quality and to diagnose acute or chronic lung rejection, invasive infections and eventually to perform interventional procedures such as dilatation or stenting of bronchial stenosis.

One of the most common radiological findings after TBB is pneumothorax (incidence between 0.1%–3%), which is easily recognized on a chest radiograph. Postbioptic haemorrhage can present as small nodules or ground glass opacifications. They are most often seen in the periphery of the lung and may contain a small cavity. Clearing is generally seen over a 2-week period. The same picture can be seen after BAL taken mostly from the middle lobe or the lingula, when about 100 ml of saline is instilled but not completely removed.

References

Alexander BD, Tapson VF (2001) Infectious complications of lung transplantation. Transpl Infect Dis 3(3):128–137

Baldi S, Rapellino M, Ruffini E, Cavello A, Mancusco M (1997) Atypical mycobacteriosis in a lung transplant recipient. Eur Respir J 10:952–954

Bankier A, Van Muylem A, Knoop C, Estenne M, Gevenois PA (2001) Bronchiolitis obliterans syndrome in heart-lung. Radiology 218:533–539

Boe J, Estenne M, Weder W (2003) Lung transplantation. European Respiratory Monograph 26. Maney, London

Boehler A (2001) Lung transplantation for cystic lung diseases: lymphangioleiomyomatosis, histiocytosis x, and sarcoidosis. Semin Respir Crit Care Med 22(5):509–516

Collins J (2000) Imaging of the chest after lung transplantation. J Thorac Imaging 55:332–339

Collins J, Muller NL, Kazerooni EA, Paciocco G (2000) CT findings of pneumonia after lung transplantation. AJR Am J Roentgenol 175:811–818

Collins J, Kazerooni EA, Lacomis J, McAdams HP, Leung AN, Shiau M, Semenkovich J, Love RB (2002) Bronchogenic carcinoma after lung transplantation: frequency, clinical characteristics, and imaging findings. Radiology 224:131–138

Dauriat G, Mal H, Thabut G, Mornex JF, Bertocchi M, Tronc F, Leroy-Ladurie F, Dartevelle P, Reynaud-Gaubert M, Thomas P, Pison C, Blin D, Stern M, Bonnette P, Dromer C, Velly JF, Brugiere O, Leseche G, Fournier M (2006) Lung transplantation for pulmonary Langerhans' cell histiocytosis: a multicenter analysis. Transplantation 15;81(5):746–750

Ferdinande P, Bruyninckx F, Van Raemdonck D, Daenen W, Verleden G; Leuven Lung Transplant Group (2004) Phrenic nerve dysfunction after heart-lung transplantation. J Heart Lung Transplant 23:105–109

Ferrer J, Roldan J, Roman A, Bravo C, Monteforte V, Pallissa E, Gic I, Sole J, Morell F (2003) Acute and chronic pleural complications in lung transplantation. J Heart Lung Transplant 22:1217–1225

Garrean S, Massad MG, Tshibaka M, Hanhan Z, Caines AE, Benedetti E (2005) Sirolimus-associated interstitial pneumonitis in solid organ transplant recipients. Clin Transplant 19(5):698–703

Garver RI Jr., Zorn GL, Wu X, McGiffin DC, Young KR Jr., Pinkard NB (1999) Recurrence of bronchioloalveolar carcinoma in transplanted lungs. N Engl J Med 340(14):1071–1074

Glanville A, Estenne M (2003) Indications, patient selection and timing of referral for lung transplantation. Eur Respir J 22:845–852

Hardy J, Webb WR, Dalton ML, Walker GR (1963) Lung homotransplantation in man: report of the initial case. J Am Med Assoc 186:1065–1074

Herber S, Kalden P, Kreitner KF, Riedel C, Rompe JD, Thelen M (2001) Akute und chronische Transplantatabstoßung? HRCT des Thorax nach Lungentransplantation. Fortschr Röntgenstr 173:822–829

Herridge MS, de Hoyos AL, Chaparro C, Winton TL, Keston S, Maurer JR (1995) Pleural complications in lung transplant recipients. J Thorac Cardiovasc Surg 110:22–26

Hertz MI, Taylor DO, Trulock EP et al (2002) The Registry of the International Society for Heart and Lung Transplantation: nineteenth official report – 2002. J Heart Lung Transplant 21:950–970

Hosenpud JD, Bennett LE, Keck BM, Boucek MM, Novick RJ (2000) The Registry of the International Society for Heart and Lung Transplantation: Seventeenth Official Report – 2000. J Heart Lung Transplant 19:909–931

Judson MA, Handy JR, Sahn SA (1996) Pleural effusions following lung transplantation. Time course, characteristics, and clinical implications. Chest 109:1190–1194

Knoop C, Haverich A, Fischer A (2003) Immunosuppressive therapy after human lung transplantation. European Respiratory Monograph 26. Maney, London, pp 105–129

Konen E, Weisbrod GL, Pakhale S, Chung T, Paul NS, Hutcheon MA (2003) Fibrosis of the upper lobes: a newly identified late-onset complication after lung transplantation? AJR Am J Roentgenol 181:1539–1543

Kubak BM (2002) Fungal infection in lung transplantation. Transpl Infect Dis 4 [Suppl 3]:24–31

Lau CL, Patterson GA, Palmer SM (2004) Critical care aspects of lung transplantation. J Intensive Care Med 19:83–104

Malouf MA, Glanville AFR (1999) The spectrum of mycobacterial infection after lung transplantation. Am J Respir Crit Care Med 160(5 Pt 1):1611–1616

Massard G, Badier M, Guillot C et al (1993) Lung size matching for double lung transplantation based on the submammary thoracic perimeter: accuracy and functional results. J Thorac Cardiovasc Surg 105:9–14

McAdams HP, Erasmus JJ, Palmer SM (2001) Complications (excluding hyperinflation) involving the native lung after single-lung transplantation: incidence, radiologic features, and clinical importance. Radiology 218:233–241

McWilliams TJ, Levvey BJ, Russell PA, Milne DG, Snell GI (2003) Interstitial pneumonitis associated with sirolimus: a dilemma for lung transplantation. J Heart Lung Transplant 22:210–213

Miller RA, Lanza LA, Kline JN, Geist LJ (1995) Mycobacterium tuberculosis in lung transplant recipients. Am J Respir Crit Care Med 152(1):374–376

Milman N, Burton C, Andersen CB, Carlsen J, Iversen M (2005) Lung transplantation for end-stage pulmonary sarcoidosis: outcome in a series of seven consecutive patients. Sarcoidosis Vasc Diffuse Lung Dis 22(3):222–228

Montefusco CM, Veith FJ (1986) Lung transplantation. Surg Clin North Am 66:503–515

Morales P, Briones A, Torres JJ, Sole A, Perez D, Pastor A (2005) Pulmonary tuberculosis in lung and heart-lung transplantation: fifteen years of experience in a single center in Spain. Transplant Proc 37(9):4050–4055

Penn I (1993) Incidence and treatment of neoplasia after transplantation. J Heart Lung Transplant 12(Suppl 6, part 2):S328–S336

Saleem I, Moss J, Egan JJ (2005) Lung transplantation for rare pulmonary diseases. Sarcoidosis Vasc Diffuse Lung Dis 22 [Suppl 1]:S85–S90

Schulman LL, Scully B, McGregor CC, Austin JH (1997) Pulmonary tuberculosis after lung transplantation. Chest 111:1459–1462

Schulman LL, Htun T, Staniloae C, McGregor CC, Austin JH (2000) Pulmonary nodules and masses after lung and heart-lung transplantation. J Thorac Imaging 15(3):173–179

Sheridan PH Jr, Cheriyan A, Doud J, Dornseif SE, Montoya A, Houck J, Flisak ME, Walsh JM, Garrity ED Jr. (1995) Incidence of phrenic neuropathy after isolated lung transplantation. The Loyola University Lung Transplant Group. J Heart Lung Transplant 14:684–691

Slone RM, Gievada DS, Yusen RD (1998) Preoperative and postoperative imaging in the surgical management of pulmonary emphysema. Radiol Clin North Am 36:57–89

Toronto Lung Transplantation Group (1986) Unilateral lung transplantation for pulmonary fibrosis. N Engl J Med 314:1140–1145

Verleden GM (2005) Is it bronchiolitis obliterans syndrome or is it chronic rejection: a reappraisal? Eur Respir J 25:221–224

Ward S, Muller NL (2000) Pulmonary complications following lung transplantation. Clin Radiol 55:332–339

Yousem SA, Berry GJ, Cagle PT et al (1996) Revision of the 1990 working formulation for the classification of pulmonary allograft rejection: Lung Rejection Study Group. J Heart Lung Transplant 15:1–15

Zenati M, Yousem SA, Dowling RD, Stein KL, Griffith BP (1990) Primary graft failure following pulmonary transplantation. Transplantation 50:165–167

Zorn GL, McGiffin DC, Young KR Jr., Alexander CB, Weill D, Kirklin JK (2003) Pulmonary transplantation for advanced bronchioloalveolar carcinoma. J Thorac Cardiovasc Surg 125:45–48

5.2 Imaging of Lung Transplantation

Sheida Mehrain, Daniela Kienzl, and Alexander Bankier

CONTENTS

S. Mehrain, MD
D. Kienzl, MD
Department of Radiology, Medical University of Vienna, Waehringer Guertel 18–20, 1090 Vienna, Austria
A. A. Bankier, MD
Director of Functional Respiratory Imaging, Beth Israel Deaconess Medical Center, Harvard Medical School, 330 Brookline Avenue, Boston, MA 02215, USA

5.2.1 Introduction

Between the performance of the first successful lung transplantation in 1988 (Hosenpud et al. 2000) and June 2004, there have been 3154 heart-lung and 19,296 lung transplantations recorded in the Registry of the International Society for Heart and Lung Transplantation (Trulock et al. 2005). The procedure has gained widespread acceptance as a therapeutic option for a diverse array of lung diseases. However, complications are frequent and result in constraints on long-term preservation of graft function and patient survival.

5.2.1.1 Indications and Contraindications

Lung transplantation is indicated for patients with end-stage lung disease who demonstrate declining function despite of optimal therapy (Trulock et al. 2005). Candidates for lung transplantation should have a chronic disease that is refractory to other medical or surgical therapies, and for which survival is limited to usually less than 2–3 years (Trulock et al. 2005). During the period from January 1995 to June 2004 the most frequent indications for lung transplantation were chronic obstructive pulmonary disease (COPD, 38%), idiopathic pulmonary fibrosis (IPF, 17%), cystic fibrosis (CF, 17%) and 1-anti-trypsin deficiency emphysema (9%) (Trulock et al. 2005) (Fig. 5.2.1). Critically ill patients in desperate clinical situations such as significant cardiac, renal, or hepatic impairment are rarely appropriate candidates for transplantation (Maurer et al. 1998). Further contraindications include uncontrolled infection, uncured malignancies as well as active cigarette smoking and/or other drug/alcohol dependency (Collins

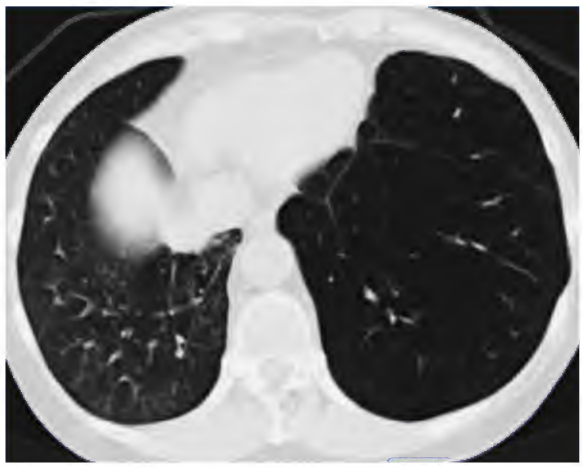

Fig. 5.2.1. Transverse CT section in a single right-lung transplant recipient. Native emphysematous lung (*left*) is overinflated, while the transplanted lung shows normal density

Fig. 5.2.2. Transverse CT section in a single-lung transplant recipient. Native fibrotic lung (*right*) shows increased density, whereas the density of the transplanted left lung is normal

2002). Important considerations are also irresolvable psychosocial problems or noncompliance with medical management (Collins 2002).

5.2.1.2 Transplant Allocation

Prioritization on the waiting list according to the recipient's primary disease is considered the fairest allocation of donor lungs, since obvious waiting-list mortality differences depending on the primary disease exist (Glanville and Estenne 2003). For example, patients with IPF (Fig. 5.2.2), who have disproportionately high mortality rates while on the waiting list, are currently assigned a bonus of 90 days by the United Network for Organ Sharing of the USA upon registration on the active list (Glanville and Estenne 2003).

5.2.1.3 Surgical Procedures

The number of combined heart-lung transplantations has been rapidly declining, while the recently more common double-lung procedure has been surpassing in number the earlier dominating single-lung procedure since 2002 (Trulock et al. 2005) (Fig. 5.2.3). The decrease in donor organ pool by performing double-lung procedures is unsatisfactory considering the long waiting time of more than 18 months to receive lung transplantation (Trulock et al. 2005). This trend is, however, most likely motivated by better overall survival results, by better lung function and fewer occurring complications after double-lung transplantation (Trulock et al. 2005). To date, the procedure of choice is single or bilateral lung transplantation, with the limited number of donor organs determining the surgical approach in individual situations. The formerly common heart-lung transplantation under cardiopulmonary bypass is now rarely performed. Bilateral transplantation is usually performed sequentially with two single-lung transplants. If the rarely employed extracorporeal support is necessitated, it is instituted through the femoral approach. The surgical approach has been modified and the original clamshell incision has been replaced by two small anterior thoracotomies (Venuta et al. 2005). Donor shortage has led to the development of living lobar transplantation. In living lobar transplantation, one donor provides a right lower lobe, the other donor a left lower lobe to a single bilateral lobar recipient (Fig. 5.2.4). One transplant center describes an overall significant morbidity of 4.6% and no donor mortality in living donor transplantation (Starnes et al. 2004). The shortage of donor lungs suitable for children and small adults has led to the development of the "split-lung" technique. In this procedure, the left lung is separated into two lobes. The left lower lobe is used for left lung transplant and the left upper lobe for

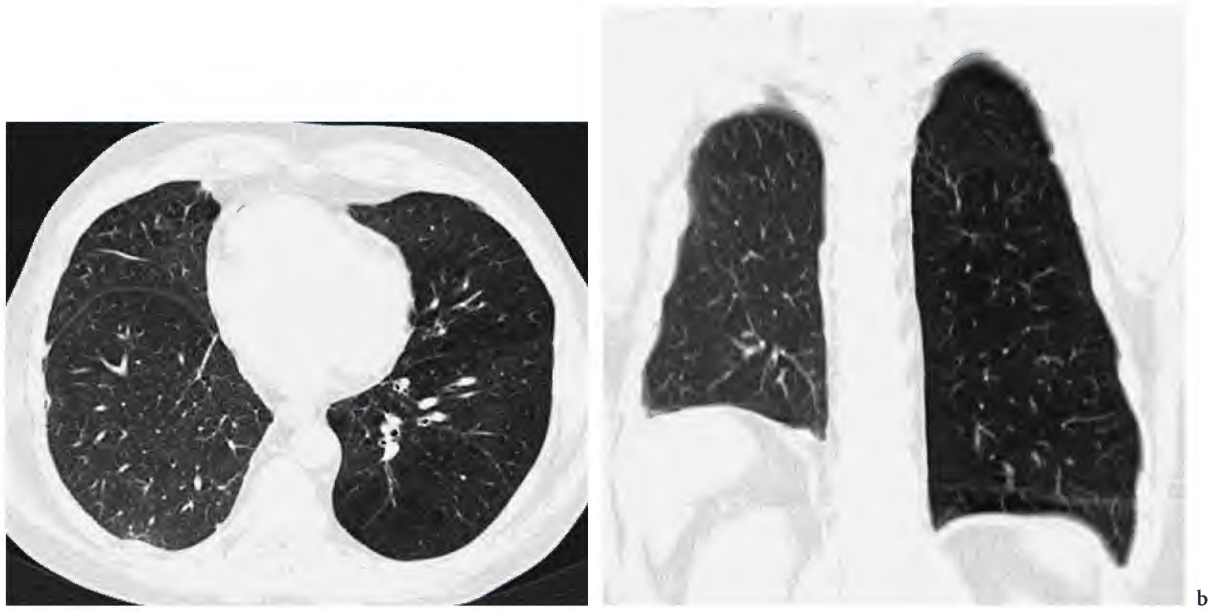

Fig. 5.2.3. a Transverse CT section in a single-lung transplant recipient. Transplanted lung and native lung show marked differences in size and density. **b** Coronal multiplanar reconstructed CT section in a different single-lung transplant recipient as **a**. Transplanted lung and native lung show marked differences in size and density

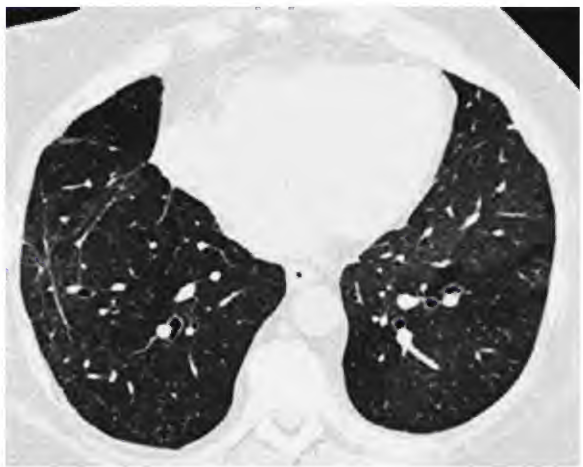

Fig. 5.2.4. Transverse CT scan in double-lung transplant recipient with two sequentially performed single-lung transplants. Lungs of different donors in the same patient show different sizes and densities

right lung transplant. The rotation of the left upper lobe into the right pleural space requires anastomizing the membranous portion of the bronchus to the cartilaginous ring on each of the donor and recipient side. This technique allows bilateral lung transplantation to be performed in a small-size recipient with excellent short- and long-term outcome (Artemiou et al. 1999; Couetil et al. 1997).

5.2.1.4 Survival and Morbidity

Survival rates have been improving consistently since the beginnings of lung transplantations. To date, the 1-year survival rate of lung transplantation is approximately 76%, as opposed to 70% in 2000, and the 5-year survival rate of lung transplantation is 49%, as opposed to 45% in 2000 (Trulock et al. 2005). Repeated hospitalization after lung transplantation is further declining, but is still affecting a substantial percentage of patients (Trulock et al. 2005). The most common morbidities among the 1- and 5-year survivors are hypertension, renal dysfunction, hyperlipidemia, diabetes and bronchiolitis obliterans (BO). Infection and BO, presumed to reflect chronic allograft rejection, are the leading causes of mortality. Complications of lung transplantation can be divided in perioperative and postoperative complications, of which the leading causes relate to surgical technique, primary graft failure, infection, acute and chronic rejection and malignancy as well as recurrence of the primary disease (Trulock et al. 2005).

5.2.2 Preoperative Imaging

5.2.2.1 Preoperative Planning

Evaluation of both the donor and the recipient prior to transplantation is needed, to match donor and recipient lung size and, in cases of single-lung transplantation, to select which side of the recipient's lung ought to be removed (Winton 1992). Postero-anterior and lateral chest radiographs are effective in estimating the donor lung situation in terms of obvious disease or/and injury as well as size matching between donor lung and recipient thorax. Size matching is approximated by comparing the height from the lung apex to the diaphragm at the midclavicular line and the width at the level of the dome of the diaphragms of the donor and recipient's lung; a 10%–20% difference in size is acceptable (Winton 1992). In the so-called split-lung technique, the donor lung is downsized by peripheral nonanatomic segmental resections and transplanted in recipients with smaller thorax size (Wisser et al. 1996).

5.2.2.2 Preoperative Screening

Other than obvious disease, it is important to not only exclude clinically occult disease preoperatively in the recipient patient, but also to perform routine chest radiographical check-ups while on the waiting list to exclude occult disease such as small interval malignancies. Routine CT of the thorax is also recommended in recipients while on the waiting list to differentiate potential opacities seen in routine interval radiographs as well as for the preoperative assessment for lung transplantation. Rarely noninvasive evaluation with positron emission tomography using [^{18}F]fluorodeoxyglucose (FDG) is performed in cases where there are suspicious nodules shown at CT examination (Kazerooni et al. 1995).

Right and left heart catheterizations, quantitative ventilation–perfusion scanning as well as multiple-gated acquisition radionuclide ventriculography are also obtained if clinically relevant (Kazerooni et al. 1995).

5.2.3 Postoperative Complications

After overcoming the surgical procedure, a new pool of complications must be dealt with by the patients undergoing lung transplantation. One challenge facing the medical team involved is determining the correct differential diagnosis and consequently assessing the complication with the right treatment strategy. The similarity of the clinical presentations and radiological features of acute complications such as infection, early graft dysfunction and acute lung transplant rejection complicates the diagnosis. Another reason for the diagnostic difficulty is the timely occurrence overlap between "normal" postoperative complications such as mild, transient pulmonary edema, post-biopsy nodules (Fig. 5.2.5), or postoperative atelectasis (Fig. 5.2.6), or chest wall defects (Fig. 5.2.7), and the potentially serious complications related to transplantation such as severe reperfusion edema and adult respiratory distress syndrome (ARDS) (Fig. 5.2.8). The time of occurrence of post transplantation complications is one of the key factors in helping to narrow the differential diagnosis, when "normal" postoperative features are ruled out and the patient presents with nonspecific clinical signs of postoperative complications such as low-grade fever, dyspnea, cough and impaired oxygenation.

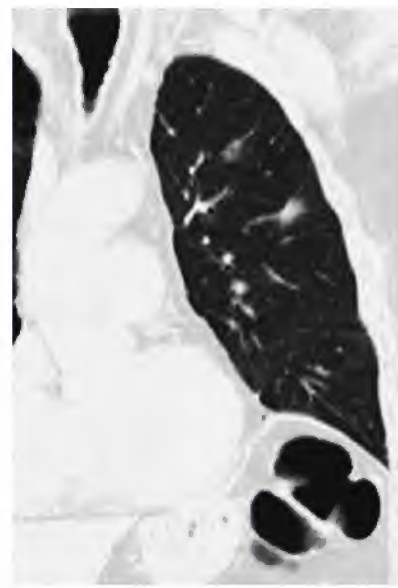

Fig. 5.2.5. Coronal multiplanar reconstructed CT section of left lung. CT section shows a postbiopsy nodule

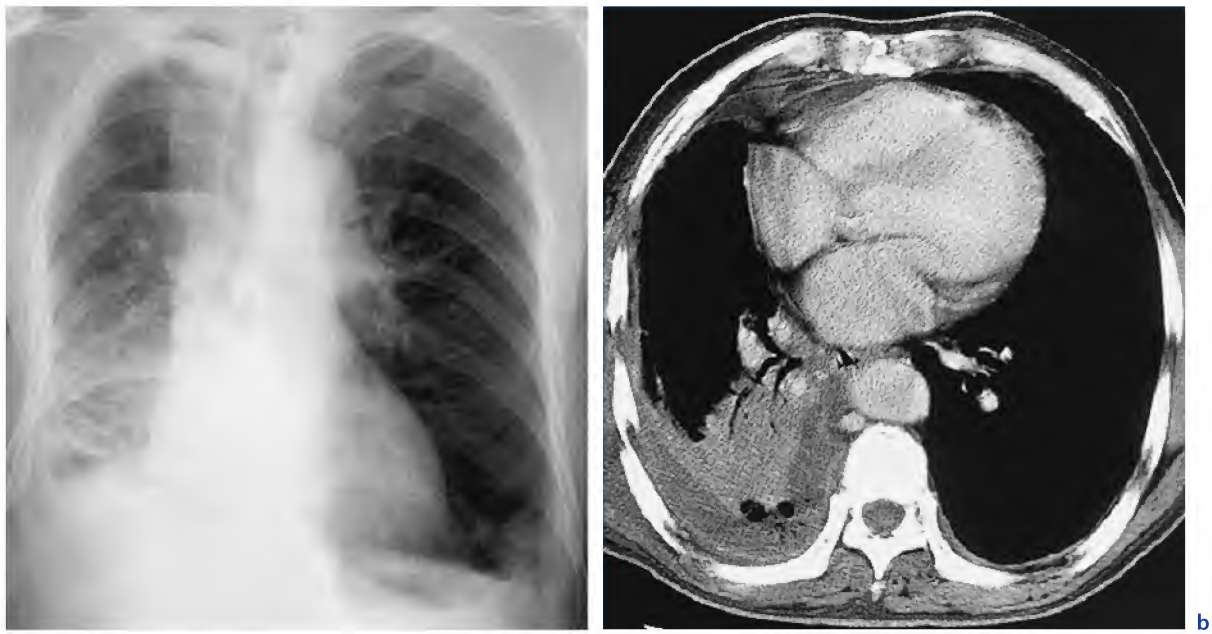

a b

Fig. 5.2.6. a Chest radiograph and **b** in a double-lung transplant recipient. Both modalities show postoperative atelectasis

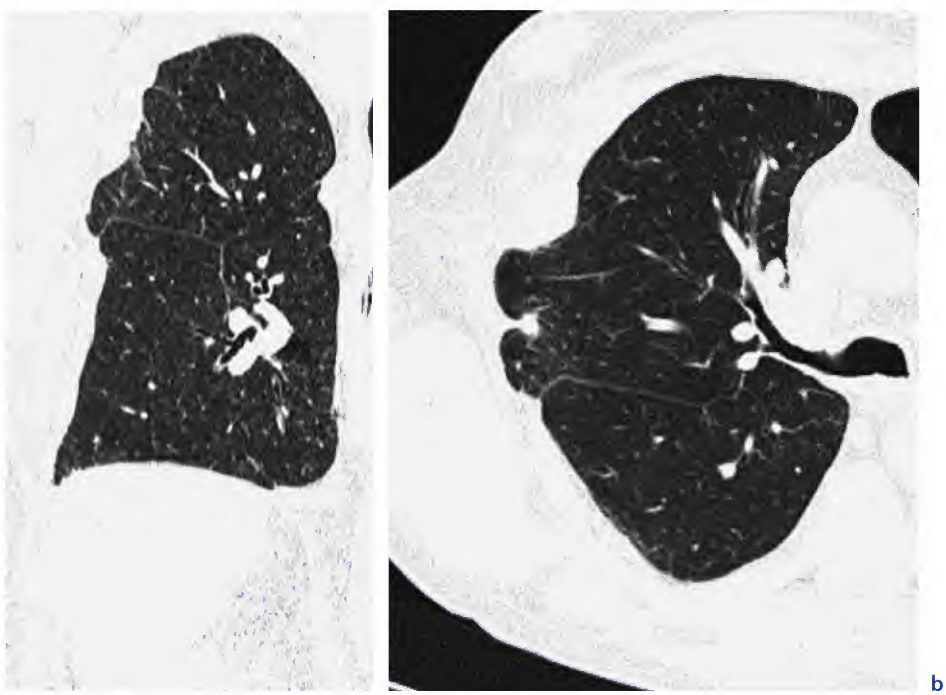

a b

Fig. 5.2.7. a Transverse CT section through right lung. CT section shows postoperative chest wall defect. **b** Coronal multiplanar reconstructed CT section through right lung. CT section shows postoperative chest wall defect

Fig. 5.2.8. Transverse CT section shows ground glass opacities and reticulations in an ARDS-affected lung

5.2.3.1 Complications in the Acute Phase

Complications in the acute phase occur in a time window between the first few hours and 3 months after transplantation. Usually patients are extubated within 24–48 h of transplantation. The intubation time can be prolonged and a tracheostomy may be necessitated if a complication such as early graft dysfunction or infection arises.

The most common causes of death in the initial hospitalization period or within the first 60 days right after patients are discharged are cardiac-related and primary graft failure (Meyers et al. 1999). Other common causes include parenchyma bleeding, ARDS, sepsis, bacterial pneumonia, and pulmonary embolism and neurological injury (Meyers et al. 1999). Anastomotic dehiscence, a previously common postoperative complication, is now very rare because of improved surgical techniques (Date et al. 1995). Treatment usually consists of overstenting the anastomotic dehiscence via bronchoscopy (Fig. 5.2.9) (Susanto et al. 1998).

5.2.3.1.1 Early Graft Dysfunction

Early graft dysfunction (EGD) is defined as a clinical scenario that includes radiographic abnormalities, poor oxygenation, and, if biopsies are performed, a histological pattern of diffuse alveolar damage or organizing pneumonia (Paradis et al. 1992). In the first 3 days and decreasing thereafter, up to 98% of patients present with a form of EGD in their first radiographic routine check-ups (Anderson et al. 1995; Kundu et al. 1998). Causes for EGD may include ischemia–reperfusion injury, implantation response, acute lung injury and hyperacute rejection (Paradis et al. 1992). The most common contributing factor of EGD is the reperfusion edema that reflects the increased capillary permeability and occurs to some degree in all transplanted lungs (Kaplan et al. 1992). The cause of reperfusion edema is multifactorial, including interruption of lymphatic drainage in the donor lung, preexisting donor lung injury, surfactant deficiency, abnormalities of coagulant factors, and ischemic damage to pulmonary capillaries (Kaplan et al. 1992).

The chest radiographic findings of reperfusion injury are nonspecific and are similar to those in patients who have left ventricular failure, fluid overload and acute rejection (Anderson et al. 1995). The findings range from a subtle perihilar haze to patchy or confluent airspace consolidation (Anderson et al. 1995). Also, peribronchial and perivascular thickening and a pattern of reticular interstitial lung opacities are seen in most patients. Up to 98% of patients present with these radiological findings in the first postoperative chest radiograph (Anderson et al. 1995; Kundu et al. 1998). Simultaneously, patients who had mild interstitial abnormalities on the initial chest radiograph usually present with normal findings by day 10 (Davis and Pasque 1995). There is poor correlation between the severity of radiographic findings and the alveolar-arterial oxygen gradient (Davis and Pasque 1995). Although most patients experience radiographic changes from reperfusion edema, only 5%–10% of patients with radiologically apparent moderate or severe early graft dysfunction develop early graft failure (Davis and Pasque 1995). Overall, the early postoperative radiological findings are poorly predictive when it comes to ruling out early graft failure. They are, however, diagnostically relevant when assessing infections, which are also frequent complications in the acute postoperative phase (Trulock 1997).

5.2.3.1.2 Infection in the Acute Postoperative Phase

Infection is the most common cause of morbidity and mortality in the acute and subacute phase af-

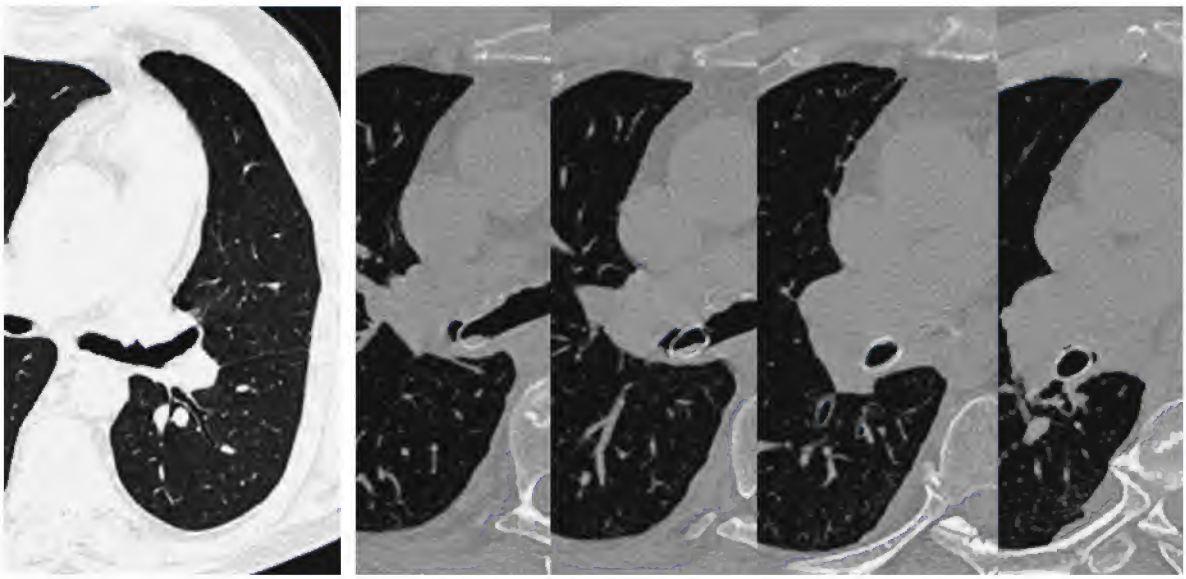

a b

Fig. 5.2.9a,b. Transverse CT scan in double-lung transplant recipient shows irregularities of the bronchial anastomosis (**a**) and a stent bridging this irregularity (**b**)

ter lung transplantation and the second most common cause of late death after lung transplantation (Williams and Snell 1997). Because in the lung transplant patient population respiratory infection may progress rapidly to respiratory failure and death, correct and quick diagnosis is crucial. The rate of infection among lung transplant recipients is significantly higher than in recipients of other solid-organ transplants. This is most likely due to the exposure of the allograft to the external environment (Kramer et al. 1993a). Other reasons for the high incidence of respiratory infection include impaired mucociliary clearance because of diffuse ischemic injury to the bronchial mucosa, blunted cough due to postoperative pain, altered phagocytosis in alveolar macrophages and poor lymphatic drainage.

The lung allograft can become infected by passive transfer of organisms with the donor organ and by persistent recipient's organisms in the proximal airways, the sinuses, or the remaining native lung. Infection can also occur by de novo acquisition following transplantation, especially due to augmented immunosuppression to suppress the allograft rejection (Kramer et al. 1993a).

5.2.3.1.2.1 Bacterial Infection

Bacterial infection with Gram-negative bacteria of the lower respiratory tract is the most common in the early post transplant phase, and typically *Pseudomonas aeruginosa* are isolated (Cahill et al. 1997; Paradowski 1997). Although the incidence of bacterial pneumonia is highest in the first 3 months after transplantation and especially in the first month, the risk persists throughout the recipient's life (Trulock 1997).

The most frequent patterns seen in CT examinations with bacterial pneumonia are consolidation and ground glass opacification (Fig. 5.2.10) (Collins et al. 2000).

Other common findings are nodules varying in size and distribution and "tree-in-bud" patterns. If only ground glass opacification is seen on CT examinations, the differential diagnosis must include *Pneumocystis jiroveci* (PCP), formerly known as *Pneumocystis carinii* pneumonia (Agarwal et al. 2006), and acute rejection. One helpful hint at eliminating PCP is the fact that PCP has been virtually eliminated in lung-transplant recipients by the use of antibiotic prophylaxis and that if it does occur it is almost always associated with noncompliance with prescribed medication (Collins 2002).

5.2.3.1.2.2 Cytomegalovirus Infection

The second most common cause of infection in lung-transplant recipients is cytomegalovirus (CMV) (Trulock 1997). CMV is common in the general

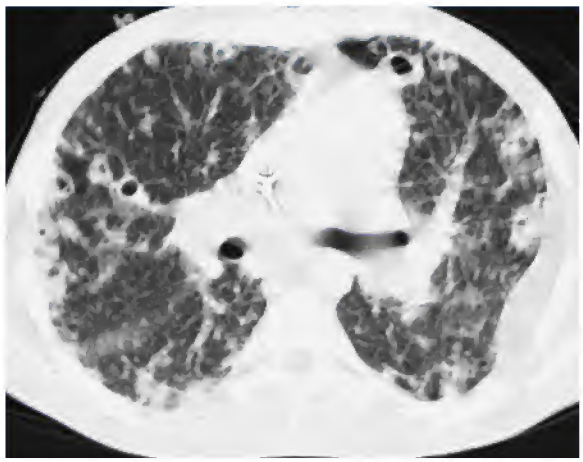

Fig. 5.2.10. Transverse CT scan in double-lung transplant recipient. CT scan shows multiple cavitary lesions corresponding to pneumatoceles after staphylococcal infection

population, and not all patients who present with CMV infection (i.e., identification of the organism in material obtained from any body site in the absence of symptoms and histological changes associated with CMV) also have CMV disease (i.e., identification of the organism in the material obtained from any body site in the presence of histological evidence of tissue damage). Patients who are seronegative for CMV before the procedure and in whom primary infection occurs as the result of the transplantation of an organ from a seropositive recipient are at greatest risk for severe infection, particularly pneumonitis (Ettinger et al. 1993). Pneumonitis is the most common presentation in CMV disease following lung transplantation, although hepatitis, gastroenteritis, or colitis can also occur (Shreeniwas et al. 1996).

A common way to prevent primary CMV infection in the lung-transplant recipient when either the donor or the recipient is seropositive is the initiation of ganciclovir prophylactically at the time of transplantation or preemptively when an increasing viral burden is detected (Palmer et al. 2004; Soghikian et al. 1996). Another strategy to prevent infection with CMV in the recipient is the use of seronegative donors and screened blood products. Unfortunately, although this reduces the risk of infection to negligible levels, this strategy is logically associated with increased waiting times before transplantation, since the majority of donors have been exposed to CMV (Arcasoy and Kotloff 1999).

5.2.3.1.3 Acute Rejection

5.2.3.1.3.1 Clinical and Imaging Diagnosis

Acute graft rejection is rare before the fifth postoperative day after lung transplantation, and the incidence is greatest within the first 100 days, usually within 3 weeks of surgery (Bando et al. 1995a). The clinical manifestations of acute rejection are poorly specific and include malaise, low-grade fever, dyspnea and coughing as well as impaired oxygenation and leukocytosis. Radiological findings which suggest acute rejection are new, worsening or persisting opacities 5–10 days after transplantation, new or increasing pleural effusions and septal lines without other signs of left ventricular failure (Fig. 5.2.11) (Bergin et al. 1990). Although these radiographic changes in the chest radiograph are common in early episodes of rejection, the chest film alone as a follow-up is nonspecific in early post transplant recipients. On the other hand, a "normal" postoperative chest radiograph does not rule out acute rejection. In a study by Kundu et al. for

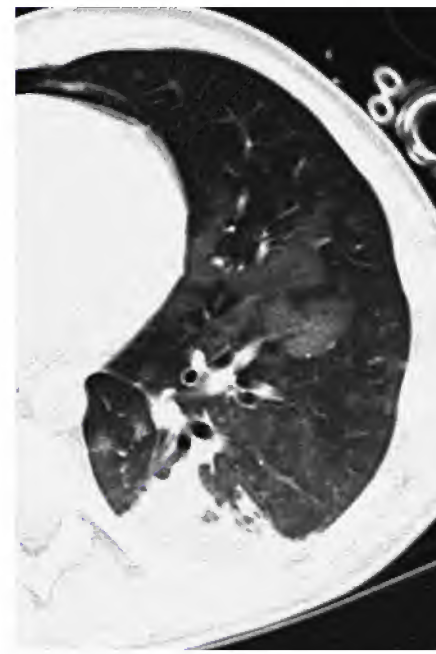

Fig. 5.2.11. Transverse CT scan of the left lung in a lung transplant recipient. The combination of ground glass opacities and gravity-dependent consolidations are highly suggestive of acute rejection and resemble features seen in early ARDS

instance, chest radiograph findings were found to be abnormal in only about 50% of instances of biopsy-proven acute rejection (Kundu et al. 1999). Because of poorly specific manifestations and chronological overlapping of other likely complications such as failure or infection, it is often very difficult to diagnose acute rejection and differentiate it from other complications that are also clinically similar. Further, retrospective epidemiologic analyses have demonstrated that three or more episodes of acute rejection are the major risk factors for the subsequent development of bronchiolitis obliterans (BO), which puts even more weight on correctly diagnosing and effectively treating acute rejection (Keller et al. 1995).

5.2.3.1.3.2 Histological Diagnosis of Acute Rejection

The diagnosis of acute rejection is made on the basis of histological findings. The histological hallmark is the presence of perivascular lymphocytic infiltrates, which in more severe cases spread over into the interstitium and alveolar air spaces (Yousem et al. 1996). When performing transbronchial biopsy, at least five pieces of alveolated parenchyma containing bronchioles and more than 100 air sacs should be obtained for optimal and accurate diagnosis of acute rejection (Yousem et al. 1996).

To ease the differential diagnosis when rejection is suspected, most institutions perform routine surveillance biopsies. A representative surveillance biopsy schedule is: 3 weeks; 3, 6, 9, 12 months; and annually thereafter (Trulock 1997).

If performed when based on clinical indications, transbronchial biopsy has been reported to reach a sensitivity for the detection of acute rejection of up to 94% (Trulock 1997). The rationale for surveillance biopsy protocols is based upon retrospective evidence that up to one-third of surveillance biopsies demonstrate evidence of allograft rejection (Chakinala et al. 2004) whereas only 40% of histologically confirmed grades II–IV acute rejections are associated with clinical signs or symptoms (Baz et al. 1996). There are reports in the literature however that suggest a much lower yield after 24 months, and some centers do not routinely perform biopsies after this point (Dransfield et al. 2004). In the study of Tamm et al. (1997) the benefit of surveillance biopsies was questioned. In this study, 51 heart-lung transplant recipients who underwent surveillance transbronchial biopsies were compared with 75 patients who received heart-lung transplants without routine surveillance biopsies. No significantly long patient survival rate was noted between the two groups, although the surveillance biopsy group received more steroid pulses (Tamm et al. 1997).

A less controversial method of monitoring allograft function is patient-administered home spirometry. Once postoperative function has been stabilized, the forced expiratory volume in one second (FEV_1) and forced vital capacity (FVC) should vary less than 5% from the baseline FEV_1 and FVC right after transplantation (Bjortuft et al. 1993; Morlion et al. 2002). A decline of 10% or more in spirometric values that persists for more than 2 days has been reported to indicate either rejection or infection.

5.2.3.1.3.3 Treating Acute Rejection

Treatment of acute rejection consists of high-dose parenteral corticosteroids, such as intravenous methylprednisolone (0.5–1.0 g IV per day) for 3 days. This is usually done in the inpatient setting, although selected patients who are clinically stable can be treated as outpatients. The outpatient regimen is the same, with intravenous methylprednisolone at home or in a chemotherapy infusion center (Chakinala and Trulock 2003). Resolution occurs rapidly in patients with clinical signs and symptoms of rejection. The clinical symptoms of acute rejection usually improve over 24–48 h, and the physiologic abnormalities begin to improve in the same time frame and return to baseline over several weeks. Since the risk of developing CMV is higher in patients receiving augmented immunosuppression, many centers administer ganciclovir (5 mg/kg IV bid) during the period of augmented immunosuppression. This practice has been successful in renal transplant recipients, for whom the risk of CMV disease is reduced when antiviral therapy is administered during intravenous steroid therapy for acute rejection (Hibberd et al. 1995).

5.2.3.1.3.4 Infection – Acute Rejection Surveillance

The clinical presentation of acute rejection and acute infection alone is nonspecific. Manifestations can include low-grade fever, shortness of breath, nonproductive cough, and changes in measured pulmonary function. In both entities, the chest radiograph may demonstrate perihilar infiltrates, interstitial edema,

focal consolidation, or pleural effusions (Shreeniwas et al. 1996). The point in time at which a disease manifests radiographically may provide clues to its etiology. CMV infection is rarely detected before the second week after transplantation, and the mean time to the initial episode of CMV pneumonitis is 55 days (Smith et al. 1998). In comparison, acute rejection has a variable time course, but may occur within the first 2–3 weeks after lung transplantation, when CMV infection would not be expected. For this reason, surveillance fiber optic bronchoscopy is usually performed whenever there is a clinical indication and decline of spirometric values in the absence of recently untreated organisms identified by sputum culture (Kukafka et al. 1997). However, it should be noted that even histologically the differentiation of rejection from infection can be at times difficult, since features suggesting rejection are also present in viral infection, and, most commonly, in CMV infection (Chakinala and Trulock 2003). In particular, the lymphocytic infiltrate that accompanies such infections or the presence of acute inflammatory cells, such as polymorphonuclear leukocytes, make the histological diagnosis difficult. Alveolar inflammation – as opposed to vascular or airway-centered inflammation – in combination with viral inclusions or the presence of infectious pathogens on special staining is more indicative of infection. In the presence of active infection, it is impossible to make the diagnosis of rejection with certainty. The approach in such situations is to treat the infection and then repeat the biopsies to assess any contribution of rejection to the patient's clinical syndrome (Chakinala and Trulock 2003). For all the above-mentioned reasons it is essential to understand the importance of interdisciplinary work-up of patients presenting with postoperative complications to achieve the correct diagnosis and treatment.

5.2.3.2 Complications in the Nonacute Phase

5.2.3.2.1 Bronchiolitis Obliterans

5.2.3.2.1.1 Definition, Cause and Clinical Presentation

Chronic rejection, histologically defined as a fibroproliferative process that targets the small airways, is a major limiting factor in the long-term survival of lung-transplant patients (Sundaresan et al. 1995). Synonymous with bronchiolitis obliterans (BO), it leads to a submucosal fibrosis of the small airways, and consequently to luminal obliteration and often to obstructive airflow limitation (Arcasoy and Kotloff 1999; Boehler and Estenne 2000; Chamberlain et al. 1994). This chronic lymphoproliferative process is multifocal and may spare whole parts of the affected lung, while literally destroying the lung function (Boehler and Estenne 2000). Therefore, while the diagnosis of BO is based on the histological findings obtained at biopsy, a negative transbronchial biopsy does not exclude BO (Boehler and Estenne 2000; Chamberlain et al. 1994). Therefore, the International Society for Heart and Lung Transplantation devised a standardized nomenclature proposing the use of a spirometric definition for a clinical diagnosis (Cooper et al. 1993; Estenne et al. 2002). They also made a distinction between histologically proven BO and bronchiolitis obliterans syndrome (BOS). The latter is a clinical term and is applied to the situation in which there is "graft deterioration secondary to progressive airways disease for which there is no other cause" in the absence of histological evidence of BO with sustained fall in FEV_1 to a level of 80% or less of the peak value after transplantation (Estenne et al. 2002). The mortality rate associated with BOS ranges from 25% to 56%; the risk increases with the time elapsed after diagnosis has been made (Bando et al. 1995a; Keller et al. 1995; Nathan et al. 1995; Sundaresan et al. 1995). Because the occurrence of BOS increases with time, centers with a longer experience report higher prevalence rates, and centers that have presented their results in multiple publications report higher prevalence rates in a later publication (Trulock et al. 2003). Usually the onset of BOS is at 3 months after transplantation. The natural evolution of BOS has been described to follow one of three patterns: (1) rapid, relentless decline after onset; (2) initial rapid deterioration followed by stabilization; and (3) subtle onset and slow, relentless progression (Levine and Bryan 1995; Nathan et al. 1995). Retrospective epidemiologic analyses have demonstrated that three or more episodes of acute rejection are the major risk factor for the subsequent development of BO (Bando et al. 1995b; Boehler et al. 1998; Keller et al. 1995).

Gastroesophageal reflux (GER) appears to be common in patients following lung transplantation, and may contribute to chronic allograft rejection.

The frequency and clinical importance of GER were evaluated in a study of 128 lung-transplant recipients at a single institution: 93 (73%) had abnormal esophageal acid contact times based upon 24-hambulatory pH probe monitoring (Davis et al. 2003). From this group, 26 patients met diagnostic criteria for BO and underwent fundoplication. Following the procedure, 16 patients had lower BOS scores, and 13 no longer met criteria for the diagnosis of BOS. Long-term follow-up of these patients suggests that early fundoplication can result in a lower incidence of BOS and improved survival (Cantu et al. 2004).

5.2.3.2.1.2
Histological Diagnosis

Transbronchial biopsy is still considered the final proof of BO. However, the reported sensitivity and sensibility of transbronchial biopsy in diagnosing BOS have been diverting (Chamberlain et al. 1994). For example, one study reported a sensitivity of 17% and a specificity of 94.5% for a single set of transbronchial biopsies (Chamberlain et al. 1994). Another study reported a rate of 15% histological confirmation in patients clinically diagnosed with BOS (Kramer et al. 1993b). Another study concluded that transbronchial biopsies confirmed the diagnosis in 82% of their patients who developed clinical BOS (Bando et al. 1995b). In contrast Sundaresan et al. (1995) noted that among 77 patients diagnosed with chronic rejection, the diagnosis was made on the basis of declining FEV_1 in 52%. Only 9% of patients had a histologically proven diagnosis without the typical clinical physiologic abnormalities, whereas 39% had both positive histology and declining spirometry (Sundaresan et al. 1995). Because of these differing data, centers have adopted different approaches to making the diagnosis of BOS. Although the use of transbronchial biopsy in this setting is debated, many lung transplantation centers feel that it may aid in earlier diagnosis and therefore facilitate earlier therapy (Kukafka et al. 1997). Reasons for a confirming biopsy include exclusion of other causes of the clinical syndrome and establishment of the diagnosis prior to attempting therapy and/or retransplantation. Although no therapy has a good track record, many institutions have clinical protocols examining the efficacy of new approaches such as photopheresis, total lymphoid irradiation, plasmapheresis, and inhaled ciclosporin (Iacono et al. 2004).

5.2.3.2.1.3
Imaging of BO

Areas of air trapping caused by small airways are seen as regional inhomogeneities that fail to decrease in volume and remain relative lucent compared to normal lung parenchyma on expiratory CT sections. Areas of decreased attenuation, very often in the early onset of disease not seen on inspiratory CT sections, are easier detected on end-expiratory CT sections (Figs. 5.2.12, 5.2.13) (Arakawa and Webb 1998; Desai and Hansell 1997; Lucidarme et al. 1998; Ng et al. 1999; Verschakelen et al. 1998). The unchanging low attenuation in expiratory CT sections, and also the absence of a decreasing cross-sectional area of the affected part of the lung are helpful in detecting air trapping (Stern and Frank 1994). Expiratory CT can also be used in differentiating between the three main causes of a mosaic pattern (small airways disease, i.e., BO, infiltrative lung disease, and occlusive pulmonary vascular disease) in cases where inspiratory CT is problematic (Arakawa and Webb 1998; Stern et al. 1995). It is important however to keep in mind that in patients with widespread BO, end-expiratory CT sections may appear almost identical to the inspiratory CT sections, simply because of the severity of the air trapping (Fig. 5.2.14). In these cases there is no inhomogeneity of attenuation or change in cross-sectional area of any part of the lung. This important sign of air trapping on HRCT sections obtained at end-expiration in comparison to inspiratory HRCT sections is becoming a routinely performed examination (Arakawa and Webb 1998).

5.2.3.2.1.4
Developing Role of HRCT in the Diagnosis of BO

In one of the first CT studies of BO, Turton et al. (1981) examined 15 patients who fulfilled the criteria of "obliterative bronchiolitis" with thin-section CT (interspaced 3-mm sections, contiguous 10-mm sections). In 5 of the 15 patients the chest radiographs were normal and the remaining 10 patients showed "limited vascular attenuation and hyperinflation". In 13 of the 15 patients "patchy irregular areas of high and low attenuation in variable proportions, accentuated in expiration" were observed. These findings, together with two cases by Eber et al. (1993) were the first reports to identify regional inhomogeneity of the density of the lung parenchyma as the key CT feature of BO. This noninvasive ap-

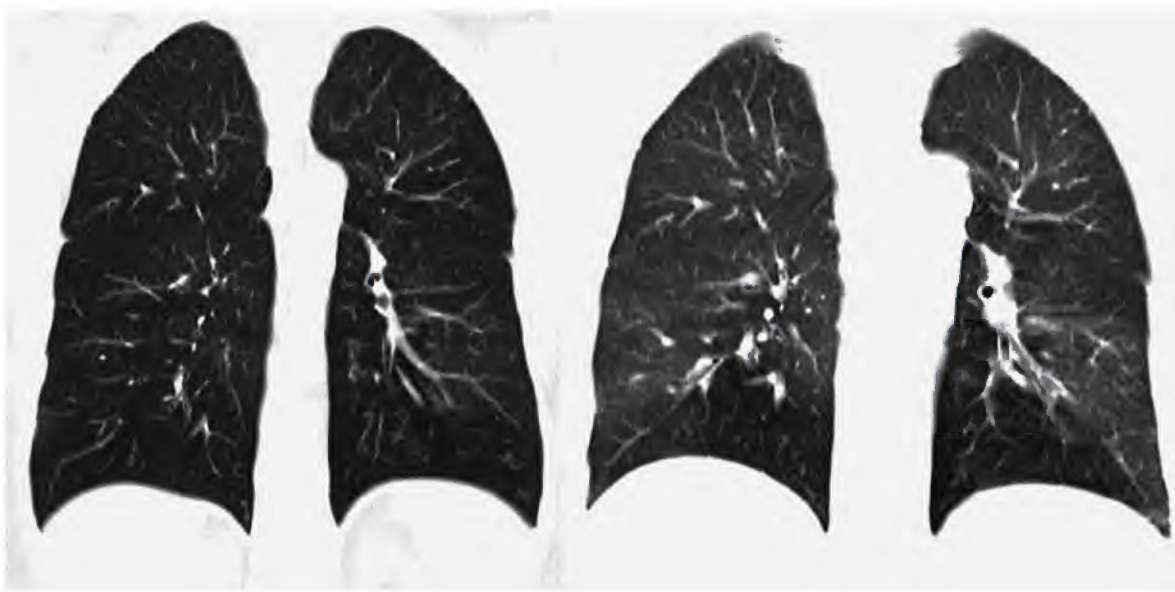

Fig. 5.2.12. Coronal multiplanar reformation CT section of a double-lung transplantation recipient in inspiration (*left*) and expiration (*right*). Whereas lung density in inspiration is normal, expiration shows extensive basal air trapping

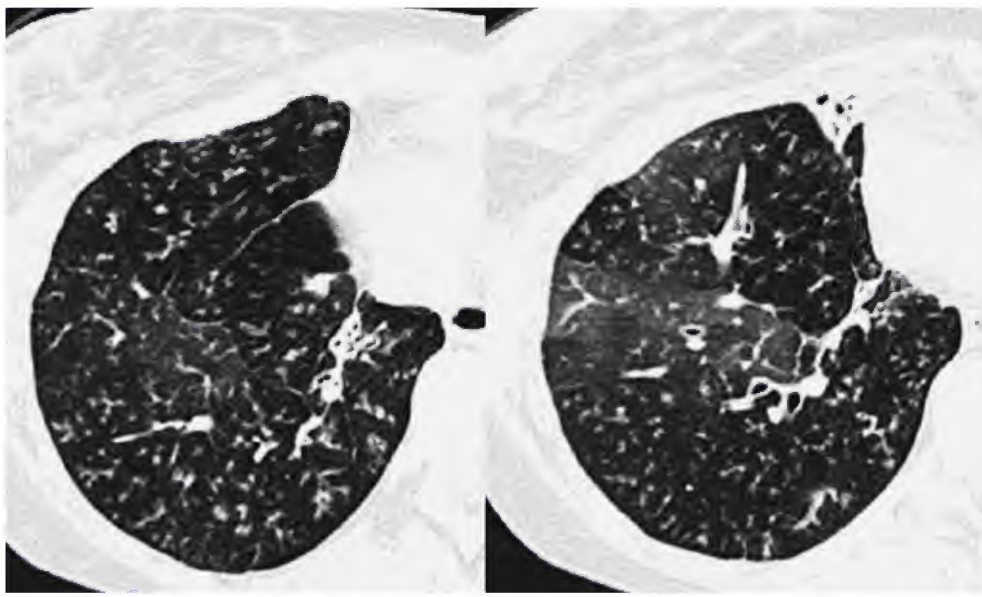

Fig. 5.2.13. Transverse CT section through the right lower lobe in a lung transplantation recipient in inspiration (*left*) and expiration (*right*). Inspiration section shows peripheral tree-in-bud and subtle inhomogeneity of the lung density. Inhomogeneities are accentuated in expiration and extended air trapping becomes apparent

proach to early diagnosis and follow-up of air trapping on HRCT scans has become more accepted recently (Bankier et al. 2001; Knollmann et al. 2004; Konen et al. 2004). The identification of areas of ground glass opacification on HRCT after transplantation, with an inclining incidence 6 months after transplantation, was described as very suggestive but nonspecific (Loubeyre et al. 1995). The reported sensitivity and specificity of HRCT for diagnosing BO associated with numerous other predisposing conditions or causative agents has already been presented; for example, MacLeod's syndrome,

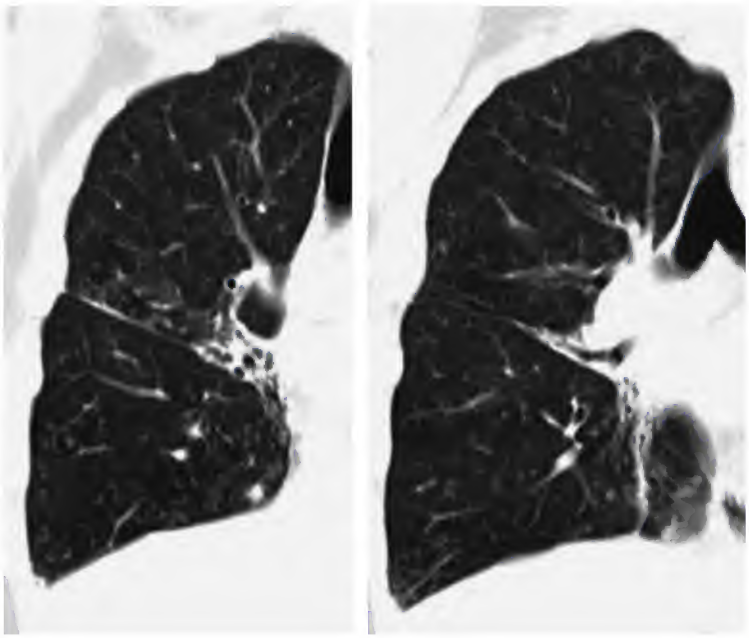

Fig. 5.2.14a, b. Coronal multiplanar reformation CT section of the right lung in lung transplantation recipient in inspiration (**a**) and expiration (**b**). Images show perihilar scarring and extensive peripheral tree-in-bud without any significant decrease in cross-sectional area in expiration

a form of constrictive bronchiolitis that occurs typically following a viral infection acquired in childhood. Here the inhomogeneous nature of lung involvement, similar to the post transplant lung, is particularly well demonstrated on CT (Lucaya et al. 1998; Marti-Bonmati et al. 1989; Moore et al. 1992; Zhang et al. 1999). Later studies went further to apply these findings specifically to BO in lung-transplant patients and provided further evidence that air trapping on expiratory CT scans is an accurate indicator of BO (Leung et al. 1998; Worthy et al. 1997). These findings were, however, based on a small number of patients and a control group was not used. Later on larger study groups reported the reliable accuracy of expiratory thin-section CT to diagnose BOS and complemented the clinical follow-up of lung-transplant recipients (Fig. 5.2.15) (Bankier et al. 2001). Other studies found that the diagnosis of BOS on expiratory thin-section CT was not accurate enough to warrant a role in the follow-up of these patients (Konen et al. 2004; Lee et al. 2000; Miller et al. 2001). These diverting findings however, for the most part, probably reflect differences in examination protocols and scoring systems, and varying patient populations. Bankier et al. (2001) took on this uncertainty by examining more patients and analyzing longer periods of follow-up CT examination, and proved that air trapping at a certain threshold is a relatively sensitive, specific, and accurate method for diagnosing BOS. In a later study Bankier et al. (2003) also examined whether changes in air trapping at sequential CT examinations result from an inherent variability of air trapping or from the variability of the underlying BOS. In this study, Bankier et al. (2003) showed that the anatomic distribution and extent of air trapping in functionally stable heart-lung transplant patients are reproducible characteristics and hence may contribute to the early detection of subclinical chronic rejection of the allograft lung and may be a major tool in the follow-up of such patients (Bankier et al. 2003).

Although some lung transplant centers use HRCT and air trapping in the screening of possible BO, there are still many more centers that doubt these findings because of the lack of a multi-center study proving the value and impact on clinical management of the above-mentioned findings.

5.2.3.2.1.5 Treatment of BO

A variety of treatments have been tried for BO. A study of 32 patients with BO found that conversion from ciclosporin to tacrolimus was associated with spirometric stabilization over 12 months of follow-up (Cairn et al. 2003), and a second study of 13 patients reported similar outcomes when mycophenolate mofetil was introduced (Whyte et al. 1997). Other studies have reported similar results after in-

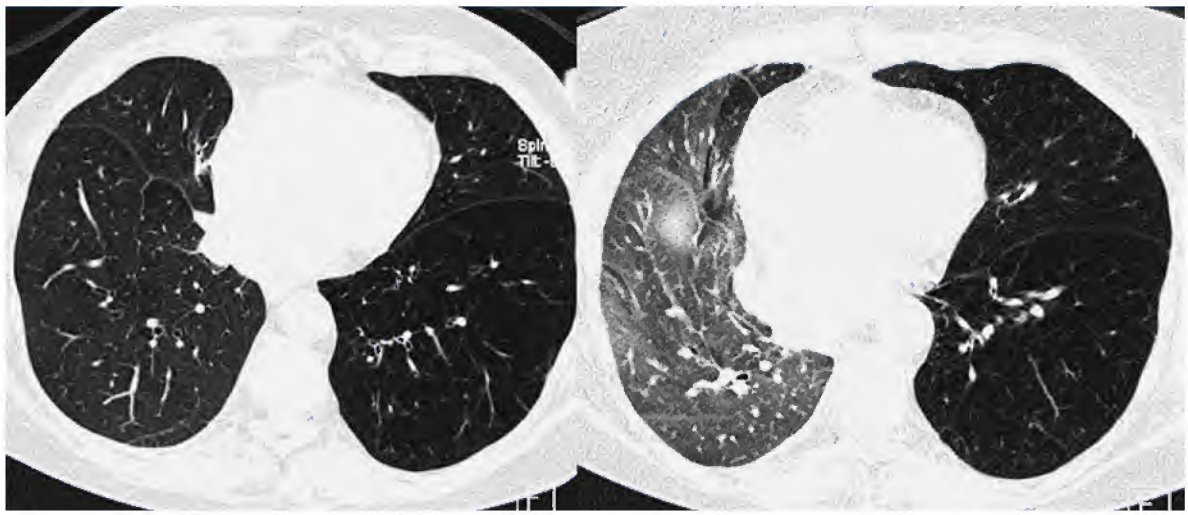

Fig. 5.2.15. Transverse CT section after right single-lung transplantation in inspiration (*left*) and expiration (*right*). Native emphysematous lung does not change in density between inspiration and expiration, suggestive of extensive air trapping. Transplanted right lung increases in density in expiration and shows only a peripheral area of air trapping

troducing substitutions in the immunosuppression regimen (Revell et al. 2000; Verleden et al. 2003). Limited evidence suggests that high-dose inhaled corticosteroids are not effective in slowing or preventing the development of BOS (Whitford et al. 2002). Two reports assessed the value of prolonged oral azithromycin therapy (250 mg PO × 5 days, then 250 mg PO every other day) in patients with BOS (Gerhardt et al. 2003; Verleden and Dupont 2004; Yates et al. 2005). This approach was associated with significant improvements in FEV_1 for some, but not all, patients. These reports have involved only small numbers of patients, and there is little convincing evidence that any of the treatment modalities can be considered effective therapy that dramatically changes the natural history of BOS. It seems that the best strategy to deal with BOS is attempted primary prevention, i.e., aggressive early immunosuppression to eliminate early episodes of acute rejection, since there is no reliable therapy once patients develop symptomatic airflow obstruction.

The issue of retransplantation after the development of BOS is controversial. Early experience suggested that the outcome was not as good as with the first transplant, and some believe that BOS tends to recur in retransplant recipients in an accelerated fashion (Novick et al. 1998). The risk, however, does not appear to be significantly different from that with the first transplant. In a review of 230 retransplantation cases performed in 47 centers between 1985 and 1996 1-year survival was significantly lower (47%) than for the initial transplant (Novick et al. 1998). Among the long-term survivors, however, the risk of developing BO by 2 years was 38%, a rate similar to that of first transplants. Similarly in a single-center series of 15 patients undergoing retransplantation for BOS it was noted that 60% were still alive at 1 year. Surviving patients had a 28% likelihood of recurrent BOS within 3 years after transplantation (Brugiere et al. 2003). Opinions concerning the appropriateness of retransplantation as a treatment of BOS vary widely, in part shaped by the recognition that most centers have more potential first-time recipients than donors, and that mortality on the waiting list is a significant problem. As a result of these considerations, transplant programs vary in policy concerning the availability of retransplantation as a therapeutic option.

5.2.3.2.2 Infection in the Nonacute Phase

5.2.3.2.2.1 Fungal Infections

The isolation of *Candida* or *Aspergillus* species from pulmonary specimens is not unusual. The majority of isolates represent colonization without invasive or clinically apparent disease, but these fungi also may produce major complications and death (Fig. 5.2.16)

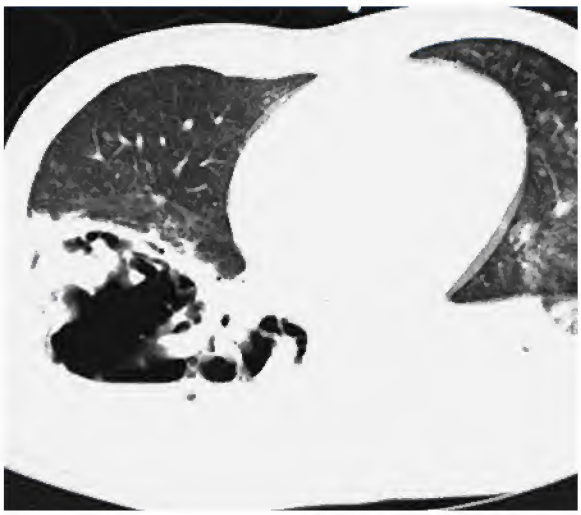

Fig. 5.2.16. Transverse CT section after double-lung transplantation. CT shows extensive cavitation in the right lower lobe following necrotizing pneumonia

(Dauber et al. 1990; End et al. 1995; Kramer et al. 1993a; Mannes et al. 1995; Maurer et al. 1992; McDougall et al. 1993; Paradis and Williams 1993; Westney et al. 1996; Winter et al. 1994; Yeldandi et al. 1995). Since effective, nontoxic antifungal drugs have become increasingly available, most centers have had a low threshold for preventive or preemptive treatment (Dummer et al. 2004).

5.2.3.2.2.2 Candida *Infection*

Candida infection occurs relative frequently, perhaps because colonization is common both in donor lungs and in hospitalized, immunosuppressed patients (Low et al. 1993; Zenati et al. 1990). Before the era of prophylaxis or preemptive therapy, *Candida* infection in the donor was associated with fatal, invasive complications in the recipient (Dauber et al. 1990; Zenati et al. 1990). Although *Candida* is often isolated from respiratory tract specimens, pneumonitis is rare. Disseminated or locally invasive infection with *Candida* can be treated with fluconazole or amphotericin B.

5.2.3.2.2.3 Aspergillus *Infection*

Aspergillus is a ubiquitous organism and is transmitted by inhalation of spores. It can be a devastating pathogen in an immunocompromised host. Surveys have reported a frequency of infection in lung-transplant recipients in the range of 20%–45% (Cahill et al. 1997; Flume et al. 1994; Nunley et al. 1998; Westney et al. 1996; Yeldandi et al. 1995). *Aspergillus* infection after lung transplantation can be classified into two major categories, saprophytic colonization and disease. Particularly devitalized cartilage and foreign suture material of the fresh bronchial anastomosis may create vulnerable sites for *Aspergillus*. *Aspergillus* may also diffusely infect the airways and cause mucosal edema, ulceration and the formation of pseudomembranes (Kramer et al. 1991). One series including 101 patients reported the development of invasive aspergillosis in 14% (Husni et al. 1998). The primary site of lung disease is usually the allograft, but the native lung has been the nidus in some single-lung recipients (McDougall et al. 1993; Westney et al. 1996; Yeldandi et al. 1995). The infection itself has not always been reported to be the ultimate cause of death, however up to 30%–75% mortality rates have been connected with *Aspergillus* disease. Most of the deaths have occurred in recipients with pneumonia or disseminated aspergillosis (Cahill et al. 1997; Kramer et al. 1991; Westney et al. 1996; Yeldandi et al. 1995).

Risk factors for *Aspergillus* infection have not been extensively analyzed, but a strong association with CMV disease was noted in several studies (Husni et al. 1998; Monforte et al. 2001; Yeldandi et al. 1995). No relationship of *Aspergillus* infection to rejection or augmented immunosuppression has been proven, and retransplantation infection with *Aspergillus* does not predict post transplantation illness (Flume et al. 1994). The risk of developing an invasive disease, however, is strongly associated with early post transplant colonization. One study of 151 lung transplant recipients found that patients who had *Aspergillus fumigatus* isolated from the airway within the first 6 months of transplantation had an 11-fold greater risk of developing invasive disease compared with those not colonized during this period (Cahill et al. 1997).

The diagnosis of aspergillus bronchitis is usually made on the basis of a compatible bronchoscopic appearance and isolation of the organism from a biopsy or lavage specimen (Kramer et al. 1991). The definitive diagnosis of pneumonia requires biopsy demonstration of invasion, but a presumptive diagnosis may be made if *Aspergillus* is present in bronchoalveolar lavage (BAL) or sputum and the clinical picture is consistent. The most common CT findings

in patients with fungal pneumonia in general are a combination of nodules, consolidation, and ground glass opacities (Collins et al. 2000). Nodules are mostly multiple and vary in size, have irregular margins and involve all lung zones (Fig. 5.2.17). Bronchitis due to *Aspergillus* infection has responded well to itraconazole or aerosolized amphotericin (Kramer et al. 1991; Mehrad et al. 2001; Westney et al. 1996; Yeldandi et al. 1995). The standard treatment for pneumonia or disseminated aspergillosis is intravenous amphotericin B, but the outcome has been disappointing.

The threat of serious complications and the availability of effective, nontoxic drugs has led the majority of centers to undertake preventive therapy for *Candida* or *Aspergillus* infection (Dummer et al. 2004). The protocols are typically based on fluconazole for *Candida* and itraconazole for *Aspergillus*. Such strategies undoubtedly result in over treatment but have been justified by the reduction in serious fungal infections (Hamacher et al. 1999; Paradis and Williams 1993). The treatment of all respiratory isolates of *Candida* and *Aspergillus* infection with fluconazole or itraconazole reduced the lifetime incidence of fungal infections from 14% to 5% (Paradis and Williams 1993).

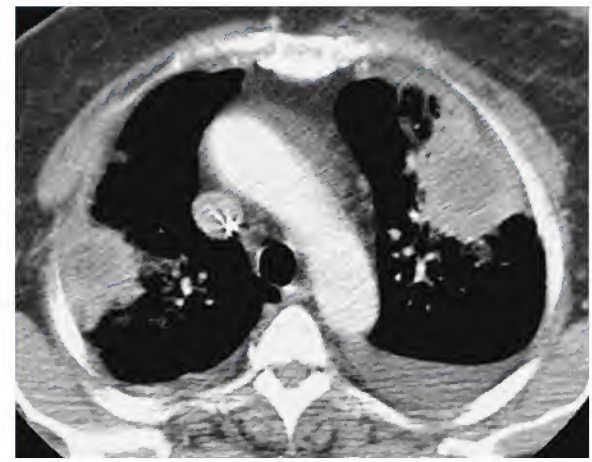

Fig. 5.2.17. Transverse CT section after double-lung transplantation. CT shows large peripheral enhancing masses corresponding to fungal infection

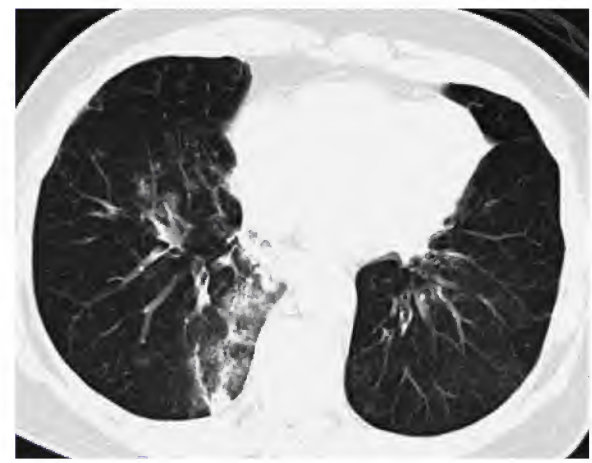

Fig. 5.2.18. Transverse CT section after double-lung transplantation. CT shows partly consolidated, partly ground-glass-like opacities in the right lung, corresponding to *Mycobacterium xenopi*

5.2.3.2.2.4
Other Fungal Infections

Other fungi, including *Cryptococcus*, *Mucor*, and endemically restricted organisms such as *Coccidioides immitis* or *Xenopi* (Fig. 5.2.18), have occasionally caused pulmonary or disseminated disease following lung transplantation (Dauber et al. 1990; Kramer et al. 1991; Paradis and Williams 1993). Prophylaxis should be considered for recipients who live within endemic areas.

5.2.3.2.2.5
Tuberculosis

The incidence of pulmonary tuberculosis after lung transplantation is estimated to be between 2% and 3.8% (Kesten and Chaparro 1999; Schulman et al. 1997). The transmission of pulmonary tuberculosis after lung transplantation is probably via the donor allograft (Collins 2002). The infection typically occurs 1.5–9 months after surgery. CT finding are nonspecific and include subtle bronchial narrowing, pleural effusions and bilateral small nodules, multiple bilateral upper and lower lobe cavitary lesions and consolidations as well as mediastinal lymph node enlargement (Collins 2002).

5.2.3.2.2.6
Bacterial Infection in the Nonacute Phase

Although bacterial infection is more common in the acute phase after lung transplantation, as mentioned above, it also reemerges as a late complication (Trulock 1997). Especially among patients in whom BOS develops, recurrent episodes of purulent tracheobronchitis are common (Arcasoy and Kotloff 1999). Radiographically these episodes of

bacterial infection are often associated with evidence of bronchiectasis (Kramer et al. 1993b).

5.2.3.2.3 Post Transplantation Malignancy

The chronic use of immunosuppressive agents to prevent allograft rejection increases the long-term risk of malignancy compared with that of the general population.

The most frequent malignancy in lung transplant recipients is post transplantation lymphoproliferative disease (PTLD) and occurs in 5%–20% of patients (Trulock 1997). The histological findings range from benign polymorphic hyperplasia of lymphocytes to malignant lymphoma. PTLD is thought to be caused by proliferation of Epstein–Barr-virus-infected donor B-lymphocytes and is more common in Epstein–Barr-virus-seronegative recipients who receive an Epstein–Barr-virus-seropositive donor lung (Collins et al. 1998). Patients may respond to a reduction in immunosuppressive therapy, but this response must be balanced against increasing allograft rejection.

Common radiographic findings of PTLD consist of single or multiple pulmonary nodules, hilar or mediastinal lymphadenopathy, pleural or pericardial effusions, and parenchymal consolidation (Fig. 5.2.19) (Collins et al. 1998; Dodd et al. 1992). Other neoplasms are skin and lip carcinomas, vulvar or perineal carcinomas, in situ cervical cancer, and Kaposi's sarcoma. The risk for cancers that are common in the general population (e.g., lung, breast, prostate, colon) is not increased in transplant recipients (Penn 1993). When lung cancer has occurred in patients undergoing lung transplantation, it has typically been described in patients with strong risk factors for lung cancer prior to transplantation (Fig. 5.2.20) (Arcasoy et al. 2001). In rare cases, the

Fig. 5.2.20. Transverse CT section of a double-lung transplant recipient shows a large subcarinal mass suggestive of post transplant lymphoproliferative disease

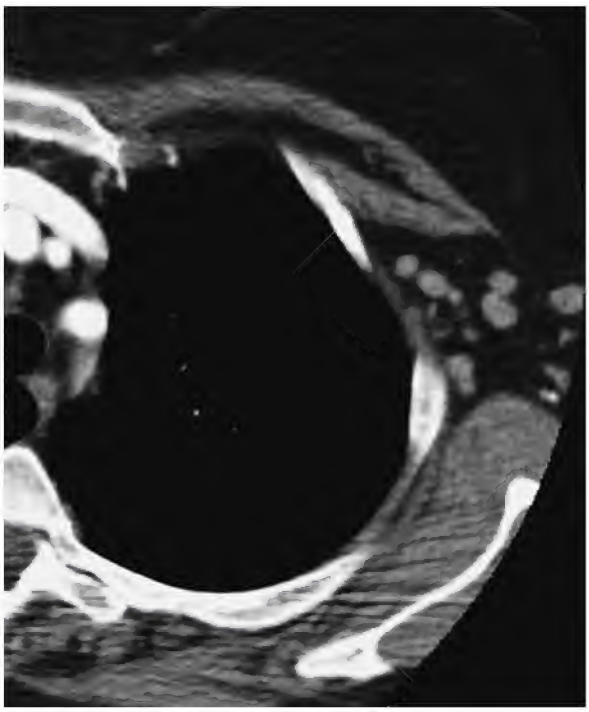

a

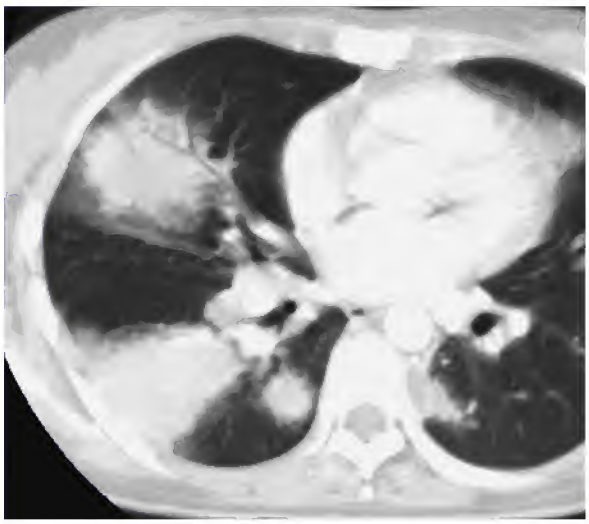

b

Fig. 5.2.19a,b. CT shows large axillary lymph nodes (**a**) and focal pulmonary consolidation (**b**) in a patient with lymphoproliferative disease

tumor represents recurrent disease in patients who were transplanted for bronchoalveolar carcinoma (de Perrot et al. 2003; Garver et al. 1999). A single-center review of outcomes following lung transplantation identified bronchogenic carcinoma in 6 of 251 patients (2.4%). All 6 patients had a history of heavy smoking (mean of nearly 80 pack years), and 5 patients had COPD as their indication for transplantation (Arcasoy et al. 2001).

5.2.3.2.4 Recurrence of Primary Disease

A number of diseases have been reported to recur in the lung allograft, including sarcoidosis (Bjortuft et al. 1994; Johnson et al. 1993; Kazerooni et al. 1994; Milman et al. 2005; Walker et al. 1998), and bronchioloalveolar carcinoma (Dransfield et al. 2004; Paloyan et al. 2000). Other less frequently observed but reported disease recurrences after lung transplantation are idiopathic pulmonary hemosiderosis (Calabrese et al. 2002; Wroblewski et al. 1997), alpha-1-antitrypsin deficiency (Mal et al. 2004), pulmonary veno-occlusive disease (Izbicki et al. 2005), diffuse panbronchiolitis (Baz et al. 1995), pulmonary Langerhans' cell histiocytosis (Fig. 5.2.21) (Etienne et al. 1998; Gabbay et al. 1998; Habib et al. 1998), lymphangioleiomyomatosis (Nine et al. 1994; O'Brien et al. 1995), desquamative interstitial pneumonia (Verleden 1998), and pulmonary alveolar proteinosis (Parker and Novotny 1997). Particularly sarcoidosis has been described to have a high pathologic recurrence rate in some small series (Collins et al. 2001). It usually is discovered incidentally when granulomas are noted on lung biopsy specimens, but these pathologic recurrences have not adversely affected the long-term outcome (Johnson et al. 1993). As an example, a series of 12 patients found post transplantation recurrence of sarcoidosis in 3, but reported 3- and 5-year survival rates comparable to those of patients transplanted for other diseases (Walker et al. 1998). Because the history of lung transplantation is brief compared with the natural history of the underlying diseases, it would not be surprising for recurrence of other diseases to be described in the future among long-term surviving patients.

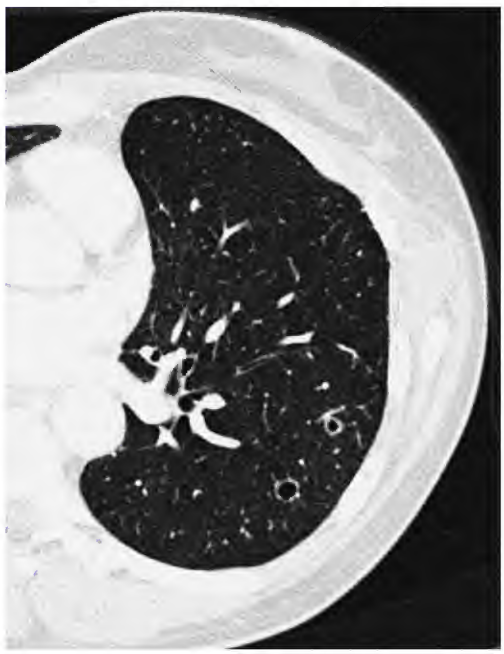

Fig. 5.2.21. Transverse CT section through the left lower lobe. Recurrence of histocytosis X in transplanted lung

References

Agarwal R, Reddy C, Aggarwal AN, Saxena AK (2006) It's *Pneumocystis jiroveci* not *Pneumocystis carinii*. Chest 129:498; author reply 498

Anderson DC, Glazer HS, Semenkovich JW, Pilgram TK, Trulock EP, Cooper JD, Patterson GA (1995) Lung transplant edema: chest radiography after lung transplantation – the first 10 days. Radiology 195:275–281

Arakawa H, Webb WR (1998) Air trapping on expiratory high-resolution CT scans in the absence of inspiratory scan abnormalities: correlation with pulmonary function tests and differential diagnosis. AJR Am J Roentgenol 170:1349–1353

Arcasoy SM, Kotloff RM (1999) Lung transplantation. N Engl J Med 340:1081–1091

Arcasoy SM, Hersh C, Christie JD, Zisman D, Pochettino A, Rosengard BR, Blumenthal NP, Palevsky HI, Bavaria JE, Kotloff RM (2001) Bronchogenic carcinoma complicating lung transplantation. J Heart Lung Transplant 20:1044–1053

Artemiou O, Birsan T, Taghavi S, Eichler I, Wisser W, Wolner E, Klepetko W (1999) Bilateral lobar transplantation with the split lung technique. J Thorac Cardiovasc Surg 118:369–370

Bando K, Paradis IL, Komatsu K, Konishi H, Matsushima M, Keena RJ, Hardesty RL, Armitage JM, Griffith BP (1995a) Analysis of time-dependent risks for infection, rejection, and death after pulmonary transplantation. J Thorac Cardiovasc Surg 109:49–57; discussion 57–49

Bando K, Paradis IL, Similo S, Konishi H, Komatsu K, Zullo TG, Yousem SA, Close JM, Zeevi A, Duquesnoy RJ et al (1995b) Obliterative bronchiolitis after lung and heart-lung transplantation. An analysis of risk factors and management. J Thorac Cardiovasc Surg 110:4–13; discussion 13–14

Bankier AA, Van Muylem A, Knoop C, Estenne M, Gevenois PA (2001) Bronchiolitis obliterans syndrome in heart-lung transplant recipients: diagnosis with expiratory CT. Radiology 218:533–539

Bankier AA, Van Muylem A, Scillia P, De Maertelaer V, Estenne M, Gevenois PA (2003) Air trapping in heart-lung transplant recipients: variability of anatomic distribution and extent at sequential expiratory thin-section CT. Radiology 229:737–742

Baz MA, Kussin PS, Van Trigt P, Davis RD, Roggli VL, Tapson VF (1995) Recurrence of diffuse panbronchiolitis after lung transplantation. Am J Respir Crit Care Med 151:895–898

Baz MA, Layish DT, Govert JA, Howell DN, Lawrence CM, Davis RD, Tapson VF (1996) Diagnostic yield of bronchoscopies after isolated lung transplantation. Chest 110:84–88

Bergin CJ, Castellino RA, Blank N, Berry GJ, Sibley RK, Starnes VA (1990) Acute lung rejection after heart-lung transplantation: correlation of findings on chest radiographs with lung biopsy results. AJR Am J Roentgenol 155:23–27

Bjortuft O, Johansen B, Boe J, Foerster A, Holter E, Geiran O (1993) Daily home spirometry facilitates early detection of rejection in single lung transplant recipients with emphysema. Eur Respir J 6:705–708

Bjortuft O, Foerster A, Boe J, Geiran O (1994) Single lung transplantation as treatment for end-stage pulmonary sarcoidosis: recurrence of sarcoidosis in two different lung allografts in one patient. J Heart Lung Transplant 13:24–29

Boehler A, Estenne M (2000) Obliterative bronchiolitis after lung transplantation. Curr Opin Pulm Med 6:133–139

Boehler A, Kesten S, Weder W, Speich R (1998) Bronchiolitis obliterans after lung transplantation: a review. Chest 114:1411–1426

Brugiere O, Thabut G, Castier Y, Mal H, Dauriat G, Marceau A, Leseche G (2003) Lung retransplantation for bronchiolitis obliterans syndrome: long-term follow-up in a series of 15 recipients. Chest 123:1832–1837

Cahill BC, Hibbs JR, Savik K, Juni BA, Dosland BM, Edin-Stibbe C, Hertz MI (1997) Aspergillus airway colonization and invasive disease after lung transplantation. Chest 112:1160–1164

Cairn J, Yek T, Banner NR, Khaghani A, Hodson ME, Yacoub M (2003) Time-related changes in pulmonary function after conversion to tacrolimus in bronchiolitis obliterans syndrome. J Heart Lung Transplant 22:50–57

Calabrese F, Giacometti C, Rea F, Loy M, Sartori F, Di Vittorio G, Abudureheman A, Thiene G, Valente M (2002) Recurrence of idiopathic pulmonary hemosiderosis in a young adult patient after bilateral single-lung transplantation. Transplantation 74:1643–1645

Cantu E 3rd, Appel JZ 3rd, Hartwig MG, Woreta H, Green C, Messier R, Palmer SM, Davis RD Jr (2004) J. Maxwell Chamberlain Memorial Paper. Early fundoplication prevents chronic allograft dysfunction in patients with gastroesophageal reflux disease. Ann Thorac Surg 78:1142–1151; discussion 1142–1151

Chakinala MM, Trulock EP (2003) Acute allograft rejection after lung transplantation: diagnosis and therapy. Chest Surg Clin N Am 13:525–542

Chakinala MM, Ritter J, Gage BF, Lynch JP, Aloush A, Patterson GA, Trulock EP (2004) Yield of surveillance bronchoscopy for acute rejection and lymphocytic bronchitis/bronchiolitis after lung transplantation. J Heart Lung Transplant 23:1396–1404

Chamberlain D, Maurer J, Chaparro C, Idolor L (1994) Evaluation of transbronchial lung biopsy specimens in the diagnosis of bronchiolitis obliterans after lung transplantation. J Heart Lung Transplant 13:963–971

Collins J (2002) Imaging of the chest after lung transplantation. J Thorac Imaging 17:102–112

Collins J, Muller NL, Leung AN, McGuinness G, Mergo PJ, Flint JD, Warner TF, Poirier C, Theodore J, Zander D, Yee HT (1998) Epstein-Barr-virus-associated lymphoproliferative disease of the lung: CT and histologic findings. Radiology 208:749–759

Collins J, Muller NL, Kazerooni EA, Paciocco G (2000) CT findings of pneumonia after lung transplantation. AJR Am J Roentgenol 175:811–818

Collins J, Hartman MJ, Warner TF, Muller NL, Kazerooni EA, McAdams HP, Slone RM, Parker LA (2001) Frequency and CT findings of recurrent disease after lung transplantation. Radiology 219:503–509

Cooper JD, Billingham M, Egan T, Hertz MI, Higenbottam T, Lynch J, Mauer J, Paradis I, Patterson GA, Smith C et al (1993) A working formulation for the standardization of nomenclature and for clinical staging of chronic dysfunction in lung allografts. International Society for Heart and Lung Transplantation. J Heart Lung Transplant 12:713–716

Couetil JP, Tolan MJ, Loulmet DF, Guinvarch A, Chevalier PG, Achkar A, Birmbaum P, Carpentier AF (1997) Pulmonary bipartitioning and lobar transplantation: a new approach to donor organ shortage. J Thorac Cardiovasc Surg 113:529–537

Date H, Trulock EP, Arcidi JM, Sundaresan S, Cooper JD, Patterson GA (1995) Improved airway healing after lung transplantation. An analysis of 348 bronchial anastomoses. J Thorac Cardiovasc Surg 110:1424–1432; discussion 1432–1423

Dauber JH, Paradis IL, Dummer JS (1990) Infectious complications in pulmonary allograft recipients. Clin Chest Med 11:291–308

Davis RD Jr., Pasque MK (1995) Pulmonary transplantation. Ann Surg 221:14–28

Davis RD Jr., Lau CL, Eubanks S, Messier RH, Hadjiliadis D, Steele MP, Palmer SM (2003) Improved lung allograft function after fundoplication in patients with gastroesophageal reflux disease undergoing lung transplantation. J Thorac Cardiovasc Surg 125:533–542

de Perrot M, Fischer S, Waddell TK, Strueber M, Harringer W, Pierre AF, Spiliopoulos A, Haverich A, Keshavjee S (2003) Management of lung transplant recipients with bronchogenic carcinoma in the native lung. J Heart Lung Transplant 22:87–89

Desai SR, Hansell DM (1997) Small airways disease: expiratory computed tomography comes of age. Clin Radiol 52:332–337

Dodd GD 3rd, Ledesma-Medina J, Baron RL, Fuhrman CR (1992) Posttransplant lymphoproliferative disorder: intrathoracic manifestations. Radiology 184:65–69

Dransfield MT, Garver RI, Weill D (2004) Standardized guidelines for surveillance bronchoscopy reduce compli-

cations in lung transplant recipients. J Heart Lung Transplant 23:110–114
Dummer JS, Lazariashvilli N, Barnes J, Ninan M, Milstone AP (2004) A survey of anti-fungal management in lung transplantation. J Heart Lung Transplant 23:1376–1381
Eber CD, Stark P, Bertozzi P (1993) Bronchiolitis obliterans on high-resolution CT: a pattern of mosaic oligemia. J Comput Assist Tomogr 17:853–856
End A, Helbich T, Wisser W, Dekan G, Klepetko W (1995) The pulmonary nodule after lung transplantation. Cause and outcome. Chest 107:1317–1322
Estenne M, Maurer JR, Boehler A, Egan JJ, Frost A, Hertz M, Mallory GB, Snell GI, Yousem S (2002) Bronchiolitis obliterans syndrome 2001: an update of the diagnostic criteria. J Heart Lung Transplant 21:297–310
Etienne B, Bertocchi M, Gamondes JP, Thevenet F, Boudard C, Wiesendanger T, Loire R, Brune J, Mornex JF (1998) Relapsing pulmonary Langerhans cell histiocytosis after lung transplantation. Am J Respir Crit Care Med 157:288–291
Ettinger NA, Bailey TC, Trulock EP, Storch GA, Anderson D, Raab S, Spitznagel EL, Dresler C, Cooper JD (1993) Cytomegalovirus infection and pneumonitis. Impact after isolated lung transplantation. Washington University Lung Transplant Group. Am Rev Respir Dis 147:1017–1023
Flume PA, Egan TM, Paradowski LJ, Detterbeck FC, Thompson JT, Yankaskas JR (1994) Infectious complications of lung transplantation. Impact of cystic fibrosis. Am J Respir Crit Care Med 149:1601–1607
Gabbay E, Dark JH, Ashcroft T, Milne D, Gibson GJ, Healy M, Corris PA (1998) Recurrence of Langerhans' cell granulomatosis following lung transplantation. Thorax 53:326–327
Garver RI Jr., Zorn GL, Wu X, McGiffin DC, Young KR Jr., Pinkard NB (1999) Recurrence of bronchioloalveolar carcinoma in transplanted lungs. N Engl J Med 340:1071–1074
Gerhardt SG, McDyer JF, Girgis RE, Conte JV, Yang SC, Orens JB (2003) Maintenance azithromycin therapy for bronchiolitis obliterans syndrome: results of a pilot study. Am J Respir Crit Care Med 168:121–125
Glanville AR, Estenne M (2003) Indications, patient selection and timing of referral for lung transplantation. Eur Respir J 22:845–852
Habib SB, Congleton J, Carr D, Partridge J, Corrin B, Geddes DM, Banner N, Yacoub M, Burke M (1998) Recurrence of recipient Langerhans' cell histiocytosis following bilateral lung transplantation. Thorax 53:323–325
Hamacher J, Spiliopoulos A, Kurt AM, Nicod LP (1999) Pre-emptive therapy with azoles in lung transplant patients. Geneva Lung Transplantation Group. Eur Respir J 13:180–186
Hibberd PL, Tolkoff-Rubin NE, Conti D, Stuart F, Thistlethwaite JR, Neylan JF, Snydman DR, Freeman R, Lorber MI, Rubin RH (1995) Preemptive ganciclovir therapy to prevent cytomegalovirus disease in cytomegalovirus antibody-positive renal transplant recipients. A randomized controlled trial. Ann Intern Med 123:18–26
Hosenpud JD, Bennett LE, Keck BM, Boucek MM, Novick RJ (2000) The Registry of the International Society for Heart and Lung Transplantation: seventeenth official report – 2000. J Heart Lung Transplant 19:909–931
Husni RN, Gordon SM, Longworth DL, Arroliga A, Stillwell PC, Avery RK, Maurer JR, Mehta A, Kirby T (1998) Cytomegalovirus infection is a risk factor for invasive aspergillosis in lung transplant recipients. Clin Infect Dis 26:753–755
Iacono AT, Corcoran TE, Griffith BP, Grgurich WF, Smith DA, Zeevi A, Smaldone GC, McCurry KR, Johnson BA, Dauber JH (2004) Aerosol cyclosporin therapy in lung transplant recipients with bronchiolitis obliterans. Eur Respir J 23:384–390
Izbicki G, Shitrit D, Schechtman I, Bendayan D, Fink G, Sahar G, Saute M, Ben-Gal T, Kramer MR (2005) Recurrence of pulmonary veno-occlusive disease after heart-lung transplantation. J Heart Lung Transplant 24:635–637
Johnson BA, Duncan SR, Ohori NP, Paradis IL, Yousem SA, Grgurich WF, Dauber JH, Griffith BP (1993) Recurrence of sarcoidosis in pulmonary allograft recipients. Am Rev Respir Dis 148:1373–1377
Kaplan JD, Trulock EP, Cooper JD, Schuster DP (1992) Pulmonary vascular permeability after lung transplantation. A positron emission tomographic study. Am Rev Respir Dis 145:954–957
Kazerooni EA, Jackson C, Cascade PN (1994) Sarcoidosis: recurrence of primary disease in transplanted lungs. Radiology 192:461–464
Kazerooni EA, Chow LC, Whyte RI, Martinez FJ, Lynch JP (1995) Preoperative examination of lung transplant candidates: value of chest CT compared with chest radiography. AJR Am J Roentgenol 165:1343–1348
Keller CA, Cagle PT, Brown RW, Noon G, Frost AE (1995) Bronchiolitis obliterans in recipients of single, double, and heart-lung transplantation. Chest 107:973–980
Kesten S, Chaparro C (1999) Mycobacterial infections in lung transplant recipients. Chest 115:741–745
Knollmann FD, Kapell S, Lehmkuhl H, Schulz B, Bottcher H, Hetzer R, Felix R (2004) Dynamic high-resolution electron-beam CT scanning for the diagnosis of bronchiolitis obliterans syndrome after lung transplantation. Chest 126:447–456
Konen E, Gutierrez C, Chaparro C, Murray CP, Chung T, Crossin J, Hutcheon MA, Paul NS, Weisbrod GL (2004) Bronchiolitis obliterans syndrome in lung transplant recipients: can thin-section CT findings predict disease before its clinical appearance? Radiology 231:467–473
Kramer MR, Denning DW, Marshall SE, Ross DJ, Berry G, Lewiston NJ, Stevens DA, Theodore J (1991) Ulcerative tracheobronchitis after lung transplantation. A new form of invasive aspergillosis. Am Rev Respir Dis 144:552–556
Kramer MR, Marshall SE, Starnes VA, Gamberg P, Amitai Z, Theodore J (1993a) Infectious complications in heart-lung transplantation. Analysis of 200 episodes. Arch Intern Med 153:2010–2016
Kramer MR, Stoehr C, Whang JL, Berry GJ, Sibley R, Marshall SE, Patterson GM, Starnes VA, Theodore J (1993b) The diagnosis of obliterative bronchiolitis after heart-lung and lung transplantation: low yield of transbronchial lung biopsy. J Heart Lung Transplant 12:675–681
Kukafka DS, O'Brien GM, Furukawa S, Criner GJ (1997) Surveillance bronchoscopy in lung transplant recipients. Chest 111:377–381
Kundu S, Herman SJ, Winton TL (1998) Reperfusion edema after lung transplantation: radiographic manifestations. Radiology 206:75–80

Kundu S, Herman SJ, Larhs A, Rappaport DC, Weisbrod GL, Maurer J, Chamberlain D, Winton T (1999) Correlation of chest radiographic findings with biopsy-proven acute lung rejection. J Thorac Imaging 14:178–184

Lee ES, Gotway MB, Reddy GP, Golden JA, Keith FM, Webb WR (2000) Early bronchiolitis obliterans following lung transplantation: accuracy of expiratory thin-section CT for diagnosis. Radiology 216:472–477

Leung AN, Fisher K, Valentine V, Girgis RE, Berry GJ, Robbins RC, Theodore J (1998) Bronchiolitis obliterans after lung transplantation: detection using expiratory HRCT. Chest 113:365–370

Levine SM, Bryan CL (1995) Bronchiolitis obliterans in lung transplant recipients. The "thorn in the side" of lung transplantation. Chest 107:894–897

Loubeyre P, Revel D, Delignette A, Loire R, Mornex JF (1995) High-resolution computed tomographic findings associated with histologically diagnosed acute lung rejection in heart-lung transplant recipients. Chest 107:132–138

Low DE, Kaiser LR, Haydock DA, Trulock E, Cooper JD (1993) The donor lung: infectious and pathologic factors affecting outcome in lung transplantation. J Thorac Cardiovasc Surg 106:614–621

Lucaya J, Gartner S, Garcia-Pena P, Cobos N, Roca I, Linan S (1998) Spectrum of manifestations of Swyer-James-MacLeod syndrome. J Comput Assist Tomogr 22:592–597

Lucidarme O, Coche E, Cluzel P, Mourey-Gerosa I, Howarth N, Grenier P (1998) Expiratory CT scans for chronic airway disease: correlation with pulmonary function test results. AJR Am J Roentgenol 170:301–307

Mal H, Guignabert C, Thabut G, d'Ortho MP, Brugiere O, Dauriat G, Marrash-Chahla R, Rangheard AS, Leseche G, Fournier M (2004) Recurrence of pulmonary emphysema in an alpha-1 proteinase inhibitor-deficient lung transplant recipient. Am J Respir Crit Care Med 170:811–814

Mannes GP, van der Bij W, de Boer WJ (1995) Liposomal amphotericin B in three lung transplant recipients. The Groningen Lung Transplantation Group. J Heart Lung Transplant 14:781–784

Marti-Bonmati L, Ruiz Perales F, Catala F, Mata JM, Calonge E (1989) CT findings in Swyer-James syndrome. Radiology 172:477–480

Maurer JR, Tullis DE, Grossman RF, Vellend H, Winton TL, Patterson GA (1992) Infectious complications following isolated lung transplantation. Chest 101:1056–1059

Maurer JR, Frost AE, Estenne M, Higenbottam T, Glanville AR (1998) International guidelines for the selection of lung transplant candidates. The International Society for Heart and Lung Transplantation, the American Thoracic Society, the American Society of Transplant Physicians, the European Respiratory Society. Transplantation 66:951–956

McDougall JC, Vigneswaran WT, Peters SG, Marshall WT, McGregor CG (1993) Fungal infection of the contralateral native lung after single-lung transplantation. Ann Thorac Surg 56:176–178

Mehrad B, Paciocco G, Martinez FJ, Ojo TC, Iannettoni MD, Lynch JP 3rd (2001) Spectrum of Aspergillus infection in lung transplant recipients: case series and review of the literature. Chest 119:169–175

Meyers BF, Lynch J, Trulock EP, Guthrie TJ, Cooper JD, Patterson GA (1999) Lung transplantation: a decade of experience. Ann Surg 230:362–370; discussion 370–361

Miller WT Jr., Kotloff RM, Blumenthal NP, Aronchick JM, Gefter WB, Miller WT (2001) Utility of high resolution computed tomography in predicting bronchiolitis obliterans syndrome following lung transplantation: preliminary findings. J Thorac Imaging 16:76–80

Milman N, Andersen CB, Burton CM, Iversen M (2005) Recurrent sarcoid granulomas in a transplanted lung derive from recipient immune cells. Eur Respir J 26:549–552

Monforte V, Roman A, Gavalda J, Bravo C, Tenorio L, Ferrer A, Maestre J, Morell F (2001) Nebulized amphotericin B prophylaxis for Aspergillus infection in lung transplantation: study of risk factors. J Heart Lung Transplant 20:1274–1281

Moore AD, Godwin JD, Dietrich PA, Verschakelen JA, Henderson WR Jr. (1992) Swyer-James syndrome: CT findings in eight patients. AJR Am J Roentgenol 158:1211–1215

Morlion B, Knoop C, Paiva M, Estenne M (2002) Internet-based home monitoring of pulmonary function after lung transplantation. Am J Respir Crit Care Med 165:694–697

Nathan SD, Ross DJ, Belman MJ, Shain S, Elashoff JD, Kass RM, Koerner SK (1995) Bronchiolitis obliterans in single-lung transplant recipients. Chest 107:967–972

Ng CS, Desai SR, Rubens MB, Padley SP, Wells AU, Hansell DM (1999) Visual quantitation and observer variation of signs of small airways disease at inspiratory and expiratory CT. J Thorac Imaging 14:279–285

Nine JS, Yousem SA, Paradis IL, Keenan R, Griffith BP (1994) Lymphangioleiomyomatosis: recurrence after lung transplantation. J Heart Lung Transplant 13:714–719

Novick RJ, Stitt LW, Al-Kattan K, Klepetko W, Schafers HJ, Duchatelle JP, Khaghani A, Hardesty RL, Patterson GA, Yacoub MH (1998) Pulmonary retransplantation: predictors of graft function and survival in 230 patients. Pulmonary Retransplant Registry. Ann Thorac Surg 65:227–234

Nunley DR, Ohori P, Grgurich WF, Iacono AT, Williams PA, Keenan RJ, Dauber JH (1998) Pulmonary aspergillosis in cystic fibrosis lung transplant recipients. Chest 114:1321–1329

O'Brien JD, Lium JH, Parosa JF, Deyoung BR, Wick MR, Trulock EP (1995) Lymphangiomyomatosis recurrence in the allograft after single-lung transplantation. Am J Respir Crit Care Med 151:2033–2036

Palmer SM, Grinnan DC, Diane Reams B, Steele MP, Messier RH, Duane Davis R (2004) Delay of CMV infection in high-risk CMV mismatch lung transplant recipients due to prophylaxis with oral ganciclovir. Clin Transplant 18:179–185

Paloyan EB, Swinnen LJ, Montoya A, Lonchyna V, Sullivan HJ, Garrity E (2000) Lung transplantation for advanced bronchioloalveolar carcinoma confined to the lungs. Transplantation 69:2446–2448

Paradis IL, Williams P (1993) Infection after lung transplantation. Semin Respir Infect 8:207–215

Paradis IL, Duncan SR, Dauber JH, Yousem S, Hardesty R, Griffith B (1992) Distinguishing between infection, rejection, and the adult respiratory distress syndrome after human lung transplantation. J Heart Lung Transplant 11: S232–S236

Paradowski LJ (1997) Saprophytic fungal infections and lung transplantation – revisited. J Heart Lung Transplant 16:524–531

Parker LA, Novotny DB (1997) Recurrent alveolar proteinosis following double lung transplantation. Chest 111:1457–1458

Penn I (1993) Incidence and treatment of neoplasia after transplantation. J Heart Lung Transplant 12:S328–S336

Revell MP, Lewis ME, Llewellyn-Jones CG, Wilson IC, Bonser RS (2000) Conservation of small-airway function by tacrolimus/cyclosporine conversion in the management of bronchiolitis obliterans following lung transplantation. J Heart Lung Transplant 19:1219–1223

Schulman LL, Scully B, McGregor CC, Austin JH (1997) Pulmonary tuberculosis after lung transplantation. Chest 111:1459–1462

Shreeniwas R, Schulman LL, Berkmen YM, McGregor CC, Austin JH (1996) Opportunistic bronchopulmonary infections after lung transplantation: clinical and radiographic findings. Radiology 200:349–356

Smith MA, Sundaresan S, Mohanakumar T, Trulock EP, Lynch JP, Phelan DL, Cooper JD, Patterson GA (1998) Effect of development of antibodies to HLA and cytomegalovirus mismatch on lung transplantation survival and development of bronchiolitis obliterans syndrome. J Thorac Cardiovasc Surg 116:812–820

Soghikian MV, Valentine VG, Berry GJ, Patel HR, Robbins RC, Theodore J (1996) Impact of ganciclovir prophylaxis on heart-lung and lung transplant recipients. J Heart Lung Transplant 15:881–887

Starnes VA, Bowdish ME, Woo MS, Barbers RG, Schenkel FA, Horn MV, Pessotto R, Sievers EM, Baker CJ, Cohen RG, Bremner RM, Wells WJ, Barr ML (2004) A decade of living lobar lung transplantation: recipient outcomes. J Thorac Cardiovasc Surg 127:114–122

Stern EJ, Frank MS (1994) Small-airway diseases of the lungs: findings at expiratory CT. AJR Am J Roentgenol 163:37–41

Stern EJ, Swensen SJ, Hartman TE, Frank MS (1995) CT mosaic pattern of lung attenuation: distinguishing different causes. AJR Am J Roentgenol 165:813–816

Sundaresan S, Trulock EP, Mohanakumar T, Cooper JD, Patterson GA (1995) Prevalence and outcome of bronchiolitis obliterans syndrome after lung transplantation. Washington University Lung Transplant Group. Ann Thorac Surg 60:1341–1346; discussion 1346–1347

Susanto I, Peters JI, Levine SM, Sako EY, Anzueto A, Bryan CL (1998) Use of balloon-expandable metallic stents in the management of bronchial stenosis and bronchomalacia after lung transplantation. Chest 114:1330–1335

Tamm M, Sharples LD, Higenbottam TW, Stewart S, Wallwork J (1997) Bronchiolitis obliterans syndrome in heart-lung transplantation: surveillance biopsies. Am J Respir Crit Care Med 155:1705–1710

Trulock EP (1997) Lung transplantation. Am J Respir Crit Care Med 155:789–818

Trulock EP, Edwards LB, Taylor DO, Boucek MM, Mohacsi PJ, Keck BM, Hertz MI (2003) The Registry of the International Society for Heart and Lung Transplantation: twentieth official adult lung and heart-lung transplant report – 2003. J Heart Lung Transplant 22:625–635

Trulock EP, Edwards LB, Taylor DO, Boucek MM, Keck BM, Hertz MI (2005) Registry of the International Society for Heart and Lung Transplantation: twenty-second official adult lung and heart-lung transplant report – 2005. J Heart Lung Transplant 24:956–967

Turton CW, Williams G, Green M (1981) Cryptogenic obliterative bronchiolitis in adults. Thorax 36:805–810

Venuta F, Diso D, Anile M, Aratari MT, Francioni F, Pugliese F, Rendina EA, Coloni GF (2005) Evolving techniques and perspectives in lung transplantation. Transplant Proc 37:2682–2683

Verleden GM (1998) Recurrence of desquamative interstitial pneumonia after lung transplantation. Am J Respir Crit Care Med 157:1349–1350

Verleden GM, Dupont LJ (2004) Azithromycin therapy for patients with bronchiolitis obliterans syndrome after lung transplantation. Transplantation 77:1465–1467

Verleden GM, Dupont LJ, Van Raemdonck D, Vanhaecke J (2003) Effect of switching from cyclosporine to tacrolimus on exhaled nitric oxide and pulmonary function in patients with chronic rejection after lung transplantation. J Heart Lung Transplant 22:908–913

Verschakelen JA, Scheinbaum K, Bogaert J, Demedts M, Lacquet LL, Baert AL (1998) Expiratory CT in cigarette smokers: correlation between areas of decreased lung attenuation, pulmonary function tests and smoking history. Eur Radiol 8:1391–1399

Walker S, Mikhail G, Banner N, Partridge J, Khaghani A, Burke M, Yacoub M (1998) Medium term results of lung transplantation for end stage pulmonary sarcoidosis. Thorax 53:281–284

Westney GE, Kesten S, De Hoyos A, Chapparro C, Winton T, Maurer JR (1996) Aspergillus infection in single and double lung transplant recipients. Transplantation 61:915–919

Whitford H, Walters EH, Levvey B, Kotsimbos T, Orsida B, Ward C, Pais M, Reid S, Williams T, Snell G (2002) Addition of inhaled corticosteroids to systemic immunosuppression after lung transplantation: a double-blind, placebo-controlled trial. Transplantation 73:1793–1799

Whyte RI, Rossi SJ, Mulligan MS, Florn R, Baker L, Gupta S, Martinez FJ, Lynch JP 3rd (1997) Mycophenolate mofetil for obliterative bronchiolitis syndrome after lung transplantation. Ann Thorac Surg 64:945–948

Williams TJ, Snell GI (1997) Early and long-term functional outcomes in unilateral, bilateral, and living-related transplant recipients. Clin Chest Med 18:245–257

Winter JB, Gouw AS, Groen M, Wildevuur C, Prop J (1994) Respiratory viral infections aggravate airway damage caused by chronic rejection in rat lung allografts. Transplantation 57:418–422

Winton TL (1992) Lung transplantation: donor selection. Semin Thorac Cardiovasc Surg 4:79–82

Wisser W, Klepetko W, Wekerle T, Laufer G, Stift A, Hiesmayr M, Schlick W (1996) Tailoring of the lung to overcome size disparities in lung transplantation. J Heart Lung Transplant 15:239–242

Worthy SA, Park CS, Kim JS, Muller NL (1997) Bronchiolitis obliterans after lung transplantation: high-resolution CT findings in 15 patients. AJR Am J Roentgenol 169:673–677

Wroblewski BM, Stefanovic CR, McDonough VM, Kidik PJ (1997) The challenges of idiopathic pulmonary hemosiderosis and lung transplantation. Crit Care Nurse 17:39–44

Yates B, Murphy DM, Forrest IA, Ward C, Rutherford RM,

Fisher AJ, Lordan JL, Dark JH, Corris PA (2005) Azithromycin reverses airflow obstruction in established bronchiolitis obliterans syndrome. Am J Respir Crit Care Med 172:772–775

Yeldandi V, Laghi F, McCabe MA, Larson R, O'Keefe P, Husain A, Montoya A, Garrity ER Jr. (1995) Aspergillus and lung transplantation. J Heart Lung Transplant 14:883–890

Yousem SA, Berry GJ, Cagle PT, Chamberlain D, Husain AN, Hruban RH, Marchevsky A, Ohori NP, Ritter J, Stewart S, Tazelaar HD (1996) Revision of the 1990 working formulation for the classification of pulmonary allograft rejection: Lung Rejection Study Group. J Heart Lung Transplant 15:1–15

Zenati M, Dowling RD, Dummer JS, Paradis IL, Arena VC, Armitage JM, Kormos RL, Hardesty RL, Griffith BP (1990) Influence of the donor lung on development of early infections in lung transplant recipients. J Heart Transplant 9:502–508; discussion 508–509

Zhang L, Irion K, da Silva Porto N, Abreu e Silva F (1999) High-resolution computed tomography in pediatric patients with postinfectious bronchiolitis obliterans. J Thorac Imaging 14:85–89

Fisher AJ, Lordan JL, Dark JH, Corris PA (2005) Azithromycin reverses airflow obstruction in established bronchiolitis obliterans syndrome. Am J Respir Crit Care Med 172:772–775

Yeldandi V, Laghi F, McCabe MA, Larson R, O'Keefe P, Husain A, Montoya A, Garrity ER Jr. (1995) Aspergillus and lung transplantation. J Heart Lung Transplant 14:883–890

Yousem SA, Berry GJ, Cagle PT, Chamberlain D, Husain AN, Hruban RH, Marchevsky A, Ohori NP, Ritter J, Stewart S, Tazelaar HD (1996) Revision of the 1990 working formulation for the classification of pulmonary allograft rejection: Lung Rejection Study Group. J Heart Lung Transplant 15:1–15

Zenati M, Dowling RD, Dummer JS, Paradis IL, Arena VC, Armitage JM, Kormos RL, Hardesty RL, Griffith BP (1990) Influence of the donor lung on development of early infections in lung transplant recipients. J Heart Transplant 9:502–508; discussion 508–509

Zhang L, Irion K, da Silva Porto N, Abreu e Silva F (1999) High-resolution computed tomography in pediatric patients with postinfectious bronchiolitis obliterans. J Thorac Imaging 14:85–89

Bone Marrow Transplantation

6

6.1 Hematopoietic Transplantation

Jorge Sierra

CONTENTS

J. Sierra, MD, PhD
Professor of Medicine, Director, Clinical Hematology and Hematopoietic Transplantation Program, Hospital de la Santa Creu i Sant Pau, Universitat Autónoma de Barcelona, Barcelona, Spain

6.1.1 Introduction

Hematopoietic transplantation is increasingly being used as treatment for a variety of severe diseases. Data from International Registries indicate that more than 25,000 transplants are performed every year in Europe, and a similar number in the United States (US) (Copelan 2006; Gratwohl et al. 2007). The objectives of this procedure are: (1) to replace hematopoiesis affected by a severe and irreversible disorder, (2) to rescue the patient from intense marrow toxicity induced by high-dose chemotherapy and/or radiation, and (3) to use a fraction of cells contained in the graft as anti-tumor immunotherapy. Of note, one or more of these objectives may be pursued in a particular situation; for example, in a patient with acute leukemia, transplantation aims to replace the neoplastic hematopoiesis by administering high-dose cytotoxic therapy and taking advantage of the graft-versus-leukemia effect of donor T-lymphocytes from the graft. In contrast, in aplastic anemia the only goal of the procedure is to restore an adequate hematopoiesis.

There are several transplantation modalities, depending on the type of donor and the source of hematopoietic cells. In all cases, the donor has to be identical or very similar to the recipient in the major histocompatibility system of human leukocyte antigens (HLA). If the donor is an identical twin of the recipient the transplant is named syngeneic, whereas if the donor is another type of individual the denomination is allogeneic; in the latter circumstance the donor may be related or unrelated to the patient. Frequently, the patient acts as his own hematopoietic donor and the name for such an approach is autologous transplantation. In this situation, the transplanted cells have to be collected and cryopreserved before the administration of high-dose therapy.

Regarding the source of hematopoietic stem cells, the transplant may be from bone marrow, mobilized peripheral blood or umbilical cord blood.

6.1.2 History

In 1939, Osgood administered repeated injections of a small amount of intravenous bone marrow to treat aplastic anemia without observing a response (Thomas 1999). One year later, Morrison unsuccessfully treated another aplastic anemia patient by infusing marrow cells into the sternum. During the Second World War, the Atomic Energy Commission of the US promoted investigations on the intravenous administration of bone marrow cells to irradiated dogs. The low dose of radiation, 350 rads or 3.5 Gy, was insufficient to facilitate the engraftment of infused marrow.

Between 1949 and 1954, Jacobson, Lorenz, Barnes and Loutit made important experiments in mice showing that cells from the spleen or the bone marrow protected from death caused by radiation. Of note, a different evolution was observed after syngeneic and allogeneic transplantation, since mice in the latter group usually died due to complications defined as "secondary disease". This experience anticipated the most relevant problem after this type of transplantation, graft-versus-host disease (GVHD).

In 1957, Thomas and Ferrebee published a report on six patients with end-stage hematologic cancer who received extensive radiation and intravenous marrow cells from healthy donors (Thomas et al. 1957). This pioneering experience in human hematopoietic transplantation led to engraftment in only one case. One year later, Kurnick described the first two cases of autologous transplantation of human marrow cells to treat radiation toxicity.

In 1959 Thomas published the first series of successful bone marrow transplants in humans using identical twin donors. One year before, Dausset and van Rood had discovered the HLA system, enabling the possibility of performing allogeneic transplantation with a reasonable chance of success. In 1965, Mathé et al. were the first to obtain a sustained allogeneic engraftment, although the patient subsequently died from chronic GVHD.

In 1969, the Seattle transplant team, under the leadership of Donnall Thomas, established the program of hematopoietic transplantation as a treatment for severe aplastic anemia and advanced-stage acute leukemia. These investigators demonstrated that this treatment allowed long-term survival in a small fraction of otherwise incurable patients. The results encouraged this group to investigate this approach in earlier phases of disease evolution. In 1972 and 1974 the Seattle team published two reports in aplastic anemia patients achieving 40% long-term survival. These experiences increased the interest about marrow transplantation in other Western countries during the second half of the 1970s.

The first unrelated donor marrow transplantation was performed in 1972 (Thomas 1999). In 1973, the Anthony Nolan Registry of the United Kingdom (UK) was created to increase the access to HLA-typed unrelated volunteers. However, due to the initial complexity of donor search, these transplants were infrequent until the second half of the 1980s.

In 1989, Gluckman et al. performed the first human transplantation with hematopoietic cells from the umbilical cord blood of a newborn, in a patient with Fanconi anemia. One year later, in 1990, Donnall Thomas was awarded with the Nobel Prize of Medicine for his pioneer work and achievements in hematopoietic transplantation field.

Until the late 1980s, bone marrow was the stem cell source in practically all transplants. In those days it became evident that large numbers of hematopoietic progenitors could be obtained from peripheral blood during the recovery phase following chemotherapy. The introduction of colony-stimulating factors (CSF) in clinical practice led to the same observation: these agents were able to mobilize large amounts of hematopoietic progenitor cells to peripheral blood. Of note, the combination of chemotherapy and CSF increased the harvestable cells by means of apheresis devices compared with either alone. In autologous transplants, peripheral blood rapidly replaced bone marrow as the source of hematopoietic progenitors. In contrast, in allogeneic procedures the introduction of peripheral blood was slower. The reason was the particular concern that GVHD could be very frequent and severe, since peripheral blood contains 10 times more T-lymphocytes than bone marrow. However, this drawback was not confirmed by clinical experience and since 1995 the proportion of peripheral blood transplants has progressively increased, accounting now for more than 70% of allogeneic procedures.

6.1.3 Indications

Hematopoietic transplantation is mostly indicated for hematologic malignancies that can be treated with high doses of cytotoxic agents (Copelan 2006). Figure 6.1.1 reflects the most frequent diagnoses in patients with neoplastic diseases. Current indications and practice of this treatment have been recently reviewed (Gratwohl et al. 2007). Patients with lymphoma, myeloma, acute leukemia or myelodysplasia may benefit from this procedure, among others. Hematopoietic transplantation is also useful for replacing insufficient or defective cells derived from the marrow progenitors. This is the case in patients with marrow aplasia, central cytopenias, paroxysmal nocturnal hemoglobinuria, marrow myelofibrosis or inherited disorders of metabolism. Depending on the disease and degree of marrow involvement, patients will be suitable for allogeneic, autologous transplantation, or both. Of note, progress in non-transplant therapies is limiting some classical indications for this procedure. A good example of this is chronic myelogenous leukemia, where the introduction of imatinib, a bcr-abl tyrosine kinase inhibitor, has dramatically decreased the number of transplants for this disease (Baccarani et al. 2006). On the other hand, studies showing no superiority of autologous transplantation over conventional treatment in patients with breast cancer mean that the former is almost never used now.

6.1.4 Transplantation Technique

The main phases of hematopoietic transplantation procedure are as follows (Fig. 6.1.2): (1) identification of stem cell donor and stem cell source, followed in autologous transplants by the harvest of hematopoietic cells, (2) administration of a preparative regimen (conditioning) to damage the recipient's hematopoiesis and immune system, to create marrow space, and eventually to treat the neoplastic disease, (3) collection and infusion of hematopoietic progenitors from the donor, or thawing and administration of the autologous stem cells, (4) supportive measures until hematologic and immune recoveries are achieved, (5) in allogeneic transplants, management of the immune interaction between donor cells and recipient tissues potentially leading to graft rejection and/or GVHD.

6.1.4.1 Donor Selection in Allogeneic Transplants

HLA compatibility between donor and recipient may be studied by serologic methods or DNA techniques. The required resolution of HLA-typing methods is lower when recipient and donor are siblings compared to unrelated donor transplantation. In the latter circumstance, high-resolution allele typing is necessary for an adequate HLA matching. HLA-A,

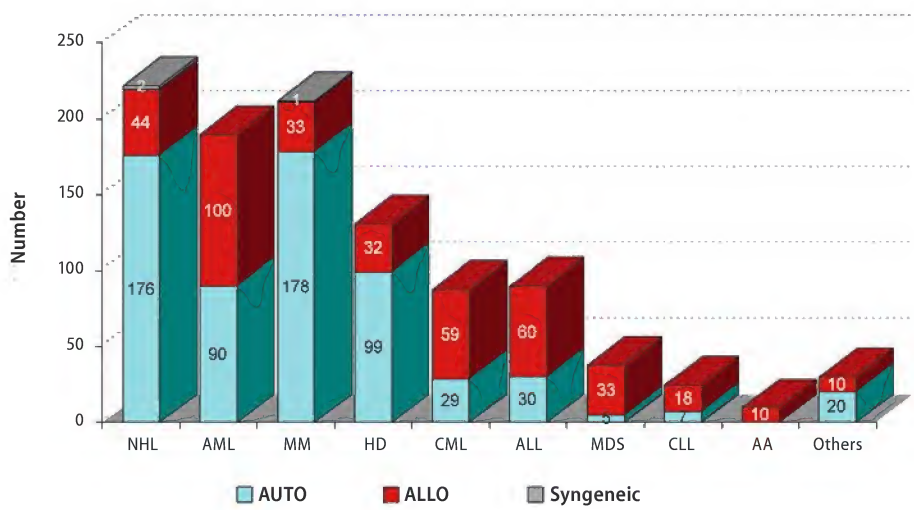

Fig. 6.1.1. Indications of autologous, allogeneic or syngeneic hematopoietic transplantation at the Hospital de la Santa Creu i Sant Pau in Barcelona. (*AA*, Aplastic anemia; *ALL*, acute lymphoblastic leukemia; *AML*, acute myeloid leukemia; *CLL*, chronic lymphocytic leukemia; *CML*, chronic myelogenous leukemia; *HD*, Hodgkin's disease; *MDS*, myelodysplastic syndrome; *MM*, multiple myeloma; *NHL*, non-Hodgkin's lymphoma)

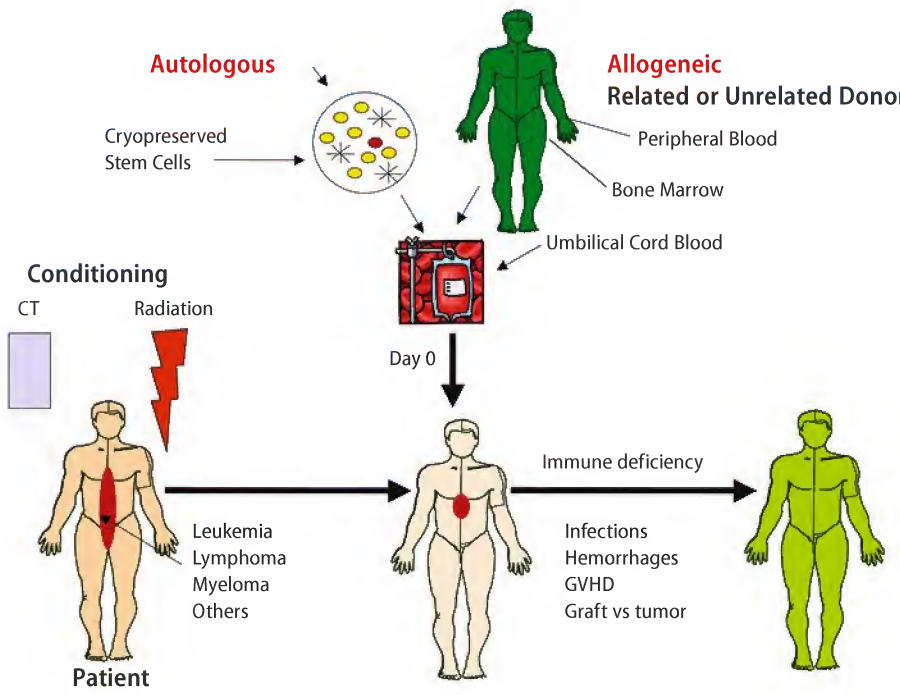

Fig. 6.1.2. Schema of hematopoietic stem cell transplantation. The patient receives conditioning regimen with chemotherapy (*CT*) and/or radiation to create marrow space and reduce the tumor. On day 0, autologous or allogeneic hematopoietic cells are administered through a right atrial catheter. The patient experiences profound aplasia and immune suppression. During this period immediate toxicity and opportunistic infections appear. After hematologic recovery, recipient tissues are recognized by immune-competent donor-derived T-cells and graft-versus-host disease (*GVHD*) develops. Graft-versus-tumor effect contributes to the eradication of residual neoplastic cells

-B, and -DR antigens are analyzed in transplants between siblings, whereas HLA-A, -B, -C, DRB1 and DQB1 alleles are studied in unrelated pairs. No more than one antigen mismatch is acceptable if the donor is a relative of the recipient, and no more than one allele mismatch in transplants from unrelated volunteers. In umbilical cord blood transplantation, units are selected by HLA-A and -B serologic or low-resolution DNA typing, whereas allele identification is required for matching at HLA-DRB1. Up to two HLA disparities are acceptable in this type of transplantation.

6.1.4.2 Hematopoietic Stem Cell Harvest

Multiple punctures in the iliac crests (more than 100–150) are necessary to aspirate enough marrow cells for transplantation. This procedure is made under general or less frequently regional anesthesia. Harvest of marrow cells from the sternum is exceptional. Marrow blood (1000–1500 ml) has to be obtained and subsequently filtered to eliminate bone fragments. This product is collected in transfusion bags with red cells being removed in case of donor–recipient major ABO incompatibility. The amount of hematopoietic progenitors of an adequate marrow product is at least 1×10^6 CD34-positive cells/kg of the recipient. Administering a high marrow cell dose is particularly relevant for improving the outcome after unrelated transplantation.

Hematopoietic stem cells may also be obtained from the peripheral blood by means of apheresis machines. These devices are sophisticated centrifuges which separate circulating blood cells and allow their selective aspiration. To mobilize hematopoietic progenitor cells from marrow to blood, CSF have to be administered to the donor. In autologous harvesting chemotherapy is frequently combined with CSF. The usual dose of granulocyte CSF (G-CSF) is 10 μg/kg daily if used alone and 5 μg/kg when combined with chemotherapy. This chemotherapy may be the patient's standard treatment or consist of a single high dose of cyclophosphamide (1–3 g IV). In chemotherapy-plus-CSF mobilization, peripheral blood stem cell collection usually begins on day 11–14 after the start of treatment, whereas in CSF priming alone harvesting is initiated on day 4 or 5 of therapy. In most instances, one to four apheresis sessions are required to obtain at least 2×10^6 CD34+ cells/kg, the adequate number of cells for transplantation. In autologous collection from heavily pretreated patients it is relatively frequent to observe a low

number of circulating CD34+ cells during the mobilization attempt. This circumstance is known as mobilization failure.

Collection of cord blood stem cells consists of canalization of the umbilical vein after delivery to obtain, by gravidity and pressure on the placenta, 100–150 ml of blood. An adequate cord blood unit for transplantation contains at least 5×10^6 total CD34+ cells. The infused cell dose has to be at least 1×10^5 CD34 cells/kg or 2×10^7 nucleated cells (NC)/kg.

All cell products for transplantation have to be bacteriologically and virologically tested. In autologous and in cord blood transplantation the cells collected are cryopreserved and stored for future use.

6.1.4.3 Conditioning Regimen

The conditioning or preparative regimen includes chemotherapy, radiation or both. There are two categories of conditioning: (1) high-dose conditioning also known as myeloablative, and (2) reduced intensity conditioning or non-myeloablative.

High-dose conditioning has a powerful antineoplastic effect but significant toxicity precluding its administration to elderly or debilitated patients. This type of regimen leads to early full engraftment of donor cells. Reduced intensity conditioning has an immunosuppressive effect with low anti-tumor activity (Martino et al. 2001). This modality of preparative approach has improved short-term toxicity in old and sick patients. Engraftment of donor cells is progressive with full replacement of recipient hematopoiesis and lymphopoiesis (chimerism) being achieved after several weeks or months (Fig. 6.1.3). In some circumstances, complete hematopoietic and immune recovery from transplanted cells requires the infusion of additional donor T-lymphocytes.

Cytotoxic drugs commonly administered in conditioning regimens are alkylating agents such as cyclophosphamide, busulphan or melphalan, topoisomerase inhibitors, antimetabolites such as cytarabine, nitrosoureas such as BCNU and purine analogs such as fludarabine. Total body irradiation is frequently added in high dose (8–12 Gy) or as part of reduced-intensity conditioning (2 Gy). Polyclonal [antithymocyte globulin (ATG)] or monoclonal (Campath 1H) antibodies may also be incorporated into the preparative regimen to facilitate engraftment and decrease GVHD after transplantation.

6.1.4.4 Stem Cell Infusion

A right atrial catheter has to be placed in the recipient of hematopoietic transplantation. The collected cells are infused freshly, or after rapid thawing in autologous or cord blood transplantation. Infusion duration is variable, from minutes to more than 1 h, depending on the volume to be administered. Vitals have to be monitored every 10–15 min. The main complications of cell infusion are chills, fluid overload and, infrequently, fat emboli in the lungs.

6.1.4.5 Graft-Versus-Host Disease Prophylaxis in Allogeneic Transplantation

Allogeneic stem cell infusion without post-transplant immunosuppression or T-cell depletion of the graft is followed by hyperacute and lethal GVHD. In T-cell replete transplantation, prophylaxis of this complication has to be administered. This consists of cyclosporine or tacrolimus together with methotrexate, prednisone, mycophenolate mofetil (MMF), rapamycin or the combination of two of these drugs. Adverse effects of cyclosporine and tacrolimus are renal and central nervous system toxicities, hyperbilirubinemia and thrombotic microangiopathy. Methotrexate prophylaxis is associated with mucositis, delayed engraftment, and liver toxicity. Prednisone facilitates the development of fungal and viral infections. Mycophenolate and rapamycin lead to gastrointestinal secondary effects.

6.1.4.6 Post-Transplant Supportive Measures

Transplanted patients develop profound aplasia and immunosuppression as a consequence of the conditioning regimen. During the neutropenic period it is recommended to keep the patients in isolated rooms equipped with high-efficiency particulate air (HEPA) filters. Diet has to be free of germ contamination, and oral antibacterial, antifungal, and

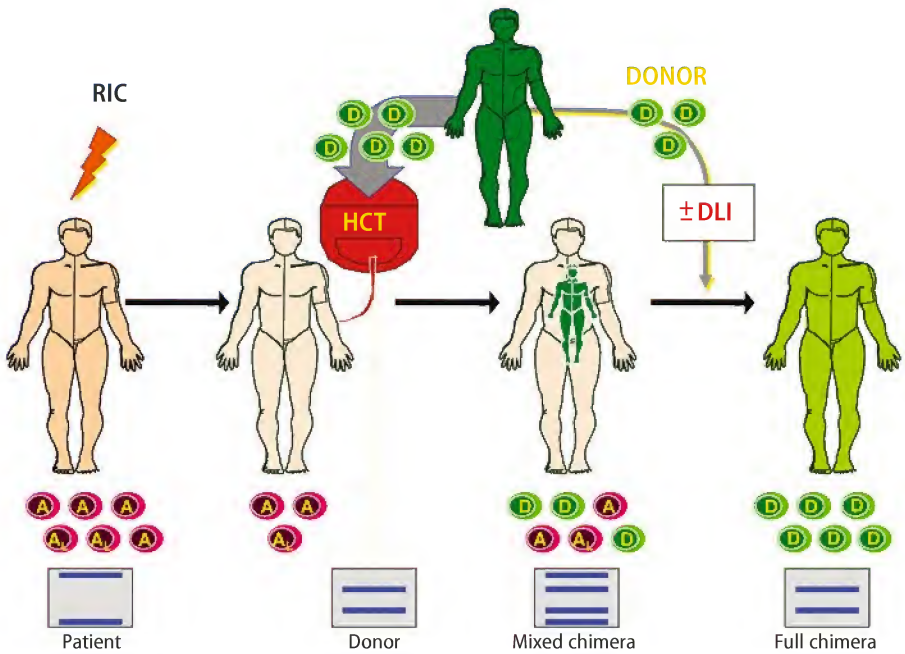

Fig. 6.1.3. Allogeneic hematopoietic cell transplantation (HCT) after reduced intensity conditioning (*RIC*). In the first weeks after transplant there is coexistence of donor and recipient hematopoietic cells (mixed chimerism). Spontaneously or after donor lymphocyte infusions (*DLI*) full donor chimerism is established

antiviral prophylaxis is administered. Red cell and platelet transfusions are given until these cells are produced by the graft. In some circumstances, CSF are administered to accelerate hematological recovery. In patients with severe hypogammaglobulinemia the substitutive intravenous supply of immunoglobulins is recommended.

6.1.4.7 Hematopoietic and Immune Reconstitution from Transplanted Cells

More than 0.5×10^9/l neutrophils are achieved at a median of 10–14 days after transplantation of peripheral blood progenitor cells, 21–28 days after marrow infusion, and 25–35 days when umbilical cord blood is the hematopoietic source. A self-sustained platelet count above 20×10^9/l is usually reached 5 days to 3 weeks after neutrophil recovery. Full immune reconstitution is slow and takes several months. CD4+ cell counts are low after transplantation. B-cell production and function are also impaired after the procedure. New ontogeny of the immune system after allogeneic transplantation requires vaccination against the most common pathogens, once the ability to effectively produce antibodies is restored.

As soon as hematopoietic cells appear in marrow and in blood, their origin from the donor may be demonstrated by several techniques. These include, among others, studies of red cell antigens, sex disparities, and molecular methods such as analysis of the variable number of tandem repeats (VNTR). The circumstance of donor hematopoiesis in the recipient is known as chimerism. This chimerism may be full donor or mixed with the persistence of a variable proportion of host cells. Chimerism is early and complete when high-dose conditioning is administered. In contrast, mixed chimerism for weeks or months may be observed after reduced-intensity conditioning transplantation. Persistent mixed chimerism is frequently associated with disease recurrence or graft rejection. On the other hand, full donor chimerism is usually a requisite for developing GVHD.

6.1.5 Transplant Complications

6.1.5.1 Graft Failure

Lack of engraftment (or primary graft failure) is exceptional in transplantation after full-dose conditioning for neoplastic diseases, provided that the patients receive an adequate hematopoietic cell dose of autologous origin or from an HLA-identical sibling. Transplantation from unrelated donors, par-

ticularly if there is some degree of HLA disparity, and from umbilical cord blood increases the risk of graft failure, as well as the administration of reduced-intensity conditioning. Graft failure is also more frequent if the patient has preserved immune integrity before the procedure, such as in aplastic anemia or chronic myeloid leukemia without prior intensive treatment. In the high-risk circumstances mentioned, the frequency of this complication ranges between 5% and 20%.

Secondary graft failure, also known as poor graft function, develops in patients with severe systemic infections early post-transplant and in those with CMV replication after the procedure. Parvovirus B19 is another pathogen that has to be investigated in cases of secondary graft failure. Certain drugs used after transplantation such as methotrexate, cotrimoxazole, ganciclovir, amphotericin B, and mycophenolate mofetil are myelotoxic and may cause or contribute to poor graft function.

6.1.5.2 Opportunistic Infections

A wide variety of infectious complications may develop after transplantation (Fig. 6.1.4). During the neutropenic period, fever appears in practically all patients. The causative pathogens are usually Gram positive cocci entering the body through the intravenous catheter or as a consequence of severe oral mucositis. Gram-negative sepsis may also occur with the more frequent entry route being the gastrointestinal tract.

Bacterial, viral or fungal pneumonia is also relatively common after transplantation. Computed tomography of the thorax is useful for early detection of this complication and the radiologic findings will be extensively reviewed in this book. In patients with pulmonary infection, bacteria, fungi, community viruses, CMV, and *Pneumocystis carinii* have to be investigated by antigenemia or polymerase chain reaction (PCR) in blood, nasopharyngeal cultures and direct staining and cultures of bronchoalveolar brushing and lavage. Transbronchial or transparietal lung biopsy may be necessary for an etiologic diagnosis. If the pulmonary complication is not under adequate control severe respiratory failure may develop requiring mechanical ventilation.

Viral infections that occur after transplantation are not limited to the lung. Herpes simplex infections are frequent early after the procedure, manifesting as oral vesicles or ulcerations. Less frequent is genital involvement by herpes simple virus, hepatitis or encephalitis. Herpes zoster and varicella reactivate in most patients, particularly if aciclovir prophylaxis is discontinued. Occasionally, severe cerebral arteritis or pneumonia caused by this virus may occur. CMV infection is frequent after transplantation and has to be regularly monitored by antigenemia and/or PCR for early treatment avoiding CMV disease. Epstein Barr virus (EBV) infection and EBV-associated lymphoproliferative disorders have also to be tested on a regular basis, especially in transplants with "in

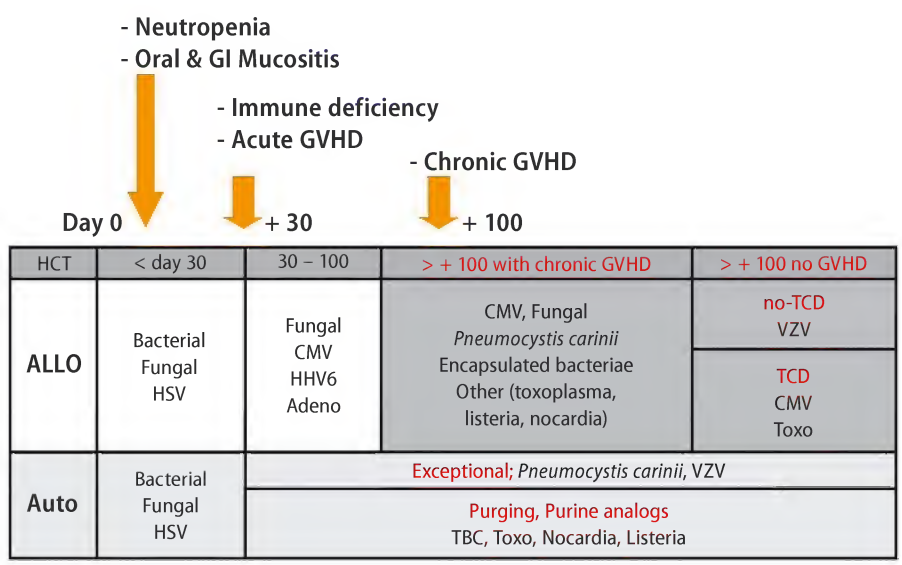

Fig. 6.1.4. Pattern of infections after hematopoietic cell transplantation (*HCT*). (*Adeno*, adenovirus; *CMV*, cytomegalovirus; *GVHD*, graft-versus-host disease; *HHV6*, human herpes virus 6; *HSV*, herpes simple virus; *TCD*, T-cell depletion; *TOXO*, toxoplasma; *VZV*, varicella zoster virus)

vivo" or "ex vivo" T-cell depletion. Rituximab™, a monoclonal antibody against cells expressing CD20 antigen, is an effective treatment of post-transplant EBV-related disorders.

Aspergillus infection is frequent after transplantation, despite galactomannan antigen monitoring and antifungal prophylaxis. Prolonged neutropenia, GVHD, and immunosuppressive treatment predispose to this complication. Angioinvasive pulmonary involvement is the most frequent clinical picture. Bronchial aspergillosis and solitary lung lesions are less common. If the disease does not respond to treatment, widespread aspergillosis may occur with cerebral disease. In the latter situation, mortality is practically constant.

Other filamentous fungi and *Candida* sp. infection are much less frequent than aspergillosis, although they have also to be taken into account in the differential diagnosis of patients with suspected fungal infection.

Occasional post-transplant infections include toxoplasma or tuberculosis of the lungs and/or central nervous system disease, and *Pneumocystis carinii* pneumonia. These diseases respond well to treatment and because of that early and precise diagnosis is mandatory.

6.1.5.3 Graft-Versus-Host Disease

The recognition of several tissues of the recipient by the immune-competent T-cells from the donor causes GVHD. This phenomenon occurs in 50%–90% of allogeneic transplants, being more frequent in cases of HLA disparity, transplantation from unrelated donors, and in male recipients transplanted from female donors. There are two forms of GVHD with a different clinical picture. The acute form develops before day 100 after transplant and involves skin, liver, and gastrointestinal tract. Patients have erythema, papulae (Fig. 6.1.5a) or epidermolysis (Fig. 6.1.5b), hepatitis and/or cholestasis, vomiting and diarrhea. Chronic GVHD is diagnosed when present after day 100. This complication manifests as lichenoid, sclerodermiform or hypopigmented skin lesions, mucosal and ocular involvement (Sicca syndrome), restrictive or obstructive (obliterans bronchiolitis) lung disease, chronic hepatitis and/or cholestasis, and less frequently muscular or fasciae inflammation. The treatment of GVHD consists of immunosuppressive and immunomodulatory drugs such as steroids, cyclosporine or tacrolimus, mycophenolate mofetil, thalidomide, rapamycin, and polyclonal or monoclonal anti T-cell antibodies. The overall complete response rate to treatment for GVHD is higher than 50%. In contrast, patients who do not respond or have a relapse have poor outcome in terms of long-term survival. In patients transplanted for malignancies, the best scenario is to develop moderate and sustained GVHD which


a

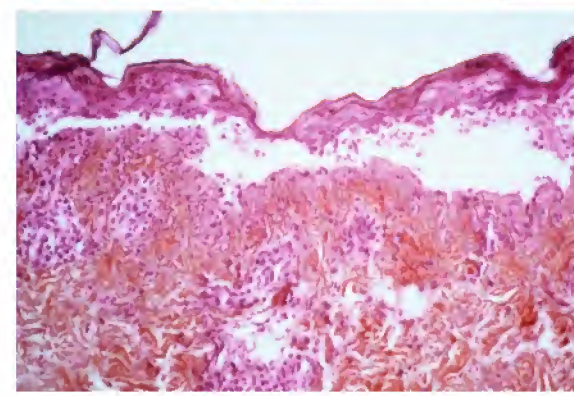
b

Fig. 6.1.5a,b. Acute graft-versus-host disease of the skin with **a** papulae and **b** epidermolysis

responds to treatment. This circumstance is associated with decreased recurrence of the neoplastic disease due to the powerful graft-versus-tumor effect (Martino et al. 2002).

6.1.5.4 Other Complications

Liver veno occlusive disease, recently defined as sinusoid obstruction syndrome (SOS), may develop in the first 40 days after transplantation as a consequence of a high-dose conditioning regimen. Prior liver disease predisposes to this complication which manifests as cholestasis and fluid retention secondary to portal hypertension and renal dysfunction. Current treatment of SOS consists of fluid restriction, diuretics, and defibrotide. Although transiently severe, the evolution is favorable in most cases.

Renal insufficiency, usually reversible, is common after the procedure and commonly related to the use of nephrotoxic drugs such as ciclosporin, tacrolimus, vancomycin or amphotericin B. In a minority of instances dialysis may be required. Microangiopathic hemolysis and thrombocytopenia secondary to ciclosporin or tacrolimus may further impair renal function. Hemorrhagic cystitis is also a possible complication of the transplant and is related to the use of high-dose cyclophosphamide, bacterial or viral infection (adenovirus) or mucosal GVHD. Infertility is almost inevitable after transplantation, unless a reduced-intensity conditioning regimen is administered.

With the improvement of long-term results of hematopoietic transplantation, late complications of the procedure are becoming evident. Cataracts, hypothyroidism, growth retardation, impaired hair growth, sexual dysfunction, and depression among other disorders have to be carefully evaluated and treated. However, more than 80% of transplant survivors are asymptomatic and able to carry on with a normal life.

6.1.6 Results

The results of hematopoietic transplantation depend mainly on age, disease stage, and type of procedure (Copelan 2006). The results are best in young pa-

Table 6.1.1. Results according to type of hematopoietic transplantation and disease-stage (modified from reference Copelan 2006). (CP, Chronic phase; NHL, non-Hodgkin's lymphoma)

	100-Day mortality	5-Year relapse	5-Year event-free survival
Autologous			
Diffuse large-cell NHL			
1st CT-sensitive relapse	3–5	45–52	45–50
2nd CT-sensitive relapse	5–8	47–65	30–35
Refractory	10–20	70–85	5–10
Allogeneic			
Acute myeloid leukemia			
1st complete remission	7–10	25–38	55–65
2nd complete remission	10–20	40–60	30–40
Refractory	30–40	40–55	15–20
Chronic myeloid leukemia			
CP<1 year after diagnosis	5–10	10–25	70–80
CP>1 year after diagnosis	10–15	25–40	50–60
Accelerated	15–20	45–55	30–35
Blastic	35–45	40–60	5–15

tients with early disease transplanted from HLA-identical siblings. The use of adult unrelated donors has an approximately 15% higher procedure-related mortality and decreased survival as compared to HLA-identical sibling transplants. An additional 10% mortality should be generally predicted if the stem cell source is umbilical cord blood. Autografting has a lower procedure-related mortality but a higher relapse rate than allogeneic transplantation. The same phenomenon is observed after reduced-intensity conditioning compared to conventional allogeneic transplant, a lower mortality but more recurrences. The main results obtained in the different disease categories are summarized in Table 6.1.1.

6.1.7 Future Developments

Hematopoietic transplantation is a field of active research. New methods are being developed to refine the transplantation technique to make it safer and more effective. Conditioning regimens targeted to neoplastic and/or immune cells and to preserve extrahematological tissues are under investigation. Antigen or molecularly targeted treatment may also be useful for eradicating minimal residual disease after the procedure (Ravandi et al. 2004). Improved knowledge of the mechanism of GVHD and the graft-versus-tumor effect may allow them to be separated, to achieve control over the neoplasia without undesirable toxicity. Progress in the field of immune tolerance may allow the surpassing of HLA barriers in some donor–recipient pairs, and the safe performance of HLA-haploidentical transplants. Finally, the selective use of hematopoietic and mesenchymal cell subsets may improve engraftment and allow further exploitation of these cells for tissue repair or as a form of immune modulation and therapy (Xia et al. 2004; Lazarus et al. 2005).

References

Baccarani M, Saglio G, Goldman J, Hochhaus A, Simonsson B, Appelbaum F et al (2006) Evolving concepts in the management of chronic myeloid leukemia: recommendations from an expert panel on behalf of the European LeukemiaNet. Blood 108:1809–1820

Copelan EA (2006) Hematopoietic stem-cell transplantation. N Engl J Med 354:1813–1826

Gratwohl A, Baldomero H, Frauendorfer K, Urbano-Ispizua A, Niederwieser D for the Joint Accreditation Committee of the International Society for Cellular Therapy ISCT and the European Group for Blood and Marrow Transplantation EBMT (JACIE) (2007). Results of the EBMT activity survey 2005 on haematopoietic stem cell transplantation: focus on increasing use of unrelated donors. Bone Marrow Transplant 39:71–87

Lazarus HM, Koc ON, Devine SM, Curtin P, Maziarz RT, Holland HK et al (2005) Cotransplantation of HLA-identical sibling culture-expanded mesenchymal stem cells and hematopoietic stem cells in hematologic malignancy patients. Biol Blood Marrow Transplant 11:389–398

Martino R, Caballero MD, Canals C, Simon JA, Solano C, Urbano-Ispizua A et al (2001) Allogeneic peripheral blood stem cell transplantation with reduced-intensity conditioning: results of a prospective multicentre study. Br J Haematol 115:653–659

Martino R, Caballero MD, Simon JA, Canals C, Solano C, Urbano-Ispizua A et al (2002) Evidence for a graft-versus-leukemia effect after allogeneic peripheral blood stem cell transplantation with reduced intensity conditioning in acute myelogenous leukemia and myelodysplastic syndromes. Blood 100:2243–2245

Ravandi F, Kantarjian H, Giles F, Cortés J (2004) New agents in acute myeloid leukemia and other myeloid disorders. Cancer 100:441–454

Thomas ED (1999) A history of haemopoietic cell transplantation. Br J Haematol 105:330–339

Thomas ED, Lochte HL, Ching-Lu W, Ferrebee J (1957) Intravenous infusion of bone marrow in patients receiving radiation and chemotherapy. N Engl J Med 257:491–496

Xia G, Kovochich M, Truitt RL, Johnson BD (2004) Tracking ex vivo-expanded CD4+CD25+ and CD8+CD25+ regulatory T cells after infusion to prevent donor lymphocyte infusion-induced lethal acute graft-versus-host disease. Biol Blood Marrow Transplant 10:748–760

6.2 Imaging in Bone Marrow Transplantation

Tomas Franquet

CONTENTS

6.2.1 Introduction

The term "hematopoietic stem cell transplantation" has supplanted the previously employed term "bone marrow transplantation" to reflect the broader range of donor stem cell sources that are now available: bone marrow, fetal cord blood, and growth-factor-stimulated peripheral blood (Kotloff et al. 2004). Hematopoietic stem cell (HSC) transplantation is being used with increasing frequency for the treatment of leukemia, aplastic anemia, myeloma, and some forms of lymphoma and solid tumors. It is estimated that more than 50,000 marrow and HSC transplantations are performed annually worldwide (Tabbara et al. 2002).

Although HSC transplantation is a well-established procedure, thoracic complications are common (Winer-Muram et al. 1996; Yen et al. 2004) and occur in a significant number of patients after marrow transplantation (Krowka et al. 1985; Chan et al. 1990; Soubani et al. 1996; Worthy et al. 1997; Kotloff et al. 2004).

Pulmonary complications are a common cause of morbidity and mortality after HSC transplantation occurring in 40%–60% of recipients and accounting for more than 90% of mortality (Yen et al. 2004). The spectrum of pulmonary complications has been influenced by changes in transplantation technique, prophylactic treatment for infections, and the use of new chemotherapeutic drugs that contribute to lung injury. Allogeneic recipients develop pulmonary complications at a much higher frequency than those receiving autologous HSC transplant (Tabbara et al. 2002).

Marrow grafting is preceded by intense immunosuppressive treatment to prevent rejection of the

T. Franquett, MD
Professor, Hospital de Saint Pau, Department of Radiology, Avenida S. Antonio Maria Claret 167, Barcelona 08021, Spain

transplanted marrow. Preparative regimens cause a spectrum of pulmonary acute toxicities and complications that may be either infectious and related to the degree of ongoing immunosuppression, or non-infectious and related to previous chemotherapy, degree of immunosuppression, and, in allogeneic transplants, the presence of graft-versus-host disease (GVHD) (Chan et al. 1990).

Pneumonia remains a common life-threatening complication in HSC recipients occurring as a direct result of transplantation-induced immune suppression (Aronchick 2000). Non-infectious complications include pulmonary edema, engraftment syndrome, alveolar hemorrhage, drug-induced lung injury, idiopathic pneumonia, obliterative bronchiolitis, cryptogenic organizing pneumonia, pulmonary veno-occlusive disease, and post-transplant lymphoproliferative disorder (Alam and Chan 1996; Soubani et al. 1996; Worthy et al. 1997). As the number of survivors increases, several late effects of treatment are becoming evident. Sarcoidosis has been sporadically reported as a rare complication following either autologous or allogeneic HSC transplantation (Bhagat et al. 2004). In these patients the prevalence of sarcoidosis may be tenfold higher than that of the normal population (Bhagat et al. 2004).

In this chapter, imaging features of various infectious and non-infectious pulmonary complications following HSC transplantation are discussed and illustrated.

6.2.2 Clinical Considerations

Specific pulmonary complications tend to occur during identifiable phases that correspond with the state of immune reconstitution after the marrow transplant. It is useful to divide the post-transplant period into three phases: (1) neutropenic phase (the first 30 days); (2) early phase (days 31–100); and (3) late phase (more than 100 days after the transplant). Although this division is clinically useful, overlap occurs in the timing of specific complications (Chan et al. 1990; Soubani et al. 1996; Worthy et al. 1997).

Signs and symptoms of pulmonary disorders related to HSC transplantation are often non-specific and rapid and accurate diagnosis is essential in these life-threatening disorders.

6.2.3 Integrating Clinical Factors, Imaging Findings, and Other Diagnostic Procedures

Although imaging has a limited role before HSC transplantation, it is important after transplantation when it may support the clinical diagnosis of a variety of complications. It may also be used to monitor the effect of therapy and to detect recurrence of the underlying disease if the transplant is unsuccessful (Evans et al. 2003). The most useful imaging modalities available for the evaluation of the patient with known or suspected post-transplant pulmonary complications are chest radiography and computed tomography (Wah et al. 2003).

Combining clinical factors, including the type of transplant and the point of time during the post-transplantation course, with characteristic imaging features yields the most specific and accurate differential diagnosis for radiologic findings in these patients (Nusair et al. 2004; Coy et al. 2005; Franquet et al. 2005a). In the absence of clinical information, radiologists cannot reliably distinguish between pneumonia and other non-infectious pulmonary processes.

Diffuse parenchymal infiltrates are common radiographic findings in HSC transplant recipients. In the neutropenic phase, < 30 days after transplantation, infectious causes of pulmonary infiltrates have been documented in fewer than 20% of recipients who underwent open lung biopsy (Crawford et al. 1988). In this phase, pulmonary edema secondary to cardiac decompensation, intravascular volume excess, acute respiratory distress syndrome, or pulmonary capillary leak is the major reason for diffuse parenchymal infiltrates. However, between 30 and 180 days after transplantation, infections are the commonest cause of diffuse parenchymal abnormalities (Crawford et al. 1988; Cunningham 1992). Pulmonary edema and the idiopathic pulmonary syndrome (IPS) are the most common conditions to be distinguished from bronchopneumonia when a generalized pulmonary abnormality is radiographically demonstrated (Cardozo and Hagenbeek 1985; Crawford 1999).

Focal parenchymal infiltrates are frequently due to infection regardless of the time of presentation after transplant; however, distinction of localized pneumonia from other pulmonary processes cannot be made with certainty on radiologic grounds (Janzen et al. 1993). Unfortunately, the clinical data

and imaging findings often fail to lead to a definitive diagnosis of pneumonia because an extensive number of non-infectious processes associated with febrile pneumonitis – i.e., drug-induced pulmonary disease, IPS, and organizing pneumonia – mimic pulmonary infection (Janzen et al. 1993). Localized pulmonary disease of a lobar or segmental distribution can also be produced by pulmonary edema and hemorrhage.

6.2.3.1 Conventional Chest Radiography

A posteroanterior (PA) (and lateral when possible) chest radiograph is the primary imaging modality used in the initial evaluation and follow-up of HSC transplant recipients with fever. Other roles for chest radiography are an enhanced ability to assess the extent of disease, to detect complications (i.e., cavitation, abscess formation, pneumothorax, pleural effusion), and to detect additional or alternative diagnoses and sometimes to guide invasive diagnostic procedures. The non-specificity of radiographic findings as well as the wide range of potential causes often lead to frustration when evaluating the imaging findings of a patient with a suspected thoracic complication.

6.2.3.2 Computed Tomography

Although CT is not recommended for the initial evaluation of patients with pneumonia, it is useful in the detection, differential diagnosis, and management of the HSC transplanted recipient with acute pulmonary disease when chest radiographs show non-specific abnormal findings or when the radiographic findings are normal with clinical findings of pulmonary disease (Worthy et al. 1997; Tanaka et al. 2002; Franquet et al. 2005a).

There is a large literature indicating that CT is a sensitive method capable of imaging the lung with excellent spatial resolution providing anatomical detail similar to that seen by gross pathological examination. Differences in tissue attenuation and parenchymal changes caused by an acute inflammatory process can be seen readily by CT. Unlike chest radiography, CT provides cross-sectional images and the pattern and distribution of pulmonary processes are therefore much more readily appreciated than on conventional examinations. The findings of air-space disease, air-space (acinar) nodules, ground-glass opacities, consolidation, air bronchograms, and centrilobular or perilobular distribution are seen better by CT than by conventional radiography. Air-space nodules represent the size of the acinus (6–10 mm) and are centrilobular in distribution. They are best appreciated in early disease and best seen at the edge of the pathologic process where consolidation is incomplete.

6.2.3.3 Non-Invasive and Bronchoscopic Diagnostic Procedures

The clinical and radiographic presentation of pulmonary disease in HSC transplant recipients often fails to allow the specific identification of a causative pathogen or to permit the distinction between infectious and non-infectious processes (Ettinger 1993; Starobin et al. 2003).

Non-invasive and bronchoscopic procedures have been shown to be safe and useful techniques for evaluating pulmonary infiltrates in immunocompromised patients. Fiber-optic bronchial aspirates (FBAS) and broncho-alveolar lavage (BAL) are the procedures of choice for evaluating pulmonary infiltrates in HSC transplant recipients and they have the highest diagnostic yield and impact on therapeutic decisions (Young et al. 1984; Springmeyer et al. 1986; Heurlin et al. 1991; Soubani et al. 2001). BAL has proved valuable even in patients who have severe thrombocytopenia (Stover et al. 1984; Huaringa et al. 2000). Negative results do not exclude angioinvasive fungal infections, such as aspergillosis.

6.2.3.4 Invasive Diagnostic Procedures

Diagnostic information may also be obtained by transbronchial or percutaneous needle aspiration. Transbronchial biopsy may be unsafe to perform in severely thrombocytopenic patients.

Despite its reported results in the diagnosis of pulmonary infection being variable (11.7%–73%), percutaneous fine needle aspiration is an alternative method used to identify causative pathogens in selected patients with pneumonia (Jantunen et al. 2002). Transthoracic needle aspiration should be considered for patients who have not responded to

initial therapy, who may have nosocomial superinfection, who are immunocompromised, or in whom TB is suspected but has not been confirmed by examination of the sputum or gastric lavage. It is not clear whether use of transthoracic needle aspiration results in a reduction in mortality and morbidity in a cost-effective fashion, compared to a less invasive approach.

6.2.3.5 Open Lung Biopsy

Surgical lung biopsy (SLB), by way of either thoracotomy or video-assisted thoracoscopy, may be diagnostic (Crawford et al. 1988; Snyder et al. 1990). SLB provides a specific diagnosis in the majority of patients with hematologic malignancy or HSC transplant recipients and unexplained pulmonary infiltrates (Wong et al. 2002; Zihlif et al. 2005). Even in severely immunosuppressed patients, the morbidity and mortality that are associated with this technique seem to be acceptable, especially when the biopsy is performed thoracoscopically (Roviaro et al. 2002).

6.2.4 Infectious Complications

Although the incidence of pulmonary infection after HSC transplantation has declined, pneumonia remains a common life-threatening complication in these patients and occurs as a direct result of transplantation-induced immune suppression (Crawford et al. 1988; Choi and Leung 1999). During the initial post-transplant period, patients are profoundly neutropenic (absolute neutrophil count < 500 cells/μl) and the majority of microbiologically documented pneumonias are caused by fungi or bacteria (Cunningham 1992). If neutropenia is prolonged beyond 2 weeks, *Aspergillus* spp. as well as other opportunistic moulds may cause life-threatening infections (Kaiser et al. 1998; Fukuda et al. 2004). While fungi are the most common cause of pulmonary infection in the early pre-engraftment phase, viruses most commonly occur in the post-engraftment phase (Kapoor et al. 1989; Giacchino et al. 1993). Conversely, in the late post-engraftment phase, from day 100 until the patient regains normal immunity usually 1–2 years later, there is no predominant pathogen and the majority of infections are usually bacterial (Paulin et al. 1987; Kotloff et al. 2004).

6.2.4.1 Bacterial Infection

Bacterial infections are responsible for approximately 90% of infections during the early phase of neutropenia and are not lethal as often as are viral and fungal infections (Maschmeyer 2001). The list of pathogens that can cause bacterial pneumonia in HSC transplant recipients is extensive, but a narrow spectrum accounts for most cases. During the first few days after transplantation, the organisms involved are aerobic bacteria found in the bowels (*Escherichia coli*, *Klebsiella*, *Pseudomonas*) and those found on the skin or intravenous catheters (*Staphylococcus aureus*, coagulase-negative staphylococci); other causative organisms are *Legionella*, *Haemophilus influenza*, Viridans streptococci, *Enterobacter*, and *Nocardia* (Villablanca et al. 1990; Kumar and Jimenez 2001; Lin et al. 2004). Viridans streptococcal shock syndrome may occur early in the transplantation course (6 or 7 days post-transplantation) in patients with severe neutropenia and viridans streptococcal bacteremia (Martino et al. 1995).

Clinical symptoms of bacterial infection include fever, cough, and progressive dyspnea that is present in more than 90% of patients. Although the pulmonary examination may reveal rhonchi and crackles, the examination may be normal in 50% of patients.

The radiographic findings in bacterial infections are non-specific. Plain radiographs most commonly show focal alveolar infiltrates, but may be normal in 30% of patients, most likely because of the routine use of broad-spectrum antibiotics for febrile patients (Maschmeyer 2001). On high-resolution CT, a focal air-space consolidation, which typically presents in either a segmental or lobar distribution, is frequently identified. Differentiation from atypical patterns of opportunistic infections is often impossible on the basis of radiographic findings. Conversely, atypical patterns, including bilateral diffuse opacities, are not uncommon manifestations of bacterial pneumonia.

Pyogenic airways disease, including infectious bronchitis and bronchiolitis, are increasingly seen in HSC transplant recipients. Histologically, they are characterized by an active cellular bronchiolitis

with mononuclear cell inflammation of the respiratory bronchioles and the presence of an inflammatory exudate and mucus in the bronchiolar lumen (Aquino et al. 1996). Bronchogenic dissemination of pyogenic bacteria can result in dilatation and thickening of bronchiolar walls. Chest radiography may have normal or non-specific findings consisting of heterogeneous ill-defined opacities, especially visible in the lower lung regions. Other common radiographic findings are peribronchial thickening occasionally observed as "tram tracking".

Associated airway abnormalities can also be depicted by CT. Characteristic CT findings include: (1) small ill-defined centrilobular densities representing bronchioles impacted with inflammatory material and peribronchiolar inflammation ("tree-in-bud"), (2) branching linear opacities corresponding to inflammatory cells in the walls of the airways, and (3) focal areas of consolidation due to bronchopneumonia (Fig. 6.2.1) (Aquino et al. 1996). Although these findings are reversible in the majority of cases, recurrent and persistent infections may lead to bronchiolectasis.

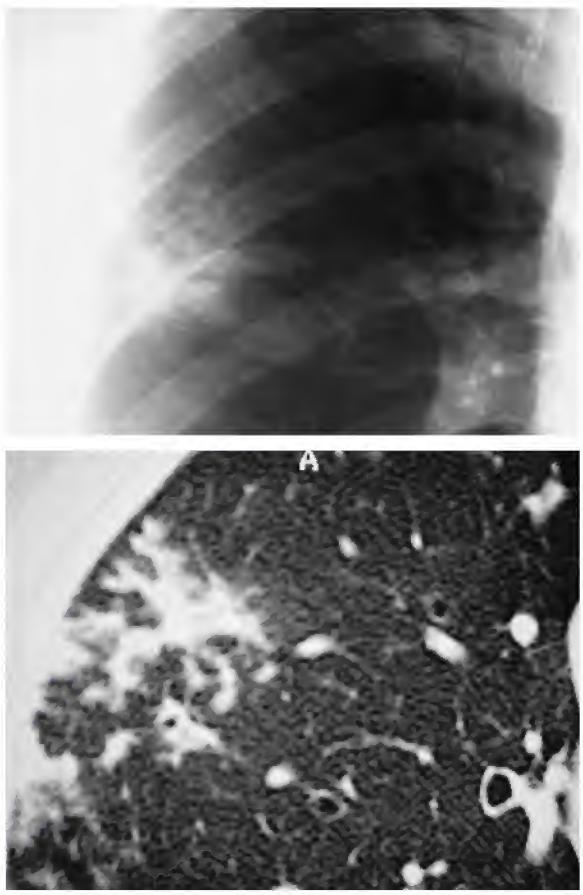

Fig. 6.2.1a,b. A 48-year-old man with *Pseudomonas aeruginosa* pneumonia after allogeneic hematopoietic stem cell transplantation. **a** Close-up view of an anteroposterior chest radiograph shows an ill-defined opacity in the right upper lobe. **b** Corresponding HRCT scan at the same level shows multiple branching linear opacities and some areas of lobular consolidation

6.2.4.1.1 Mycobacterial Infection

Infection with *Mycobacterium tuberculosis* and a variety of non-tuberculous mycobacteria has been observed in HSC transplant recipients (Navari et al. 1983; Mohite et al. 2001). *Mycobacterium tuberculosis* infection can occur after HSC transplantation, but the incidence in the reported series is lower than that of other infections (Roy and Weisdorf 1997; Aljurf et al. 1999; Mohite et al. 2001). Overall, the incidence of tuberculosis has bee reported to be between 0.19% and 5.5% of cases (Martino et al. 1996; Roy and Weisdorf 1997). Reports of non-tuberculous mycobacterial disease in both HSC and solid organ transplant recipients have also increased (Ozkaynak et al. 1990; Busch et al. 1991; Doucette and Fishman 2004).

6.2.4.2 Fungal Infections

A major infectious cause of death in HSC transplant recipients is invasive fungal infection (Allan et al. 1988; Bodey and Vartivarian 1989; Bag 2003). Beyond the first week after transplantation, fungal infections become increasingly common, being identified as a cause of pneumonia in 12%–50% of patients (Connolly et al. 1999). With increased use of prophylactic fluconazole, infections with resistant fungi have become more common. Other less common pulmonary mycoses (e.g., *Penicillium purpurogenum*, *Acremonium strictum* and *Scedosporium apiospermum*) have been also observed.

6.2.4.2.1 Pneumocystis Jiroveci (Formerly Pneumocystis Carinii)

The disease known as *Pneumocystis* pneumonia (PCP) is a major cause of illness and death in persons with impaired immune systems. Pneumocystis organisms from different host species have very dif-

ferent DNA sequences, indicating multiple species. In recognition of its genetic and functional distinctness, the organism that causes human *Pneumocystis carinii* pneumonia is now named *Pneumocystis jiroveci* (Stringer et al. 2002).

Pneumocystis jiroveci has been reported to be a rare cause of pulmonary infection in HSC transplant recipients (Saito et al. 2001; Chen et al. 2003; Resnick et al. 2005). The manifestations of disease depend on the severity of infection. Clinical symptoms of PCP include non-productive cough, shortness of breath, and hypoxia on room air.

Abnormal chest radiographs have been reported in up to 90% of patients with suspected PCP showing the typical findings of diffuse bilateral interstitial infiltrates most marked in a perihilar distribution (Soubani et al. 1996; Worthy et al. 1997; Resnick et al. 2005). As the disease progresses, alveolar infiltrates may also develop. The widespread use of *Pneumocystis* prophylaxis has led to a larger proportion of patients that present with normal radiographs. However, normal radiographs do not exclude the diagnosis (Boiselle et al. 1997).

Computed tomography is the imaging modality of choice to evaluate those symptomatic patients with a clinical suspicion of PCP but with an otherwise normal or equivocal chest radiograph. Characteristic CT features are perihilar ground-glass opacity, often in a patchy or geographical distribution, with areas of affected lung interspersed by normal lung parenchyma (Fig. 6.2.2). In addition to the ground-glass pattern, there is often associated thickening of the interlobular septa giving a "crazy paving" appearance. Other less common radiographic patterns of PCP are parenchymal consolidation, mass lesions, multiple pulmonary nodules, pleural effusion, and lymph node enlargement (Boiselle et al. 1999).

Fig. 6.2.2. A 36-year-old female patient with *Pneumocystis* pneumonia (*PCP*) after allogeneic hematopoietic stem cell transplantation. HRCT scan at the level of the lower lobes demonstrates diffuse bilateral patchy areas of ground-glass attenuation

6.2.4.2.2 Aspergillosis

Aspergillus are ubiquitous organisms that are part of the normal environmental flora and abound in the soil around us (Denning 2000, 2001). Aspergillosis is a mycotic disease caused by *Aspergillus* species, usually *A. fumigatus*. Other pathogenic species include *A. flavus*, *A. niger*, and *A. terreus*. *Aspergillus* infections can result in a variety of clinical, radiologic, and histologic manifestations (Aquino et al. 1994; Gotway et al. 2002). Although all humans beings are commonly exposed to these organisms, the type and severity of pulmonary involvement are influenced by the patient's immunologic status and the presence of pre-existing lung disease. Disseminated and invasive forms most often occur in immunologically compromised hosts representing a common cause of life-threatening opportunistic infection in neutropenic patients (Allan et al. 1988; Alangaden et al. 2002; Bag 2003).

The definitive diagnosis of invasive pulmonary aspergillosis is traditionally based on the histologic evidence of tissue invasion by branched septate hyphae. In recent years it has been shown that *Aspergillus* infection can result in a broad range of airway complications (Gotway et al. 2002; Franquet et al. 2004).

6.2.4.2.2.1 Angioinvasive Aspergillosis

Angioinvasive aspergillosis is commonly seen in immunocompromised patients with severe neutropenia (Denning 2000; Fukuda et al. 2004). There has been a substantial increase in the number of patients at risk of developing invasive aspergillosis for many reasons, including the development of new intensive chemotherapy regimens for solid tumors, difficult-to-treat lymphoma, myeloma, and resistant leukemia as well as an increase in the number of solid organ transplantations and increased use of immunosuppressive regimens for other autoimmune diseases. Angioinvasive aspergillosis is the most common fungal pulmonary infection in severe neutropenic patients. It is much more common in allogeneic than in autologous HCT recipients and in patients with acute leukemia (Denning 2000; Fukuda et al. 2004).

The diagnosis of angioinvasive aspergillosis is based on clinical, radiological, and mycological data. Although a febrile neutropenic patient with pulmonary infiltrates should be evaluated for aspergillosis, a conclusive diagnosis of angioinvasive aspergillosis is seldom straightforward and remains a significant clinical problem. Disseminated aspergillosis occurs in up to 60% of patients with invasive pulmonary aspergillosis; sites of involvement include the brain, kidney, liver, thyroid, heart, and spleen.

The consensus criteria for angioinvasive aspergillosis developed by the European Organization for Research and Treatment of Cancer/Mycoses Study Group (EORTC/MSG) were intended to provide uniform criteria for inclusion and evaluation of oncohematologic patients with suspected angioinvasive aspergillosis enrolled in clinical trials (Ascioglu et al. 2002).

Newer techniques, such as polymerase chain reaction and the galactomannan test, may change the current diagnostic approach. Galactomannan and nucleic acid detection in serum or in bronchoalveolar lavage (BAL) fluid are useful for the early identification of invasive aspergillosis in the immunocompromised host; however, a definite diagnosis of invasive aspergillosis still requires the demonstration of the fungus in tissue specimens (Maertens et al. 2001). The value of early diagnostic criteria such as the galactomannan test needs to be proven in prospective trials.

Angioinvasive aspergillosis is characterized histologically by invasion and the occlusion of small to medium pulmonary arteries by fungal hyphae. This leads to the formation of necrotic hemorrhagic nodules or pleural-based wedge-shaped hemorrhagic infarcts. The clinical diagnosis is difficult, and the mortality rate is approximately 85%. The characteristic CT findings consist of nodules surrounded by a halo of ground-glass attenuation (halo sign) or pleural-based wedge-shaped areas of consolidation (Fig. 6.2.3) (Kuhlman et al. 1985). These findings correspond to hemorrhagic infarcts. In severely neutropenic patients the halo sign is highly suggestive of angioinvasive aspergillosis (Kuhlman et al. 1985, 1987, 1988).

However, a similar appearance has been described in a number of other conditions including infection by *Mucorales*, *Candida*, Herpes simplex and cytomegalovirus, Wegener's granulomatosis, Kaposi's sarcoma and hemorrhagic metastases (Primack et al. 1994). Separation of fragments of necrotic lung (pulmonary sequestra) from adjacent parenchyma results in air-crescents similar to those seen in mycetomas. The air-crescent sign in angioinvasive aspergillosis is usually seen during convalescence, i.e., 2–3 weeks after onset of treatment and concomitant with resolution of the neutropenia (Franquet et al. 2001; Gotway et al. 2002).

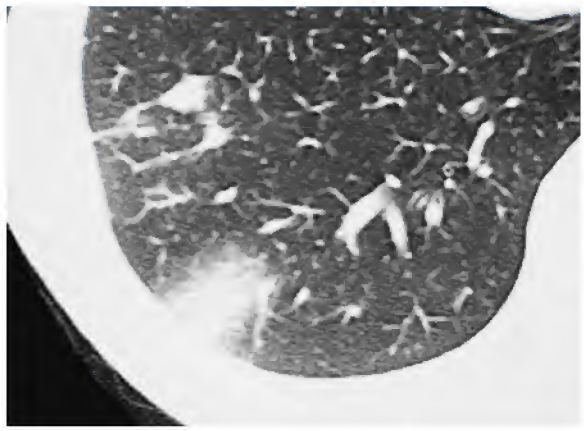

Fig. 6.2.3. Halo sign due to angioinvasive aspergillosis in a 47-year-old woman after allogeneic hematopoietic stem cell transplantation. Close-up view of a HRCT scan at the right lower lobe shows a peripheral nodular opacity with a surrounding halo of ground-glass attenuation. These findings correspond to a nodular area of infarction surrounded by hemorrhage

6.2.4.2.2.2 Airway Invasive Aspergillosis

Aspergillus bronchopneumonia, also known as airway invasive aspergillosis, occurs in up of 10% of cases of invasive pulmonary aspergillosis. It is characterized histologically by the presence of *Aspergillus* organisms deep to the airway basement membrane (Franquet et al. 2004). Airway invasive aspergillosis occurs most commonly in immunocompromised neutropenic patients and in patients with acquired immunodeficiency syndrome (AIDS) (Franquet et al. 2002). Clinical manifestations include acute tracheobronchitis, bronchiolitis, and bronchopneumonia. Patients with acute tracheobronchitis usually have normal radiologic findings. Occasionally tracheal or bronchial wall thickening may be seen. Bronchiolitis is characterized on high-resolution CT by the presence of centrilobular nodules and branching linear or nodular opacities giving an appearance resembling a "tree-in-bud". The centrilobular nodules have a patchy distribution in the lung. *Aspergillus* bronchopneumonia

results in predominantly peribronchial areas of consolidation. Rarely, the consolidation may have a lobar distribution.

Centrilobular nodular opacities similar to those seen in *Aspergillus* bronchiolitis have been described in a number of conditions, including endobronchial spread of pulmonary tuberculosis, *M. avium-intracellulare*, viral and mycoplasma pneumonia (Aquino et al. 1996). The radiologic manifestations of *Aspergillus* bronchopneumonia are indistinguishable from those of bronchopneumonias caused by other microorganisms (Aquino et al. 1996; Franquet et al. 2004).

A similar appearance has been described in bronchocentric mycosis. Although this process is histologically somewhat similar to bronchocentric granulomatosis, a high index of suspicion of infection needs to be maintained when this pathologic process is identified in a transplant host (Tazelaar et al. 1989).

6.2.4.2.3 Mucormycosis

The *Mucor* species are ubiquitous , saprophytic molds, usually found in soil and in decaying food. Infection occurs by either inhalation of airborne fungal spores or through hematogenous spread from a distant focus. The spectrum of disease includes rhinocerebral and pulmonary, gastrointestinal, cutaneous, and disseminated manifestations (Connolly et al. 1999; Maertens et al. 1999).

The most common associated conditions include diabetes mellitus, solid organ transplantation, renal failure, chemotherapy, and hematologic malignant neoplasms (Gaziev et al. 1996). Lung involvement occurs in more than 30% of cases. Radiographic manifestations are non-specific and include consolidation, cavitation or abscess formation, nodules and masses. Lesions are most often unifocal affecting more frequently the upper lobes. As occur in other angioinvasive fungal infections such as aspergillosis and candidiasis, the "air-crescent" sign and the "halo" sign may also be seen in patients with mucormycosis (McAdams et al. 1997; Connolly et al. 1999).

6.2.4.2.4 Cryptococcal Pneumonia

Cryptococcus neoformans is an encapsulated non-mycelial, budding yeast found worldwide, particularly in soil contaminated by bird droppings (Cameron et al. 1991). *Cryptococcus* is a common pulmonary fungal pathogen in the AIDS population usually when the CD4 count is below 100 cells/mm^3 (Sider and Westcott 1994). Although the central nervous system is the most commonly affected organ, the lungs are also involved (Vilchez et al. 2001). In a series of 31 HIV-infected patients with cryptococcal infection, 12 (39%) had cryptococcal pneumonia (Sider and Westcott 1994). Presenting symptoms are non-specific and include fever, cough, dyspnea, sputum production, and pleuritic chest pain. The most common radiographic findings consist of a reticular or reticulonodular interstitial pattern. Less common manifestations include ground-glass attenuation, air-space consolidation, "tree-in-bud" opacities, and miliary nodules (Fig. 6.2.4) (Khoury et al. 1984). The CT pattern in immunocompromised non-AIDS patients seems to differ from that in AIDS

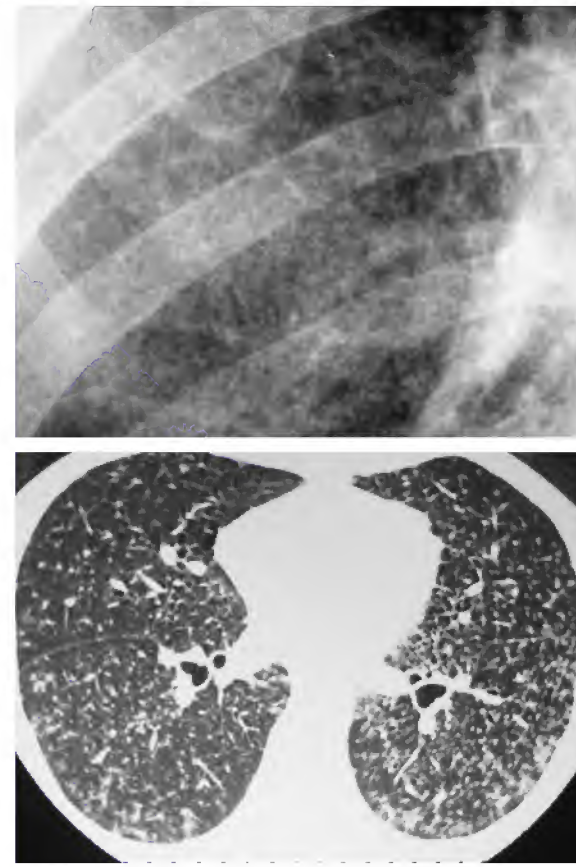

Fig. 6.2.4a,b. A 39-year-old woman with acute myelocytic leukemia and miliary cryptoccocosis. **a** Close-up view of an anteroposterior radiograph shows a diffuse miliary pattern. **b** Corresponding HRCT scan confirms numerous small miliary nodules in a random distribution

patients by the presence of nodules and the absence of reticular or reticulonodular interstitial infiltrates (Zinck et al. 2002).

6.2.4.2.5 Histoplasmosis

Histoplasma capsulatum is a pathogenic dimorphic yeast found in temperate regions throughout the world. Histoplasmosis is rare in Europe and occurs in endemic areas in North America such as the Ohio-Mississippi and St Lawrence River valleys (Conces et al. 1993; McAdams et al. 1995). Histoplasmosis is rare, but often a life-threatening infection in patients with AIDS and hematologic malignancies. Most cases of disseminated histoplasmosis occur either as a result of new infection after an environmental exposure or as a result of reactivation of a remote infection (Conces et al. 1993; Kauffman 2002). The radiographic findings of disseminated histoplasmosis are varied and non-specific; approximately 40% of patients with pulmonary disseminated histoplasmosis have a normal chest radiograph (Conces et al. 1993). CT can be helpful in the assessment of patients who have symptoms of pulmonary disease and normal or non-specific radiographic findings. The most common radiographic findings are diffuse nodular opacities 3 mm or less in diameter, nodules greater than 3 mm in diameter, small linear opacities, and focal or patchy areas of consolidation (McAdams et al. 1995).

6.2.4.2.6 Candidiasis

Pulmonary candidiasis is a relatively uncommon complication seen in immunocompromised patients and is rarely reported in patients without predisposing conditions. *Candida* sp. have been increasingly recognized as an important source of fungal pneumonia in patients with hematologic malignancies (acute leukemia and lymphoma) and allogeneic bone marrow transplant recipients (Buff et al. 1982; Allan et al. 1988; Connolly et al. 1999; Franquet et al. 2005b, 2005c). Factors that predispose bone marrow transplant recipients to *Candida* infections include allogeneic bone marrow transplantation, increased age, and a prolonged neutropenia (Verfaillie et al. 1991). A definitive diagnosis of pulmonary candidiasis requires demonstration of the organism in tissue. Pathologically, areas of consolidation represent areas of bronchopneumonia, intra-alveolar hemorrhage, exudates, and hyaline membranes. Chest radiographic and CT abnormalities consist of multifocal patchy areas of consolidation, focal cavitation, and multiple pulmonary nodules (Franquet et al. 2005b).

6.2.4.3 Viral Infection

Viruses have been increasingly recognized as important causes of serious respiratory illnesses in HSC transplant recipients. Most respiratory viral infections produce acute symptoms such as fever, non-productive cough, dyspnea, and hypoxemia. These infections may result from reactivation of a latent process or reflect newly acquired infection.

6.2.4.3.1 Community Respiratory Viruses

Community respiratory viruses particularly respiratory syncytial virus (RSV), influenza, parainfluenza, and adenovirus have been recognized as potential causes of severe pneumonia, accounting for the majority of non-CMV pulmonary infections in both autologous and allogeneic HCT recipients (Krinzman et al. 1998; Markovic et al. 1998; Ghosh et al. 1999; Nichols et al. 2001; Chakrabarti et al. 2002; Ison et al. 2003; Nichols et al. 2004). In these patients, respiratory viral infections can be mild and self-limited, but also can lead to severe, life-threatening disease more frequently than in normal immune hosts. The prevalence of respiratory viral infections in HSC transplanted patients is variable. In a prospective study conducted by the European Group for Blood and Marrow Transplantation, 40 respiratory virus infections (2%) were diagnosed in 1863 patients (Ljungman 2001). In another study, Leung et al. (1999) found respiratory viral infections in only three (5%) of the 59 infectious episodes (two RSV and one influenza B).

Human metapneumovirus (HMPV) is a recently identified new RNA respiratory virus that belongs to the *Paramyxoviridae* family and to the larger *Pneumovirinae* subfamily (Boivin et al. 2002; Williams et al. 2004). Their clinical manifestations are virtually indistinguishable from those associated with other respiratory viruses. Clinical symptoms typically consist of fever exceeding > 38°C, non-productive cough, progressive dyspnea, and hypoxemia (Boivin et al. 2002). Despite the fact that HMPV may

cause serious pneumonia in high-risk patients, it is often unsuspected in an immunocompromised host because their clinical features are indistinguishable from those associated with other respiratory viruses.

The descriptions of the thin-section CT appearances in respiratory viral infections have been limited to very few studies. Oikonomou et al. (2003) reviewed the thin-section CT findings in four patients with hematologic malignancies and influenza A pneumonitis and found that the predominant CT findings were ground-glass opacities and centrilobular nodules lesser than 10 mm in diameter (Fig. 6.2.5). Gasparetto et al. (2004) reviewed the thin-section CT findings in 20 patients with RSV pneumonitis after HSC transplantation and found that the most common thin-section CT findings consisted of small centrilobular nodules and multifocal areas of consolidation and ground-glass opacities in a bilateral asymmetric distribution. The CT appearances of HMPV infection were patchy areas of ground-glass attenuation, small nodules, and multifocal areas of consolidation in a bilateral asymmetric distribution (Fig. 6.2.6) (Franquet et al. 2005c). Similar findings have been described in patients with CMV, Herpes simplex virus, and Herpes varicella-zoster virus pulmonary infections (Foot et al. 1993; Kang et al. 1996; Franquet et al. 2003a; Gasparetto et al. 2005).

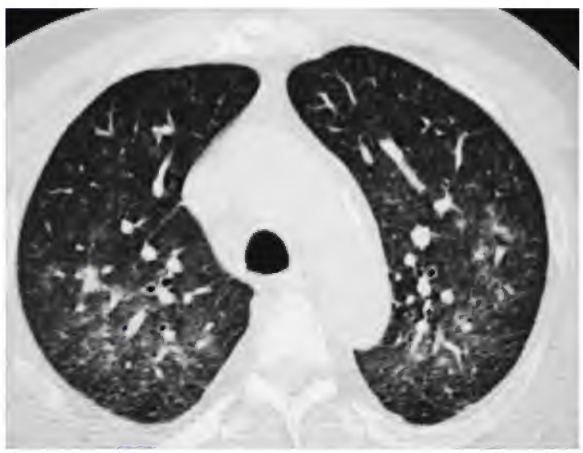

Fig. 6.2.5. *Parainfluenza 3* infection in a 60-year-old man who had severe neutropenia secondary to chemotherapy and HSC transplant for myelodysplastic syndrome. Transverse thin-section (1-mm collimation, lung window) CT scan at the level of the aortic arch shows bilateral areas of ground-glass opacity in the upper lobes

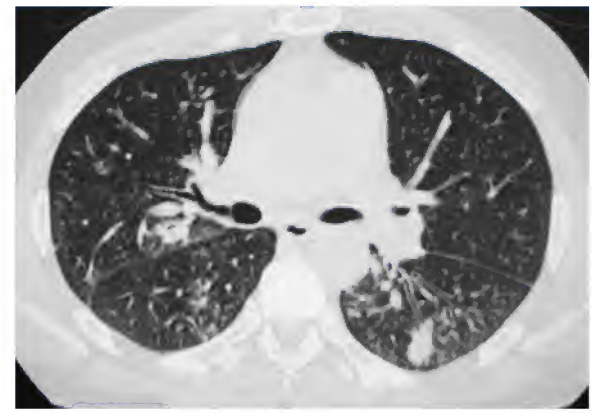

Fig. 6.2.6. *Human metapneumovirus* pneumonia in a 58-year-old man with neutropenia following HSC transplantation. Transverse thin-section (1-mm collimation) CT scan obtained at level of the carina shows bilateral areas of ground-glass attenuation and multiple ill-defined nodules affecting the posterior segment of the right upper lobe and both superior segments of the lower lobes

6.2.4.3.2 Cytomegalovirus (CMV)

The incidence of CMV pneumonia has been significantly reduced with the use of ganciclovir prophylaxis. Nevertheless, CMV remains one of the major complications in the post-engraftment phase, mostly within the first 4 months, being responsible for up to 50% of cases of pneumonia occurring in 50%–70% of allogeneic bone marrow transplant recipients (Cordonnier 1990; Kotloff et al. 2004). CMV disease rarely develops earlier than 14 days after transplantation and may become evident as late as 4 months after the procedure. CMV infection may be related to primary acquisition or to reactivation of latent infection or reinfection with a different strain in a previously seropositive patient.

CT findings of CMV pneumonia are diverse and consist of unilateral or bilateral interstitial infiltrates, alveolar consolidation, ground-glass opacities, and multiple small nodules with associated areas of ground-glass attenuation ("halo") (Fig. 6.2.7) (Kang et al. 1996; Franquet et al. 2003a). It has recently been reported that nodule size is helpful in the differential diagnosis of infectious causes of nodules in immunocompromised patients (Franquet et al. 2003b).

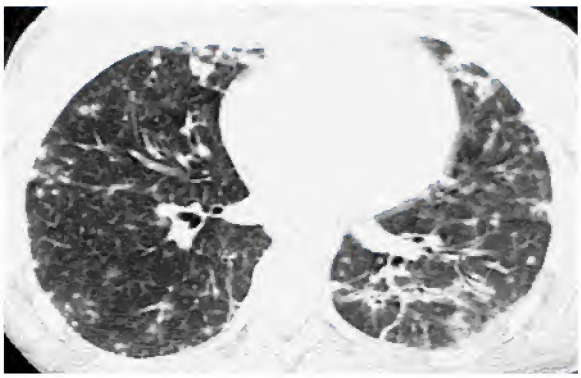

Fig. 6.2.7. Cytomegalovirus (*CMV*) infection in a 23-year-old man with acute myeloid leukemia and allogeneic HSC transplantation. CT scan obtained at the level of the inferior pulmonary veins shows diffuse ground-glass attenuation and multiple small ill-defined nodules in both lungs

6.2.5 Non-Infectious Complications

Non-infectious causes of lung injury after HSC transplantation include a spectrum of syndromes: pulmonary edema, engraftment syndrome, alveolar hemorrhage, drug-induced lung injury, idiopathic pneumonia syndrome (IPS), bronchiolitis obliterans (BO), cryptogenic organizing pneumonia (COP), pulmonary veno-occlusive disease (VOD), and post-transplantation lymphoproliferative disorder (PTLD) (Worthy et al. 1997; Khurshid and Anderson 2002).

Most of these causes are attributed to treatment-related toxicities and are influenced by the myeloablative conditioning regimens used before transplantation, the degree of immunosuppression, and the interaction of the graft with the host. Therefore, these causes tend also to occur within specific time periods after transplantation. "Early" complications occur within the first 100 days after transplantation and "late" complications occur beyond day 100 (Worthy et al. 1997).

6.2.5.1 Early Complications

Early complications can be further subdivided into those that appear in the neutropenic phase (first 30 days of transplantation) or in the early phase (within 30–100 days of transplantation).

During the period of neutropenia, patients have a significant risk of developing non-infectious pulmonary complications such as pulmonary edema, engraftment syndrome, alveolar hemorrhage, and drug-induced lung injury.

6.2.5.1.1 Neutropenic Phase

6.2.5.1.1.1 Pulmonary Edema

Pulmonary edema is one of the earliest complications following HSC transplantation and may occur even in those patients with normal cardiac function. It is usually secondary to the large volumes of fluids infused to minimize the toxicity of conditioning regimens, and to transfusion of blood products (Worthy et al. 1997). Characteristic chest radiographic findings include diffuse interstitial lines such as Kerley A and Kerley B. The HRCT findings include enlarged pulmonary vessels, septal lines, peribronchial cuffing, ground-glass opacities, and small pleural effusions (Evans et al. 2003; Wah et al. 2003) (Fig. 6.2.8). The ground-glass opacities tend to involve mainly the dependent lung regions.

Fig. 6.2.8. Pulmonary edema due to fluid overload in a 28-year-old woman after allogeneic HSC transplantation. HRCT scan through upper lobes shows smooth septal thickening in a gravity-dependent distribution. The left interlobar fissure is also prominent due to subpleural edema. (With permission from Franquet et al. 2005a)

6.2.5.1.1.2 Engraftment Syndrome

Engraftment syndrome is a non-infectious pulmonary complication that represents a form of diffuse capillary leak associated with lung injury and pul-

monary edema. It has been described, during recovery from neutropenia, in autologous HSC transplantation. The median time of onset is 7 days after HSC transplantation (Khurshid and Anderson 2002). Clinically, as occurs with other non-infectious pulmonary complications, patients are febrile and may also present with skin rash similar to that in acute GVHD, and hypoxia. Chest radiograph findings are non-specific and range from normality to bilateral air-space opacification, diffuse vascular redistribution, and pleural effusions (Fig. 6.2.9). On CT, engraftment syndrome usually manifests as bilateral ground-glass opacification, air-space consolidation distributed at the hilar or peribronchial regions, and smooth thickening of interlobular septa (Evans et al. 2003; Wah et al. 2003).

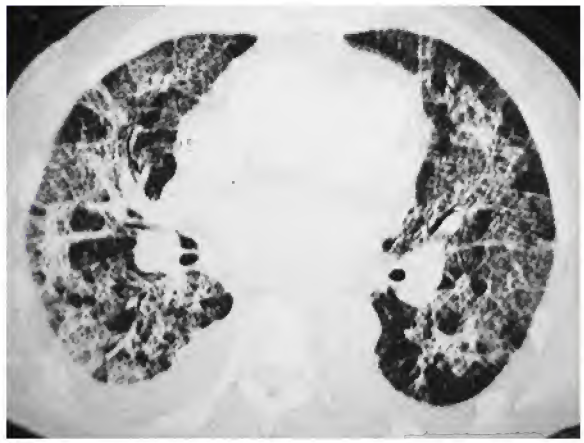

Fig. 6.2.9. Engraftment syndrome in a 46-year-old woman with non-Hodgkin lymphoma 3 weeks following allogeneic HSC transplantation. HRCT scan shows bilateral areas of consolidation having a peribronchovascular and subpleural distribution. Note a right pleural effusion. (With permission from Franquet et al. 2005a)

6.2.5.1.1.3 Diffuse Alveolar Hemorrhage (DAH)

Diffuse pulmonary alveolar hemorrhage (DAH) is a life-threatening complication following bone marrow transplantation with a reported mortality of approximately 70%–100% (Afessa et al. 2002; Ben-Abraham et al. 2003). The overall incidence of DAH is higher following autologous (20%) than allogeneic (10%) HSC transplantation. It typically occurs as a diffuse process in the first month after transplant, often at the time of granulocyte recovery (Schmidt-Wolf et al. 1993; Alam and Chan 1996; Afessa et al. 2002). Although its pathogenesis is not entirely understood, predisposing risk factors include intensive pre-transplantation chemotherapy and total body and thoracic irradiation (Worthy et al. 1997). The HRCT findings consist of extensive bilateral ground-glass opacities with or without superimposed intralobular linear opacities ("crazy-paving" pattern) (Fig. 6.2.10) (Evans et al. 2003; Wah et al. 2003).

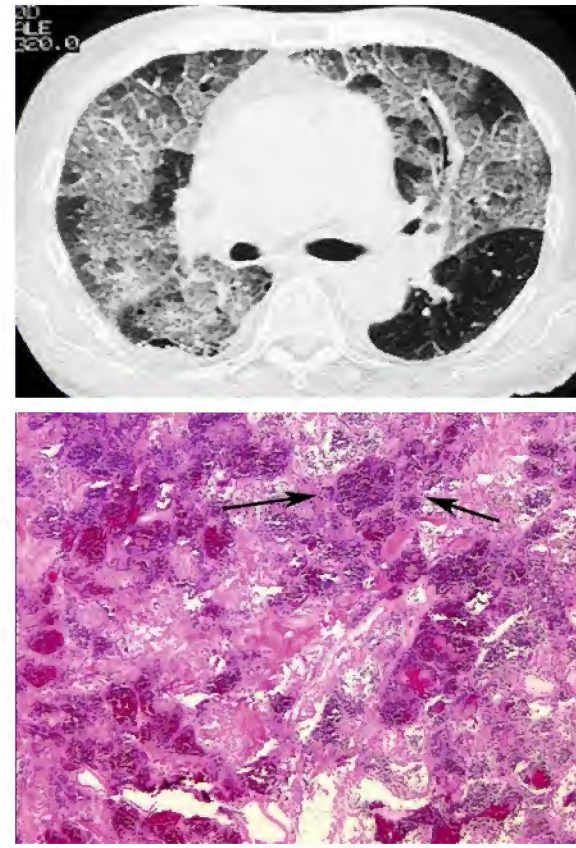

Fig. 6.2.10a,b. Diffuse alveolar hemorrhage in a 46-year-old woman with non-Hodgkin lymphoma 3 weeks after allogeneic HSC transplantation. **a** HRCT scan at the level of carina shows diffuse ground-glass opacity in addition to septal thickening ("crazy-paving"). **b** Histologically, macrophages containing hemosiderin are present within the alveolar spaces (*arrows*). (H and E, ×100; with permission from Franquet et al. 2005a)

6.2.5.1.1.4 Drug-Induced Lung Injury

Drug-induced lung disease occurs in up to 10% of patients following autologous or allogeneic HSC transplantation and must always be considered in the differential diagnosis of pulmonary infiltrates in transplant recipients. A wide range of histologic re-

action patterns can be seen, the most common being diffuse alveolar damage, hypersensitivity reaction, non-specific interstitial pneumonia, and organizing pneumonia (Ellis et al. 2000).

Plain chest radiography is likely to underestimate subclinical forms of drug-induced lung disease, compared with HRCT. The CT manifestations are non-specific and reflect the histologic findings. CT features have been divided into four categories according to their dominant pattern and distribution of disease: fibrosis (irregular linear opacities with architectural distortion) with or without consolidation, ground-glass opacities, widespread bilateral consolidation, and bronchial wall thickening with areas of decreased attenuation (Fig. 6.2.11) (Evans et al. 2003; Wah et al. 2003).

6.2.5.2 Early Phase

6.2.5.2.1 Idiopathic Pneumonia Syndrome (IPS)

Idiopathic pneumonia syndrome (IPS) is defined as diffuse lung injury occurring after HSC transplantation in the absence of active lower respiratory tract infection even in the presence of non-lobar radiographic infiltrates and physiologic changes consistent with pneumonia (Kantrow et al. 1997). Thus, the diagnosis of IPS is one of exclusion, which requires the elimination of potential infectious agents as a cause of the patient's respiratory status. Idiopathic pneumonia is the most common cause of diffuse radiographic abnormalities between 30 days and 180 days after HSC transplantation. Clinical symptoms include dyspnea, cough, and fever. The mortality rate of IPS remains greater than 70%, and two-thirds of all deaths are associated with progressive respiratory failure (Kantrow et al. 1997). The histologic features of IPS range from a primarily interstitial reaction with diffuse or focal widening of the alveolar septa and interstitial spaces by mononuclear inflammatory cells and edema to diffuse alveolar damage with intra-alveolar hyaline membranes, edema, and hemorrhage. Other associated patterns such as organizing pneumonia and vascular damage have also been described. The pathologic findings of IPS are similar to those found in acute interstitial pneumonia and acute respiratory distress syndrome (ARDS) and can be separated into acute exudative, subacute proliferative, and chronic fibrotic phases. Characteristic CT findings include focal or diffuse ground-glass opacity and air-space consolidation with a basilar predominance (Fig. 6.2.12), a pattern consistent with non-cardiogenic pulmonary edema (Kantrow et al. 1997). Pleural effusions may be present. Architectural distortion, traction bronchiectasis, and the presence of honeycombing are indicative of the fibrotic phase of IPS.

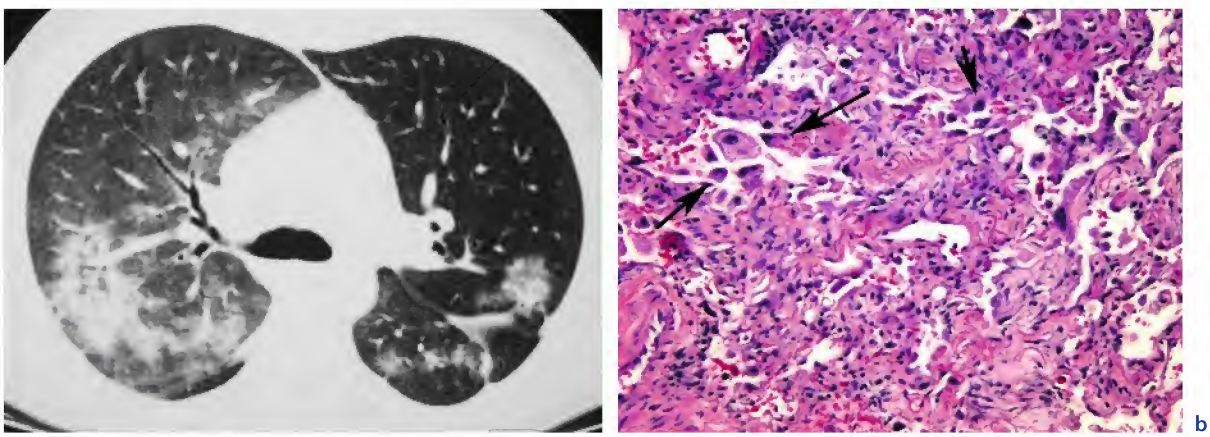

Fig. 6.2.11a,b. Vincristine-induced interstitial pneumonitis in a 63-year-old man with myeloma. **a** HRCT scan at the level of the carina shows diffuse ground-glass attenuation in the right lung and bilateral patchy areas of consolidation. **b** Photomicrograph of histopathologic section shows patchy expansion of the interstitium by lymphocytic infiltrate, mild interstitial fibrosis, and reactive hyperplastic type II pneumocytes (*arrows*) (H and E, ×250) (with permission from Franquet et al. 2005a)

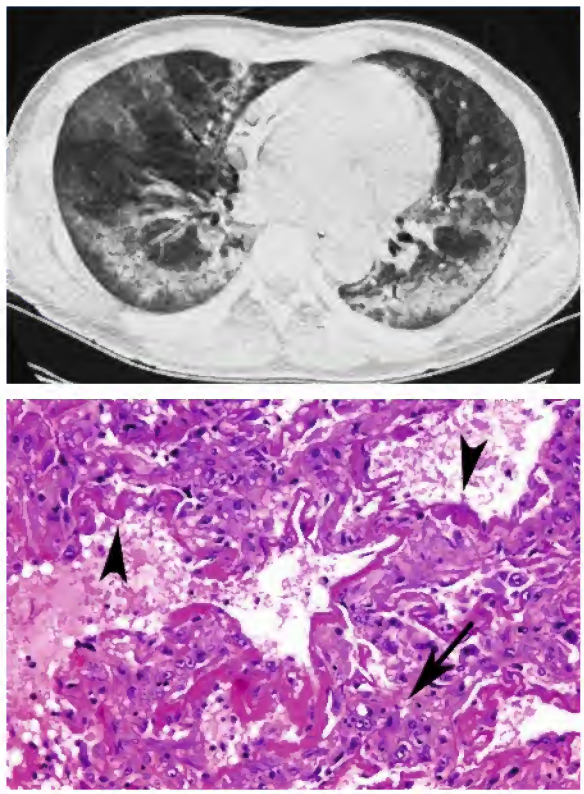

Fig. 6.2.12a,b. Idiopathic pneumonia syndrome in a 40-year-old man with AML 4 weeks following allogeneic HSC transplantation. **a** HRCT scan at the level of lower lung zones shows bilateral patchy areas of consolidation and ground-glass attenuation. **b** Histologically, the alveolar septa are thickened by edema and round cell infiltration (*arrow*). Hyperplasia and desquamation of the alveolar lining cells, fibrinous exudation, and hyaline membranes (*arrowheads*) are seen within the alveolar spaces. (H and E, ×250) (with permission from Franquet et al. 2005a)

Fig. 6.2.13. Acute graft-versus-host disease in a 34-year-old man with CML 5 weeks following allogeneic HSC transplantation. HRCT at the level of the inferior pulmonary veins shows small areas of consolidation (*arrow*) in association with discrete right pleural effusion. (With permission from Franquet et al. 2005a)

6.2.5.2.2 Acute GVHD

GVHD is an immune reaction mediated by donor T-lymphocytes that recognize the recipient's tissue as a foreign body. It may present as acute or chronic pulmonary complication after HSC transplantation (Cooke and Yanik 2004). Acute GVHD develops in 20%–75% of patients (Tabbara et al. 2002; Freudenberger et al. 2003). The most commonly affected tissue systems are the skin, liver, and gastrointestinal system. Pulmonary involvement is rare. The median time of onset of respiratory symptoms is 5 months (range 1–13 months). The reported radiologic manifestations include mild perihilar or diffuse interstitial fibrosis, cysts, and lung nodules (Fig. 6.2.13).

6.2.5.2.3 Pleuro-pericardial Effusion/Hepatic Veno-occlusive Disease

Pleuro-pericardial effusion has been reported in approximately 16% of patients in the first few weeks after receiving HSC transplantation (Freudenberger et al. 2003). The most common non-infectious cause of pleural effusion is aggressive treatment with fluids, blood, and blood product transfusion. The effusion is usually bilateral or right sided and rarely related to an identifiable infectious source. Hepatic veno-occlusive disease, an occasional complication in allogeneic HSC transplantation recipients, is characterized by jaundice, hepatic enlargement, right upper quadrant pain, and ascites (Barker et al. 2003; Freudenberger et al. 2003). Pleural effusion has been reported in up to 50% of HSC transplantation recipients with hepatic veno-occlusive disease. Patients with veno-occlusive disease and pleural effusions have either no or minimal respiratory symptoms. Hepatic veno-occlusive disease usually precedes the development of pleural effusion (Fig. 6.2.14). Although pleural and pericardial effusions may be detected on conventional chest radiographs, they are better evaluated with CT and MR.

Fig. 6.2.14. Pleuro-pericardial effusion in a 28-year-old woman after allogeneic HSC transplantation. HRCT scan photographed using mediastinal window shows the presence of bilateral pleural and small pericardial effusions. (With permission from Franquet et al. 2005a)

6.2.5.2.4 Pulmonary Cytolytic Thrombi (PCT)

A rare early pulmonary vascular complication consisting of endothelial swelling with arteriolar, venular, and capillary thrombi has been described after allogeneic HSC transplantation with acute GVHD (Gulbahce et al. 2000, 2004). Active GVHD shortly before or at the time of PCT in all patients is indicative of the presence of alloreactive donor cells and supports an etiologic association. Pathologically it is characterized by intravascular formation of basophilic thrombi frequently accompanied by pulmonary infarcts (Gulbahce et al. 2000, 2004). The median time of onset of PCT is 2 months after transplantation although cases have been reported as early as 2 weeks. Although its pathogenesis is unknown, PCT may be a manifestation of acute GVHD. CT findings consist of multiple pulmonary nodules (Fig. 6.2.15).

6.2.5.2.5 Post-Radiation Thoracic Injuries

Radiation-induced thoracic injures can usually be diagnosed from characteristic imaging appearances and knowledge of the radiation port, radiation dose, and time interval since therapy. Commonest thoracic complications are acute radiation pneumonitis and fibrosis. Rare complications include spontaneous pneumothorax, thymic cysts, calcified lymph

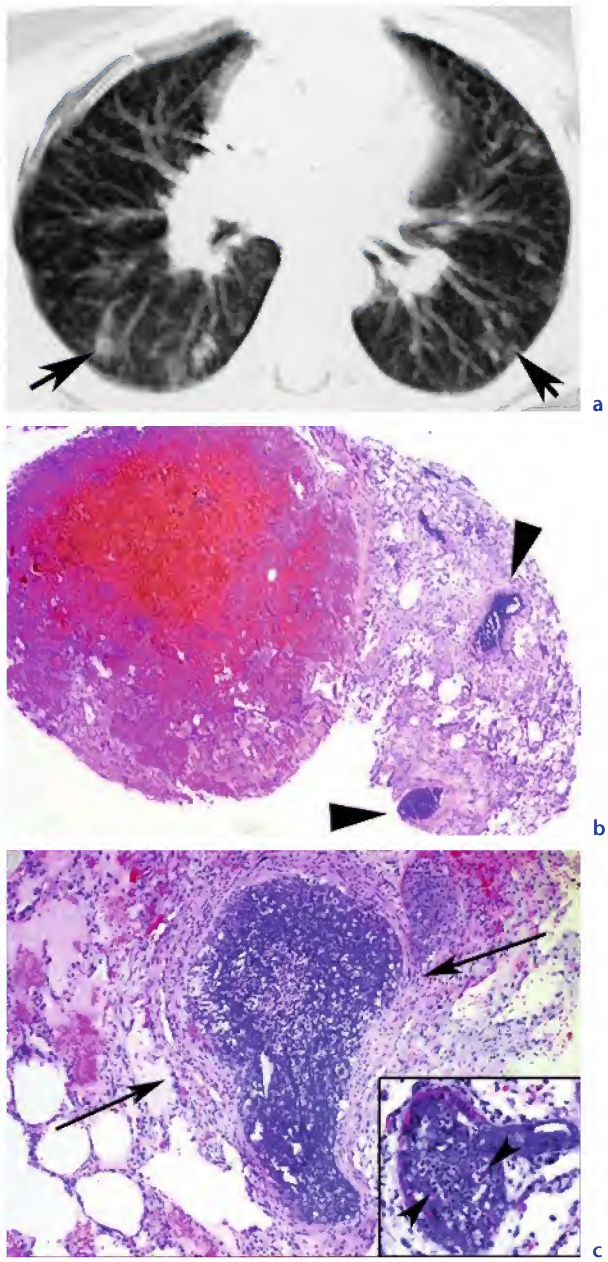

Fig. 6.2.15a–c. Pulmonary cytolytic thrombi in an 11-year-old patient after allogeneic HSC transplantation for an ALL. **a** CT scan with discrete peripheral pulmonary nodules suggestive of opportunistic infection (*arrows*). **b** Histologically, the nodules consisted primarily of hemorrhagic infarcts (*asterisk*). Occlusive vascular lesions were present within, adjacent to, and away from the hemorrhagic infarct (*arrowheads*). (H and E, ×40). **c** Intensely basophilic, tenacious, amorphous material occludes the lumen of the vessels (*arrows*). Few intact cells recognized as leukocytes (*arrowheads*) are also seen (*inset*) (H and E, ×400). (Courtesy of Gulbahce HE, Minneapolis, Mn., USA). (With permission from Franquet et al. 2005a)

nodes, vascular calcifications, and osseous sarcomas (Bluemke et al. 1991).

6.2.5.2.5.1 Radiation Pneumonitis

Radiation to the chest can result in acute pneumonitis or chronic fibrosis. Risk factors for radiation injury include total dose delivered, preexisting lung disease, and concurrent treatment with agents that sensitize the lung to radiation damage. Radiation pneumonitis presents 6 weeks to 6 months after completion of radiation therapy (Evans et al. 2003; Wah et al. 2003). In patients who progress to a clinically evident radiation pneumonitis, the radiographic findings range from normal to mild perivascular haziness. Over time, these initial lesions may develop into alveolar infiltrates. Radiologic changes may be observed in completely asymptomatic patients.

Clinical symptoms of radiation pneumonitis can be separated into early and late phases. During the early phase, 1–3 months after treatment, patients present with fever and leukocytosis making radiation injury a clinical syndrome difficult to distinguish from infection. Computed tomography is helpful in distinguishing radiation pneumonitis from pulmonary infiltrates of other causes. Given that radiation changes rarely occur outside the treated field, a characteristic CT finding consists of sharply marginated ground-glass opacities that do not follow an anatomic border (Fig. 6.2.16) (Evans et al. 2003; Wah et al. 2003).

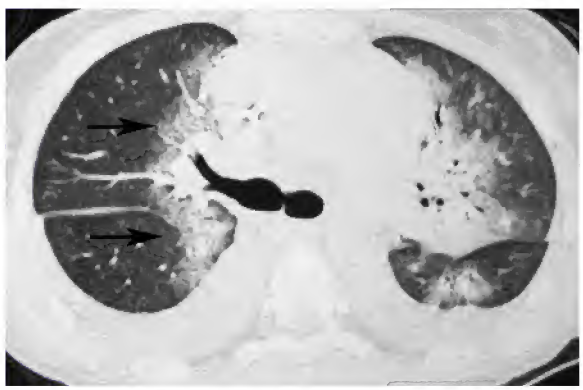

Fig. 6.2.16. Acute radiation pneumonitis in a 28-year-old woman after allogeneic HSC transplantation. HRCT shows paramediastinal ground-glass attenuation with associated broncho-vascular distortion. Notice the sharp border between the radiated area and the normal lung parenchyma (*arrowheads*). (With permission from Franquet et al. 2005a)

6.2.5.3 Late Complications

6.2.5.3.1 Chronic GVHD

Chronic GVHD is the most common non-relapse problem, occurring in approximately 60%–80% of long-term survivors of allogeneic HSC transplant and is a major cause of late morbidity and mortality. Onset is usually between 100 days and 6 months after transplantation, although earlier and later development are possible (Patriarca et al. 2004). The disease is more common in older patients, in recipients of mismatched or unrelated stem cells, and in those with a preceding episode of acute GVHD. Pulmonary complications include bronchiolitis obliterans (BO) and cryptogenic organizing pneumonia (COP). Moreover, patients with chronic GVHD have a particularly high risk of infections due to hypogammaglobulinemia and immune dysfunction. These patients must be re-immunized at 1 and 2 years for tetanus, diphtheria, polio, pneumococcus, meningococcus, and *Haemophilus influenzae* type B. In most patients, chronic GVHD resolves but it may require 1–3 years of immunosuppressive treatment.

6.2.5.3.1.1 Bronchiolitis Obliterans (BO)

Bronchiolitis obliterans, an obstructive pulmonary disorder that affects the small airways, has been reported in between 2% and 14% of allogeneic HSC transplantation recipients who survive more than 3 months (Freudenberger et al. 2003). Bronchiolitis obliterans is associated with high mortality (up to 60%) at 3 years post HSC transplantation (Freudenberger et al. 2003). Presenting symptoms include gradual dyspnea accompanied by persistent cough and expiratory wheeze. Pulmonary function testing shows new obstructive lung defects defined by a forced expiratory volume in 1 s (FEV1) $< 80\%$ of predicted or a decrease of FEV1/forced vital capacity by $\geq 10\%$ within a period of less than 1 year.

Histologically, there is a predominantly constrictive bronchiolitis with destruction and narrowing of the bronchiolar lumen by fibrous tissue. This association suggests an immunologic mechanism that includes bronchial epithelial injury. High-resolution CT findings include areas of decreased attenuation and vascularity (mosaic perfusion), air

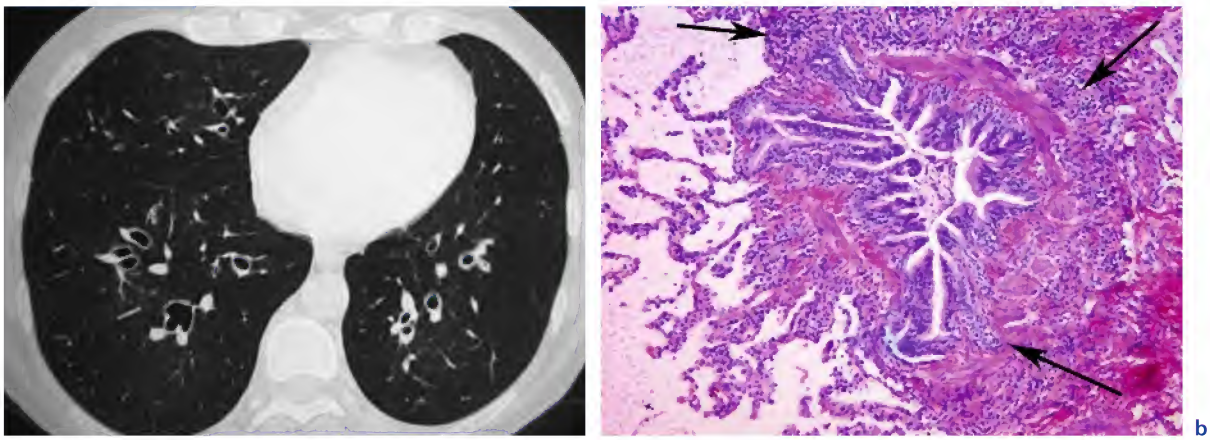

Fig. 6.2.17a,b. Chronic (obliterative) bronchiolitis in a 48-year-old woman 5 months following allogeneic HSC transplantation. **a** HRCT scan at the level of lower lobes shows a striking dilatation of subsegmental airways in the right lower lobe. A general reduction in lung parenchymal density is also noted. **b** Histologic section of lung parenchyma shows a moderately severe mononuclear inflammatory cell infiltrate in the peribronchiolar interstitial tissue (*arrows*). (With permission from Franquet et al. 2005a)

(Winer-Muram et al. 1996) trapping, and bronchial dilatation (Fig. 6.2.17) (Urbanski et al. 1987; Ooi et al. 1998).

6.2.5.3.1.2 Organizing Pneumonia (OP)

Organizing pneumonia (OP), also known as bronchiolitis obliterans organizing pneumonia (BOOP), is defined as granulated tissue plugs within lumens of small airways that extend into alveolar ducts and alveoli (Epler 1995). Organizing pneumonia is increasingly recognized as an important cause of diffuse infiltrative lung disease and is a well-known late manifestation of chronic GVHD occurring in up to 10% of stem cell transplantation (Freudenberger et al. 2003). Risk factors for OP include allogeneic HSC transplantation and GVHD (Winer-Muram et al. 1996; Khurshid and Anderson 2002). CT findings consist of patchy consolidation frequently in a subpleural or peribronchial location, ground-glass opacities, and, occasionally, centrilobular nodules (Franquet et al. 2005a) (Fig. 6.2.18).

6.2.5.3.1.3 Air-Leak Syndromes

Although air-leak syndromes have not been recognized as a fatal complication in HSC transplant recipients, pneumothorax, pneumomediastinum and subcutaneous emphysema are potential complications of patients with chronic GVHD and BO.

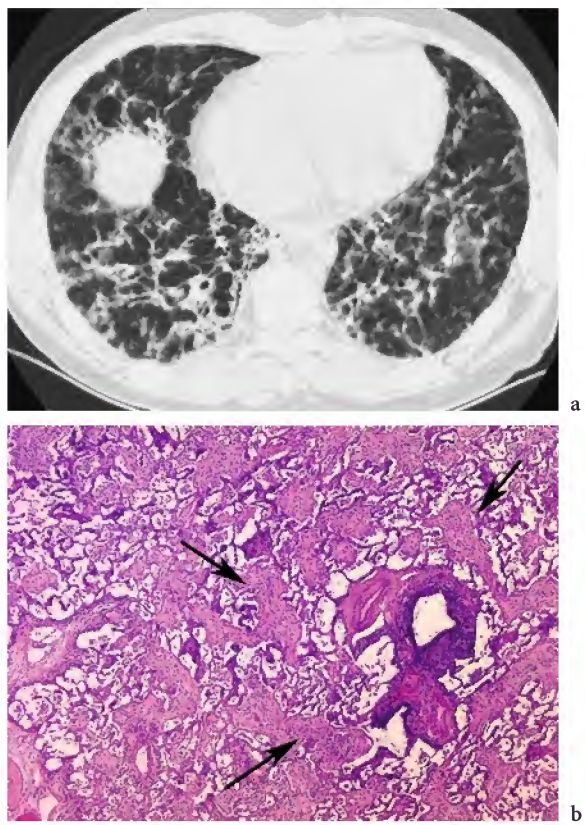

Fig. 6.2.18a,b. Organizing pneumonia after allogeneic HSC transplantation. **a** HRCT scan at the level of lower lung zones shows bilateral patchy areas of consolidation in a predominantly peribronchial distribution. **b** Photomicrograph shows the presence of fibroblastic tissue in the lumens of peribronchial alveoli (*arrows*). (H and E, ×100) (with permission from Franquet et al. 2005a)

In these patients, air in the peribronchial sheets (pulmonary interstitial emphysema) can be associated with impairment of respiratory function and/or chest pain, possibly resulting from compression of small vessels by the interstitial air. In most patients, pulmonary interstitial emphysema is transient and it is well known that this process is difficult, if not impossible, to detect by chest radiograph. Chest CT should be performed in any HSC transplant recipient with known or suspected cGVHD who present with acute clinical symptoms, especially chest pain, to rule out associated air-leak syndromes. Therefore, suspicion of BO should be high and prompt therapy should be initiated in long-term HSC transplant recipients presenting with spontaneous pneumomediastinum, pneumothorax or subcutaneous emphysema (Franquet et al. 2007).

6.2.5.3.2 Post-Transplant Malignancies

Post-transplant malignancies in HSC transplantation patients are seven times more common than primary cancer in the general population. Post-transplant malignancies include solid tumors, hematologic neoplasms, and post-transplantation lymphoproliferative disorder (PTLD) (Libshitz et al. 1978; Worthy et al. 1997).

Solid tumors have been attributed to radiation therapy with most of them occurring within or adjacent to the directly irradiated tissues or radiation ports (Bluemke et al. 1991; Bhatia et al. 2001). The risk of radiation-associated solid tumor development after HSC transplantation appears to rise with increasing levels of irradiation and is likely to increase with longer follow-up. This underscores the importance of close monitoring of patients who undergo bone marrow transplantation (Bhatia et al. 2001).

Bone and soft-tissue sarcomas and breast carcinoma are the most common radiation-induced tumors. Radiation-induced sarcoma of bone should be considered when bone destruction and an associated soft-tissue mass are shown on CT, or when changes occur in the appearance of previously stable irradiated bone (Lorigan et al. 1989). Radiation-induced mesothelioma, lung carcinoma, and esophageal carcinoma have also been described.

Post-transplantation lymphoproliferative disorder (PTLD) represents a heterogeneous group of Epstein–Barr-virus-related lymphoid tumors that occur in the setting of ineffective T-cell function because of pharmacologic immunosuppression after solid-organ transplant and HSC transplantation recipients (Worthy et al. 1997). Post-transplantation lymphoproliferative disorder occurs in approximately 2% of HSC transplantation patients, especially after heart-lung and renal transplantation. On chest radiograph or CT, PTLD usually consists of multiple pulmonary nodules and/or hilar or mediastinal lymph node enlargement (Fig. 6.2.19) (Bragg et al. 1994; Rappaport et al. 1998; Pickhardt et al. 2000).

Fig. 6.2.19. Post-transplantation lymphoproliferative disorder (*PTLD*) in a 54-year-old man with multiple myeloma, 2 months after allogeneic HSC transplantation. CT scans shows multiple axilar and mediastinal adenopathies. (With permission from Franquet et al. 2005a)

6.2.5.3.3 Radiation Fibrosis

Radiation fibrosis typically occurs 6 months or more after radiation therapy. Fibrotic changes are variably present between 30 and 40 Gy, and are always seen after 40 Gy. Permanent scarring resulting in respiratory compromise may develop if the dose and volume of lung irradiated are excessive. The HRCT findings consist of a reticular pattern with associated traction bronchiectasis limited to the radiation portal (Worthy et al. 1997; Wah et al. 2003) (Fig. 6.2.20).

6.2.5.3.4 Calcification of Mediastinal Lymph Nodes and Thymic Cysts

Calcification of lymph nodes and pre-sternal soft tissue disease may be seen after radiotherapy for Hodgkin's disease (Worthy et al. 1997). Calcification of non-enlarged nodes in HD signifies a favorable response to therapy (Fig. 6.2.21). Thymic

Fig. 6.2.20a,b. Radiation fibrosis in a 48-year-old man after radiation therapy for lymphoma. **a** Chest radiograph obtained 1 year after radiation therapy shows bilateral fibrotic changes in the paramediastinal lung zone (*arrows*). **b** CT scan confirms bilateral paramediastinal fibrosis in the field of irradiation (*arrowheads*). (With permission from Franquet et al. 2005a)

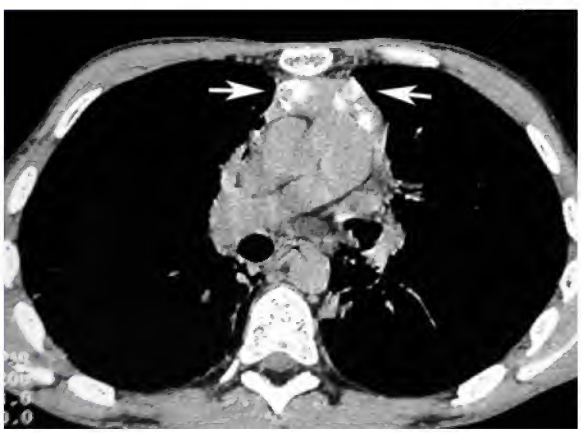

Fig. 6.2.21. Mediastinal lymph node calcification in a 38-year-old man after radiation therapy for lymphoma. Close-up view of CT shows multiple calcified retrosternal lymphadenopathy (*arrows*). The patient had undergone radiotherapy for Hodgkin's disease 3 years previously. (With permission from Franquet et al. 2005a)

Fig. 6.2.22a–c. Calcified thymic cyst in a 30-year-old man after radiotherapy for Hodgkin's disease. **a** Posteroanterior and lateral **b** chest radiograph show a well-defined anterior mediastinal mass with a thin rim of calcification (*arrows*). **c** CT scan clearly shows a well-defined anterior mediastinal mass with a thin rim of calcification. (With permission from Franquet et al. 2005a)

cysts, sometimes with a thin rim of calcification, may develop as an inflammatory response after radiotherapy for Hodgkin's disease (Fig. 6.2.22); occasionally they enlarge and simulate recurrent tumor (Worthy et al. 1997).

6.2.6 Conclusion

The radiologist plays an important role in the diagnosis and management of HSC transplant recipients with suspected pulmonary complications. Conventional chest radiography remains the first imaging procedure in the imaging work-up of patients. Although CT is not recommended for the initial evaluation, it is frequently appropriate in those cases with normal, equivocal, or non-specific radiographic findings. High-resolution CT is helpful in the differential diagnosis of infectious from non-infectious acute parenchymal lung disease. A combination of the clinical information and HRCT findings, which are sometimes characteristic of several entities, may help the radiologist in forming a meaningful differential diagnosis of these disorders. Familiarity with the appearance of more typical pulmonary complications should improve diagnosis and patient care.

References

Afessa B, Tefferi A, Litzow MR, Peters SG (2002) Outcome of diffuse alveolar hemorrhage in hematopoietic stem cell transplant recipients. Am J Respir Crit Care Med 166:1364–1368

Alam S, Chan KM (1996) Noninfectious pulmonary complications after organ transplantation. Curr Opin Pulm Med 2:412–418

Alangaden GJ, Wahiduzzaman M, Chandrasekar PH (2002) Aspergillosis: the most common community-acquired pneumonia with Gram-negative Bacilli as copathogens in stem cell transplant recipients with graft-versus-host disease. Clin Infect Dis 35:659–664

Aljurf M, Gyger M, Alrajhi A, Sahovic E, Chaudhri N, Musa M, Ayoub O, Seth P, Aslam M, Al-Fiar F (1999) *Mycobacterium tuberculosis* infection in allogeneic bone marrow transplantation patients. Bone Marrow Transplant 24:551–554

Allan BT, Patton D, Ramsey NK, Day DL (1988) Pulmonary fungal infections after bone marrow transplantation. Pediatr Radiol 18:118–122

Aquino SL, Kee ST, Warnock ML, Gamsu G (1994) Pulmonary aspergillosis: imaging findings with pathologic correlation. AJR Am J Roentgenol 163:811–815

Aquino SL, Gamsu G, Webb WR, Kee ST (1996) Tree-in-bud pattern: frequency and significance on thin section CT. J Comput Assist Tomogr 20:594–599

Aronchick JM (2000) Pulmonary infections in cancer and bone marrow transplant patients. Semin Roentgenol 35:140–151

Ascioglu S, Rex JH, de Pauw B, Bennett JE, Bille J, Crokaert F, Denning DW, Donnelly JP, Edwards JE, Erjavec Z, Fiere D, Lortholary O, Maertens J, Meis JF, Patterson TF, Ritter J, Selleslag D, Shah PM, Stevens DA, Walsh TJ (2002) Defining opportunistic invasive fungal infections in immunocompromised patients with cancer and hematopoietic stem cell transplants: an international consensus. Clin Infect Dis 34:7–14

Bag R (2003) Fungal pneumonias in transplant recipients. Curr Opin Pulm Med 9:193–198

Barker CC, Butzner JD, Anderson RA, Brant R, Sauve RS (2003) Incidence, survival and risk factors for the development of veno-occlusive disease in pediatric hematopoietic stem cell transplant recipients. Bone Marrow Transplant 32:79–87

Ben-Abraham R, Paret G, Cohen R, Szold O, Cividalli G, Toren A, Nagler A (2003) Diffuse alveolar hemorrhage following allogeneic bone marrow transplantation in children. Chest 124:660–664

Bhagat R, Rizzieri DA, Vredenburgh JJ, Chao NJ, Folz RJ (2004) Pulmonary sarcoidosis following stem cell transplantation: is it more than a chance occurrence? Chest 126:642–644

Bhatia S, Louie AD, Bhatia R, O'Donnell MR, Fung H, Kashyap A, Krishnan A, Molina A, Nademanee A, Niland JC, Parker PA, Snyder DS, Spielberger R, Stein A, Forman SJ (2001) Solid cancers after bone marrow transplantation. J Clin Oncol 19:464–471

Bluemke DA, Fishman EK, Kuhlman JE, Zinreich ES (1991) Complications of radiation therapy: CT evaluation. Radiographics 11:581–600

Bodey GP, Vartivarian S (1989) Aspergillosis. Eur J Clin Microbiol Infect Dis 8:413–437

Boiselle PM, Tocino I, Hooley RJ, Pumerantz AS, Selwyn PA, Neklesa VP, Lange RC (1997) Chest radiograph interpretation of *Pneumocystis carinii* pneumonia, bacterial pneumonia, and pulmonary tuberculosis in HIV-positive patients: accuracy, distinguishing features, and mimics. J Thorac Imaging 12:47–53

Boiselle PM, Crans CA Jr, Kaplan MA (1999) The changing face of *Pneumocystis carinii* pneumonia in AIDS patients. AJR Am J Roentgenol 172:1301–1309

Boivin G, Abed Y, Pelletier G, Ruel L, Moisan D, Cote S, Peret TC, Erdman DD, Anderson LJ (2002) Virological features and clinical manifestations associated with human metapneumovirus: a new paramyxovirus responsible for acute respiratory-tract infections in all age groups. J Infect Dis 186:1330–1334

Bragg DG, Chor PJ, Murray KA, Kjeldsberg CR (1994) Lymphoproliferative disorders of the lung: histopathology, clinical manifestations, and imaging features. AJR Am J Roentgenol 163:273–281

Buff SJ, McLelland R, Gallis HA, Matthay R, Putman CE (1982) *Candida albicans* pneumonia: radiographic appearance. AJR Am J Roentgenol 138:645–648

Busch FW, Bautz W, Dierkesmann R, Toomes H, Schalk KP, Rusch-Gerdes S, Ehninger G (1991) [Lung changes caused by *Mycobacterium xenopi* infection in a patient with bone marrow transplantation: problems in differential diagnosis]. Pneumologie 45:340–342

Cameron ML, Bartlett JA, Gallis HA, Waskin HA (1991) Manifestations of pulmonary cryptococcosis in patients with acquired immunodeficiency syndrome. Rev Infect Dis 13:64–67

Cardozo BL, Hagenbeek A (1985) Interstitial pneumonitis following bone marrow transplantation: pathogenesis and therapeutic considerations. Eur J Cancer Clin Oncol 21:43–51

Chakrabarti S, Avivi I, Mackinnon S, Ward K, Kottaridis PD, Osman H, Waldmann H, Hale G, Fegan CD, Yong K, Goldstone AH, Linch DC, Milligan DW (2002) Respiratory virus infections in transplant recipients after reduced-intensity conditioning with Campath-1H: high incidence but low mortality. Br J Haematol 119:1125–1132

Chan CK, Hyland RH, Hutcheon MA (1990) Pulmonary complications following bone marrow transplantation. Clin Chest Med 11:323–332

Chen CS, Boeckh M, Seidel K, Clark JG, Kansu E, Madtes DK, Wagner JL, Witherspoon RP, Anasetti C, Appelbaum FR, Bensinger WI, Deeg HJ, Martin PJ, Sanders JE, Storb R, Storek J, Wade J, Siadak M, Flowers ME, Sullivan KM (2003) Incidence, risk factors, and mortality from pneumonia developing late after hematopoietic stem cell transplantation. Bone Marrow Transplant 32:515–522

Choi YH, Leung AN (1999) Radiologic findings: pulmonary infections after bone marrow transplantation. J Thorac Imaging 14:201–206

Conces DJ Jr, Stockberger SM, Tarver RD, Wheat LJ (1993) Disseminated histoplasmosis in AIDS: findings on chest radiographs. AJR Am J Roentgenol 160:15–19

Connolly JE Jr, McAdams HP, Erasmus JJ, Rosado-de-Christenson ML (1999) Opportunistic fungal pneumonia. J Thorac Imaging 14:51–62

Cooke KR, Yanik G (2004) Acute lung injury after allogeneic stem cell transplantation: is the lung a target of acute graft-versus-host disease? Bone Marrow Transplant 34:753–765

Cordonnier C (1990) [Clinical, diagnostic and physiopathological aspects of cytomegalovirus pneumonia after bone marrow transplantation]. Rev Pneumol Clin 46:244–250

Coy DL, Ormazabal A, Godwin JD, Lalani T (2005) Imaging evaluation of pulmonary and abdominal complications following hematopoietic stem cell transplantation. Radiographics 25:305–317; discussion 318

Crawford SW (1999) Noninfectious lung disease in the immunocompromised host. Respiration 66:385–395

Crawford SW, Hackman RC, Clark JG (1988) Open lung biopsy diagnosis of diffuse pulmonary infiltrates after marrow transplantation. Chest 94:949–953

Cunningham I (1992) Pulmonary infections after bone marrow transplant. Semin Respir Infect 7:132–138

Denning DW (2000) Early diagnosis of invasive aspergillosis. Lancet 355:423–424

Denning DW (2001) Chronic forms of pulmonary aspergillosis. Clin Microbiol Infect 7 [Suppl 2]:25–31

Doucette K, Fishman JA (2004) Nontuberculous mycobacterial infection in hematopoietic stem cell and solid organ transplant recipients. Clin Infect Dis 38:1428–1439

Ellis SJ, Cleverley JR, Muller NL (2000) Drug-induced lung disease: high-resolution CT findings. AJR Am J Roentgenol 175:1019–1024

Epler GR (1995) Bronchiolitis obliterans organizing pneumonia. Semin Respir Infect 10:65–77

Ettinger NA (1993) Invasive diagnostic approaches to pulmonary infiltrates. Semin Respir Infect 8:168–176

Evans A, Steward CG, Lyburn ID, Grier DJ (2003) Imaging in haematopoietic stem cell transplantation. Clin Radiol 58:201–214

Foot AB, Caul EO, Roome AP, Darville JM, Oakhill A (1993) Cytomegalovirus pneumonitis and bone marrow transplantation: identification of a specific high risk group. J Clin Pathol 46:415–419

Franquet T, Muller NL, Gimenez A, Guembe P, de La Torre J, Bague S (2001) Spectrum of pulmonary aspergillosis: histologic, clinical, and radiologic findings. Radiographics 21:825–837

Franquet T, Serrano F, Gimenez A, Rodriguez-Arias JM, Puzo C (2002) Necrotizing Aspergillosis of large airways: CT findings in eight patients. J Comput Assist Tomogr 26:342–345

Franquet T, Lee KS, Muller NL (2003a) Thin-section CT findings in 32 immunocompromised patients with cytomegalovirus pneumonia who do not have AIDS. AJR Am J Roentgenol 181:1059–1063

Franquet T, Muller NL, Gimenez A, Martinez S, Madrid M, Domingo P (2003b) Infectious pulmonary nodules in immunocompromised patients: usefulness of computed tomography in predicting their etiology. J Comput Assist Tomogr 27:461–468

Franquet T, Muller NL, Oikonomou A, Flint JD (2004) Aspergillus infection of the airways: computed tomography and pathologic findings. J Comput Assist Tomogr 28:10–16

Franquet T, Muller NL, Lee KS, Gimenez A, Flint JD (2005a) High-resolution CT and pathologic findings of noninfectious pulmonary complications after hematopoietic stem cell transplantation. AJR Am J Roentgenol 184:629–637

Franquet T, Muller NL, Lee KS, Oikonomou A, Flint JD (2005b) Pulmonary candidiasis after hematopoietic stem cell transplantation: thin-section CT findings. Radiology 236: 332–337

Franquet T, Rodriguez S, Martino R, Salinas T, Gimenez A, Hidalgo A (2005c) Human metapneumovirus infection in hematopoietic stem cell transplant recipients: high-resolution computed tomography findings. J Comput Assist Tomogr 29:223–227

Franquet T, Rodríguez S, Hernández JM, Martino R, Giménez A, Hidalgo A, Domingo P (2007) Air-leak syndromes in hematopoietic stem cell transplant recipients with chronic GVHD. High-resolution CT findings. J Thorac Imaging (in press)

Freudenberger TD, Madtes DK, Curtis JR, Cummings P, Storer BE, Hackman RC (2003) Association between acute and chronic graft-versus-host disease and bronchiolitis obliterans organizing pneumonia in recipients of hematopoietic stem cell transplants. Blood 102:3822–3828

Fukuda T, Boeckh M, Guthrie KA, Mattson DK, Owens S, Wald A, Sandmaier BM, Corey L, Storb RF, Marr KA (2004) Invasive aspergillosis before allogeneic hematopoietic stem cell transplantation: 10-year experience at a single transplant center. Biol Blood Marrow Transplant 10:494–503

Gasparetto EL, Escuissato DL, Marchiori E, Ono S, Frare e Silva RL, Muller NL (2004) High-resolution CT findings of respiratory syncytial virus pneumonia after bone marrow transplantation. AJR Am J Roentgenol 182:1133–1137

Gasparetto EL, Escuissato DL, Inoue C, Marchiori E, Muller NL (2005) Herpes simplex virus type 2 pneumonia after bone marrow transplantation: high-resolution CT findings in 3 patients. J Thorac Imaging 20:71–73

Gaziev D, Baronciani D, Galimberti M, Polchi P, Angelucci E, Giardini C, Muretto P, Perugini S, Riggio S, Ghirlanda S, Erer B, Maiello A, Lucarelli G (1996) Mucormycosis after bone marrow transplantation: report of four cases in thalassemia and review of the literature. Bone Marrow Transplant 17:409–414

Ghosh S, Champlin R, Couch R, Englund J, Raad I, Malik S, Luna M, Whimbey E (1999) Rhinovirus infections in myelosuppressed adult blood and marrow transplant recipients. Clin Infect Dis 29:528–532

Giacchino M, Busca A, Miniero R, Defilippi C, Massara FM, Vassallo E, Madon E (1993) [Pulmonary complications after bone marrow transplantation]. Minerva Pediatr 45:141–150

Gotway MB, Dawn SK, Caoili EM, Reddy GP, Araoz PA, Webb WR (2002) The radiologic spectrum of pulmonary Aspergillus infections. J Comput Assist Tomogr 26:159–173

Gulbahce HE, Manivel JC, Jessurun J (2000) Pulmonary cytolytic thrombi: a previously unrecognized complication of bone marrow transplantation. Am J Surg Pathol 24:1147–1152

Gulbahce HE, Pambuccian SE, Jessurun J, Woodard P, Steiner ME, Manivel JC, Hite S, Ramsay NK, Baker KS (2004) Pulmonary nodular lesions in bone marrow transplant recipients: impact of histologic diagnosis on patient management and prognosis. Am J Clin Pathol 121:205–210

Heurlin N, Brattstrom C, Lonnqvist B, Westman L, Lidman C, Andersson J (1991) Aetiology of pulmonary diseases in immunocompromised patients. Eur Respir J 4:10–18

Huaringa AJ, Leyva FJ, Signes-Costa J, Morice RC, Raad I, Darwish AA, Champlin RE (2000) Bronchoalveolar lavage in the diagnosis of pulmonary complications of bone marrow transplant patients. Bone Marrow Transplant 25:975–979

Ison MG, Hayden FG, Kaiser L, Corey L, Boeckh M (2003) Rhinovirus infections in hematopoietic stem cell transplant recipients with pneumonia. Clin Infect Dis 36:1139–1143

Jantunen E, Piilonen A, Volin L, Ruutu P, Parkkali T, Koukila-Kahkola P, Ruutu T (2002) Radiologically guided fine needle lung biopsies in the evaluation of focal pulmonary lesions in allogeneic stem cell transplant recipients. Bone Marrow Transplant 29:353–356

Janzen DL, Padley SP, Adler BD, Muller NL (1993) Acute pulmonary complications in immunocompromised non-AIDS patients: comparison of diagnostic accuracy of CT and chest radiography. Clin Radiol 47:159–165

Kaiser L, Huguenin T, Lew PD, Chapuis B, Pittet D (1998) Invasive aspergillosis. Clinical features of 35 proven cases at a single institution. Medicine (Baltimore) 77:188–194

Kang EY, Patz EF Jr, Muller NL (1996) Cytomegalovirus pneumonia in transplant patients: CT findings. J Comput Assist Tomogr 20:295–299

Kantrow SP, Hackman RC, Boeckh M, Myerson D, Crawford SW (1997) Idiopathic pneumonia syndrome: changing spectrum of lung injury after marrow transplantation. Transplantation 63:1079–1086

Kapoor N, Copelan EA, Tutschka PJ (1989) Cytomegalovirus infection in bone marrow transplant recipients: use of intravenous gamma globulin as a prophylactic and therapeutic agent. Transplant Proc 21:3095–3096

Kauffman CA (2002) Endemic mycoses in patients with hematologic malignancies. Semin Respir Infect 17:106–112

Khoury MB, Godwin JD, Ravin CE, Gallis HA, Halvorsen RA, Putman CE (1984) Thoracic cryptococcosis: immunologic competence and radiologic appearance. AJR Am J Roentgenol 142:893–896

Khurshid I, Anderson LC (2002) Non-infectious pulmonary complications after bone marrow transplantation. Postgrad Med J 78:257–262

Kotloff RM, Ahya VN, Crawford SW (2004) Pulmonary complications of solid organ and hematopoietic stem cell transplantation. Am J Respir Crit Care Med 170:22–48

Krinzman S, Basgoz N, Kradin R, Shepard JA, Flieder DB, Wright CD, Wain JC, Ginns LC (1998) Respiratory syncytial virus-associated infections in adult recipients of solid organ transplants. J Heart Lung Transplant 17:202–210

Krowka MJ, Rosenow EC 3rd, Hoagland HC (1985) Pulmonary complications of bone marrow transplantation. Chest 87:237–246

Kuhlman JE, Fishman EK, Siegelman SS (1985) Invasive pulmonary aspergillosis in acute leukemia: characteristic findings on CT, the CT halo sign, and the role of CT in early diagnosis. Radiology 157:611–614

Kuhlman JE, Fishman EK, Burch PA, Karp JE, Zerhouni EA, Siegelman SS (1987) Invasive pulmonary aspergillosis in acute leukemia. The contribution of CT to early diagnosis and aggressive management. Chest 92:95–99

Kuhlman JE, Fishman EK, Burch PA, Karp JE, Zerhouni EA, Siegelman SS (1988) CT of invasive pulmonary aspergillosis. AJR Am J Roentgenol 150:1015–1020

Kumar K, Jimenez V (2001) Pulmonary nocardiosis after bone marrow transplantation successfully treated with doxycycline. Int J Infect Dis 5:222–224

Leung AN, Gosselin MV, Napper CH, Braun SG, Hu WW, Wong RM, Gasman J (1999) Pulmonary infections after bone marrow transplantation: clinical and radiographic findings. Radiology 210:699–710

Libshitz HI, Zornoza J, McLarty JW (1978) Lung cancer in chronic leukemia and lymphoma. Radiology 127:297–300

Lin JT, Lee MY, Hsiao LT, Yang MH, Chao TC, Chen PM, Chiou TJ (2004) Pulmonary nocardiosis in a patient with CML relapse undergoing imatinib therapy after bone marrow transplantation. Ann Hematol 83:444–446

Ljungman P (2001) Respiratory virus infections in stem cell transplant patients: the European experience. Biol Blood Marrow Transplant Suppl 7:5S–7S

Lorigan JG, Libshitz HI, Peuchot M (1989) Radiation-induced sarcoma of bone: CT findings in 19 cases. AJR Am J Roentgenol 153:791–794

Maertens J, Demuynck H, Verbeken EK, Zachee P, Verhoef GE, Vandenberghe P, Boogaerts MA (1999) Mucormycosis in allogeneic bone marrow transplant recipients: report of five cases and review of the role of iron overload in the pathogenesis. Bone Marrow Transplant 24:307–312

Maertens J, Verhaegen J, Lagrou K, Van Eldere J, Boogaerts M (2001) Screening for circulating galactomannan as a

noninvasive diagnostic tool for invasive aspergillosis in prolonged neutropenic patients and stem cell transplantation recipients: a prospective validation. Blood 97:1604–1610

Markovic SN, Adlakha A, Smith TF, Walker RC (1998) Respiratory syncytial virus pneumonitis-induced diffuse alveolar damage in an autologous bone marrow transplant recipient. Mayo Clin Proc 73:153–156

Martino R, Manteiga R, Sanchez I, Brunet S, Sureda A, Badell I, Argiles B, Subira M, Bordes R, Domingo-Albos A (1995) Viridans streptococcal shock syndrome during bone marrow transplantation. Acta Haematol 94:69–73

Martino R, Martinez C, Brunet S, Sureda A, Lopez R, Domingo-Albos A (1996) Tuberculosis in bone marrow transplant recipients: report of two cases and review of the literature. Bone Marrow Transplant 18:809–812

Maschmeyer G (2001) Pneumonia in febrile neutropenic patients: radiologic diagnosis. Curr Opin Oncol 13:229–235

McAdams HP, Rosado-de-Christenson ML, Lesar M, Templeton PA, Moran CA (1995) Thoracic mycoses from endemic fungi: radiologic-pathologic correlation. Radiographics 15:255–270

McAdams HP, Rosado de Christenson M, Strollo DC, Patz EF Jr (1997) Pulmonary mucormycosis: radiologic findings in 32 cases. AJR Am J Roentgenol 168:1541–1548

Mohite U, Das M, Saikia T, Parikh P, Gopal R, Kelkar R, Advani S (2001) Mycobacterial pulmonary infection post allogeneic bone marrow transplantation. Leuk Lymphoma 40:675–678

Navari RM, Sullivan KM, Springmeyer SC, Siegel MS, Meyers JD, Buckner CD, Sanders JE, Stewart PS, Clift RA, Fefer A et al (1983) Mycobacterial infections in marrow transplant patients. Transplantation 36:509–513

Nichols WG, Corey L, Gooley T, Davis C, Boeckh M (2001) Parainfluenza virus infections after hematopoietic stem cell transplantation: risk factors, response to antiviral therapy, and effect on transplant outcome. Blood 98:573–578

Nichols WG, Guthrie KA, Corey L, Boeckh M (2004) Influenza infections after hematopoietic stem cell transplantation: risk factors, mortality, and the effect of antiviral therapy. Clin Infect Dis 39:1300–1306

Nusair S, Breuer R, Shapira MY, Berkman N, Or R (2004) Low incidence of pulmonary complications following nonmyeloablative stem cell transplantation. Eur Respir J 23:440–445

Oikonomou A, Muller NL, Nantel S (2003) Radiographic and high-resolution CT findings of influenza virus pneumonia in patients with hematologic malignancies. AJR Am J Roentgenol 181:507–511

Ooi GC, Peh WC, Ip M (1998) High-resolution computed tomography of bronchiolitis obliterans syndrome after bone marrow transplantation. Respiration 65:187–191

Ozkaynak MF, Lenarsky C, Kohn D, Weinberg K, Parkman R (1990) *Mycobacterium avium-intracellulare* infections after allogeneic bone marrow transplantation in children. Am J Pediatr Hematol Oncol 12:220–224

Patriarca F, Skert C, Sperotto A, Damiani D, Cerno M, Geromin A, Zaja F, Stocchi R, Prosdocimo S, Fili C, Fanin R (2004) Incidence, outcome, and risk factors of late-onset noninfectious pulmonary complications after unrelated donor stem cell transplantation. Bone Marrow Transplant 33:751–758

Paulin T, Ringden O, Nilsson B, Lonnqvist B, Gahrton G (1987) Variables predicting bacterial and fungal infections after allogeneic marrow engraftment. Transplantation 43:393–398

Pickhardt PJ, Siegel MJ, Hayashi RJ, Kelly M (2000) Post-transplantation lymphoproliferative disorder in children: clinical, histopathologic, and imaging features. Radiology 217:16–25

Primack SL, Hartman TE, Lee KS, Muller NL (1994) Pulmonary nodules and the CT halo sign. Radiology 190:513–515

Rappaport DC, Chamberlain DW, Shepherd FA, Hutcheon MA (1998) Lymphoproliferative disorders after lung transplantation: imaging features. Radiology 206:519–524

Resnick IB, Averbuch D, Aker M, Engelhard D (2005) Is *Pneumocystis carinii* pneumonia after stem cell transplantations a contagious disease? Clin Transplant 19:427–431

Roviaro G, Varoli F, Francese M, Caminiti R, Vergani C, Maciocco M (2002) Thoracoscopy and transplantation: a new attractive tool. Transplantation 73:1013–1018

Roy V, Weisdorf D (1997) Mycobacterial infections following bone marrow transplantation: a 20 year retrospective review. Bone Marrow Transplant 19:467–470

Saito T, Seo S, Kanda Y, Shoji N, Ogasawara T, Murakami J, Tanosaki R, Tobinai K, Takaue Y, Mineishi S (2001) Early onset *Pneumocystis carinii* pneumonia after allogeneic peripheral blood stem cell transplantation. Am J Hematol 67:206–209

Schmidt-Wolf I, Schwerdtfeger R, Schwella N, Gallardo J, Schmid HJ, Huhn D, Siegert W (1993) Diffuse pulmonary alveolar hemorrhage after allogeneic bone marrow transplantation. Ann Hematol 67:139–141

Sider L, Westcott MA (1994) Pulmonary manifestations of cryptococcosis in patients with AIDS: CT features. J Thorac Imaging 9:78–84

Snyder CL, Ramsay NK, McGlave PB, Ferrell KL, Leonard AS (1990) Diagnostic open-lung biopsy after bone marrow transplantation. J Pediatr Surg 25:871–876; discussion 876–877

Soubani AO, Miller KB, Hassoun PM (1996) Pulmonary complications of bone marrow transplantation. Chest 109:1066–1077

Soubani AO, Qureshi MA, Baynes RD (2001) Flexible bronchoscopy in the diagnosis of pulmonary infiltrates following autologous peripheral stem cell transplantation for advanced breast cancer. Bone Marrow Transplant 28:981–985

Springmeyer SC, Hackman RC, Holle R, Greenberg GM, Weems CE, Myerson D, Meyers JD, Thomas ED (1986) Use of bronchoalveolar lavage to diagnose acute diffuse pneumonia in the immunocompromised host. J Infect Dis 154:604–610

Starobin D, Fink G, Shitrit D, Izbicki G, Bendayan D, Bakal I, Kramer MR (2003) The role of fiberoptic bronchoscopy evaluating transplant recipients with suspected pulmonary infections: analysis of 168 cases in a multi-organ transplantation center. Transplant Proc 35:659–660

Stover DE, Zaman MB, Hajdu SI, Lange M, Gold J, Armstrong D (1984) Bronchoalveolar lavage in the diagnosis of diffuse pulmonary infiltrates in the immunosuppressed host. Ann Intern Med 101:1–7

Stringer JR, Beard CB, Miller RF, Wakefield AE (2002) A new

name (*Pneumocystis jiroveci*) for Pneumocystis from humans. Emerg Infect Dis 8:891–896
Tabbara IA, Zimmerman K, Morgan C, Nahleh Z (2002) Allogeneic hematopoietic stem cell transplantation: complications and results. Arch Intern Med 162:1558–1566
Tanaka N, Matsumoto T, Miura G, Emoto T, Matsunaga N (2002) HRCT findings of chest complications in patients with leukemia. Eur Radiol 12:1512–1522
Tazelaar HD, Baird AM, Mill M, Grimes MM, Schulman LL, Smith CR (1989) Bronchocentric mycosis occurring in transplant recipients. Chest 96:92–95
Urbanski SJ, Kossakowska AE, Curtis J, Chan CK, Hutcheon MA, Hyland RH, Messner H, Minden M, Sculier JP (1987) Idiopathic small airways pathology in patients with graft-versus-host disease following allogeneic bone marrow transplantation. Am J Surg Pathol 11:965–971
Verfaillie C, Weisdorf D, Haake R, Hostetter M, Ramsay NK, McGlave P (1991) Candida infections in bone marrow transplant recipients. Bone Marrow Transplant 8:177–184
Vilchez RA, Linden P, Lacomis J, Costello P, Fung J, Kusne S (2001) Acute respiratory failure associated with pulmonary cryptococcosis in non-aids patients. Chest 119:1865–1869
Villablanca JG, Steiner M, Kersey J, Ramsay NK, Ferrieri P, Haake R, Weisdorf D (1990) The clinical spectrum of infections with viridans streptococci in bone marrow transplant patients. Bone Marrow Transplant 5:387–393
Wah TM, Moss HA, Robertson RJ, Barnard DL (2003) Pulmonary complications following bone marrow transplantation. Br J Radiol 76:373–379
Williams JV, Harris PA, Tollefson SJ, Halburnt-Rush LL, Pingsterhaus JM, Edwards KM, Wright PF, Crowe JE Jr (2004) Human metapneumovirus and lower respiratory tract disease in otherwise healthy infants and children. N Engl J Med 350:443–450
Winer-Muram HT, Gurney JW, Bozeman PM, Krance RA (1996) Pulmonary complications after bone marrow transplantation. Radiol Clin North Am 34:97–117
Wong PW, Stefanec T, Brown K, White DA (2002) Role of fine-needle aspirates of focal lung lesions in patients with hematologic malignancies. Chest 121:527–532
Worthy SA, Flint JD, Muller NL (1997) Pulmonary complications after bone marrow transplantation: high-resolution CT and pathologic findings. Radiographics 17:1359–1371
Yen KT, Lee AS, Krowka MJ, Burger CD (2004) Pulmonary complications in bone marrow transplantation: a practical approach to diagnosis and treatment. Clin Chest Med 25:189–201
Young JA, Hopkin JM, Cuthbertson WP (1984) Pulmonary infiltrates in immunocompromised patients: diagnosis by cytological examination of bronchoalveolar lavage fluid. J Clin Pathol 37:390–397
Zihlif M, Khanchandani G, Ahmed HP, Soubani AO (2005) Surgical lung biopsy in patients with hematological malignancy or hematopoietic stem cell transplantation and unexplained pulmonary infiltrates: improved outcome with specific diagnosis. Am J Hematol 78:94–99
Zinck SE, Leung AN, Frost M, Berry GJ, Muller NL (2002) Pulmonary cryptococcosis: CT and pathologic findings. J Comput Assist Tomogr 26:330–334

Imaging in Pancreas and Intestinal Transplantation

7

Martin C. Freund and Karin M. Unsinn

CONTENTS

M. C. Freund, MD, Professor
K. M. Unsinn, MD
Department of Radiology, Medical University Innsbruck, Anichstr. 35, 6020 Innsbruck, Austria

7.1 Introduction to Pancreas Transplantation

Successful pancreas transplantation is currently the only known therapy that establishes an insulin-independent euglycemic state with normalization of glycosylated hemoglobin levels. Insulin-secreting cells are part of the pancreatic islets, which are predominantly located in the tail (Williams 1995). In the majority of cases, pancreas transplantation is performed together with the kidney from the same donor as simultaneous pancreas–kidney transplantation in patients with coexisting end-stage diabetic nephropathy, and less frequently as sequential pancreas after kidney transplantation or pancreas transplantation alone. In all modifications of pancreas transplantation the recipient's native pancreas is left untouched. The first human pancreas transplantation was performed at the University of Minnesota in 1966 (Kelly et al. 1967). Since then, pancreas graft survival has improved consistently, especially in the last decade, thanks to refined surgical techniques and the introduction of better immunosuppressive regimens including tacrolimus and mycophenolate mofetil, which have decreased technical and immunological failure rates. In total, over 90% of pancreas transplantations are performed as simultaneous pancreas–kidney transplantations from the same donor, with the remaining cases classified as sequential pancreas after previous kidney transplantation, and rarely as pancreas transplantation alone. Today the international pancreas transplant registry reports a 1-year patient survival rate of greater than 95%, a 1-year pancreas graft survival rate of greater than 80% for simultaneous pancreas–kidney transplantation, and of nearly 80% for pancreas after previous kidney transplantation and pancreas transplantation alone (Gruessner and Sutherland 2001; International Pancreas Transplant Registry 2004). Although the majori-

ty of transplant centers formerly used exocrine bladder drainage to divert pancreatic juice, an increasing proportion of simultaneous pancreas–kidney transplantations are being performed with the more physiologic enteric drainage and either systemic or portal endocrine drainage.

Knowledge of the transplantation procedure and postoperative imaging anatomy of the pancreas allograft are basic requirements for radiologists. Early diagnosis of organ-related complications after pancreas transplantation is essential for short- and long-term results (Moulton et al. 1989; Dachmann et al. 1998). For these reasons the following sections schematically illustrate the intraoperative appearance during the most important steps of the pancreas transplantation procedure performed in patients with standard vascular anatomy, i.e., organ procurement, back-table reconstruction, and pancreas implantation (Fig. 7.1).

7.2 Organ Procurement

The growing organ shortage together with the establishment of pancreas transplantation caused multiorgan procurement, including liver and whole pancreas from the same donor, to become standard. This requires either en bloc retrieval of liver and pancreas followed by back-table separation (de Ville et al. 1995) or separate procurement of the liver prior to the pancreas (Imagawa et al. 1996). For procurement of the donor's pancreas (Fig. 7.1a) together with a duodenal segment, various vascular structures have to be ligated and transected in an ordered temporal and spatial sequence. These are the proximal gastroduodenal artery, proximal splenic artery, proximal portal vein, superior and inferior mesenteric vein at the mesenteric root and lower rim of the pancreas, respectively, proximal superior mesenteric artery distal to the origin of the inferior pancreaticoduodenal artery including the proximal vascular root of the mesentery and the splenic vascular pedicle at the pancreatic tail. Also, the distal common bile duct is ligated and transected, the duodenum is stapled and transected distal to the pylorus and at the third segment, and the spleen is excised. Additionally, the donor's iliac artery bifurcation is procured for reconstruction of the arterial conduit.

7.3 Back-Table Reconstruction

The procured pancreatic graft, attached to a small portion of the duodenum containing the ampulla of Vater, is then further prepared in lactated Ringer's solution at 4°C under sterile conditions at the back-table (Fig. 7.1b) (Gill et al. 1997). Minimal requirements for successful arterial reconstruction of the pancreatic graft are a full-length splenic artery and a proximal superior mesenteric artery including the inferior pancreaticoduodenal artery. Arterial reconstruction is performed with the donor's iliac artery bifurcation. The donor's external iliac artery is anastomosed in an end-to-end fashion to the donor's proximal superior mesenteric artery and the donor's internal iliac artery to the donor's splenic artery. The donor's common iliac artery serves as a common arterial conduit for the donor's pancreas and connects two formerly unrelated arterial territories, i.e., mesenteric and splenic. Moreover, excess tissue, especially fat, is carefully removed from the pancreatic borders without injuring the parenchyma and vessels. The distal portion of the duodenum is kept sufficiently long until the side-to-side duodenojejunostomy is completed in the recipient.

7.4 Pancreas Transplantation

A midline abdominal incision is used for intraperitoneal placement. The donor's pancreas is placed laterally in the pelvis with the duodenal segment facing either preferentially cephalad for enteric exocrine diversion or sometimes caudad for bladder drainage. Whenever possible, the graft is revascularized in an end-to-side fashion connecting the donor's portal vein to the recipient's right common iliac vein or distal inferior vena cava and the donor's arterial conduit to the recipient's right common iliac artery (Fig. 7.1c). The side-to-side duodenojejunostomy connects the donor's duodenal segment to the recipient's upper jejunum, approximately 30–40 cm distal to the ligament of Treitz, using a circular stapler for a circular, radio-opaque suture line (Fig. 7.1d). The second portion of the duodenum is then shortened in situ to its final length of approximately 10 cm and closed distally with a stapling device. Modifications to this approach

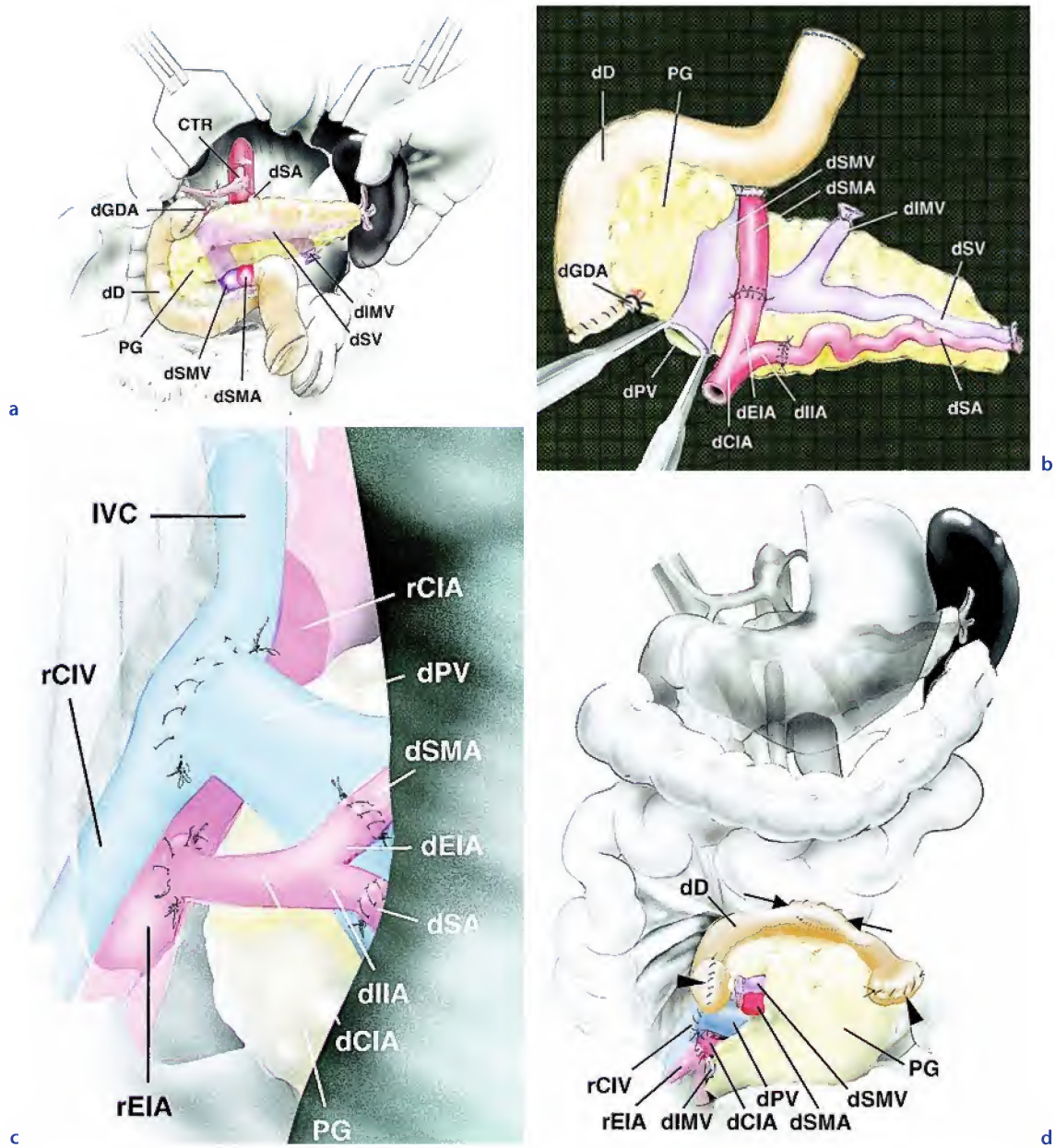

Fig. 7.1a–d. Colored drawings schematically illustrate the transplantation procedure for whole cadaveric pancreatic graft with enteric exocrine drainage. (d Donor's, CIA common iliac artery, CIV common iliac vein, CTR celiac trunk, D duodenum,EIA external iliac artery, GDA gastroduodenal artery, IIA internal iliac artery, IMV inferior mesenteric vein, IVC inferior vena cava, PG, black arrow pancreatic graft, PV portal vein, SA splenic artery, SMA superior mesenteric artery, SMV superior mesenteric vein, SV splenic vein). **a** Drawing shows intraoperative appearance at the end of pancreas procurement before splenectomy but after dissection of the gastroduodenal artery, splenic artery, superior and inferior mesenteric vein, superior mesenteric artery at the line of the mesenteric root, and proximal and distal duodenum. Dissected common bile duct not shown due to superposition of donor's pancreatic head and duodenum. **b** Drawing shows back-table procedure with display of pancreatic graft from behind and emphasis on arterial reconstruction. End-to-end anastomosis of donor's external iliac artery to donor's superior mesenteric artery and donor's internal iliac artery to donor's splenic artery is performed; donor's common iliac artery serves as common arterial conduit of the pancreatic graft. **c** Colored scheme shows magnified intraoperative appearance following revascularization. End-to-side anastomosis is utilized to connect the donor's portal vein to the recipient's right common iliac vein and the donor's arterial conduit to the recipient's right common iliac artery. Surgical drapings cover the recipient's intestine. **d** Colored drawing illustrates the intraoperative appearance at the end of the transplantation procedure. The pancreatic graft is placed intraperitoneally in the pelvis in cephalad orientation with side-to-side duodenojejunostomy connecting the donor's duodenal segment to the recipient's upper jejunum; donor's duodenum is closed on both ends using sutures (*arrowhead*) or staples. Recipient's native pancreas in the upper abdomen is left untouched

include portal rather than systemic venous drainage of the endocrine pancreas, and bladder rather than enteric diversion of the pancreatic juice. For portal drainage the graft is placed parapancreatic, and an end-to-side anastomosis is performed to join the donor's portal vein to the recipient's infrapancreatic superior mesenteric vein and the donor's arterial conduit to the recipient's proximal common iliac artery. Using this approach, exocrine diversion is completed by end-to-end anastomosis of the donor's distal duodenum with a Roux-en-Y loop. For exocrine bladder drainage the pancreas graft with the duodenal segment faces caudad with subsequent side-to-side duodenocystostomy. The recipient's native pancreas is left untouched.

The examples below illustrate the normal postoperative imaging anatomy following pancreas transplantation with systemic venous and exocrine enteric or portal drainage using sonography, computed tomography (CT), magnetic resonance imaging (MRI), angiography and small bowel follow-through examination (Figs. 7.2–7.12). Additionally, an example shows the normal postoperative imaging anatomy following segmental pancreas transplantation with systemic venous and vesical exocrine drainage (Fig. 7.13). All imaged patients underwent pancreas transplantation for long-standing type 1 diabetes mellitus.

7.5 Posttransplantation Complications

Knowledge of the transplantation procedure and postoperative imaging anatomy of the pancreas allograft are basic requirements for radiologists. Graft survival, among other factors, corresponds to early diagnosis and therapy for specific graft-related complications including thrombosis, leakage of enteric anastomosis, hematoma, abscess, pancreatitis, pseudocyst formation, rejection, and posttransplantation lymphoproliferative disorder.

7.6 Imaging Techniques

Various imaging modalities are routinely used to detect early and late posttransplantation complications. In contrast to other solid organ transplants, for instance liver and kidney, imaging of the pancreas allograft by sonography and color-coded sonography is hampered by superposition of intestinal gas. This results from the heterotopic position of the graft in the right pelvis adjacent to the iliac vessels and surrounded by air-filled intestinal loops. For this reason complete evaluation of the vascular and enteric anastomoses as well as the parenchyma of the pancreatic graft can be best accomplished by contrast-enhanced helical CT (Dachmann et al. 1998). Additionally, contrast-enhanced multidetector CT enables 3D reconstruction of the vascular anatomy with respect to neighboring anatomic structures. MRI without contrast application (Vahey et al. 1988), with static (Fernandez et al. 1991) and especially with dynamic (Krebs et al. 1999) contrast enhancement enables better evaluation of the pancreatic parenchymal graft. However, MR angiography is inferior to CT angiography due to its limited spatial resolution. Moreover, evaluation of the enteric anastomosis by MRI is difficult. Additionally, renal function also determines the selection of an appropriate cross-sectional imaging modality after simultaneous pancreas–kidney transplantation. In case of decreased renal function, contrast-enhanced MRI and not contrast-enhanced CT represents the preferred examination in order to preserve the renal graft. MR pancreaticography is a complementary examination for detection of duct abnormalities. Catheter angiography is used to confirm vascular complications while permitting immediate endovascular therapy. Other imaging-guided interventions are employed to treat localized fluid collections percutaneously, for instance seroma, hematoma, abscess. Occasionally, small bowel follow-up studies are performed to detect complications of the enteral anastomosis.

7.7 Imaged Abnormalities

The following complications after pancreas transplantation with enteric anastomosis can be observed: vascular graft complications including rejection, pancreatic graft complications including infection, and other transplantation-associated complications.

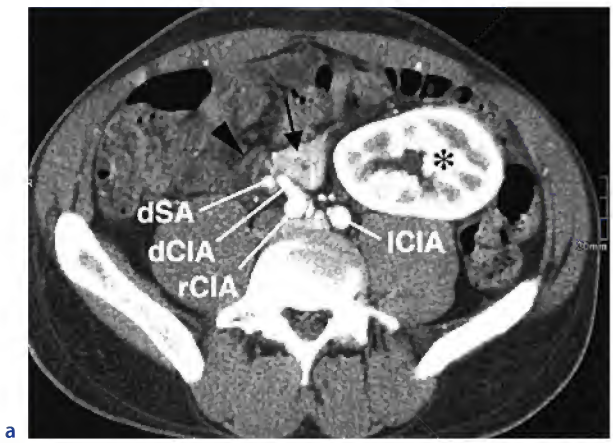

a

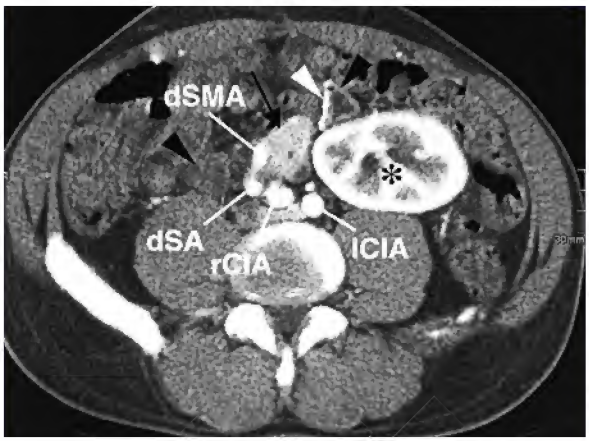

b

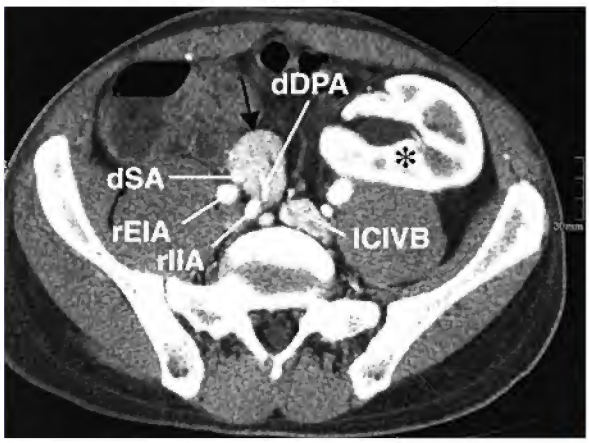

c

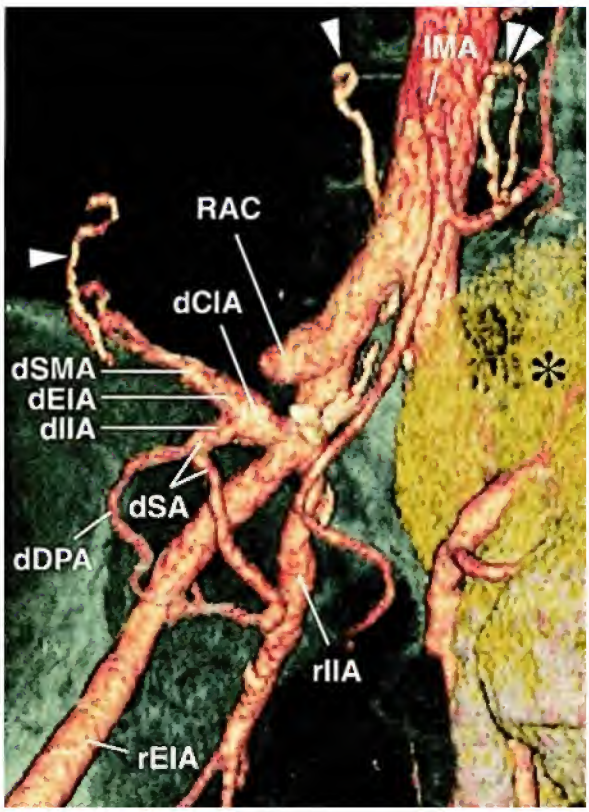

d

Fig. 7.2a–d. A 33-year-old man with a history of two separate pancreas transplantations at different times. (CIA Common iliac artery, CIVB common iliac vein bifurcation, d donor's„DPA dorsal pancreatic artery, EIA external iliac artery, IIA internal iliac artery, IMA inferior mesenteric artery, l left, r right, SA splenic artery, SMA superior mesenteric artery). Annotation: pancreatic graft (*black arrow*), renal graft (*black asterisk*). **a–c** Contrast-enhanced helical CT scans obtained 36 months after initial simultaneous pancreas–kidney transplantation and normal pancreatic graft function at the time of examination. Dominant arterial phase at the line of arterial anastomosis (**a**), and cephalad (**b**) and caudad (**c**) to the arterial anastomosis displays normal posttransplant arterial anatomy, homogeneous enhancement of pancreatic graft (*arrow*), and donor's normal duodenum (black arrowhead) with hyperdense staple line (white arrowhead). **d** 3D volume-rendering display of contrast-enhanced MDCT during dominant arterial phase (obtained 5 days after sequential pancreas-after-kidney retransplantation after vascular failure and pancreatectomy of initial pancreatic graft) shows normal posttransplant arterial anatomy, residual arterial conduit (RAC) after pancreatectomy of initial pancreatic graft, hyperdense staple line (*single arrowheads*) of donor's duodenum, and hyperdense circular staple line (*double arrowheads*) of duodenojejunostomy (intestinal wall structures and grafted pancreatic parenchyma are not seen due to applied electronic thresholds)

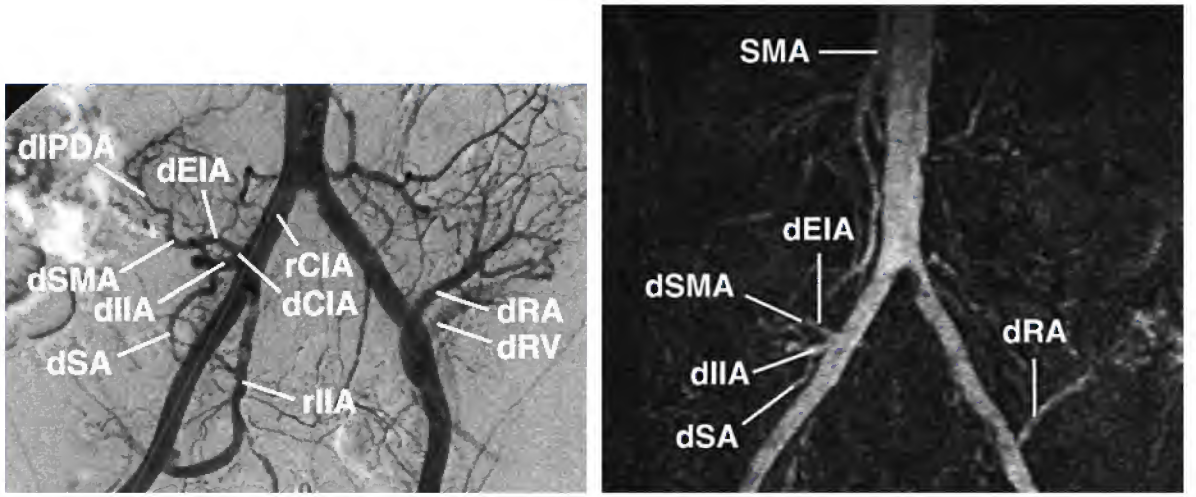

Fig. 7.3a,b. A 53-year-old man after simultaneous pancreas–kidney transplantation. (CIA Common iliac artery, d donor's, EIA external iliac artery, IIA internal iliac artery, IPDA inferior pancreaticoduodenal artery, r right, RA renal artery, RV renal vein, SA splenic artery, SMA superior mesenteric artery). **a** Angiogram obtained 31 months after operation shows normal posttransplant arterial anatomy with right-sided pancreatic and left-sided renal graft. **b** Maximum-intensity-projection reconstruction of contrast-enhanced MR imaging obtained 47 months after operation with normal posttransplant arterial anatomy

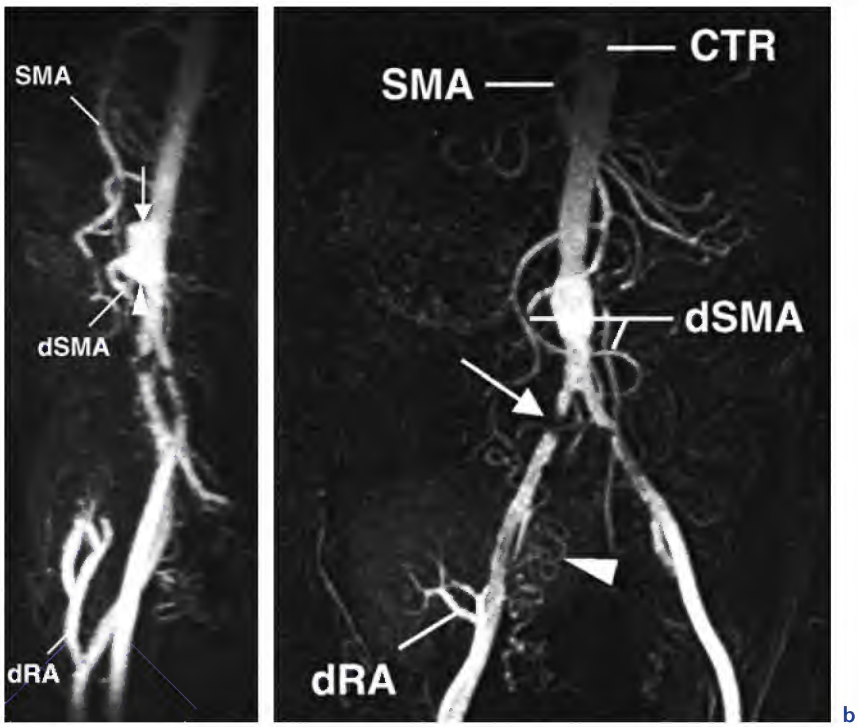

Fig. 7.4a,b. A 39-year-old woman; image obtained 56 months after simultaneous pancreas-kidney transplantation. Arterial revascularization of pancreatic graft was performed with donor's arterial conduit to recipient's infrarenal aorta and right-sided renal transplantation due to advanced calcifying arthrosclerosis. (CTR Celiac trunk, d donor's, RA renal artery, SMA superior mesenteric artery). **a** Lateral view of maximum-intensity-projection reconstruction of contrast-enhanced MRI displays normal enhancement of donor's arterial conduit (*between arrow and arrowhead*) and originating donor's superior mesenteric artery. **b** Frontal view of maximum-intensity-projection reconstruction of contrast-enhanced MRI shows additional high-grade stenosis of right common iliac artery (*arrow*) and serpentine arterial collateral between median sacral artery and internal iliac artery territory (*arrowhead*)

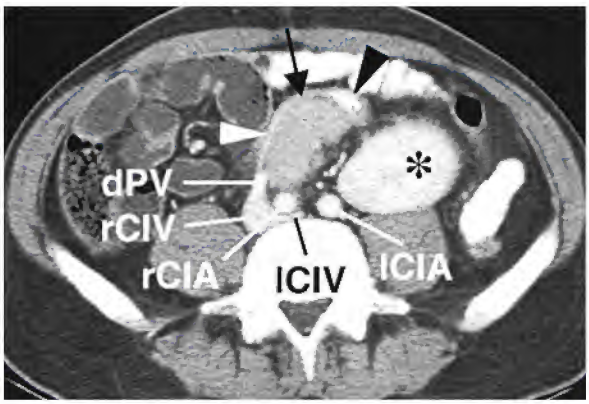

a

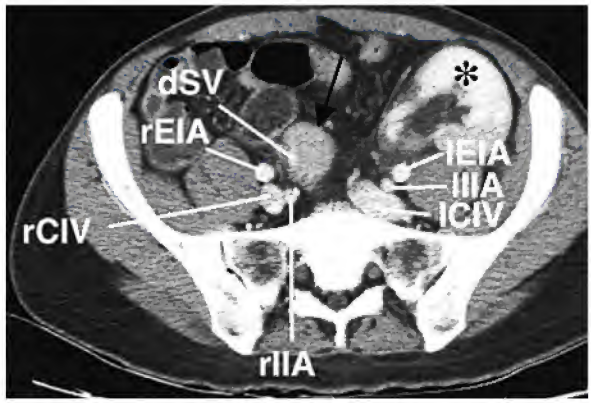

c

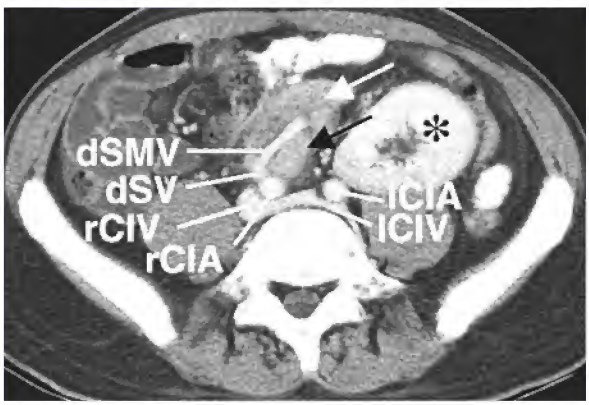

b

Fig. 7.5a–c. A 40-year-old man; image obtained 14 days after simultaneous pancreas–kidney transplantation. (CIA Common iliac artery, CIV common iliac vein, d donor's, EIA external iliac artery, IIA internal iliac artery, l left, PV portal vein, r right, SMV superior mesenteric vein, SV splenic vein). Annotations: pancreatic graft (*black arrow*), renal graft (*black asterisk*). **a–c** Contrast-enhanced multidetector CT during dominant parenchymal phase at level of venous anastomosis (a), cephalad (b) and caudad (c) to venous anastomosis displays normal posttransplant venous anatomy, homogeneous enhancement of pancreatic graft (*black arrow*), donor's normal duodenum with hyperdense staple line (*black arrowhead*), hyperdense mesenteric staple line (white arrowhead), and intermediate density of donor's mesenteric fat (*white arrow*) at level of superior mesenteric vein (b)

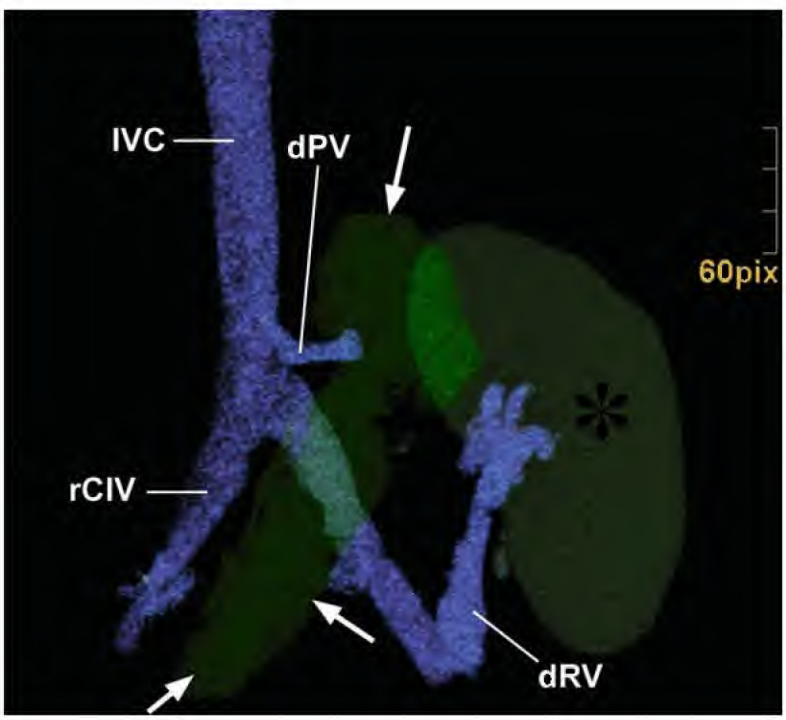

Fig. 7.6. A 28-year-old man; image obtained 3 weeks after simultaneous pancreas-kidney transplantation with systemic venous drainage. 3D volume-rendering display of contrast-enhanced MDCT during dominant venous phase shows normal posttransplant venous anatomy. (CIV Common iliac vein, d donor's, IVC inferior vena cava, PV portal vein, r right, RV renal vein.) Annotations: pancreatic graft (*arrow*), renal graft (*black asterisk*)

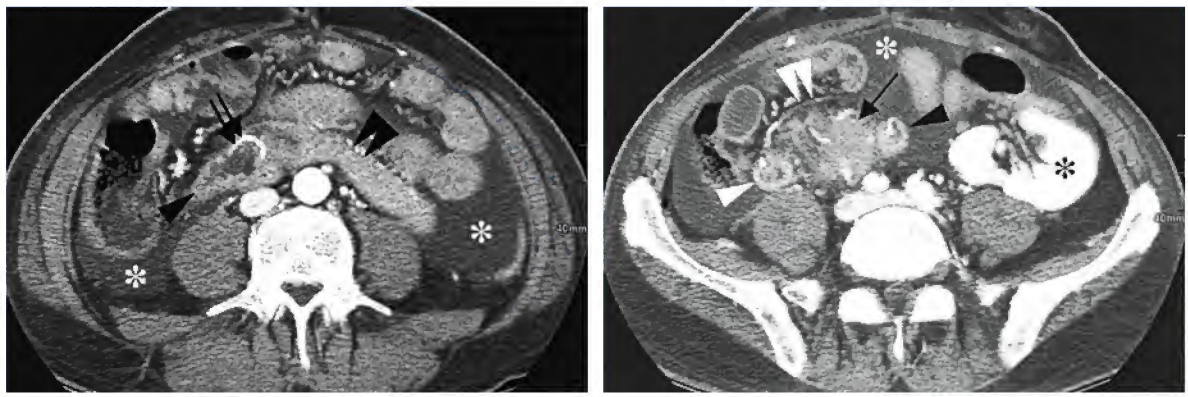

Fig. 7.7a,b. A 58-year-old man; image obtained 9 days after sequential pancreas-after-kidney transplantation. **a** Contrast-enhanced multidetector CT shows normal side-to-side duodenojejunostomy with hyperdense, circular staple line (*arrows*), donor's duodenum (*black arrowhead*), recipient's jejunum (*black arrowheads*), and ascites (*white asterisk*). **b** Contrast-enhanced multidetector CT 5 cm caudal of duodenojejunostomy displays donor's duodenum closed proximally (*black arrowhead*) and distally (*white arrowhead*) with hyperdense staple line, hyperdense mesenteric staple line (*arrowheads*), pancreatic graft (*arrow*), renal graft (*black asterisk*) and ascites (*white asterisk*)

Fig. 7.8. A 42-year-old man; image obtained 7 days after simultaneous pancreas-kidney transplantation. Small bowel follow-through examination with water-soluble contrast material shows duodenojejunostomy (*single arrow*) and partly contrasted donor's duodenum (*arrowheads*). Contrast-filled small bowel loops and partially air-filled descending colon indirectly outline pancreas graft. Also seen are radiopaque cutaneous staples (*double arrows*) resulting from median laparotomy

Fig. 7.9. An 18-year-old man; image obtained 15 days after simultaneous pancreas-kidney transplantation. Coronal T2-weighted turbo spin-echo MRI displays normal pancreatic graft (*arrow*) in pelvis. Annotation: renal graft (*black asterisk*)

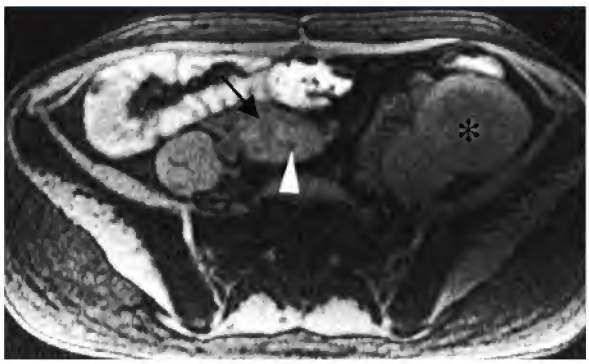

a

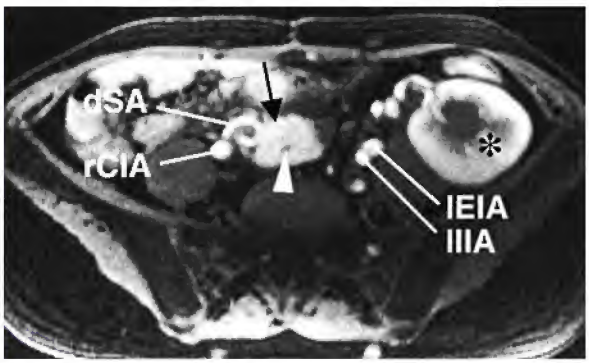

b

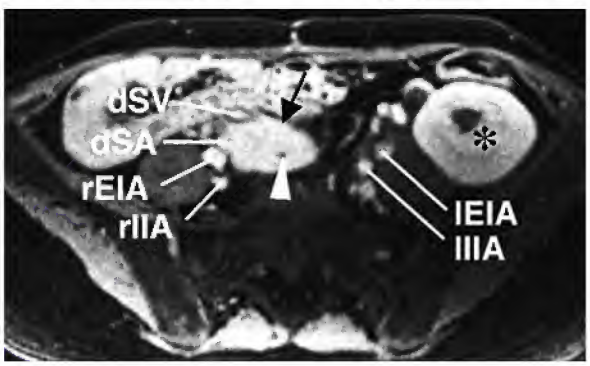

c

d

Fig. 7.10a–d. A 25-year-old woman; image obtained 14 days after simultaneous pancreas-kidney transplantation. (CIA common iliac artery, d donor's, EIA external iliac artery, IIA internal iliac artery, l left, r right, SA splenic artery, SV splenic vein). Annotations: pancreatic graft (*black arrow*), renal graft (*black asterisk*). **a–c** MRI with fat-suppressed T1-weighted gradient-echo sequences without contrast enhancement (a) and with contrast enhancement during dominant arterial phase (b) and during dominant parenchymal phase (c) show normal vascular anatomy, homogeneous parenchymal enhancement of pancreatic graft (arrow), and major pancreatic duct (*arrowhead*). **d** MR pancreaticography shows vertically oriented major pancreatic duct (*arrow*), donor's duodenum (*between arrowhead and arrowheads*) and ascites (*white asterisk*) in pelvis

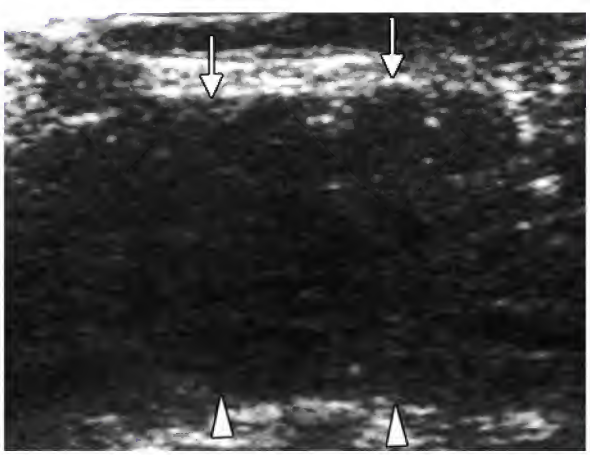

a

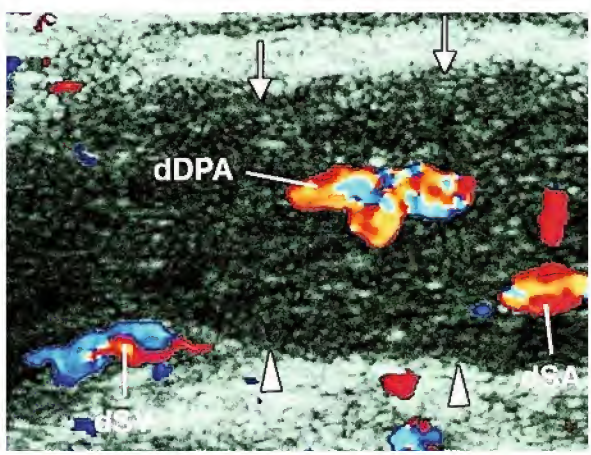

b

Fig. 7.11a,b. A 40-year-old woman; image obtained 63 months after a simultaneous pancreas-kidney transplantation. (d Donor's, DPA dorsal pancreatic artery, SA splenic artery). **a** High-resolution sonography (longitudinal section) displays normal hypoechogeneic parenchyma of pancreatic graft (*between arrow and arrowhead*). **b** Color-coded sonography (longitudinal section) shows normal arterial and venous anatomy to better advantage

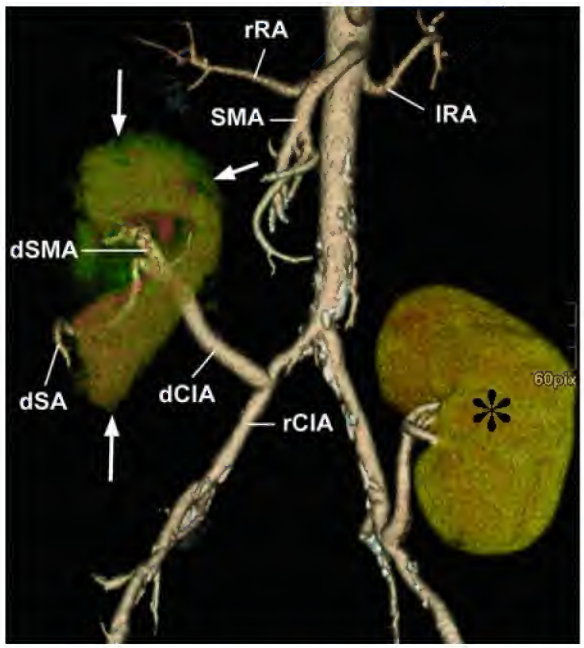

a

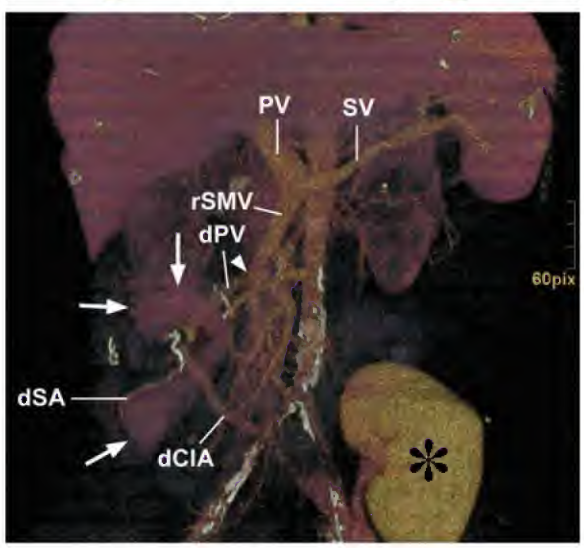

b

Fig. 7.12a,b. A 41-year-old woman; image obtained 5 weeks after simultaneous pancreas-kidney transplantation with enteric exocrine drainage and portal endocrine drainage. (*d* donor's, *CIA* common iliac artery, *l* left, *r* right, *RA* renal artery, *SA* splenic artery, *SMA* superior mesenteric artery.). Annotations: pancreatic graft (*arrow*), renal graft (*asterisk*). **a** Three-dimensional volume-rendering image of contrast-enhanced MDCT during dominant arterial phase. Arterial revascularization of segmental pancreatic graft was performed with long segment of donor's common iliac artery to recipient's right external iliac artery and systemic endocrine drainage (not shown). **b** Three-dimensional volume-rendering image of contrast-enhanced MDCT during dominant portal–venous phase. Venous revascularization was performed with donor's portal vein to recipient's superior mesenteric vein

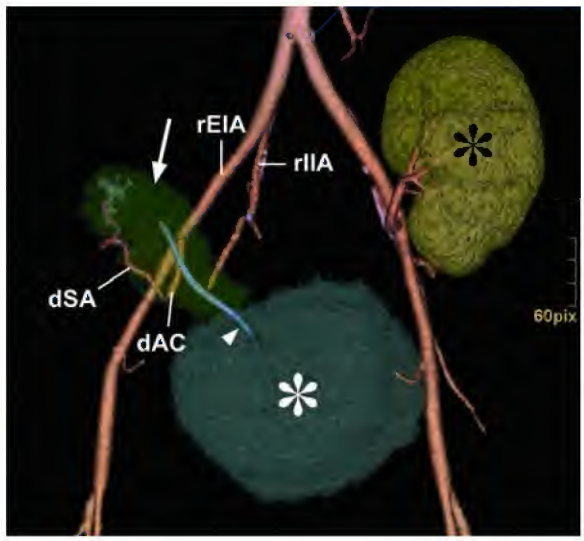

Fig. 7.13. A 33-year-old woman with history of segmental pancreas transplantation with vesical exocrine drainage. Three-dimensional volume-rendering image of contrast-enhanced MDCT during dominant arterial phase obtained after 20 days after simultaneous pancreas-kidney transplantation. Arterial revascularization of segmental pancreatic graft was performed with donor's arterial conduit to recipient's right external iliac artery and systemic endocrine drainage (not shown). (*AC* Arterial conduit, *d* donor's, *EIA* external iliac artery, *IIA* internal iliac artery, *r* right, *white asterisk* urinary bladder.) Annotations: segmental pancreatic graft (*arrow*), pancreatic vesical splint (*arrowhead*), renal graft (*black asterisk*)

7.8 Vascular Graft Complications Including Rejection

The most serious vascular complication is venous and arterial graft thrombosis and results in pancreatic graft necrosis and pancreatectomy in the majority of cases. Typically, contrast-enhanced CT displays an intraluminal filling defect in the larger graft veins (Fig. 7.14). Arterial thrombosis results in complete occlusion of the vessel with non-enhancement of the parenchymal graft indicating graft necrosis (Fig. 7.15). Further progression can result in an emphysematous transformation of the pancreatic graft; in a patient without clinical signs of local infection or sepsis this is described as an innocuous gas collection in the pancreatic graft (Vas et al. 1989). But image-guided biopsy represents the only definite test to distinguish an infected from non-infected pancreatic graft with

gas collection (Fig. 7.16). Risk factors for early graft loss due to arterial occlusion after pancreas transplantation are mainly posed by technical complications involving back-table preparation or the vascular anastomosis in the recipient. In the later course graft loss due to arterial occlusion represents the endpoint of graft rejection due to alloimmune vasculitis, resulting in occlusion of small vessels, progressing to larger vessels and finally involving the anastomosed greater donor's vessels (Krebs et al. 1999). For this reason, dynamic contrast-enhanced MRI appears to be a promising means of assessing parenchymal enhancement in order to detect early changes of vascular rejection (Krebs et al. 1999); other MRI protocols or other imaging modalities including sonography, color-coded sonography and contrast-enhanced CT did not meet expectations. However, considering the absence of reliable clinical markers and the persistent uncertainty regarding imaging examinations, image-guided biopsy of the pancreatic graft (Fig. 7.17) still represents the gold standard for the diagnosis of graft rejection (Lee et al. 2000).

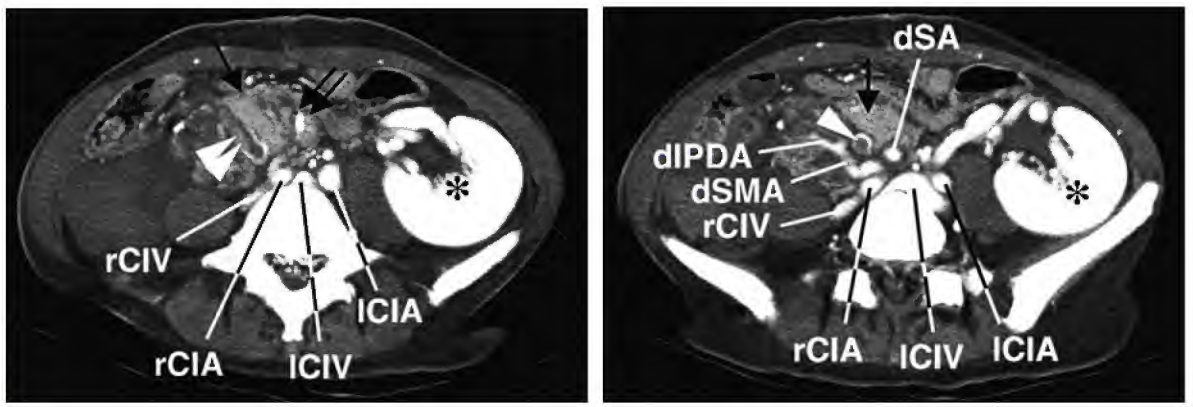

a b

Fig. 7.14a,b. A 43-year-old woman with abdominal discomfort; image obtained 12 days after simultaneous pancreas–kidney transplantation. **a**, **b** Contrast-enhanced multidetector CT displays acute thrombosis of superior mesenteric vein (*arrowheads*) and splenic vein (*arrowhead*) but homogeneous contrast enhancement of pancreatic graft (*arrow*) with donor's duodenum (*arrows*) and renal graft (*asterisk*). (*CIA* common iliac artery, *CIV* common iliac vein, *d* donor's, *IPDA* inferior pancreaticoduodenal artery, *l* left, *r* right, *SA* splenic artery, *SMA* superior mesenteric artery)

a b

Fig. 7.15a,b. A 36-year-old woman with newly developed hyperglycemia, graft necrosis and subsequent graft pancreatectomy; image obtained 8 months after pancreas transplantation alone. **a** Contrast-enhanced multidetector CT during dominant arterial phase shows enhancement of donor's arterial conduit (*arrowhead*) but non-visualization of graft arteries and non-enhancement of pancreas graft (*arrow*) indicating arterial occlusion and absent parenchymal perfusion. (*CIA* Common iliac artery, *l* left, *r* right.) **a** Angiogram verifies CT findings with residual enhancement of donor's arterial conduit (*arrowhead*) but non-visualization of graft arteries and absent parenchymal enhancement of pancreatic graft

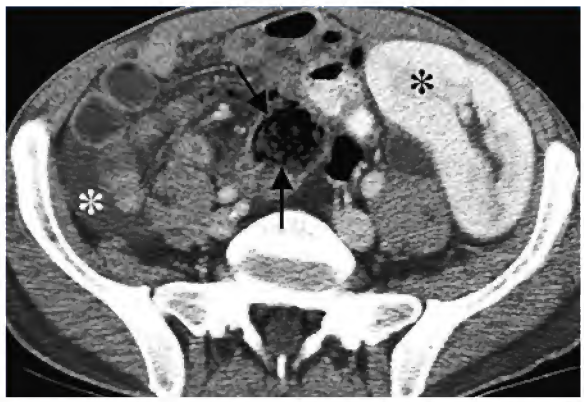

Fig. 7.16. Image from a 44-year-old man obtained 9 months after simultaneous pancreas–kidney transplantation with graft necrosis but without local infection or sepsis and subsequent graft extirpation. Contrast-enhanced multidetector CT shows absent parenchymal enhancement and emphysematous transformation of pancreatic graft (*arrow*) consistent with innocuous gas collection. Annotation: renal graft (*black asterisk*) and ascites (*white asterisk*)

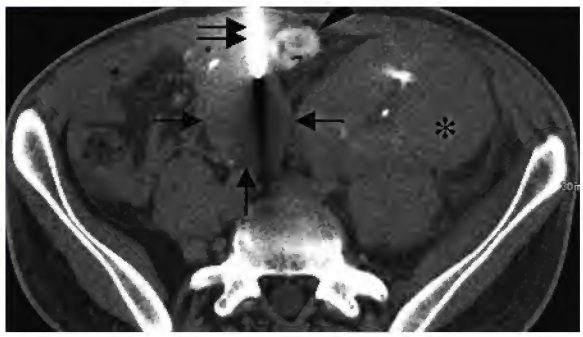

Fig. 7.17. Image from a 33-year-old man obtained 20 months after simultaneous pancreas–kidney transplantation with pancreatic graft dysfunction and acute rejection verified by histopathological examination. Helical CT is used for image-guided percutaneous biopsy (*arrows*) of pancreatic graft (*arrow*) adjacent to contrast-medium-filled small bowel (*arrowhead*) and renal graft (*asterisk*)

7.9 Pancreatic Graft Complications Including Infection

Complications of the pancreatic graft itself are an important cause of morbidity in the early posttransplant period. These complications include pancreatitis, pseudocyst formation including expansion, infection with abscess formation, pseudoaneurysm formation, leakage of the enteric anastomosis or duodenal stump, and small bowel obstruction. Self-limited edematous pancreatitis (Fig. 7.18) occurs preferentially in the early posttransplant period due to reperfusion injury and typically involves the entire graft. Focal edematous swelling of the donor's remaining mesenteric fat attached to the superior mesenteric arterial stump should not be misdiagnosed as focal edematous pancreatitis (Fig. 7.19); presumably this condition results from ligation of the donor's lymphatic vessels. Necrotizing pancreatitis is the most severe form of pancreatitis (Fig. 7.20) and necessitates graft pancreatectomy. Pseudocyst formation develops later in the clinical course after onset of graft pancreatitis and can occur in various sizes, contours, and septations inside or outside the pancreatic graft. Sonography is the imaging modality of choice for large pseudocysts (Fig. 7.21), whereas complex pseudocysts (Fig. 7.22), infected pseudocysts (Fig. 7.23a) as well as percutaneous catheter drainage of pseudocysts (Fig. 7.23b) are best imaged by contrast-enhanced CT (Patel et al. 1991). Infection of pseudocysts after pancreas transplantation is a frequent occurrence and can cause pseudoaneurysm formation in arteries (Fig. 7.24) and veins (Tan et al. 2002). Finally, fistula formation can result from pancreatitis with communication to the skin (Fig. 7.23c) or peritoneal cavity (Fig. 7.24), and sinus tract formation can involve the retroperitoneum (Figs. 7.25, 7.26) and gut (Fig. 7.26).

Enteric complications manifest either as leakage of the duodenojejunostomy or duodenal stump with ensuing abscess and peritonitis or sometimes as volvulus from twisting of the small bowel around the longitudinal axis of the graft (Fig. 7.27).

7.10 Other Transplantation-Associated Complications

Pseudothrombosis of the iliac vein (Fig. 7.28) has been described following simultaneous pancreas–kidney transplantation with bilateral revascularization to the respective iliac vessels (Gupta et al. 2002). Pseudothrombosis results from delayed venous opacification of the iliac vein ipsilateral to the pancreatic graft as compared to the contralateral side of the renal graft. This phenomenon results from longer transit time and reduced blood flow to the pancreas as compared to the kidney. Pseudothrombosis can also involve the ipsilateral iliac vein below the vascular anastomoses of the pancre-

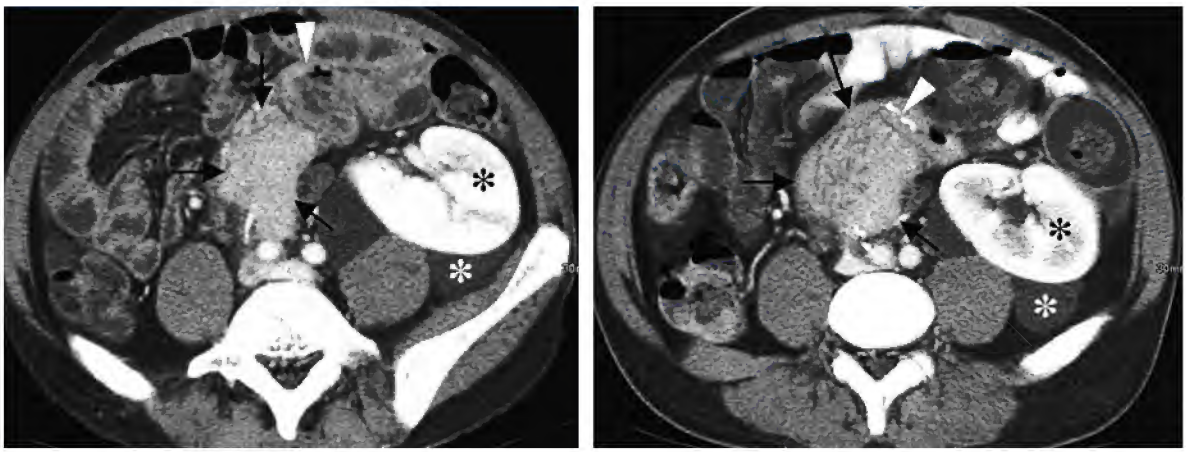

a b

Fig. 7.18a,b. Image from a 40-year-old man obtained 16 days after simultaneous pancreas–kidney transplantation and graft pancreatitis. Annotations: pancreatic graft (*arrow*), donor's duodenum (*arrowhead*), renal graft (*black asterisk*), and perirenal fluid (*white asterisk*). **a** Contrast-enhanced multidetector CT shows homogeneous contrast enhancement of pancreatic graft (*arrow*). **b** Contrast-enhanced multidetector CT performed 5 days after initial CT displays inhomogeneous contrast enhancement and increasing size of pancreatic graft (*arrow*) indicating edematous pancreatitis

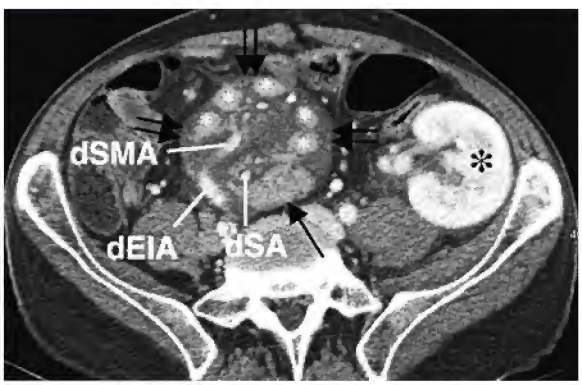

Fig. 7.19. Image from a 51-year-old man obtained 4 weeks after simultaneous pancreas–kidney transplantation. Contrast-enhanced multidetector CT shows edematous swelling of donor's remaining mesenteric fat (*arrows*) and lymph nodes (*white asterisk*) attached to unremarkable, homogeneous contrast-enhancing pancreatic graft (*arrow*). Condition presumably results from ligature of donor's lymphatic vessels. CT also shows normal enhancement of donor's (*d*) vessels including superior mesenteric artery (*SMA*), external iliac artery (*EIA*), splenic artery (*SA*) and renal graft (*black asterisk*)

Fig. 7.20. Image from a 38-year-old man obtained 5 weeks after simultaneous pancreas–kidney transplantation with necrotizing graft pancreatitis and subsequent graft extirpation. Contrast-enhanced helical CT displays remnants of contrast-enhanced pancreatic graft (*arrow*) surrounded by fluid and thin-walled membrane (*arrowhead*) representing pseudocyst formation due to necrotizing pancreatitis. Ascites (*white asterisk*) and renal graft (*black asterisk*) are also seen

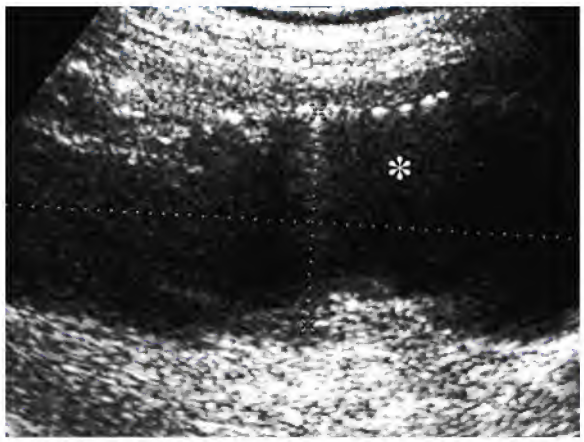

Fig. 7.21. Image from a 54-year-old man obtained 5 months after simultaneous pancreas–kidney transplantation with graft pancreatitis and pseudocyst formation. Sonography shows large, partly septated cyst (*white asterisk*) adjacent to pancreatic graft (not shown) consistent with peripancreatic pseudocyst

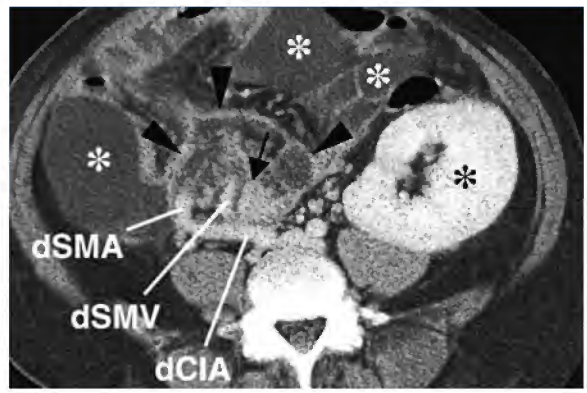

Fig. 7.22. Image from a 34-year-old woman obtained 5 months after simultaneous pancreas-kidney transplantation with exudative pancreatitis and pseudocyst formation. Contrast-enhanced helical CT displays homogeneous enhancement of small pancreatic graft (*arrow*) surrounded by thin-walled peripancreatic pseudocyst (*arrowhead*) and various intra-abdominal pseudocysts (*white asterisk*). Annotations: renal graft (*black asterisk*). (*CIA* Common iliac artery, *d* donor's, *SMA* superior mesenteric artery, *SMV* superior mesenteric vein)

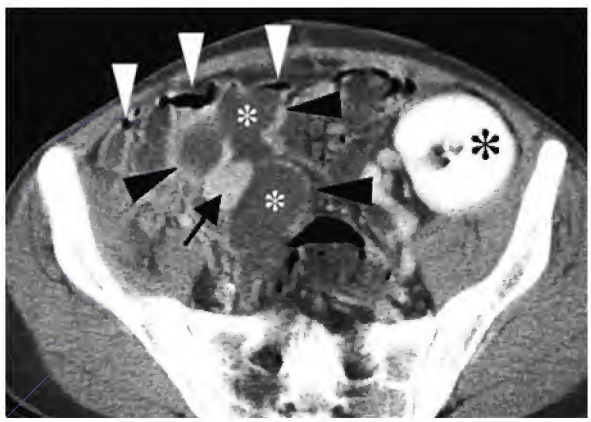

a

b

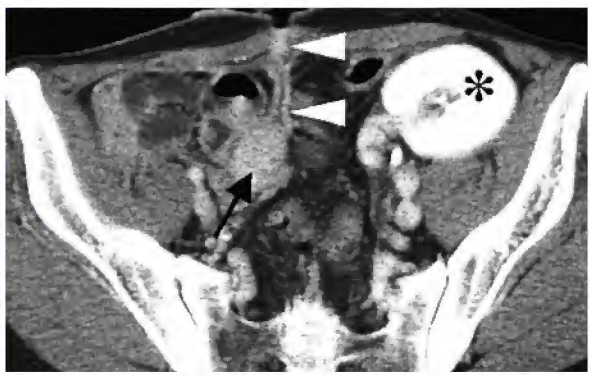

c

Fig. 7.23a–c. Images from a 27-year-old man obtained 4 weeks after simultaneous pancreas–kidney transplantation with infected peripancreatic pseudocyst requiring percutaneous drainage, and pancreatic–cutaneous fistula. **a** Contrast-enhanced helical CT shows homogeneous contrast enhancement of pancreatic graft (*arrow*) surrounded by septated, peripancreatic fluid collection (*white asterisk*) combined with air-fluid level (*white arrowhead*) and thin, contrast-enhanced wall (*black arrowhead*) consistent with infected pseudocyst. Annotation: renal graft (*black asterisk*). **b** Subsequent CT-guided percutaneous drainage was performed with pigtail catheter (*arrows*) for treatment of infected peripancreatic pseudocyst. Pancreatic graft (*arrow*) and renal graft (*asterisk*) are seen. **c** Contrast-enhanced helical CT performed 10 weeks after initial CT, after CT-guided percutaneous drainage and ultimately operative debridement of recurrently infected pseudocyst, shows pancreatic–cutaneous fistula (*arrowhead*) originating from pancreatic graft (*arrow*). Annotation: renal graft (*asterisk*)

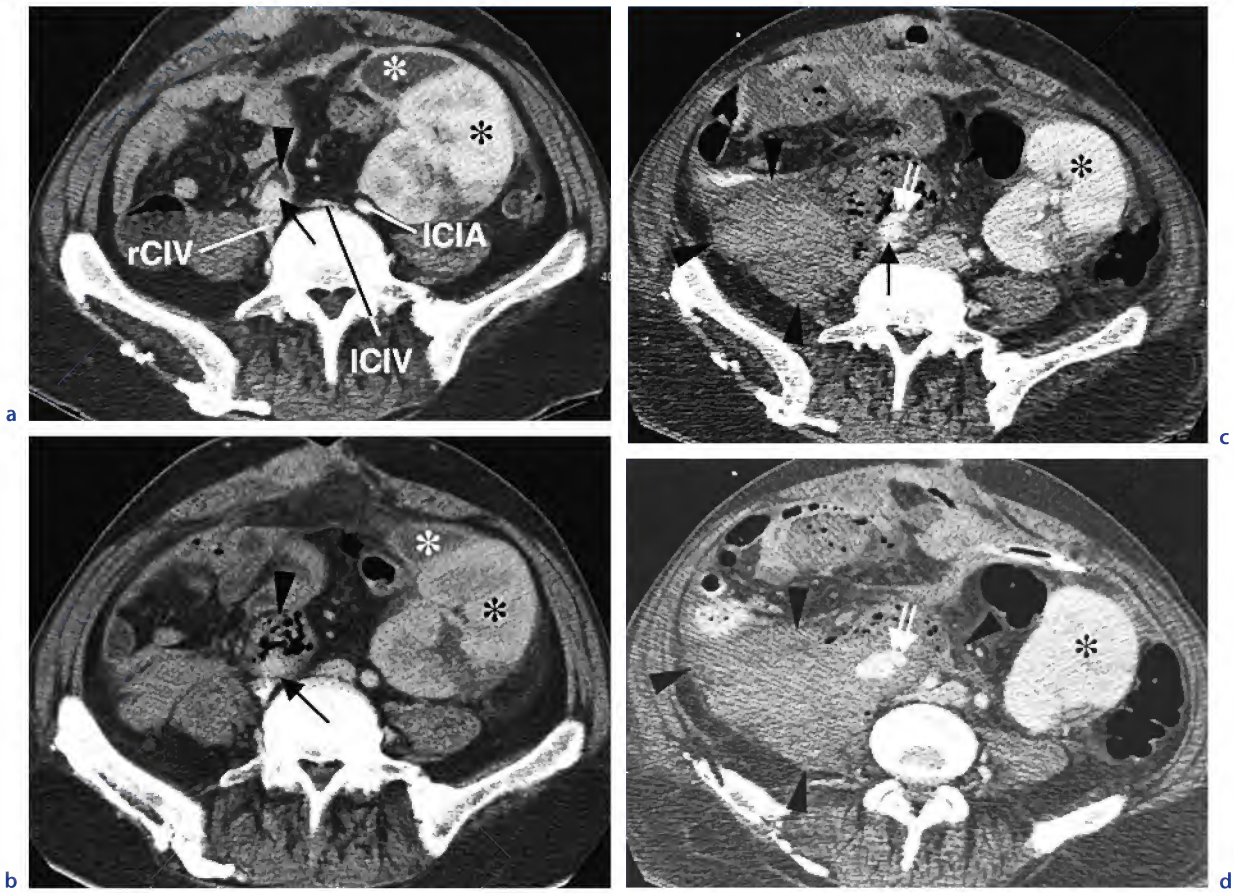

Fig. 7.24a–d. Image from a 50-year-old man obtained 18 days after simultaneous pancreas–kidney transplantation and after pancreatic graft extirpation (5 days after operation) due to infected graft pancreatitis with localized retroperitoneal and intra-abdominal abscesses, and subsequent surgical arterial repair of symptomatic mycotic pseudoaneurysm. **a** Contrast-enhanced helical CT shows residual donor's arterial conduit (*arrow*) after pancreatic graft extirpation surrounded by small fluid collection with thin-walled contrast-enhanced membrane (*arrowhead*). Also residual fluid collection (*white asterisk*) in perirenal location is seen. (*CIA* Common iliac artery, *CIV* common iliac vein, *l* left, *r* right.) Annotation: renal graft (*black asterisk*). **b** Contrast-enhanced multidetector CT with dominant late parenchymal phase performed 9 days after initial CT displays donor's residual arterial conduit (*arrow*) and newly developed emphysematous transformation (*arrowhead*) of adjacent fluid collection, indicating recurrent abscess. Decrease in fluid (*white asterisk*) adjacent to renal graft (*black asterisk*) is noted. **c, d** Contrast-enhanced multidetector CT performed 12 days after initial CT shows newly developed mycotic pseudoaneurysm (*arrows*) originating from donor's arterial conduit (*arrow*) and recently developed large retroperitoneal hematoma (*arrowhead*). Annotation: renal graft (*black asterisk*)

Fig. 7.25. Image from a 29-year-old man obtained 3 weeks after simultaneous pancreas-kidney transplantation with infected peripancreatic pseudocyst and complex pancreatic-cutaneous fistula. Drainage catheter (*arrows*) was placed through a cutaneous fistula opening, and sonogram displays large central cavity (*arrow*) with communication to peritoneal cavity (*black arrowhead*) and sinus tracts (*white arrowhead*) in retroperitoneal location

atic graft due to more peripheral implantation of the renal graft on the contralateral side and longer transit time of the lower extremity as compared to the renal graft. Posttransplant lymphoproliferative disorder (Fig. 7.29) is a serious but rare complication of pancreas transplantation. It manifests predominantly as a diffuse enlargement of the pancreatic graft, which is indistinguishable from acute pancreatitis for imaging modalities, or rarely as intra- or extra-allograft focal masses, lymphadenopathy or organomegaly (Meader et al. 2000).

A comprehensive pictorial essay of imaging findings after pancreas transplantation with enteric exocrine drainage was published by the authors of this book chapter (Freund et al. 2004a, 2004b).

7.11 Introduction to Intestinal Transplantation

Intestinal transplantation represents an alternative in patients with irreversible, chronic intestinal failure in order to restore enteral absorption of ingested food and fluid. In adults the most common cause of chronic intestinal failure results from extensive resection of the small bowel due to occlusion of the superior mesenteric vessels, inflammatory bowel disease, or abdominal trauma. In children the causes of short-

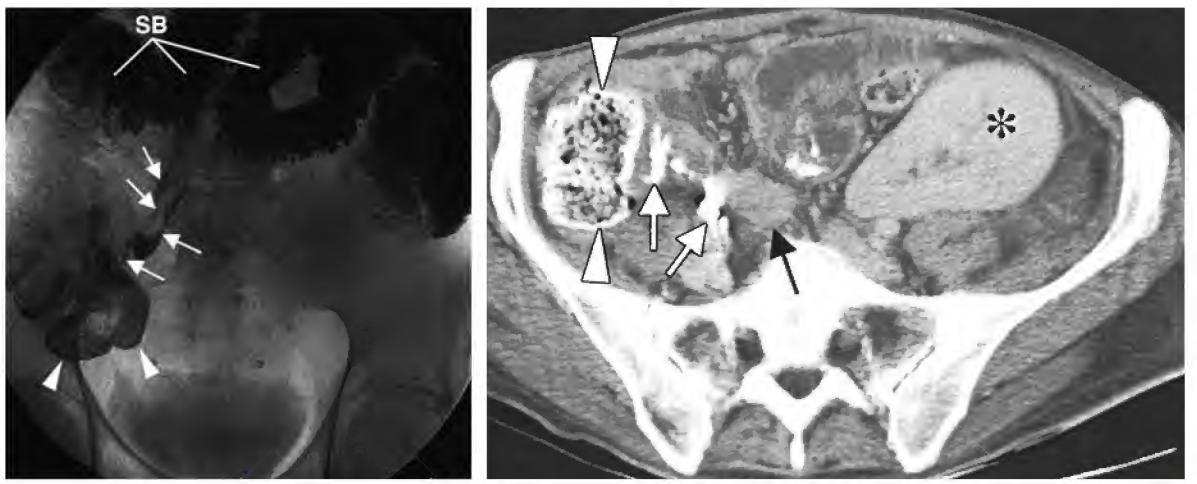

Fig. 7.26a,b. Image from a 43-year-old man obtained 10 weeks after simultaneous pancreas-kidney transplantation complicated by pancreatitis, infection of peripancreatic pseudocyst, and subsequent surgical debridement and drainage tube placement. **a** Spot film during small bowel follow-through examination shows contrast-filled small bowel loops (*SB*), cecum (*arrowhead*) and two partly contrast-filled sinus tracts (*arrow*) opening to cecum. **b** Contrast-enhanced helical CT confirms retroperitoneal location of partly contrast-filled sinus tracts (*white arrow*) adjacent to cecum (*arrowhead*) and pancreatic graft (*black arrow*), indicating previously existing pancreatic-colic fistula. Annotation: renal graft (*asterisk*)

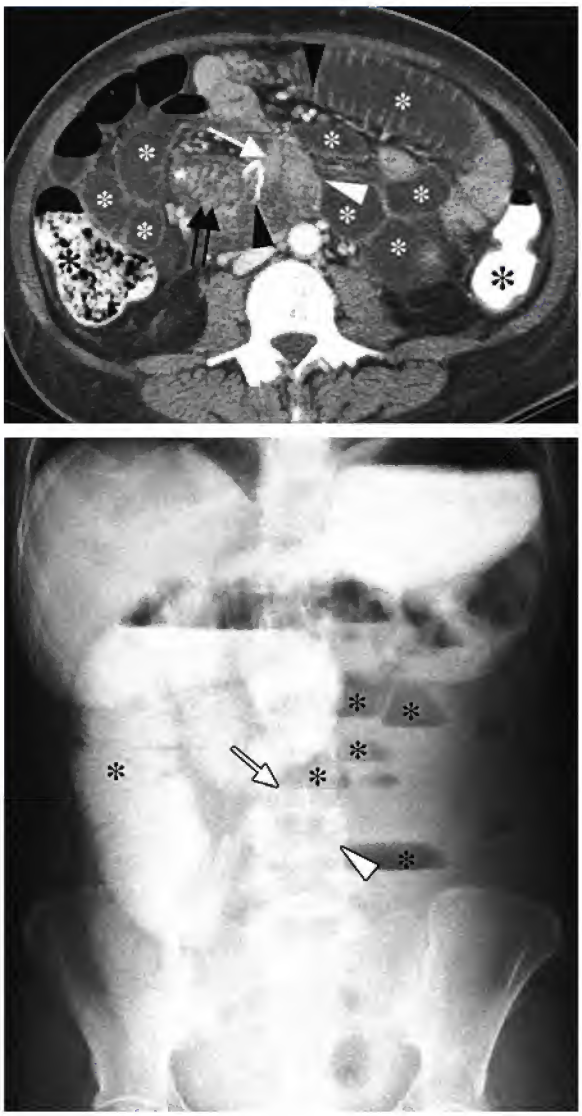

Fig. 7.27a,b. Image from a 39-year-old woman obtained 14 days after simultaneous pancreas-kidney transplantation with clinical signs of upper intestinal obstruction due to intermittent small bowel volvulus and subsequent surgical reduction. **a** Contrast-enhanced multidetector CT shows prestenotic, dilated, fluid-filled loops of small bowel (*white asterisk*), twisted segment of small bowel (*between arrow and arrowhead*) consisting of collapsed loop of small intestine located adjacent to donor's duodenum (*arrows*) with hyperdense staple line (*arrowhead*), and poststenotic, non-dilated colon (*black asterisk*) filled with intraluminal contrast material from prior unremarkable small bowel follow-through. **b** Upright abdominal radiograph after repeat small bowel follow-through with water-soluble contrast material verifies mechanical small bowel obstruction at level of presumed location of head of pancreatic graft (*between arrow and arrowhead*) with dilatation and pathological air-fluid levels of partly contrast-filled, prestenotic small intestinal loops (*asterisk*) including stomach

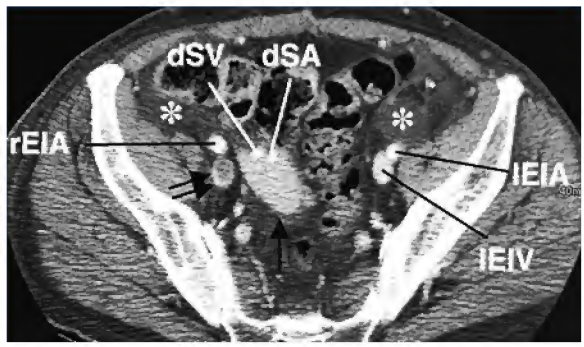

Fig. 7.28. Image from a 54-year-old man obtained 9 months after simultaneous pancreas-kidney transplantation. Contrast-enhanced multidetector CT shows pseudothrombosis of right external iliac vein (*arrows*) as compared to left side. This is due to delayed venous opacification on right side resulting from longer transit time and reduced blood flow of right-sided pancreatic graft as compared to left-sided renal graft, as well as due to more peripheral implantation of renal graft and longer transit time of the lower extremity as compared to renal graft. Homogeneous contrast enhancement of pancreatic graft (*arrow*) and ascites (*white asterisk*) is seen. (*d* Donor's, *EIA* external iliac artery, *EIV* external iliac vein, *l* left, *r* right, *SA* splenic artery, *SV* splenic vein)

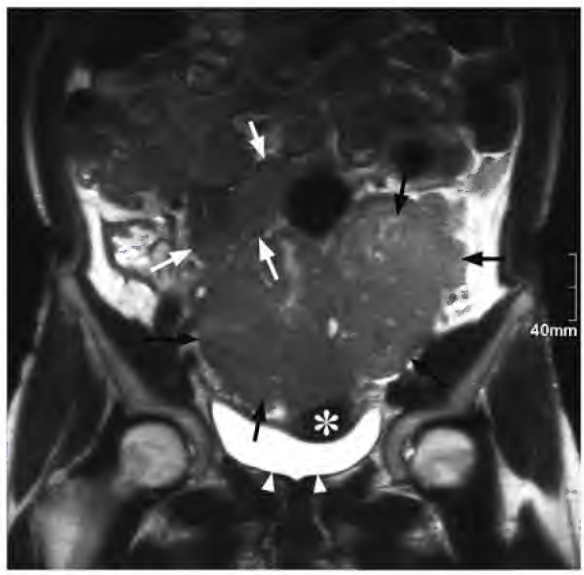

Fig. 7.29. Image from a 45-year-old woman after sequential pancreas-after-kidney transplantation with enteric exocrine drainage and systemic endocrine drainage. Coronal T2-weighted turbo spin-echo MRI obtained 16 years after kidney transplantation and 7 years after pancreas transplantation shows soft tissue mass (*black arrow*) between displaced pancreatic graft (*white arrow*), uterus (*white asterisk*) and urinary bladder (*arrowhead*). Histologic evaluation of image-guided biopsy (not shown) revealed CD20-positive, EBV-negative diffuse large B-cell lymphoma consistent with posttransplantation lymphoproliferative disorder (*PTLD*)

bowel syndrome are midgut volvulus, gastroschisis, intestinal atresia, and necrotizing enterocolitis. Infrequently intestinal failure results from permanent intestinal dysfunction despite normal intestinal length. This occurs more frequently in children and includes aganglionosis, malabsorption syndromes, particularly microvillus inclusion disease, and motility disorders, particularly intestinal pseudo-obstruction (Mazariegos and Kocoshis 1998). Intestinal transplantation with ciclosporin-based immunosuppression started in the 1980s in North America (Cohen et al. 1986) and Europe (Deltz et al. 1989) and was followed by multivisceral transplantation (Starzl et al. 1989; Margreiter et al. 1992) and liver–intestinal transplantation (Grant et al. 1990). Isolated intestinal transplantation is indicated for patients with irreversible intestinal failure without liver dysfunction and serious total parenteral nutrition-related complications, mostly lack of venous access due to recurrent thrombosis. Liver–intestinal transplantation is primarily indicated for patients with intestinal failure and total parenteral nutrition-related cholestatic liver failure. Multivisceral transplantation is indicated for patients with irreversible failure of small bowel and liver combined with portomesenteric thrombosis or Gardner's syndrome with intra-abdominal desmoid tumor (Furukawa et al. 1998).

Proper interpretation of imaging studies after transplantation depends on familiarity with surgical anatomy (Bach et al. 1991, 1992; Campbell et al. 1993, 1995; Furukawa et al. 1998). For this reason this pictorial essay schematically illustrates the intraoperative appearance during the most important steps of the main intestinal transplantation procedures performed in children and adults. Each procedure is supplemented with examples of typical anatomy as shown by various imaging modalities including sonography, CT, MRI, gastrointestinal contrast examination, and angiography.

The various procedures of small bowel transplantation are described and illustrated in the following order: intestinal, multivisceral, and liver–intestinal transplantation.

7.12 Intestinal Transplantation

In order to understand the postoperative anatomy the time sequence of isolated transplantation of the small bowel is schematically shown in a cadaveric donor (Fig. 7.30) (Furukawa et al. 1998) although living-related intestinal transplantation has already been performed (Gruessner and Sharp 1997). During procurement the size-matched donor small bowel together with an arterial and venous main stem are excised. The ileum is transected proximal to the ileocecal valve and the jejunum is divided close to the Treitz ligament; especially the ileal branches of the ileocolic artery should be preserved. If the pancreas is not to be used as a graft, the origin of the superior mesenteric artery is excised. The splenic vein is transected next to the venous confluence and the portal vein is transected above the confluence of the superior mesenteric and splenic veins. In the case of pancreas procurement the superior mesenteric vein is transected at the lower rim of the pancreas. In the recipient all adhesions from previous surgical procedures are dissected and the infrarenal abdominal aorta as well as the venous confluence or inferior vena cava are exposed. In the case of orthotopic transplantation the intestinal allograft is revascularized in an end-to-side fashion connecting the donor superior mesenteric artery to the recipient infrarenal abdominal aorta above the origin of the inferior mesenteric artery, and the donor superior mesenteric vein to the recipient superior mesenteric vein or portal vein. In the case of heterotopic transplantation vascular continuity is restored in end-to-side fashion connecting the donor superior mesenteric artery to the recipient infrarenal abdominal aorta below the origin of the inferior mesenteric artery or common iliac artery and the donor superior mesenteric vein to the recipient inferior vena cava or common iliac vein. Proximal intestinal continuity is established between the most distal level of the recipient upper gastrointestinal remnant and the donor jejunum, duodenum, or stomach. A gastrojejunal anastomosis is usually performed in end-to-side fashion. The type of duodenojejunal or jejunojejunal anastomosis, either end-to-end or side-to-side, is dictated by anatomic and surgical considerations. The distal enteric anastomosis varies depending on recipient anatomy. In patients with an intact terminal ileum, an ileoileal anastomosis can be performed, which preserves the ileocecal valve. In patients with only parts of the colon remaining, the donor ileum can be anastomosed to the residual recipient colon. In every case a temporary ileostomy is performed

for direct inspection of graft mucosa and for access of surveillance endoscopy and biopsies; it is surgically closed 3–6 months after transplantation. For patients with previous proctocolectomy a terminal ileostomy is performed.

Typical examples of regular anatomy are shown below using CT, catheter angiography, and gastrointestinal contrast studies (Figs. 7.31–7.35).

7.13 Multivisceral Transplantation

A multivisceral graft usually employs the liver, pancreas, part of the stomach, duodenum, and small bowel (Fig. 7.36) (Starzl et al. 1989; Margreiter et al. 1992). During explantation the various donor

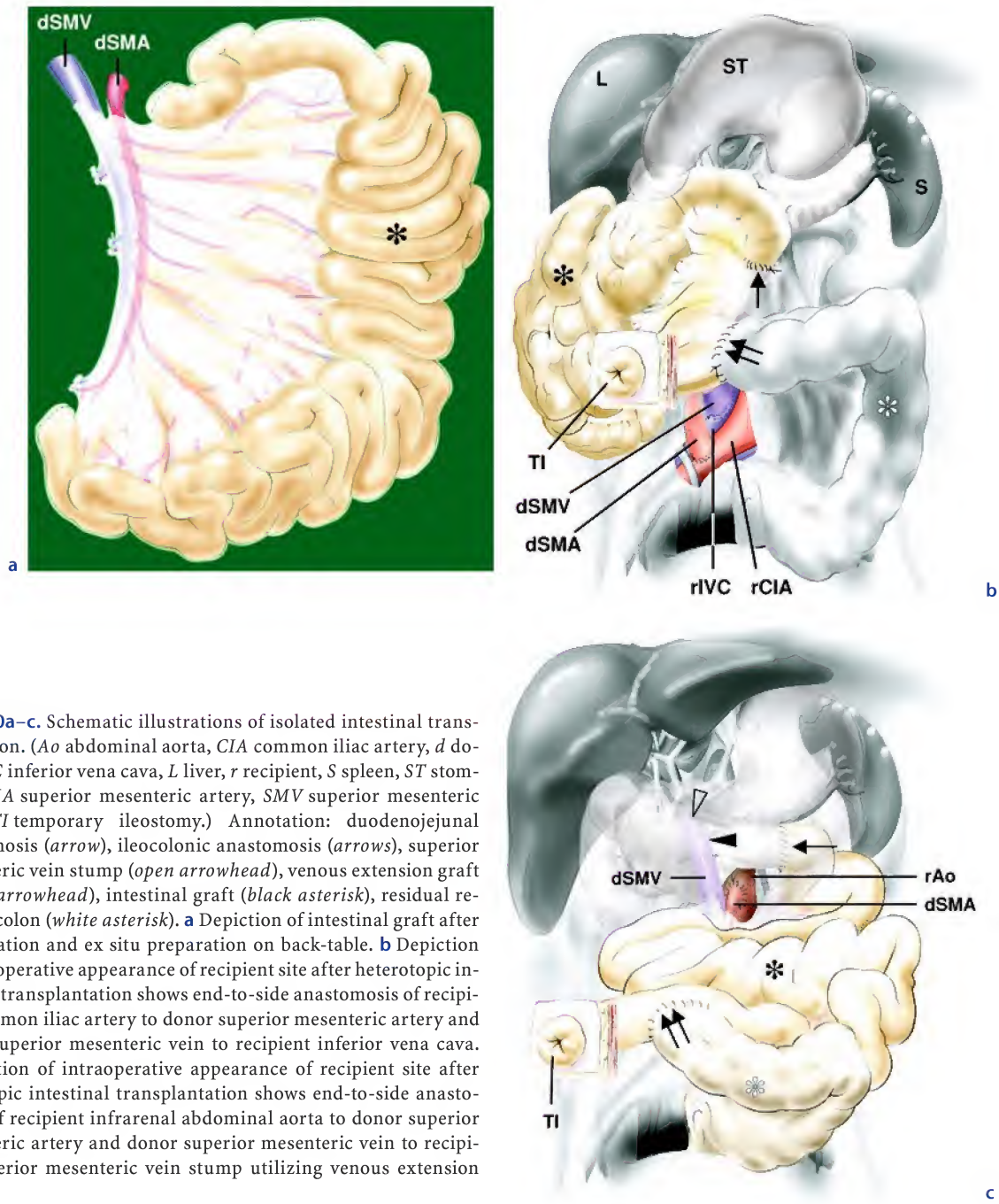

Fig. 7.30a–c. Schematic illustrations of isolated intestinal transplantation. (*Ao* abdominal aorta, *CIA* common iliac artery, *d* donor, *IVC* inferior vena cava, *L* liver, *r* recipient, *S* spleen, *ST* stomach, *SMA* superior mesenteric artery, *SMV* superior mesenteric vein, *TI* temporary ileostomy.) Annotation: duodenojejunal anastomosis (*arrow*), ileocolonic anastomosis (*arrows*), superior mesenteric vein stump (*open arrowhead*), venous extension graft (*closed arrowhead*), intestinal graft (*black asterisk*), residual recipient colon (*white asterisk*). **a** Depiction of intestinal graft after explantation and ex situ preparation on back-table. **b** Depiction of intraoperative appearance of recipient site after heterotopic intestinal transplantation shows end-to-side anastomosis of recipient common iliac artery to donor superior mesenteric artery and donor superior mesenteric vein to recipient inferior vena cava. **c** Depiction of intraoperative appearance of recipient site after orthotopic intestinal transplantation shows end-to-side anastomosis of recipient infrarenal abdominal aorta to donor superior mesenteric artery and donor superior mesenteric vein to recipient superior mesenteric vein stump utilizing venous extension graft

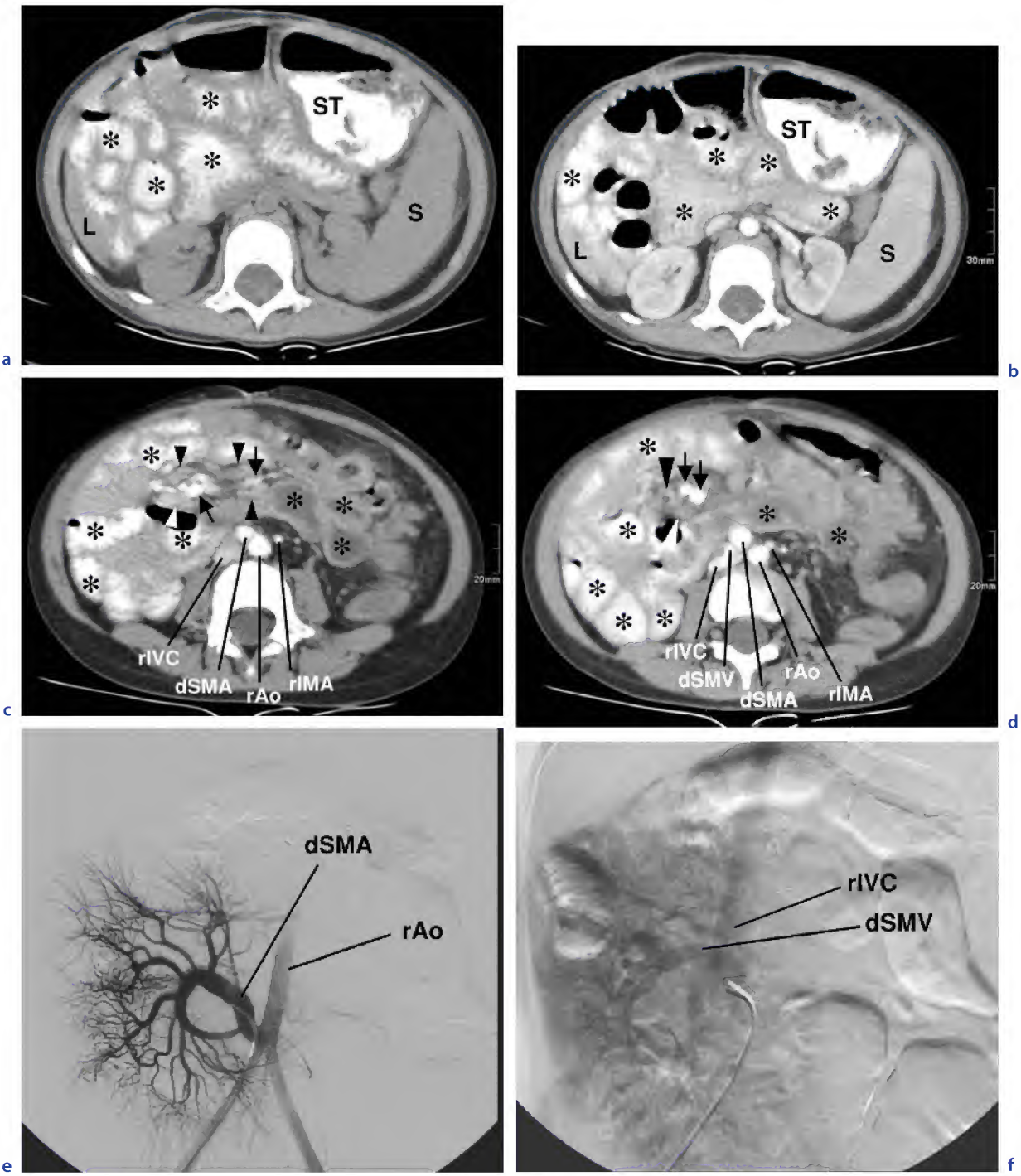

Fig. 7.31a–f. Images obtained 14 months after heterotopic intestinal transplantation in 3-year-old girl with short-bowel syndrome. (*Ao* abdominal aorta, *d* donor, *IMA* inferior mesenteric artery, *IVC* inferior vena cava, *L* liver, *r* recipient, *S* spleen, *ST* stomach, *SMA* superior mesenteric artery, *SMV* superior mesenteric vein.) Annotations: intestinal graft lumen (*black asterisk*), subsegmental arteries and veins in mesenteric fat of intestinal graft (*arrow*), donor lymph node (*arrowhead*). **a, b** MDCT with only oral (**a**) and with oral and intravenous contrast application (**b**) shows normal wall, mucosal folds, and contrast enhancement of intestinal graft. **c, d** MDCT with oral and intravenous contrast application at level of arterial anastomosis (**c**) and venous anastomosis (**d**) shows dSMA arising from recipient infrarenal aorta and dSMV draining in rIVC. **e, f** Selective catheter angiogram during dominant arterial phase (**e**) shows arterial anastomosis of dSMA to recipient infrarenal aorta. Angiogram during dominant venous phase (**f**) displays venous anastomosis of dSMV to rIVC

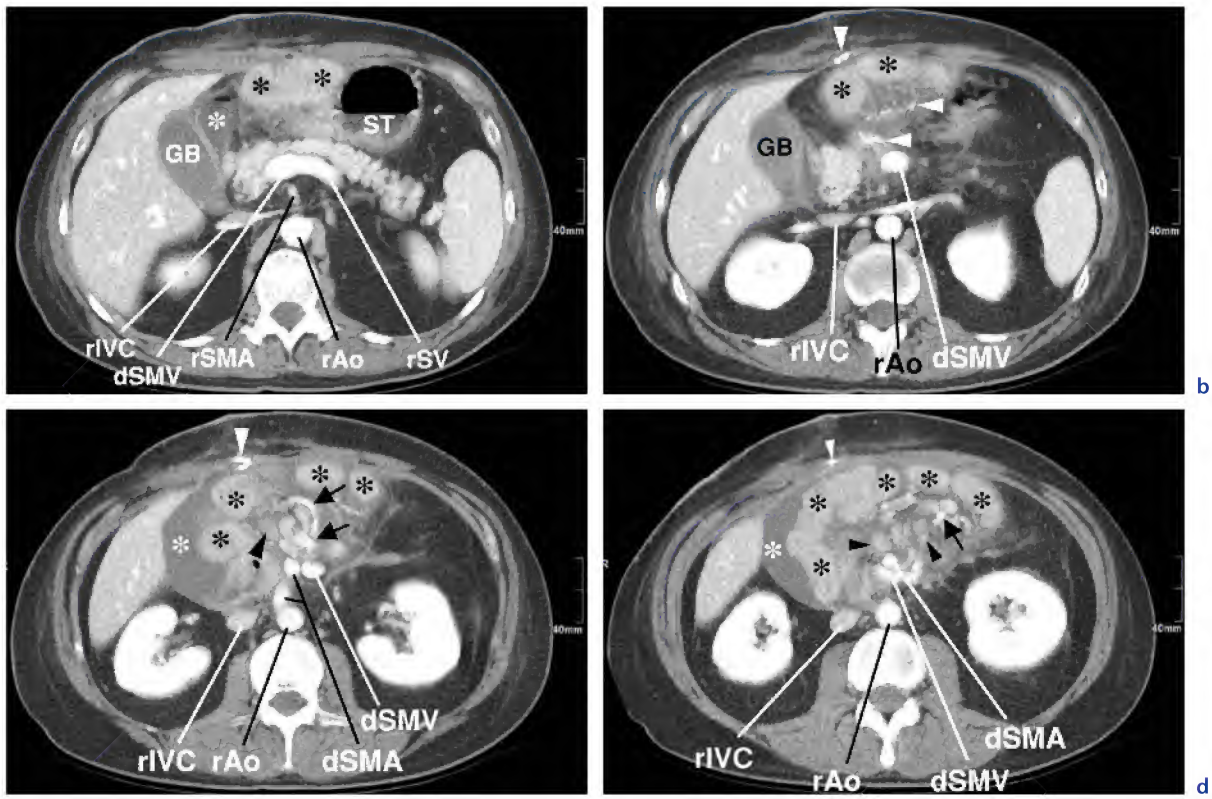

Fig. 7.32a–d. Contrast-enhanced MDCT obtained 14 months after orthotopic intestinal transplantation in 39-year-old man with short-bowel syndrome and normal graft function. (*Ao* abdominal aorta, *d* donor, *GB* gallbladder, *IVC* inferior vena cava, *r* recipient, *SV* splenic vein, *ST* stomach, *SMA* superior mesenteric artery stump, *SMV* superior mesenteric vein.) Annotations: intestinal graft lumen (*black asterisk*), loculated fluid (*white asterisk*), subsegmental arteries and veins in mesenteric fat of intestinal graft (*arrow*), donor lymph node (black *arrowhead*), hyperdense staple line (white arrowhead). **a–d** Images show dSMV draining in recipient portal venous confluence (**a, b**) and dSMA arising from recipient infrarenal aorta (**c, d**)

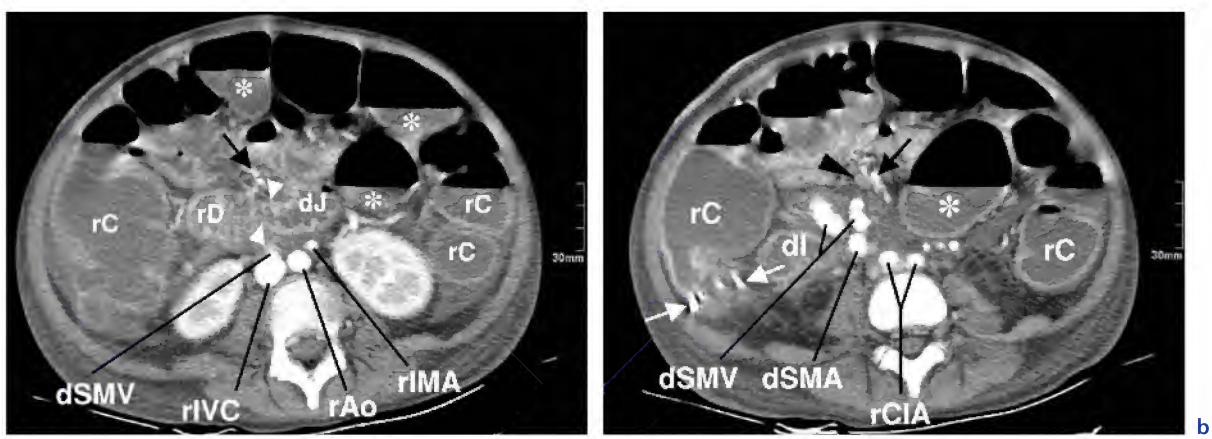

Fig. 7.33a,b. Contrast-enhanced MDCT obtained 4 months after operation in 5-year-old girl with short-bowel syndrome after intestinal transplantation. (*Ao* abdominal aorta, *C* colon, *CIA* common iliac artery, *d* donor, *D* duodenum, *I* ileum, *IMA* inferior mesenteric artery, *IVC* inferior vena cava, *J* jejunum, *r* recipient, *SMV* superior mesenteric vein.) Annotations: intestinal graft lumen (*white asterisk*), subsegmental arteries and veins in mesenteric fat of intestinal graft (*arrow*), donor lymph node (*black arrowhead*), proximal intestinal anastomosis (*between white arrowheads*), distal intestinal anastomosis (*between white arrows*). **a, b** Images show (**a**) proximal intestinal end-to-end anastomosis (*between white arrowheads*) between recipient duodenum and donor jejunum as well as (**b**) distal intestinal end-to-end anastomosis (*between white arrows*) marked by hyperdense staple line between donor ileum and recipient ascending colon

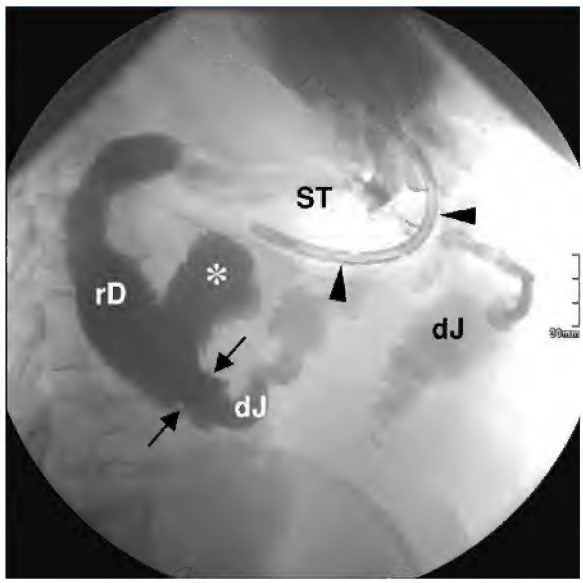

Fig. 7.34. Upper gastrointestinal series with water-soluble contrast material obtained 4 weeks after intestinal transplantation in 39-year-old man with short-bowel syndrome. Image shows proximal intestinal side-to-end anastomosis (*between arrows*) between recipient duodenum and donor jejunum. (*d* donor, *D* duodenum, *J* jejunum, *r* recipient, *ST* stomach.) Annotations: recipient duodenal stump (*asterisk*), proximal intestinal anastomosis (*between arrows*), gastric tube (*arrowhead*)

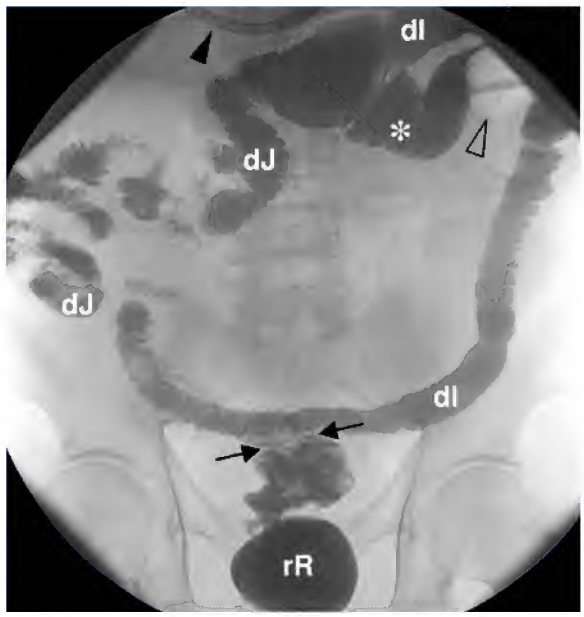

Fig. 7.35. Retrograde intestinal enema study obtained 3 months after intestinal transplantation in 59-year-old man with short-bowel syndrome shows blocked Foley's catheter (*open arrowhead*) within isolated donor intestinal loop (*asterisk*) and distal intestinal end-to-side anastomosis (*between arrows*) between donor ileum and recipient rectum. (*d* donor, *I* ileum, *J* jejunum, *r* recipient, *R* rectum.) Annotation: intestinal tube (*arrowhead*)

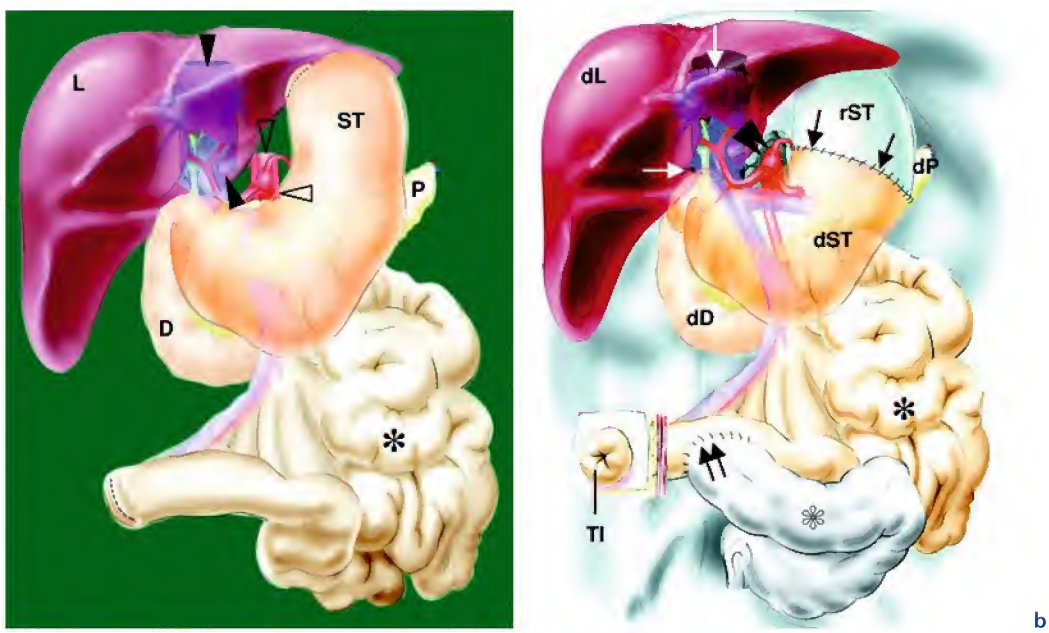

a b

Fig. 7.36a,b. Schematic illustrations of multivisceral transplantation. (*d* donor, *L* liver, *P* pancreas, *r* recipient, *S* spleen, *ST* stomach, *TI* temporary ileostomy.) Annotations: gastrogastric anastomosis (*black arrow*), cavocaval anastomosis (*white arrow*), ileocolonic anastomosis (*arrows*), aortic segment together with celiac trunk and superior mesenteric artery (*open arrowhead*), inferior vena cava segment together with hepatic veins (*closed arrowhead*), aortoaortic anastomosis (*arrowheads*), intestinal graft (*black asterisk*), residual recipient colon (*white asterisk*). **a** Depiction of multivisceral graft on back-table after explantation. **b** Depiction of intraoperative appearance of recipient site after implantation

organs are mobilized en bloc without manipulation of the portal venous system. If the stomach is utilized the greater gastric curvature is mobilized with preservation of the gastroepiploic arch; the short gastric vessels are transected and the greater omentum is resected. Cholecystectomy and splenectomy are performed either in situ or ex situ on the back-table. During procurement the donor liver is typically removed together with the inferior vena cava. For arterial revascularization 10 cm of donor aorta is excised above the celiac trunk and directly below the superior mesenteric artery in order to preserve the origins of the renal arteries for further renal transplantation. The procured aorta is suture-closed below the origin of the superior mesenteric artery. This creates an aortic conduit with the celiac trunk and superior mesenteric artery; the proximal part of the aortic conduit is designated for aortoaortic anastomosis. Formerly, the combined origins of the celiac trunk and superior mesenteric artery were excised for arterial revascularization. This technique was abandoned because it was more technically demanding and unpredictable due to anastomotic scarring and ensuing arterial stenosis. Transection of the small bowel is performed in a way similar to that used in intestinal transplantation except for dissection of venous and arterial vessels. In the recipient exenteration of the abdominal organs is performed; this includes the liver with or without the intrahepatic vena cava, pancreas, spleen, part of the stomach, and small bowel. The infrarenal abdominal aorta is exposed. The arterial anastomosis is restored in end-to-side fashion connecting the large donor aortic conduit to the recipient infrarenal abdominal aorta. The venous anastomosis is restored in end-to-end fashion connecting the suprahepatic and infrahepatic inferior vena. Sometimes the piggyback technique is employed as follows: in the recipient the liver is removed without inferior vena cava; after implantation the infrahepatic portion of the vena cava of the graft is stapled resulting in a caval stump. The donor suprahepatic vena cava is anastomosed in end-to-side fashion at the level of the hepatic veins or in side-to-side fashion to the recipient vena cava. Proximal gastrointestinal reconstruction of the multivisceral graft is performed by connecting the proximal portion of the recipient stomach to the donor stomach. Distal intestinal continuity of the multivisceral graft is established analogous to intestinal transplantation as described, utilizing one of the various types of intestinointestinal anastomosis. Also a pyloroplasty is performed to prevent gastric outlet obstruction resulting from denervation of the stomach.

Typical examples of the regular anatomy are shown below using various imaging modalities after multivisceral transplantation (Figs. 7.37–7.39).

7.14 Liver-Intestinal Transplantation

A combined liver–intestinal graft employs at least the small bowel attached to the liver. In the early period of liver–intestinal transplantation only the portal vein was left intact; the bile duct was transected and its distal portion together with the donor duodenum and pancreas was removed during back-table preparation in order to avoid donor pancreatitis (Grant et al. 1990). This technique has been discarded because of surgical problems related to difficult preparation in pediatric donors, bile leaks after biliary anastomosis, and the risk of torsion of the portal vein. Nowadays liver and small bowel with the attached, intact, proximal stapled duodenum and the adjacent rim of the pancreatic head are transplanted en bloc. This modification simplifies graft preparation, eliminates dissection of the bile duct within the hepatoduodenal ligament, omits biliary anastomotic complications, and obviates vascular torsion (Sudan et al. 2001). This technique also enables procurement of a reduced and size-matched liver and intestinal graft from donors who are larger than the recipient (de Goyet et al. 2000). For this reason the range of possible donors for children on the waiting list is extended. Size reduction is achieved by resection of segments II and III or segments II, III, and IV or extended right hemihepatectomy and, if necessary, by resection of a distal segment of the ileum. In the recipient the procedure starts with hepatectomy and preserves stomach, duodenum, and pancreas. The residual native portal vein draining the remnant viscera is anastomosed to the native suprarenal inferior vena cava in end-to-side fashion (Fig. 7.40). After implantation the donor graft is revascularized analogous to multivisceral transplantation. Proximal intestinal continuity is established between the remaining recipient duodenum or jejunum and the donor proximal jejunum; distal intestinal continuity is established analogous to intestinal transplantation as described, utilizing one of the various types of intestinointestinal anastomosis.

Typical examples of regular anatomy are shown below using sonography (Fig. 7.41).

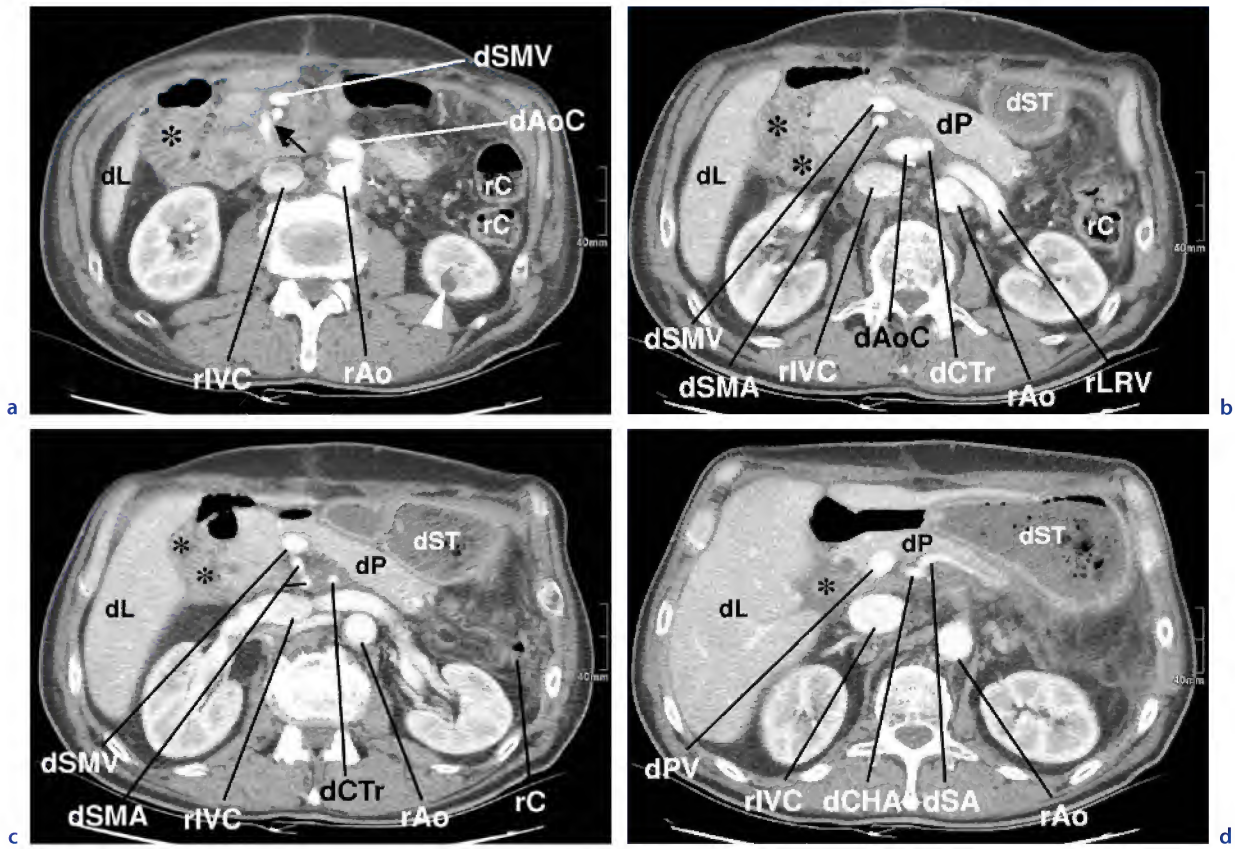

Fig. 7.37a–d. Contrast-enhanced MDCT during dominant arterial phase obtained 5 weeks after multivisceral transplantation in 61-year-old man with liver cirrhosis, hepatocellular carcinoma, and portomesenteric thrombosis. (*Ao* abdominal aorta, *AoC* aortic conduit, *C* colon, *CHA* common hepatic artery, *CTr* celiac trunk, *d* donor, *IVC* inferior vena cava, *LRV* left renal vein, *L* liver, *P* pancreas, *PV* portal vein, *r* recipient, *SA* splenic artery, *ST* stomach, *SMA* superior mesenteric artery, *SMV* superior mesenteric vein.) Annotations: intestinal graft lumen (*black asterisk*), subsegmental arteries and veins in mesenteric fat of intestinal graft (*arrow*), renal cyst (*white arrowhead*). **a–d** Images show normal anatomy at level of arterial anastomosis (**a**), origin of celiac trunk (**b**), origin of superior mesenteric artery (**c**), and bifurcation of celiac trunk (**d**)

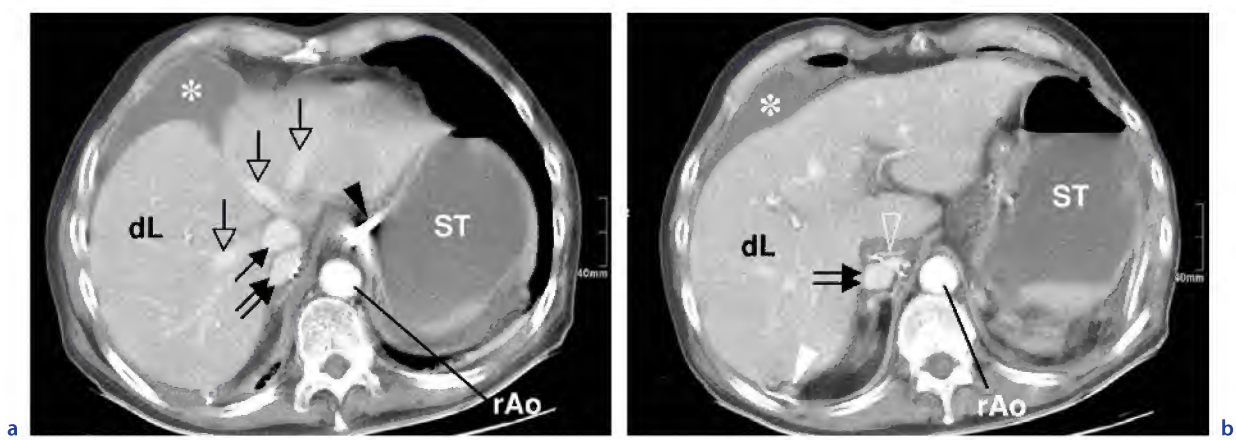

Fig. 7.38a,b. Contrast-enhanced helical CT obtained 7 days after multivisceral transplantation with piggyback technique in 67-year-old man with liver cirrhosis, hepatocellular carcinoma, and portomesenteric thrombosis. (*Ao* aorta, *d* donor, *L* liver, *r* recipient, *ST* stomach.) Annotations: ascites (*white asterisk*), donor inferior vena cava (*arrow*), liver vein (*open arrow*), recipient inferior vena cava with hyperdense staple line (*arrows*), gastric tube (*black arrowhead*), subphrenic drain (*white closed arrowhead*), staple line of donor caval stump (*white open arrowhead*). Images at level of hepatic veins (**a**) show side-by-side location of donor and recipient inferior vena cava as well as stapled caval stump caudally (**b**)

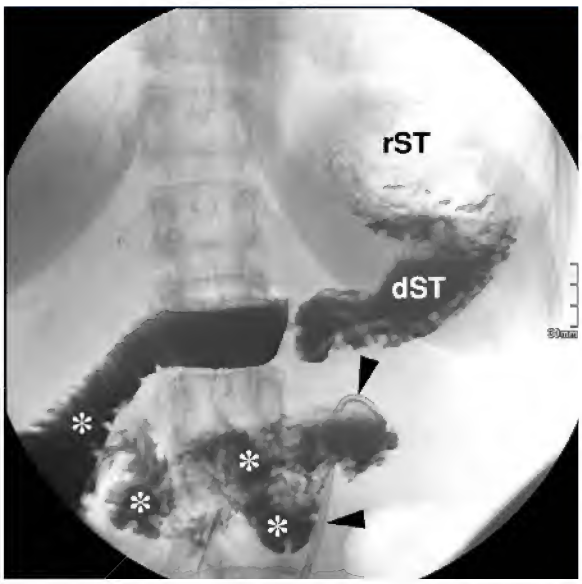

Fig. 7.39. Upper gastrointestinal series with water-soluble contrast material obtained 5 years after multivisceral transplantation in 41-year-old woman with Gardner's syndrome and intra-abdominal desmoid tumor. (*d* donor, *r* recipient, *ST* stomach.) Annotations: intestinal graft (*asterisk*), urethral drainage tube (*arrowhead*). Image shows normal postoperative anatomy after end-to-end gastrogastrostomy with normal intestinal contrast passage (exact position of end-to-end gastrogastrostomy not discernible)

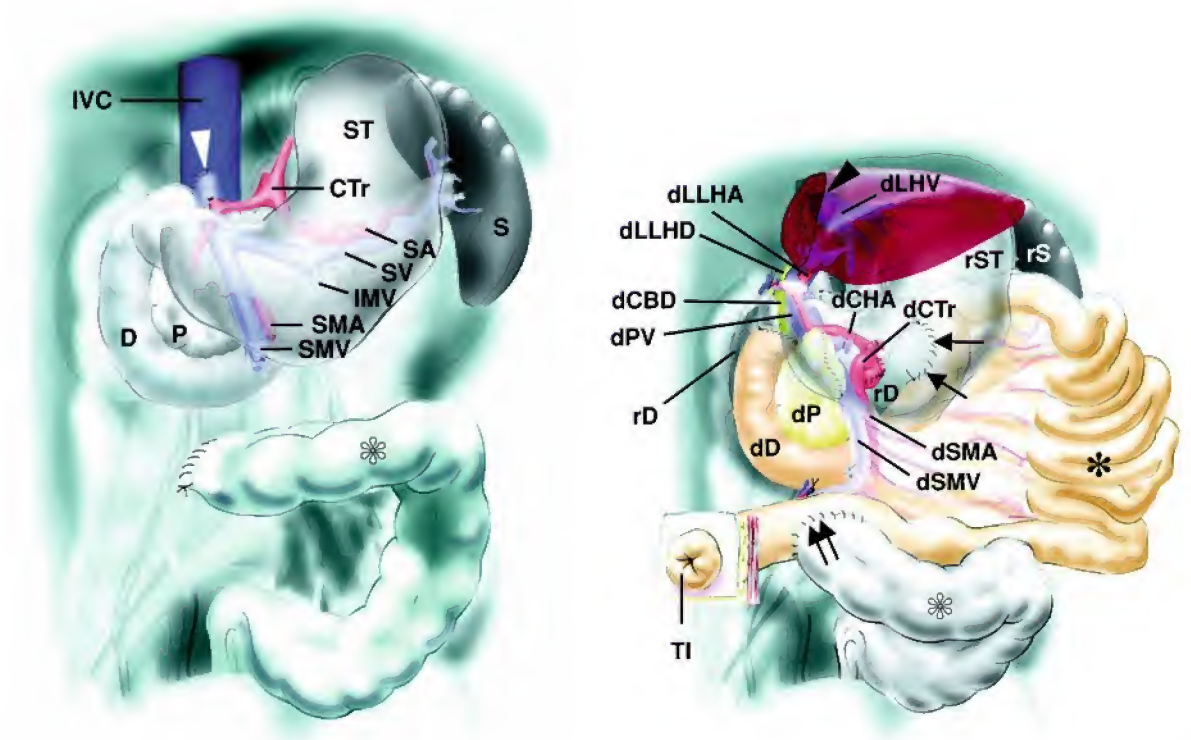

a b

Fig. 7.40a,b. Schematic illustrations of liver-intestinal transplantation. (*CBD* common bile duct, *CHA* common hepatic artery, *CTr* celiac trunk, *d* donor, *D* duodenum, *IMV* inferior mesenteric vein, *IVC* inferior vena cava, *L* liver, *LHV* left hepatic vein, *LLHA* left lateral hepatic artery, *LLHD* left lateral hepatic duct, *P* pancreas, *PV* portal vein, *r* recipient, *S* spleen, *SA* splenic artery, *SMA* superior mesenteric artery, *SMV* superior mesenteric vein, *ST* stomach, *SV* splenic vein, *TI* temporary ileostomy.) Annotations: duodenoduodenal anastomosis (*arrow*), ileocolonic anastomosis (*arrows*), portocaval anastomosis (*white arrowhead*), intestinal graft (*black asterisk*), residual recipient colon (*white asterisk*). **a** Depiction of intraoperative appearance of recipient site after removal of diseased liver in patient with short-bowel syndrome shows end-to-side anastomosis between portal vein and inferior vena cava. **b** Depiction of intraoperative appearance of recipient site after implantation of size-reduced liver–intestinal graft utilizing extended right hemihepatectomy and distal segmental small bowel resection

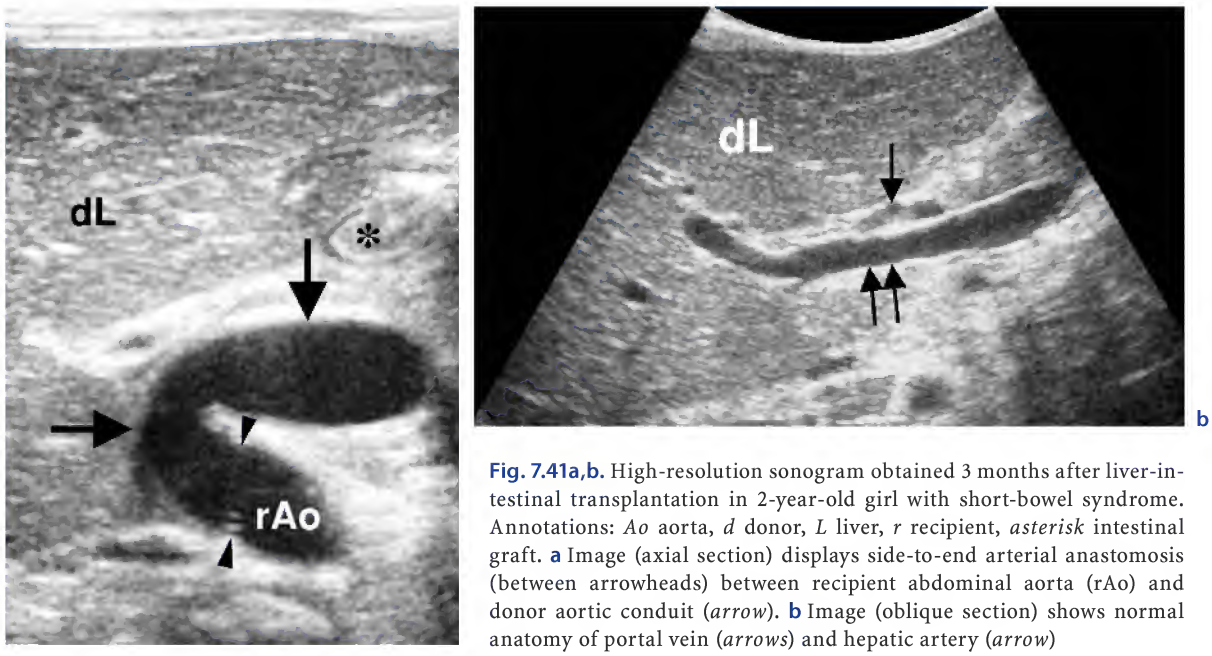

a b

Fig. 7.41a,b. High-resolution sonogram obtained 3 months after liver-intestinal transplantation in 2-year-old girl with short-bowel syndrome. Annotations: *Ao* aorta, *d* donor, *L* liver, *r* recipient, *asterisk* intestinal graft. **a** Image (axial section) displays side-to-end arterial anastomosis (between arrowheads) between recipient abdominal aorta (rAo) and donor aortic conduit (*arrow*). **b** Image (oblique section) shows normal anatomy of portal vein (*arrows*) and hepatic artery (*arrow*)

7.15 Posttransplantation Complications

Compared to other solid organ transplantations intestinal transplantation is hampered by the presence of a large number of immunocompetent donor lymphocytes in gut-associated lymphoid tissue and mesenteric nodes as well as bacterial contamination, all of which increase the risk for rejection and infection. In the last decade patient and intestinal graft survival have improved consistently thanks to refined surgical techniques, introduction of better immunosuppressive regimens including tacrolimus, and better antimicrobial therapy of opportunistic infections. These advances decreased technical and immunological failure rates as well as infection rate. Today transplantation centers report 1-year patient and graft survival rates of 81% and 63%, respectively (Port 2003). This compares less favorably to other solid organ transplantations of the heart, liver, kidney, and pancreas with 1-year patient and graft survival approaching or exceeding 90% (Port 2003).

Knowledge of the transplantation procedure and postoperative imaging anatomy of the intestinal graft are basic requirements for radiologists. Graft survival, among other factors, corresponds to early diagnosis and therapy for specific graft-related complications including leakage of enteric anastomosis, abdominal abscess, peritonitis, thrombosis of graft vessels, hematoma, and posttransplantation lymphoproliferative disorder. This pictorial essay uses various imaging modalities to show the imaging spectrum of diseases after isolated intestinal, combined liver–intestinal or multivisceral transplantation.

7.16 Imaging Modalities

Various imaging modalities are routinely used to detect early or late posttransplantation complications. During the initial period of intestinal transplantation in the early 1990s gastrointestinal contrast studies with barium or water-soluble contrast material were performed to evaluate the integrity of the intestinal graft; for example, upper gastrointestinal and small bowel series, enteroclysis, and contrast enema (Bach et al. 1991; Campbell et al. 1993). Particularly a Foley's catheter blocked within the isolated intestinal loop after its introduction through the temporary ileostomy facilitates a retrograde contrast enema examination. Today gastrointestinal contrast studies are performed only occasionally to detect complications of the enteric anastomosis or to evaluate gastrointestinal motility. Due to the accumulated knowledge of the clinical pattern of complications cross-sectional imaging studies are

currently utilized to detect pathologies of the vessels, intestinal wall, and abdominal cavity (Bach et al. 1992; Campbell et al. 1995). The use of sonography and color-coded sonography to image the vascular system, entire intestinal graft, and abdominal cavity is hampered by intraluminal intestinal gas (Campbell et al. 1995), but postoperative motility of the intestinal graft can be sufficiently evaluated by sonography due to its real-time display. Contrast-enhanced helical CT represents the primary imaging modality for complete evaluation of the vascular and enteric anastomoses, vessels, intestinal graft, and abdominal cavity (Lappas 2003). MRI without and with intravenous contrast application may also be useful in evaluating the intestinal graft, but evaluation of the enteric anastomosis by MRI is difficult. Sometimes patients have coexistent impaired renal function before and after intestinal transplantation; renal function determines the selection of the appropriate cross-sectional imaging modality. In order to preserve renal function contrast-enhanced MRI and not contrast-enhanced CT represents the preferred examination. Catheter angiography is used to confirm vascular complications while permitting immediate endovascular therapy (Lappas 2003). Other imaging-guided interventions are employed to treat localized fluid collections percutaneously, for instance seroma, hematoma, abscess.

Imaging modalities are not utilized to detect rejection and graft-versus-host disease. Acute rejection is diagnosed by endoscopy combined with mucosal biopsies from donor stomach, duodenum or distal ileum via the ileostomy. Graft-versus-host disease manifests most commonly as skin lesions or mucosal lesions in the recipient's residual gastrointestinal tract; both sites are best amenable for visual or endoscopic inspection and biopsies.

7.17 Imaged Abnormalities

Organ-specific complications after combined liver–intestinal and multivisceral transplantation concern mainly the intestinal graft and therefore resemble complications after isolated intestinal transplantation. These complications rarely involve the hepatic or pancreatic graft due to lack of operative manipulation of the hepatobiliary and portal venous system.

Mainly the following complications are observed after intestinal transplantation by imaging modalities: intestinal graft complications including infection, vascular complications, and other transplantation-associated complications.

7.18 Intestinal Graft Complications Including Infection

Typical graft complications include graft dysmotility, dehiscence, and stricture of the enteric anastomosis as well as abdominal infections. Intestinal graft dysmotility occurs frequently in the early postoperative period and can be observed directly by real-time sonography or gastrointestinal studies; it is also suspected on abdominal radiographs and CT by the appearance of a gasless abdomen or increased numbers of air-fluid levels and luminal dilatation (Fig. 7.42c). Anastomotic complications manifest either as dehiscence or stricture and can involve any anastomosis encountered in intestinal transplantation procedures. For proper interpretation of an imaging study the radiologist must be familiar with the presence, location, and fashion of the various enteroanastomoses including end-to-end, end-to-side, and side-to-side reconstruction of intestinal tract continuity. Gastrointestinal contrast studies are performed with water-soluble contrast material in the case of a suspected anastomotic dehiscence. Typically, a contrast leakage is observed either contained or with free communication within the abdominal cavity (Fig. 7.43). An anastomotic stenosis presents as luminal narrowing on gastrointestinal contrast studies and may exhibit prestenotic dilatation and dysmotility (Fig. 7.42d).

Abdominal infections represent a frequent complication after intestinal transplantation and manifest as abscess, peritonitis or fistula formation. The typical findings for an intra-abdominal abscess include localized fluid collection with or without gas formation, air-fluid level, and contrast-enhancing abscess membrane (Fig. 7.45a). Imaging-guided biopsy is required for definite diagnosis and for differentiation between abscess and seroma or hematoma. An abscess can also occur in intra-abdominal parenchymal organs; the liver is especially prone to abscess formation because of its filter function of portal venous drainage from the intestinal graft (Fig. 7.45b). The diagnosis of localized or general-

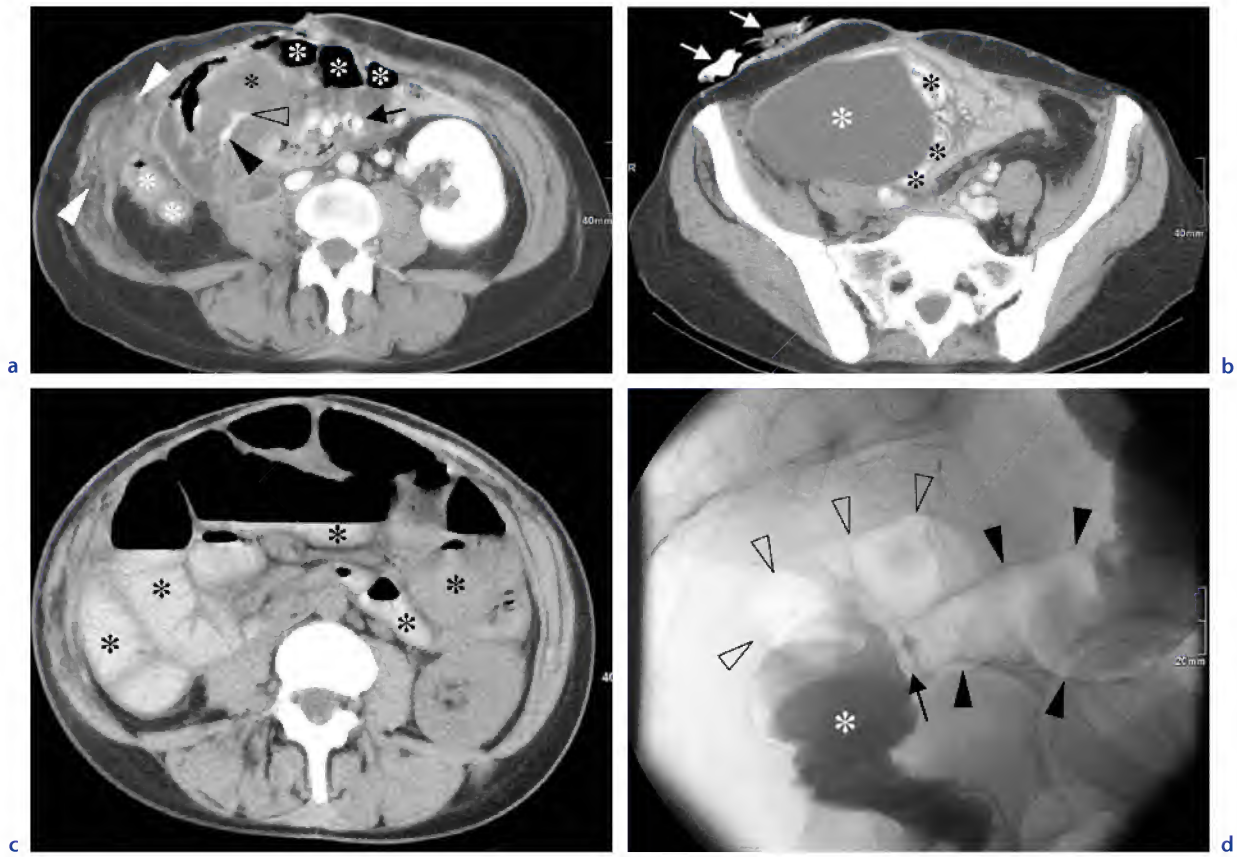

Fig. 7.42a–d. Image from a 41-year-old woman after multivisceral transplantation necessitated by Gardner's syndrome with intra-abdominal desmoid tumor. **a** Ten days after operation with laboratory evidence of acute hemorrhage. Contrast-enhanced helical CT displays mesenteric pseudoaneurysm (*closed black arrowhead*) with localized contrast extravasation (*open black arrowhead*) and mesenteric hematoma (*black asterisk*). Annotations: intestinal graft lumen (*white asterisk*), mesenteric arteries and veins of intestinal graft (*arrow*), postoperative changes in abdominal wall (*between white arrowhead*). **b** Six weeks after operation with normal intestinal graft function. Helical CT after oral and intravenous contrast application shows large loculated fluid collection (*white asterisk*) with displacement of intestinal graft loops (*black asterisk*). Subsequent image-guided drainage revealed lymphocele. Annotations: postoperative dressing of ileostomy (*arrow*). **c** Eight months after operation with clinical evidence of intestinal obstruction. Helical CT without intravenous but with oral contrast administration shows dilated, non-thickened loops of intestinal graft (*asterisk*) with air-fluid level consistent with intestinal dysmotility. **d** Clinical evidence of intestinal obstruction at 34 months after operation. Radiograph obtained during enema with water-soluble contrast material displays concentric high-grade stenosis of ileorectal, end-to-side anastomosis (*arrow*). Annotations: air-filled recipient rectal stump (*open arrowhead*), contrast-filled distal rectum (*white asterisk*), donor ileum (*closed arrowhead*)

ized peritonitis is challenging, even by contrast-enhanced CT or MR imaging; imaging findings include edematous infiltration of the mesenterial fat as well as increased contrast enhancement of the intestinal wall and involved mesenterium (Fig. 7.46). Fistula formation results from an abdominal infection with communication to the skin; sinus tract formation involves the retroperitoneum including the psoas muscle.

Contrast-enhanced CT sometimes shows an unspecific diffuse thickening of the intestinal wall and mucosal folds early after transplantation presumably due to edema related to organ procurement and interruption of draining lymphatic vessels combined with an unspecific enlargement of the donor's mesenteric lymph nodes (Fig. 7.47b). CT can also detect an unspecific focal wall thickening of the small bowel but cannot delineate the

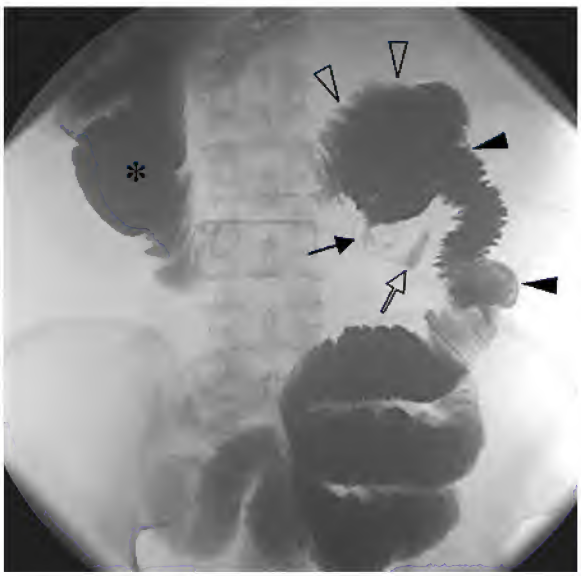

Fig. 7.43. Upper gastrointestinal examination with water-soluble contrast material obtained 17 days after intestinal transplantation utilizing side-to-end jejunojejunal anastomosis in 59-year-old man with short-bowel syndrome. Image shows contained contrast leakage (*open arrow*) of recipient jejunal stump with staple line (*closed arrow*). Annotations: donor jejunum (*closed arrowhead*), recipient duodenum (*asterisk*), recipient jejunum (*open arrowhead*)

underlying cause (Fig. 7.44a). This requires further clinical or short-term imaging evaluation and especially exclusion of rejection or opportunistic infection.

7.19 Vascular Graft Complications

The most serious vascular complication is arterial and venous graft thrombosis and can result in intestinal graft necrosis necessitating graft enterectomy. Typically, contrast-enhanced CT displays either an intraluminal filling defect or complete occlusion of the involved artery with non-enhancement of the intestinal wall indicating graft necrosis (Fig. 7.44d). Sometimes an intraluminal membrane can be observed on imaging (Fig. 7.44f); this finding is suggestive of arterial dissection. In patients with venous thrombosis, contrast-enhanced CT shows an intraluminal-filling defect of the involved vein. Segmental venous thrombosis of the intestinal graft may result in intestinal pneumatosis (Fig. 7.45c). Thrombotic occlusion of the portal vein is followed by portal hypertension, venous congestion syndrome, and splenic infarction (Fig. 7.44b). Hematomas can also be detected by various imaging modalities (Fig. 7.42a); these either indicate a localized vascular abnormality including pseudoaneurysm (Fig. 7.42a) and vascular anastomotic dehiscence or result from clotting disorders.

7.20 Other Transplantation-Associated Complications

Varying degrees of fluid collection are observed after intestinal transplantation including lymphocele (Fig. 7.42b) and seroma; ascites is often located between the intestinal graft loops. In most cases these fluid collections regress in size without treatment, but sometimes percutaneous diagnostic aspiration or therapeutic drainage is necessary. Posttransplantation lymphoproliferative disorder represents a serious but rare complication of isolated intestinal, multivisceral and combined liver–intestinal transplantation, and manifests often as involvement of the intestinal or parenchymal organ graft (Fig. 7.47) or infrequently as involvement of the recipient's remaining native gastrointestinal tract or as an extra-allograft lymphadenopathy (Reyes et al. 1996). Complications after combined liver–intestinal and multivisceral transplantation rarely involve extra-intestinal graft organs but may include fatty liver degeneration (Fig. 7.47a), pancreatitis (Fig. 7.48a) and pancreatic pseudocyst (Fig. 7.44c) as well as thrombosis of the inferior vena cava (Fig. 7.44e).

A comprehensive pictorial essay of the spectrum of imaging findings after intestinal, liver–intestinal, or multivisceral transplantation was published by the authors of this book chapter (Unsinn et al. 2004a, 2004b).

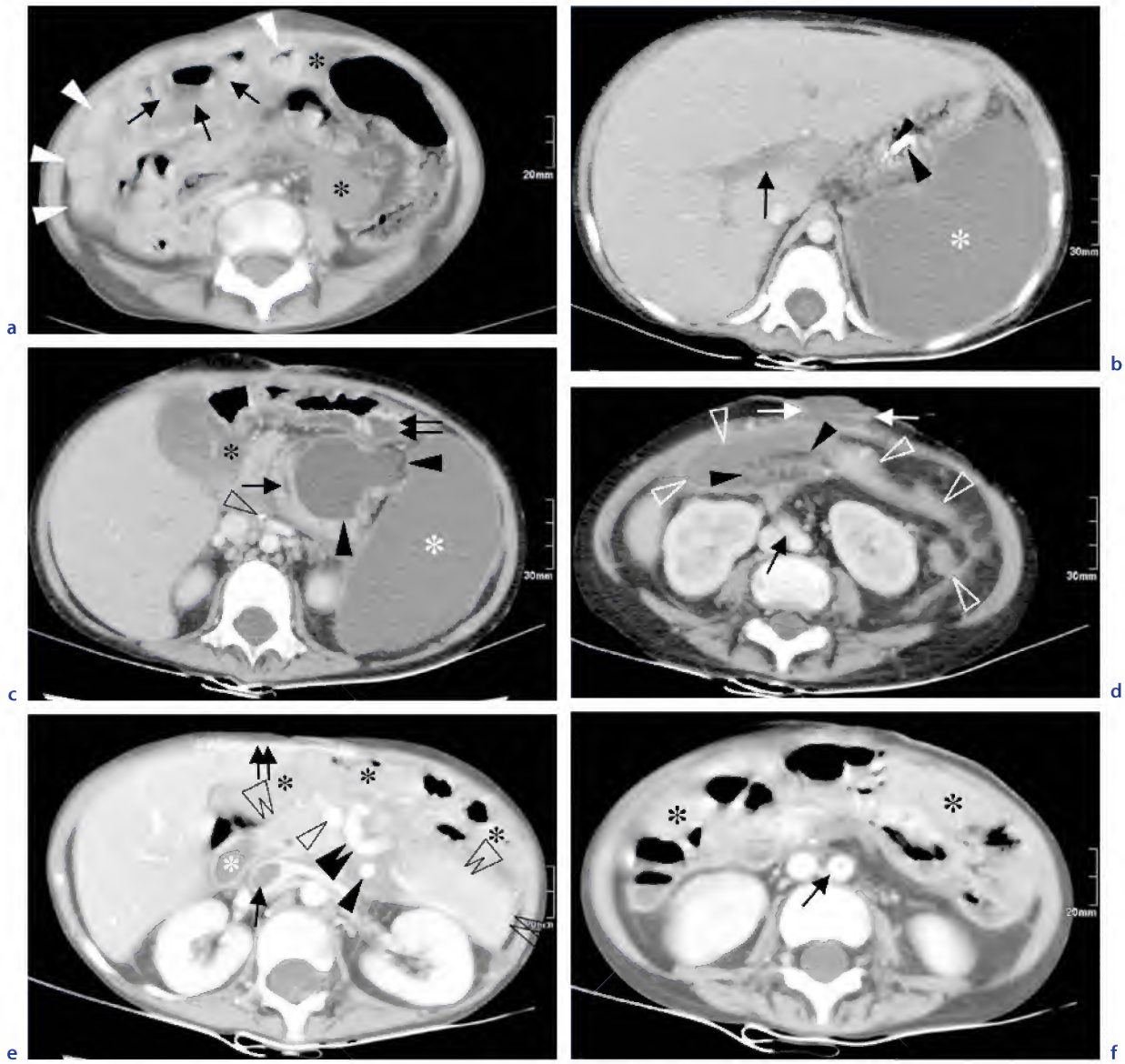

Fig. 7.44a–f. Images from 3-year-old girl after intestinal transplantation necessitated by short-bowel syndrome (**a–d**), graft failure (**b–d**) and subsequent retransplantation utilizing multivisceral graft (**e, f**). **a** Contrast-enhanced helical CT obtained 26 months after operation shows unspecific focal wall thickening of intestinal graft with reduced contrast enhancement (*arrow*) compared to non-thickened, regular contrast-enhanced intestinal loops (*arrowhead*) consistent with focal intestinal ischemia. Annotation: ascites (*asterisk*). **b–d** Contrast-enhanced MDCT obtained 3 years after operation in patient with chronic intestinal graft failure. **b** Image displays complete acute thrombotic occlusion of portal vein (*arrow*) with non-enhancement of spleen (*asterisk*) indicating infarction. Annotation: gastric tube (*arrowhead*). **c** Image additionally shows thin-walled pancreatic pseudocyst (*arrowhead*) and focal ductal dilatation of pancreatic body (*arrow*). Annotations: ascites (*black asterisk*), splenic infarct (*white asterisk*), surgical clip (*open arrowhead*), unspecific focal gastric wall thickening (*arrows*). **d** Image shows contrast enhancement of donor superior mesenteric artery (*arrow*) but non-enhancement of graft arteries and intestinal wall (*arrowhead*), indicating chronic vascular occlusion. Additional intra-abdominal abscess (*open arrowhead*) with cutaneous fistula (*between arrows*). **e, f** Contrast-enhanced MDCT obtained 3 years after initial intestinal transplantation with graft failure and 8 weeks after subsequent multivisceral transplantation with normal graft function. **e** Image shows acute thrombosis of inferior vena cava (*arrow*) at level of renal veins. Normal enhancement and appearance of intestinal graft (*black asterisk*) as well as hyperdense prosthetic mesh inlay (*arrows*) for abdominal wall repair are noted. Annotation of donor anatomic structures: celiac trunk (*closed arrowhead*), duodenum (*white asterisk*), pancreas (*open arrowheads*), superior mesenteric artery (*closed arrowheads*), superior mesenteric vein (*open arrowhead*). **f** Image displays dissection membrane in abdominal aorta (*arrow*). Annotation: intestinal graft loops (*asterisk*)

a

b

c

Fig. 7.45a–c. Images from 39-year-old woman after intestinal transplantation necessitated by Gardner's syndrome with intra-abdominal desmoid tumor (**a**), graft failure and subsequent retransplantation utilizing multivisceral graft (**b, c**). **a** Contrast-enhanced MDCT obtained 2 months after initial intestinal transplantation displays multiple intra-abdominal abscesses (*asterisks*) with air-fluid level and contrast-enhancing abscess membrane. Mesenteric lymphadenopathy (*open arrowhead*), partly thickened wall of intestinal graft (*solid arrowhead*), recipient descending colon (*double arrows*) are depicted. **b** Contrast-enhanced MDCT obtained 2 months after retransplantation displays multiple intrahepatic focal hypodensities consistent with nocardial abscesses (*arrow*). Annotations: fluid-filled stomach (*asterisk*), small intra-abdominal abscess (*arrowhead*). **c** Contrast-enhanced MDCT obtained 3 months after retransplantation that used multivisceral graft shows non-enhancement of intestinal graft (*lower white arrows*) except proximal jejunum (*black arrow*), focal intramural pneumatosis (*white arrowhead*) and free intra-abdominal air bubble (*black arrowhead*) due to arterial thrombosis with ischemia and perforation. Localized fluid (*white asterisk*) with cutaneous fistula (*between upper white arrows*) is also depicted

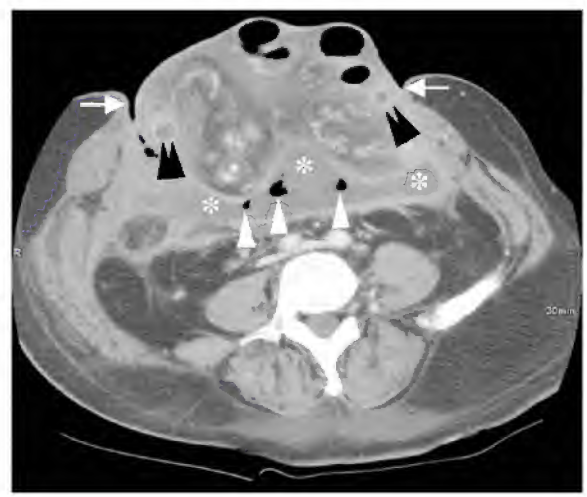

Fig. 7.46. Contrast-enhanced MDCT obtained 6 weeks after intestinal transplantation in 39-year-old man with short-bowel syndrome who presented with acute sepsis syndrome. Image shows large ventral abdominal wall defect (*between arrows*) due to dehiscence and subsequent operative widening of median laparotomy, intra-abdominal abscess (*asterisk*) with air bubbles (*white arrowheads*) and cutaneous drainage (*arrows*). Also seen are intestinal graft enlargement due to edematous infiltration, engorgement of mesenteric vessels, and increased contrast enhancement of intestinal wall (*black arrowheads*), all of which are consistent with surgically proven peritonitis

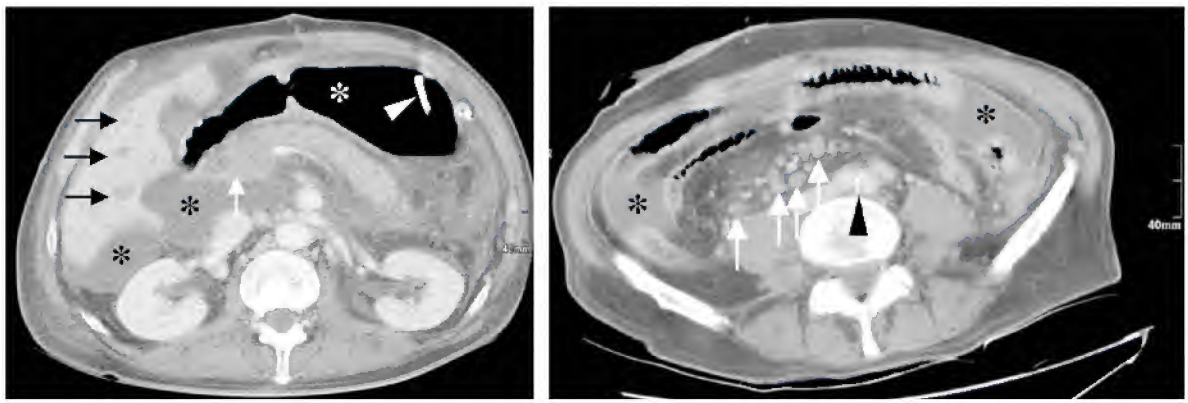

Fig. 7.47a,b. 67-year-old man after multivisceral transplantation necessitated by liver cirrhosis with intrahepatic hepatocellular carcinoma and chronic thrombotic occlusion of portomesenteric venous system with clinical evidence of infection. **a** Contrast-enhanced helical CT obtained 2 weeks after operation shows enlargement of pancreatic head with reduced contrast enhancement (*white arrow*) consistent with edematous pancreatitis. Annotation: ascites (*black asterisk*), gastric tube (*white arrowhead*), periportal lymphedema (*black arrow*), stomach (*white asterisk*). **b** Contrast-enhanced helical CT obtained 4 weeks after operation displays unspecific enlargement of mesenteric lymph nodes (*arrow*) of intestinal graft. Annotations: ascites (*asterisk*), calcification of iliac artery (*arrowhead*)

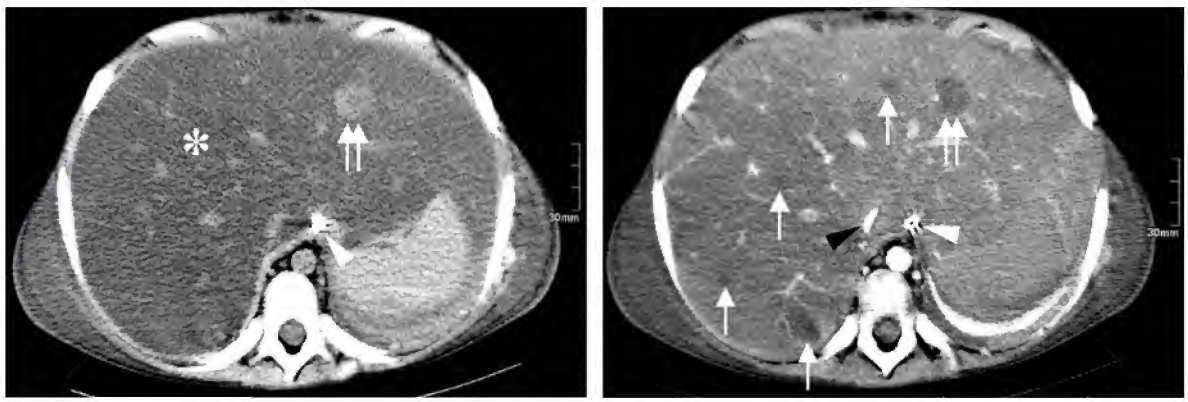

Fig. 7.48a,b. MDCT of 5-year-old girl with short-bowel syndrome obtained 4 months after intestinal transplantation and newly developed ascites. Annotation: gastric tube (*arrowhead*). **a** Non-enhanced study shows fatty liver degeneration (*white asterisk*) and focal hyperdensity (*arrow*) in left liver lobe. **b** After contrast enhancement additional focal intrahepatic hypodensities (*arrows*) are seen representing pathologically proven multifocal posttransplantation lymphoproliferative disorder. Contrast-enhancing inferior vena cava (*black arrowhead*)

References

Bach DB, Hurlbut JJ, Romano WM et al (1991) Human orthotopic small intestine transplantation: radiologic assessment. Radiology 180:37–41

Bach DB, Levin MF, Vellet AD et al (1992) CT findings in patients with small-bowel transplants. AJR Am J Roentgenol 159:311–315

Campbell WL, Abu-Elmagd K, Federle MP et al (1993) Contrast examination of the small bowel in patients with small-bowel transplants: findings in 16 patients. AJR Am J Roentgenol 161:969–974

Campbell WL, Abu-Elmagd K, Furukawa H, Todo S (1995) Intestinal and multivisceral transplantation. Radiol Clin North Am 33:595–614

Cohen Z, Silverman RE, Wassef R et al (1986) Small intestinal transplantation using cyclosporine. Report of a case. Transplantation 42:613–621

Dachmann AH, Newmark GM, Thistlethwaite JR, Oto A, Bruce DS, Newell KA (1998) Imaging of pancreatic transplantation using portal venous and enteric exocrine drainage. AJR Am J Roentgenol 171:157–163

de Goyet JDV, Mitchell A, Mayer AD et al (2000) En bloc combined reduced-liver and small bowel transplants: from large donors to small children. Transplantation 69:555–559

de Ville de Goyet J, Redinig R, Hausleither V, Lerut J, Otte JB (1995) Standarized quick en bloc technique for procurement of cadaveric liver graft for pediatric transplantation. Transpl Int 8:280–285

Deltz E, Schroeder P, Gebhardt H et al (1989) Successful clinical small bowel transplantation: report of a case. Clin Transpl 3:89–91

Fernandez NP, Bernadino ME, Neylan JF, Olson PR (1991) Diagnosis of pancreatic transplant dysfunction: value of gadopentate dimeglumine-enhanced MR imaging. AJR Am J Roentgenol 156:1171–1176

Freund MC, Steurer W, Gassner EM et al (2004a) Spectrum of imaging findings after pancreas transplantation with enteric exocrine drainage: part 1, posttransplantation anatomy. AJR Am J Roentgenol 182:911–917

Freund MC, Steurer W, Gassner EM et al (2004b) Spectrum of imaging findings after pancreas transplantation with enteric exocrine drainage: part 2, posttransplantation complications. AJR Am J Roentgenol 182:919–925

Furukawa H, Todo S, Reyes J, Abu-Elmagd K, Starzl TE (1998) Technical aspects of small bowel transplantation. Curr Opin Organ Transpl 3:279–285

Gill IS, Sindhi R, Jerius JT, Sudan D, Stratta RJ (1997) Bench reconstruction of pancreas for transplantation: experience with 192 cases. Clin Transpl 11:104–109

Grant D, Wall W, Mimeault R et al (1990) Successful small-bowel/liver transplantation. Lancet 335:181–184

Gruessner RWG, Sharp HL (1997) Living related intestinal transplantation – first report of a standardized surgical technique. Transplantation 64:1605–1607

Gruessner AC, Sutherland DE (2001) Analysis of United States (US) and non-US pancreas transplants reported to the United Network for Organ Sharing (UNOS) and the International Pancreas Transplant Registry (IPTR) as of October 2001. Clin Transpl 2001:41–72

Gupta R, Rottenberg G, Taylor J (2002) Pseudothrombosis of the iliac vein in patients following combined kidney and pancreas transplantation. Br J Radiol 75:692–694

Imagawa DK, Olthoff KM, Yersiz H (1996) Rapid en bloc technique for pancreas-liver procurement. Improved early liver function. Transplantation 61:1605–1609

International Pancreas Transplant Registry at the University of Minnesota (2004) http://www.iptr.umn.edu/IPTR/annual_reports/2004_annual_report.html (Accessed Jan 01, 2007)

Kelly WD, Lillehei RC, Merkel FK, Idezuki Y, Goetz FC (1967) Allotransplantation of the pancreas and duodenum along with the kidney in diabetic nephropathy. Surgery 61:827–837

Krebs TL, Daly B, Wong-You-Cheong JJ, Carrol K, Bartlett ST (1999) Acute pancreatic transplant rejection: evaluation with dynamic contrast-enhanced MR imaging compared with histopathologic analysis. Radiology 210:437–442

Lappas JC (2003) Imaging of the postsurgical small bowel. Radiol Clin North Am 41:305–326

Lee BC, McGahan JP, Perez RV, Boone JM (2000) The role of percutaneous biopsy in detection of pancreatic transplant rejection. Clin Transpl 14:493–498

Margreiter R, Konigsrainer A, Schmid T et al (1992) Successful multivisceral transplantation. Transplant Proc 24:1226–1227

Mazariegos GV, Kocoshis S (1998) Patient selection for intestinal transplantation. Curr Opin Organ Transplant 3:293–297

Meador TL, Krebs TL, Wong-You-Cheong JJ, Daly B, Keay S, Bartlett S (2000) Imaging features of posttransplantation lymphoproliferative disorder in pancreas transplant recipients. AJR Am J Roentgenol 174:121–124

Moulton JS, Munda R, Weiss MA, Lubbers DJ (1989) Pancreatic transplants: CT with clinical and pathologic correlation. Radiology 172:21–26

Patel BK, Garvin PJ, Aridge DL, Chenoweth JL, Markivee CR (1991) Fluid collections developing after pancreatic transplantation: radiologic evaluation and intervention. Radiology 181:215–220

Port FK (2003) Organ donation and transplantation trends in the United States, 2001. Am J Transpl 3 [Suppl 4]:7–12

Reyes J, Green M, Bueno J et al (1996) Epstein-Barr virus associated posttransplant lymphoproliferative disease after intestinal transplantation. Transplant Proc 28:2768–2769

Starzl TE, Rowe MI, Todo S et al (1989) Transplantation of multiple abdominal viscera. J Am Med Assoc 261:1449–1457

Sudan DL, Iyer KR, Geroover A et al (2001) A new technique for combined liver/small intestinal transplantation. Transplantation 72:11–13

Tan M, Di Carlo A, Stein LA, Cantarovich M, Tchervenkov J, Metrakos P (2002) Pseudoaneurysm of the superior mesenteric artery after pancreas transplantation treated by endovascular stenting. Transplantation 72:336–338

Unsinn KM, Koenigsrainer A, Rieger M et al (2004a) Spectrum of imaging findings after intestinal, liver-intestinal, or multivisceral transplantation: part 1, posttransplantation anatomy. AJR Am J Roentgenol 183:1275–1283

Unsinn KM, Koenigsrainer A, Rieger M et al (2004b) Spectrum of imaging findings after intestinal, liver-intestinal, or multivisceral transplantation: part 2, posttransplantation complications. AJR Am J Roentgenol 183:1285–1291

Vahey TN, Glazer GM, Francis MR et al (1988) MR diagnosis of pancreatic transplant rejection. AJR Am J Roentgenol 150:557–560

Vas W, Patel B, Mahanta B, Salimi Z, Markivee C, Garvin P (1989) Innocuous gas collections in pancreatic allografts demonstrated by computed tomography. Gastrointest Radiol 14:118–122

Williams PL (1995) Gray's anatomy, 38th edn. Churchill Livingstone, New York, p 1791

Subject Index

C

D

E

F

G

H

I

J

K

L

M

N

O

P

R

List of Contributors

Herwig Antretter, MD
Professor, Klinische Abteilung für Herzchirurgie
Universitätsklinik für Chirurgie
Anichstrasse 35
6020 Innsbruck
Austria

Alexander A. Bankier, MD
Director of Functional Respiratory Imaging
Beth Israel Deaconess Medical Center
Harvard Medical School
330 Brookline Avenue
Boston, MA 02215
USA

Tomas Franquet, MD
Professor, Hospital de Saint Pau
Department of Radiology
Avenida S. Antoni Maria Claret 167
Barcelona 08025
Spain

Martin C. Freund, MD
Professor, Department of Radiology
Medical University Innsbruck
Anichstrasse 35
6020 Innsbruck
Austria

Nicolas Grenier, MD
Professor, Service d'Imagerie Diagnostique et
Interventionelle de l'Adulte
Groupe Hospitalier Pellegrin
Place Amélie Raba-Léon
33076 Bordeaux Cedex
France

Nigel Heaton, MB, BS, FRCS
Professor of Transplant Surgery
Institute of Liver Studies
King's College Hospital
Denmark Hill
London SE5 9RS
UK

Peter Jaksch, MD
Department of Thoracic Surgery
Transplantation Unit
Medical University of Vienna
Waehringer Guertel 18–20
1090 Vienna
Austria

Daniela Kienzl, MD
Department of Anesthesia
Medical University of Vienna
Waehringer Guertel 18–20
1090 Vienna
Austria

Jonathan B. Kruskal, MD
Professor, Department of Radiology
Beth Israel Deaconess Medical Center
330 Brookline Ave
Boston, MA 02215
USA

Janet E. Kuhlman, MD
Professor, Department of Radiology
Thoracic Imaging Section
University of Wisconsin Medical School
E3/311 CSC
600 Highland Avenue
Madison WI 53792-3252
USA

Christiane Kulinna-Cosentini, MD
Department of Radiology
Medical University of Vienna
Waehringer Guertel 18–20
1090 Vienna
Austria

Guenther Laufer, MD
Klinische Abteilung für Herzchirurgie
Universitätsklinik für Chirurgie
Anichstrasse 35
6020 Innsbruck
Austria

Sheida Mehrain, MD
Professor, Department of Radiology
Medical University of Vienna
Waehringer Guertel 18–20
1090 Vienna
Austria

Pierre Merville, MD
Professor, Département de Néphrologie
Unité Médicale de Néphrologie
Transplantation Rénale
Groupe Hospitalier Pellegrin
Place Amélie Raba-Léon
33076 Bordeaux Cedex
France

Gilles Pasticier, MD
Département d'Urologie
Groupe Hospitalier Pellegrin
Place Amélie Raba-Léon
33076 Bordeaux Cedex
France

Ivan Pedrosa, MD
Department of Radiology
Beth Israel Deaconess Medical Center
330 Brookline Ave
Boston, MA 02215
USA

Vassilios Raptopoulos, MD
Professor, Department of Radiology
Beth Israel Deaconess Medical Center
330 Brookline Ave
Boston, MA 02215
USA

Jorge Sierra, MD, PhD
Professor of Medicine
Director, Clinical Hematology and
Hematopoietic Transplantation Program
Hospital de la Santa Creu i Sant Pau
Universitat Autónoma de Barcelona
Barcelona
Spain

Olga Tucker, MD, FRCSI
Specialist Registrar
Institute of Liver Studies
King's College Hospital
Denmark Hill
London SE5 9RS
UK

Karin M. Unsinn, MD
Department of Radiology
Medical University Innsbruck
Anichstrasse 35
6020 Innsbruck
Austria

Giulia A. Zamboni, MD
Department of Radiology
Beth Israel Deaconess Medical Center
330 Brookline Ave
Boston, MA 02215
USA

Medical Radiology Diagnostic Imaging and Radiation Oncology

Titles in the series already published

Diagnostic Imaging

Innovations in Diagnostic Imaging
Edited by J. H. Anderson

Radiology of the Upper Urinary Tract
Edited by E. K. Lang

The Thymus - Diagnostic Imaging, Functions, and Pathologic Anatomy
Edited by E. Walter, E. Willich, and W. R. Webb

Interventional Neuroradiology
Edited by A. Valavanis

Radiology of the Pancreas
Edited by A. L. Baert, co-edited by G. Delorme

Radiology of the Lower Urinary Tract
Edited by E. K. Lang

Magnetic Resonance Angiography
Edited by I. P. Arlart, G. M. Bongartz, and G. Marchal

Contrast-Enhanced MRI of the Breast
S. Heywang-Köbrunner and R. Beck

Spiral CT of the Chest
Edited by M. Rémy-Jardin and J. Rémy

Radiological Diagnosis of Breast Diseases
Edited by M. Friedrich and E.A. Sickles

Radiology of the Trauma
Edited by M. Heller and A. Fink

Biliary Tract Radiology
Edited by P. Rossi, co-edited by M. Brezi

Radiological Imaging of Sports Injuries
Edited by C. Masciocchi

Modern Imaging of the Alimentary Tube
Edited by A. R. Margulis

Diagnosis and Therapy of Spinal Tumors
Edited by P. R. Algra, J. Valk, and J. J. Heimans

Interventional Magnetic Resonance Imaging
Edited by J. F. Debatin and G. Adam

Abdominal and Pelvic MRI
Edited by A. Heuck and M. Reiser

Orthopedic Imaging
Techniques and Applications
Edited by A. M. Davies and H. Pettersson

Radiology of the Female Pelvic Organs
Edited by E. K.Lang

Magnetic Resonance of the Heart and Great Vessels
Clinical Applications
Edited by J. Bogaert, A.J. Duerinckx, and F. E. Rademakers

Modern Head and Neck Imaging
Edited by S. K. Mukherji and J. A. Castelijns

Radiological Imaging of Endocrine Diseases
Edited by J. N. Bruneton in collaboration with B. Padovani and M.-Y. Mourou

Trends in Contrast Media
Edited by H. S. Thomsen, R. N. Muller, and R. F. Mattrey

Functional MRI
Edited by C. T. W. Moonen and P. A. Bandettini

Radiology of the Pancreas
2nd Revised Edition
Edited by A. L. Baert. Co-edited by G. Delorme and L. Van Hoe

Emergency Pediatric Radiology
Edited by H. Carty

Spiral CT of the Abdomen
Edited by F. Terrier, M. Grossholz, and C. D. Becker

Liver Malignancies
Diagnostic and Interventional Radiology
Edited by C. Bartolozzi and R. Lencioni

Medical Imaging of the Spleen
Edited by A. M. De Schepper and F. Vanhoenacker

Radiology of Peripheral Vascular Diseases
Edited by E. Zeitler

Diagnostic Nuclear Medicine
Edited by C. Schiepers

Radiology of Blunt Trauma of the Chest
P. Schnyder and M. Wintermark

Portal Hypertension
Diagnostic Imaging-Guided Therapy
Edited by P. Rossi
Co-edited by P. Ricci and L. Broglia

Recent Advances in Diagnostic Neuroradiology
Edited by Ph. Demaerel

Virtual Endoscopy and Related 3D Techniques
Edited by P. Rogalla, J. Terwisscha Van Scheltinga, and B. Hamm

Multislice CT
Edited by M. F. Reiser, M. Takahashi, M. Modic, and R. Bruening

Pediatric Uroradiology
Edited by R. Fotter

Transfontanellar Doppler Imaging in Neonates
A. Couture and C. Veyrac

Radiology of AIDS
A Practical Approach
Edited by J.W.A.J. Reeders and P.C. Goodman

CT of the Peritoneum
Armando Rossi and Giorgio Rossi

Magnetic Resonance Angiography
2nd Revised Edition
Edited by I. P. Arlart, G. M. Bongratz, and G. Marchal

Pediatric Chest Imaging
Edited by Javier Lucaya and Janet L. Strife

Applications of Sonography in Head and Neck Pathology
Edited by J. N. Bruneton in collaboration with C. Raffaelli and O. Dassonville

Imaging of the Larynx
Edited by R. Hermans

3D Image Processing
Techniques and Clinical Applications
Edited by D. Caramella and C. Bartolozzi

Imaging of Orbital and Visual Pathway Pathology
Edited by W. S. Müller-Forell

Pediatric ENT Radiology
Edited by S. J. King and A. E. Boothroyd

Radiological Imaging of the Small Intestine
Edited by N. C. Gourtsoyiannis

Imaging of the Knee
Techniques and Applications
Edited by A. M. Davies and V. N. Cassar-Pullicino

Perinatal Imaging
From Ultrasound to MR Imaging
Edited by Fred E. Avni

Radiological Imaging of the Neonatal Chest
Edited by V. Donoghue

Diagnostic and Interventional Radiology in Liver Transplantation
Edited by E. Bücheler, V. Nicolas, C. E. Broelsch, X. Rogiers, and G. Krupski

Radiology of Osteoporosis
Edited by S. Grampp

Imaging Pelvic Floor Disorders
Edited by C. I. Bartram and J. O. L. DeLancey
Associate Editors: S. Halligan, F. M. Kelvin, and J. Stoker

Imaging of the Pancreas
Cystic and Rare Tumors
Edited by C. Procacci and A. J. Megibow

High Resolution Sonography of the Peripheral Nervous System
Edited by S. Peer and G. Bodner

Imaging of the Foot and Ankle
Techniques and Applications
Edited by A. M. Davies, R. W. Whitehouse, and J. P. R. Jenkins

Radiology Imaging of the Ureter
Edited by F. Joffre, Ph. Otal, and M. Soulie

Imaging of the Shoulder
Techniques and Applications
Edited by A. M. Davies and J. Hodler

Radiology of the Petrous Bone
Edited by M. Lemmerling and S. S. Kollias

Interventional Radiology in Cancer
Edited by A. Adam, R. F. Dondelinger, and P. R. Mueller

Duplex and Color Doppler Imaging of the Venous System
Edited by G. H. Mostbeck

Multidetector-Row CT of the Thorax
Edited by U. J. Schoepf

Functional Imaging of the Chest
Edited by H.-U. Kauczor

Radiology of the Pharynx and the Esophagus
Edited by O. Ekberg

Radiological Imaging in Hematological Malignancies
Edited by A. Guermazi

Imaging and Intervention in Abdominal Trauma
Edited by R. F. Dondelinger

Multislice CT
2nd Revised Edition
Edited by M. F. Reiser, M. Takahashi, M. Modic, and C. R. Becker

Intracranial Vascular Malformations and Aneurysms
From Diagnostic Work-Up to Endovascular Therapy
Edited by M. Forsting

Radiology and Imaging of the Colon
Edited by A. H. Chapman

Coronary Radiology
Edited by M. Oudkerk

Dynamic Contrast-Enhanced Magnetic Resonance Imaging in Oncology
Edited by A. Jackson, D. L. Buckley, and G. J. M. Parker

Imaging in Treatment Planning for Sinonasal Diseases
Edited by R. Maroldi and P. Nicolai

Clinical Cardiac MRI
With Interactive CD-ROM
Edited by J. Bogaert, S. Dymarkowski, and A. M. Taylor

Focal Liver Lesions
Detection, Characterization, Ablation
Edited by R. Lencioni, D. Cioni, and C. Bartolozzi

Multidetector-Row CT Angiography
Edited by C. Catalano and R. Passariello

Paediatric Musculoskeletal Diseases
With an Emphasis on Ultrasound
Edited by D. Wilson

Contrast Media in Ultrasonography
Basic Principles and Clinical Applications
Edited by Emilio Quaia

MR Imaging in White Matter Diseases of the Brain and Spinal Cord
Edited by M. Filippi, N. De Stefano, V. Dousset, and J. C. McGowan

Diagnostic Nuclear Medicine
2nd Revised Edition
Edited by C. Schiepers

Imaging of the Kidney Cancer
Edited by A. Guermazi

Magnetic Resonance Imaging in Ischemic Stroke
Edited by R. von Kummer and T. Back

Imaging of the Hip & Bony Pelvis
Techniques and Applications
Edited by A. M. Davies, K. J. Johnson, and R. W. Whitehouse

Imaging of Occupational and Environmental Disorders of the Chest
Edited by P. A. Gevenois and P. De Vuyst

Contrast Media
Safety Issues and ESUR Guidelines
Edited by H. S. Thomsen

Virtual Colonoscopy
A Practical Guide
Edited by P. Lefere and S. Gryspeerdt

Vascular Embolotherapy
A Comprehensive Approach
Volume 1: *General Principles, Chest, Abdomen, and Great Vessels*
Edited by J. Golzarian. Co-edited by S. Sun and M. J. Sharafuddin

Vascular Embolotherapy
A Comprehensive Approach
Volume 2: *Oncology, Trauma, Gene Therapy, Vascular Malformations, and Neck*
Edited by J. Golzarian. Co-edited by S. Sun and M. J. Sharafuddin

Head and Neck Cancer Imaging
Edited by R. Hermans

Vascular Interventional Radiology
Current Evidence in Endovascular Surgery
Edited by M. G. Cowling

Ultrasound of the Gastrointestinal Tract
Edited by G. Maconi and G. Bianchi Porro

Imaging of Orthopedic Sports Injuries
Edited by F. M. Vanhoenacker, M. Maas, J. L. M. A. Gielen

Parallel Imaging in Clinical MR Applications
Edited by S. O. Schoenberg, O. Dietrich, and F. M. Reiser

MR and CT of the Female Pelvis
Edited by B. Hamm and R. Forstner

Ultrasound of the Musculoskeletal System
S. Bianchi and C. Martinoli

Spinal Imaging
Diagnostic Imaging of the Spine and Spinal Cord
Edited by J. W. M. Van Goethem, L. Van den Hauwe, and P. M. Parizel

Radiation Dose from Adult and Pediatric Multidetector Computed Tomography
Edited by D. Tack and P. A. Gevenois

Computed Tomography of the Lung
A Pattern Approach
J. A. Verschakelen and W. De Wever

Clinical Functional MRI
Presurgical Functional Neuroimaging
Edited bei C. Stippich

Imaging in Transplantation
Edited by A. A. Bankier

Radiological Imaging of the Digestive System in Infants and Children
Edited by A. Devos and J. G. Blickman

Springer

MEDICAL RADIOLOGY Diagnostic Imaging and Radiation Oncology

Titles in the series already published

RADIATION ONCOLOGY

Lung Cancer
Edited by C.W. Scarantino

Innovations in Radiation Oncology
Edited by H. R. Withers
and L. J. Peters

Radiation Therapy
of Head and Neck Cancer
Edited by G. E. Laramore

Gastrointestinal Cancer –
Radiation Therapy
Edited by R.R. Dobelbower, Jr.

Radiation Exposure
and Occupational Risks
Edited by E. Scherer, C. Streffer,
and K.-R. Trott

Radiation Therapy of Benign Diseases
A Clinical Guide
S. E. Order and S. S. Donaldson

Interventional Radiation
Therapy Techniques – Brachytherapy
Edited by R. Sauer

Radiopathology of Organs and Tissues
Edited by E. Scherer, C. Streffer,
and K.-R. Trott

Concomitant Continuous Infusion
Chemotherapy and Radiation
Edited by M. Rotman
and C. J. Rosenthal

Intraoperative Radiotherapy –
Clinical Experiences and Results
Edited by F. A. Calvo, M. Santos,
and L.W. Brady

Radiotherapy of Intraocular
and Orbital Tumors
Edited by W. E. Alberti and
R. H. Sagerman

Interstitial and Intracavitary
Thermoradiotherapy
Edited by M. H. Seegenschmiedt
and R. Sauer

Non-Disseminated Breast Cancer
Controversial Issues in Management
Edited by G. H. Fletcher and S.H. Levitt

Current Topics in
Clinical Radiobiology of Tumors
Edited by H.-P. Beck-Bornholdt

Practical Approaches to
Cancer Invasion and Metastases
A Compendium of Radiation
Oncologists' Responses to 40 Histories
Edited by A. R. Kagan with the
Assistance of R. J. Steckel

Radiation Therapy in Pediatric Oncology
Edited by J. R. Cassady

Radiation Therapy Physics
Edited by A. R. Smith

Late Sequelae in Oncology
Edited by J. Dunst and R. Sauer

Mediastinal Tumors. Update 1995
Edited by D. E. Wood and C. R. Thomas, Jr.

Thermoradiotherapy
and Thermochemotherapy
Volume 1:
Biology, Physiology, and Physics
Volume 2:
Clinical Applications
Edited by M.H. Seegenschmiedt,
P. Fessenden, and C.C. Vernon

Carcinoma of the Prostate
Innovations in Management
Edited by Z. Petrovich, L. Baert,
and L.W. Brady

Radiation Oncology
of Gynecological Cancers
Edited by H.W. Vahrson

Carcinoma of the Bladder
Innovations in Management
Edited by Z. Petrovich, L. Baert,
and L.W. Brady

Blood Perfusion and
Microenvironment of Human Tumors
Implications for Clinical Radiooncology
Edited by M. Molls and P. Vaupel

Radiation Therapy of Benign Diseases
A Clinical Guide
2nd Revised Edition
S. E. Order and S. S. Donaldson

Carcinoma of the Kidney and Testis,
and Rare Urologic Malignancies
Innovations in Management
Edited by Z. Petrovich, L. Baert,
and L.W. Brady

Progress and Perspectives in the
Treatment of Lung Cancer
Edited by P. Van Houtte,
J. Klastersky, and P. Rocmans

Combined Modality Therapy of
Central Nervous System Tumors
Edited by Z. Petrovich, L. W. Brady,
M. L. Apuzzo, and M. Bamberg

Age-Related Macular Degeneration
Current Treatment Concepts
Edited by W. A. Alberti, G. Richard,
and R. H. Sagerman

Radiotherapy of Intraocular
and Orbital Tumors
2nd Revised Edition
Edited by R. H. Sagerman,
and W. E. Alberti

Modification of Radiation Response
Cytokines, Growth Factors,
and Other Biolgical Targets
Edited by C. Nieder, L. Milas,
and K. K. Ang

Radiation Oncology for Cure and Palliation
R. G. Parker, N. A. Janjan,
and M. T. Selch

Clinical Target Volumes in Conformal and
Intensity Modulated Radiation Therapy
A Clinical Guide to Cancer Treatment
Edited by V. Grégoire, P. Scalliet,
and K. K. Ang

Advances in Radiation Oncology
in Lung Cancer
Edited by Branislav Jeremić

New Technologies in Radiation Oncology
Edited by W. Schlegel, T. Bortfeld,
and A.-L. Grosu

Technical Basis of Radiation Therapy
4th Revised Edition
Edited by S. H. Levitt, J. A. Purdy,
C. A. Perez, and S. Vijayakumar

Late Effects of Cancer Treatment
on Normal Tissues
Edited by P. Rubin, L. S. Constine,
L. B. Marks, and P. Okunieff

Clinical Practice of Radiation Therapy for
Benign Diseases
Contemporary Concepts and Clical
Results
Edited by M. H. Seegenschmiedt,
H.-B. Makoski, K.-R. Trott, and
L. W. Brady

Springer